frontiers | Research Topics

Exploring the role of immune cells and cell therapy in liver cancer

Edited by
Yue Wang, Yan-Ru Lou and Zhiying He

Coordinated by
Wencheng Zhang and Xicheng Wang

Published in
Frontiers in Immunology

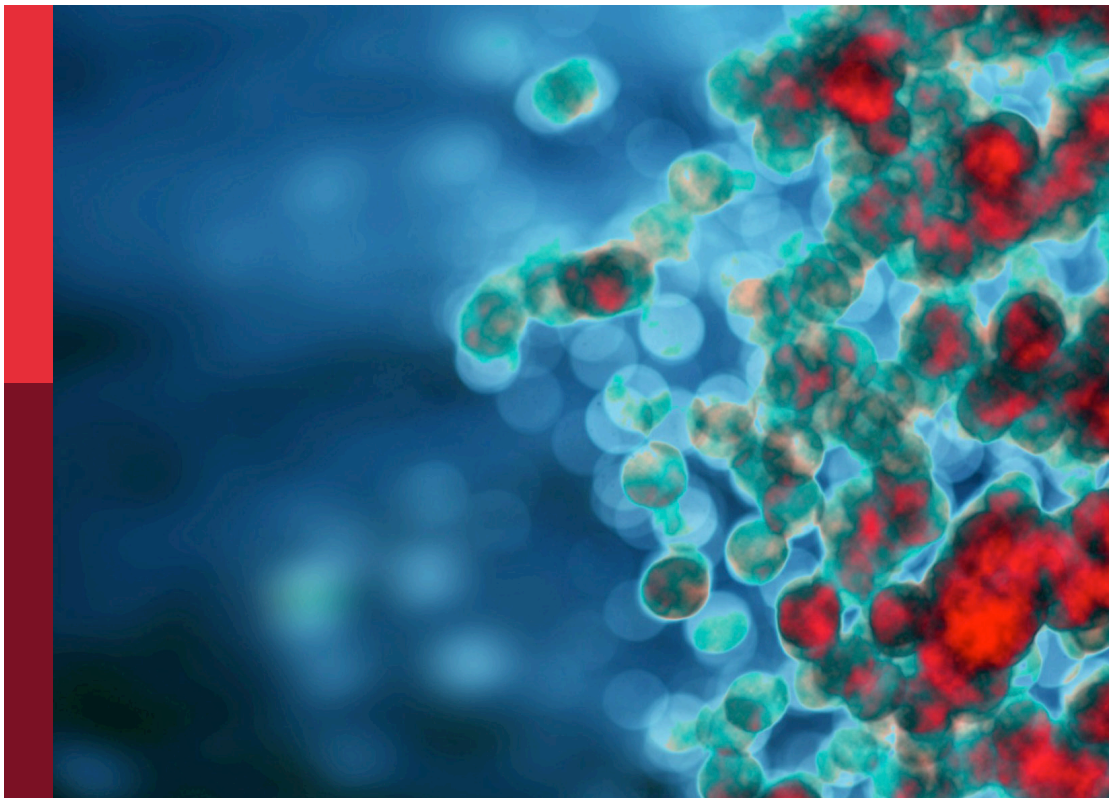

ISSN 1664-8714
ISBN 978-2-8325-7328-0
DOI 10.3389/978-2-8325-7328-0

Generative AI statement
Any alternative text (Alt text) provided alongside figures in the articles in this ebook has been generated by Frontiers with the support of artificial intelligence and reasonable efforts have been made to ensure accuracy, including review by the authors wherever possible. If you identify any issues, please contact us.

About Frontiers

Frontiers is more than just an open access publisher of scholarly articles: it is a pioneering approach to the world of academia, radically improving the way scholarly research is managed. The grand vision of Frontiers is a world where all people have an equal opportunity to seek, share and generate knowledge. Frontiers provides immediate and permanent online open access to all its publications, but this alone is not enough to realize our grand goals.

Frontiers journal series

The Frontiers journal series is a multi-tier and interdisciplinary set of open-access, online journals, promising a paradigm shift from the current review, selection and dissemination processes in academic publishing. All Frontiers journals are driven by researchers for researchers; therefore, they constitute a service to the scholarly community. At the same time, the *Frontiers journal series* operates on a revolutionary invention, the tiered publishing system, initially addressing specific communities of scholars, and gradually climbing up to broader public understanding, thus serving the interests of the lay society, too.

Dedication to quality

Each Frontiers article is a landmark of the highest quality, thanks to genuinely collaborative interactions between authors and review editors, who include some of the world's best academicians. Research must be certified by peers before entering a stream of knowledge that may eventually reach the public - and shape society; therefore, Frontiers only applies the most rigorous and unbiased reviews. Frontiers revolutionizes research publishing by freely delivering the most outstanding research, evaluated with no bias from both the academic and social point of view. By applying the most advanced information technologies, Frontiers is catapulting scholarly publishing into a new generation.

What are Frontiers Research Topics?

Frontiers Research Topics are very popular trademarks of the *Frontiers journals series*: they are collections of at least ten articles, all centered on a particular subject. With their unique mix of varied contributions from Original Research to Review Articles, Frontiers Research Topics unify the most influential researchers, the latest key findings and historical advances in a hot research area.

Find out more on how to host your own Frontiers Research Topic or contribute to one as an author by contacting the Frontiers editorial office: frontiersin.org/about/contact

Exploring the role of immune cells and cell therapy in liver cancer

Topic editors
Yue Wang — Second Military Medical University, China
Yan-Ru Lou — Shanghai Jiao Tong University, China
Zhiying He — Tongji University, China

Topic coordinators
Wencheng Zhang — Tongji University, China
Xicheng Wang — Tongji University, China

Citation
Wang, Y., Lou, Y.-R., He, Z., Zhang, W., Wang, X., eds. (2026). *Exploring the role of immune cells and cell therapy in liver cancer*. Lausanne: Frontiers Media SA.
doi: 10.3389/978-2-8325-7328-0

Table of contents

frontiers | Frontiers in Immunology

TYPE Editorial
PUBLISHED 15 December 2025
DOI 10.3389/fimmu.2025.1752606

OPEN ACCESS

EDITED AND REVIEWED BY
Peter Brossart,
University of Bonn, Germany

*CORRESPONDENCE
Zhiying He
zyhe@tongji.edu.cn

RECEIVED 23 November 2025
ACCEPTED 08 December 2025
PUBLISHED 15 December 2025

CITATION
Zhang W, Lou Y-R, Wang Y, Wang X and He Z (2025) Editorial: Exploring the role of immune cells and cell therapy in liver cancer.
Front. Immunol. 16:1752606.
doi: 10.3389/fimmu.2025.1752606

Editorial: Exploring the role of immune cells and cell therapy in liver cancer

Wencheng Zhang[1,2,3], Yan-Ru Lou[4], Yue Wang[5,6], Xicheng Wang[1,2,3] and Zhiying He[1,2,3]*

[1]Institute for Regenerative Medicine, Medical Innovation Center and State Key Laboratory of Cardiovascular Diseases, Shanghai East Hospital, School of Life Sciences and Technology, Tongji University, Shanghai, China, [2]Shanghai Engineering Research Center of Stem Cells Translational Medicine, Shanghai, China, [3]Shanghai Institute of Stem Cell Research and Clinical Translation, Shanghai, China, [4]Shanghai Children's Hospital, School of Medicine, Shanghai Jiao Tong University, Shanghai, China, [5]Research Center of Developmental Biology Department of Histology and Embryology College of Basic Medicine, Second Military Medical University, Shanghai, China, [6]Shanghai Key Laboratory of Cell Engineering Second Military Medical University, Shanghai, China

KEYWORDS

chimeric antigen receptor (CAR) T-cell therapy, immunotherapy, liver cancer (LC), natural killer cells (NK cells), programmed cell death protein-1 (PD-1), tumor microenvironment (TME), tumor organoids

Editorial on the Research Topic
Exploring the role of immune cells and cell therapy in liver cancer

Hepatocellular carcinoma (HCC) is one of the most common cancers worldwide, underscoring the urgent need for improved diagnosis and treatment. One of the most critical aspect for the complexity of the HCC is its tumor microenvironment (TME), a complex structure composed of various immune cells, cancer-associated fibroblasts, endothelial cells, and other tissue-resident cells., The TME plays a crucial role in the occurrence, development, invasion, infiltration, metastasis, spread, and growth of tumors. Understanding the complex interactions between tumor cells and the TME is not only a prerequisite for the rational development of effective anti-tumor therapies but also key to targeted therapy and effective drug delivery. This Research Topic of *Frontiers in Immunology* explores the latest advances in developing cell or immunotherapies with stable quality and significant efficacy in the context of tumor and immune microenvironment. These innovations offer promising strategies for treating liver tumors that are currently untreatable in clinical practice and provide useful research and translational directions for cell therapy against other solid tumors.

Immunotherapy for liver cancer can be broadly categorized into traditional targeted therapy and novel immune cell therapy. Regarding traditional treatments, Dong et al. conducted a retrospective real-world study on the poor prognosis and ineffectiveness of existing treatments for advanced intrahepatic cholangiocarcinoma (ICC). Analysis of data from 95 ICC patients revealed that chemotherapy combined with lenvatinib and programmed cell death protein-1 (PD-1) inhibitors was significantly effective and well-tolerated, representing a potentially better treatment option for advanced unresectable intrahepatic cholangiocarcinoma. However, this conclusion still requires validation through larger-scale prospective cohort studies. Chen et al. also conducted a systemic

meta-analysis to examine the efficacy and safety of transarterial chemoembolization (TACE) plus lenvatinib with or without PD-1 inhibitors (TLP group) compared with TACE + lenvatinib (TL group) for unresectable hepatocellular carcinoma (uHCC). And their result concluded that the TLP group had better efficacy for uHCC than that of the TL group, with an acceptable safety profile.

Beyond classic sites like PD-1, many studies have focused on novel targets. Chen et al. elucidated the crucial role of caspase-8 in the development, progression, and drug resistance of HCC, and explored the prospects of targeting caspase-8 as a treatment for HCC. However, the authors also noted that the regulatory role of caspase-8 in the complex TME of HCC is not fully understood. Furthermore, the clinical translation of this approach faces significant technical hurdles, including the lack of highly specific and selective caspase-8 activators and inhibitors, as well as the lack of effective delivery to tumor tissues and the ability to penetrate the vascularized TME of HCC.

As of the immune cell therapy, Zhang et al. reviewed the application of cell therapy in HCC, covering different cell types, their effective mechanisms, the latest advances in clinical trials, and current challenges. Their work provides useful insights for future research and clinical applications in the treatment of HCC. To date, the chimeric antigen receptor (CAR) T-cell therapy has been known as a key advancement in cancer treatment, but many challenges remain in using CAR-T cells to treat solid tumors such as HCC. Key issues that still need to be addressed include improving T-cell migration, combating the immunosuppressive TME, and enhancing safety. A mini-review by Zhou et al. summarizes the latest research findings and clinical progress of CAR-T cell therapy in the treatment of HCC, providing a comprehensive overview of the current status, challenges, and future prospects of CAR-T cell immunotherapy in HCC treatment.

The development of alternative immune cell therapy is based on clarifying the composition and dynamic changes in immune cell populations in disease states compared to healthy condition. Natural killer cells (NK cells) play a role in both innate and adaptive immune responses. Multiple studies have confirmed that NK cell phenotype and specific functions are influenced by the microenvironment. Hepatic NK cells undergo functional and phenotypic changes during liver cancer progression, affecting disease prognosis. To explore the effects of immune cells or immune signaling pathways on the behavior of tumor cells and tumor-initiating cells, Antonia Paul et al. established a 37-color flow cytometry method incorporating 41 markers to perform in-depth phenotypic analysis of human peripheral and hepatic NK cells. This high-parameter, high-resolution detection platform provides a key tool for in-depth analysis of different NK cell subsets in peripheral blood and liver under healthy and disease states.

Other than NK cells, dendritic cells (DCs), a diverse class of professional antigen-presenting cells, also holds promise as an effective strategy to improve the efficacy of anti-tumor immunotherapy and enhance tolerance to autoantigens in autoimmune diseases. Wang et al. found that oral administration of a Toll-like 2 receptor (TLR2)- activating lactic acid-producing probiotics (LAP) can effectively and significantly induce the accumulation of regulatory dendritic cells (rDCs) in the liver of mice. This accumulation inhibited the function of cytotoxic T cells and alleviated diethylnitrosamine (DEN)-induced liver injury, fibrosis, and tumorigenesis. Considering the role of LAP in stimulating regulatory DCs, this therapeutic strategy may also have good clinical application value in the prevention or treatment of autoimmune diseases (arthritis and asthma), inflammatory bowel disease, and alcoholic or non-alcoholic chronic liver disease.

Of course, any immunotherapy, while establishing the effectiveness of drugs and cells, must also acknowledge the unique immune microenvironment of the liver. The liver's immune microenvironment not only inhibits the efficacy of immunotherapeutic drugs but also creates a barrier, leading to drug resistance and reducing the overall effectiveness of treatment. Liu et al. summarized recent research progress on the immune profile of liver cancer, pointing out that future treatment strategies include combining immunotherapy with other therapies, utilizing targeted therapies to modulate the immune microenvironment, and developing novel drugs that can bypass or counteract liver inhibitory mechanisms, thereby improving the treatment outcomes of liver cancer.

In addition to focusing on the progress of immunotherapy for HCC, this Research Topic also summarizes models for liver cancer research and prognostic assessment. Song et al. summarized the current research and treatment progress for fibrolamellar carcinoma (FLC), a rare tumor. They particularly elucidated the crucial role of the interaction between FLC epithelial cells, endothelial progenitor cells, stellate cells, and the host's immune microenvironment in the construction of FLC organoids. The review emphasized the key role of the interaction between tumor cells and multiple cell types within the TME in tumor organoid construction, and the concepts mentioned in this review also apply to the construction of organoids for HCC and cholangiocarcinoma.

Lastly, as a direct manifestation of the role of the tumor immune microenvironment in tumor recurrence and metastasis, microvascular invasion (MVI) is an independent risk factor for recurrence and metastasis of HCC, highly associated with poor prognosis. Mu et al. identified characteristic genes of MVI and constructed a novel prognostic prediction model for HCC using spatial transcriptome sequencing. This model suggests an increased proportion of macrophages in high-risk patients, indicating that HCC tumor cells may promote HCC metastasis through macrophage cell interactions via activating "migration inhibitory factor (MIF)-CD74" signaling. This study not only provides an assessment model for the prognosis of patients with HCC but also has important clinical significance in differentiating patient types and selecting appropriate treatment options.

In summary, this Research Topic provides a systematic and comprehensive overview of the current progress, breakthroughs, existing problems, and solutions in traditional drug immunotherapy and cell therapy for HCC. It underscores the development of sequencing for targeted therapy and cell therapy, as well as combined systemic therapies, for solid tumors such as HCC.

Author contributions

WZ: Writing – original draft, Funding acquisition, Writing – review & editing. Y-RL: Writing – review & editing. YW: Writing – review & editing. XW: Writing – review & editing, Funding acquisition. ZH: Funding acquisition, Writing – review & editing.

Funding

The author(s) declared that financial support was received for this work and/or its publication. Authors were supported by the National Natural Science Foundation of China (82471592, 82270638, 82300718, 82301904), Shanghai Clinical Research Center for Cell Therapy (23J41900100), Shanghai Engineering Research Center of Stem Cells Translational Medicine (20DZ2255100), Peak Disciplines (Type IV) of Institutions of Higher Learning in Shanghai, and China Postdoctoral Science Foundation (2025M772275).

Acknowledgments

We thank the authors of the publications collected in this Research Topic for their contributions.

Conflict of interest

The authors declared that this work was conducted in the absence of any commercial or financial relationships that could be construed as a potential conflict of interest.

Generative AI statement

The author(s) declared that generative AI was not used in the creation of this manuscript.

Any alternative text (alt text) provided alongside figures in this article has been generated by Frontiers with the support of artificial intelligence and reasonable efforts have been made to ensure accuracy, including review by the authors wherever possible. If you identify any issues, please contact us.

Publisher's note

frontiers | Frontiers in Immunology

TYPE Systematic Review
PUBLISHED 30 August 2024
DOI 10.3389/fimmu.2024.1466113

OPEN ACCESS

EDITED BY
Yan-Ru Lou,
University of Helsinki, Finland

REVIEWED BY
Elena Niculet,
Dunarea de Jos University, Romania
Kazuto Tajiri,
University of Toyama University Hospital, Japan

*CORRESPONDENCE
Tao Luo
Taoluo35@126.com

RECEIVED 17 July 2024
ACCEPTED 15 August 2024
PUBLISHED 30 August 2024

CITATION
Chen Y, Jia L, Li Y, Cui W, Wang J, Zhang C, Bian C and Luo T (2024) Efficacy and safety of transarterial chemoembolization plus lenvatinib combined with PD-1 inhibitors versus transarterial chemoembolization plus lenvatinib for unresectable hepatocellular carcinoma: a meta-analysis.
Front. Immunol. 15:1466113.
doi: 10.3389/fimmu.2024.1466113

Efficacy and safety of transarterial chemoembolization plus lenvatinib combined with PD-1 inhibitors versus transarterial chemoembolization plus lenvatinib for unresectable hepatocellular carcinoma: a meta-analysis

Yue Chen[1], Luyao Jia[1], Yu Li[1], Wenhao Cui[2], Jukun Wang[1], Chao Zhang[1], Chunjing Bian[1] and Tao Luo[1]*

[1]Department of General Surgery, Xuanwu Hospital, Capital Medical University, Beijing, China, [2]Emergency Medicine Department, Xuanwu Hospital, Capital Medical University, Beijing, China

Background: Locoregional treatment combined with systemic therapy is expected to play a synergistic anticancer role. We conducted this systemic meta-analysis to examine the efficacy and safety of transarterial chemoembolization (TACE) plus lenvatinib with or without programmed cell death protein-1 (PD-1) inhibitors (TLP group) compared with TACE + lenvatinib (TL group) for unresectable hepatocellular carcinoma (uHCC).

Methods: From the inception date to April 2024, the data from PubMed, EMBASE, the Cochrane Library, Ovid, Web of Science, and Clinical Trials. gov were used for meta-analysis. All clinical outcomes of interest included overall survival (OS), progression-free survival (PFS), objective response rate (ORR), disease control rate (DCR), and adverse events (AEs). The hazard ratio (HR) and risk ratio (RR) with 95% confidence intervals (CI) were used to measure the pooled effect.

Results: This study included 10 retrospective cohort studies, including 1128 patients. The OS (HR=0.51; 95% CI: 0.43–0.60, $P < 0.05$), PFS (HR=0.52; 95% CI: 0.45–0.61, $P < 0.05$), ORR (RR = 1.58; 95% CI: 1.37–1.83; $P < 0.05$) and DCR (RR = 1.31; 95% CI: 1.20–1.43; $P < 0.05$) were significantly higher in TLP group than in the TL group. The incidence of AEs was acceptable. Prognostic factor analysis identified that ECOG PS (1/0), Child-Pugh class (B/A), BCLC stage (C/B) and main portal vein invasion (yes/no) were independent prognostic factors for OS. BCLC stage (C/B) and main portal vein invasion (yes/no) were independent prognostic factors for PFS.

Conclusion: The TLP group had better efficacy for uHCC than that of the TL group, with acceptable safety.

Systematic review registration: PROSPERO, identifier (CRD42023420093).

KEYWORDS

transarterial chemoembolization, lenvatinib, programmed cell death protein-1 inhibitors, unresectable, hepatocellular carcinoma

Introduction

The morbidity and mortality of hepatocellular carcinoma (HCC) remain high worldwide, among which primary liver cancer is the most common. It ranks fifth in the incidence rate and is the third leading cause of cancer death in the world (1). Because of the strong compensatory ability of liver, most patients are diagnosed with HCC when the disease progresses to the middle and late stage. Patients eventually lost the opportunity of surgery, ablation and liver transplantation, resulting in poor prognosis (2). Therefore, the combined treatment of unresectable HCC (uHCC) has attracted much attention.

In SHARP and REFLECT trials, tyrosine kinase inhibitors (TKIs) sorafenib and lenvatinib were recommended as the first-line treatment drugs for advanced HCC respectively (3, 4). Among them, subsequent trials proved that the effect of lenvatinib was not inferior to sorafenib for HCC (5). However, it is found that systemic therapy alone cannot achieve satisfactory survival time for advanced HCC. According to the treatment strategy of Barcelona Clinic Liver Cancer (BCLC), transitional chemoembolization (TACE) is recognized as the first preferred treatment for uHCC (6). But TACE alone has certain limitations. Subsequent clinical trials have proved that the combination of TACE and lenvatinib is more effective than single therapy, with potential effectiveness and safety (7).

With the emergence of refractory and drug-resistant HCC, blocking immune checkpoint pathway by immune checkpoint inhibitors (ICIs) has been found to be a new cancer treatment strategy (8). At present, the most widely studied ICIs is anti-programmed cell death 1 (PD-1)/programmed cell death protein ligand 1 (PD-L1), which can enhance the function of T cells and exert an anti-tumor activity (9). A recent clinical trial (IMbrave150) showed that compared with sorafenib or lenvatinib, the combination of atilizumab (PD-L1) and bevacizumab (anti-vascular endothelial growth factor, VEGF) was a better first-line choice for advanced HCC, and the overall survival(OS) of HCC was significantly prolonged (10). Since then, the beginning of targeted immunotherapy for HCC has begun, and PD-1 has become the second-line therapy for advanced HCC. Therefore, adding PD-1 on the basis of TACE + lenvatinib may optimize the efficacy of the triple therapy and produce more desirable synergistic effect (11, 12).

In the past two years, the efficacy of TACE + lenvatinib + PD-1 triple therapy has achieved encouraging results in many trials. Therefore, we conducted this systemic meta-analysis to compare the efficacy and safety of TACE + lenvatinib + PD-1 triple therapy and TACE + lenvatinib dual therapy in multiple trials, so as to determine a better treatment plan for uHCC patients.

Materials and methods

Ethical approval was not required for this study, and the article has been reported in line with the PRISMA (Preferred Reporting Items for systemic Reviews and Meta Analyses) checklist (13). This meta-analysis was registered at PROSPERO (CRD42023420093).

Literature search strategy

The publication time was limited to when the databases were established until April, 2024. We conducted a systemic search of PubMed, EMBASE, the Cochrane Library, Ovid, Web Of Science, and Clinical Trials.gov databases to identify useful literatures related to this meta-analysis. The MESH terms used in these databases included ("carcinoma, hepatocellular" or "liver cancer" or "HCC" or "liver neoplasm"), ("transarterial chemoembolization" or "TACE"), ("PD-1" or "immunotherapy therapies") ("Lenvatinib" or "Lenvima"). There are no restrictions on the language of selected literatures. After that, two authors (**XX** and **XX**) independently extracted and confirmed relevant data. The flowchart of the article screening and selection process is presented in the Figure 1.

Study selection

Inclusion criteria: 1) the patients diagnosed with uHCC by imaging and biopsy evidence; 2) the uHCC patients received TACE + lenvatinib + PD-1(TLP) group compared with TACE + lenvatinib (TL) group; 3) the types of study include randomized controlled trials (RCT) and retrospective cohort studies (RCS); 4) the clinical outcomes evaluated were OS, progression-free survival (PFS),

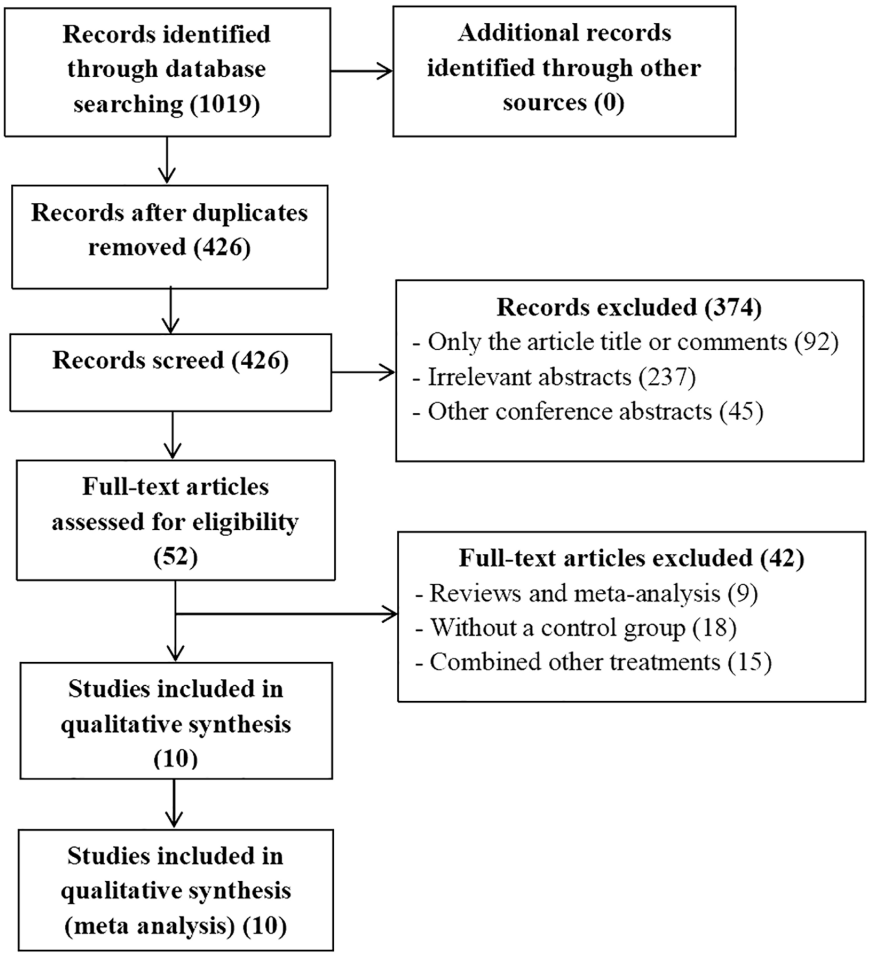

FIGURE 1
Flowchart of article screening and selection process.

objective response rate (ORR), disease control rate (DCR), and adverse events (AEs), which include at least one valuable survival outcome.

Exclusion criteria: 1) the study types included a review, a meta-analysis, a conference abstract, a letter, and a case report; 2) the study lacked effective outcomes data or reported irrelevant outcomes; 3) There is no control group.

Data extraction and quality assessment

Two reviewers (**XX** and **XX**) independently screened the studies and evaluated the quality of the included studies in a standardized way. Any discrepancy was resolved through a discussion. A third reviewer (**XX**) would decide if necessary. The data extracted from each study include the name of the first author, the year of publication, the design of the study population, the nationality and the clinical characteristics of patients (including sex, age, Child-Pugh class, ECOG PS, BCLC stage). The Newcastle-Ottawa Scale (NOS) was applied for RCS (14). Additionally, tumor responses were determined by the modified response evaluation criteria in solid tumors (mRECIST) or RECIST. The quality assessment of each literature is presented in Table 1.

Statistical analysis

Hazard ratios (HRs) with 95% confidence intervals (CIs) were calculated to analyze OS and PFS. The risk ratios (RR) with 95% CIs were calculated to analyze ORR, DCR and AEs. A fixed effect model was used for data pooling if no significant heterogeneity among included trials was observed. Otherwise, a random effect model was used. The I^2 statistic ($I^2 > 50\%$ was deemed to have significant heterogeneity) and $\chi 2$ test ($P < 0.10$ was deemed to suggest significant heterogeneity) were used to assess the heterogeneity among the trials. The funnel plots were performed to detect the existence of publication bias ($P < 0.10$ was deemed to represent significant publication bias). All analyses were performed using the Revman5.4 software. Statistical test was a two-tailed test, and $p < 0.05$ was statistically significant.

TABLE 1 Baseline characteristics of the studies.

Study	Country	Design	Patients (M/F)		Age (years)		Child-Pugh class (A/B)		ECOG PS (0/1/2)		BLCL (B/C)		PD-1	NOS SCORE
			TACE-L-P	L-P	TACE-L-P	L-P	TACE-L-P	L-P	TACE-L-P	L-P	TACE-L-P	L-P		
Cai 2022 (15)	China	RCS	41 (37/4)	40 (33/7)	51.9 ± 10.3	54.6 ± 11.0	37/4	33/7	33/8/0	28/ 12/0	/	/	Sintilimab, Tislelizumab, Camrelizumab	8
Chen 2021	China	RCS	70 (37/33)	72 (38/ 34)	54.2	50	/	/	47/23/0	30/42	47/23	45/27	Pembrolizumab	8
Guo 2022 (16)	China	RCS	75 (65/10)	91 (88/3)	≤60: 66 >60: 25	≤60: 60 >60: 15	13/78	2/73	58/33/0	69/6/0	20/71	20/55	Camrelizumab, Sintilimab	8
Qu 2022 (17)	China	RCS	30 (26/4)	21 (20/1)	55.5 (47.8, 64.3)	50.0 (45.0, 61.0)	28/2	21/0	/	/	1/29	3/18	/	7
Sheng 2024 (18)	China	RCS	113 (95/18)	128 (108/ 20)	64.48 ± 10.83	62.59 ± 10.58	88/25	99/29	62/36/15	66/ 42/20	54/59	63/65	Sintilimab, Camrelizumab, Tislelizumab	8
Wang yy 2023 (19)	China	RCS	45 (42/3)	20 (15/5)	54 (18 - 79)	62 (26 - 75)	30/15	18/2	26/19/0	7/13/0	11/34	5/15	Camrelizumab, Sintilimab, Pembrolizumab, Tislelizumab, Nivolumab	7
Wang wj 2023 (20)	China	RCS	54 (49/5)	45 (43/2)	57.0 ± 9.9	60.8 ± 9.4	49/5	42/3	46/8/0	41/4/0	/	/	Sintilimab, Camrelizumab, Toripalimab	8
Wu 2024 (21)	China	RCS	18 (15/3)	23 (18/5)	56.9 ± 8.1	58.1 ± 9.4	18/0	21/2	7/11/0	7/16/0	/	/	Sintilimab, Camrelizumab, Nivolumab, Tislelizumab	8
Xiang 2023 (22)	China	RCS	33 (28/5)	49 (45/4)	51.0 ± 12.2	51.7 ± 11.2	25/8	41/8	22/11	38/11	10/23	22/27	camrelizumab	8
Zou 2023 (23)	China	RCS	70 (59/11)	90 (77/ 13)	53.6 ± 15.1	52.3 ± 14.8	46/24	61/29	17/53/0	28/ 62/0	0/70	0/90	Pembrolizumab, Sintilimab	8

M, male; F, female; TACE; transarterial chemoembolization; L, lenvatinib; P, programmed cell death protein-1; ECOG, Eastern Cooperative Oncology Group; BCLC, Barcelona Clinic Liver Cancer; NOS, the Newcastle–Ottawa Scale; RCS, retrospective cohort study; /, not reported.

10.3389/fimmu.2024.1466113

Results

Search results

A total of 10 articles met the inclusion and exclusion criteria, of which 426 were selected after removing duplicates. We excluded 374 articles after reviewing the titles and abstracts of 426 articles. The full text of the remaining 52 articles were evaluated. According to the inclusion and exclusion criteria, 42 studies were excluded. Ultimately, 10 articles including 1128 patients were included in the current meta-analysis, which all studies included were RCS (15–24).

Study characteristics

The included study characteristics are summarized in Table 1. All included articles were published in China from 2022 to 2024. Of the 1128 patients included in our meta-analysis, 848 were male and 280 were female. Furthermore, 549 patients with uHCC received TLP triple therapy, while 579 patients received TL dual therapy. The PD-1 included in all selected articles were mainly Sintilimab, Tislelizumab, Camrelizumab, Pembrolizumab and Nivolumab, which was also depicted in Table 1. There were some significant variables which were analyzed in subgroups in the two groups.

Risk of bias

NOS was used to assess RCS. It contains the selection of subjects, comparability of the groups, and assessment of outcomes, with a maximum of 9 points. Studies with a score of more than 6 were determined to be high quality.

Meta-analysis outcomes

Overall survival and progression-free survival

Only nine articles provided the outcomes of OS and 10 articles provided the outcomes of PFS for the two groups, including the point estimate (HR) and its 95% CI. The meta-analysis indicated that patients with uHCC in the TLP group had significantly longer OS (HR=0.51; 95% CI: 0.43–0.60, $P < 0.05$) and PFS (HR=0.52; 95% CI: 0.45–0.61, $P < 0.05$) than those in the TL group. The findings indicated that the TLP triple therapy could significantly prolonged survival time (Figure 2).

Disease control rate and objective response rate

Ten articles have provided the outcomes of ORR and only nine articles have provided the outcomes of DCR for the two groups, including the point estimate (RR) and its 95% CI. The meta-analysis indicated that patients with uHCC in the TLP group had

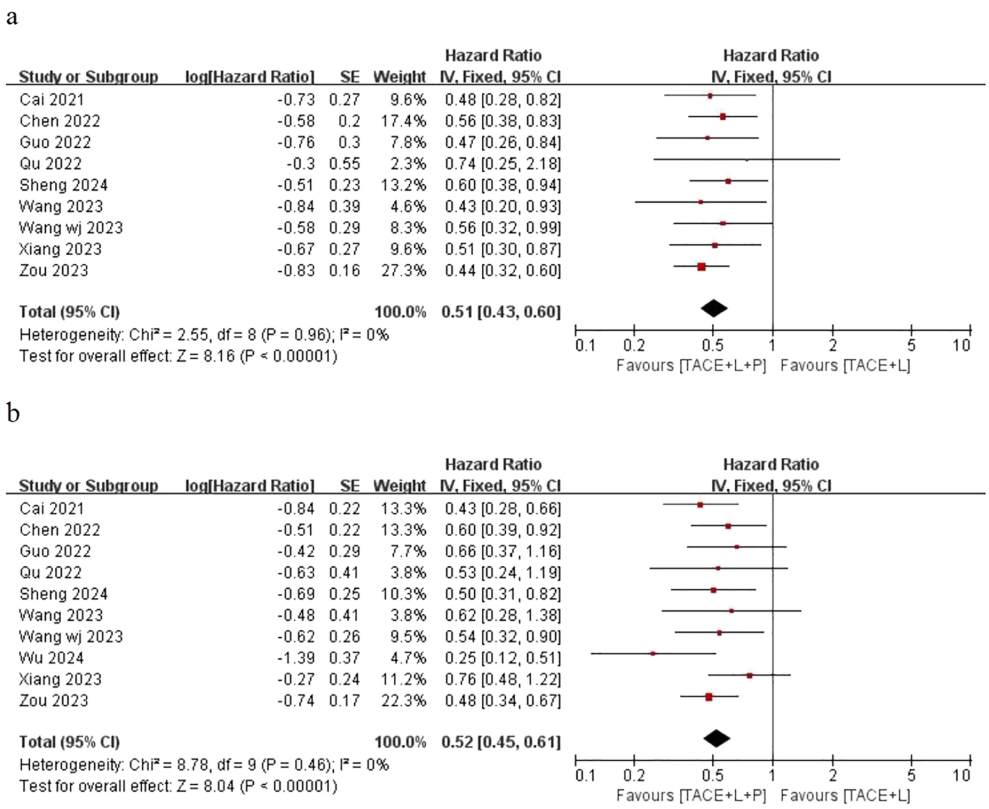

FIGURE 2
Fixed effect model of OS **(A)** and PFS **(B)** for uHCC with TLP vs TL. OS: overall survival, PFS: progression-free survival, uHCC: unresectable hepatocellular carcinoma, T: transarterial chemoembolization, L: lenvatinib, P: programmed cell death protein-1, CI: confidence intervals.

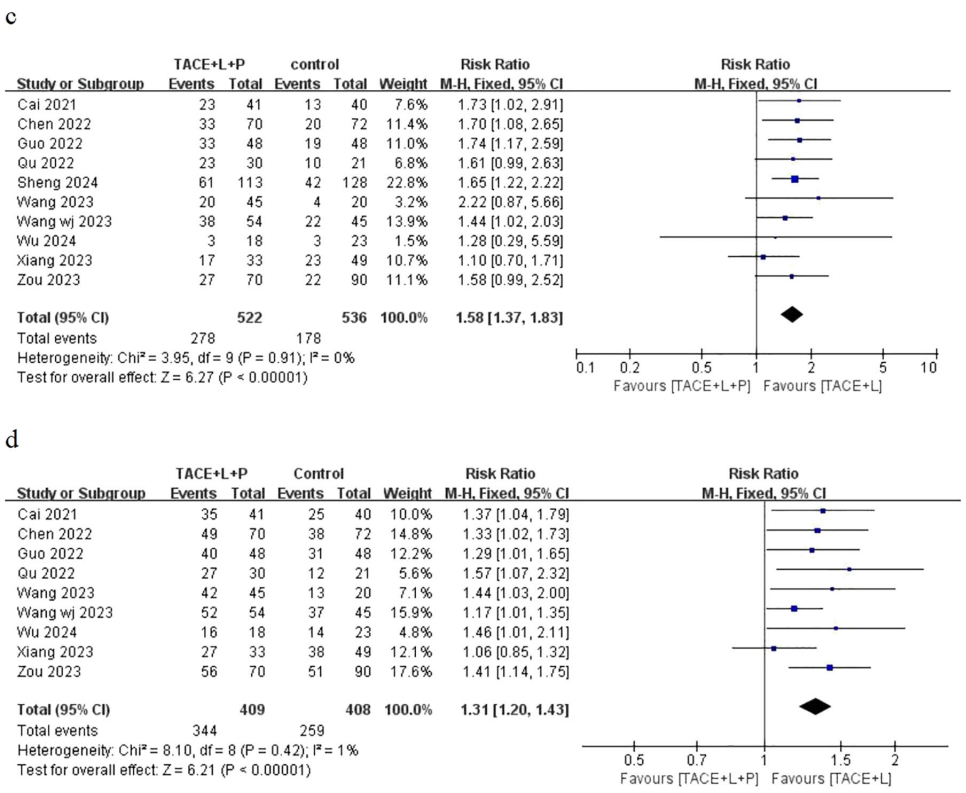

FIGURE 3
Fixed effect model of ORR **(C)** and DCR **(D)** for uHCC with TLP vs TL. ORR: objective response rate, DCR: disease control rate, uHCC: unresectable hepatocellular carcinoma, T: transarterial chemoembolization, L: lenvatinib, P: programmed cell death protein-1, CI: confidence intervals.

significantly better ORR (RR = 1.58; 95% CI: 1.37–1.83; $P < 0.05$) and DCR (RR = 1.31; 95% CI: 1.20–1.43; $P < 0.05$) than those in the TL group (Figure 3). Similarly, the results also showed that the TLP triple therapy was more effective than the TL dual therapy.

Prognostic factor analysis for overall survival and progression-free survival

The results based on univariate and multivariate analysis data from included trials in both groups showed that ECOG PS (1/0): (HR=1.18; 95% CI: 1.02-1.36, $P<0.05$), Child-Pugh class (B/A): (HR=1.83; 95% CI: 1.54-2.17, $P<0.05$), BCLC stage (C/B): (HR=1.85; 95% CI: 1.29-2.66, $P<0.05$) and main portal vein invasion (yes/no): (HR=1.25; 95% CI: 1.05-1.50, $P<0.05$) were independent prognostic factors for OS. Similarly, the results showed that BCLC stage (C/B): (HR=1.60; 95% CI: 1.04-2.46, $P<0.05$) and main portal vein invasion (yes/no): (HR=1.27; 95% CI: 1.02-1.59, $P<0.05$) were independent prognostic factors for PFS (Table 2).

Adverse events

Ten included studies reported the incidence of grade 3/4 AEs and only 9 studies reported all grades AEs. The common incidence of grade 3-4 AEs and all grade AEs included abdominal pain, decreased appetite, hypertension, nausea, diarrhea, rash, hand-foot syndrome, elevated aspartate aminotransferase (AST), elevated alanine aminotransferase (ALT), thrombocytopenia, thyroid dysfunction (Table 3). The frequency of all grades AEs was similar in both groups. The incidence of 3/4 grade nausea (RR = 4.40; 95% CI: 1.42-13.61; $P < 0.05$), rash (RR = 2.75; 95% CI: 1.13-6.70; $P < 0.05$), hand-foot syndrome (RR = 2.51; 95% CI: 1.29-4.89; $P < 0.05$) and thyroid dysfunction (RR = 6.12; 95% CI: 1.49, 25.19; $P < 0.05$) were more frequent in the TLP group than in the TL group.

Publication bias

The funnel plots were applied to show the publication bias of this meta-analysis. The funnel plots of outcomes for OS, PFS, ORR, and DCR are shown in the Supplementary Materials. In general, the probability of publication bias is low as the scatter points were distributed symmetrically in the inverted funnel.

Discussion

With the widespread concern of locoregional treatment combined with systemic targeted immunotherapy in the treatment of uHCC, more experiments have been conducted to study the efficacy of TACE plus lenvatinib combined with PD-1 for advanced HCC. The results of our meta-analysis showed that compared with the TL group, the TLP group achieved longer OS and PFS, better ORR and DCR, with low heterogeneity. Treatment-

TABLE 2 Analyses of prognostic factors for OS and PFS of TLP group vs TL group.

Factor	Analysis of OS			Analysis of PFS		
	No.	HR [95% CI]	P	No.	HR [95% CI]	P
AFP((μg/L) ≥400/<400	4	1.23 [0.96, 1.56]	0.1	5	1.05 [0.86, 1.29]	0.62
ECOG PS 1/0	4	1.18 [1.02, 1.36]	**0.03**	5	1.45 [0.96, 2.19]	0.07
Child-Pugh class B/A	5	1.83 [1.54, 2.17]	**<0.001**	4	1.32 [0.81, 2.14]	0.27
BCLC stage C/B	3	1.85 [1.29, 2.66]	**0.001**	2	1.60 [1.04, 2.46]	**0.03**
main portal vein invasion yes/no	4	1.25 [1.05, 1.50]	**0.01**	5	1.27 [1.02, 1.59]	**0.03**
Extrahepatic metastasis yes/no	4	1.42 [0.89, 2.26]	0.15	3	1.44 [0.88, 2.33]	0.14

OS, overall survival; PFS, progression-free survival; T; transarterial chemoembolization; L, lenvatinib; P, programmed cell death protein-1; AFP, alpha fetoprotein; ECOG, Eastern Cooperative Oncology Group; BCLC, Barcelona Clinic Liver Cancer; No., number; HR, hazard ratio; CI, confidence intervals.
Bold values indicate significant risk factors affecting OS and PFS for uHCC patients in the TLP group vs. TLP group.

related AEs were acceptable. Prognostic factor analysis identified ECOG PS (1/0), Child Pugh class (B/A), BCLC stage (C/B), and main portal vein invasion (yes/no) as independent prognostic factors for OS. BCLC stage (C/B) and main portal vein invasion (yes/no) were identified as independent prognostic factors for PFS. As far as we know, our meta-analysis is a relatively comprehensive study at present, providing more reliable evidence for uHCC patients.

Lenvatinib is a multi-targeted receptor TKI that targets VEGFR1-3, as well as fibroblast growth factor receptors (FGFR)1-4 (25). The LAUNCH trial showed TACE + lenvatinib had longer OS and PFS than lenvatinib alone for uHCC (7). Experts agree that hypoxia caused by TACE therapy can up-regulate VEGF. TACE combined with lenvatinib can reverse the high secretion of antigen factors and inhibit the recurrence and metastasis of residual tumors (26, 27).

Currently, our meta-analysis compared TLP triple therapy with TL dual therapy, and the latter had better results in TLP group. The results of pooled analyses showed a low degree of heterogeneity for the outcomes, using the fixed effect models. The results are consistent with previous studies comparing the combination of TLP versus TL. In a real-world study, TACE combined with PD-1 and TKI significantly improved OS, PFS and ORR for Chinese patients with advanced HCC, with acceptable safety (28). Recently, a prospective study has shown that the triple therapy of TACE + lenvatinib + camrelizumab had satisfactory clinical effect and controllable safety, which further confirmed the clinical efficacy of

TABLE 3 Adverse events of TLP group vs TL group.

Adverse Events	All grades			Grade 3/4		
	No.	RR [95% CI]	P	No.	RR [95% CI]	P
Abdominal pain	7	0.92 [0.73, 1.17]	0.52	7	1.00 [0.47, 2.11]	0.99
Decreased appetite	6	1.22 [0.55, 2.72]	0.63	7	1.33 [0.65, 2.70]	0.44
Hypertension	8	1.23 [0.96, 1.59]	0.1	8	1.74 [1.10, 2.74]	0.51
Nausea	5	0.84 [0.50, 1.40]	0.5	6	4.40 [1.42, 13.61]	**0.01**
Diarrhea	9	1.09 [0.80, 1.48]	0.58	10	1.45 [0.77, 2.71]	0.25
Rash	6	1.39 [0.90, 2.15]	0.14	7	2.75 [1.13, 6.70]	**0.03**
Hand-foot syndrome	5	1.00 [0.70, 1.42]	1	6	2.51 [1.29, 4.89]	**0.007**
Elevated AST	5	1.18 [0.90, 1.56]	0.23	6	1.32 [0.76, 2.31]	0.32
Elevated ALT	5	1.05 [0.83, 1.32]	0.71	6	0.95 [0.47, 1.93]	0.89
Thrombocytopenia	7	1.19 [0.84, 1.70]	0.32	8	1.31 [0.70, 2.46]	0.40
Thyroid dysfunction	7	1.48 [0.89, 2.47]	0.13	7	6.12 [1.49, 25.19]	**0.01**

T, transarterial chemoembolization; L, lenvatinib; P, programmed cell death protein-1; AST, aspartate aminotransferase; ALT, alanine aminotransferase; No., number; RR, relative risk; CI, confidence intervals.
The bold values indicate that compared to the TLP group, the TL group of uHCC patients experienced more frequent and severe grade 3-4 adverse events, which should be taken seriously.

locoregional treatment combined with targeted immunotherapy for uHCC (29). Better outcomes of TACE + lenvatinib + PD-1 are considered to be attributed to the synergistic antitumor activity of the three combination therapies. PD-1 was added to the TACE + lenvatinib combination therapy to enhance the anti-tumor immune effect. On the one hand, the possible mechanism is that lenvatinib can inhibit IFN-γ signal transduction in tumor cells by targeting FGFR, and the combination of PD-1 and lenvatinib can reverse the immunosuppressive state of the tumor microenvironment, thus improving the immune response rate of PD-1 inhibitors (12, 30). On the other hand, TACE can cause ischemic necrosis of tumor tissue and release a large number of tumor-specific antigens, thus enhancing the anti-tumor immune effect of PD-1 inhibitors (31, 32). In addition, TACE has relatively reduced the adverse reactions of HCC patients to systemic targeted immunotherapy and avoided the frequent drug resistance (33).

In a pooled analysis of all the studies we included, multiple factors were found to be risk factors for OS and PFS for uHCC, which was consistent with previous studies (34). For patients with uHCC, BCLC stage C and major portal vein invasion are both risk factors for OS and PFS of TLP group vs TP group. Both ECOG PS 0 and Child Pugh class A are applied to uHCC patients of TLP group vs TP group. Of note, liver function was evaluated with Child Pugh scores after the treatment procedure, which is significant for prognosis (35). Only patients with better liver function have the ability to tolerate subsequent target immunotherapy and fully utilize the advantages of combination therapy (36).

In addition, the treatment-related AEs were controllable and acceptable in both groups. It is worth noting that the results of our meta-analysis showed that the occurrence frequency of grade 3-4 AEs was higher in the TLP group than that in the TL group, which was safe with appropriate symptomatic treatment (37). The reason why the degree of nausea is more severe in the TLP group is that the triple combination therapy has greater toxic effects. Rash, hand-foot syndrome, and thyroid dysfunction are the most common immune-related adverse events (irAEs), mainly related to the therapeutic mechanism of PD-1 blockade of immune checkpoints. Importantly, the combination therapy for uHCC can lead to inevitable adverse reactions, and its long-term safety requires ongoing attention.

Although the results of this meta-analysis are satisfactory, there are still several limitations. Firstly, due to all the included literatures are retrospective studies, it is difficult to avoid recall bias. Secondly, only 10 studies were included, and there were not enough cases to analyze. Thirdly, considering that all published studies are from China, the conclusion is not applicable to western populations. Last but not least, most of the etiology of HCC are mainly related to hepatitis B virus infection in China. The benefits of combined PD-1 treatment may be related to the etiologies of disease in our study. Therefore, independent prospective clinical trials are needed to further verify the evaluation results.

Conclusion

This meta-analysis demonstrated that the triple therapy of TACE + lenvatinib +PD-1 was superior to the dual therapy of TACE + lenvatinib with respect to OS, PFS, ORR and DCR, with less occurrence of AEs.

Data availability statement

The original contributions presented in the study are included in the article/Supplementary Material. Further inquiries can be directed to the corresponding author.

Author contributions

YC: Writing – original draft, Conceptualization, Data curation, Formal analysis, Investigation, Methodology, Resources, Software. LJ: Data curation, Writing – review & editing. YL: Data curation, Writing – review & editing. WC: Data curation, Writing – review & editing. CZ: Data curation, Writing – review & editing. JW: Data curation, Writing – review & editing. CB: Supervision, Writing – review & editing. TL: Validation, Funding acquisition, Writing – review & editing.

Funding

The author(s) declare that no financial support was received for the research, authorship, and/or publication of this article.

Acknowledgments

We thank all teams and individuals which involved in this work.

Conflict of interest

The authors declare that the research was conducted in the absence of any commercial or financial relationships that could be construed as a potential conflict of interest.

Publisher's note

Supplementary material

The Supplementary Material for this article can be found online at: https://www.frontiersin.org/articles/10.3389/fimmu.2024.1466113/full#supplementary-material

References

1. Sung H, Ferlay J, Siegel RL, Laversanne M, Soerjomataram I, Jemal A, et al. Global cancer statistics 2020: GLOBOCAN estimates of incidence and mortality worldwide for 36 cancers in 185 counties. *CA Cancer J Clin*. (2021) 71:209–49. doi: 10.3322/caac.21660

2. Zhou J, Sun H, Wang Z, Cong W, Wang J, Zeng M, et al. Guidelines for the diagnosis and treatment of hepatocellular carcinoma (2019 edition). *Liver Cancer*. (2020) 9:682–720. doi: 10.1159/000509424

3. Llovet JM, Ricci S, Mazzaferro V, Hilgard P, Gane E, Blanc JF, et al. Sorafenib in advanced hepatocellular carcinoma. *N Engl J Med*. (2008) 359:378–90. doi: 10.1056/NEJMoa0708857

4. Llovet JM, Montal R, Sia D, Finn RS. Molecular therapies and precision medicine for hepatocellular carcinoma. *Nat Rev Clin Oncol*. (2018) 15:599–616. doi: 10.1038/s41571-018-0073-4

5. Kudo M, Finn RS, Qin S, Han KH, Ikeda K, Piscaglia F, et al. Lenvatinib versus sorafenib in first-line treatment of patients with unresectable hepatocellular carcinoma: a randomised phase 3 non-inferiority trial. *Lancet*. (2018) 391:1163–73. doi: 10.1016/S0140-6736(18)30207-1

6. Reig M, Forner A, Rimola J, Ferrer-F à brega J, Ferrer-Fàbrega J, Burrel M, Garcia-Criado Á, et al. BCLC strategy for prognosis prediction and treatment recommendation: The 2022 update. *J Hepatol*. (2022) 76:681–93. doi: 10.1016/j.jhep.2021.11.018

7. Peng Z, Fan W, Zhu B, Wang G, Sun J, Xiao C, et al. Lenvatinib combined with transarterial chemoembolization as first-line treatment for advanced hepatocellular carcinoma: A phase III, randomized clinical trial (LAUNCH). *J Clin Oncol*. (2023) 41:117–27. doi: 10.1200/JCO.22.00392

8. Cheng AL, Hsu C, Chan SL, Choo SP, Kudo M. Challenges of combination therapy with immune checkpoint inspectors for hepatocellular carcinoma. *J Hepatol*. (2020) 72:307–19. doi: 10.1016/j.jhep.2019.09.025

9. Blank C, Gajewski TF, Mackensen A. Interaction of PD-L1 on tumor cells with PD-1 on tumor-specific T cells as a mechanism of immune evasion: implications for tumor immunotherapy. *Cancer Immunol Immunother*. (2005) 54:307–14. doi: 10.1007/s00262-004-0593-x

10. Finn RS, Qin S, Ikeda M, Galle PR, Ducreux M, Kim TY, et al. Atezolizumab plus bevacizumab in unresectable hepatocellular carcinoma. *N Engl J Med*. (2020) 382:1894–905. doi: 10.1056/NEJMoa1915745

11. Rimassa L, Finn RS, Sangro B. Combination immunotherapy for hepatocellular carcinoma. *J Hepatol*. (2023) 79:506–15. doi: 10.1016/j.jhep.2023.03.003

12. Yi C, Chen L, Lin Z, Liu L, Shao W, Zhang R, et al. Lenvatinib targets FGF receptor 4 to enhance antitumor immune response of anti-programmed cell death-1 in HCC. *Hepatology*. (2021) 74:2544–60. doi: 10.1002/hep.31921

13. Page MJ, Moher D, Bossuyt PM, Liu L, Shao W, Zhang R, et al. PRISMA 2020 explanation and elaboration: updated guidance and exemplars for reporting systematic reviews. *BMJ*. (2021) 372:n160. doi: 10.1136/bmj.n160

14. Lo CK, Mertz D, Loeb M. Newcastle-Ottawa Scale: comparing reviewers' to authors' assessments. *BMC Med Res Methodol*. (2014) 14:45. doi: 10.1186/1471-2288-14-45

15. Cai M, Huang W, Huang J, Shi W, Guo Y, Liang L, et al. Transarterial chemoembolization combined with lenvatinib plus PD-1 inhibitor for advanced hepatocellular carcinoma: A retrospective cohort study. *Front Immunol*. (2022) 13:848387. doi: 10.3389/fimmu.2022.848387

16. Guo P, Pi X, Gao F, Li Q, Li D, Feng W, et al. Transarterial chemoembolization plus lenvatinib with or without programmed death-1 inhibitors for patients with unresectable hepatocellular carcinoma: A propensity score matching study. *Front Oncol*. (2022) 12:945915. doi: 10.3389/fonc.2022.945915

17. Qu WF, Ding ZB, Qu XD, Tang Z, Zhu GQ, et al. Conversion therapy for initially unresectable hepatocellular carcinoma using a combination of toripalimab, lenvatinib plus TACE: real-world study. *BJS Open*. (2022) 6:zrac114. doi: 10.1093/bjsopen/zrac114

18. Sheng Y, Wang Q, Liu H, Wang Q, Chen W, Xing W. Prognostic nomogram model for selecting between transarterial chemoembolization plus lenvatinib, with and without PD-1 inhibitor in unresectable hepatocellular carcinoma. *Br J Radiol*. (2024) 97:668–79. doi: 10.1093/bjr/tqae018

19. Wang YY, Yang X, Wang YC, Long JY, Sun HS, Li YR, et al. Clinical outcomes of lenvatinib plus transarterial chemoembolization with or without programmed death receptor-1 inhibitors in unresectable hepatocellular carcinoma. *World J Gastroenterol*. (2023) 29:1614–26. doi: 10.3748/wjg.v29.i10.1614

20. Wang WJ, Liu ZH, Wang K, Yu HM, Cheng YQ, Xiang YJ, et al. Efficacy and safety of TACE combined with lenvatinib and PD-1 inhibitors for unresectable recurrent HCC: A multicenter, retrospective study. *Cancer Med*. (2023) 12:11513–24. doi: 10.1002/cam4.5880

21. Wu HX, Ding XY, Xu YW, Yu MH, Li XM, Deng N, et al. Transcatheter arterial chemoembolization combined with PD-1 inhibitors and Lenvatinib for hepatocellular carcinoma with portal vein tumor thrombus. *World J Gastroenterol*. (2024) 30:843–54. doi: 10.3748/wjg.v30.i8.843

22. Xiang Z, Li G, Mu L, Wang H, Zhou C, Yan H, et al. TACE combined with lenvatinib and camrelizumab for unresectable multiple nodular and large hepatocellular carcinoma (>5 cm). *Technol Cancer Res Treat*. (2023) 22:15330338231200320. doi: 10.1177/15330338231200320

23. Zou X, Xu Q, You R, Yin G. Correlation and efficacy of TACE combined with lenvatinib plus PD-1 inhibitor in the treatment of hepatocellular carcinoma with portal vein tumor thrombus based on immunological features. *Cancer Med*. (2023) 12:11315–33. doi: 10.1002/cam4.5841

24. Chen S, Wu Z, Shi F, Mai Q, Wang L, Wang F, et al. Lenvatinib plus TACE with or without pembrolizumab for the treatment of initially unresectable hepatocellular carcinoma harbouring PD-L1 expression: a retrospective study. *J Cancer Res Clin Oncol*. (2022) 148:2115–25. doi: 10.1007/s00432-021-03767-4

25. Yamamoto Y, Matsui J, Matsushima T, Obaishi H, Miyazaki K, Nakamura K, et al. Lenvatinib, an angiogenesis inhibitor targeting VEGFR/FGFR, shows broad antitumor activity in human tumor xenograft models associated with microvessel density and pericyte coverage. *Vasc Cell*. (2014) 6:18. doi: 10.1186/2045-824X-6-18

26. Nahm JH, Rhee H, Kim H, Yoo JE, San Lee J, Jeon Y, et al. Increased expression of stemness markers and altered tumor stroma in hepatocellular carcinoma under TACE-induced hypoxia: A biopsy and resection matched study. *Oncotarget*. (2017) 8:99359–71. doi: 10.18632/oncotarget.22078

27. Shim JH, Park JW, Kim JH, An M, Kong SY, Nam BH, et al. Association between increment of serum VEGF level and prognosis after transcatheter arterial chemoembolization in hepatocellular carcinoma patients. *Cancer Sci*. (2008) 99:2037–44. doi: 10.1111/j.1349-7006.2008.00909.x

28. Zhu HD, Li HL, Huang MS, Yang WZ, Yin GW, Zhong BY, et al. Transarterial chemoembolization with PD-(L)1 inhibitors plus molecular targeted therapies for hepatocellular carcinoma (CHANCE001). *Signal Transduct Target Ther*. (2023) 8:58. doi: 10.1038/s41392-022-01235-0

29. Wu XK, Yang LF, Chen YF, Chen ZW, Lu H, Shen XY, et al. Transcatheter arterial chemoembolisation combined with lenvatinib plus camrelizumab as conversion therapy for unresectable hepatocellular carcinoma: a single-arm, multicentre, prospective study. *EClinicalMedicine*. (2023) 67:102367. doi: 10.1016/j.eclinm.2023.102367

30. Huinen ZR, Huijbers EJM, van Beijnum JR, Nowak-Sliwinska P, Griffioen AW. Anti-angiogenic agents - overcoming tumour endothelial cell anergy and improving immunotherapy outcomes. *Nat Rev Clin Oncol*. (2021) 18:527–40. doi: 10.1038/s41571-021-00496-y

31. Cheu JW, Wong CC. Mechanistic rationales guiding combination hepatocellular carcinoma therapies involving immune checkpoint inhibitors. *Hepatology*. (2021) 74:2264–76. doi: 10.1002/hep.31840

32. Fukumura D, Kloepper J, Amoozgar Z, Duda DG, Jain RK. Enhancing cancer immunotherapy using antiangiogenics: opportunities and challenges. *Nat Rev Clin Oncol*. (2018) 15:325–40. doi: 10.1038/nrclinonc.2018.29

33. Sangro B, Chan SL, Meyer T, Reig M, El-Khoueiry A, Galle PR. Diagnosis and management of toxicities of immune checkpoint inhibitors in hepatocellular carcinoma. *J Hepatol*. (2020) 72:320–41. doi: 10.1016/j.jhep.2019.10.021

34. Duan X, Li H, Kuang D, Chen P, Zhang K, et al. Transcatheter arterial chemoembolization plus apatinib with or without camrelizumab for unresectable hepatocellular carcinoma: a multicenter retrospective cohort study. *Hepatol Int*. (2023) 17:915–26. doi: 10.1007/s12072-023-10519-8

35. Katzke V, Johnson T, Sookthai D, Hüsing A, Kühn T, Kaaks R. Circulating liver enzymes and risks of chronic diseases and mortality in the prospective EPIC-Heidelberg case-cohort study. *BMJ Open*. (2020) 10:e033532. doi: 10.1136/bmjopen-2019-033532

36. D'Avola D, Granito A, Torre-Aláez M, Piscaglia F. The importance of liver functional reserve in the non-surgical treatment of hepatocellular carcinoma. *J Hepatol*. (2022) 76:1185–98. doi: 10.1016/j.jhep.2021.11.013

37. Khoja L, Day D, Wei-Wu Chen T, Siu LL, Hansen AR. Tumour- and class-specific patterns of immune-related adverse events of immune checkpoint inhibitors: a systematic review. *Ann Oncol*. (2017) 28:2377–85. doi: 10.1093/annonc/mdx286

frontiers | Frontiers in Immunology

TYPE Original Research
PUBLISHED 03 September 2024
DOI 10.3389/fimmu.2024.1463574

OPEN ACCESS

EDITED BY
Yue Wang,
Second Military Medical University, China

REVIEWED BY
Jie Shen,
Nanjing Drum Tower Hospital, China
Anrong Mao,
Fudan University, China

*CORRESPONDENCE
Binghua Dai
daibinghua@smmu.edu.cn
Kui Wang
wangkuiykl@163.com
Li Geng
luokunl2011@126.com

†These authors have contributed equally to this work and share first authorship

RECEIVED 12 July 2024
ACCEPTED 19 August 2024
PUBLISHED 03 September 2024

CITATION
Dong Z, Sui C, Lu J, Guo J, Duan K, Wang K, Geng L, Dai B and Yang J (2024) Chemotherapy combined with lenvatinib and PD-1 may be a potential better alternative option for advanced unresectable intrahepatic cholangiocarcinoma: a retrospective real-world study. *Front. Immunol.* 15:1463574. doi: 10.3389/fimmu.2024.1463574

Chemotherapy combined with lenvatinib and PD-1 may be a potential better alternative option for advanced unresectable intrahepatic cholangiocarcinoma: a retrospective real-world study

Zhitao Dong[1†], Chengjun Sui[1†], Jiongjiong Lu[1†], Junwu Guo[1], Kecai Duan[1], Kui Wang[2*], Li Geng[1*], Binghua Dai[1*] and Jiamei Yang[1]

[1]Department of Special Treatment, Shanghai Eastern Hepatobiliary Surgery Hospital, Shang Hai, China, [2]Department of Hepatic Surgery, Shanghai Eastern Hepatobiliary Surgery Hospital, Shang Hai, China

Background: Currently, the prognosis of advanced intrahepatic cholangiocarcinoma (ICC) is poor, and the current treatment methods are not effective.

Objective: The aim of this study was to evaluate the anticancer efficacy of chemotherapy combined with PD-1 inhibitors and tyrosine kinase inhibitors (TKIs) in patients with ICC.

Methods: We retrospectively screened patients with advanced intrahepatic cholangiocarcinoma (ICC) who received chemotherapy combined with lenvatinib and PD-1. We evaluated overall survival (OS), progression-free survival (PFS), the objective response rate (ORR), the disease control rate (DCR), the tumor shrinkage rate, and safety.

Results: We enrolled 95 patients with ICC and divided them into three groups with a median follow-up duration of 15.1 months. The chemotherapy group (chemo-regimen group), chemotherapy combined with immune checkpoint inhibitors (dual-regimen group), and chemotherapy combined with lenvatinib (triple-regimen group) had median OS times of 13.1 months, 20.8 months, and 39.6 months, respectively. Notably, the triple-regimen group had a significantly longer OS than did the chemo-regimen and dual-regimen groups. The chemo-regimen group, dual-regimen group, and triple-regimen group reported median PFS durations of 4.8 months, 11.9 months, and 23.4 months, respectively. Both combination groups exhibited significantly longer PFS than the chemotherapy-only group ($P<0.05$). The ORRs of the chemo-regimen, dual-regimen, and triple-regimen groups were 18.2%, 55.5%, and 54.7%, respectively. The DCRs were 72.7%, 90%, and 96.2%, respectively, indicating significantly better outcomes in the combination therapy groups.

Conclusion: The combination of chemotherapy with PD-1 inhibitors and lenvatinib demonstrates considerable efficacy and tolerability as a treatment strategy for patients with advanced ICC.

KEYWORDS

unresectable ICC, programmed cell death protein 1 (PD-1), tyrosine kinase, PD-1 inhibitor, systematic therapy

1 Introduction

Gemcitabine plus cisplatin (GC) therapy has been established as the first-line treatment for advanced ICC; however, the objective response rate (ORR) remains relatively low. The ABC-002 study reported an ORR of 21%-37% for biliary tract cancer (BTC) (1). The median overall survival (OS) was 11.7 months, whereas it was 8.1 months in the control group (OR=0.64; 95% CI=0.52-0.80, P<0.001). The median progression-free survival (PFS) in the GC group was 8.0 months, whereas it was 5.0 months in the control group. Furthermore, the ABC-06 study demonstrated that FOLFOX chemotherapy (a regimen of folinic acid (2), fluorouracil, and oxaliplatin) marginally improved overall survival (OS) in patients with advanced BTC compared with active symptom control (6.2 months vs. 5.3 months). The efficacy of chemotherapy is notably limited, and alternative treatment options are scarce, particularly after the development of resistance or disease progression.

Immune checkpoint inhibitors (ICIs) have shown some degree of clinical efficacy in liver cancer; however, the effectiveness of single-agent immunotherapy is often constrained by the high heterogeneity and immunosuppressive nature of the TME (3). An emerging strategy involves combining PD-1/PD-L1 inhibitors with antiangiogenic drugs or chemotherapies that possess immunomodulatory properties to counteract TME immunosuppression. This approach is superior to standard treatments. For example, a single-arm phase II clinical trial demonstrated that the combination of lenvatinib and pembrolizumab induced a tumor response (4), with an ORR of 25% in advanced BTC patients and a median progression-free survival (PFS) and OS of 4.9 months and 11.0 months, respectively. A similar trial evaluating camrelizumab combined with GEMOX reported an ORR of 54%, with a median PFS and OS of 6.1 months and 11.8 months, respectively (5).

The integration of ICIs with antiangiogenic drugs and chemotherapy has led to significant advancements in the treatment of advanced BTC. A notable phase II clinical trial conducted by Shi et al. included 30 patients with pathologically confirmed advanced ICC. These patients received first-line treatment comprising Gemox chemotherapy combined with anti-PD-1 antibodies and lenvatinib (6). The outcomes of this trial were promising, with a median PFS of 10.0 months, a median OS that was not reached, and an ORR of 80%. Similarly, Li et al. reported the efficacy of tislelizumab combined with lenvatinib and the Gemox regimen as conversion therapy for potentially resectable locally advanced BTC, yielding an ORR of 56% and a disease control rate (DCR) of 92%. These studies underscore the potential of combining immunotherapy with targeted therapy and systemic chemotherapy as a viable and effective treatment approach for advanced BTC characterized by favorable ORRs.

Therefore, we conducted a retrospective study using preclinical data to assess the safety and efficacy of lenvatinib in conjunction with PD-1 inhibitors and chemotherapy regimens in a real-world setting in patients with advanced ICC.

2 Methods

2.1 Participants

In this study, we enrolled consecutive patients who presented to Shanghai Eastern Hepatobiliary Surgery Hospital between February 2019 and October 2022. Eligible patients were diagnosed with advanced ICC on the basis of imaging data, including computed tomography (CT), magnetic resonance imaging (MRI), and magnetic resonance cholangiopancreatography (MRCP), in conjunction with pathological biopsy. Biopsy methods included cytological sampling of the perihilar cholangiocarcinoma by brushing or endoscopic retrograde cholangiopancreatography.

For inclusion in the study, patients had to meet specific criteria as per the Response Evaluation Criteria in Solid Tumors (RECIST) version 1.1, which necessitated the presence of at least one measurable lesion. Patients who had previously received treatment were excluded from this study.

The criteria for diagnosing advanced ICC were as follows (7, 8): (1) biopsy indicative of poor differentiation, (2) evidence of portal vein or inferior vena cava invasion, and (3) multiple lymph nodes or distant metastases confirmed by imaging.

2.2 Inclusion criteria

Eligible participants were required to have an Eastern Cooperative Oncology Group performance status (ECOG PS) of 0 or 1, a life expectancy of at least one month, and at least one measurable lesion, as defined by RECIST 1.1. Additionally, patients were required to have a

Child–Pugh grade of A or B. For patients presenting with obstructive jaundice, initial biliary drainage was performed to ensure the safety of the subsequent treatment regimen.

2.3 Exclusion criteria

Patients with a history of prior treatments such as Transarterial Chemoembolization (TACE), radiation therapy, ablation, or Hepatic Arterial Infusion Chemotherapy (HAIC) were excluded. Similarly, those who had received PD-1, PD-L1, or MEK inhibitors, as well as those with a history of autoimmune diseases or other malignancies, did not meet the study's inclusion criteria. The study also excluded patients lacking the comprehensive imaging data required for accurate tumor response evaluation. Furthermore, patients who were lost to follow-up or had uncontrolled intercurrent illnesses were also excluded.

2.4 Ethical considerations and patient consent

This study was conducted in strict accordance with the principles of the Declaration of Helsinki and the International Conference on Harmonization Good Clinical Practice guidelines. This study was approved by the Ethics Committee of Eastern Hepatobiliary Hospital (ethics code: EHBHKY2019-K-027.1/3/2020). Before the commencement of treatment, informed consent was obtained from all participants, and their data were anonymized for clinical research. The confidentiality and anonymity of the patients' information were rigorously maintained, ensuring that patient identities were not discernible in any reports or publications. This report aligns with the Strengthening the Reporting of Observational Studies in Epidemiology (STROBE) statement.

2.5 Treatment regimen

In this study, the participants were stratified into three distinct treatment groups, each receiving a different therapeutic regimen.

2.5.1 Triple-regimen group (chemo+ICI+TKI)

This group received a combination of lenvatinib, PD-1 inhibitors, and chemotherapy. The lenvatinib dosage was determined on the basis of body weight: patients weighing ≥60 kg received 12 mg of lenvatinib orally once daily, whereas those weighing <60 kg received 8 mg of lenvatinib. PD-1 inhibitor therapy involved a fixed dose of 200 mg administered every three weeks, with three different PD-1 drugs available (tislelizumab, toripalimab, and sintilimab). The chemotherapy regimens included gemcitabine plus cisplatin (GC) administered intravenously every three weeks for a total of six cycles. Following the completion of chemotherapy, immunotherapy and targeted therapy were continued until the disease progressed.

2.5.2 Dual-regimen group (chemo+ICI)

Patients in this group received a combination of a GC regimen and PD-1 inhibitors. The chemotherapy regimens used were similar to those used in the three-drug combination group.

2.5.3 Control group (chemo)

This group was treated with a GC regimen.

The treatment continued until disease progression or unacceptable toxicity occurred or some other conditions were judged by the investigator as inappropriate for continuing the treatment. Once severe toxicity occurred, the administration would be delayed and/or the dose would be reduced according to the drug's instructions.

2.6 Evaluation methods

The tumor response in this study was meticulously evaluated by a panel of three experienced radiologists using RECIST version 1.1 and mRECIST criteria. Imaging assessments, predominantly conducted via MRI (or CT when MRI was unavailable), were performed at baseline and subsequently every 4–8 weeks following each treatment cycle. Radiological assessments were performed at least four weeks after the initial observation to confirm complete remission (CR) and partial remission (PR).

Adverse events (AEs) were comprehensively documented from the commencement of treatment until one month after its conclusion. These events were classified and graded according to the National Cancer Institute Common Terminology Criteria for Adverse Events (CTCAE), version 4.03.

2.7 Treatment endpoints

The primary endpoints defined for this study were PFS and OS. The secondary endpoints included the ORR and DCR, along with safety evaluations. The ORR was defined as the aggregate percentage of patients who achieved CR or PR. Both the ORR and DCR were calculated on the basis of the standards set by RECIST 1.1 and mRECIST, respectively.

2.8 Statistical analysis

The data are described herein as means ± standard errors for normally distributed values and as medians (interquartile ranges [IQRs]) for nonnormally distributed values. Categorical variables of the baseline characteristics are presented as numbers (n) and ratios (%). The Wilcoxon rank-sum test, Student's t test, Pearson's chi-square test, and Fisher's exact test were used as appropriate to compare baseline characteristics between groups. The median PFS and OS rates and 95% confidence intervals (CIs) in the total population and subgroups were estimated by using the Kaplan–Meier method, and the log-rank test was used to analyze the differences in the survival curves. Unadjusted hazard ratios (HRs)

were initially derived via Cox regression without including covariates or propensity scores in the model. The ORR was calculated as a percentage with two-sided 95% confidence intervals (CIs) via the Clopper–Pearson method. Programming and statistical analyses were performed with SPSS (version 20.0). All the statistical analyses were two-sided, and p values less than 0.05 were considered to indicate statistical significance.

3 Results

3.1 General characteristics of the patients

Among the initial pool of 158 patients screened for this study, a subset of patients was excluded on the basis of the following criteria: 37 patients had undergone transarterial chemoembolization (TACE), radiofrequency ablation, or hepatic arterial infusion (HAIC) chemotherapy; 3 patients had a history of other malignant tumors; 9 patients lacked complete imaging data; and 14 patients were lost to follow-up. A research flowchart is shown in Figure 1.

Consequently, 95 patients were enrolled in this study. Among the 95 enrolled patients, 22 received chemotherapy (chemotherapy group), 20 received a chemotherapy regimen plus PD-1 inhibitor treatment (dual-combination group), and 53 received a chemotherapy regimen plus PD-1 inhibitor plus lenvatinib treatment. The PD-1 inhibitors predominantly included tislelizumab, toripalimab, and sintilimab.

3.2 Baseline characteristics

Table 1 presents a detailed summary of the demographic and baseline characteristics of all the enrolled patients. The median patient age at the initiation of treatment was 58 years. Most patients were male, constituting 64.2% of the cohort (61/95), whereas 25.8% were female (34/95).

A significant majority of patients (94.7% (90/95) had an Eastern Cooperative Oncology Group (ECOG) performance status of 0-1), indicating relatively good physical functioning. Nearly all patients (98.9%, 94/95) were classified as Child–Pugh stage A, reflecting relatively preserved liver function. At baseline, 63.2% of the patients (60/95) had abnormal levels of the tumor antigen CA19-9. Furthermore, 45.3% of patients (43 of 95) had a history of hepatitis B infection. A total of 30.5% (29/87) had a poorly differentiated histology, 24 patients had a well-differentiated histology, and 42 patients had a moderately differentiated histology. Prior to treatment, 31 patients had distant metastases, predominantly in the lungs (22 patients, 26.3%), bones (five patients, 5.26%), and brain (two patients, 2.10%). There were also multiple organ metastases (two patients, 2.10%). Thirty-seven patients (38.9%, 30/95) had positive lymph nodes at the beginning of the study.

3.3 Efficacy

3.3.1 The median treatment duration

The median treatment duration across the three study groups was 8.0 months, with an IQR of 5.7 to 12.0 months. This duration varied among the groups; patients in the chemo-regimen group underwent a median of 4.0 chemotherapy cycles (IQR 3.0–6.0). In the dual-regimen group, patients received a median of five treatment cycles (IQR 4.0–8.0). Patients in the triple-regimen group had a median of six treatment cycles (IQR 3.0–9.0) (Table 2).

3.3.2 Follow-up duration

The median follow-up duration for the chemo-regimen group was 36.6 months (IQR: 34.4-38.7), that for the dual-regimen group was 32.6 months (IQR: 30.2-34.9), and that for the triple-regimen group was 33.1 months (IQR: 30.8-35.3). At the last follow-up, ten patients in the triple-therapy group did not exhibit disease progression and continued maintenance-targeted immunotherapy. There were no significant differences in the follow-up times among the three groups (P > 0.05) (Table 2).

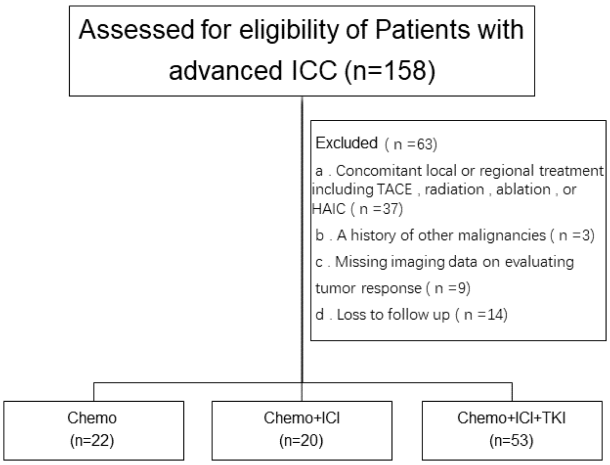

FIGURE 1
The flow chart of the study illustrates the enrollment procedure.

10.3389/fimmu.2024.1463574

TABLE 1 Baseline demographic and clinical characteristics (n=95).

Character	Factor	Chemo (N=22)	Chemo+ICI (N=20)	Chemo+ICI+TKI (N=53)	Overall (N=95)	P-value
Sex	Male	13 (59.1%)	10 (50.0%)	38 (71.7%)	61 (64.2%)	0.1919
	Female	9 (40.9%)	10 (50.0%)	15 (28.3%)	34 (35.8%)	
Age	Mean / Std	59.9 / 11.20	56.5 / 8.99	58.4 / 8.98	58.3 / 9.50	0.5792
	Median	62	57	57	58	
	Inter Quartile Range	52, 69	51, 60	53, 65	52, 65	
Child-Pugh stage	A	22 (100%)	19 (95.0%)	53 (100%)	94 (98.9%)	0.1503
	B	0	1 (5.0%)	0	1 (1.1%)	
Lymph node	No	13 (59.1%)	11 (55.0%)	34 (64.2%)	58 (61.1%)	0.7567
	Yes	9 (40.9%)	9 (45.0%)	19 (35.8%)	37 (38.9%)	
Metastasis	No	14 (63.6%)	12 (60.0%)	38 (71.7%)	64 (67.4%)	0.5812
	Yes	8 (36.4%)	8 (40.0%)	15 (28.3%)	31 (32.6%)	
Maximum tumor diameter	Mean / Std	80.373 / 46.8786	83.099 / 42.6172	81.600 / 49.4813	81.631 / 47.0460	0.9629
	Median	77.00	76.35	75.00	75.00	
	Inter Quartile Range	46.00, 102.00	49.35, 119.94	54.00, 96.92	52.70, 102.00	
HBV	Positive	16 (72.7%)	8 (40.0%)	19 (35.8%)	43 (45.3%)	0.0143
	Negative	6 (27.3%)	12 (60.0%)	34 (64.2%)	52 (54.7%)	
Hepatolithiasis	No	0	1 (5.0%)	1 (1.9%)	2 (2.1%)	0.5224
	Yes	22 (100%)	19 (95.0%)	52 (98.1%)	93 (97.9%)	
Diabetes	No	20 (90.9%)	17 (85.0%)	43 (81.1%)	80 (84.2%)	0.5685
	Yes	2 (9.1%)	3 (15.0%)	10 (18.9%)	15 (15.8%)	
Hypertension	No	17 (77.3%)	17 (85.0%)	45 (84.9%)	79 (83.2%)	0.7018
	Yes	5 (22.7%)	3 (15.0%)	8 (15.1%)	16 (16.8%)	
Differentiated degree	Low differentiation	10 (45.5%)	9 (45.0%)	10 (18.9%)	29 (30.5%)	0.0771
	Middle to low differentiation	3 (13.6%)	4 (20.0%)	17 (32.1%)	24 (25.3%)	
	moderately differentiated	9 (40.9%)	7 (35.0%)	26 (49.1%)	42 (44.2%)	
Tumor number	=1	12 (54.5%)	11 (55.0%)	22 (41.5%)	45 (47.4%)	0.2070
	≥2	6 (27.3%)	9 (45.0%)	29 (54.7%)	44 (46.3%)	
CA199	<37	5 (22.7%)	7 (35.0%)	23 (43.4%)	35 (36.8%)	0.1430
	≥37	17 (77.3%)	13 (65.0%)	30 (56.6%)	60 (63.2%)	
NLR	Mean / Std	4.59/3.69	3.49 / 1.90	4.57 / 3.15	4.35 / 3.07	0.3728
	Median	3.72	2.77	3.66	3.35	
	Inter Quartile Range	2.26, 5.71	2.24, 4.58	2.49, 5.99	2.36, 5.71	
PLR	Mean / Std	195.93 / 123.16	177.21 / 75.39	161.61 / 90.30	172.96/ 96.22	0.3690
	Median	154.16	178.75	146.03	152.34	
	Inter Quartile Range	115.08, 229.93	112.25, 228.41	101.53, 222.73	104.73, 227.47	

NLR, Neutrophil-to-Lymphocyte Ratio; PLR, Platelet-to-Lymphocyte Ratio.

3.3.3 Overall survival (OS)

In the present study, the median OS varied across the treatment groups. For the group that received chemotherapy alone, the median OS was 13.1 months, with an IQR of 8.8–17.5 months. In the dual-regimen group, the median OS was 20.8 months (IQR: 16.1–25.4). The triple-regimen group had a further extended median OS of 39.6 months (IQR: 33.2 to 45.9) (Figure 2A). The dual-regimen and triple-regimen groups had significantly different OS rates (chemo-regimen group vs. dual-regimen group, P=0.024; dual-regimen group vs. triple-regimen group, P=0.045; chemo-regimen group vs. triple-regimen group, P<0.001).

3.3.4 Progression-free survival (PFS)

The median PFS time for patients who received chemotherapy alone was 4.8 months (IQR 3.0–6.7 months) (Figure 2B). In the dual-regimen group, the median PFS time was 11.9 months (IQR 9.0–14.8 months). The median PFS of patients in the triple-regimen group was slightly greater at 23.4 months (IQR 18.2–28.7 months). Statistical analysis revealed significant differences in PFS between the chemotherapy group and the other two therapy groups (chemo-regimen group vs. dual-regimen group, P <0.001; dual-regimen group vs. triple-regimen group, P <0.001; chemo-regimen group vs. triple-regimen group, P=0.036).

3.3.5 Optimal response time

The median response time to tumor treatment in the chemo-regimen group was 3.65 months, with an IQR of 2.40–5.40 months (Figure 3A). Patients in the dual-regimen group had a median response time of 5.25 months, with an IQR of 3.075–7.45 months. The median response time in the triple-regimen group was 4.60 months, with an IQR of 3.15 to 6.40 months. Statistical analysis revealed no significant differences in the median response times between the chemo-regimen and triple-regimen groups (P=0.5281). Similarly, no significant differences were detected between the chemo-regimen and dual-regimen groups or between the dual-regimen and triple-regimen groups (P=0.3652 and P=0.5049, respectively).

3.3.6 Early tumor regression rate (early tumor shrinkage, ETS)

This study characterized early tumor shrinkage (ETS) as tumor regression of ≥20% after 6–8 weeks of treatment initiation. The median ETS rates observed in the chemo-, dual-, and triple-regimen treatment groups were 24%, 61%, and 63%, respectively. Comparative analysis indicated that the dual regimen and triple regimens yielded significantly higher ETS rates than the chemotherapy regimen did (P<0.05). However, no significant differences were observed between the dual-regimen group and the triple-regimen group (P=0.3652).

TABLE 2 Confirmed anti-tumour activity (evaluated by modified RECIST).

	Chemo (n=22)	Chemo+ICI (n=20)	Chemo+ICI+TKI (n=53)
Tumor Response			
Complete response	0% (0)	10% (2)	9.4% (5)
Partial response	18.2% (4)	45% (9)	47.2% (25)
Stable disease	31.8% (7)	40% (8)	39.6% (21)
Progressive disease	50% (11)	5% (1)	3.8% (2)
Objective Response	18.2% (4/22)	55.0% (11/20)	56.6% (30/53)
Disease Control Rate	50% (11/22)	95% (19/20)	96.2% (51/53)
Median duration of response (months)	8.9m (IQR:5.50-14.03)	10.7 m (IQR:9.05-15.85)	14.2 m (IQR:10.65-25.15)
Tumour Shrinkage Duration			
< 6 months	1	1	1
≥ 6 months	1	6	9
≥ 12 months	2	3	19
Median treatment duration (Cycles)	4 (IQR:3-6)	5 (IQR:4-8)	6 (IQR:3-9)
Median treatment duration (Months)		8.0 (IQR:5.7-12.0)	
Median follow-up duration (Months)	36.6 (IQR: 34.4-38.7)	32.6 (IQR: 30.2-34.9)	33.1 (IQR: 30.8-35.3)

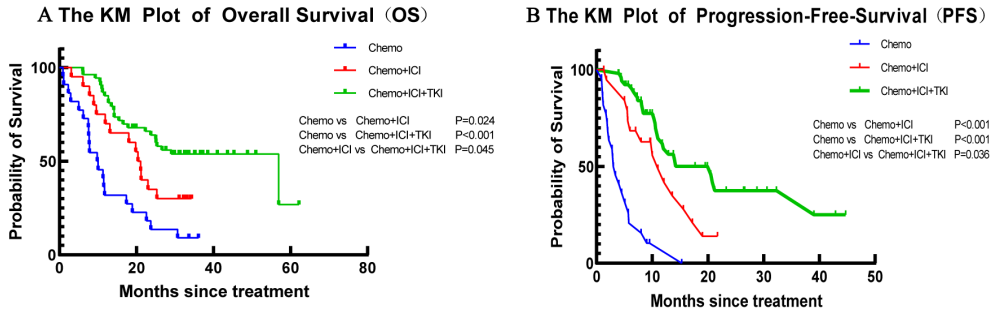

FIGURE 2
The Kaplan–Meier curves of **(A)** OS and **(B)** PFS in patients of the Chemo group, the Dual-regimen group, and the Triple group, respectively.

3.3.7 Average tumor shrinkage depth (DpR)

The average tumor shrinkage depths in the chemo-regimen, dual-regimen, and triple-regimen groups were -1.676% (IQR: -18.86 ~ -22.78%), -36.55% (IQR: -72.06 ~ -11.62%), and 34.22% (IQR: -60.21 ~ -11.33%), respectively (Figure 3B). A statistically significant difference was observed between the patients who received chemotherapy alone and those who received chemotherapy and ICI therapy (p = 0.0018). There was also a statistically significant difference between the chemo- and triple-regimen groups, as indicated by a P value of 0.0004.

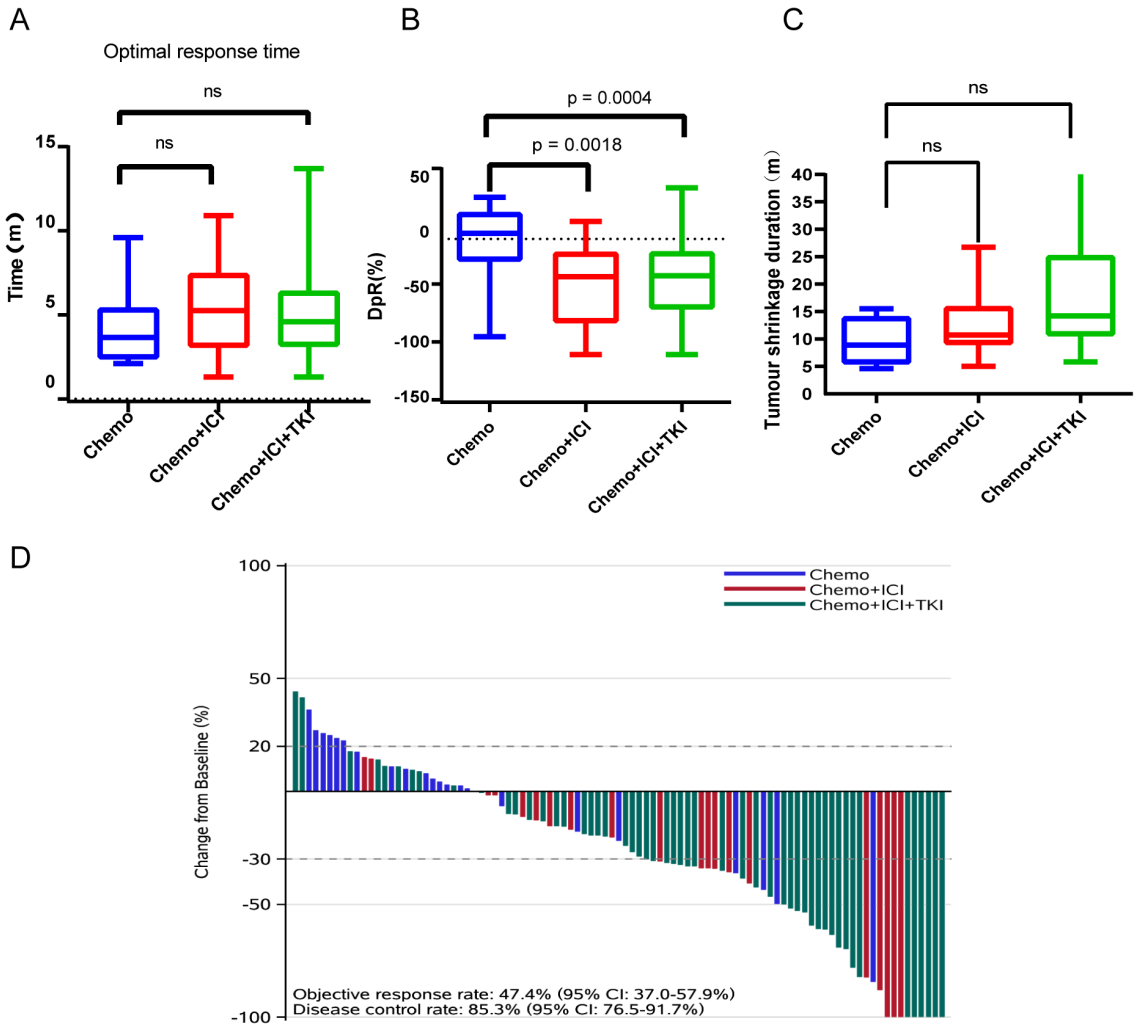

FIGURE 3
Analysis of optimal response time **(A)**, average tumor shrinkage depth (DpR) **(B)**, tumor shrinkage duration **(C)**, and treatment effect **(D)**. NS: not significant.

However, no statistically significant difference was found between the dual- and triple-regimen groups, as evidenced by a P value of 0.8109.

3.3.8 DpR duration (months)/tumor shrinkage duration

The median durations of tumor shrinkage in the chemo-regimen, Dual-regimen, and triple-regimen groups were 8.9 months (IQR: 5.50–14.03), 10.7 months (IQR: 9.05–15.85), and 14.2 months (IQR: 10.65–25.15), respectively (Figure 3C). Statistical analysis revealed no significant differences in the duration of tumor shrinkage among the three groups. The P values for the comparisons were as follows: between the chemo-regimen group and the dual-regimen group, 0.39; between the chemo-regimen group and the triple-regimen group, 0.10; and between the dual-regimen group and the triple-regimen group, 0.11.

3.3.9 Treatment effect

After treatment, the patients' overall DCR was reported to be 89.5%, with an IQR of 82.7–95.9%. The ORR for the entire cohort was 46.3%, with an IQR of 37.4%–59.2%. The ORRs of patients in the chemo-regimen, dual-regimen, and triple-regimen groups were 18.2% (4/22), 55.5% (11/20), and 54.7% (29/53), respectively. The DCRs of the three groups were 72.7% (16/22), 90% (18/20), and 96.2% (51/53), respectively (Figure 3D; Table 2). In the dual-regimen group, 10.0% of the patients achieved CR, whereas 9.4% of the patients reached CR in the triple-regimen group (Figure 4).

After treatment, the observed response duration varied across the three treatment groups. In the chemo-regimen group, 75% of the patients had a response duration exceeding six months, and 50% experienced a response lasting more than one year. In the dual-regimen group, 90.0% of the patients sustained a response for more than half a year, and 30% had a response duration extending beyond one year. The triple-regimen group included a majority (96.6%) of patients with response durations exceeding six months, and 65.5% of patients in this group experienced responses lasting more than one year.

Within the triple-regimen group, two patients exhibited notable posttreatment outcomes, enabling them to undergo radical surgical intervention (Figure 5).

The first patient achieved a 50% reduction in tumor size after five cycles of the combined treatment regimen, which was classified as a partial response (PR) according to the mRECIST criteria. This significant shrinkage allowed for successful radical resection of the liver tumor, after which the patient was discharged. Similarly, the second patient completed six cycles of combined treatment, resulting in a 40% reduction in tumor size, and was also deemed a PR according to the mRECIST criteria. This reduction facilitated radical resection of the liver tumor, followed by subsequent discharge. These instances highlight the efficacy of the triple-therapy regimen in significantly reducing tumor size, thereby making patients eligible for potentially curative surgical procedures.

3.3.10 Subgroup analysis

A comprehensive subgroup analysis was conducted to compare the survival outcomes among the three patient groups, with a focus on the median PFS and median OS across different stratifications, as illustrated in the forest plot (Figures 6, 7). The three groups were compared and analyzed, but no clear high-risk factors were found.

3.3.11 Safety analysis

Throughout the treatment in this study, all 95 patients (representing 100% of the cohort) reported experiencing AEs, but notably, there were no instances of grade 5 AEs (Table 3). The incidence and nature of Grade ≥ 3 tumors varied across different treatment groups. In the chemo-regimen group, 22.7% (5/22) of the patients had Grade 3 or higher AEs, predominantly involving myelosuppression. Thirty percent (6/20) of the patients in the dual-regimen group AEs of similar severity, with palmoplantar erythema being the most common. In the triple-regimen group, which received combined chemotherapy, immune checkpoint inhibitors, and targeted therapy, 32.1% (17/53) of the patients experienced grade 3 or higher AEs, mainly palmoplantar erythema and pneumonia (Table 3). Nevertheless, the AEs in the

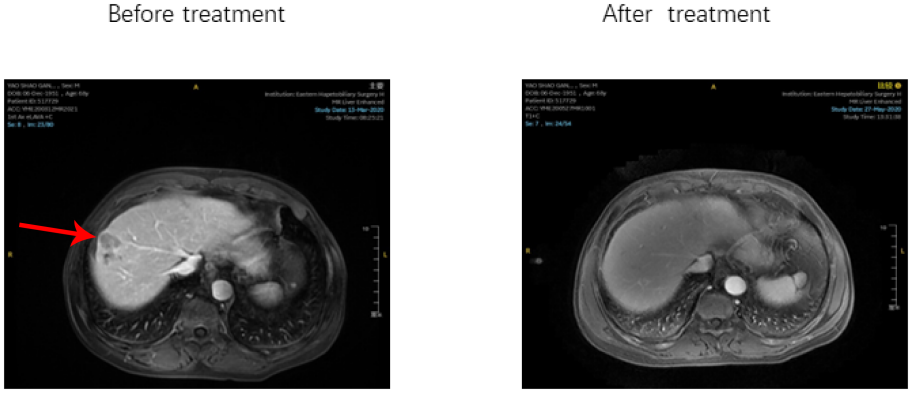

FIGURE 4
After receiving Triple regimen treatment, the patient's lesion completely disappeared.

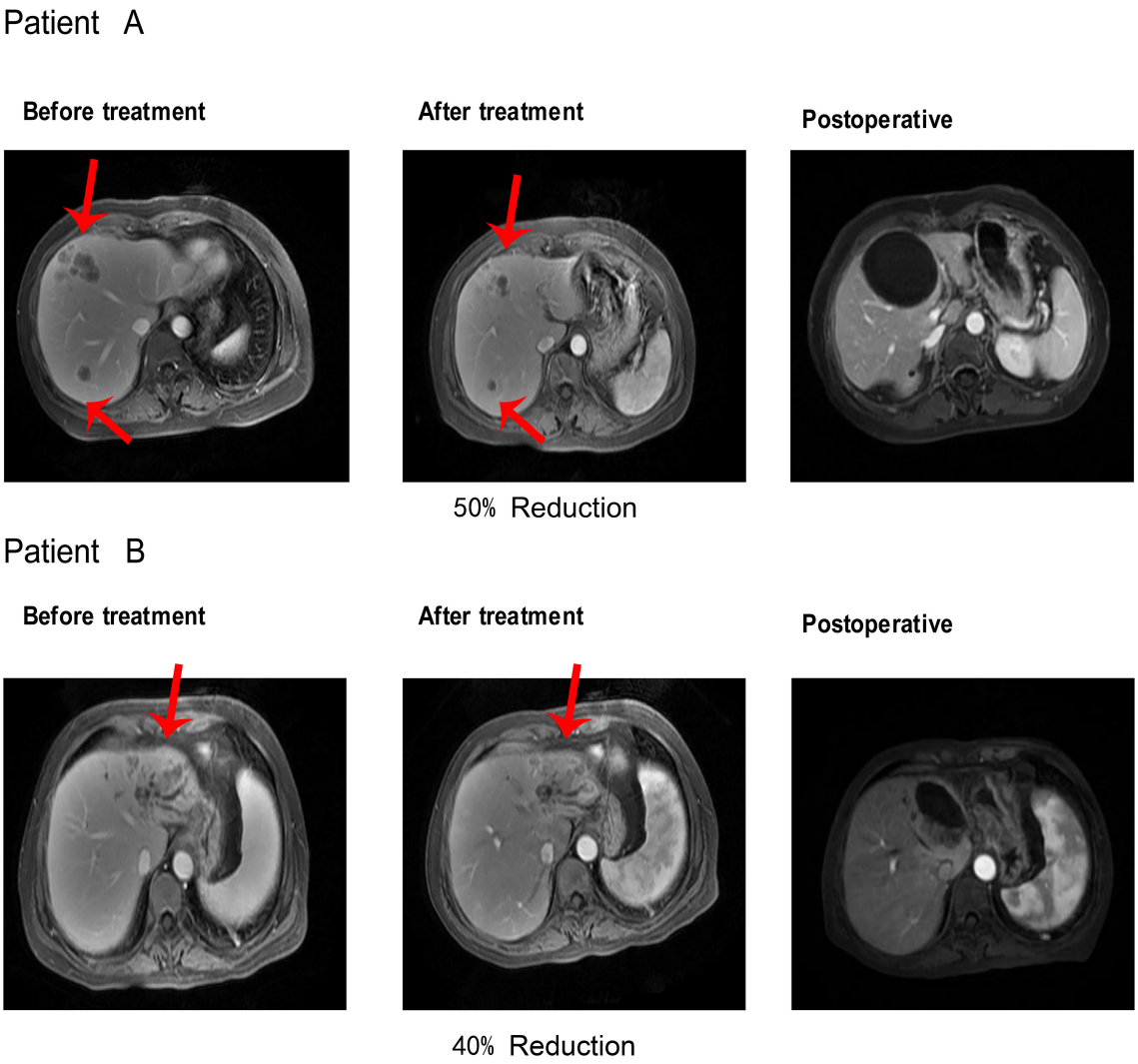

FIGURE 5
After receiving Triple regimen treatment, patients A and B significantly reduced lesion size and underwent radical surgical resection.

combination therapy groups were generally safe, well tolerated, and manageable.

4 Discussion

4.1 Effectiveness analysis

ICC is a highly malignant tumor with a poor prognosis and a low response rate. This is the first study to compare the efficacy and safety of three treatment regimens (chemotherapy alone, chemotherapy+PD-1, and chemotherapy+TKI+PD-1) in real-world patients with advanced ICC. Our results indicated that triple therapy (chemotherapy + TKI + PD-1) as a first-line treatment yielded better PFS and (OS than the other regimens. This approach demonstrated significant antitumor activity in patients with ICC, with notable median PFS and OS rates and high ORRs, DCRs, and CBRs. These findings suggest that a combination of targeted therapy, immunotherapy, and systemic chemotherapy is effective for BTC treatment, which aligns with the outcomes reported in other studies of similar regimens.

The recent advancements in combination therapies for unresectable or advanced malignant biliary tract tumors have been significant (9). The TOPAZ-1 trial (NCT03875235) highlighted the efficacy of combining durvalumab with gemcitabine and cisplatin (chemotherapy regimens) as first-line treatment. As of February 25, 2022, the OS survival rate was 76.9%. The median OS (95% CI) was 12.9 (11.6–14.1) months in the experimental group and 11.3 (10.1–12.5) months in the control group.

These findings reflect the ongoing commitment of researchers to improve therapeutic strategies for challenging biliary tract cancers (10).

Antiangiogenesis targeted therapy inhibits tumor angiogenesis and tumor cell proliferation and improves the tumor immune microenvironment, resulting in a synergistic enhancement mechanism with immunotherapy. In the treatment of advanced liver cancer, the combination of antiangiogenic targeted therapy and immunotherapy has become the preferred first-line treatment strategy. In the treatment of biliary tract tumors, a combination of

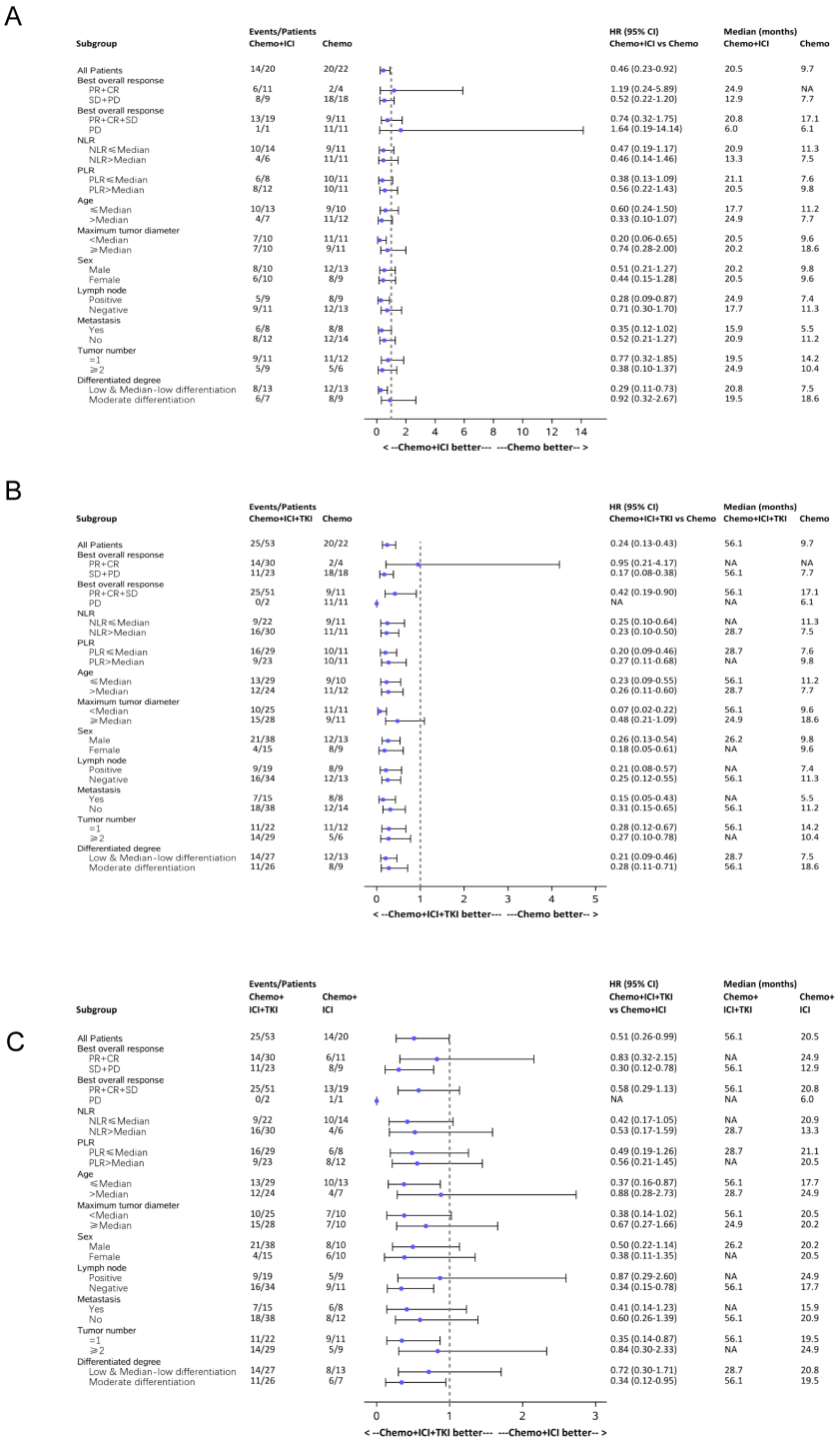

FIGURE 6
Forest plot analysis of subgroups of PFS in all the three group patients. **(A)** Forest plot analysis of subgroups of PFS between the chemo-regimen and dual-regimen group. **(B)** Forest plot analysis of subgroups of PFS between the chemo-regimen and triple-regimen group. **(C)** Forest plot analysis of subgroups of PFS between the dual-regimen and triple-regimen group.

chemotherapy, immunotherapy, and antiangiogenic targeted therapy has also been actively explored.

In 2020, the European Society for Medical Oncology (ESMO) reported a phase II clinical study conducted in China for locally advanced or metastatic ICC: a combination of toripalimab, lenvatinib, gemcitabine, and the oxaliplatin and gemcitabine (GEMOX) chemotherapy regimen (11), followed by maintenance therapy with toripalimab and lenvatinib after six cycles of treatment. The results revealed that the ORR was as high as 80.0% (24/30), the DCR was 93.3% (28/30), the median PFS was 10.0 months, and the incidence of ≥ grade 3 AEs was 50%. In a phase II randomized controlled study reported by the American

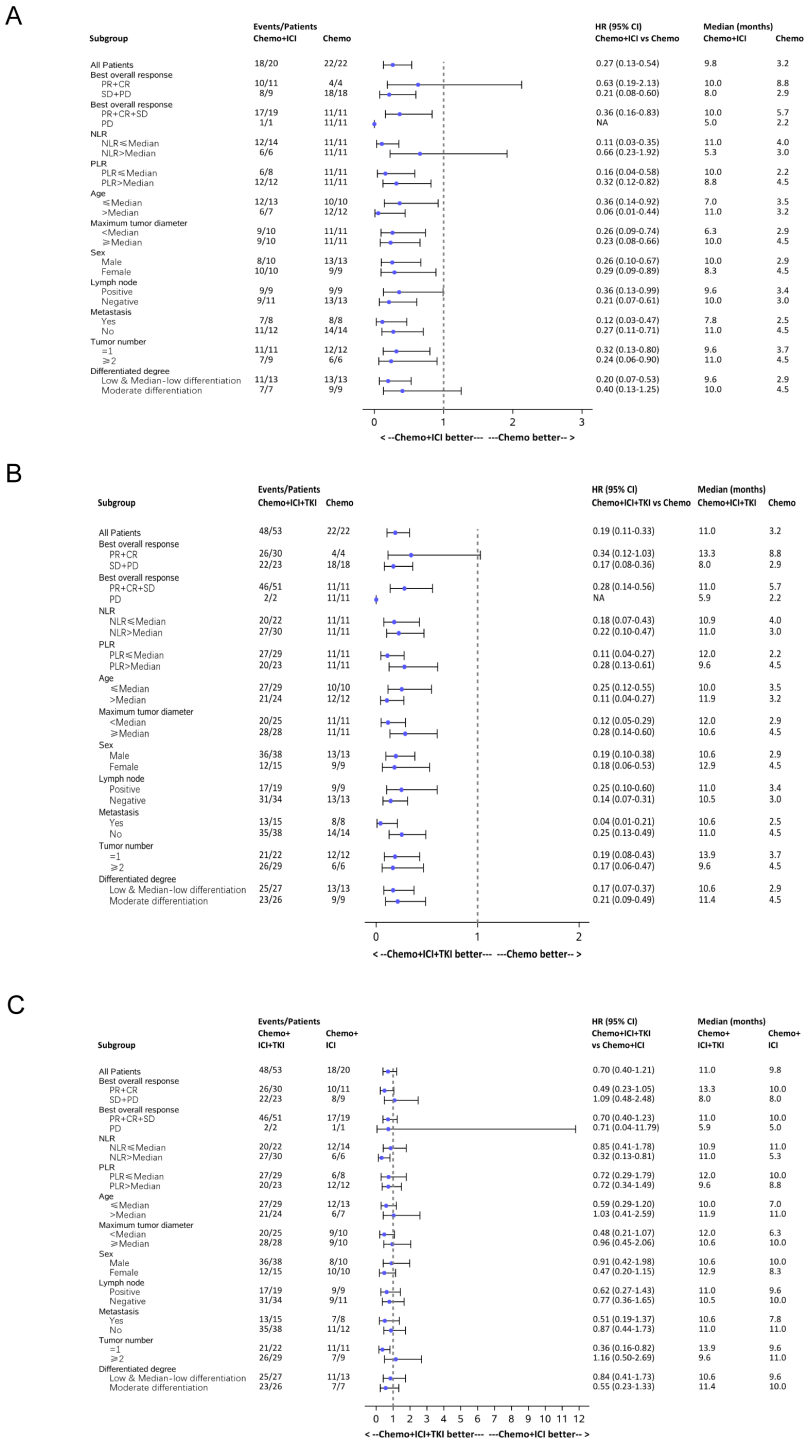

FIGURE 7
Forest plot analysis of subgroups of OS in all the three group patients. **(A)** Forest plot analysis of subgroups of OS between the chemo-regimen and dual-regimen group. **(B)** Forest plot analysis of subgroups of OS between the chemo-regimen and triple-regimen group. **(C)** Forest plot analysis of subgroups of OS between the dual-regimen and triple-regimen group.

Society of Clinical Oncology (ASCO) in 2023 (12), 80 patients with nonsurgically resectable or metastatic BTC were enrolled. The results revealed that the combination therapy group had a significantly longer median PFS (8.6 months vs. 6.2 months, P<0.01), higher ORR (52.8% vs. 29.4%), and median response duration (9.4 months vs. 3.4 months) but also had higher rates of grade 3/4 TRAEs (77.5% vs. 40%).

According to the above studies, the use of chemotherapy combined with immunotherapy and tyrosine kinase inhibitors as antivascular targeted drugs has good prospects, especially with an ORR ranging from 52.8% to 80.0%, indicating the potential for translational therapy. Further phase III clinical studies are needed to confirm its efficacy and safety.

10.3389/fimmu.2024.1463574

TABLE 3 Summary of the TRAEs in patients (n=95).

	Complications											
	Chemo(n=22)				Chemo+ICI(n=20)				Chemo+ICI+TKI(n=53)			
	<3		≥3		<3		≥3		<3		≥3	
Weakness	2	9.09%	0	0.00%	2	10.00%	0	0.00%	4	7.55%	0	0.00%
Decreased Appetite	3	13.64%	0	0.00%	3	15.00%	0	0.00%	5	9.43%	0	0.00%
Fever	1	4.55%	0	0.00%	1	5.00%	0	0.00%	2	3.77%	0	0.00%
Rash	2	9.09%	0	0.00%	2	10.00%	1	5.00%	6	11.32%	2	3.77%
Palmar And Plantar Erythema	1	4.55%	0	0.00%	2	10.00%	2	10.00%	8	15.09%	4	7.55%
Elevated ALT Or AST	1	4.55%	0	0.00%	1	5.00%	0	0.00%	2	3.77%	0	0.00%
Proteinuria	1	4.55%	0	0.00%	1	5.00%	0	0.00%	3	5.66%	0	0.00%
Anemia	2	9.09%	0	0.00%	1	5.00%	0	0.00%	2	3.77%	0	0.00%
Thrombocytopenia	1	4.55%	2	9.09%	2	10.00%	1	5.00%	3	5.66%	2	3.77%
Abdominal Pain	1	4.55%	0	0.00%	1	5.00%	0	0.00%	1	1.89%	0	0.00%
Hypothyroidism	0	0.00%	0	0.00%	0	0.00%	0	0.00%	3	5.66%	1	1.89%
Pruritus	0	0.00%	0	0.00%	0	0.00%	0	0.00%	4	7.55%	0	0.00%
Elevated Blood Bilirubin	1	4.55%	0	0.00%	1	5.00%	0	0.00%	2	3.77%	0	0.00%
Hypertension	0	0.00%	0	0.00%	1	5.00%	0	0.00%	2	3.77%	1	1.89%
Diarrhea	2	9.09%	1	4.55%	2	10.00%	0	0.00%	5	9.43%	1	1.89%
Nausea	2	9.09%	0	0.00%	2	10.00%	0	0.00%	4	7.55%	0	0.00%
Neutropenia	2	9.09%	2	9.09%	2	10.00%	1	5.00%	3	5.66%	2	3.77%
Vomit	1	4.55%	0	0.00%	1	5.00%	0	0.00%	2	3.77%	0	0.00%
Pneumonia	0	0.00%	0	0.00%	1	5.00%	1	5.00%	5	9.43%	3	5.66%
Myocardial Damage	0	0.00%	0	0.00%	0	0.00%	0	0.00%	2	3.77%	2	3.77%

ALT, alanine aminotransferase; AST, aspartate transaminase; TRAE, treatment-related AE.

Predicting the efficacy of immunotherapy via biomarkers is also an important direction for research and exploration of BTC immunotherapy. Subgroup analysis of the TOPAZ-1 and KEYNOTE-966 studies suggested that it may not be possible to predict the survival benefit of combined immunotherapy with chemotherapy by dividing patients according to PD-L1 expression. In the TOPAZ-1 study, patients with tumor area positivity (TAP) ≥1% who received combined immunotherapy had an HR of 0.79 (95% CI: 0.61~1.00) for OS, whereas patients with TAP <1% who received combined immunotherapy had an HR of 0.86 (95% CI: 0.60~1.23) for OS. In the KEYNOTE-966 study, patients with a combined positive score (CPS) ≥1 who received combined immunotherapy had an HR of 0.85 (95% CI: 0.72~1.00) for OS, whereas patients with a CPS <1 who received combined immunotherapy had an HR of 0.84 (95% CI: 0.62~1.14) for OS.

4.2 Surgical treatment after downstaging with target-free therapy

In this study, two ICC patients achieved significant tumor shrinkage after target-free therapy and were classified as having a PR according to the mRECIST criteria. Both patients underwent conversion therapy, followed by successful radical liver tumor resection. After surgery, the patients recovered well without severe complications, and pathological examinations revealed a 40%-50% tumor shrinkage rate with no residual cancer cells at the tumor margins or lymph nodes. The Multi-Disciplinary Treatment (MDT) team deemed the patients suitable for surgery after downstaging, leading to complete tumor removal and positive postoperative recovery. These cases highlight that a significant treatment response can open up surgical options for ICC patients, emphasizing the need for more clinical studies to explore this approach further.

4.3 Evaluation indicators of tumor efficacy

As dynamic methods for assessing tumor treatment efficacy, the early tumor shrinkage rate and depth have significant clinical importance and value. In our study, Groups 2 and 3 presented notably higher early tumor shrinkage rates than did Group 1 ($P<0.05$). There were also significant differences in the average tumor shrinkage depth between Groups 1 and 2 and between

Groups 1 and 3 (P<0.05). These findings suggest that the tumor shrinkage rate and depth are critical indicators of treatment efficacy. Although the triple-regimen group had a longer duration of tumor shrinkage than Groups 2 and 1 did, these differences were not statistically significant (P>0.05). The early tumor shrinkage rate and depth have been reported to correlate positively with OS and PFS in patients. Clinical trials have demonstrated that patients who achieve a significantly early tumor shrinkage rate and depth tend to have better OS and PFS rates. These measures can serve as adjunctive indicators for evaluating treatment efficacy and for enhancing precision and objectivity when used along with traditional static parameters. For example, in metastatic colorectal cancer (mCRC) and non-small cell lung cancer (NSCLC), early tumor shrinkage (ETS) and depth of response (DpR) can stratify patients into distinct subgroups for tailored treatment plans (13). However, the specific values and time points of these indicators vary according to the tumor type and treatment, necessitating further research to standardize and optimize their use.

4.4 Mechanism analysis

Chemotherapy enhances the effects of immunotherapy via several mechanisms. First, cytotoxic agents such as platinum and gemcitabine activate apoptosis in monocytes/macrophages, reduce the number of myeloid-derived suppressor cells, and bolster anticancer immunity (14). Second, cytokines from chemotherapy-damaged cells recruit antigen-presenting cells (APCs) (15), facilitating phagocytosis and proinflammatory cytokine secretion by dendritic cells (DCs) (16). Additionally, epigenetic modulators upregulate antigen processing and presentation mechanisms and stimulate cytokine production, further enhancing the immune response (17). Patients resistant to chemotherapy may respond to a rechallenge after anti-PD-1 treatment. Targeted drugs such as the multitarget tyrosine kinase inhibitor lenvatinib, which acts on VEGFR1-3, induce immunogenic cell death (ICD) and modulate the immune response via the VEGF-VEGFR pathway (3). This action directly attacks cancer cells, mitigates immunosuppressive factors, and enhances immunotherapy efficacy (18). Therefore, the early combined use of targeted therapy, immunotherapy, and systemic chemotherapy is recommended (19).

4.5 Safety

Although targeted therapy and immunotherapy combined with chemotherapy may lead to more adverse reactions, these complications are generally controllable (20, 21). In our study, all patients experienced some AEs; however, no grade 5 AEs occurred. Approximately 45.6% of the patients had Grade 3 AEs, and 3.5% experienced Grade 4 AEs. Common AEs included fatigue, myelosuppression, and decreased appetite. The higher incidence of myelosuppression was attributed to chemotherapy. In comparison, adding chemotherapy to targeted therapy and immunotherapy in this study did not significantly increase the incidence of AEs (22).

4.6 Limitations

Although insightful, this study has several limitations, including its single-center, real-world design and small sample size, which necessitate cautious interpretation. Future research should involve larger, multicenter, prospective studies. The use of various immunotherapeutic drugs, including anti-PD-1 agents, requires further investigation through prospective, single-drug studies. Additionally, our study utilized only lenvatinib, a TKI drug. In future studies, we will explore the application of other targeted drugs in the treatment of ICC. Furthermore, the effectiveness of targeted therapy combined with immunotherapy and chemotherapy in different tumor classifications requires further confirmation; for example, we can investigate the effects of the expression of different genes on the efficacy of targeted therapies. Despite these limitations, this study offers valuable insights for future clinical research and the development of treatment strategies.

4.7 Conclusion

The combination of PD-1 inhibitors, TKIs, and chemotherapy is effective, safe, and tolerable for the treatment of advanced ICC. This combined treatment regimen outperforms the chemotherapy regimen alone, thereby extending the survival of patients with advanced ICC. However, further research with larger prospective cohorts is necessary to validate these findings more comprehensively.

Data availability statement

The raw data supporting the conclusions of this article will be made available by the authors, without undue reservation.

Ethics statement

The studies involving humans were approved by This study was approved by the Ethics Committee of Eastern Hepatobiliary Hospital (ethics code: EHBHKY2019-K-027.1/3/2020). The studies were conducted in accordance with the local legislation and institutional requirements. The participants provided their written informed consent to participate in this study.

Author contributions

ZD: Writing – original draft. CS: Conceptualization, Data curation, Writing – review & editing. JL: Investigation, Software, Writing – review & editing. JG: Methodology, Supervision, Writing – review & editing. KD: Data curation, Formal analysis, Writing – review & editing. KW: Formal analysis, Project administration, Validation, Writing – review & editing. LG: Project administration, Validation, Writing – review & editing. JY: Project administration, Resources,

Writing – review & editing. BD: Funding acquisition, Resources, Visualization, Writing – original draft.

Funding

The author(s) declare financial support was received for the research, authorship, and/or publication of this article. (1) Shanghai Municipal Health Commission (202240313); (2) National Natural Science Foundation of China (82174145); (3) Shanghai Natural Science Foundation (21ZR1478400).

Acknowledgments

Acknowledgments were extended to the patients and their families for their participation in the study, as well as to Mr. Zhongtao Sun and Ms. Yalin Wang from MSD Medical Affairs for their assistance with statistical analysis of the data and other efforts.

Conflict of interest

The authors declare that the research was conducted in the absence of any commercial or financial relationships that could be construed as a potential conflict of interest.

Publisher's note

References

1. Valle J, Wasan H, Palmer DH, Cunningham D, Anthoney A, Maraveyas A, et al. Cisplatin plus gemcitabine versus gemcitabine for biliary tract cancer. *N Engl J Med*. (2010) 362:1273–81. doi: 10.1056/NEJMoa0908721

2. Lamarca A, Palmer DH, Wasan HS, Ross PJ, Ma YT, Arora A, et al. Second-line FOLFOX chemotherapy versus active symptom control for advanced biliary tract cancer (ABC-06): a phase 3, open-label, randomised, controlled trial. *Lancet Oncol*. (2021) 22:690–701. doi: 10.1016/S1470-2045(21)00027-9

3. Tomlinson JL, Valle JW, Ilyas SI. Immunobiology of cholangiocarcinoma. *J Hepatol*. (2023) 79:867–75. doi: 10.1016/j.jhep.2023.05.010

4. Zhang Q, Liu X, Wei S, Zhang L, Tian Y, Gao Z, et al. Lenvatinib plus PD-1 inhibitors as first-line treatment in patients with unresectable biliary tract cancer: A single-arm, open-label, phase II study. *Front Oncol*. (2021) 11:751391. doi: 10.3389/fonc.2021.751391

5. Zhang YQ, Wang K, Feng JK, Yuan LY, Liang C, Xiang YJ, et al. Camrelizumab plus gemcitabine and oxaliplatin for the treatment of advanced intrahepatic cholangiocarcinoma: a bi-centric observational retrospective study. *Front Oncol*. (2023) 13:1101038. doi: 10.3389/fonc.2023.1101038

6. Shi GM, Huang XY, Wu D, Sun HC, Liang F, Ji Y, et al. Toripalimab combined with lenvatinib and GEMOX is a promising regimen as first-line treatment for advanced intrahepatic cholangiocarcinoma: a single-center, single-arm, phase 2 study. *Signal Transduct Target Ther*. (2023) 8:106. doi: 10.1038/s41392-023-01317-7

7. Benson AB, D'Angelica MI, Abrams T, Abbott DE, Ahmed A, Anaya DA, et al. NCCN guidelines® Insights: biliary tract cancers, version 2.2023. *J Natl Compr Cancer Network*. (2023) 21:694–704. doi: 10.1097/HEP.0000000000000688

8. Rimini M, Fornaro L, Rizzato MD, Antonuzzo L, Rossari F, Satake T, et al. Durvalumab plus gemcitabine and cisplatin in advanced biliary tract cancer: A large real-life worldwide population. *Eur J Cancer*. (2024) 208:114199. doi: 10.1016/j.ejca.2024.114199

9. Moris D, Palta M, Kim C, Allen PJ, Morse MA, Lidsky ME. Advances in the treatment of intrahepatic cholangiocarcinoma: An overview of the current and future therapeutic landscape for clinicians. *CA Cancer J Clin*. (2023) 73:198–222. doi: 10.3322/caac.21759

10. Fan A, Wang B, Wang X, Nie Y, Fan D, Zhao X, et al. Immunotherapy in colorectal cancer: current achievements and future perspective. *Int J Biol Sci*. (2021) 17:3837–49. doi: 10.7150/ijbs.64077

11. Zhou J, Fan J, Shi G, Huang X, Wu D, Yang G, et al. 56P Anti-PD1 antibody toripalimab, lenvatinib and gemox chemotherapy as first-line treatment of advanced and unresectable intrahepatic cholangiocarcinoma: A phase II clinical trial. *Ann Oncol*. (2020) 31:S262–3. doi: 10.1016/j.annonc.2020.08.034

12. Li H. 65P A single-arm, open-label, phase II study of tislelizumab combined with lenvatinib and Gemox regimen for conversion therapy of potentially resectable locally advanced biliary tract cancers. *Ann Oncol*. (2022) 33:570. doi: 10.1016/j.annonc.2022.07.093

13. Sung H, Ferlay J, Siegel RL, Laversanne M, Soerjomataram I, Jemal A, et al. Global cancer statistics 2020: GLOBOCAN estimates of incidence and mortality worldwide for 36 cancers in 185 countries. *CA Cancer J Clin*. (2021) 71:209–49. doi: 10.3322/caac.21660

14. Sung H, Ferlay J, Siegel RL, Laversanne M, Soerjomataram I, Jemal A, et al. Rational development of combination therapies for biliary tract cancers. *J Hepatol*. (2023) 78:217–28. doi: 10.1016/j.jhep.2022.09.004

15. Wang J, Zhu Y, Chen Y, Huang Y, Guo Q, Wang Y, et al. Three-in-one oncolytic adenovirus system initiates a synergetic photodynamic immunotherapy in immune-suppressive cholangiocarcinoma. *Small*. (2023) 19:e2207668. doi: 10.1002/smll.202207668

16. Serra-Camprubí Q, Verdaguer H, Oliveros W, Lupión-Garcia N, Llop-Guevara A, Molina C, et al. Human metastatic cholangiocarcinoma patient-derived xenografts and tumoroids for preclinical drug evaluation. *Clin Cancer Res*. (2023) 29:432–45. doi: 10.1158/1078-0432.CCR-22-2551

17. Gehl V, O'Rourke CJ, Andersen JB. Immunogenomics of cholangiocarcinoma. *Hepatology*. (2023). doi: 10.1097/HEP.0000000000000688

18. Pinter M, Scheiner B, Pinato DJ. Immune checkpoint inhibitors in hepatocellular carcinoma: emerging challenges in clinical practice. *Lancet Gastroenterol Hepatol*. (2023) 8:760–70. doi: 10.1016/S2468-1253(23)00147-4

19. Greten TF, Schwabe R, Bardeesy N, Ma L, Goyal L, Kelley RK, et al. Immunology and immunotherapy of cholangiocarcinoma. *Nat Rev Gastroenterol Hepatol*. (2023) 20:349–65. doi: 10.1038/s41575-022-00741-4

20. Merters J, Lamarca A. Integrating cytotoxic, targeted and immune therapies for cholangiocarcinoma. *J Hepatol*. (2023) 78:652–7. doi: 10.1016/j.jhep.2022.11.005

21. Kelley RK, Ueno M, Yoo C, Finn RS, Furuse J, Ren Z, et al. Pembrolizumab in combination with gemcitabine and cisplatin compared with gemcitabine and cisplatin alone for patients with advanced biliary tract cancer (KEYNOTE-966): a randomised, double-blind, placebo-controlled, phase 3 trial. *Lancet*. (2023) 401:1853–65. doi: 10.1016/S0140-6736(23)00727-4

22. Gandhy SU, Casak SJ, Mushti SL, Cheng J, Subramaniam S, Zhao H, et al. FDA approval summary: futibatinib for unresectable advanced or metastatic, chemotherapy refractory intrahepatic cholangiocarcinoma with FGFR2 fusions or other rearrangements. *Clin Cancer Res*. (2023) 29:4027–31. doi: 10.1158/1078-0432.CCR-23-1042

frontiers | Frontiers in Immunology

TYPE Review
PUBLISHED 03 September 2024
DOI 10.3389/fimmu.2024.1460282

OPEN ACCESS

EDITED BY
Yue Wang,
Second Military Medical University, China

REVIEWED BY
Gautam Sethi,
National University of Singapore, Singapore
Yongsheng Xiao,
Fudan University, China

*CORRESPONDENCE
Tian Li
fmmult@foxmail.com
Na Zhang
na.zhang.weifang@outlook.com

RECEIVED 05 July 2024
ACCEPTED 21 August 2024
PUBLISHED 03 September 2024

CITATION
Liu Y, Yang H, Li T and Zhang N (2024) Immunotherapy in liver cancer: overcoming the tolerogenic liver microenvironment. *Front. Immunol.* 15:1460282. doi: 10.3389/fimmu.2024.1460282

Immunotherapy in liver cancer: overcoming the tolerogenic liver microenvironment

Yanju Liu[1], Hongyuan Yang[1], Tian Li[2]* and Na Zhang[1]*

[1]Department of Infectious Diseases, Weifang People's Hospital, Weifang, Shandong, China, [2]School of Basic Medicine, Fourth Military Medical University, Xi'an, China

Liver cancer is a major global health concern, ranking among the top causes of cancer-related deaths worldwide. Despite advances in medical research, the prognosis for liver cancer remains poor, largely due to the inherent limitations of current therapies. Traditional treatments like surgery, radiation, and chemotherapy often fail to provide long-term remission and are associated with significant side effects. Immunotherapy has emerged as a promising avenue for cancer treatment, leveraging the body's immune system to target and destroy cancer cells. However, its application in liver cancer has been limited. One of the primary challenges is the liver's unique immune microenvironment, which can inhibit the effectiveness of immunotherapeutic agents. This immune microenvironment creates a barrier, leading to drug resistance and reducing the overall efficacy of treatment. Recent studies have focused on understanding the immunological landscape of liver cancer to develop strategies that can overcome these obstacles. By identifying the specific factors within the liver that contribute to immune suppression and drug resistance, researchers aim to enhance the effectiveness of immunotherapy. Prospective strategies include combining immunotherapy with other treatments, using targeted therapies to modulate the immune microenvironment, and developing new agents that can bypass or counteract the inhibitory mechanisms in the liver. These advancements hold promise for improving outcomes in liver cancer treatment.

KEYWORDS

immunotherapy, liver cancer, cancer microenvironment, combinational therapy, therapeutic advances

1 Introduction

Neoplasms remain the main killer worldwide (1–3). Among which, liver cancer, predominantly hepatocellular carcinoma (HCC), stands as one of the leading causes of cancer-related deaths worldwide (4–9). Despite advances in oncological therapies, the prognosis for liver cancer patients remains dire, especially in cases diagnosed at advanced stages (10). Traditional treatments, such as resection, transplantation, and systemic chemotherapy, offer limited efficacy and often come with significant side effects (11).

This backdrop underscores the urgent need for innovative therapeutic approaches, among which immunotherapy has emerged as a promising candidate (12).

Immunotherapy, which harnesses the body's immune system to fight cancer, has significantly transformed the treatment of various malignancies (13–16), marking a shift from traditional therapies by focusing on the interactions between cancer cells and the immune system (17). Applying immunotherapy in liver cancer, however, poses distinct challenges, primarily due to the liver's unique immunological characteristics (18). The liver is not only a crucial metabolic organ but also plays a significant role in immunology (19). Its specialized microenvironment, inherently inclined towards tolerance for normal functioning, paradoxically provides a protective environment for tumor cells, complicating the effectiveness of immunotherapy in liver cancer (20).

The tolerogenic nature of the liver is characterized by a distinct array of immune cells and regulatory pathways (21). This environment is adept at maintaining immune homeostasis and preventing overactive responses to the myriad of antigens constantly presented to it, primarily from the gut via the portal circulation (22). In the context of HCC, this immunological landscape facilitates immune evasion, allowing cancer cells to thrive and proliferate under the radar of immune surveillance (23, 24).

Addressing these challenges requires a deep understanding of the liver's immune milieu and the complex interplay between tumor biology and host immunity (25). This review aims to dissect the intricacies of the liver's immune environment and explore how current and emerging immunotherapeutic strategies are being tailored to overcome these barriers (26). We delve into the latest research underscoring the potential of immunotherapy in liver cancer (27). This review not only highlights the progress in immunotherapy but also delves into the multifaceted nature of tumor drug resistance, exploring genetic alterations, immune evasion, and the influence of the tumor microenvironment.

2 Immunological landscape of liver cancer

The tumor microenvironment (TME) is a complex network comprising cancer cells, immune cells, fibroblasts, endothelial cells, and the extracellular matrix, actively influencing cancer progression and response to therapies like immunotherapy (28–31). The TME supports tumor growth through angiogenesis, immune evasion, and modifying drug responses, playing a critical role in immunotherapy tolerance by mechanisms such as cytokine secretion (e.g., TGF-β, IL-10) that suppress immune responses, and the expression of checkpoint molecules like PD-L1 that help tumors evade immune detection (32). Additionally, direct interactions between tumors and immune cells can deactivate effector immune cells, contributing to the TME's immune-suppressive nature (33). Understanding and manipulating the TME is essential for developing effective cancer therapies, combining tumor-targeting strategies with approaches to alter the TME, aiming for improved therapeutic outcomes.

The liver's immune system is uniquely adapted to its exposure to food antigens and gut-derived microbial products via the portal vein (34, 35). This exposure necessitates a predominantly tolerogenic environment to avoid an overactive immune response, which could lead to tissue damage and impaired liver function (36). The liver achieves this through a complex network of cells and signals that promote tolerance rather than immunity (37) (Figure 1).

2.1 The antigenicity of HCC

The antigenic landscape of HCC is characterized by the presence of tumor-specific antigens (TSAs) and neoantigens, essential for the immune system's recognition and attack on cancer cells (38). While TSAs, including alpha-fetoprotein (AFP), glypican-3 (GPC3), and melanoma-associated gene 1 (MAGE-1) in HCC, are predominantly cancer-centric, their presence, albeit in lower quantities, is not exclusive to cancer cells (39). The immune system, adept at identifying abnormalities, flags these antigens, especially when overexpressed or coupled with other tumor-associated signals (40). In contrast, neoantigens, borne out of tumor-specific genetic alterations such as point mutations and chromosomal rearrangements, are exclusive to cancer cells, rendering them precise targets for immune attacks (41).

Central to immune surveillance, TSAs and neoantigens underpin various immunotherapeutic strategies for HCC, including the deployment of cancer vaccines, the transfer of adoptive T cells, and the application of checkpoint blockade therapies (42, 43). However, targeting these antigens is fraught with challenges, given the liver's natural inclination towards immune tolerance, the heterogeneous expression of antigens across tumors, and the cancer cells' adeptness at evading immune detection (44, 45). Moreover, the liver's altered immune landscape, often a consequence of underlying conditions like hepatitis or cirrhosis, can significantly impact the efficacy of antigen-targeted therapies (46). Thus, delving deep into the antigenic profile of HCC, through meticulous identification and functional analysis of TSAs and neoantigens, is imperative for refining immunotherapeutic approaches and enhancing treatment precision and effectiveness against liver cancer (47).

2.2 Specialized immune cell populations

The liver's immune environment is intricately composed of various specialized cell types that play pivotal roles in maintaining immune homeostasis and regulating immune responses (48). In the context of liver cancer, particularly hepatocellular carcinoma (HCC), these cells contribute to a tolerogenic milieu that can impede effective immunotherapeutic interventions (49).

Cytotoxic T Cells (CTLs) are essential for the direct killing of cancer cells. In healthy immune responses, these cells recognize and destroy cells expressing specific antigens, including tumor cells. However, in HCC, the activity of CTLs is often suppressed due to

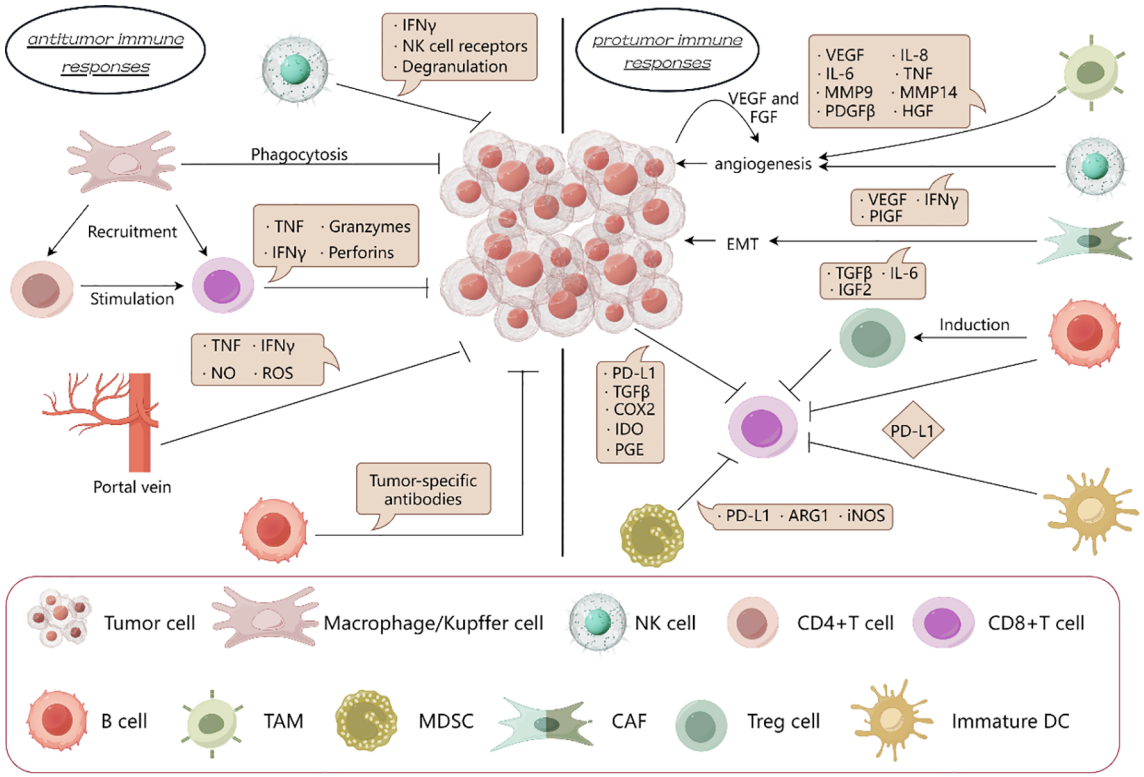

FIGURE 1
Protumor immune responses is dominant in liver cancer. In the immune microenvironment of liver cancer, the protumor immune response is superior to the anti-tumor immune response. By secreting cytokines, TAM and NK cells promote angiogenesis, CAF promotes epithelial mesenchymal transformation; Treg cells, immature DC cells, MDSCs and tumor cells suppresses the effect of CD8+T cells on tumors. And the killing effect on tumor by macrophages, NK cells and CD8+T cells is inhibited.

the immunosuppressive signals within the liver (50). Factors such as the upregulation of PD-L1 on tumor cells and the secretion of immunosuppressive cytokines like IL-10 and TGF-beta inhibit CTL activation and proliferation (51). Moreover, the presence of regulatory elements such as Tregs and myeloid-derived suppressor cells (MDSCs) further dampens the CTL response, allowing tumor cells to evade immune detection (52).

Regulatory T Cells (Tregs) play a critical role in maintaining immune tolerance by suppressing autoimmunity and excessive immune responses that could damage host tissues. In liver cancer, Tregs are recruited and expanded within the tumor microenvironment, where they inhibit the function of CTLs and NK cells through the secretion of suppressive cytokines like TGF-beta and IL-10 (53). This suppression helps the tumor evade immune surveillance. The enrichment of Tregs in the liver is also facilitated by the liver's exposure to antigens from the gut, which promotes a generally tolerogenic environment (54).

As the liver's resident macrophages, Kupffer cells are involved in clearing pathogens and cellular debris. However, in HCC, their role shifts towards promoting tumor growth and survival. They achieve this by secreting pro-tumorigenic cytokines and growth factors that enhance tumor cell proliferation, angiogenesis, and metastasis (55). Kupffer cells also contribute to the immunosuppressive environment by producing IL-10 and TGF-beta, which inhibit the functions of dendritic cells and CTLs. Additionally, they engage in crosstalk with hepatic stellate cells and cancer-associated fibroblasts to remodel the extracellular matrix, further facilitating tumor progression (56).

Dendritic Cells (DCs) are crucial for antigen presentation and the activation of T cells. However, in the liver tumor microenvironment, the function of DCs is often compromised. They are either numerically decreased or functionally impaired, which hampers their ability to present tumor antigens effectively and initiate a robust anti-tumor immune response (57). The impaired functionality of DCs in HCC is partly due to the suppressive cytokines produced by other immune cells and the tumor cells themselves.

Natural Killer (NK) and NKT Cells are important for their roles in immune surveillance and the early response to tumor formation. These cells can recognize and kill transformed cells without the need for prior sensitization to specific antigens. In liver cancer, however, their cytotoxic activity is often inhibited by the immunosuppressive cytokines in the microenvironment and by direct interactions with tumor cells that express inhibitory molecules (58).

Each of these cell populations plays a significant role in the immunological landscape of liver cancer, contributing to the complexity and challenge of developing effective immunotherapeutic strategies. Understanding and manipulating the functions and interactions of these cells is key to enhancing the immune response against liver cancer (Figure 2).

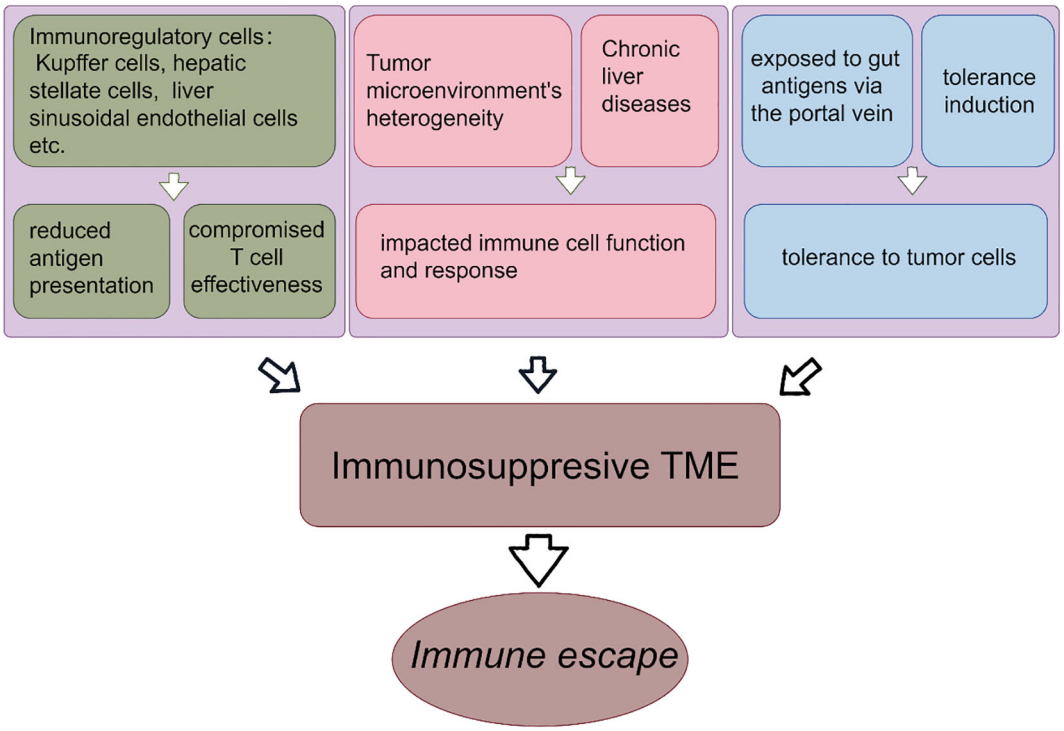

FIGURE 2
Formation of liver immunosuppressive tumor microenvironment. The formation of immunosuppressive microenvironment of liver cancer promotes the immune escape. The reduced antigen presentation by immunoregulatory cells leads to the impaired T cell effects. The heterogeneity of TME and chronic liver diseases lead to the suppression of immune function and immune response. Liver is exposed to intestinal antigens and obtains immune tolerance.

2.3 Key cytokines in immune suppression

Among the cytokines that play critical roles in the liver's immune landscape, TGF-beta and IL-10 stand out due to their potent immunosuppressive effects. TGF-beta is a multifunctional cytokine that primarily facilitates an immunosuppressive environment conducive to tumor growth and metastasis in the context of liver cancer. It acts by inhibiting the proliferation and activation of T cells and by promoting the conversion of effector T cells into regulatory T cells, thus enhancing immune tolerance (59).

IL-10, another immunosuppressive cytokine, further contributes to the complexity of the immune landscape in liver cancer by inhibiting the synthesis of pro-inflammatory cytokines, thus reducing the effectiveness of the immune response against tumor cells. It also promotes the differentiation of Tregs and hampers the antigen-presenting capabilities of dendritic cells, reducing the overall immune surveillance in HCC (60).

2.4 Impact of liver microenvironment on immune surveillance

The liver's unique immunological landscape, pivotal for metabolism and detoxification, significantly shapes liver cancer immunotherapy (61). Tasked with tolerance induction, the liver, constantly exposed to gut antigens via the portal vein, distinguishes between harmful and benign substances (62). This mechanism, however, may inadvertently extend tolerance to tumor cells, complicating immunotherapy (63).

Immunoregulatory cells such as the liver sinusoidal endothelial cells, the Kupffer cells, and the hepatic stellate cells, integral to the liver's immune tolerance, can suppress the immune response against HCC cells (64). This suppression leads to reduced antigen presentation and compromises T cell effectiveness in targeting cancer cells (65). Additionally, the liver harbors unique immune cells like NK, NKT, and γδ T cells, each with specific roles in immune surveillance, offering avenues for immunotherapy (66).

The roles of specific immune cells such as macrophages, neutrophils, and regulatory T cells (Tregs) are critical in mediating immunotherapy resistance, particularly to immune checkpoint inhibitors (ICIs). Within the liver TME, macrophages contribute significantly to ICI resistance. Their interaction with tumor cells often results in the secretion of various chemokines and cytokines that not only protect the tumor from immune attack but also enhance the recruitment of other immunosuppressive cell types. This activity establishes a feedback loop that sustains and amplifies immune suppression, diminishing the therapeutic efficacy of ICIs (67). The role of neutrophils extends beyond traditional pathogen defense to influencing the balance of the immune response in the TME. They support a suppressive environment by interacting with other immune cells and modulating their activity towards tolerance rather than immunity. Their presence in the TME correlates with poorer outcomes in immunotherapy, suggesting their potential as therapeutic targets to enhance ICI

response (68). Tregs directly impact the effectiveness of ICIs by maintaining a high threshold for T cell activation. They utilize various mechanisms to suppress effector T cell function, crucially dampening the immune response against the tumor. Manipulating Treg activity or selectively reducing their numbers within the TME could potentially restore immune activity and improve responses to immunotherapies (69).

The liver tumor microenvironment's heterogeneity, influenced by individual patient factors, affects immunotherapy's effectiveness (70). Chronic liver diseases, often precursors to liver cancer, alter the immune landscape, impacting immune cell function and response (71).

The challenge in liver cancer immunotherapy lies in effectively activating an anti-tumor immune response without disrupting the liver's essential tolerance mechanisms (72). Understanding the intricate balance of liver immunity is crucial for designing effective immunotherapeutic strategies (73). This involves identifying targets within the liver's immune milieu that can be modulated to enhance the immune response against HCC cells while preserving the liver's vital functions (74).

In conclusion, the liver's immunological microenvironment, with its unique cellular composition and tolerance-promoting mechanisms, presents both a challenge and an opportunity for the development of effective immunotherapies for liver cancer (75). Strategies that can navigate and modulate this complex environment hold the key to successful immunotherapeutic interventions in HCC (76).

3 Current immunotherapeutic approaches for liver cancer

3.1 Genetic and molecular landscape of liver cancer

Liver cancer, particularly HCC, is characterized by distinct genetic mutations that influence both tumor behavior and interaction with the immune system. Key mutations often involve genes like TP53, known for its role in cell cycle regulation and apoptosis, and CTNNB1, which affects the Wnt/beta-catenin signaling pathway (77). These genetic abnormalities are not only pivotal for cancer progression but also modulate the tumor microenvironment to favor immune evasion and resistance to therapy.

TP53, the most commonly mutated gene in human cancers, plays a crucial role in DNA repair, cell cycle regulation, and apoptosis. Mutations in TP53 are associated with poor prognosis in liver cancer and can lead to an accumulation of genomic instability, making tumors more aggressive and resistant to conventional therapies (78).

Mutations in CTNNB1, which encodes beta-catenin, are prevalent in liver cancer. These mutations lead to the activation of the Wnt/beta-catenin signaling pathway, promoting cell proliferation and survival. Importantly, beta-catenin activation is linked to immune evasion mechanisms, such as the suppression of cytokine production and inhibition of T cell infiltration into the tumor microenvironment (79).

The genetic makeup of HCC significantly influences the effectiveness of immunotherapeutic approaches. Tumors with extensive mutational burdens may present a higher number of neoantigens, potentially enhancing their visibility to the immune system. However, the same mutations often enhance the expression of immune checkpoints like PD-L1, contributing to an immunosuppressive tumor milieu (80).

3.2 Checkpoint inhibitors

The use of drugs targeting immune checkpoints like PD-L1, PD-1, and CTLA-4, has been a significant development in the treatment of liver cancer, particularly hepatocellular carcinoma (HCC) (81). These immune checkpoint inhibitors (ICIs) are designated to inhibit cancer cells' mechanisms to evade the immune system (82).

Nivolumab was among the first PD-1 inhibitors being utilized in HCC (83). Clinical trials have shown it effective in patients with advanced HCC, particularly in those who had previous treatment with the standard treatment sorafenib (84). The response rates in these trials varied but showed promising results, with some patients experiencing significant tumor reduction and prolonged survival (85).

Pembrolizumab has also been tested in HCC patients, especially those who did not respond to first-line therapies like sorafenib (86). Clinical trials reported moderate response rates, with a certain subset of patients achieving durable responses (87). Unfortunately, the overall effectiveness and best patient selection criteria for pembrolizumab in HCC are still areas of active research (88).

Atezolizumab has been studied in combination with bevacizumab, an anti-angiogenic agent. This combination has shown enhanced effectiveness compared to atezolizumab alone or other standard therapies in HCC (89). This combination has shown a promising response rate and satisfying survival rate in patients, leading to changes in first-line treatment recommendations for some HCC patients (90).

Ipilimumab, a CTLA4 monoclonal antibody, often used in combination with nivolumab, has shown effectiveness in HCC, particularly in patients who failed to respond to previous treatments. The combination of nivolumab and ipilimumab appears to have significant synergistic effect, leading to higher response rates compared to either drug alone (91).

While the response rates for ICIs in HCC vary, a significant number of patients have shown partial or complete responses. These drugs have also been associated with improved overall survival rates in certain patient groups (92). Importantly, ICIs tend to have a lasting effect for those who do respond, leading to longer periods of disease control (93).

Various clinical trials are focused on optimizing the utilization of ICIs in liver cancer, including determining the best combinations of drugs, the ideal sequencing of therapies, and identifying biomarkers to predict the most likely group of patients to benefit from these treatments (94).

3.3 Adoptive cell therapy

CAR-T cell therapy, a form of immunotherapy that genetically engineers the patients' T cells to express a Chimeric Antigen Receptor (CAR) to be more capable of recognizing and killing cancer cells, is becoming a potential candidate as a treatment option for liver cancer, including hepatocellular carcinoma (HCC) (95). The current application of CAR-T cell therapy in liver cancer is primarily in the research and clinical trial phases (96). Various studies are focused on identifying suitable targets specific to liver carcinoma cells and engineering CAR-T cells to recognize these targets (97). These targets might include, for instance, GPC3 (glypican-3), which is often overexpressed in HCC (98). While still in the early stages, initial results from clinical trials suggest potential for CAR-T cell therapy in treating liver cancer. The field of CAR-T cell therapy for liver cancer is rapidly evolving, and future findings from ongoing basic and clinical research and trials are expected to provide more insights to the effectiveness and practical application of this therapy in liver cancer treatment.

3.4 Vaccine-based therapies

Therapeutic vaccines for liver cancer are an emerging area of research, focusing on stimulating the immune system itself to generate potent inhibition of cancer. These vaccines differ from traditional vaccines; instead of preventing disease, they are designed to treat existing cancer (42, 99).

Oncolytic virus vaccines attracted great attention of researchers and clinicians. The development of these vaccines involves genetically modifying viruses that selectively infect the cancer cells and kill them (100). Once the virus infects the tumor cells, it triggers an immune response not only against the virus but also against the tumor cells. This dual action helps in directly destroying the cancer cells and also in priming the immune system to recognize the cancer cells and induce cell death in the tumor (101).

Peptide-based vaccines serve as another strategy to treat cancer. These vaccines use specific peptides (short chains of amino acids) that are found on the outer membrane of cancer cells. After injecting these peptides, the immune system is trained to recognize and kill cells displaying these peptides, which, in most cases, are typically tumor cells in HCC (102).

The primary function of therapeutic vaccines in liver cancer is to boost the immune system's capacity to identify and destroy cancer cells. They work by either introducing specific antigens associated with liver cancer into the body or by modifying existing immune cells to be more effective against cancer cells (42, 103). The general idea is to trigger specifically targeted immune response that leads to the destruction of cancer cells while sparing normal tissue. These therapeutic vaccines stand for a promising area of research in the treatment of liver cancer, offering potential benefits such as targeted therapy with fewer side effects compared to traditional treatments. However, most of these vaccines are still in clinical trials, and more research is needed for us to better understand their efficacy and safety in treating liver cancer.

3.5 Clinical trials

Several significant clinical trials have been conducted focusing on novel immunotherapeutic approaches for liver cancer, particularly hepatocellular carcinoma (HCC). Here's an overview of some key trials and their preliminary results:

CheckMate 040 and 459 evaluated the efficacy of nivolumab, a PD-1 inhibitor, in advanced HCC patients. CheckMate 040 reported encouraging results in terms of overall response rate (ORR) and survival benefits in HCC patients, including those previously treated with sorafenib. CheckMate 459 compared first-line use of nivolumab with sorafenib. Although it failed to meet the pre-set primary endpoint of improved overall survival, nivolumab demonstrated a favorable safety profile (104, 105).

KEYNOTE-224, -240, and -394 focused on pembrolizumab in HCC. KEYNOTE-224 trial demonstrated encouraging results for pembrolizumab in sorafenib-treated patients. KEYNOTE-240 and KEYNOTE-394 trials aimed to confirm these findings in a larger cohort. The results demonstrated a better overall survival (OS) and progression-free survival (PFS), although the statistical significance varied (106–108).

The IMbrave150 trial, a pivotal phase III study, demonstrated significant advancements in treating advanced hepatocellular carcinoma (HCC) by combining atezolizumab, an anti-PD-L1 antibody, with bevacizumab, an anti-VEGF antibody, showcasing superior overall survival and progression-free survival compared to the standard treatment with sorafenib. This combination leverages dual mechanisms to modulate the tumor microenvironment, enhancing immune cell infiltration and activity while simultaneously inhibiting angiogenesis crucial for tumor growth. Despite its effectiveness, challenges such as therapy resistance—mediated by alternative immune pathways or adaptive resistance mechanisms within the tumor—persist, highlighting the need for predictive biomarkers to identify likely responders and optimize treatment regimens. Future directions include exploring synergies with other therapies and tailoring approaches based on comprehensive molecular profiling to overcome immunotolerance and improve outcomes in liver cancer treatment (109, 110).

Various ongoing trials have been exploring CAR-T cell therapy targeting specific antigens in liver cancer, such as GPC3 (111, 112). These trials are still in early phases, and results are awaited to understand the efficacy and, importantly, safety of CAR-T cells in HCC.

Trials are ongoing for vaccines targeting tumor antigens in liver cancer, such as AFP. Early-phase trials have shown some promise, but more intensive exploration is needed to establish their foundation in HCC treatment (103).

In addition, recent clinical trial updates from prominent oncology conferences, such as ASCO and ESMO, showed that the field of immunotherapy in liver cancer is rapidly advancing. The EMERALD-1 trial, combining durvalumab with bevacizumab and TACE, has shown encouraging results, significantly elongating PFS compared to TACE monotherapy (113). This underscores the potential of combining ICIs with locoregional therapies to enhance therapeutic outcomes. Furthermore, the LEAP-002 study highlights the

effectiveness of combining lenvatinib with pembrolizumab, marking a step forward in dual-therapy regimens (114). Additionally, the innovative approach of the REVERT LIVER CANCER Phase 2 trial, exploring, a STAT3 inhibitor, as monotherapy and in combination, opens new avenues in targeting the liver's immunosuppressive environment (115, 116). These developments reflect a growing exploration of the liver's immune tolerance mechanisms and the potential of tailored combination therapies to overcome these barriers, offering new hope for patients battling liver cancer.

The most recent 2024 ASCO annual meeting reported updates on important clinical trials, such as KEYNOTE-224 and EMERALD-1, showing encouraging survival data (117, 118). CAR-T cell therapies showed promising efficacy, especially in heavily treated advanced HCC cases (119). Additionally, the oncolytic virus VG161 reported substantial disease control rates in refractory HCC (120). These studies emphasize the ongoing shift towards precision medicine, leveraging advanced genomic profiling and novel therapeutic combinations to improve outcomes for HCC patients. There are currently more than 70 ongoing clinical trials regarding immunotherapy in liver cancer (Table 1).

4 Strategies to overcome the tolerogenic microenvironment

4.1 Combination therapies

The rationale for combining other therapies with immunotherapy in liver cancer treatment stems from several key factors. Firstly, immunotherapies alone might not be fully effective due to the liver's immune-tolerant nature and the complex tumor microenvironment in conditions like hepatocellular carcinoma (HCC) (121). Combining these therapies can enhance overall efficacy and overcome the resistance that often develops against single-treatment modalities. Moreover, liver cancer involves various biological pathways, and a combination approach allows for a more comprehensive targeting of the disease. Such combinations can also produce synergistic effects; for instance, certain chemotherapy induces immunogenic cell death, potentially enhancing the immune system's recognition and attack on tumor cells (122). Additionally, this strategy might allow for lower dosages of each treatment, potentially reducing side effects while maintaining or improving efficacy. Finally, certain therapies can modify the tumor's immune microenvironment, which becomes more susceptible to an immune attack, thus supporting the effectiveness of immunotherapy. This multi-modal approach is central to current research in liver cancer, aiming to significantly improve patient outcomes.

Combining Immunotherapy with Chemotherapy leverages the direct tumor-killing effect of chemotherapy and the immune-modulating properties of immunotherapy. Chemotherapy can release cancer antigens, making tumor cells easier to recognize by the immune system, while immunotherapy can strengthen the immune response against these exposed antigens.

Another important strategy is to combine immunotherapy and targeted therapy. Targeted therapies work by acting on specific molecular targets related to cancer. When combined with immunotherapy, these therapies can disrupt cancer cell mechanisms that suppress the antitumor immunity, enhancing the function of immunotherapeutic agents. Overcoming resistance to immune checkpoint inhibitors (ICIs) is significantly enhanced by incorporating anti-angiogenic drugs, which target the vascular

TABLE 1 Ongoing clinical trials of immunotherapy on liver cancer.

NCT Number	Study Type	Phase	Status	Sample Size(n)	Conditions	Outcome Measures
NCT05109052	Interventional	I/II	Withdrawn	48	HCC	Safety and Tolerability
NCT05185505	Interventional	IV	Recruiting	24	HCC	1 Acute Rejection 2 AE 3 ORR 4 atezolizumab/bevacizumab therapy 5 liver transplantation 6 necrotic tumors 7 RFS 8 OS 9 Tumor biomarkers 10 Immune Cell Biomarkers
NCT05609695	Observational	NA	Not yet recruiting	100	HCC	1 OS 2 TR 3 PFS
NCT05942560	Interventional	NA	Not yet recruiting	160	Depression, Anxiety, HCC, CBT	1 Depression symptoms 2 Anxiety symptoms 3 Quality of life score 4 Immune variables 5 OS
NCT05873244	Interventional	II	Recruiting	44	HCC	1 PFS 2 OS 3 radiological response rate 4 time-to-progression 5 AE
NCT05443230	Observational	NA	Enrolling by invitation	200	HCC, Sarcopenia	1 Short-term results 2 Long-term results
NCT05717400	Interventional	IV	Recruiting	15	HCC	1 Overall Response Rate

(Continued)

TABLE 1 Continued

NCT Number	Study Type	Phase	Status	Sample Size(n)	Conditions	Outcome Measures
NCT05484908	Interventional	NA	Not yet recruiting	60	HCC, Liver Failure, Immune-Mediated Hepatitis	1 Mortality rate 2 Model for end-stage liver disease (MELD) score variation
NCT06045286	Interventional	I	Recruiting	30	Colorectal Liver Metastases	1 ORR 2 PFS 3 OS
NCT06199232	Interventional	NA	Not yet recruiting	47	Liver Metastasis Colon Cancer, Failed From Standard Treatment, MSS, ctDNA Genotype	1 PFS 2 OS 3 ORR 4 DCR 5 AE
NCT05550090	Observational	NA	Recruiting	40	Metastatic Breast Cancer in the Liver	1 Correlation between DCE-MRI parameters combined with IVIM parameters and efficacy of chemotherapy in patients with liver metastasis of breast cancer
NCT05438420	Interventional	I/II	Recruiting	120	HCC, Cervical Cancer, Esophageal Cancer, Gastric Cancer	1 AE 2 TR 3 Change in the area under curve (AUC) of Q702 and its primary metabolites
NCT06047015	Interventional	I/II	Not yet recruiting	12	Liver Metastasis Colon Cancer	1 Complications 2 Abscopal effect 3 Tumor-specific immune response 4 PFS 5 Quality of life questionnaire
NCT05677113	Interventional	II	Recruiting	115	Liver Metastases, Colorectal Cancer	1 PFS 2 Clearance of ctDNA 3 Side-effect profile of QBECO 4 Quality of recovery 5 Five-year overall survival
NCT05833126	Interventional	II	Recruiting	25	Recurrent Liver Cancer After Liver Transplantation	1 Acute graft rejection rate 2 ORR 3 OS 4 PFS 5 Time to Progression 6 SAE 7 Graft Rejection
NCT05451043	Interventional	II	Not yet recruiting	62	HCC, Biliary Tract Cancer, Pancreatic Cancer, Cholangiocarcinoma	1 Investigating and establishing the efficacy of propranolol in boosting the effects of immunotherapy 2 Feasibility of study therapy 3 Safety/tolerability 4 PFS 5 OS
NCT05039736	Interventional	II	Withdrawn	0	HCC	1 overall response rate
NCT05893056	Interventional	II	Recruiting	25	Gastric Cancer Metastatic to Liver	1 ORR 2 DOR 3 PFS 4 OS 5 DCR 6 Number of participants with treatment-related adverse events as assessed by CTCAE v5.0
NCT05169957	Interventional	I	Recruiting	18	Liver Metastases, Melanoma, Cutaneous, Melanoma, Mucosal, Melanoma, Ocular, Metastatic Melanoma	1 Percentage of patients who receive all planned radiotherapy 2 Proportion of patients who develop grade 3 or higher toxicity 3 OS 4 PFS 5 Proportion of patients with local control 6 ORR 7 BOR
NCT06117891	Observational	NA	Recruiting	300	Unresectable Hepatocellular Carcinoma	1 OS 2 Discriptive analysis 3 DOT 4 PFS 5 ORR 6 Treatment sequences post first-line AB or other IO combinations
NCT05588297	Interventional	II	Not yet recruiting	12	Colorectal Cancer Liver Metastases	1 R0 recession rate 2 Pathological complete response rate 3 TRG 4 ORR 5 EFS 6 DFS 7 OS 7 AE 8 Quality of life score
NCT05322187	Interventional	II/III	Not yet recruiting	15	HCC, Hepatoblastoma, Pediatric Cancer, Pediatric Solid Tumor, Transitional Cell Tumor	1 ORR 2 dynamic α-fetoprotein response (AFP-R) 3 AE 4 Health outcomes as assessed by the

(Continued)

TABLE 1 Continued

NCT Number	Study Type	Phase	Status	Sample Size(n)	Conditions	Outcome Measures
						PROMIS® Pediatric Scale v1.0 Global Health 7 + 2 scores at baseline
NCT05510427	Interventional	I	Withdrawn	0	HCC, Cholangiocarcinoma	1 AE 2 MTD
NCT05984511	Interventional	NA	Not yet recruiting	234	HCC, Tumor Thrombus, Hepatic Portal Vein Tumor Invasion	1 OS 2 PFS 3 ORR 4 Duration of portal patency 5 AE
NCT05653531	Interventional	NA	Withdrawn	0	Liver Biomarkers, ICI, Lung Cancer, Transaminases	1 basal ALT blood concentration in lung cancer patients treated with ICI determined
NCT05233358	Interventional	NA	Not yet recruiting	176	HCC	1 PFS 2 OS 3 To Tumor Untreatable Progression 4 ORR 5 DCR 6 DOR 7 AE
NCT05339581	Interventional	NA	Not yet recruiting	78	HCC, Liver Transplant; Complications, Portal Vein Thrombosis, Radiotherapy; Complications	1 PVTT RR/NR 2 Alpha Fetoprotein Response (AFP-R) 3 PFS 4 ORR 5 TTP 6 DOR
NCT05411133	Interventional	I	Recruiting	68	HCC, Cholangiocarcinoma, Colorectal Adenocarcinoma, Esophageal Adenocarcinoma, Gastric Cancer, Gastroesophageal Junction, Gastrointestinal Cancer, Pancreatic Cancer	1 AE 2 Amount of Cabotamig (ARB202) in plasma 3 Biochemical and physiological effects 4 Effect of Cabotamig (ARB202) on tumour
NCT05937295	Interventional	I	Recruiting	20	Fibrolamellar Hepatocellular Carcinoma	1 To assess immunogenicity in terms of induction of peptide specific T-cell responses 2 Safety and Tolerability
NCT05332496	Observational [Patient Registry]	NA	Recruiting	220	HCC	1 PFS 2 OS 3 ORR 4 DOR 5 DCR 6 AE
NCT05332821	Observational [Patient Registry]	NA	Recruiting	474	HCC	1 OS 2 PFS 3 ORR 4 DOR 5 DCR 6 AE
NCT05647954	Interventional	III	Not yet recruiting	350	Melanoma Neuroendocrine Tumors Neuroectodermal Tumors, Neoplasms Germ Cell and Embryonal Neoplasms by Histologic Type, Neoplasms Neoplasms	1 PFS 2 OS 3 ORR 4 DCR 5 DOR 6 PFS 7 OS 8 AE
NCT05810402	Interventional	NA	Not yet recruiting	60	HCC, ICI, Liquid Biopsy	1 Percentage of patients with CTCs-PD-L1+ by CellSearch® technique 2 OS 3 PFS
NCT06031480	Interventional	II	Not yet recruiting	55	HCC	1 ORR
NCT04430452	Interventional	II	Recruiting	21	HCC	1 ORR 2 AE 3 PFS 4 DOR 5 OS
NCT06040177	Interventional	I/II	Recruiting	30	HCC Non-resectable, ICI, Portal Vein Tumor Thrombus	1 ORR 2 PFS 3 DCR 4 DOR 5 OS
NCT06205706	Interventional	I/II	Recruiting	104	HCC, Non Small Cell Lung Cancer, Solid Tumors	1 AE 2 SAE 3 Frequency of dose interruptions and dose reductions 4 DLT
NCT05278195	Observational	NA	Recruiting	300	HCC	1 OS 2 Specificity 3 Sensitivity 4 The area under curve (AUC) of Receiver Operating Characteristic (ROC) curves of the radiomics artificial intelligence mode 5 Accuracy

(Continued)

10.3389/fimmu.2024.1460282

TABLE 1 Continued

NCT Number	Study Type	Phase	Status	Sample Size(n)	Conditions	Outcome Measures
NCT05406466	Interventional	II	Recruiting	25	Melanoma	1 ORR 2 DCR 3 DOR 4 TTR 5 PFS 6 OS 7 AE
NCT05070247	Interventional	I/II	Recruiting	313	HCC, Breast Cancer, Esophageal Cancer, Gastric Cancer, Kidney Cancer, Mesothelioma, Nasopharyngeal Cancer, Non-small Cell Lung Cancer (NSCLC), Non-squamous, Pancreatic Cancer, Squamous Cell Cancer of Head and Neck (SCCHN)	1 Dose Escalation 2 Dose Expansion: Overall Response Rate (ORR) 3 DCR 4 DOR 5 TTR 6 PFS 7 OS 8 AE
NCT05665348	Interventional	II/III	Not yet recruiting	574	HCC, Metastatic Tumor	1 Objective response of treatment 2 OS 3 PFS 4 OR
NCT05879328	Observational	NA	Recruiting	12	HCC	1 RFS 2 TR 3 Complication rate 4 OS 5 Patients' reported outcomes (PROs) 6 Comparison with historical series
NCT04777851	Interventional	III	Recruiting	496	HCC	1 PFS 2 OS 3 ORR 4 Time to unTACEable Progression (TTUP) 5 DOR
NCT04965714	Interventional	II	Withdrawn	0	Resectable HCC	1 AE 2 Rate of pathologic complete response 3 Necrosis of tumors 4 TTP 5 RFS 6 OS
NCT06041477	Interventional	III	Recruiting	540	HCC, Chemotherapeutic Toxicity, Chemotherapy Effect	1 PFS 2 OS 3 ORR 4 DCR 5 CRR 6 Safety profiles of all participants
NCT05897268	Interventional	II	Recruiting	25	HCC	1 ORR 2 PFS 3 OS 4 DOR 5 DCR 6 ORR 7 PFS 8 OS 9 AE
NCT05096715	Interventional	I	Not yet recruiting	20	Unresectable HCC	1 Dose Limiting Toxicity Rate 2 PFS 3 OS 4 In-field response rate 5 Change in Child-Pugh Score 6 Out of field response rate
NCT05092373	Interventional	I	Recruiting	36	too much	1 To assess the safety and tolerability of TTF, including the maximum tolerated dose (MTD) 2 ORR 3 PFS 4 OS
NCT05578430	Interventional	II	Not yet recruiting	54	Resectable HCC	1 MPR 2 RFS 3 ORR 4 AE
NCT05044676	Observational	NA	Recruiting	120	HCC	1 OS
NCT05516628	Interventional	II	Not yet recruiting	30	HCC	1 RFS 2 TTR 3 RFS 4 OS
NCT06218511	Interventional	I	Recruiting	10	HCC	1 DFS 2 PFS 3 OS 4 AE
NCT05625893	Interventional	II	Recruiting	63	HCC, Portal Vein Thrombosis	1 PFS 2 AE 3 OS 4 Time-to-progression 5 ORR 6 DCR 7 Local tumor progression rate
NCT04965454	Interventional	II	Recruiting	80	HCC Non-resectable	1 ORR 2 DCR
NCT05337137	Interventional	I/II	Recruiting	162	HCC	1 DLT 2 ORR 3 PFS
NCT06133062	Interventional	II	Recruiting	45	HCC Non-resectable	1 PFS 2 LC 3 TTP 4 ORR 5 OS 6 AE
NCT05537402	Interventional	II	Recruiting	204	HCC	1 PFS 2 ORR 3 OS
NCT05717738	Observational	NA	Recruiting	300	HCC Non-resectable	1 Response Rate measured by mRECIST criteria 2 Number of Patients Amendable to Curative

(Continued)

10.3389/fimmu.2024.1460282

TABLE 1 Continued

NCT Number	Study Type	Phase	Status	Sample Size(n)	Conditions	Outcome Measures
						Surgical Interventions 3 TTP 4 PFS 5 OS 6 Pathological response 7 DCR 8 Quality of Life (QoL)
NCT05168163	Interventional	II	Recruiting	122	HCC	1 OS 2 PFS 3 ORR 4 DOR 5 AE
NCT05620771	Interventional	II	Recruiting	84	HCC	1 PFS 2 TTP 23 ORR 4 DOR 5 CBR 6 OS 7 AE
NCT05389527	Interventional	II	Active, not recruiting	43	HCC	1 MPR 2 PCR 3 Pathologic complete response (pCR) 4 ORR 5 R0 resection rate 6 DFS 7 OS 8 AE
NCT05488522	Interventional	I	Recruiting	18	HCC	1 Primary Objective 2 Secondary Objective 3 OS 4 PFS
NCT05101629	Interventional	II	Active, not recruiting	32	HCC	1 ORR 2 OS 3 Safety and toxicity
NCT05199285	Interventional	II	Recruiting	40	HCC	1 ORR 2 OS 3 PFS 4 Disease control 5 AE
NCT05822752	Interventional	II	Recruiting	120	HCC	1 BOR 2 DOR 3 PFS 4 OS
NCT05269381	Interventional	I	Recruiting	36	too much	1 AE 2 The number and percentage of participants who completed the sequencing with satisfactory data quality registration and identified at least 10 actionable peptides, meet the eligibility criteria for registration, and able to initiate vaccine production 3 Immunogenicity responders
NCT05327738	Interventional	II	Withdrawn	0	HCC	1 Proportion of progression-free participants 2 ORR 3 DCR 4 TTP 5 PFS 6 OS 7 Incidence of grade >= 3 adverse events
NCT05377034	Interventional	II	Recruiting	176	Locally Advanced Hepatocellular Carcinoma	1 BOR 2 DOR 3 TOR 4 PFS 5 OS
NCT05286320	Interventional	I/II	Not yet recruiting	27	Unresectable Hepatocellular Carcinoma, Lenvatinib, Pembrolizumab, Stereotactic Body Radiotherapy	1 safety rate 2 ORR 3 PFS 4 OS 5 Immune biomarkers
NCT06024252	Observational	NA	Not yet recruiting	200	HCC	1 OS 2 PFS 3 ORR 4 One-year survival rate 5 Immune-TACE PFS 6 DCR 7 Treatment pattern
NCT05448677	Interventional	II	Recruiting	196	HCC	1 PFS 2 ORR
NCT05223816	Interventional	II	Recruiting	97	HCC, Intrahepatic Cholangiocarcinoma	1 Safety in Cohort1 2 ORR 3 PFS
NCT05797805	Interventional	I/II	Recruiting	108	Advanced Hepatocellular Carcinoma	1 AE 2 DLT 3 Evaluate efficacy of tegavivint as a single agent
NCT05776875	Interventional	II	Recruiting	24	HCC	1 AE 2 Response rate 3 Time to progression 4 Time to TACE progression (TTTP) 5 Time to untaceable progression
NCT05908786	Interventional	I/II	Recruiting	150	HCC	1 MPR 2 PCR 3 Relapse-Free Survival (RFS) 4 Event-Free Survival (EFS) 5 OS

(Continued)

TABLE 1 Continued

NCT Number	Study Type	Phase	Status	Sample Size(n)	Conditions	Outcome Measures
NCT05396937	Interventional	II	Recruiting	42	HCC	1 ORR 2 Duration of Objective Response (DoR) 3 DCR 4 TTP 5 PFS 6 OS
NCT05903456	Interventional	II	Not yet recruiting	20	HCC	1 ORR 2 PFS 3 OS 4 DCR 5 Disease Control Rate 6 DOR 7 AE
NCT06066333	Interventional	II	Recruiting	12	ACC, Adrenocortical Carcinoma, Metastatic Adrenocortical Carcinoma	1 AE

endothelial growth factor (VEGF) pathway (123). These drugs aid in normalizing the tumor's abnormal vasculature, which not only improves blood flow and oxygenation within the tumor, thereby reducing hypoxia, but also facilitates the infiltration of effector T cells into the tumor microenvironment (124). This process enhances the immune system's capacity to target and destroy tumor cells. Additionally, anti-angiogenic therapies help reduce the recruitment of immunosuppressive cells such as regulatory T cells (Tregs) and myeloid-derived suppressor cells (MDSCs) to the tumor site and alter immune-related signaling, including the modulation of PD-L1 expression on tumor and immune cells (125). The combination of the immune checkpoint inhibitor atezolizumab (PD-L1 inhibitor) with bevacizumab (VEGF inhibitor) has become the recommended first-line systemic treatment for advanced HCC (109). A case study reported the successful treatment of brain metastasis in intrahepatic cholangiocarcinoma with a combination of the PD-1 inhibitor camrelizumab and a multi-kinase inhibitor lenvatinib. The patient showed a complete response (CR) and a PFS of 17.5 months without serious side effects, suggesting the potential of this combination therapy (126).

Dual Immune Checkpoint Inhibition is another widely-used approach. Using two different immune checkpoint inhibitors can have a synergistic effect. This combination can enhance T-cell activation and more effectively attack cancer cells than single-agent therapy (127). In the HIMALAYA study, Tremelimumab and durvalumab show potential in treating unresectable, advanced liver cancer, offering a new choice for inflammation-driven cancer (128).

Techniques like radiofrequency ablation (RFA) or transarterial chemoembolization (TACE) can also be combined with immunotherapy (129, 130). These local treatments can increase antigen presentation and inflammation, potentially making immunotherapy more effective (131).

In addition, therapeutic cancer vaccines can be combined with immunotherapies to enhance the immune response specifically against liver cancer cells (132).

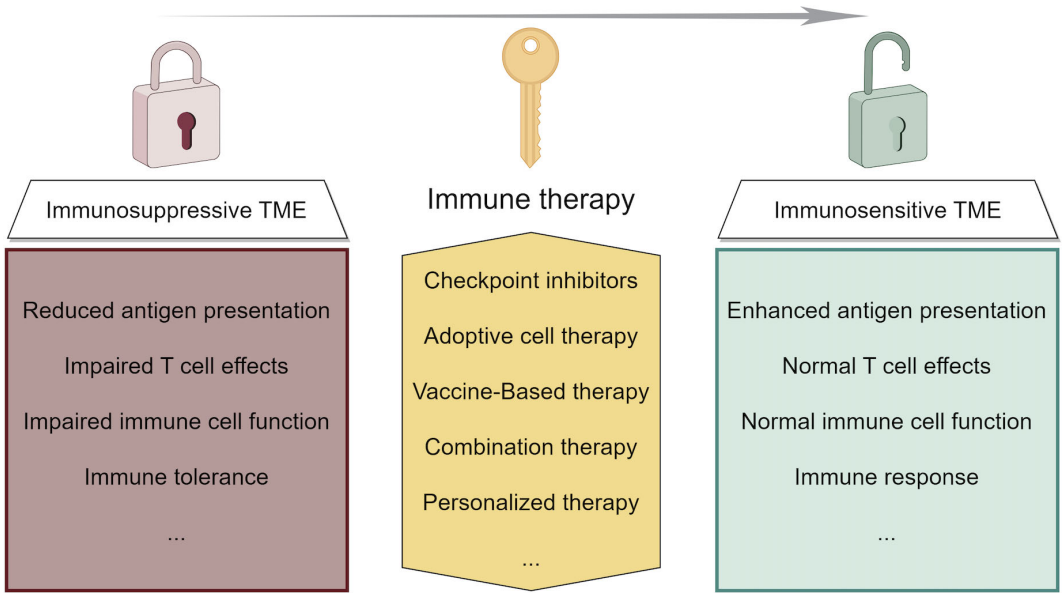

FIGURE 3
Strategies of immunotherapy in liver cancer and their function of modifying the tumor microenvironment.

These combination therapies aim to capitalize on the strengths of each treatment modality, aiming for a more robust and targeted attack on liver cancer cells (12). Clinical trials are still being carried out to find out the most effective combinations and protocols (42).

Preclinical studies also gave sight to novel strategies to enhance the effect of immunotherapy. For instance, a recent study reported that antitumor immunity can be enhanced by targeting cGas/STING pathway (133). Targeting fibrinogen-like protein 1 can also enhance immunotherapy in hepatocellular carcinoma (134).

4.2 Personalized medicine by immune classification

Personalized approaches, including the development of biomarkers for the prediction of immunotherapy outcome, are increasingly important in liver cancer treatment, allowing for more targeted and effective treatments (135).

The immune microenvironment of liver cancer can be classified based on molecular features and immunogenicity into distinct types, reflecting the heterogeneity and complexity of tumor immune interactions (22). Based on the differentiated infiltration of the cytotoxic immune cells, primary liver cancers are categorized into inflamed tumors, which are immunologically active, and non-inflamed tumors, which are immunologically inactive (136). Recent studies further identified four immune subclasses of liver cancer according to their immunosuppression mechanisms and genomic alterations, namely, 1) Tumor-associated macrophage (TAM): This subclass shows increased levels of extracellular matrix genes, and is associated with poor survival (137). 2) CTNNB1: characterized by CTNNB1 mutations (138). 3) Cytolytic activity (CYT): Represents inflamed tumors with high cytolytic activity (139). 4) Regulatory T cell (Treg): Also represents inflamed tumors but with increased presence of Treg cells (140). The TAM and CTNNB1 subclasses are seen as non-inflamed, while the CYT and Treg subclasses represent inflamed tumors (141). Further classification based on immunogenomic features has led to the identification of three HCC subtypes based on immune characteristics: immunity high (referred as Immunity_H), medium (Immunity_M), and low (Immunity_L). This classification is effectively predictive of patient prognosis, with the Immunity_H subtype indicating a better survival rate due to higher immune and stromal scores (85, 89).

The classifications of the liver cancer immune microenvironment based on molecular features and immunogenicity enabled personalized therapeutic strategies (142). Understanding the specific immune subclass of a liver tumor allows for selecting patients more likely to respond to immunotherapies, as well as developing targeted therapies (143). For instance, patients with inflamed tumors might have a higher responding rate to Immunotherapies due to the presence of active immune cells in the tumor (144). Tumors in the TAM subclass might benefit from therapies targeting TAMs or the extracellular matrix to reverse immunosuppression and enhance immune activity against the tumor (145). Moreover, the identification of Immunity subclasses can serve as predictive biomarkers for patient prognosis. Patients with the Immunity_H subtype, characterized by higher stromal and immune scores, have a better survival rate, indicating that these patients might respond better to immunotherapies (137, 146). This information is crucial for clinical decision-making and modifying treatment approaches based on individual tumor features (99, 147). By identifying the specific mechanisms of immune resistance in different liver cancer subclasses, therapies can be tailored to counteract these mechanisms (148). For instance, if a tumor employs specific checkpoint pathways to evade immune surveillance, checkpoint inhibitors targeting those pathways can be used (149).

Strategies based on the immune classification enables a more precise and personalized approach to liver cancer treatment (150). By understanding the molecular and immunological landscape of individual tumors, treatments can be tailored to target specific pathways and immune cells involved in tumor progression, leading to more effective and less toxic treatment options (151).

5 Conclusion and future directions

Recent advances in liver cancer immunotherapy, particularly in HCC, have highlighted several key findings, including the efficacy of novel ICIs, the potential of combination therapies, and the importance of personalized approaches based on biomarkers (152). These developments suggest a future where liver cancer treatments are more tailored and effective (153). The focus is shifting toward understanding the liver's unique immune environment and developing therapies to overcome its inherent challenges (Figure 3). The future outlook for liver cancer immunotherapy is promising, with ongoing research aimed at improving response rates and patient outcomes through more targeted, personalized treatment. Future research in immunotherapy for liver cancer should focus on combination therapies that merge different immunotherapeutic strategies or pair them with traditional treatments to overcome the immunosuppressive tumor microenvironment. Personalized immunotherapies based on genomic profiling, alongside the development of predictive biomarkers, could tailor treatments to individual patient profiles for improved efficacy. Targeting regulatory T cells, exploring new immunotherapeutic targets, and enhancing T cell responsiveness within the suppressive liver environment are promising directions. Studies should also address inherent or acquired resistance mechanisms to optimize therapeutic outcomes. Innovative clinical trial designs that incorporate dynamic endpoints and real-time biomarker analysis can expedite the advancement of effective treatments. An integrative approach combining genomic, proteomic, and clinical data might offer a comprehensive understanding of disease mechanisms and therapy interactions, paving the way for breakthroughs in liver cancer immunotherapy.

Author contributions

YL: Investigation, Writing – original draft. HY: Data curation, Investigation, Writing – original draft. TL: Methodology, Supervision, Writing – review & editing. NZ: Conceptualization, Data curation, Formal analysis, Funding acquisition, Investigation, Methodology, Project administration, Resources, Software, Supervision, Validation, Visualization, Writing – review & editing.

Funding

The author(s) declare that no financial support was received for the research, authorship, and/or publication of this article.

Conflict of interest

The authors declare that the research was conducted in the absence of any commercial or financial relationships that could be construed as a potential conflict of interest.

Publisher's note

References

1. Tang Z, Dong H, Li T, Wang N, Wei X, Wu H, et al. The synergistic reducing drug resistance effect of cisplatin and ursolic acid on osteosarcoma through a multistep mechanism involving ferritinophagy. *Oxid Med Cell Longev 2021*. (2021), 5192271. doi: 10.1155/2021/5192271

2. Hu W, Yang Y, Fan C, Ma Z, Deng C, Li T, et al. Clinical and pathological significance of N-Myc downstream-regulated gene 2 (NDRG2) in diverse human cancers. *Apoptosis*. (2016) 21:675–82. doi: 10.1007/s10495-016-1244-3

3. Hu C, Cao Y, Li P, Tang X, Yang M, Gu S, et al. Oleanolic acid induces autophagy and apoptosis via the AMPK-mTOR signaling pathway in colon cancer. *J Oncol*. (2021) 2021:8281718. doi: 10.1155/2021/8281718

4. Siegel RL, Giaquinto AN, Jemal A. Cancer statistics, 2024. *CA Cancer J Clin*. (2024) 74:12–49. doi: 10.3322/caac.21820

5. Zongyi Y, Xiaowu L. Immunotherapy for hepatocellular carcinoma. *Cancer Lett*. (2020) 470:8–17. doi: 10.1016/j.canlet.2019.12.002

6. Wang J, Peng Y, Jing S, Han L, Li T, Luo J. A deep-learning approach for segmentation of liver tumors in magnetic resonance imaging using UNet+. *BMC Cancer*. (2023) 23:1060. doi: 10.1186/s12885-023-11432-x

7. Fu XT, Qie JB, Chen JF, Gao Z, Li XG, Feng SR, et al. Inhibition of SIRT1 relieves hepatocarcinogenesis via alleviating autophagy and inflammation. *Int J Biol Macromol*. (2024) 278(Pt 1):134120. doi: 10.1016/j.ijbiomac.2024.134120

8. Qu X, Zhang L, Li S, Li T, Zhao X, Wang N, et al. m(6)A-related angiogenic genes to construct prognostic signature, reveal immune and oxidative stress landscape, and screen drugs in hepatocellular carcinoma. *Oxid Med Cell Longev*. (2022) 2022:8301888. doi: 10.1155/2022/8301888

9. Luo J, Huang Z, Wang M, Li T, Huang J. Prognostic role of multiparameter MRI and radiomics in progression of advanced unresectable hepatocellular carcinoma following combined transcatheter arterial chemoembolization and lenvatinib therapy. *BMC Gastroenterol*. (2022) 22:108. doi: 10.1186/s12876-022-02129-9

10. Rashid T, Bennett JE, Muller DC, Cross AJ, Pearson-Stuttard J, Asaria P, et al. Mortality from leading cancers in districts of England from 2002 to 2019: a population-based, spatiotemporal study. *Lancet Oncol*. (2024) 25:86–98. doi: 10.1016/S1470-2045(23)00530-2

11. Maki H, Hasegawa K. Advances in the surgical treatment of liver cancer. *Biosci Trends*. (2022) 16:178–88. doi: 10.5582/bst.2022.01245

12. Llovet JM, Kelley RK, Villanueva A, Singal AG, Pikarsky E, Roayaie S, et al. Hepatocellular carcinoma. *Nat Rev Dis Primers*. (2021) 7:6. doi: 10.1038/s41572-020-00240-3

13. Li T, Qiao T. Unraveling tumor microenvironment of small-cell lung cancer: Implications for immunotherapy. *Semin Cancer Biol*. (2022) 86:117–25. doi: 10.1016/j.semcancer.2022.09.005

14. Guo W, Qiao T, Dong B, Li T, Liu Q, Xu X. The effect of hypoxia-induced exosomes on anti-tumor immunity and its implication for immunotherapy. *Front Immunol*. (2022) 13:915985. doi: 10.3389/fimmu.2022.915985

15. Zeng L, Liang L, Fang X, Xiang S, Dai C, Zheng T, et al. Glycolysis induces Th2 cell infiltration and significantly affects prognosis and immunotherapy response to lung adenocarcinoma. *Funct Integr Genomics*. (2023) 23:221. doi: 10.1007/s10142-023-01155-4

16. Guo W, Qiao T, Li T. The role of stem cells in small-cell lung cancer: evidence from chemoresistance to immunotherapy. *Semin Cancer Biol*. (2022) 87:160–9. doi: 10.1016/j.semcancer.2022.11.006

17. Oliveira G, Wu CJ. Dynamics and specificities of T cells in cancer immunotherapy. *Nat Rev Cancer*. (2023) 23:295–316. doi: 10.1038/s41568-023-00560-y

18. Yi M, Li T, Niu M, Mei Q, Zhao B, Chu Q, et al. Exploiting innate immunity for cancer immunotherapy. *Mol Cancer*. (2023) 22:187. doi: 10.1186/s12943-023-01885-w

19. Heymann F, Tacke F. Immunology in the liver–from homeostasis to disease. *Nat Rev Gastroenterol Hepatol*. (2016) 13:88–110. doi: 10.1038/nrgastro.2015.200

20. Gottwick C, Carambia A, Herkel J. Harnessing the liver to induce antigen-specific immune tolerance. *Semin Immunopathol*. (2022) 44:475–84. doi: 10.1007/s00281-022-00942-8

21. Zou Y, Ye F, Kong Y, Hu X, Deng X, Xie J, et al. The single-cell landscape of intratumoral heterogeneity and the immunosuppressive microenvironment in liver and brain metastases of breast cancer. *Adv Sci (Weinh)*. (2023) 10:e2203699. doi: 10.1002/advs.202203699

22. Rizvi S, Gores GJ. Pathogenesis, diagnosis, and management of cholangiocarcinoma. *Gastroenterology*. (2013) 145:1215–29. doi: 10.1053/j.gastro.2013.10.013

23. Prieto J, Melero I, Sangro B. Immunological landscape and immunotherapy of hepatocellular carcinoma. *Nat Rev Gastroenterol Hepatol*. (2015) 12:681–700. doi: 10.1038/nrgastro.2015.173

24. Kim E, Viatour P. Hepatocellular carcinoma: old friends and new tricks. *Exp Mol Med*. (2020) 52:1898–907. doi: 10.1038/s12276-020-00527-1

25. Yahoo N, Dudek M, Knolle P, Heikenwälder M. Role of immune responses in the development of NAFLD-associated liver cancer and prospects for therapeutic modulation. *J Hepatol*. (2023) 79:538–51. doi: 10.1016/j.jhep.2023.02.033

26. Foerster F, Gairing SJ, Ilyas SI, Galle PR. Emerging immunotherapy for HCC: A guide for hepatologists. *Hepatology*. (2022) 75:1604–26. doi: 10.1002/hep.32447

27. Geh D, Leslie J, Rumney R, Reeves HL, Bird TG, Mann DA. Neutrophils as potential therapeutic targets in hepatocellular carcinoma. *Nat Rev Gastroenterol Hepatol*. (2022) 19:257–73. doi: 10.1038/s41575-021-00568-5

28. Giovannetti E, Li T. Extracellular vesicles in cancer: Shaping the intricate network of metabolic reprogramming and immune interactions in the tumor microenvironment. *Cytokine Growth Factor Rev*. (2023) 73:1–2. doi: 10.1016/j.cytogfr.2023.09.001

29. Zhang X, Yu S, Li X, Wen X, Liu S, Zu R, et al. Research progress on the interaction between oxidative stress and platelets: Another avenue for cancer? *Pharmacol Res*. (2023) 191:106777. doi: 10.1016/j.phrs.2023.106777

30. Bao G, Li T, Guan X, Yao Y, Liang J, Xiang Y, et al. Development of a prognostic alternative splicing signature associated with tumor microenvironment immune profiles in lung adenocarcinoma. *Front Oncol*. (2022) 12:880478. doi: 10.3389/fonc.2022.880478

31. Wu G, Ma Z, Cheng Y, Hu W, Deng C, Jiang S, et al. Targeting Gas6/TAM in cancer cells and tumor microenvironment. *Mol Cancer*. (2018) 17:20. doi: 10.1186/s12943-018-0769-1

32. Mellman I, Chen DS, Powles T, Turley SJ. The cancer-immunity cycle: Indication, genotype, and immunotype. *Immunity*. (2023) 56:2188–205. doi: 10.1016/j.immuni.2023.09.011

33. Bader JE, Voss K, Rathmell JC. Targeting metabolism to improve the tumor microenvironment for cancer immunotherapy. *Mol Cell*. (2020) 78:1019–33. doi: 10.1016/j.molcel.2020.05.034

34. Zhang W, He H, Zang M, Wu Q, Zhao H, Lu LL, et al. Genetic features of aflatoxin-associated hepatocellular carcinoma. *Gastroenterology*. (2017) 153:249–262.e2. doi: 10.1053/j.gastro.2017.03.024

35. Sharma A, Seow JJW, Dutertre CA, Pai R, Blériot C, Mishra A, et al. Onco-fetal reprogramming of endothelial cells drives immunosuppressive macrophages in hepatocellular carcinoma. *Cell*. (2020) 183:377–394.e21. doi: 10.1016/j.cell.2020.08.040

36. Pfister D, Núñez NG, Pinyol R, Govaere O, Pinter M, Szydlowska M, et al. NASH limits anti-tumour surveillance in immunotherapy-treated HCC. *Nature*. (2021) 592:450–6. doi: 10.1038/s41586-021-03362-0

37. Wu YQ, Zhang CS, Xiong J, Cai DQ, Wang CZ, Wang Y, et al. Low glucose metabolite 3-phosphoglycerate switches PHGDH from serine synthesis to p53 activation to control cell fate. *Cell Res*. (2023) 33:835–50. doi: 10.1038/s41422-023-00874-4

38. He J, Xiong X, Yang H, Li D, Liu X, Li S, et al. Defined tumor antigen-specific T cells potentiate personalized TCR-T cell therapy and prediction of immunotherapy response. *Cell Res*. (2022) 32:530–42. doi: 10.1038/s41422-022-00627-9

39. Pang BY, Leng Y, Wang X, Wang YQ, Jiang LH. A meta-analysis and of clinical values of 11 blood biomarkers, such as AFP, DCP, and GP73 for diagnosis of

hepatocellular carcinoma. *Ann Med*. (2023) 55:42–61. doi: 10.1080/07853890.2022.2153163

40. Grosjean I, Roméo B, Domdom MA, Belaid A, D'Andréa G, Guillot N, et al. Autophagopathies: from autophagy gene polymorphisms to precision medicine for human diseases. *Autophagy*. (2022) 18:2519–36. doi: 10.1080/15548627.2022.2039994

41. Gao Q, Zhu H, Dong L, Shi W, Chen R, Song Z, et al. Integrated proteogenomic characterization of HBV-related hepatocellular carcinoma. *Cell*. (2019) 179:561–577.e22. doi: 10.1016/j.cell.2019.08.052

42. Llovet JM, Zucman-Rossi J, Pikarsky E, Sangro B, Schwartz M, Sherman M, et al. Hepatocellular carcinoma. *Nat Rev Dis Primers*. (2016) 2:16018. doi: 10.1038/nrdp.2016.18

43. Dong S, Guo X, Han F, He Z, Wang Y. Emerging role of natural products in cancer immunotherapy. *Acta Pharm Sin B*. (2022) 12:1163–85. doi: 10.1016/j.apsb.2021.08.020

44. Shiraki K, Yamanaka T, Inoue H, Kawakita T, Enokimura N, Okano H, et al. Expression of TNF-related apoptosis-inducing ligand in human hepatocellular carcinoma. *Int J Oncol*. (2005) 26:1273–81. doi: 10.3892/ijo

45. Cheng AL, Hsu C, Chan SL, Choo SP, Kudo M. Challenges of combination therapy with immune checkpoint inhibitors for hepatocellular carcinoma. *J Hepatol*. (2020) 72:307–19. doi: 10.1016/j.jhep.2019.09.025

46. Pinter M, Jain RK, Duda DG. The current landscape of immune checkpoint blockade in hepatocellular carcinoma: A review. *JAMA Oncol*. (2021) 7:113–23. doi: 10.1001/jamaoncol.2020.3381

47. Sun Y, Wu P, Zhang Z, Wang Z, Zhou K, Song M, et al. Integrated multi-omics profiling to dissect the spatiotemporal evolution of metastatic hepatocellular carcinoma. *Cancer Cell*. (2024) 42:135–156.e17. doi: 10.1016/j.ccell.2023.11.010

48. Ringelhan M, Pfister D, O'Connor T, Pikarsky E, Heikenwalder M. The immunology of hepatocellular carcinoma. *Nat Immunol*. (2018) 19:222–32. doi: 10.1038/s41590-018-0044-z

49. Oura K, Morishita A, Tani J, Masaki T. Tumor immune microenvironment and immunosuppressive therapy in hepatocellular carcinoma: A review. *Int J Mol Sci*. (2021) 22. doi: 10.3390/ijms22115801

50. Zheng C, Zheng L, Yoo JK, Guo H, Zhang Y, Guo X, et al. Landscape of infiltrating T cells in liver cancer revealed by single-cell sequencing. *Cell*. (2017) 169:1342–1356.e16. doi: 10.1016/j.cell.2017.05.035

51. Lu C, Rong D, Zhang B, Zheng W, Wang X, Chen Z, et al. Current perspectives on the immunosuppressive tumor microenvironment in hepatocellular carcinoma: challenges and opportunities. *Mol Cancer*. (2019) 18:130. doi: 10.1186/s12943-019-1047-6

52. Santagata S, Rea G, Castaldo D, Napolitano M, Capiluongo A, D'Alterio C, et al. Hepatocellular carcinoma (HCC) tumor microenvironment is more suppressive than colorectal cancer liver metastasis (CRLM) tumor microenvironment. *Hepatol Int*. (2024) 18:568–81. doi: 10.1007/s12072-023-10537-6

53. Lee JC, Mehdizadeh S, Smith J, Young A, Mufazalov IA, Mowery CT, et al. Regulatory T cell control of systemic immunity and immunotherapy response in liver metastasis. *Sci Immunol*. (2020) 5. doi: 10.1126/sciimmunol.aba0759

54. Riaz F, Wei P, Pan F. Fine-tuning of regulatory T cells is indispensable for the metabolic steatosis-related hepatocellular carcinoma: A review. *Front Cell Dev Biol*. (2022) 10:949603. doi: 10.3389/fcell.2022.949603

55. Liu W, Zhou X, Yao Q, Chen C, Zhang Q, Ding K, et al. In situ expansion and reprogramming of Kupffer cells elicit potent tumoricidal immunity against liver metastasis. *J Clin Invest*. (2023) 133. doi: 10.1172/JCI157937

56. Tacke F. Targeting hepatic macrophages to treat liver diseases. *J Hepatol*. (2017) 66:1300–12. doi: 10.1016/j.jhep.2017.02.026

57. Sun Y, Wu L, Zhong Y, Zhou K, Hou Y, Wang Z, et al. Single-cell landscape of the ecosystem in early-relapse hepatocellular carcinoma. *Cell*. (2021) 184:404–421.e16. doi: 10.1016/j.cell.2020.11.041

58. Zhang S, Saha B, Kodys K, Szabo G. IFN-γ production by human natural killer cells in response to HCV-infected hepatoma cells is dependent on accessory cells. *J Hepatol*. (2013) 59:442–9. doi: 10.1016/j.jhep.2013.04.022

59. Bissell DM. Chronic liver injury, TGF-beta, and cancer. *Exp Mol Med*. (2001) 33:179–90. doi: 10.1038/emm.2001.31

60. Shiri AM, Zhang T, Bedke T, Zazara DE, Zhao L, Lücke J, et al. IL-10 dampens antitumor immunity and promotes liver metastasis via PD-L1 induction. *J Hepatol*. (2024) 80:634–44. doi: 10.1016/j.jhep.2023.12.015

61. Cogliati B, Yashaswini CN, Wang S, Sia D, Friedman SL. Friend or foe? The elusive role of hepatic stellate cells in liver cancer. *Nat Rev Gastroenterol Hepatol*. (2023) 20:647–61. doi: 10.1038/s41575-023-00821-z

62. Vandierendonck A, Degroote H, Vanderborght B, Verhelst X, Geerts A, Devisscher L, et al. NOX1 inhibition attenuates the development of a pro-tumorigenic environment in experimental hepatocellular carcinoma. *J Exp Clin Cancer Res*. (2021) 40:40. doi: 10.1186/s13046-021-01837-6

63. Umemura A, Park EJ, Taniguchi K, Lee JH, Shalapour S, Valasek MA, et al. Liver damage, inflammation, and enhanced tumorigenesis after persistent mTORC1 inhibition. *Cell Metab*. (2014) 20:133–44. doi: 10.1016/j.cmet.2014.05.001

64. Ji G, Ma L, Yao H, Ma S, Si X, Wang Y, et al. Precise delivery of obeticholic acid via nanoapproach for triggering natural killer T cell-mediated liver cancer immunotherapy. *Acta Pharm Sin B*. (2020) 10:2171–82. doi: 10.1016/j.apsb.2020.09.004

65. Zhou C, Weng J, Liu C, Liu S, Hu Z, Xie X, et al. Disruption of SLFN11 deficiency-induced CCL2 signaling and macrophage M2 polarization potentiates anti-PD-1 therapy efficacy in hepatocellular carcinoma. *Gastroenterology*. (2023) 164:1261–78. doi: 10.1053/j.gastro.2023.02.005

66. Sun H, Sun C, Xiao W, Sun R. Tissue-resident lymphocytes: from adaptive to innate immunity. *Cell Mol Immunol*. (2019) 16:205–15. doi: 10.1038/s41423-018-0192-y

67. Casari M, Siegl D, Deppermann C, Schuppan D. Macrophages and platelets in liver fibrosis and hepatocellular carcinoma. *Front Immunol*. (2023) 14:1277808. doi: 10.3389/fimmu.2023.1277808

68. Scheiner B, Pinato DJ. Tumor-infiltrating neutrophils: gatekeepers in liver cancer immune control. *Gastroenterology*. (2023) 164:1338–9. doi: 10.1053/j.gastro.2023.01.025

69. Ji D, Song C, Li Y, Xia J, Wu Y, Jia J, et al. Combination of radiotherapy and suppression of Tregs enhances abscopal antitumor effect and inhibits metastasis in rectal cancer. *J Immunother Cancer*. (2020) 8. doi: 10.1136/jitc-2020-000826

70. Lee TK, Guan XY, Ma S. Cancer stem cells in hepatocellular carcinoma - from origin to clinical implications. *Nat Rev Gastroenterol Hepatol*. (2022) 19:26–44. doi: 10.1038/s41575-021-00508-3

71. Seitz HK, Bataller R, Cortez-Pinto H, Gao B, Gual A, Lackner C, et al. Alcoholic liver disease. *Nat Rev Dis Primers*. (2018) 4:16. doi: 10.1038/s41572-018-0014-7

72. Cai Z, Su X, Qiu L, Li Z, Li X, Dong X, et al. Personalized neoantigen vaccine prevents postoperative recurrence in hepatocellular carcinoma patients with vascular invasion. *Mol Cancer*. (2021) 20:164. doi: 10.1186/s12943-021-01467-8

73. Zhu Y, Yang J, Xu D, Gao XM, Zhang Z, Hsu JL, et al. Disruption of tumour-associated macrophage trafficking by the osteopontin-induced colony-stimulating factor-1 signalling sensitises hepatocellular carcinoma to anti-PD-L1 blockade. *Gut*. (2019) 68:1653–66. doi: 10.1136/gutjnl-2019-318419

74. Finkin S, Yuan D, Stein I, Taniguchi K, Weber A, Unger K, et al. Ectopic lymphoid structures function as microniches for tumor progenitor cells in hepatocellular carcinoma. *Nat Immunol*. (2015) 16:1235–44. doi: 10.1038/ni.3290

75. Craig AJ, von Felden J, Garcia-Lezana T, Sarcognato S, Villanueva A. Tumour evolution in hepatocellular carcinoma. *Nat Rev Gastroenterol Hepatol*. (2020) 17:139–52. doi: 10.1038/s41575-019-0229-4

76. Yang XM, Wang XQ, Hu LP, Feng MX, Zhou YQ, Li DX, et al. Nucleolar HEAT repeat containing 1 up-regulated by the mechanistic target of rapamycin complex 1 signaling promotes hepatocellular carcinoma growth by dominating ribosome biogenesis and proteome homeostasis. *Gastroenterology*. (2023) 165:629–46. doi: 10.1053/j.gastro.2023.05.029

77. Comprehensive and integrative genomic characterization of hepatocellular carcinoma. *Cell*. (2017) 169:1327–1341.e23. doi: 10.1016/j.cell.2017.05.046

78. Hussain SP, Schwank J, Staib F, Wang XW, Harris CC. TP53 mutations and hepatocellular carcinoma: insights into the etiology and pathogenesis of liver cancer. *Oncogene*. (2007) 26:2166–76. doi: 10.1038/sj.onc.1210279

79. Calderaro J, Ziol M, Paradis V, Zucman-Rossi J. Molecular and histological correlations in liver cancer. *J Hepatol*. (2019) 71:616–30. doi: 10.1016/j.jhep.2019.06.001

80. Losic B, Craig AJ, Villacorta-Martin C, Martins-Filho SN, Akers N, Chen X, et al. Intratumoral heterogeneity and clonal evolution in liver cancer. *Nat Commun*. (2020) 11:291. doi: 10.1038/s41467-019-14050-z

81. Greten TF, Villanueva A, Korangy F, Ruf B, Yarchoan M, Ma L, et al. Biomarkers for immunotherapy of hepatocellular carcinoma. *Nat Rev Clin Oncol*. (2023) 20:780–98. doi: 10.1038/s41571-023-00816-4

82. Dong LQ, Peng LH, Ma LJ, Liu DB, Zhang S, Luo SZ, et al. Heterogeneous immunogenomic features and distinct escape mechanisms in multifocal hepatocellular carcinoma. *J Hepatol*. (2020) 72:896–908. doi: 10.1016/j.jhep.2019.12.014

83. Kang YK, Chen LT, Ryu MH, Oh DY, Oh SC, Chung HC, et al. Nivolumab plus chemotherapy versus placebo plus chemotherapy in patients with HER2-negative, untreated, unresectable advanced or recurrent gastric or gastro-oesophageal junction cancer (ATTRACTION-4): a randomised, multicentre, double-blind, placebo-controlled, phase 3 trial. *Lancet Oncol*. (2022) 23:234–47. doi: 10.1016/S1470-2045(21)00692-6

84. Abdu S, Juaid N, Amin A, Moulay M, Miled N. Therapeutic effects of crocin alone or in combination with sorafenib against hepatocellular carcinoma: *in vivo* & *In vitro* insights. *Antioxidants (Basel)*. (2022) 11. doi: 10.3390/antiox11091645

85. Llovet JM, Castet F, Heikenwalder M, Maini MK, Mazzaferro V, Pinato DJ, et al. Immunotherapies for hepatocellular carcinoma. *Nat Rev Clin Oncol*. (2022) 19:151–72. doi: 10.1038/s41571-021-00573-2

86. Janjigian YY, Kawazoe A, Bai Y, Xu J, Lonardi S, Metges JP, et al. Pembrolizumab plus trastuzumab and chemotherapy for HER2-positive gastric or gastro-oesophageal junction adenocarcinoma: interim analyses from the phase 3 KEYNOTE-811 randomised placebo-controlled trial. *Lancet*. (2023) 402:2197–208. doi: 10.1016/S0140-6736(23)02033-0

87. Llovet JM, De Baere T, Kulik L, Haber PK, Greten TF, Meyer T, et al. Locoregional therapies in the era of molecular and immune treatments for hepatocellular carcinoma. *Nat Rev Gastroenterol Hepatol*. (2021) 18:293–313. doi: 10.1038/s41575-020-00395-0

88. Sangro B, Sarobe P, Hervás-Stubbs S, Melero I. Advances in immunotherapy for hepatocellular carcinoma. *Nat Rev Gastroenterol Hepatol*. (2021) 18:525–43. doi: 10.1038/s41575-021-00438-0

89. Zhu AX, Abbas AR, de Galarreta MR, Guan Y, Lu S, Koeppen H, et al. Molecular correlates of clinical response and resistance to atezolizumab in combination with bevacizumab in advanced hepatocellular carcinoma. *Nat Med*. (2022) 28:1599–611. doi: 10.1038/s41591-022-01868-2

90. Hong TS, Wo JY, Yeap BY, Ben-Josef E, McDonnell EI, Blaszkowsky LS, et al. Multi-institutional phase II study of high-dose hypofractionated proton beam therapy in patients with localized, unresectable hepatocellular carcinoma and intrahepatic cholangiocarcinoma. *J Clin Oncol*. (2016) 34:460–8. doi: 10.1200/JCO.2015.64.2710

91. Gordan JD, Kennedy EB, Abou-Alfa GK, Beg MS, Brower ST, Gade TP, et al. Systemic therapy for advanced hepatocellular carcinoma: ASCO guideline. *J Clin Oncol*. (2020) 38:4317–45. doi: 10.1200/JCO.20.02672

92. El Zarif T, Nassar AH, Adib E, Fitzgerald BG, Huang J, Mouhieddine TH, et al. Safety and activity of immune checkpoint inhibitors in people living with HIV and cancer: A real-world report from the cancer therapy using checkpoint inhibitors in people living with HIV-international (CATCH-IT) consortium. *J Clin Oncol*. (2023) 41:3712–23. doi: 10.1200/JCO.22.02459

93. Meyers BM, Knox JJ, Liu DM, McLeod D, Ramjeesingh R, Tam VC, et al. The evolution of immune checkpoint inhibitor combinations in advanced hepatocellular carcinoma - A systematic review. *Cancer Treat Rev*. (2023) 118:102584. doi: 10.1016/j.ctrv.2023.102584

94. Dal Bo M, De Mattia E, Baboci L, Mezzalira S, Cecchin E, Assaraf YG, et al. New insights into the pharmacological, immunological, and CAR-T-cell approaches in the treatment of hepatocellular carcinoma. *Drug Resist Update*. (2020) 51:100702. doi: 10.1016/j.drup.2020.100702

95. Fu Q, Zheng Y, Fang W, Zhao Q, Zhao P, Liu L, et al. RUNX-3-expressing CAR T cells targeting glypican-3 in patients with heavily pretreated advanced hepatocellular carcinoma: a phase I trial. *EClinicalMedicine*. (2023) 63:102175. doi: 10.1016/j.eclinm.2023.102175

96. Rimassa L, Pressiani T, Merle P. Systemic treatment options in hepatocellular carcinoma. *Liver Cancer*. (2019) 8:427–46. doi: 10.1159/000499765

97. Sun L, Gao F, Gao Z, Ao L, Li N, Ma S, et al. Shed antigen-induced blocking effect on CAR-T cells targeting Glypican-3 in Hepatocellular Carcinoma. *J Immunother Cancer*. (2021) 9. doi: 10.1136/jitc-2020-001875

98. Yu M, Luo H, Fan M, Wu X, Shi B, Di S, et al. Development of GPC3-specific chimeric antigen receptor-engineered natural killer cells for the treatment of hepatocellular carcinoma. *Mol Ther*. (2018) 26:366–78. doi: 10.1016/j.ymthe.2017.12.012

99. Global prevalence, cascade of care, and prophylaxis coverage of hepatitis B in 2022: a modelling study. *Lancet Gastroenterol Hepatol*. (2023) 8:879–907. doi: 10.1016/S2468-1253(23)00197-8

100. Park R, Eshrat F, Al-Jumayli M, Saeed A, Saeed A. Immuno-oncotherapeutic approaches in advanced hepatocellular carcinoma. *Vaccines (Basel)*. (2020) 8. doi: 10.3390/vaccines8030447

101. Ilyas FZ, Beane JD, Pawlik TM. The state of immunotherapy in hepatobiliary cancers. *Cells*. (2021) 10. doi: 10.3390/cells10082096

102. Bauer J, Köhler N, Maringer Y, Bucher P, Bilich T, Zwick M, et al. The oncogenic fusion protein DNAJB1-PRKACA can be specifically targeted by peptide-based immunotherapy in fibrolamellar hepatocellular carcinoma. *Nat Commun*. (2022) 13:6401. doi: 10.1038/s41467-022-33746-3

103. Zuo B, Zhang Y, Zhao K, Wu L, Qi H, Yang R, et al. Universal immunotherapeutic strategy for hepatocellular carcinoma with exosome vaccines that engage adaptive and innate immune responses. *J Hematol Oncol*. (2022) 15:46. doi: 10.1186/s13045-022-01266-8

104. Yau T, Park JW, Finn RS, Cheng AL, Mathurin P, Edeline J, et al. Nivolumab versus sorafenib in advanced hepatocellular carcinoma (CheckMate 459): a randomised, multicentre, open-label, phase 3 trial. *Lancet Oncol*. (2022) 23:77–90. doi: 10.1016/S1470-2045(21)00604-5

105. El-Khoueiry AB, Sangro B, Yau T, Crocenzi TS, Kudo M, Hsu C, et al. Nivolumab in patients with advanced hepatocellular carcinoma (CheckMate 040): an open-label, non-comparative, phase 1/2 dose escalation and expansion trial. *Lancet*. (2017) 389:2492–502. doi: 10.1016/S0140-6736(17)31046-2

106. Zhu AX, Finn RS, Edeline J, Cattan S, Ogasawara S, Palmer D, et al. Pembrolizumab in patients with advanced hepatocellular carcinoma previously treated with sorafenib (KEYNOTE-224): a non-randomised, open-label phase 2 trial. *Lancet Oncol*. (2018) 19:940–52. doi: 10.1016/S1470-2045(18)30351-6

107. Finn RS, Ryoo BY, Merle P, Kudo M, Bouattour M, Lim HY, et al. Pembrolizumab as second-line therapy in patients with advanced hepatocellular carcinoma in KEYNOTE-240: A randomized, double-blind, phase III trial. *J Clin Oncol*. (2020) 38:193–202. doi: 10.1200/JCO.19.01307

108. Merle P, Kudo M, Edeline J, Bouattour M, Cheng AL, Chan SL, et al. Pembrolizumab as second-line therapy for advanced hepatocellular carcinoma: longer term follow-up from the phase 3 KEYNOTE-240 trial. *Liver Cancer*. (2023) 12:309–20. doi: 10.1159/000529636

109. Finn RS, Qin S, Ikeda M, Galle PR, Ducreux M, Kim TY, et al. Atezolizumab plus bevacizumab in unresectable hepatocellular carcinoma. *N Engl J Med*. (2020) 382:1894–905. doi: 10.1056/NEJMoa1915745

110. Cheng AL, Qin S, Ikeda M, Galle PR, Ducreux M, Kim TY, et al. Updated efficacy and safety data from IMbrave150: Atezolizumab plus bevacizumab vs. sorafenib for unresectable hepatocellular carcinoma. *J Hepatol*. (2022) 76:862–73. doi: 10.1016/j.jhep.2021.11.030

111. Waldman AD, Fritz JM, Lenardo MJ. A guide to cancer immunotherapy: from T cell basic science to clinical practice. *Nat Rev Immunol*. (2020) 20:651–68. doi: 10.1038/s41577-020-0306-5

112. Shah NN, Fry TJ. Mechanisms of resistance to CAR T cell therapy. *Nat Rev Clin Oncol*. (2019) 16:372–85. doi: 10.1038/s41571-019-0184-6

113. Fishbane S, Schiller B, Locatelli F, Covic AC, Provenzano R, Wiecek A, et al. Peginesatide in patients with anemia undergoing hemodialysis. *N Engl J Med*. (2013) 368:307–19. doi: 10.1056/NEJMoa1203165

114. Llovet JM, Kudo M, Merle P, Meyer T, Qin S, Ikeda M, et al. Lenvatinib plus pembrolizumab versus lenvatinib plus placebo for advanced hepatocellular carcinoma (LEAP-002): a randomised, double-blind, phase 3 trial. *Lancet Oncol*. (2023) 24:1399–410. doi: 10.1016/S1470-2045(23)00469-2

115. Lan L, Evan T, Li H, Hussain A, Ruiz EJ, Zaw Thin M, et al. GREM1 is required to maintain cellular heterogeneity in pancreatic cancer. *Nature*. (2022) 607:163–8. doi: 10.1038/s41586-022-04888-7

116. Bharadwaj U, Kasembeli MM, Robinson P, Tweardy DJ. Targeting janus kinases and signal transducer and activator of transcription 3 to treat inflammation, fibrosis, and cancer: rationale, progress, and caution. *Pharmacol Rev*. (2020) 72:486–526. doi: 10.1124/pr.119.018440

117. Finn RS, Kudo M, Borbath I, Edeline J, Cattan S, Vlierberghe HV, et al. Pembrolizumab (pembro) in patients (pts) with sorafenib-treated (cohort 1) and treatment (tx)-naive (cohort 2) advanced hepatocellular carcinoma (aHCC) after additional follow-up in the phase 2 KEYNOTE-224 study. *J Clin Oncol*. (2024) 42:4100–0. doi: 10.1200/JCO.2024.42.16_suppl.4100

118. Chan SL, Sangro B, Kudo M, Erinjeri JP, Qin S, Ren Z, et al. Safety analysis by treatment periods from EMERALD-1: A phase 3, randomized, placebo-controlled study of transarterial chemoembolization with durvalumab with/without bevacizumab in participants with embolization-eligible unresectable hepatocellular carcinoma. *J Clin Oncol*. (2024) 42:4122–2. doi: 10.1200/JCO.2024.42.16_suppl.4122

119. Zhang Q, Fu Q, Cao W, Wang H, Xu X, Huang J, et al. Phase I study of C-CAR031, a GPC3-specific TGFβRIIDN armored autologous CAR-T, in patients with advanced hepatocellular carcinoma (HCC). *J Clin Oncol*. (2024) 42:4019–9. doi: 10.1200/JCO.2024.42.16_suppl.4019

120. Shen Y, Liang X, Jin X, Tan Q, Zhao R, Wei G, et al. Clinical outcomes from a phase I clinical trial of a novel oncolytic virus VG161 in patients with hepatocellular carcinoma (HCC) refractory after 2 prior lines of therapy including checkpoint inhibitors (CPI). *J Clin Oncol*. (2024) 42:4105–5. doi: 10.1200/JCO.2024.42.16_suppl.4105

121. Duan H, Liu Y, Gao Z, Huang W. Recent advances in drug delivery systems for targeting cancer stem cells. *Acta Pharm Sin B*. (2021) 11:55–70. doi: 10.1016/j.apsb.2020.09.016

122. Khemlina G, Ikeda S, Kurzrock R. The biology of Hepatocellular carcinoma: implications for genomic and immune therapies. *Mol Cancer*. (2017) 16:149. doi: 10.1186/s12943-017-0712-x

123. Lee WS, Yang H, Chon HJ, Kim C. Combination of anti-angiogenic therapy and immune checkpoint blockade normalizes vascular-immune crosstalk to potentiate cancer immunity. *Exp Mol Med*. (2020) 52:1475–85. doi: 10.1038/s12276-020-00500-y

124. Song Y, Fu Y, Xie Q, Zhu B, Wang J, Zhang B. Anti-angiogenic agents in combination with immune checkpoint inhibitors: A promising strategy for cancer treatment. *Front Immunol*. (2020) 11:1956. doi: 10.3389/fimmu.2020.01956

125. McDonald PC, Chafe SC, Dedhar S. Overcoming hypoxia-mediated tumor progression: combinatorial approaches targeting pH regulation, angiogenesis and immune dysfunction. *Front Cell Dev Biol*. (2016) 4:27. doi: 10.3389/fcell.2016.00027

126. Xie P, Guo L, Zhang B, Xu Y, Song Q, Shi H, et al. Case report: immunotherapy successfully treated brain metastasis in intrahepatic cholangiocarcinoma and literature review. *Front Oncol*. (2022) 12. doi: 10.3389/fonc.2022.911202

127. Rimassa L, Finn RS, Sangro B. Combination immunotherapy for hepatocellular carcinoma. *J Hepatol*. (2023) 79:506–15. doi: 10.1016/j.jhep.2023.03.003

128. de Castria TB, Khalil DN, Harding JJ, O'Reilly EM, Abou-Alfa GK. Tremelimumab and durvalumab in the treatment of unresectable, advanced hepatocellular carcinoma. *Future Oncol*. (2022) 18:3769–82. doi: 10.2217/fon-2022-0652

129. Takayama T, Hasegawa K, Izumi N, Kudo M, Shimada M, Yamanaka N, et al. Surgery versus radiofrequency ablation for small hepatocellular carcinoma: A randomized controlled trial (SURF trial). *Liver Cancer*. (2022) 11:209–18. doi: 10.1159/000521665

130. Tan J, Fan W, Liu T, Zhu B, Liu Y, Wang S, et al. TREM2(+) macrophages suppress CD8(+) T-cell infiltration after transarterial chemoembolisation in hepatocellular carcinoma. *J Hepatol*. (2023) 79:126–40. doi: 10.1016/j.jhep.2023.02.032

131. Chen S, Huang C, Liao G, Sun H, Xie Y, Liao C, et al. Distinct single-cell immune ecosystems distinguish true and *de novo* HBV-related hepatocellular carcinoma recurrences. *Gut*. (2023) 72:1196–210. doi: 10.1136/gutjnl-2022-328428

132. Llovet JM, Pinyol R, Yarchoan M, Singal AG, Marron TU, Schwartz M, et al. Adjuvant and neoadjuvant immunotherapies in hepatocellular carcinoma. *Nat Rev Clin Oncol*. (2024) 21:294–311. doi: 10.1038/s41571-024-00868-0

133. Lv H, Zong Q, Chen C, Lv G, Xiang W, Xing F, et al. TET2-mediated tumor cGAS triggers endothelial STING activation to regulate vasculature remodeling and anti-tumor immunity in liver cancer. *Nat Commun*. (2024) 15:6. doi: 10.1038/s41467-023-43743-9

134. Lin M, He J, Zhang X, Sun X, Dong W, Zhang R, et al. Targeting fibrinogen-like protein 1 enhances immunotherapy in hepatocellular carcinoma. *J Clin Invest*. (2023) 133. doi: 10.1172/JCI164528

135. Yang X, Yang C, Zhang S, Geng H, Zhu AX, Bernards R, et al. Precision treatment in advanced hepatocellular carcinoma. *Cancer Cell*. (2024) 42:180–97. doi: 10.1016/j.ccell.2024.01.007

136. Donne R, Lujambio A. The liver cancer immune microenvironment: Therapeutic implications for hepatocellular carcinoma. *Hepatology*. (2023) 77:1773–96. doi: 10.1002/hep.32740

137. Ruf B, Bruhns M, Babaei S, Kedei N, Ma L, Revsine M, et al. Tumor-associated macrophages trigger MAIT cell dysfunction at the HCC invasive margin. *Cell*. (2023) 186:3686–3705.e32. doi: 10.1016/j.cell.2023.07.026

138. Liang B, Zhou Y, Qian M, Xu M, Wang J, Zhang Y, et al. TBX3 functions as a tumor suppressor downstream of activated CTNNB1 mutants during hepatocarcinogenesis. *J Hepatol*. (2021) 75:120–31. doi: 10.1016/j.jhep.2021.01.044

139. Tang TWH, Chen HC, Chen CY, Yen CYT, Lin CJ, Prajnamitra RP, et al. Loss of gut microbiota alters immune system composition and cripples postinfarction cardiac repair. *Circulation*. (2019) 139:647–59. doi: 10.1161/CIRCULATIONAHA.118.035235

140. Wang H, Zhang H, Wang Y, Brown ZJ, Xia Y, Huang Z, et al. Regulatory T-cell and neutrophil extracellular trap interaction contributes to carcinogenesis in non-alcoholic steatohepatitis. *J Hepatol*. (2021) 75:1271–83. doi: 10.1016/j.jhep.2021.07.032

141. Tao J, Krutsenko Y, Moghe A, Singh S, Poddar M, Bell A, et al. Nuclear factor erythroid 2-related factor 2 and β-Catenin Coactivation in Hepatocellular Cancer: Biological and Therapeutic Implications. *Hepatology*. (2021) 74:741–59. doi: 10.1002/hep.31730

142. Jia W, Xie G, Jia W. Bile acid-microbiota crosstalk in gastrointestinal inflammation and carcinogenesis. *Nat Rev Gastroenterol Hepatol*. (2018) 15:111–28. doi: 10.1038/nrgastro.2017.119

143. Yang C, Zhang H, Zhang L, Zhu AX, Bernards R, Qin W, et al. Evolving therapeutic landscape of advanced hepatocellular carcinoma. *Nat Rev Gastroenterol Hepatol*. (2023) 20:203–22. doi: 10.1038/s41575-022-00704-9

144. Sia D, Jiao Y, Martinez-Quetglas I, Kuchuk O, Villacorta-Martin C, Castro de Moura M, et al. Identification of an immune-specific class of hepatocellular carcinoma, based on molecular features. *Gastroenterology*. (2017) 153:812–26. doi: 10.1053/j.gastro.2017.06.007

145. Cassetta L, Pollard JW. Targeting macrophages: therapeutic approaches in cancer. *Nat Rev Drug Discov*. (2018) 17:887–904. doi: 10.1038/nrd.2018.169

146. Feng Z, Li H, Liu Q, Duan J, Zhou W, Yu X, et al. CT radiomics to predict macrotrabecular-massive subtype and immune status in hepatocellular carcinoma. *Radiology*. (2023) 307:e221291. doi: 10.1148/radiol.221291

147. Calderaro J, Couchy G, Imbeaud S, Amaddeo G, Letouzé E, Blanc JF, et al. Histological subtypes of hepatocellular carcinoma are related to gene mutations and molecular tumour classification. *J Hepatol*. (2017) 67:727–38. doi: 10.1016/j.jhep.2017.05.014

148. Li H, Li CW, Li X, Ding Q, Guo L, Liu S, et al. MET inhibitors promote liver tumor evasion of the immune response by stabilizing PDL1. *Gastroenterology*. (2019) 156:1849–1861.e13. doi: 10.1053/j.gastro.2019.01.252

149. Rebouissou S, Nault JC. Advances in molecular classification and precision oncology in hepatocellular carcinoma. *J Hepatol*. (2020) 72:215–29. doi: 10.1016/j.jhep.2019.08.017

150. Choi WM, Yip TC, Kim WR, Yee LJ, Brooks-Rooney C, Curteis T, et al. Chronic hepatitis B baseline viral load and on-treatment liver cancer risk: A multinational cohort study of HBeAg-positive patients. *Hepatology*. (2024) 80(2):428–39. doi: 10.1097/HEP.0000000000000884

151. Ho DW, Tsui YM, Chan LK, Sze KM, Zhang X, Cheu JW, et al. Single-cell RNA sequencing shows the immunosuppressive landscape and tumor heterogeneity of HBV-associated hepatocellular carcinoma. *Nat Commun*. (2021) 12:3684. doi: 10.1038/s41467-021-24010-1

152. Kim SC, Kim DW, Cho EJ, Lee JY, Kim J, Kwon C, et al. A circulating cell-free DNA methylation signature for the detection of hepatocellular carcinoma. *Mol Cancer*. (2023) 22:164. doi: 10.1186/s12943-023-01872-1

153. Llovet JM, Montal R, Sia D, Finn RS. Molecular therapies and precision medicine for hepatocellular carcinoma. *Nat Rev Clin Oncol*. (2018) 15:599–616. doi: 10.1038/s41571-018-0073-4

frontiers | Frontiers in Immunology

TYPE Mini Review
PUBLISHED 06 November 2024
DOI 10.3389/fimmu.2024.1489649

OPEN ACCESS

EDITED BY
Yan-Ru Lou,
University of Helsinki, Finland

REVIEWED BY
Chunwang Yuan,
Capital Medical University, China
Li-Yue Sun,
Fudan University, China

*CORRESPONDENCE
Zhonglin Zhang
13730851526@163.com
Shuo Zhang
shuomedicine@126.com

†These authors have contributed equally to this work and share first authorship

RECEIVED 01 September 2024
ACCEPTED 18 October 2024
PUBLISHED 06 November 2024

CITATION
Zhou Y, Wei S, Xu M, Wu X, Dou W, Li H, Zhang Z and Zhang S (2024) CAR-T cell therapy for hepatocellular carcinoma: current trends and challenges.
Front. Immunol. 15:1489649.
doi: 10.3389/fimmu.2024.1489649

CAR-T cell therapy for hepatocellular carcinoma: current trends and challenges

Yexin Zhou[1,2†], Shanshan Wei[3†], Menghui Xu[2†], Xinhui Wu[1], Wenbo Dou[1], Huakang Li[1], Zhonglin Zhang[3*] and Shuo Zhang[3*]

[1]Hospital of Chengdu University of Traditional Chinese Medicine, Chengdu, Sichuan, China, [2]The General Hospital of Western Theater Command, Chengdu, China, [3]Department of Radiation Oncology, Radiation Oncology Key Laboratory of Sichuan Province, Sichuan Clinical Research Center for Cancer, Sichuan Cancer Hospital & Institute, Sichuan Cancer Center, Affiliated Cancer Hospital of University of Electronic Science and Technology of China, Chengdu, Sichuan, China

Hepatocellular carcinoma (HCC) ranks among the most prevalent cancers worldwide, highlighting the urgent need for improved diagnostic and therapeutic methodologies. The standard treatment regimen generally involves surgical intervention followed by systemic therapies; however, the median survival rates for patients remain unsatisfactory. Chimeric antigen receptor (CAR) T-cell therapy has emerged as a pivotal advancement in cancer treatment. Both clinical and preclinical studies emphasize the notable efficacy of CAR T cells in targeting HCC. Various molecules, such as GPC3, c-Met, and NKG2D, show significant promise as potential immunotherapeutic targets in liver cancer. Despite this, employing CAR T cells to treat solid tumors like HCC poses considerable challenges within the discipline. Numerous innovations have significant potential to enhance the efficacy of CAR T-cell therapy for HCC, including improvements in T cell trafficking, strategies to counteract the immunosuppressive tumor microenvironment, and enhanced safety protocols. Ongoing efforts to discover therapeutic targets for CAR T cells highlight the need for the development of more practical manufacturing strategies for CAR-modified cells. This review synthesizes recent findings and clinical advancements in the use of CAR T-cell therapies for HCC treatment. We elucidate the therapeutic benefits of CAR T cells in HCC and identify the primary barriers to their broader application. Our analysis aims to provide a comprehensive overview of the current status and future prospects of CAR T-cell immunotherapy for HCC.

KEYWORDS

chimeric antigen receptor T cell, hepatocellular carcinoma, antigen, gene therapy, immunotherapy

10.3389/fimmu.2024.1489649

1 Introduction

Hepatocellular carcinoma (HCC) poses a significant global health challenge and ranks as the third most common cause of cancer-related mortality worldwide (1). While surgical resection and local ablation continue to serve as the mainstay treatment options for early-stage HCC patients, the utilization of diverse systemic therapies has become indispensable in enhancing prognosis for individuals in intermediate to advanced stages (2, 3). But current therapeutic options are seldom curative and the prognosis of patients with HCC remains grim (2, 3). Therefore, the exploration of innovative and efficient therapeutic strategies holds the utmost importance.

Recently, immunotherapy has opened up the possibility of new scenarios for treating advanced HCC (4). The immune system's access to the liver is tightly regulated, and the liver's immunosuppressive environment has evolved to defend against immune attacks (5, 6). As HCC typically expresses identifiable tumor-associated antigens, such as alpha-fetoprotein (AFP), glypican-3 (GPC3), or cellular-mesenchymal epithelial transition factor (c-MET) (7), there is a strategic opportunity where treatments could potentially stimulate or augment an anti-tumor immune response through vaccination or targeted therapeutic interventions (8, 9). Immune checkpoint inhibitors have been previously successfully employed in clinical settings for the management of HCC (10). On the contrary, chimeric antigen receptor (CAR) T cell therapy has shown significant therapeutic efficacy in patients with hematological malignancies (11, 12); nevertheless, further optimization of the technology is required for the effective and safe therapy of solid tumors including HCC (13, 14). The extensive research efforts by multiple investigators in both preclinical and clinical settings to assess CAR-T therapy against HCC underline a paradigm shift in the treatment (15). This review emphasizes the potential of applying CAR-T cells in HCC therapy, discussing aspects related to their design and delivery, recent therapeutic advancements, encountered challenges, and potential solutions.

2 Basics of CAR-T cell immunotherapy

The fundamental concept behind CAR-T cell immunotherapy is to combine the strength of a T cell with the targeting accuracy of an antibody to recognize specific tumor antigens (11). CAR-T therapy aims to introduce specific CARs into T cells in a relatively short timeframe (15). Expansion of these engineered T cells leads to the generation of memory and effector lymphocytes with high affinity *in vitro* (14, 15). Subsequently, these T cells are reinfused into the patient to undergo robust proliferation (14). The engineered CAR provides specificity, while the intracellular signaling domains trigger T cell-mediated cytotoxicity for eliminating cancer cells regardless of major histocompatibility complex (MHC) presentation (16, 17). CAR-T cells have been referred to as 'living medications' due to their ability to undergo proliferation and differentiation into durable memory cells, therefore inducing specific and enduring anti-tumor immune responses (11, 17) (Figure 1).

When viewed structurally, CARs can be divided into four distinctive components (18). There exists the antigen-binding domain and a linker region in the extracellular part of CARs (18). The antigen-binding domain typically derived from a single-chain

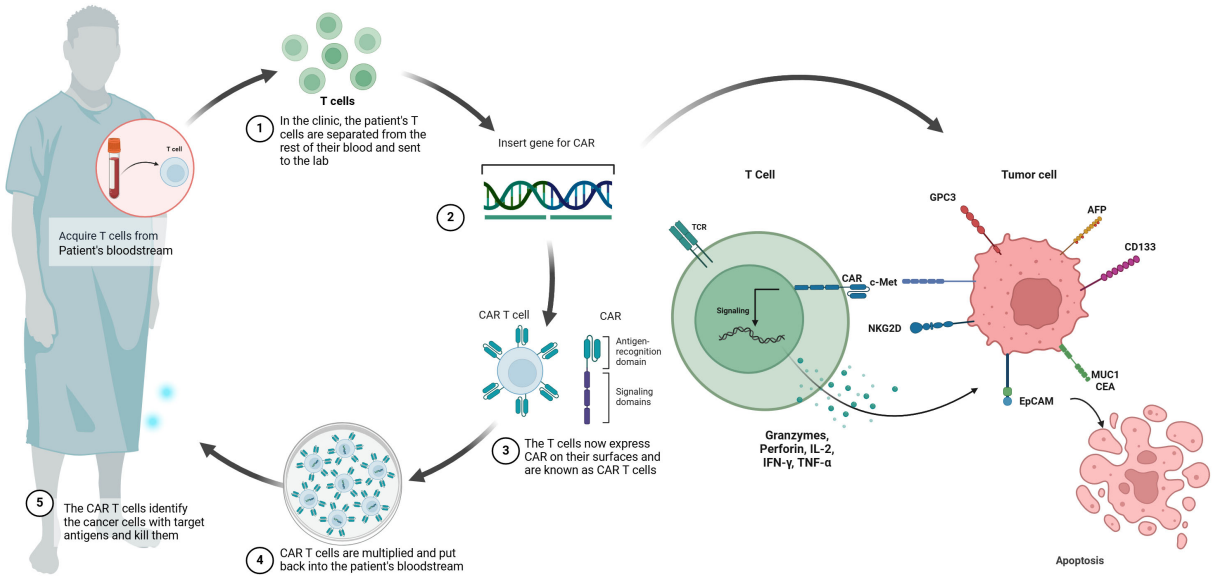

FIGURE 1
Schematic illustration of CAR-T cell therapy in HCC. chimeric antigen receptor (CAR) T cell therapy involves the initial extraction of T cells from the patient's peripheral blood, followed by the introduction of a CAR gene into the T cells using a viral vector. This process results in the production of CAR T cells. After the CAR T cells are multiplied *in vitro*, they undergo a thorough assessment for cellular quality and are then aseptically filled. The final step involves administering the CAR T cells to the patient, where they are able to selectively bind to molecular targets such as GPC3, AFP, NKG2D, CD133, EpCAM, MUC1, CEA and c-MET.

variable fragment (scFv) commonly found in antibodies, allowing the CAR to attach to the target antigen present on the tumor cells (19, 20). Following this section comes a spacer or hinge region, which is subsequently linked to a transmembrane domain (21). Finally, an intracellular domain is present to convey signals to the CAR-modified cells (22, 23).

This intracellular domain can be further categorized into costimulatory domains and signaling domains (24, 25). Specific regions of CD28, 4-1BB, ICOS, or OX40 are commonly utilized as co-stimulatory domains (24–26). The CD28 co-stimulatory receptor on T cells plays a vital role in transmitting essential signals for continuous signaling, cell growth, and preventing immune exhaustion (27). Meanwhile, 4-1BB and OX40 act as co-stimulatory receptors impacting T cell activation, maturation, and apoptosis induction (28, 29). Overall, the integration of these co-stimulatory domains has proven to enhance the effectiveness of CAR-T cells in terms of cytokine secretion, T cell expansion, proliferation, and differentiation (30, 31). CAR-T cell generations are broadly classified based on the arrangement of their intracellular signaling domains (32). The first generation of CAR consists only of the CD3ζ signaling domain, with the addition of extra co-stimulatory signaling domains in the second generation (33, 34). In the third generation, two co-stimulatory domains are combined (35). Moreover, introducing a single co-stimulatory structural domain, in conjunction with another transgene, can be utilized to amplify cytokine production and thereby strengthen the functionality of CAR-T cells in fourth-generation CAR-T cell therapy (36). Contrasting with previous generations, the fifth generation of CAR-T cells includes an additional intracellular domain (37). Full activation of T cells is exclusively attained when both CARs engage simultaneously with their corresponding target antigens expressed on the cells (14, 18). CAR-T cells will not be activated by normal cells expressing only one of the two target antigens, thus evading elimination (38).

Both clinical and preclinical evidence have highlighted the substantial roles each of these regions plays in the overall functionality of CAR-T cells (39). The design of CARs is instrumental in determining the attributes of the associated CAR-T cells, encompassing elements such as antigen specificity, activation capability, cytotoxicity, proliferation potential, expansion capacity, persistence, and safety profile (40, 41). Therefore, it is imperative to select the optimal CAR format tailored to the specific needs of individual applications.

3 Preclinical and clinical evidence of CAR-T cells against HCC

Compared to conventional antitumor pharmaceuticals, CAR-T cell therapy exhibits distinct characteristics (41). This novel therapeutic approach represents a precision-targeted strategy for the management of neoplastic growths (41). An ideal target antigen for CAR-T cell therapy in cancers should display elevated levels of expression on tumor cells while showing either insignificant or minimal expression on normal cells (42). Key target antigens investigated in preclinical studies and clinical trials encompass Mucin 1, GPC3, AFP, NK group 2D ligand (NKG2DL) and c-MET (Table 1).

3.1 GPC3

GPC3 is an embryonic glycoprotein that is tethered to the cellular membrane via a glycophosphatidylinositol anchor, which has been demonstrated upregulated expression in various malignancies, notably HCC (43, 44). Being an oncofetal antigen, GPC3 exhibits high expression in over 70% of HCC cases (43). Emerging evidence has revealed that GPC3 exerts remarkably impacts on HCC progression (43). GPC3's core protein interacts with Frizzled, the Wnt receptor, which results in amplifying Wnt/β-catenin cascade and elevated cell growth in HCC (45, 46). Moreover, GPC3 could be oncogenic activated by zinc-fingers and homeoboxes 2 (ZHX2) and C-myc, therefore promoting cell proliferation and differentiation in the setting of HCC (47, 48). Remarkably, Dargel and co-workers identified an HLA-A2-restricted peptide (GPC3-367) and employed peptide multimers to isolate GPC3-specific T cells; in this research, primary CD8+ T cells expressing the transgenic T-cell receptor recognizing GPC3 with specificity were identified. These T cells exhibited the capability to eradicate GPC3-expressing hepatoma cells *in vitro* and hinder the progression of HCC xenograft tumors in mice (49). Therefore, targeting GPC3 may be a promising strategy against HCC.

Existing evidence has mentioned that GPC3 seems to have a stronger connection with the utilization of CAR T cell therapy (50, 51). GPC3-specific CAR-T cells have demonstrated the capability to eradicate GPC3-positive HCC cells in laboratory settings and GPC3-positive HCC tumor xenografts in murine models (52, 53). The synergistic use of sorafenib in conjunction with GPC3-targeted CAR-T cells has also shown effectiveness (54, 55).

To improve therapeutic effectiveness, Sun et al. engineered GPC3-targeted CAR-T cells that overexpressed glucose transporter type 1 (GLUT1) or acylglycerol kinase (AGK) for the treatment of HCC (56). These engineered CAR-T cells demonstrated targeted and efficient elimination of GPC3-positive tumor cells *in vitro*, showcasing enhanced antitumor efficacy in comparison to the second-generation CAR-T cells (56). Additionally, the upregulation of GLUT1 or AGK conferred protection to the CAR-T cells against apoptosis following repeated encounters with tumor cells (56). In line with this, novel GPC3-CAR-T cells were engineered to express IL-7 and CCL9 for stimulating the proliferation and facilitating migration (44, 57). Significantly, in a phase I clinical trial, these modified CAR-T cells effectively eradicated the tumor upon intra-tumor administration in a patient with advanced GPC3-positive HCC (57). Zhou et al. engineered bispecific CAR-T cells targeting both fibroblast activation protein (FAP) and GPC3 simultaneously to address tumor diversity in HCC (58). The bispecific CAR-T cells displayed increased efficacy against tumor cells *in vitro*. Moreover, these bispecific CAR-T cells exhibited enhanced antitumor activity and significantly prolonged the survival of HCC mouse models, which represent a promising therapeutic approach to mitigate HCC recurrence (58).

TABLE 1 Current targets of CAR-T cell therapy in HCC.

Target	CAR construct	Mechanism	Reference
GPC3	GPC3-367-specific CAR	Eradicated GPC3-expressing HCC cells and hindered the HCC progression	(49)
GPC3	GPC3-specific CAR	Eradicated GPC3-positive HCC cells and sorafenib in conjunction with GPC3-targeted CAR-T cells has also shown effectiveness	(52–55)
GPC3	GPC3-targeted CAR-T cells expressing GLUT1 or AGK	The upregulation of GLUT1 or AGK conferred protection to the CAR-T cells against apoptosis, which significantly eradicated GPC3-expressing HCC cells	(56)
GPC3	IL-7 and CCL19-secreting GPC3-targeted CAR-T cells	GPC3-CAR-T cells were engineered to express IL-7 and CCL9 for stimulating the proliferation and facilitating migration, which effectively eradicated the tumor.	(44, 57)
GPC3	Bispecific CAR-T cells targeting FAP and GPC3	Engineered bispecific CAR-T cells targeting both FAP and GPC3 to address tumor diversity in HCC	(58)
AFP	AFP-targeted CAR	Bound to AFP peptides presented by HLA-A02:01 on tumor cells	(59, 60)
c-Met	Bispecific c-Met/PD-L1 CAR-T Cells	The bispecific CAR-T cells that target both c-Met and PD-L1 and showed notable cytotoxicity against c-Met$^+$PD-L1$^+$ HCC cells	(65)
c-Met	MET-CAR.CD28ζ	Recognized and eliminated HCC cells based on overall MET expression	(66)
NKG2D	NKG2D CAR-T	Recognized NKG2D ligands, triggering immune responses to inhibit tumor	(72)
NKG2D	NKG2D-BBz CAR	Recognized NKG2D ligands, triggering immune responses to inhibit tumor	(73)
CD133	CD133-specific CAR	Targeted delivery of a PD-1-blocking scFv by CD133-specific CAR-T cells that enhanced antitumour efficacy in HCC	(81)
CD133	CoG133-CAR	Dual antigen-binding capabilities targeting CD133 and GPC3 that ignificant eradication of HCC tumors	(82)
EpCAM	EpCAM-specific CAR	Targeted EpCAM for inhibiting tumor growth	(85)
MUC1	MUC1-specific CAR	Targeted MUC1 for inhibiting tumor growth	(89)
CEA	CEA-specific CAR	Targeted CEA for inhibiting tumor growth	(90, 91)

3.2 AFP

AFP, a fetal-specific alpha-globulin produced during fetal development and detected in fetal blood and tissues, is also observable in the HCC tumors (59). In light of the fact that CAR-T cells specifically target tumor surface antigens rather than secreted or intracellular ones, Liu et al. engineered AFP-CAR-T cells capable of selectively binding to the AFP158-166 peptide presented by HLA-A02:01 on the surface of tumor cells *in vivo* (60). AFP-targeted CAR-T cells have demonstrated the capability to significantly inhibit tumor growth both *in vivo* and vitro (60).

3.3 c-Met

c-MET is a pro-oncogene responsible for encoding the receptor for hepatocyte growth factor (HGF) (61, 62). c-MET can trigger various downstream pathways, including the RAS/MAPK and phosphoinositide 3-kinase (PI3K)/AKT pathways, promoting tumor cell proliferation, growth and metastasis in HCC (63, 64). Jiang et al. developed the bispecific CAR-T cells that target both c-Met and programmed cell death ligand (PD-L1) and showed notable cytotoxicity against c-Met$^+$PD-L1$^+$ HCC cells (65). Furthermore, dual-targeted T cells exhibited potent inhibitory effects on tumorigenesis, surpassing the effects observed with single-targeted CAR-T cells (65). Recently, Qin and colleagues designed two MET-specific CARs: CD28ζ and 4-1BB (66). In comparison with MET inhibitors that targeted MET activation, MET-CAR-T cells recognized and eliminated HCC cells based on overall MET expression, with their activity being unrelated to MET signaling pathway activation (66). While MET-CAR.CD28ζ is favored for future advancements, optimizing the CAR construct design and implementing strategies to counteract CAR-T cell exhaustion induced by the tumor microenvironment are essential to enhance the therapeutic efficacy of MET-CAR-T cells (66).

3.4 NKG2D

NKG2D serves as a vital activating receptor present on NK cells and NKT cells (67). It recognizes and binds to a range of cell surface glycoproteins known as NKG2D ligands (NKG2DL), which are distantly related to MHC class I molecules (67). These ligands are upregulated in response to malignant transformation, thereby marking “stressed” or “harmful” cells for elimination by NKG2D$^+$ lymphocytes (68, 69). The NKG2DL system offers a sophisticated immune surveillance mechanism that involves multiple layers of regulation to maintain a balance between early detection of stressed cells and prevention of autoimmunity induction (70).

In HCC, NKG2DL was elevated in tumor samples and related to aggressive carcinogenesis (71). Non-viral methods were employed in the generation of NKG2D CAR-T cells, involving the use of

electroporation to introduce CAR-carrying piggyBac transposon plasmids, followed by *in vitro* expansion with K562 artificial antigen-presenting cells (72). This strategy not only preserved the anti-tumor capabilities of NKG2D CAR-T cells in laboratory settings but also led to a decrease in the levels of exhaustion markers typically found in T cells (72). Sun et al. performed research involving the development of NKG2D-BBz CAR-T cells utilizing the CAR derived from the extracellular domain of NKG2D, combining with 4-1BB and CD3ζ (73). These modified CAR-T cells exhibited potent cytotoxicity against HCC cells in laboratory settings and demonstrated therapeutic efficacy in xenograft models (73). The findings highlight the targeted eradication of HCC cells by NKG2D-BBz CAR-T cells in an NKG2DL-dependent manner, laying the groundwork for advancing towards clinical trials involving NKG2DL-positive patients (73).

Although the preliminary findings show promise, several potential drawbacks need to be taken into account. The monitoring of tumors by NKG2D can put significant pressure on their survival (74). Thus, it is not unexpected that certain human tumors release NKG2DL from their outer layer to escape immune attacks, leading to a rise in soluble NKG2DL levels (75). When the soluble NKG2D ligand binds, it can reduce the sensitivity of NKG2D in attacking cells throughout the body and weaken their ability to fight against tumors (76, 77). Moreover, evidence suggests that NKG2D plays a role in tumor formation in cases of inflammation-induced cancers including HCC (78). The impact of NKG2D CAR-T cells on either enhancing anti-tumor activity or promoting tumor-favorable inflammation in such scenarios is awaiting to be established.

3.5 CD133

Elevated CD133 is a common feature in HCC and is typically associated with an unfavorable prognosis for patients (79). The findings of a phase II clinical trial offered initial evidence that CD133-CAR-T cells exhibited significant anti-tumor effects and posed no significant safety risks in advanced HCC cases (80). The study revealed a median overall survival of 12 months and a median progression-free survival of 6.8 months, showcasing promising results in this advanced-stage cohort (80). Moreover, Yang et al. opted for a non-viral approach to effectively generate CD133-specific CAR-T cells capable of producing PD-1 scFv checkpoint inhibitors using an SB system derived from minicircle vectors, which has demonstrated reduced immunogenicity, lower costs, and enhanced safety in comparison to viral vectors (81). Thereafter, these engineered cells exerted significantly anti-tumor effects on HCC cells and xenograft mouse models, implying that employing an approach incorporating CD133 CAR-T and PD-1 scFv cells may present a viable choice for individuals dealing with advanced HCC and upregulated expression of CD133 (81). CoG133-CAR-T cells demonstrated significant transfection efficiency and displayed dual antigen-binding capabilities targeting CD133 and GPC3 (82). Extended survival and eradication of tumors were noted in HCC xenograft mice treated with CoG133-CAR-T cells, underscoring the significant promise of dual-specificity CAR-T cells (82).

3.6 EpCAM

Epithelial Cell Adhesion Molecule (EpCAM), a transmembrane protein located on the cell surface, has traditionally served as a primary indicator for carcinomas and is commonly employed in cancer diagnostics (83, 84). EpCAM expression related to poor prognosis in patients with advanced HCC (85). At present, EpCAM CAR-T cells are in the developmental stages for cancer therapy, with their potential application in HCC remaining unexplored (86). Multiple clinical trials are currently recruiting participants to assess the effectiveness and the safe profile of EpCAM CAR-T cells in individuals with advanced HCC (NCT02729493), postoperative relapse (NCT03013712), and refractory HCC (NCT05028933).

3.7 Other targets

Mucin 1 (MUC1) is overexpressed in various cancers and contributes to tumorigenesis in HCC (87, 88). At present, an ongoing clinical trial is investigating the use of MUC1 CAR-T cells for the treatment of HCC (NCT02587689). Additionally, increased levels of carcinoembryonic antigen (CEA) in serum have been identified as prognostic biomarkers in HCC (89). In the HITM-SIR trial, six patients with CEA-positive liver metastases were treated with CEA CAR-T cells and hepatic artery infusions combined with selective internal radiation therapy (90). Notably, there were no cases of severe adverse events observed throughout the trial, additional confirmation of the safety profile of CAR-T therapy was obtained (90, 91).

4 Challenges and prospects of CAR-T cell therapy

4.1 challenges with the inefficiency of CAR-T cell trafficking and infiltration

Typically, CAR-T cells are administered via peripheral infusion, and their ability to migrate to the tumor site is essential for achieving cytolytic effects (92). However, T cells typically do not have the necessary chemokine receptors that play a key role in guiding T cells to tumor sites by interacting with chemokines released by tumor cells (93, 94). Moreover, in HCC tissue, there is a dense fibrotic structure that reduces the expression of chemokines, resulting in a significant decline in the ability of CAR-T cells to migrate and infiltrate the tumor (95). Under conditions of low oxygen levels, hypoxia-inducible factor-1 becomes activated and subsequently upregulates vascular endothelial growth factor, which interacts with receptors on endothelial cells (96). This process triggers the remodeling of the surrounding extracellular matrix and facilitates the development of

irregular blood vessels within the tumor (96). These vessels exhibit structural abnormalities, including immature basement membranes, excessive branching, and discontinuous junctions. Such aberrant morphology contributes to increased permeability and suboptimal blood flow, ultimately impairing the transport of immune cells and therapeutic agents, thereby obstructing the penetration and homing of CAR T cells (97). Strategies to improve the trafficking and infiltration capabilities include the development of CAR-T cells with chemokine receptors and CAR-T cells engineered to express heparinase (98). Additionally, local administration of CAR-T cells has shown promising enhancements in the fight against tumors (99, 100) (Figure 2).

4.2 challenges with overcoming the immunosuppressive tumor microenvironment.

After CAR-T cells have effectively penetrated into a tumor, they encounter challenges presented by the hostile tumor microenvironment (TME) including hypoxia and low levels of nutrition (101, 102). Furthermore, the compact TME encircling HCC consists of various immunosuppressive cells including Treg cells, tumor-associated macrophages (TAMs), and fibroblasts, which can inhibit effective T cell responses by the secretion of immunosuppressive molecules and activating immune checkpoints (102, 103). For example, Luo et al. utilized a folate-targeted Toll-like receptor 7 agonist (FA-TLR7-1A) to specifically revitalize TAMs and myeloid-derived suppressor cells (MDSCs), transforming them from an immunosuppressive state to a pro-inflammatory phenotype, while maintaining the characteristics of other immune cell populations (104). The combination of FA-TLR7-1A with CAR-T cell therapy not only converted TAMs and MDSCs from an M2-like anti-inflammatory phenotype to an M1-like pro-inflammatory phenotype but also enhanced the infiltration and activation of both CAR-T cells and endogenous T cells within solid tumors, which markedly improved the effectiveness of standard CAR-T cell therapy against solid tumors in immunocompetent mice. Moreover, tumor glycosylation also plays a crucial role in inhibiting antitumor immune responses. Tumor glycans can impede the recognition of peptide epitopes by antibodies through steric hindrance (105). Furthermore, they foster an immunosuppressive environment by interacting with lectins present on immune cells (such as SIGLECand MGL) and by releasing galectins that bind to inhibitory molecules (including Galectin-9 and Galectin-3) (106, 107). Additionally, branched N-glycans can support interactions between immune checkpoints (like PD-1/PD-L1), thus increasing the activation threshold for T cell receptors (108). Therefore, it is important to explore gene editing targeting immune checkpoints on CAR-T cells, along with the use of targeted drugs to counteract the immunosuppressive TME and enhance metabolism programming, which could reduce the growth of HCC by improving cytotoxic T cell responses (32, 109, 110). Moreover, numerous strategies such as combining CAR-T therapy with immune checkpoint inhibitors (ICIs) or other immunostimulatory therapies, as well as engineering CAR-T cells to resist the immunosuppressive effects of cytokines have also been implemented to improve CAR-T therapy responses within TME (111, 112).

4.3 Challenges with systemic toxicity

Slight modifications in CAR design have been found to have significant impacts, not just on durability but also on safety (113). The infusion of CAR-T cells often leads to notable adverse events, such as off-target toxicity, cytokine release syndrome (CRS), and neurotoxicity (114, 115). Genome editing is increasingly

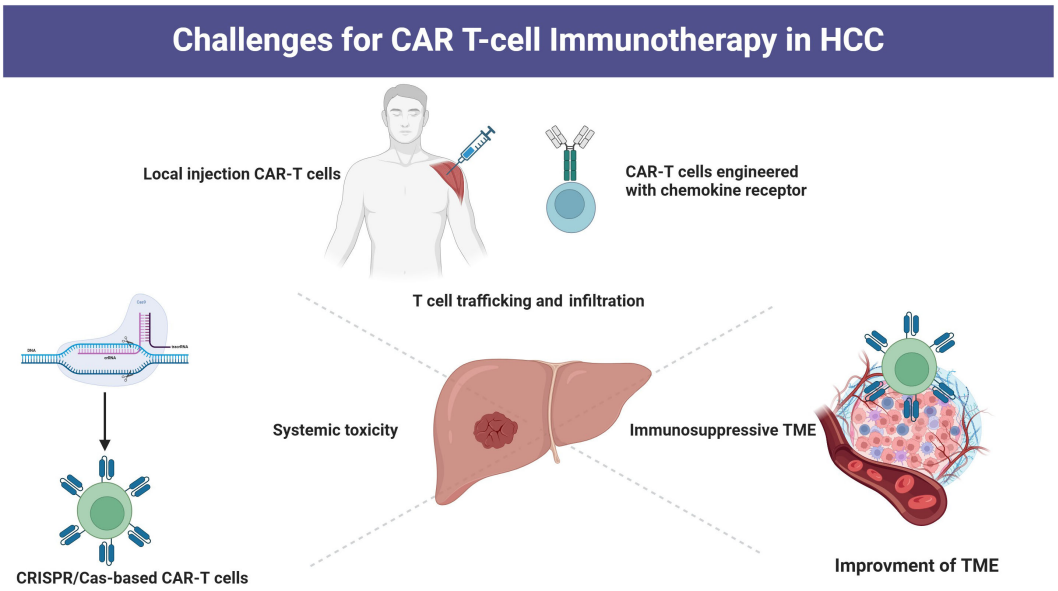

FIGURE 2
Strategies for overcoming challenges of CAR-T cell therapy.

contributing to enhancing the safety of CAR-T cells (32). TALENs and CRISPR–Cas nucleases have been utilized to target the granulocyte-macrophage colony-stimulating factor (GM-CSF) gene in CAR-T cells, aiming to inhibit GM-CSF secretion upon CAR-T cell activation, thereby potentially averting the activation of monocytes or macrophages, and subsequently reducing the risk of CRS (116, 117). Furthermore, structural alterations have shown promise in decreasing the toxicity of CAR-T cells while preserving their effectiveness in eradicating tumors (118).

5 Conclusion

CAR-T cells have emerged as a potentially revolutionary new strategy for the cancer treatment and have the potential to become a cornerstone of clinical management of HCC in the future. Despite the substantial advancements showcased by CAR-T cell therapy, there is still a considerable path ahead in CAR-T research to develop a practical treatment for HCC. To optimize CAR-T cell therapy in the future, further advancements should focus on enhancing CAR-T cell designs specific to HCC and reducing systematic toxicity. Sustained research endeavors focused on elucidating molecular mechanisms, refining treatment protocols, and overcoming therapeutic constraints are essential for driving the field forward toward achieving significant clinical results and ultimately enhancing the prognosis for patients with HCC.

Author contributions

YZ: Conceptualization, Data curation, Formal analysis, Investigation, Methodology, Project administration, Software, Writing – original draft, Writing – review & editing. SW: Conceptualization, Investigation, Writing – original draft, Writing – review & editing. MX: Conceptualization, Data curation, Investigation, Software, Writing – original draft. XW: Conceptualization, Data curation, Investigation, Methodology, Writing – review & editing. WD: Conceptualization, Data curation, Methodology, Supervision, Writing – review & editing. HL: Conceptualization, Data curation, Methodology, Supervision, Writing – review & editing. ZZ: Formal analysis, Funding acquisition, Project administration, Resources, Validation, Visualization, Writing – review & editing. SZ: Data curation, Formal analysis, Funding acquisition, Methodology, Project administration, Resources, Software, Supervision, Visualization, Writing – review & editing.

Funding

The author(s) declare financial support was received for the research, authorship, and/or publication of this article. This study was supported by the National Key R&D Program of China (2020YFC2003100, 2020YFC2003104).

Acknowledgments

We thank the BioRender drawing software (https://www.biorender.com/).

Conflict of interest

The authors declare that the research was conducted in the absence of any commercial or financial relationships that could be construed as a potential conflict of interest.

Publisher's note

References

1. Vogel A, Meyer T, Sapisochin G, Salem R, Saborowski A. Hepatocellular carcinoma. *Lancet*. (2022) 400:1345–62. doi: 10.1016/s0140-6736(22)01200-4

2. Brown ZJ, Tsilimigras DI, Ruff SM, Mohseni A, Kamel IR, Cloyd JM, et al. Management of hepatocellular carcinoma: A review. *JAMA Surg*. (2023) 158:410–20. doi: 10.1001/jamasurg.2022.7989

3. Yang JD, Hainaut P, Gores GJ, Amadou A, Plymoth A, Roberts LR. A global view of hepatocellular carcinoma: trends, risk, prevention and management. *Nat Rev Gastroenterol Hepatol*. (2019) 16:589–604. doi: 10.1038/s41575-019-0186-y

4. Sangro B, Sarobe P, Hervás-Stubbs S, Melero I. Advances in immunotherapy for hepatocellular carcinoma. *Nat Rev Gastroenterol Hepatol*. (2021) 18:525–43. doi: 10.1038/s41575-021-00438-0

5. Gottwick C, Carambia A, Herkel J. Harnessing the liver to induce antigen-specific immune tolerance. *Semin Immunopathol*. (2022) 44:475–84. doi: 10.1007/s00281-022-00942-8

6. Kubes P, Jenne C. Immune responses in the liver. *Annu Rev Immunol*. (2018) 36:247–77. doi: 10.1146/annurev-immunol-051116-052415

7. Donne R, Lujambio A. The liver cancer immune microenvironment: Therapeutic implications for hepatocellular carcinoma. *Hepatology*. (2023) 77:1773–96. doi: 10.1002/hep.32740

8. Lee JC, Green MD, Huppert LA, Chow C, Pierce RH, Daud AI. The liver-immunity nexus and cancer immunotherapy. *Clin Cancer Res*. (2022) 28:5–12. doi: 10.1158/1078-0432.Ccr-21-1193

9. Richardson N, Ng STH, Wraith DC. Antigen-specific immunotherapy for treatment of autoimmune liver diseases. *Front Immunol*. (2020) 11:1586. doi: 10.3389/fimmu.2020.01586

10. Sperandio RC, Pestana RC, Miyamura BV, Kaseb AO. Hepatocellular carcinoma immunotherapy. *Annu Rev Med*. (2022) 73:267–78. doi: 10.1146/annurev-med-042220-021121

11. Sterner RC, Sterner RM. CAR-T cell therapy: current limitations and potential strategies. *Blood Cancer J*. (2021) 11:69. doi: 10.1038/s41408-021-00459-7

12. Zhang X, Zhu L, Zhang H, Chen S, Xiao Y. CAR-T cell therapy in hematological Malignancies: current opportunities and challenges. *Front Immunol*. (2022) 13:927153. doi: 10.3389/fimmu.2022.927153

13. Flugel CL, Majzner RG, Krenciute G, Dotti G, Riddell SR, Wagner DL, et al. Overcoming on-target, off-tumour toxicity of CAR T cell therapy for solid tumours. *Nat Rev Clin Oncol*. (2023) 20:49–62. doi: 10.1038/s41571-022-00704-3

14. Ma S, Li X, Wang X, Cheng L, Li Z, Zhang C, et al. Current progress in CAR-T cell therapy for solid tumors. *Int J Biol Sci*. (2019) 15:2548–60. doi: 10.7150/ijbs.34213

15. Yu SJ. Immunotherapy for hepatocellular carcinoma: Recent advances and future targets. *Pharmacol Ther*. (2023) 244:108387. doi: 10.1016/j.pharmthera.2023.108387

16. Bao C, Gao Q, Li LL, Han L, Zhang B, Ding Y, et al. The application of nanobody in CAR-T therapy. *Biomolecules*. (2021) 11. doi: 10.3390/biom11020238

17. Zhang C, Liu J, Zhong JF, Zhang X. Engineering CAR-T cells. *biomark Res*. (2017) 5:22. doi: 10.1186/s40364-017-0102-y

18. Jayaraman J, Mellody MP, Hou AJ, Desai RP, Fung AW, Pham AHT, et al. CAR-T design: Elements and their synergistic function. *EBioMedicine*. (2020) 58:102931. doi: 10.1016/j.ebiom.2020.102931

19. Qiu Y, Liao P, Wang H, Chen J, Hu Y, Hu R, et al. Enhanced tumor immunotherapy by polyfunctional CD19-CAR T cells engineered to secrete anti-CD47 single-chain variable fragment. *Int J Biol Sci*. (2023) 19:4948–66. doi: 10.7150/ijbs.86632

20. Rahbarizadeh F, Ahmadvand D, Moghimi SM. CAR T-cell bioengineering: Single variable domain of heavy chain antibody targeted CARs. *Adv Drug Delivery Rev*. (2019) 141:41–6. doi: 10.1016/j.addr.2019.04.006

21. Li N, Quan A, Li D, Pan J, Ren H, Hoeltzel G, et al. The IgG4 hinge with CD28 transmembrane domain improves V(H)H-based CAR T cells targeting a membrane-distal epitope of GPC1 in pancreatic cancer. *Nat Commun*. (2023) 14:1986. doi: 10.1038/s41467-023-37616-4

22. Tousley AM, Rotiroti MC, Labanieh L, Rysavy LW, Kim WJ, Lareau C, et al. Co-opting signalling molecules enables logic-gated control of CAR T cells. *Nature*. (2023) 615:507–16. doi: 10.1038/s41586-023-05778-2

23. Wu L, Brzostek J, Sakthi Vale PD, Wei Q, Koh CKT, Ong JXH, et al. CD28-CAR-T cell activation through FYN kinase signaling rather than LCK enhances therapeutic performance. *Cell Rep Med*. (2023) 4:100917. doi: 10.1016/j.xcrm.2023.100917

24. Guedan S, Posey AD Jr., Shaw C, Wing A, Da T, Patel PR, et al. Enhancing CAR T cell persistence through ICOS and 4-1BB costimulation. *JCI Insight*. (2018) 3. doi: 10.1172/jci.insight.96976

25. Roselli E, Boucher JC, Li G, Kotani H, Spitler K, Reid K, et al. 4-1BB and optimized CD28 co-stimulation enhances function of human mono-specific and bi-specific third-generation CAR T cells. *J Immunother Cancer*. (2021) 9. doi: 10.1136/jitc-2021-003354

26. Singh N, Frey NV, Engels B, Barrett DM, Shestova O, Ravikumar P, et al. Antigen-independent activation enhances the efficacy of 4-1BB-costimulated CD22 CAR T cells. *Nat Med*. (2021) 27:842–50. doi: 10.1038/s41591-021-01326-5

27. Hui E, Cheung J, Zhu J, Su X, Taylor MJ, Wallweber HA, et al. T cell costimulatory receptor CD28 is a primary target for PD-1-mediated inhibition. *Science*. (2017) 355:1428–33. doi: 10.1126/science.aaf1292

28. Okuyama Y, Nagashima H, Ushio-Fukai M, Croft M, Ishii N, So T. IQGAP1 restrains T-cell cosignaling mediated by OX40. *FASEB J*. (2020) 34:540–54. doi: 10.1096/fj.201900879RR

29. Pichler AC, Carrié N, Cuisinier M, Ghazali S, Voisin A, Axisa PP, et al. TCR-independent CD137 (4-1BB) signaling promotes CD8(+)-exhausted T cell proliferation and terminal differentiation. *Immunity*. (2023) 56:1631–1648.e1610. doi: 10.1016/j.immuni.2023.06.007

30. He Y, Vlaming M, van Meerten T, Bremer E. The implementation of TNFRSF co-stimulatory domains in CAR-T cells for optimal functional activity. *Cancers (Basel)*. (2022) 14. doi: 10.3390/cancers14020299

31. Honikel MM, Olejniczak SH. Co-stimulatory receptor signaling in CAR-T cells. *Biomolecules*. (2022) 12. doi: 10.3390/biom12091303

32. Dimitri A, Herbst F, Fraietta JA. Engineering the next-generation of CAR T-cells with CRISPR-Cas9 gene editing. *Mol Cancer*. (2022) 21:78. doi: 10.1186/s12943-022-01559-z

33. Chekol Abebe E, Yibeltal Shiferaw M, Tadele Admasu F, Asmamaw Dejenie T. Ciltacabtagene autoleucel: The second anti-BCMA CAR T-cell therapeutic armamentarium of relapsed or refractory multiple myeloma. *Front Immunol*. (2022) 13:991092. doi: 10.3389/fimmu.2022.991092

34. Del Bufalo F, Becilli M, Rosignoli C, De Angelis B, Algeri M, Hanssens L, et al. Allogeneic, donor-derived, second-generation, CD19-directed CAR-T cells for the treatment of pediatric relapsed/refractory BCP-ALL. *Blood*. (2023) 142:146–57. doi: 10.1182/blood.2023020023

35. Merkt W, Freitag M, Claus M, Kolb P, Falcone V, Röhrich M, et al. Third-generation CD19.CAR-T cell-containing combination therapy in Scl70+ systemic sclerosis. *Ann Rheum Dis*. (2024) 83:543–6. doi: 10.1136/ard-2023-225174

36. Tang L, Pan S, Wei X, Xu X, Wei Q. Arming CAR-T cells with cytokines and more: Innovations in the fourth-generation CAR-T development. *Mol Ther*. (2023) 31:3146–62. doi: 10.1016/j.ymthe.2023.09.021

37. Asmamaw Dejenie T, Tiruneh GMM, Dessie Terefe G, Tadele Admasu F, Wale Tesega W, Chekol Abebe E. Current updates on generations, approvals, and clinical trials of CAR T-cell therapy. *Hum Vaccin Immunother*. (2022) 18:2114254. doi: 10.1080/21645515.2022.2114254

38. Jogalekar MP, Rajendran RL, Khan F, Dmello C, Gangadaran P, Ahn BC. CAR T-Cell-Based gene therapy for cancers: new perspectives, challenges, and clinical developments. *Front Immunol*. (2022) 13:925985. doi: 10.3389/fimmu.2022.925985

39. Zhao Z, Condomines M, van der Stegen SJC, Perna F, Kloss CC, Gunset G, et al. Structural design of engineered costimulation determines tumor rejection kinetics and persistence of CAR T cells. *Cancer Cell*. (2015) 28:415–28. doi: 10.1016/j.ccell.2015.09.004

40. Srivastava S, Riddell SR. Engineering CAR-T cells: Design concepts. *Trends Immunol*. (2015) 36:494–502. doi: 10.1016/j.it.2015.06.004

41. Zhu Y, Feng J, Wan R, Huang W. CAR T cell therapy: remedies of current challenges in design, injection, infiltration and working. *Drug Des Devel Ther*. (2023) 17:1783–92. doi: 10.2147/dddt.S413348

42. Choe JH, Watchmaker PB, Simic MS, Gilbert RD, Li AW, Krasnow NA, et al. SynNotch-CAR T cells overcome challenges of specificity, heterogeneity, and persistence in treating glioblastoma. *Sci Transl Med*. (2021) 13. doi: 10.1126/scitranslmed.abe7378

43. Zhou F, Shang W, Yu X, Tian J. Glypican-3: A promising biomarker for hepatocellular carcinoma diagnosis and treatment. *Med Res Rev*. (2018) 38:741–67. doi: 10.1002/med.21455

44. Lu LL, Xiao SX, Lin ZY, Bai JJ, Li W, Song ZQ, et al. GPC3-IL7-CCL19-CAR-T primes immune microenvironment reconstitution for hepatocellular carcinoma therapy. *Cell Biol Toxicol*. (2023) 39:3101–19. doi: 10.1007/s10565-023-09821-w

45. Hu P, Cheng B, He Y, Wei Z, Wu D, Meng Z. Autophagy suppresses proliferation of HepG2 cells via inhibiting glypican-3/wnt/β-catenin signaling. *Onco Targets Ther*. (2018) 11:193–200. doi: 10.2147/ott.S150520

46. Hu P, Ke C, Guo X, Ren P, Tong Y, Luo S, et al. Both glypican-3/Wnt/β-catenin signaling pathway and autophagy contributed to the inhibitory effect of curcumin on hepatocellular carcinoma. *Dig Liver Dis*. (2019) 51:120–6. doi: 10.1016/j.dld.2018.06.012

47. Luan F, Liu P, Ma H, Yue X, Liu J, Gao L, et al. Reduced nucleic ZHX2 involves in oncogenic activation of glypican 3 in human hepatocellular carcinoma. *Int J Biochem Cell Biol*. (2014) 55:129–35. doi: 10.1016/j.biocel.2014.08.021

48. Li L, Jin R, Zhang X, Lv F, Liu L, Liu D, et al. Oncogenic activation of glypican-3 by c-Myc in human hepatocellular carcinoma. *Hepatology*. (2012) 56:1380–90. doi: 10.1002/hep.25891

49. Dargel C, Bassani-Sternberg M, Hasreiter J, Zani F, Bockmann JH, Thiele F, et al. T cells engineered to express a T-cell receptor specific for glypican-3 to recognize and kill hepatoma cells *in vitro* and in mice. *Gastroenterology*. (2015) 149:1042–52. doi: 10.1053/j.gastro.2015.05.055

50. Nishida T, Kataoka H. Glypican 3-targeted therapy in hepatocellular carcinoma. *Cancers (Basel)*. (2019) 11. doi: 10.3390/cancers11091339

51. Zheng X, Liu X, Lei Y, Wang G, Liu M. Glypican-3: A novel and promising target for the treatment of hepatocellular carcinoma. *Front Oncol*. (2022) 12:824208. doi: 10.3389/fonc.2022.824208

52. Shi D, Shi Y, Kaseb AO, Qi X, Zhang Y, Chi J, et al. Chimeric antigen receptor-glypican-3 T-cell therapy for advanced hepatocellular carcinoma: results of phase I trials. *Clin Cancer Res*. (2020) 26:3979–89. doi: 10.1158/1078-0432.Ccr-19-3259

53. Sun L, Gao F, Gao Z, Ao L, Li N, Ma S, et al. Shed antigen-induced blocking effect on CAR-T cells targeting Glypican-3 in Hepatocellular Carcinoma. *J Immunother Cancer*. (2021) 9. doi: 10.1136/jitc-2020-001875

54. Sun H, Xing C, Jiang S, Yu K, Dai S, Kong H, et al. Long term complete response of advanced hepatocellular carcinoma to glypican-3 specific chimeric antigen receptor T-Cells plus sorafenib, a case report. *Front Immunol*. (2022) 13:963031. doi: 10.3389/fimmu.2022.963031

55. Wu X, Luo H, Shi B, Di S, Sun R, Su J, et al. Combined antitumor effects of sorafenib and GPC3-CAR T cells in mouse models of hepatocellular carcinoma. *Mol Ther*. (2019) 27:1483–94. doi: 10.1016/j.ymthe.2019.04.020

56. Sun RX, Liu YF, Sun YS, Zhou M, Wang Y, Shi BZ, et al. GPC3-targeted CAR-T cells expressing GLUT1 or AGK exhibit enhanced antitumor activity against hepatocellular carcinoma. *Acta Pharmacol Sin*. (2024). doi: 10.1038/s41401-024-01287-8

57. Pang N, Shi J, Qin L, Chen A, Tang Y, Yang H, et al. IL-7 and CCL19-secreting CAR-T cell therapy for tumors with positive glypican-3 or mesothelin. *J Hematol Oncol*. (2021) 14:118. doi: 10.1186/s13045-021-01128-9

58. Zhou L, Li Y, Zheng D, Zheng Y, Cui Y, Qin L, et al. Bispecific CAR-T cells targeting FAP and GPC3 have the potential to treat hepatocellular carcinoma. *Mol Ther Oncol*. (2024) 32:200817. doi: 10.1016/j.omton.2024.200817

59. Tayob N, Kanwal F, Alsarraj A, Hernaez R, El-Serag HB. The performance of AFP, AFP-3, DCP as biomarkers for detection of hepatocellular carcinoma (HCC): A phase 3 biomarker study in the United States. *Clin Gastroenterol Hepatol*. (2023) 21:415–423.e414. doi: 10.1016/j.cgh.2022.01.047

60. Liu H, Xu Y, Xiang J, Long L, Green S, Yang Z, et al. Targeting alpha-fetoprotein (AFP)-MHC complex with CAR T-cell therapy for liver cancer. *Clin Cancer Res*. (2017) 23:478–88. doi: 10.1158/1078-0432.Ccr-16-1203

61. Topel H, Bağırsakçı E, Yılmaz Y, Güneş A, Bağcı G, Çömez D, et al. High glucose induced c-Met activation promotes aggressive phenotype and regulates expression of glucose metabolism genes in HCC cells. *Sci Rep*. (2021) 11:11376. doi: 10.1038/s41598-021-89765-5

62. Zhou Y, Cui G, Xu H, Chun J, Yang D, Zhang Z, et al. Loss of TP53 cooperates with c-MET overexpression to drive hepatocarcinogenesis. *Cell Death Dis.* (2023) 14:476. doi: 10.1038/s41419-023-05958-y

63. Bouattour M, Raymond E, Qin S, Cheng AL, Stammberger U, Locatelli G, et al. Recent developments of c-Met as a therapeutic target in hepatocellular carcinoma. *Hepatology*. (2018) 67:1132–49. doi: 10.1002/hep.29496

64. Wang H, Rao B, Lou J, Li J, Liu Z, Li A, et al. The function of the HGF/c-met axis in hepatocellular carcinoma. *Front Cell Dev Biol*. (2020) 8:55. doi: 10.3389/fcell.2020.00055

65. Jiang W, Li T, Guo J, Wang J, Jia L, Shi X, et al. Bispecific c-met/PD-L1 CAR-T cells have enhanced therapeutic effects on hepatocellular carcinoma. *Front Oncol.* (2021) 11:546586. doi: 10.3389/fonc.2021.546586

66. Qin A, Qin Y, Lee J, Musket A, Ying M, Krenciute G, et al. Tyrosine kinase signaling-independent MET-targeting with CAR-T cells. *J Transl Med.* (2023) 21:682. doi: 10.1186/s12967-023-04521-9

67. Liu Z, Wang H, Liu H, Ding K, Shen H, Zhao X, et al. Targeting NKG2D/NKG2DL axis in multiple myeloma therapy. *Cytokine Growth Factor Rev*. (2024) 76:1–11. doi: 10.1016/j.cytogfr.2024.02.001

68. Dhar P, Wu JD. NKG2D and its ligands in cancer. *Curr Opin Immunol*. (2018) 51:55–61. doi: 10.1016/j.coi.2018.02.004

69. López-Soto A, Huergo-Zapico L, Acebes-Huerta A, Villa-Alvarez M, Gonzalez S. NKG2D signaling in cancer immunosurveillance. *Int J Cancer*. (2015) 136:1741–50. doi: 10.1002/ijc.28775

70. Wang D, Dou L, Sui L, Xue Y, Xu S. Natural killer cells in cancer immunotherapy. *MedComm (2020)*. (2024) 5:e626. doi: 10.1002/mco2.626

71. Cadoux M, Caruso S, Pham S, Gougelet A, Pophillat C, Riou R, et al. Expression of NKG2D ligands is downregulated by β-catenin signalling and associates with HCC aggressiveness. *J Hepatol.* (2021) 74:1386–97. doi: 10.1016/j.jhep.2021.01.017

72. Tay JCK, Wang J, Du Z, Ng YY, Li Z, Ren Y, et al. Manufacturing NKG2D CAR-T cells with piggyBac transposon vectors and K562 artificial antigen-presenting cells. *Mol Ther Methods Clin Dev*. (2021) 21:107–20. doi: 10.1016/j.omtm.2021.02.023

73. Sun B, Yang D, Dai H, Liu X, Jia R, Cui X, et al. Eradication of hepatocellular carcinoma by NKG2D-based CAR-T cells. *Cancer Immunol Res.* (2019) 7:1813–23. doi: 10.1158/2326-6066.Cir-19-0026

74. Paczulla AM, Rothfelder K, Raffel S, Konantz M, Steinbacher J, Wang H, et al. Absence of NKG2D ligands defines leukaemia stem cells and mediates their immune evasion. *Nature*. (2019) 572:254–9. doi: 10.1038/s41586-019-1410-1

75. Groh V, Wu J, Yee C, Spies T. Tumour-derived soluble MIC ligands impair expression of NKG2D and T-cell activation. *Nature*. (2002) 419:734–8. doi: 10.1038/nature01112

76. Maurer S, Kropp KN, Klein G, Steinle A, Haen SP, Walz JS, et al. Platelet-mediated shedding of NKG2D ligands impairs NK cell immune-surveillance of tumor cells. *Oncoimmunology*. (2018) 7:e1364827. doi: 10.1080/2162402x.2017.1364827

77. Oppenheim DE, Roberts SJ, Clarke SL, Filler R, Lewis JM, Tigelaar RE, et al. Sustained localized expression of ligand for the activating NKG2D receptor impairs natural cytotoxicity *in vivo* and reduces tumor immunosurveillance. *Nat Immunol.* (2005) 6:928–37. doi: 10.1038/ni1239

78. Sheppard S, Guedes J, Mroz A, Zavitsanou AM, Kudo H, Rothery SM, et al. The immunoreceptor NKG2D promotes tumour growth in a model of hepatocellular carcinoma. *Nat Commun*. (2017) 8:13930. doi: 10.1038/ncomms13930

79. Liu F, Qian Y. The role of CD133 in hepatocellular carcinoma. *Cancer Biol Ther*. (2021) 22:291–300. doi: 10.1080/15384047.2021.1916381

80. Dai H, Tong C, Shi D, Chen M, Guo Y, Chen D, et al. Efficacy and biomarker analysis of CD133-directed CAR T cells in advanced hepatocellular carcinoma: a single-arm, open-label, phase II trial. *Oncoimmunology*. (2020) 9:1846926. doi: 10.1080/2162402x.2020.1846926

81. Yang C, You J, Pan Q, Tang Y, Cai L, Huang Y, et al. Targeted delivery of a PD-1-blocking scFv by CD133-specific CAR-T cells using nonviral Sleeping Beauty transposition shows enhanced antitumour efficacy for advanced hepatocellular carcinoma. *BMC Med*. (2023) 21:327. doi: 10.1186/s12916-023-03016-0

82. Wang H, Wang X, Ye X, Ju Y, Cao N, Wang S, et al. Nonviral mcDNA-mediated bispecific CAR T cells kill tumor cells in an experimental mouse model of hepatocellular carcinoma. *BMC Cancer*. (2022) 22:814. doi: 10.1186/s12885-022-09861-1

83. Eyvazi S, Farajnia S, Dastmalchi S, Kanipour F, Zarredar H, Bandehpour M. Antibody based epCAM targeted therapy of cancer, review and update. *Curr Cancer Drug Targets*. (2018) 18:857–68. doi: 10.2174/1568009618666180102102311

84. Gires O, Pan M, Schinke H, Canis M, Baeuerle PA. Expression and function of epithelial cell adhesion molecule EpCAM: where are we after 40 years? *Cancer Metast Rev*. (2020) 39:969–87. doi: 10.1007/s10555-020-09898-3

85. Park DJ, Sung PS, Kim JH, Lee GW, Jang JW, Jung ES, et al. EpCAM-high liver cancer stem cells resist natural killer cell-mediated cytotoxicity by upregulating CEACAM1. *J Immunother Cancer*. (2020) 8. doi: 10.1136/jitc-2019-000301

86. Li D, Guo X, Yang K, Yang Y, Zhou W, Huang Y, et al. EpCAM-targeting CAR-T cell immunotherapy is safe and efficacious for epithelial tumors. *Sci Adv*. (2023) 9:eadg9721. doi: 10.1126/sciadv.adg9721

87. Bozkaya G, Korhan P, Cokaklı M, Erdal E, Sağol O, Karademir S, et al. Cooperative interaction of MUC1 with the HGF/c-Met pathway during hepatocarcinogenesis. *Mol Cancer*. (2012) 11:64. doi: 10.1186/1476-4598-11-64

88. Wang J, Ni WH, Hu KB, Zhai XY, Xie F, Jie J, et al. Targeting MUC1 and JNK by RNA interference and inhibitor inhibit the development of hepatocellular carcinoma. *Cancer Sci*. (2017) 108:504–11. doi: 10.1111/cas.13144

89. Verma N, Vinocha A. Role of CA 19.9 and CEA in predicting diagnosis in hepatocellular carcinoma. *J Cancer Res Ther*. (2023) 19:1356–8. doi: 10.4103/jcrt.jcrt_1280_21

90. Katz SC, Hardaway J, Prince E, Guha P, Cunetta M, Moody A, et al. HITM-SIR: phase Ib trial of intraarterial chimeric antigen receptor T-cell therapy and selective internal radiation therapy for CEA(+) liver metastases. *Cancer Gene Ther*. (2020) 27:341–55. doi: 10.1038/s41417-019-0104-z

91. Katz SC, Burga RA, McCormack E, Wang LJ, Mooring W, Point GR, et al. Phase I hepatic immunotherapy for metastases study of intra-arterial chimeric antigen receptor-modified T-cell therapy for CEA+ Liver metastases. *Clin Cancer Res*. (2015) 21:3149–59. doi: 10.1158/1078-0432.Ccr-14-1421

92. Billingsley MM, Singh N, Ravikumar P, Zhang R, June CH, Mitchell MJ. Ionizable lipid nanoparticle-mediated mRNA delivery for human CAR T cell engineering. *Nano Lett*. (2020) 20:1578–89. doi: 10.1021/acs.nanolett.9b04246

93. Spranger S, Dai D, Horton B, Gajewski TF. Tumor-residing batf3 dendritic cells are required for effector T cell trafficking and adoptive T cell therapy. *Cancer Cell*. (2017) 31:711–723.e714. doi: 10.1016/j.ccell.2017.04.003

94. Xu N, Palmer DC, Robeson AC, Shou P, Bommiasamy H, Laurie SJ, et al. STING agonist promotes CAR T cell trafficking and persistence in breast cancer. *J Exp Med*. (2021) 218. doi: 10.1084/jem.20200844

95. Caruana I, Savoldo B, Hoyos V, Weber G, Liu H, Kim ES, et al. Heparanase promotes tumor infiltration and antitumor activity of CAR-redirected T lymphocytes. *Nat Med*. (2015) 21:524–9. doi: 10.1038/nm.3833

96. Majidpoor J, Mortezaee K. Angiogenesis as a hallmark of solid tumors - clinical perspectives. *Cell Oncol (Dordr)*. (2021) 44:715–37. doi: 10.1007/s13402-021-00602-3

97. Dianat-Moghadam H, Nedaeinia R, Keshavarz M, Azizi M, Kazemi M, Salehi R. Immunotherapies targeting tumor vasculature: challenges and opportunities. *Front Immunol.* (2023) 14:1226360. doi: 10.3389/fimmu.2023.1226360

98. Liu G, Rui W, Zheng H, Huang D, Yu F, Zhang Y, et al. CXCR2-modified CAR-T cells have enhanced trafficking ability that improves treatment of hepatocellular carcinoma. *Eur J Immunol*. (2020) 50:712–24. doi: 10.1002/eji.201948457

99. Agliardi G, Liuzzi AR, Hotblack A, De Feo D, Núñez N, Stowe CL, et al. Intratumoral IL-12 delivery empowers CAR-T cell immunotherapy in a pre-clinical model of glioblastoma. *Nat Commun*. (2021) 12:444. doi: 10.1038/s41467-020-20599-x

100. Bagley SJ, Logun M, Fraietta JA, Wang X, Desai AS, Bagley LJ, et al. Intrathecal bivalent CAR T cells targeting EGFR and IL13Rα2 in recurrent glioblastoma: phase 1 trial interim results. *Nat Med*. (2024) 30:1320–9. doi: 10.1038/s41591-024-02893-z

101. Liu L, Zhang R, Deng J, Dai X, Zhu X, Fu Q, et al. Construction of TME and Identification of crosstalk between Malignant cells and macrophages by SPP1 in hepatocellular carcinoma. *Cancer Immunol Immunother*. (2022) 71:121–36. doi: 10.1007/s00262-021-02967-8

102. Sas Z, Cendrowicz E, Weinhäuser I, Rygiel TP. Tumor microenvironment of hepatocellular carcinoma: challenges and opportunities for new treatment options. *Int J Mol Sci*. (2022) 23. doi: 10.3390/ijms23073778

103. Chen C, Wang Z, Ding Y, Qin Y. Tumor microenvironment-mediated immune evasion in hepatocellular carcinoma. *Front Immunol.* (2023) 14:1133308. doi: 10.3389/fimmu.2023.1133308

104. Luo W, Napoleon JV, Zhang F, Lee YG, Wang B, Putt KS, et al. Repolarization of tumor-infiltrating myeloid cells for augmentation of CAR T cell therapies. *Front Immunol.* (2022) 13:816761. doi: 10.3389/fimmu.2022.816761

105. Munk K, Pritzer E, Kretzschmar E, Gutte B, Garten W, Klenk HD. Carbohydrate masking of an antigenic epitope of influenza virus haemagglutinin independent of oligosaccharide size. *Glycobiology*. (1992) 2:233–40. doi: 10.1093/glycob/2.3.233

106. Macauley MS, Crocker PR, Paulson JC. Siglec-mediated regulation of immune cell function in disease. *Nat Rev Immunol.* (2014) 14:653–66. doi: 10.1038/nri3737

107. Kouo T, Huang L, Pucsek AB, Cao M, Solt S, Armstrong T, et al. Galectin-3 shapes antitumor immune responses by suppressing CD8+ T cells via LAG-3 and inhibiting expansion of plasmacytoid dendritic cells. *Cancer Immunol Res*. (2015) 3:412–23. doi: 10.1158/2326-6066.Cir-14-0150

108. Lee HH, Wang YN, Xia W, Chen CH, Rau KM, Ye L, et al. Removal of N-linked glycosylation enhances PD-L1 detection and predicts anti-PD-1/PD-L1 therapeutic efficacy. *Cancer Cell*. (2019) 36:168–178.e164. doi: 10.1016/j.ccell.2019.06.008

109. Andreu-Saumell I, Rodriguez-Garcia A, Mühlgrabner V, Gimenez-Alejandre M, Marzal B, Castellsagué J, et al. CAR affinity modulates the sensitivity of CAR-T cells to PD-1/PD-L1-mediated inhibition. *Nat Commun*. (2024) 15:3552. doi: 10.1038/s41467-024-47799-z

110. Hu Y, Zu C, Zhang M, Wei G, Li W, Fu S, et al. Safety and efficacy of CRISPR-based non-viral PD1 locus specifically integrated anti-CD19 CAR-T cells in patients with relapsed or refractory Non-Hodgkin's lymphoma: a first-in-human phase I study. *EClinicalMedicine*. (2023) 60:102010. doi: 10.1016/j.eclinm.2023.102010

111. Carloni R, Sabbioni S, Rizzo A, Ricci AD, Palloni A, Petrarota C, et al. Immune-based combination therapies for advanced hepatocellular carcinoma. *J Hepatocell Carcinoma*. (2023) 10:1445–63. doi: 10.2147/jhc.S390963

112. Guo X, Jiang H, Shi B, Zhou M, Zhang H, Shi Z, et al. Disruption of PD-1 enhanced the anti-tumor activity of chimeric antigen receptor T cells against hepatocellular carcinoma. *Front Pharmacol*. (2018) 9:1118. doi: 10.3389/fphar.2018.01118

113. Peters DT, Savoldo B, Grover NS. Building safety into CAR-T therapy. *Hum Vaccin Immunother*. (2023) 19:2275457. doi: 10.1080/21645515.2023.2275457

114. Brudno JN, Kochenderfer JN. Recent advances in CAR T-cell toxicity: Mechanisms, manifestations and management. *Blood Rev*. (2019) 34:45–55. doi: 10.1016/j.blre.2018.11.002

115. Cappell KM, Kochenderfer JN. Long-term outcomes following CAR T cell therapy: what we know so far. *Nat Rev Clin Oncol*. (2023) 20:359–71. doi: 10.1038/s41571-023-00754-1

116. Sterner RM, Cox MJ, Sakemura R, Kenderian SS. Using CRISPR/cas9 to knock out GM-CSF in CAR-T cells. *J Vis Exp*. (2019) 149. doi: 10.3791/59629

117. Sterner RM, Sakemura R, Cox MJ, Yang N, Khadka RH, Forsman CL, et al. GM-CSF inhibition reduces cytokine release syndrome and neuroinflammation but enhances CAR-T cell function in xenografts. *Blood*. (2019) 133:697–709. doi: 10.1182/blood-2018-10-881722

118. Sun M, Xu P, Wang E, Zhou M, Xu T, Wang J, et al. Novel two-chain structure utilizing KIRS2/DAP12 domain improves the safety and efficacy of CAR-T cells in adults with r/r B-ALL. *Mol Ther Oncol*. (2021) 23:96–106. doi: 10.1016/j.omto.2021.08.014

frontiers | Frontiers in Immunology

TYPE Review
PUBLISHED 08 November 2024
DOI 10.3389/fimmu.2024.1459942

OPEN ACCESS

EDITED BY
Sina Naserian,
Hôpital Paul Brousse, France

REVIEWED BY
Delilah Hendriks,
Princess Maxima Center for Pediatric Oncology, Netherlands
Mohamed Essameldin Abdelgawad,
Wake Forest University, United States

*CORRESPONDENCE
Wencheng Zhang
wencheng_zhang@tongji.edu.cn;
wencheng.v.zhang@outlook.com
Zhiying He
zyhe@tongji.edu.cn

†These authors have contributed equally to this work and share first authorship

RECEIVED 05 July 2024
ACCEPTED 22 October 2024
PUBLISHED 08 November 2024

CITATION
Song J, Lu M, He Z and Zhang W (2024) Models of fibrolamellar carcinomas, tools for evaluation of a new era of treatments. *Front. Immunol.* 15:1459942. doi: 10.3389/fimmu.2024.1459942

Models of fibrolamellar carcinomas, tools for evaluation of a new era of treatments

Jinjia Song[1,2,3†], Mengqi Lu[1,4†], Zhiying He[1,2,3,4*] and Wencheng Zhang[1,2,3*]

[1]Institute for Regenerative Medicine, Medical Innovation Center and State Key Laboratory of Cardiology, Shanghai East Hospital, School of Life Sciences and Technology, Tongji University, Shanghai, China, [2]Shanghai Engineering Research Center of Stem Cells Translational Medicine, Shanghai, China, [3]Shanghai Institute of Stem Cell Research and Clinical Translation, Shanghai, China, [4]Postgraduate Training Base of Shanghai East Hospital, Jinzhou Medical University, Jinzhou, Liaoning, China

Fibrolamellar carcinoma (FLC) is a rare but fatal cancer that occurs primarily in young people. There are currently no known effective treatments, although several promising treatments appear to be in development. Genetic studies have confirmed that almost all FLC tumors have a fusion protein marker (DNAJB1-PRKACA) encoded by a fusion gene (DNAJB1-PRKACA); It is currently accepted as a diagnostic criterion for FLCs. Several research teams have established patient-derived xenograft (PDX) FLC models using immunocompromised animals as hosts and patient tissue samples (tumors or ascites) as primary sources for PDX-derived organoids. These FLC organoids are composed of FLC epithelia, endothelial progenitor cells, and stellate cells. CRISPR/Cas9 was used as a gene editing technique to modify mature hepatocytes to obtain *ex vivo* FLC-like cells expressing the fusion gene and/or other mutated genes associated with FLCs. Although these models simulate some but not all FLC features. Drug screening using these models has not proven effective in identifying clinically useful treatments. Genetic studies comparing FLCs to normal maturing endodermal cell lineages have shown that FLCs share genetic signatures not with hepatocytes, but with subpopulations of biliary tree stem cells (BTSCs), hepato/pancreatic stem/progenitor cells that consistently reside in peribiliary glands (PBGs) located in the biliary tree and are sources of stem cells for the formation and postnatal regeneration of the liver and pancreas. Therefore, it is expected that models of BTSCs, instead of hepatocytes may prove more useful. In this review, we summarize the status of the various FLC models and their features, applications, and limitations. They provide opportunities to understand the cause and characteristics of this deadly disease and are models from which effective treatments can be identified.

KEYWORDS

fibrolamellar carcinoma (FLC), biliary tree stem cells (BTSCs), tumor-derived models, organoids, DNAJB1-PRKACA fusion gene, heparan sulfate (HS)-oligosacchrides

1 Introduction

Fibrolamellar carcinoma (FLC) is named for its unique histological features, particularly the large amount of early lineage stage mesenchymal cells, which are precursors to endothelia and stellate cells, associated with FLC tumor cells (1–4). In contrast to patients with conventional hepatocellular carcinoma (HCC), patients with FLC typically have no clinical history of liver cirrhosis; few have hepatitis virus infections; and they are routinely negative for alpha-fetoprotein (AFP), an indicator of other liver tumors such as hepatoblastoma (5, 6). Currently, surgical resection is the primary clinical treatment for FLCs. The 5-year overall survival rate of FLC patients who underwent the surgical procedure ranged from 30% to 48% (7, 8). However, such treatment is not ideal because surgical resection is not suitable for patients with metastatic disease and FLC tumors are prone to recurrence and metastasis after surgical resection (9–11). Sorafenib, oxaliplatin, 5-fluorouracil, and interferon, which can be used as adjuncts to conventional chemotherapy or targeted therapies in HCC, have also been used in the treatment of patients with FLC, although with limited, if any, success; they have failed to improve long-term survival (12). It is suggested that precise immunotherapy or immunotherapy combined with chemotherapy that directly targets FLC tumor-associated proteins offers more logical strategies for effective treatment of FLCs and is increasingly the focus of researcher. However, associated clinical trials of immune checkpoint inhibitors had no impact on disease progression, and clinical trials of vaccination failed in most patients and showed only an isolated response. Therefore, new treatment methods are still in development, which requires further research.

2 Genetic signatures and mutations associated with FLC

The DNAJB1-PRKACA fusion gene is one of the markers of fibrolamellar carcinoma. The fusion of this gene is caused by a heterozygous deletion of approximately 400 kb on human chromosome 19 (Figure 1). The resulting DNAJB1-PRKACA fusion transcript is thought to activate protein kinase A through dysregulation of the catalytic portion of the protein (Figure 2). Activation of protein kinase A is also a characteristic feature of FLC. Protein kinase A consists of catalytic and regulatory subunits. Among them, PRKACA encodes the catalytic subunit and PRKAR1A encodes the regulatory subunit of protein kinase A. Honeyman et al. first identified this chimeric RNA, DNAJB1-PRKACA, which is predicted to encode a protein containing the amino-terminal domain of DNAJB1, a homolog of the molecular chaperone DNAJ fused in frame to PRKACA. PRKACA is the catalytic domain of protein kinase A and has been shown to be expressed in FLC but not in the adjacent normal liver, suggesting that this genetic alteration contributes to tumor pathogenesis (13).

This has also been confirmed by many other teams (13–15). Graham et al. developed an RT-PCR assay and an RNA *in situ* hybridization assay for paraffin-embedded tissues to detect the rearrangements of the PRKACA locus and calculated the total chimeric transcript and wild-type transcripts. Their results showed that the DNAJB1-PRKACA fusion gene is present in all FLC, while it is not detected in other tumor types. Therefore, they concluded that DNAJB1-PRKACA is an extremely sensitive and specific molecular marker for the diagnosis of FLC (16). Meanwhile, the biological function of the DNAJB1-PRKACA fusion gene and whether it is just a typical marker or a potential tumorigenic mechanism have attracted more attention. By using the gene editing tools, Engelholm et al. proved that the DNAJB1-PRKACA gene fusion can induce liver tumorigenesis with histological and cytological features of human FLCs. These features include large polygonal cells with granular, eosinophilic, and mitochondria-rich cytoplasm, prominent nucleoli, and markers of hepatocytes and cholangiocytes (17). Using a similar strategy, Kastenhuber et al. showed that either induction of the endogenous DNAJB1-PRKACA fusion gene by CRISPR/Cas9 or overexpression of the fusion gene cDNAs was sufficient to induce FLC-like tumors in young adult mice. Most importantly, their study revealed that DNAJB1-PRKACA fusion kinase interacts with β-catenin and acts as an oncogenic driving factor during FLC occurrence (18). Graham et al. further found that it is PRKAR1A loss rather than the classical DNAJB1-PRKACA fusion that is the cause of FLCs (Figure 2) (19). They identified three individuals with FLCs and a personal history of Carney complex. All three tumors showed the typical morphology of FLC and were positive for arginase, cytokeratin 7 and CD68, while all were negative for PRKAR1A protein expression. Their results suggested that FLC may be part of the Carney complex. In this case, FLCs have inactivating PRKAR1A mutations instead of the DNAJB1-PRKACA fusion gene found in sporadic FLCs, representing alternative possibilities for activating of protein kinase A.

Other teams such as Jessica Zucman-Rossi and her associates at INSERM (Paris, France) identified a homogeneous subgroup of HCC in which the BAP1 gene is inactivated and has similar features to FLCs (20). These tumors are more frequently developed in females without chronic liver disease or cirrhosis. The presence of PKA activation and T cell infiltrates suggest that these tumors could be treated with PKA inhibitors or immunomodulators. In any case, the DNAJB1-PRKACA fusion gene contributes to an increase in protein kinase activity, a key factor in the occurrence of FLC tumors. Consequently, protein kinase inhibitors may have great therapeutic potential for development and application in the treatment of these pancreatic/biliary tumors once a suitable drug is identified and developed.

3 The cellular origin of FLC and the use of gene editing techniques to generate FLC phenotypic traits from normal healthy cells

Gene editing technology generally refers to zinc-finger nucleases (ZFNs), transcription activator-like effector nucleases (TALENs), and clustered regularly interspaced short palindromic

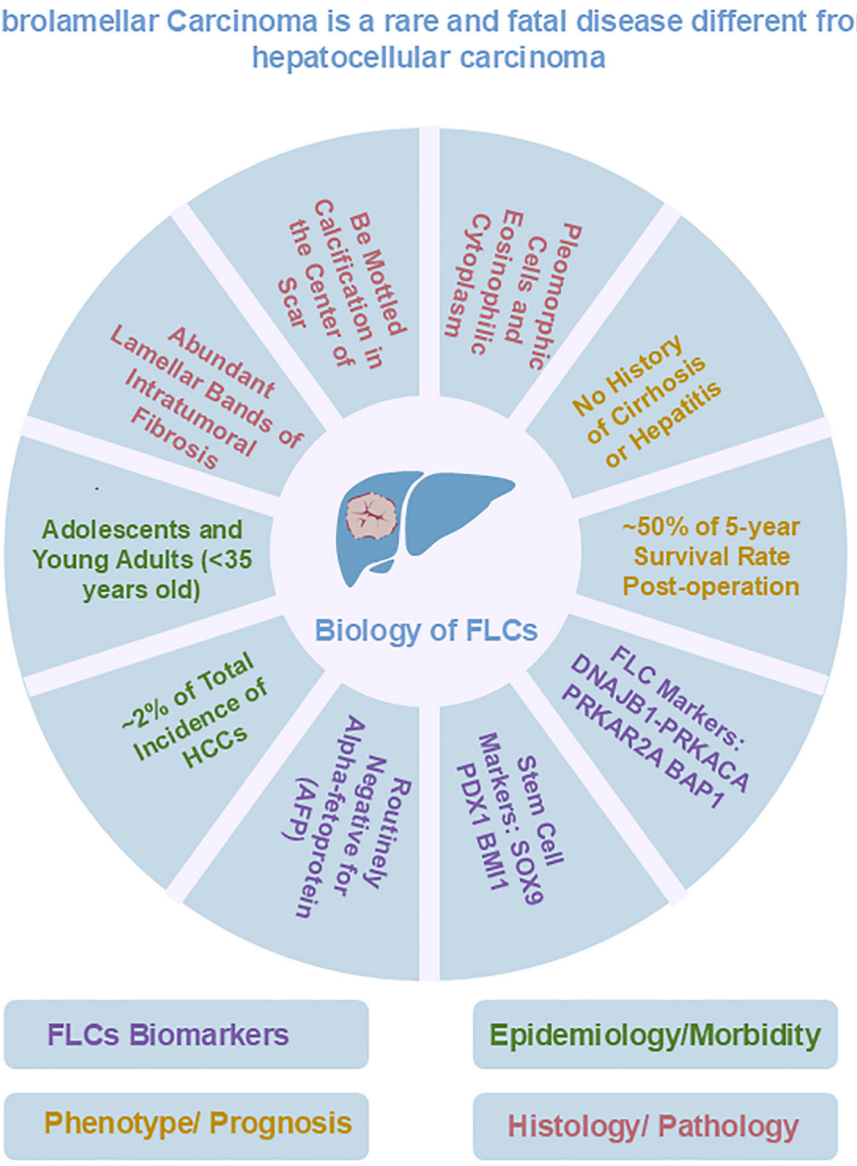

FIGURE 1
Overview of known biological features of FLC.

repeat DNA sequences (CRISPR/Cas9). CRISPR/Cas9 is considered a powerful gene editing tool that can be used to modify genes in various organisms, including humans. The CRISPR/Cas9 system is a natural immune system found in a variety of bacteria, including archaea, to protect against viral invasion (21). By developing CRISPR-associated enzymes (Cas enzyme), they can specifically target and cleave the target sequence to achieve the purpose of gene editing.

Since its first application in gene editing of mammalian cells in 2013 (22, 23), CRISPR tools have been widely developed and applied and have demonstrated their critical value in the field of tumor research. Xue et al. delivered plasmid DNA expressing Cas9 and sgRNA targeting PTEN and TP53 into mouse liver by tail vein injection and directly induced liver tumors. This study proved the feasibility of using CRISPR/Cas9 to directly target liver cancer genes and tumor suppressor genes to construct liver cancer mouse models (24). Subsequently, plasmids carrying Cas9 and multiple sgRNA targeting genes were injected into KRAS mice model using the same method, resulting in the induction of hepatocellular carcinoma and cholangiocarcinoma (25). Currently, CRISPR/Cas9 technology has been applied to the construction of mouse tumor models such as glioblastomas, pancreatic and lung cancers (26–28), providing an important tool for exploring the function of oncogenes and greatly accelerating the process of tumor research.

Previous studies have provided a comprehensive understanding of the molecular characteristics of FLC tumor tissues. However, the impact of FLC mutations on the healthy cells in the liver and the mechanisms by which different genetic backgrounds drive the occurrence of FLC are not yet known (13).

Rüland et al. constructed organoid models of human fetal hepatocytes with different FLC mutation backgrounds, including endogenous DNAJB1-PRKACA^{fus}, PRKAR2A^{KO}, BAP1^{KO} and

10.3389/fimmu.2024.1459942

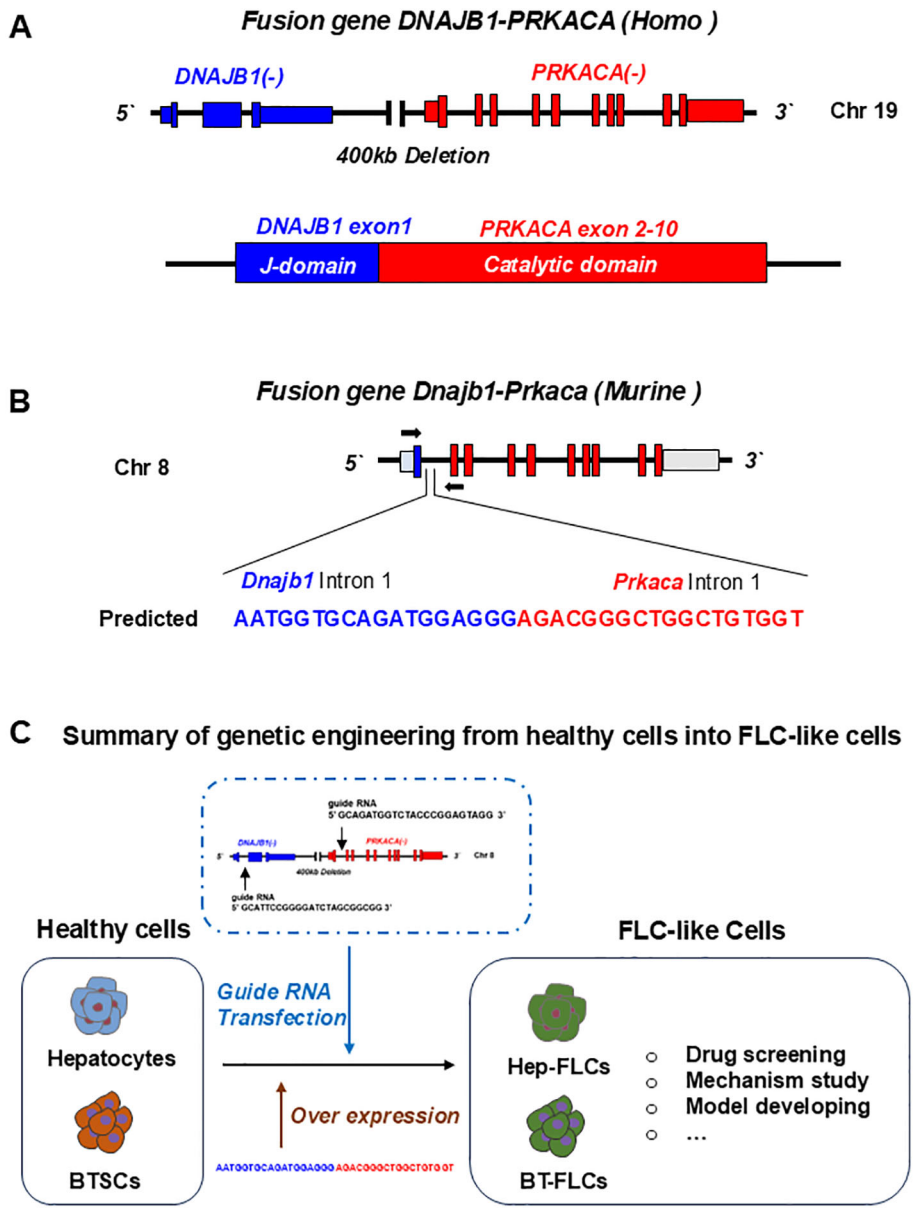

FIGURE 2
Gene editing of fusion genes in normal liver or cells for developing FLC models. **(A)** In human, fusion gene occurs on chromosome 19, when a 400Kb deletion occurs, leading to the fusion of DNAJB1 and PRKACA. The formed DNAJB1::PRKACA fusion gene can encode the DNAJB1-PRKACA fusion protein to activate protein kinase A by dysregulation of the catalytic portion of the protein. **(B)** The fusion gene can be induced by CRSPR-Cas9 on chromosome 8 in normal mice. **(C)** Normal cells including hepatocytes, biliary tree stem cells (BTSCs) or fetal liver cells can be genetic engineered into FLC-like cells by endogenic expression DNAJB1::PRKACA fusion genes or by over expressing of fusion cDNAs.

$BAP1^{KO}$;$PRKAR2A^{KO}$ organoid lines (15, 29). Transcriptomic comparison of FLC tumors and wild type fetal hepatocytes revealed that the transcriptional profile of the FLC mutant organoids was generally similar to that of FLC tumors with identical genetic backgrounds. This study suggests that FLCs can be derived from normal healthy cells in the liver after the introduction of BAP1 and PRKAR2A mutations (4). Most interestingly, this study found that various FLC mutations led to a certain degree of hepatocyte dedifferentiation, while the co-occurrence of mutations in BAP1 and PRKAR2A can significantly alter the fate of hepatocytes. The hepatocytes with double BAP1 and PRKAR2A mutations underwent de-differentiation to obtain a stem cell-stage, that has a similar phenotype to cholangiocytes or hepatic progenitor-like cells; and can be cultured under condition suitable for cholangiocytes. This indicated that either hepatocytes or cholangiocytes could be the cellular origin of FLC, in any case, they need to be in a de-differentiation stage in order to obtain the FLC feature.

Dinh et al. ran genetic signature study to identify miRNAs which are abnormal in FLC tumors. He applied RNA-seq comparison between FLCs and four cell types representing distinct maturational lineage stages in liver, including human biliary stem cells (hBTSCs), human hepatic stem cells (hHpSCs), human hepatoblasts (hHBs) and human adult mature hepatocytes (hAHEPs) (30). This genetic study brought a different voice to the

cellular origin of FLC. The results showed that FLCs have a genetic signature that overlap notably with that of the hBTSCs and to some extent that of hHpSCs or hHBs, and is significantly different from the genetic signature of mature hepatocytes or cholangiocytes (30–32). Indeed, FLCs are unique in being tumors rich in stem cells (more than 70%), while hepatocellular carcinomas are typically composed of a few percent stem cells and cholangiocarcinomas are perhaps 10% to 12% stem cells (4). However, the experimental verification of whether BTSCs expressing fusion genes through gene editing can better simulate the phenotype of FLC and confirm that BTSCs are the cellular source of FLC is still ongoing.

4 Organoid models for FLC

Conventional 2D tumor cell lines (monolayer) have proven inadequate to simulate the phenotypic traits of FLCs, which exhibit critical epithelial-mesenchymal cell-cell interactions involving paracrine signaling pathways, in addition, show aberrant mitochondrial and metabolic functions. Organoids, floating aggregates of epithelial stem/progenitor cells and the associated early maturation lineage stages of mesenchymal cells, typically precursors of endothelia and stellate cells, are widely used as more effective models for disease research.

Organoids were routinely used in the early days of cell culture in the 1930s to 1960s, but they faded from use with the advent of methods by which to establish monolayer cell cultures, especially clonal cell lines, and further enhanced in experimental usefulness with plastic cell culture dishes, developments occurring post-World War II with the development of the plastics industries. A return to studies on organoids has occurred during the last ~15 years with the remembrance of the importance of epithelial-mesenchymal cell-cell interactions, of fundamental importance to metazoans, the relevance of cell polarity and three-dimensionality, and their contribution to improvement abilities for analyzing normal and disease states in tissues were called upon (33).

As floating three-dimensional cell aggregates formed *ex vivo* by stem cells of both the epithelia and their mesenchymal cell partners, organoids are more accurate models of both normal and diseased tissues in demonstrating organ-specific and tissue-specific features than any monolayer culture model (34, 35). Tumor organoids prepared directly from human tumor tissue can be used to define their genetic signatures and phenotypic characteristics (Figure 3), making them excellent *ex vivo* research tools for normal tissues and organs compared to tumors and for cancer progression (Table 1). Referring to the construction methods of organoids from healthy donors, many studies have constructed corresponding organoids from multiple tumors, such as liver (36, 37), prostate (38), lung (39), ovaries (40), and breasts (41), etc. These tumor organoids are widely used for anti-tumor drugs screening, drug toxicity testing, disease modeling, and studying the mutational characteristics of tumors.

Sanford M. Simon and his associates had developed 21 patient-derived organoid lines from 9 patients with FLC, including 6 from adjacent non-malignant liver tissues, 3 from primary FLCs and 12 from metastatic FLCs, with the organoids system developed by Hans Clevers (Figure 3, Table 2) (42). The metastatic FLC organoid lines were derived from liver, lung, abdominal wall, omentum, ascites, and lymph node metastases at various anatomic locations. The PCR results confirmed that the DNAJB1-PRKACA fusion transcript was specifically expressed in all FLC organoid lines cultured in either hepatocyte medium or cholangiocyte medium. In terms of morphology, these FLC organoids were found to be polygonal and rich in lamellar bands of intratumoral mesenchymal cells. Through transcriptomic analysis, the FLC organoid lines established by Narayan expressed 509 genes that matched genes for a "fibrolamellar signature". The tumors in NSG mice transplanted with the FLC organoid lines showed FLC characteristics. Thus, the FLC organoid models established by Narayan have the characteristics of patient derived FLC tumor tissues.

However, the Clever`s system normally embedded tumor cells into the Matrigel, this may lead to missing critical features of FLC during the organoids formation. Therefore, different groups had revisited the Patient-Derived Xenograft (PDX) models or the combination of PDX models with organoids models for better presents the features of tumors.

5 PDX models developed for FLC

PDX models, particularly those using serial subcutaneous transplantation in immunocompromised hosts, have proven suitable for modeling FLC, but are unique among transplantable tumors in requiring long passage times on the order of months (4), which means that this experimental approach is time consuming, labor- intensive and expensive (42, 43). Compared to the exclusively animal-based PDX model, the establishment of PDX-derived organoid models is a more cost-effective and tractable approach in the study of human solid tumors.

The first-ever patient-derived PDX model of FLCs, FLC-TD-2010 (4), was developed by Oikawa and Wauthier in the Reid Lab (UNC School of Medicine, Chapel Hill, NC). It was isolated from FLC ascites tumor cells cultured briefly (one or two weeks) in serum-free Kubota's Medium (KM), designed for endodermal stem/progenitors, and used to select organoids of FLCs that partnered with their associated mesenchymal cell precursors comprised of precursors for endothelia and stellate cells; the organoids were transplanted into immunocompromised hosts (Figure 3, Table 2) (44). All transplantable FLC tumor lines established with those organoids expressed the FLC-specific fusion gene DNAJB1-PRKACA and were tumorigenic in immune-compromised hosts such as NSG mice. The FLC-TD-2010 model was validated as the first bona fide model of human FLCs and was used subsequently in research of FLCs with respect to their genetic signatures, pathogenesis and treatment strategies (30, 45, 46).

Later, Lalazar et al. established six FLC-PDX models using tumor tissue from six untreated or chemotherapy-only FLC patients (47). The model verification results confirmed that the DNAJB1-PRKACA fusion gene and its fusion protein can stably express in xenografts after multiple passages. Histological analyses showed that these PDX models had the typical morphological features of FLC, such as eosinophilic cytoplasm and areas of fibrolamellar bands. Additionally, these FLC-PDX models was proven to be outstanding for *in vitro* drugs

10.3389/fimmu.2024.1459942

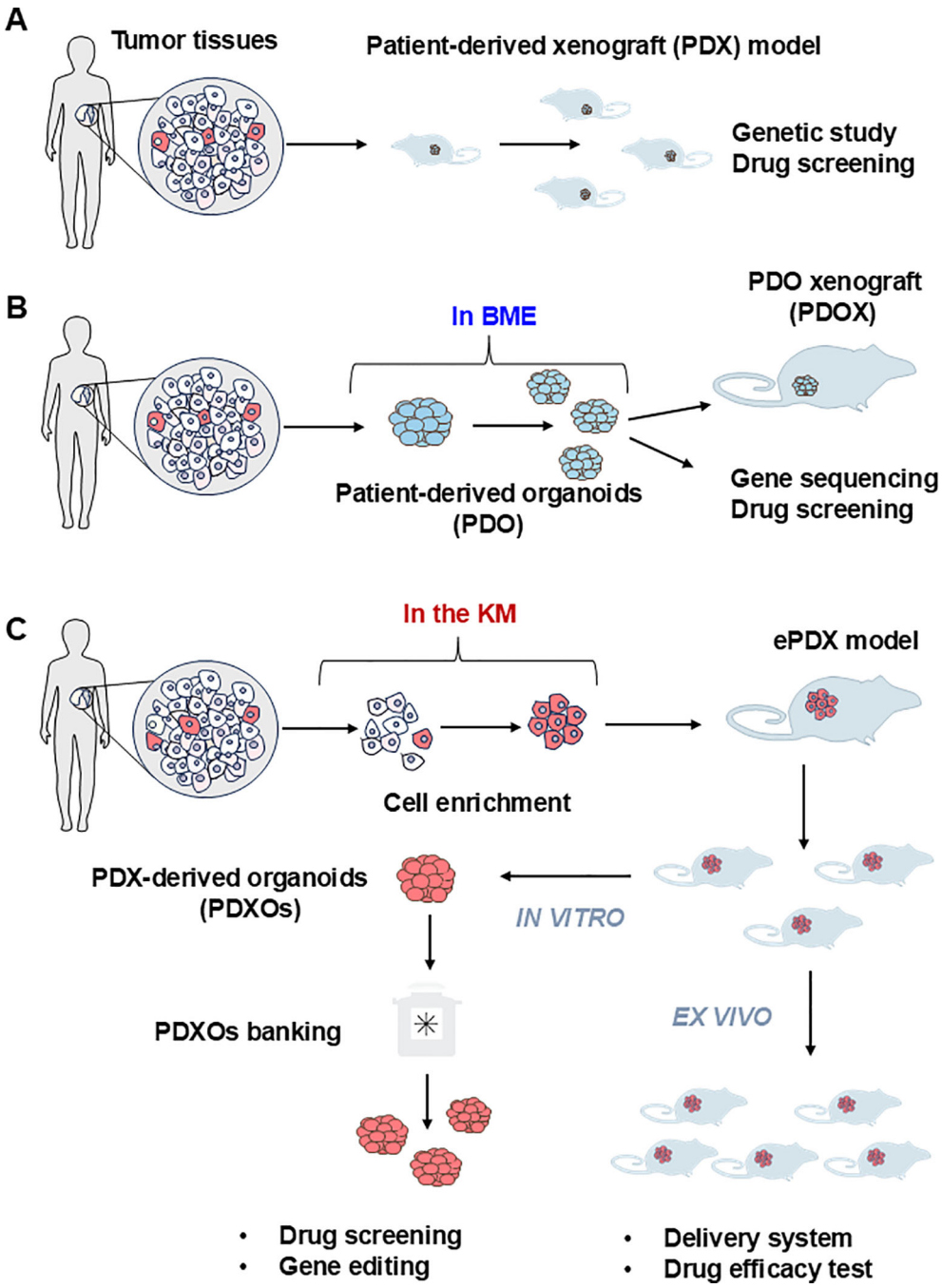

FIGURE 3
Current procedure of establishing the patient derived models of FLCs. **(A)** The patient-derived xenograft model (PDX) is the first generation of the PDX model for solid tumors. Tumor tissues are mechanically dispersed immediately after dissection with or without enzymatic treatment. The disseminated tumor can be directly injected subcutaneously into the immunocompromised NSG mice to generate the PDX model. Due to the limited amount of tumor imitating cells in the solid tumor tissue, this strategy can only be applied to limited cancer types such as breast cancer. **(B)** Patient-derived organoids (PDO) are currently the most adaptable strategy. Cell mixtures from solid tumor are mixed with basement membrane extract (BME) such as Matrigel with or without purification. The extracellular matrix provides essential nutrients for the growth of epithelial tumor cells to form three-dimensional(3D) spheroids or organoids. PDO can be used immediately or implanted into the NSG mouse to form PDO-derived xenograft model (PDOX) for further *in vivo* assay. **(C)** PDX-derived organoids (PDXOs) were developed by Reid and her associate when they established the first-ever-FLC PDX model (enriched PDX model, ePDX-model) by enriching FLC tumor cells with serum-free Kubota`s Medium (KM), and then injecting the enriched FLC patient tumor cells into NSG mice. This strategy can be applied to any solid tumor associated with cancer stem cells. The PDX-derived organoids can be obtained from the ePDX model any time they are needed for drug screening or genetic studies to develop potential new treatments.

TABLE 1 Summary of the currently available FLC *ex vivo* models.

Models	Methods	Advantage	Limitations	Reference
Patient-derived xenograft hFL-HCC model FLC-TD-2010	Ascites tumor cells derived from FLC patient were cultured briefly (a week or two) in Kubota's Medium (KM), a serum-free medium designed for endodermal stem/progenitors. Rapid culture selection resulted in organoids of FLC epithelial cells partnered with mesenchymal stem/progenitors (precursors of endothelia and stellate cells). The selected organoids were transplanted into NSG mice	**a.** The FLC organoids expressed the fusion gene DNAJB1::PRKACA and had morphological characteristics of FLCs. **b.** They are tumorigenic in immune-compromised hosts such as NSG mice	The initial tumor formation took a long time (more than 6 months), but thereafter passage took 2–3 months. All transplanted FLC organoids (100%) formed tumors even at very low inoculum concentrations (<100 cells). However, the tumorigenesis rate depended on the number of organoids transplanted; was increased by dietary supplementation (e.g. HGF and VEGF); and by transplantation of organoids embedded in hyaluronan hydrogels.	Tsunekazu Oikawa et al., *Nature Communications* 2015
Patient-derived xenograft hFL-HCC model	FLC tumor samples were donated from patients (aged 17 to 36 years; 4 women, 2 men) undergoing surgical resection. Tumor tissues were cut into pieces and transplanted subcutaneously, intrahepatically, or under the kidney capsule. A portion of the tumors were digested into single cells and injected into NSG mice intrasplenically, intrahepatically, or subcutaneously.	**a.** The DNAJB1::PRKACA fusion gene and its fusion protein remain stable expression after multiple passages of xenografts. **b.** These PDX models have the typical morphological features of FLCs, such as eosinophilic cytoplasm and areas of fibrosis. **c.** These models express 509 differentially expressed genes of FLCs.	**a.** The success rate for implantation of PDX material into NSG mice was 30-35%. **b.** The culture of PDX materials required several months to a year. **c.** The PDX tumors might not recapitulate the responses of the patients to treatments. **d.** During the evaluation of candidate agents, the response of implanted tumors to the candidate agents may differ from the tumors that has developed spontaneously in a patient.	Gadi Lalazar et al., *Cancer Discovery* 2021
Patient-derived xenograft hFL-HCC model	21 patient-derived organoid lines from 9 patients with FLCs were cultured in either the hepatocyte medium or cholangiocyte medium, including 6 from adjacent normal liver. There are 3 from primary FLCs and 12 from metastatic FLCs.	**a.** They express the fusion gene and the FLC-associated genes and have the morphological characteristics of FLCs. **b.** The organoid lines are from different sites in the patients, including adjacent non-cancerous liver, and from primary and metastatic FLCs.	**a.** The fibrolamellar bands can only be observed in the original tumor tissue. **b.** The transcriptomes of the tumor organoids clustered with each other and with the corresponding tumor tissue, was distinct from that in normal tissue and in normal organoids.	Nicole J.C. Narayan et al., *Stem cell Reports* 2022

TABLE 2 Summary of gene mutation and genetic signature of FLC.

Genetic signature	Type of mutation	Occurrence in FLC patient	Correlated treatment	Reference
DNAJB1::PRKACA	A heterozygous 400 kb deletion mutation	In almost all FLC patients	DNAJB1-PRKACA fusion kinase peptide vaccine	Joshua N. Honeyman et al., *Science* 2014 Rondell P. Graham et al., *Modern Pathology* 2015 Lars H. Engelholm et al., *Gastroenterology* 2017
PRKAR1A	PRKAR1A inactivating mutation	In FLC patients with a history of Carney complex	PKA inhibitors or immunomodulators	Rondell P. Graham et al., *Hepatology* 2017
BAP1	BAP1 inactivating mutation	More frequently in FLC female patients without chronic liver disease or cirrhosis	PKA inhibitors or immunomodulators	Théo Z Hirsch et al., *Journal of Hepatology* 2020

TABLE 3 Current clinical trials of FLCs and the latest updates.

NCT#	Description of treatment	Current outcomes	Limitations
NCT02234986	Oral ENMD-2076 for the Treatment of Patients with Advanced Fibrolamellar Carcinoma.	Of 35 patients who enrolled and received treatment, 1 (3%) had a partial response and 20 (57%) had stable disease. Three deaths were reported on-study—two due to disease progression and one due to pulmonary embolism not related to ENMD-2076.	At present, there is no comprehensive therapeutic approach supporting the further evaluation of ENMD-2076 as a single agent.
NCT01642186	A Randomized Three Arm Phase II Study of (1) Everolimus, (2) Estrogen Deprivation Therapy (EDT) With Leuprolide + Letrozole and (3) Everolimus + EDT in Patients with Unresectable Fibrolamellar Hepatocellular Carcinoma	Stable disease was observed in 9 of 26 evaluable patients (35%). PFS6 was 0%. Median overall survival (OS) was 12.4 months.	There are side effects such as nausea, vomiting, anemia, and elevated aspartate aminotransferase.
NCT05014607	DNAJB1-PRKACA neoepitope-based personalized peptide vaccine adjuvanted with the TLR1/2 agonist XS1532 and MontanideTM ISA51 VG in a single FL-HCC patient.	Patients can survive recurrence-free survival for more than 21 months after vaccination.	No released information
NCT04248569	DNAJB1-PRKACA Fusion Kinase Peptide Vaccine Combined with Nivolumab and Ipilimumab for Patients with FLC	Pending	No released information
NCT04380545	To evaluate the safety and tolerability of therapy with nivolumab + fluorouracil (5-FU) + recombinant interferon alpha 2b-like protein (IFN-alpha2b) in patients with unresectable FLC in the context of palliative systemic and prebiopsy therapy.	Pending	No released information

screening and *in vivo* drug testing. With these PDX models and the organoids generated from these models Lalazar et al. were able to test drugs including napabucasin (a novel STAT3 inhibitor), TOPO1 and HDAC inhibitors on the primary and metastatic FLCs. Their results showed that these drugs have synergistic inhibitory effects with the anti-apoptotic protein Bcl-xL. Based on their study, Lalazar suggested that eliminating oncogenes, oncotranscripts, or oncoproteins can be an effective treatment for FLC.

6 Animal models for FLCs

A reasonable and reliable animal model can simulate the microenvironment of human tumors and reflect their cellular and molecular pathological characteristics. It provides a platform to elucidate etiology and screen therapeutic drugs for effective treatments. Currently, animal models, including genetically engineered/modified mouse models (GEM) and larger animal models (especially dogs, pigs, monkeys), are used in scientific research of most tumors, such as liver cancer, pancreatic cancer, and breast cancer (48–50). Not only are GEM models efficient to operate and cost-effective, but they can also exhibit genetic heterogeneity (51). Tumors can occur naturally in a specific microenvironment, which can better simulate the molecular and pathological characteristics of human diseases. It provides a more ideal spectrum for studying the pathological properties of a particular gene *in vivo*.

6.1 Animal models of FLCs (zebrafish)

The morphological characteristics of zebrafish larvae are small and translucent, which is an ideal form for imaging (52). Therefore, zebrafish larvae are one of the valuable models for studying the cellular morphology and molecular characteristics of early-stage liver cancer (53, 54). Oliveira et al. overexpressed a pair of homologous fusion genes DNAJB1a::PRKACAa in zebrafish using the hepatocyte promoter *fabp10a* and established a stable Zebrafish line, *Tg(fabp10a:dnajb1a-pekacaa_cryaa:Cerullean)* (55). By comparing liver morphology with that in normal zebrafish, Oliveira demonstrated that zebrafish with DNAJB1a::PRKACAa overexpression displayed early malignant features, including hepatomegaly, infiltration of immune cells such as neutrophils and macrophages, and activation of caspase-a. Meanwhile, pharmacological inhibition of TNFα secretion and caspase-a with pentoxifylline and Sc-YVAD-CMK, respectively, was investigated in the liver of FLC-zebrafish, and both were found to reduce immune cell inflammation and hepatomegaly in the FLC progression. Therefore, this study suggests that TNFα and caspase-a may represent novel targets for limiting FLC progression.

6.2 Animal models of FLCs (mouse)

Mouse models are important tools for assessing the carcinogenic potential of candidate cytokines and exploring the mechanism of tumorigenesis (56). Kastenhuber et al. also used CRISPR-mediated endogenous gene deletion to create a C57 mouse model with DNAJB1-PRKACA fusion gene mutation. CRISPR.1 and CRISPR.2 guide RNA were used for gene editing in the liver of adult mouse, respectively. It was the first time that the FLC model of mature mouse liver expressing the DNAJB1-PRKACA fusion gene was constructed. Liver tumors leading to a moribund condition were observed in the gene-edited mice 16 to 24 months after injection. The liver tumors of these model mice had the

characteristics of human FLC tumor tissue, but did not express the cholangiocytic markers CK7, CK19 and CD68. It is hypothesized that this may be because the way liver tumorigenesis is achieved in mice using gene editing is different from that in humans. In addition, tumor molecular profile analyzes showed that proliferation and mitogenic signaling pathways were enhanced in FLC tumor cells, and the activation of the WNT signaling pathway cooperated with the expression of DNAJB1-PRKACA to accelerate FLC formation. Furthermore, the tumorigenicity of the DNAJB1-PRKACA fusion gene was found to be mainly dependent on the kinase domain of PRKACA.

Furthermore, Engelholm et al. designed a PX330 recombination vector that coexpresses Cas9 protein and gRNA. It was then injected into female FVB/N mice at approximately 8 weeks via hydrodynamic tail vein injection (17). In the experimental group of mice without mutagenic agents, the proportion of liver tumor formation was about 80%, and the mice with FLC tumors showed features similar to human FLC tumors, such as the increase of cell size and intracellular mitochondria. Therefore, it was suggested that expression of the fusion gene could induce the formation of FLC tumors in mice.

Although sufficient studies have shown that the DNAJB1-PRKACA fusion gene can induce FLC formation in mice, the downstream signal transduction process is still unclear. Transcriptome analyses revealed that the non-coding RNA expression profile in FLC tumor tissues is significantly different from that of adjacent normal liver and other liver tumors. The studies have provided ideas for exploring other possible tumorigenic factors in FLCs. Farber et al. identified the miRNA and lncRNA expression in FLC. The lncRNA expression profile is distinctly different from the normal liver and other liver tumor tissues. This proved that these changes in the cellular levels of miRNA are correlative with tumorigenesis of FLC (57). Similarly, Sethupathy and his associates found that expression of the DNAJB1-PRKACA fusion gene inhibits the expression of miRNA-375 and then targets YAP1 and connective tissue growth factor (CTGF) in the Hippo signaling pathway, leading to increased proliferation and invasion of FLC cells (30). Therefore, their results suggest that miRNA-375 may suppress the growth of FLC (30). The therapeutic strategy based on this is promising.

In summary, the mouse model established by Engelholm and Kastenhuber is easy to implement and reproducible and does not require the costly and time-consuming process of generating and breeding mouse strains. Therefore, it could be an effective model for further studying of the biological properties of FLC. However, as Weinberg said, “mice are not small people”, and these models can not accurately simulate all the characteristics of human diseases (58). Knocking out a gene in an organism by using gene editing can have complex consequences. Due to several confounding factors, it is impossible to precisely understand the specific function of the fusion gene that is central to FLC pathology. Before selecting the most ideal model for drug screening or new treatment innovations, a balance between feasibility and prevention of tumor function in different models should be assessed overall.

7 New treatments

Currently, surgical resection is the primary treatment for early-stage FLC patients, with surgically treated individuals having a higher survival rate (6). However, because FLC is a primary cancer without typical signs of liver damage, early predictive signals and clinical symptoms are lacking (59). There is still no standardized, effective, and systematic treatment(s) for patients with advanced FLC disease. Chemotherapeutic drugs such as gemcitabine, oxaliplatin (GEMOX), which are cisplatin and sorafenib, used in the treatment of hepatocellular carcinoma have also been used in targeted chemical therapy in patients with advanced FLC disease, but tumors had limited response to these drugs. The proliferation and metastasis of FLC tumors could not be inhibited (6). Currently, patients diagnosed with FLC are enrolled in the Pediatric Hepatic Malignancy International Therapeutic Trial (PHITT) to receive surgery in combination with cisplatin and doxorubicin (Table 3). If patients are not suitable for surgical resection, they are treated periodically with sorafenib, gemcitabine, and oxaliplatin (NCT03533582). The use of immunotherapy remains a future approach for effective treatments for FLC, and studies are underway to define logical immunotherapeutic protocols. The combination of precise immunotherapy directly targeting the FLC oncoprotein and comprehensive immune checkpoint blocking can alter the key regulatory pathways of FLCs and help improve the systemic therapeutic effect of FLCs.

The exploration of new therapeutic targets and the realization of an effective treatment is one of the current topics of FLC research. Early clinical treatments of FLC mainly focus on chemical drugs of renal cell carcinoma, hepatocellular carcinoma, and other tumors, such as Sunitinib, ENMD-2076 and other oral drug treatments. However, the therapeutic effects found so far are not ideal. According to the recent studies on the phenotypic characteristics and specific markers of FLC (13, 16), clinical trials of combined drug therapy and cellular immunotherapy for FLCs have been conducted in the past two years. For example, Nivolumab, Fluorouracil and interferon-α-2B (NCT04380545), the Glutamine Antagonist DRP-104 combined with Durvalumab (NCT06027086), and the DNAJB1-PRKACA fusion kinase peptide vaccine in combination with Nivolumab and Ipilimumab (NCT04248569) have been used in the treatment of advanced FLC patients. These clinical trials are still in the volunteer recruitment phase.

8 Glycosaminoglycan biology and FLCs

New areas of research for FLCs include glycosaminoglycan (GAG) chemistry and its regulation of FLC organoids through complexes of paracrine signals and specific GAG oligosaccharides. The ability to perform such studies is due to revolutionary breakthroughs by a team of chemists, Jian Liu (School of Pharmacy, UNC, Chapel Hill, NC). Liu have established strategies for the synthesis of chondroitin sulfate-(CS)-oligosaccharides and

heparan sulfate-(HS)-oligosaccharides. It has long been known that complexes of GAG oligosaccharides and specific proteins have dramatic regulatory effects on cell growth and differentiation. However, in the past the effects of GAGs could not be studied given the hundreds of variant chemistries extant among CS- and HS-oligosaccharides present in extracts. With synthesis of large quantities of each unique CS- or HS-oligosaccharide, one can do research on their cellular and molecular effects when in a complex with a specific protein. Jian Liu and his associates have collaborated with the molecular geneticists in Praveen Sethupathy's lab and, in parallel, with the cell and molecular biologists in the Reid lab to compare the GAG oligosaccharides in FLCs versus normal tissues and then analyzed the biological effects of some of the synthesized oligosaccharides on FLCs.

CS-oligosaccharides are sulfated GAGs comprised of disaccharides of glucuronic acid (GlcA) or iduronic acid (IdoA) and sulfated galactosamine and its associated proteoglycans, such as versican (VCAN). They were examined in normal livers compared to FLCs to determine their relative quantities. It was found that CS-oligosaccharides (but not HS-oligosaccharides) are dramatically more abundant (6-fold), and the expression index of VCAN, secreted by activated stellate cells, is significantly higher in FLC tumors as compared to normal livers. The implications are that CS-oligosaccharides and their associated proteoglycans, especially those from activated stellate cells, are a striking feature of FLCs (60). Future research will focus on assessment of the effects of complexes of specific CS-oligosaccharides and paracrine signals on organoids of stem cell subpopulations compared to FLCs compared to adult hepatocytes.

HS-oligosaccharides are sulfated glycosaminoglycans (GAGs) from the disaccharides of glucuronic acid (GlcA) or iduronic acid (IdoA) and sulfated glucosamine. HS-oligosaccharides bind to core proteins to form HS-proteoglycans (HS-PGs). Hormones or paracrine signals bind tightly to the HS-oligosaccharides on those HS-PGs and together they form three-dimensional structures that bind to receptors triggering signal transduction resulting in various cellular functions (61–64). The biological effects of HS-oligosaccharides depends on their complex sulfation motifs that dictate their binding to specific signaling proteins and that in turn to the presentation of the complex to cell receptors that trigger signal transduction (65, 66).

The effects of synthesized HS-oligosaccharides and paracrine signaling complexes on FLC organoids were examined and compared with normal BTSC organoids or HpSCs organoids (66, 67). The organoids divided steadily with a division every approximately 7 days. When spheroids were prepared, from organoids by eliminating the mesenchymal cells within, the cells the spheroids survived indefinitely in a condition of growth stagnation for several months. The mesenchymal cells, precursors to endothelia and to stellate cells, were shown to be the source of multiple paracrine signals such as fibroblast growth factors (FGFs), epidermal growth factors (EGFs), vascular endothelial growth factors (VEGFs), and Wnt ligands, etc. Distinct HS-oligosaccharides, all of them 10-12 mers or larger, could form complexes with the various paracrine factors, and each complex was able to elicit particular biological responses that proved distinct between the FLC organoids versus organoids of BTSCs or HpSCs. Some of the complexes, especially those with 3-*O* sulfated HS-oligosaccharides were able to cause the FLC organoids to go into growth arrest for weeks.

In the analyzes of the more than 50 distinct HS-oligosaccharides synthesized by Jian Liu and his associates, the HS-oligosaccharides with biological activity on the organoids were all 10-12 mers and larger. They were tightly bound to the various paracrine signals, and the complexes were found to be biologically effective on organoids of all stem cell subpopulations (66). Among the most potent proved to be those HS-oligosaccharides with 3-*O*-sulfation, a rare modification. However, this finding of 3-*O*-sulfated HS-oligosaccharides potent effects on organoids of normal and transformed hepato/pancreatic stem cells, parallels their potent biological effects in the treatment of coagulation disorders (68) and for the expansion of normal stem cells (69). In contrast to classical signal transduction pathways that are triggered only by proteins, those that are regulated by complexes of proteins and HS-oligosaccharides cannot be replaced by other alternative pathways. Furthermore, synthesized HS-oligosaccharides can be synthesized into compounds that are insensitive to heparanase, which may provide a novel and effective treatment for FLC in the future.

9 Conclusions and prospects

Although the newly discovered therapeutic targets provide new ideas for the treatment of FLCs, significant work is still needed to elucidate them. In addition, attention must be paid to the efficiency of medication administration. FLC tumors are enveloped in thick fibrolamellar bands that contain an abundance of extracellular matrix that can protect the tumor cells from various therapeutic modalities. The FLCs may exhibit features of stem cells from either the hepatic or pancreatic (or both) lineages, meaning that there will be variability in key features of FLCs depending on whether oncogenic transformation occurred in lineage stages within the biliary tree nearer to the liver versus pancreas. These variabilities are ones yet to be adjudicated in some of the ongoing research. For example, those located in the branches that can differentiate into cells with pancreatic characteristics can produce large amounts of pancreatic exocrine enzymes and matrix metalloproteinases, which pose major challenges for drug delivery and stability.

Nevertheless, there have been gratifying advances in the study of FLCs in terms of genetic and protein signature studies as well as analyzes in several *ex vivo* and *in vivo* models. There are still no fully validated treatments for FLC patients beyond surgical removal of tumors in patients with a non-metastatic tumor. Fortunately, there are multiple research directions with promising insights into novel treatments for the future, particularly in some of the ongoing research that are analyzing forms of immunotherapies.

Author contributions

JS: Writing – original draft, Writing – review & editing, Formal analysis, Visualization. ML: Writing – review & editing, Writing – original draft. ZH: Writing – review & editing, Funding acquisition,

Supervision. WZ: Writing – original draft, Writing – review & editing, Funding acquisition, Supervision, Visualization.

Funding

The author(s) declare financial support was received for the research, authorship, and/or publication of this article. This work was supported by grants to Drs. WZ and ZH including Major Program of the National Key Research and Development Project (2020YFA0112600), the National Natural Science Foundation of China (82472691, 82471592, 82270638, 82173019, 82203741), the Project of Shanghai Science and Technology Commission (22ZR1451100), the Peak Disciplines (Type IV) of Institutions of Higher Learning in Shanghai, and the Shanghai Engineering Research Center of Stem Cells Translational Medicine (20DZ2255100).

Acknowledgments

The authors would like to thank Professor Emeritus Lola M. Reid of the University of North Carolina School of Medicine for editing the manuscript and providing suggestions for the project. The Fibrolamellar Cancer Foundation (FCF) (https://fibrofoundation.org/) was founded by Tucker Davis and 3 friends and later taken cared by Tucker`s parents Marna and Charles Davis. Tucker died of FLC in 2010. Their extraordinary financial contributions to research on FLCs, primarily through the Foundation have fueled a thriving community of investigators working synergistically to clarify and characterize FLCs and to identify treatment options.

Conflict of interest

The authors declare that the research was conducted in the absence of any commercial or financial relationships that could be construed as a potential conflict of interest.

Publisher's note

References

1. Dinh TA, Utria AF, Barry KC, Ma R, Abou-Alfa GK, Gordan JD, et al. A framework for fibrolamellar carcinoma research and clinical trials. *Nat Rev Gastroenterol Hepatol.* (2022) 19:328–42. doi: 10.1038/s41575-022-00580-3

2. Torbenson M. Fibrolamellar carcinoma: 2012 update. *Scientifica.* (2012) 743790:1. doi: 10.6064/2012/743790

3. Craig JR, Peters RL, Edmondson HA, Omata M. Fibrolamellar carcinoma of the liver: a tumor of adolescents and young adults with distinctive clinico-pathologic features. *Cancer.* (1980) 46:372–9. doi: 10.1002/1097-0142(19800715)46:2<372::AID-CNCR2820460227>3.0.CO;2-S

4. Oikawa T, Wauthier E, Dinh TA, Selitsky SR, Reyna-Neyra A, Carpino G, et al. Model of fibrolamellar hepatocellular carcinomas reveals striking enrichment in cancer stem cells. *Nat Commun.* (2015) 6:8070. doi: 10.1038/ncomms9070

5. Edmondson HA. Differential diagnosis of tumors and tumor-like lesions of liver in infancy and childhood. *A.M.A. J Dis Children.* (1956) 91:168–86. doi: 10.1001/archpedi.1956.02060020170015

6. Ang CS, Kelley RK, Choti MA, Cosgrove DP, Chou JF, Klimstra D, et al. Clinicopathologic characteristics and survival outcomes of patients with fibrolamellar carcinoma: data from the fibrolamellar carcinoma consortium. *Gastrointestinal Cancer Research: GCR.* (2013) 6:3–9.

7. Eggert T, McGlynn KA, Duffy A, Manns MP, Greten TF, Altekruse SF. Fibrolamellar hepatocellular carcinoma in the USA, 2000-2010: A detailed report on frequency, treatment and outcome based on the Surveillance, Epidemiology, and End Results database. *United Eur Gastroenterol J.* (2013) 1:351–7. doi: 10.1177/2050640613501507

8. Chen X, Lu Y, Shi X, Han G, Zhang L, Ni C, et al. Epidemiological and clinical characteristics of five rare pathological subtypes of hepatocellular carcinoma. *Front In Oncol.* (2022) 12:864106. doi: 10.3389/fonc.2022.864106

9. Zakka K, Jiang R, Alese OB, Shaib WL, Wu C, Wedd JP, et al. Clinical outcomes of rare hepatocellular carcinoma variants compared to pure hepatocellular carcinoma. *J Hepatocellular Carcinoma.* (2019) 6:119–29. doi: 10.2147/JHC.S215235

10. Lemekhova A, Hornuss D, Polychronidis G, Mayer P, Rupp C, Longerich T, et al. Clinical features and surgical outcomes of fibrolamellar hepatocellular carcinoma: retrospective analysis of a single-center experience. *World J Surg Oncol.* (2020) 18:93. doi: 10.1186/s12957-020-01855-2

11. Glavas D, Bao QR, Scarpa M, Ruffolo C, Brown ZJ, Pawlik TM, et al. Treatment and prognosis of fibrolamellar hepatocellular carcinoma: a systematic review of the recent literature and meta-analysis. *J Gastrointestinal Surgery: Off J Soc For Surg Alimentary Tract.* (2023) 27:705–15. doi: 10.1007/s11605-023-05621-z

12. Ang CS, Kelley RK, Choti MA, Cosgrove DP, Chou JF, Klimstra D, et al. Clinicopathologic characteristics and survival outcomes of patients with fibrolamellar carcinoma:data from the fibrolamellar carcinoma consortium. *Gastrointestinal Cancer Res.* (2013) 6:3–9.

13. Honeyman JN, Simon EP, Robine N, Chiaroni-Clarke R, Darcy DG, Lim II, et al. Detection of a recurrent DNAJB1-PRKACA chimeric transcript in fibrolamellar hepatocellular carcinomas. *Science.* (2014) 343:1010–4. doi: 10.1126/science.1249484

14. Reid LM, Sethupathy P. The DNAJB1-PRKACA chimera: Candidate biomarker and therapeutic target for fibrolamellar carcinomas. *Hepatol (Hepatology Elsewhere).* (2015) 63:662–3. doi: 10.1002/hep.28307

15. Turnham RE, Smith FD, Kenerson HL, Omar MH, Golkowski M, Garcia I, et al. An acquired scaffolding function of the DNAJ-PKAc fusion contributes to oncogenic signaling in fibrolamellar carcinoma. *Elife.* (2019) 8:e44187. doi: 10.7554/eLife.44187.023

16. Graham RP, Jin L, Knutson DL, Kloft-Nelson SM, Greipp PT, Waldburger N, et al. DNAJB1-PRKACA is specific for fibrolamellar carcinoma. *Modern Pathology: an Off J United States Can Acad Pathology Inc.* (2015) 28:822–9. doi: 10.1038/modpathol.2015.4

17. Engelholm LH, Riaz A, Serra D, Dagnæs-Hansen F, Johansen JV, Santoni-Rugiu E, et al. CRISPR/cas9 engineering of adult mouse liver demonstrates that the dnajb1-prkaca gene fusion is sufficient to induce tumors resembling fibrolamellar hepatocellular carcinoma. *Gastroenterology.* (2017) 153:1662–73. doi: 10.1053/j.gastro.2017.09.008

18. Kastenhuber ER, Lalazar G, Houlihan SL, Tschaharganeh DF, Baslan T, Chen CC, et al. *DNAJB1-PRKACA fusion kinase interacts with β-catenin and the liver regenerative response to drive fibrolamellar hepatocellular carcinoma. Proc Natl Acad Sci U.S.A.* (2017) 114:13076–84. doi: 10.1073/pnas.1716483114

19. Graham RP, Lackner C, Terracciano L, González-Cantú Y, Maleszewski JJ, Greipp PT, et al. Fibrolamellar carcinoma in the Carney complex: PRKAR1A loss instead of the classic DNAJB1-PRKACA fusion. *Hepatol (Baltimore Md.).* (2018) 68:1441–7. doi: 10.1002/hep.29719

20. Hirsch TZ, Negulescu A, Gupta B, Caruso S, Noblet B, Couchy G, et al. BAP1 mutations define a homogeneous subgroup of hepatocellular carcinoma with fibrolamellar-like features and activated PKA. *J Hepatol.* (2020) 72:924–36. doi: 10.1016/j.jhep.2019.12.006

21. Adli M. The CRISPR tool kit for genome editing and beyond. *Nat Commun.* (2018) 9:1911. doi: 10.1038/s41467-018-04252-2

22. Mali P, Yang L, Esvelt KM, Aach J, Guell M, DiCarlo JE, et al. RNA-guided human genome engineering via Cas9. *Science*. (2013) 339:823–6. doi: 10.1126/science.1232033

23. Cong L, Ran FA, Cox D, Lin S, Barretto R, Habib N, et al. Multiplex genome engineering using CRISPR/Cas systems. *Science*. (2013) 339:819–23. doi: 10.1126/science.1231143

24. Xue W, Chen S, Yin H, Tammela T, Papagiannakopoulos T, Joshi NS, et al. CRISPR-mediated direct mutation of cancer genes in the mouse liver. *Nature*. (2014) 514:380–4. doi: 10.1038/nature13589

25. Weber J, Öllinger R, Friedrich M, Ehmer U, Barenboim M, Steiger K, et al. *CRISPR/Cas9 somatic multiplex-mutagenesis for high-throughput functional cancer genomics in mice*. *Proc Natl Acad Sci U.S.A*. (2015) 112:13982–7. doi: 10.1073/pnas.1512392112

26. Maresch R, Mueller S, Veltkamp C, Öllinger R, Friedrich M, Heid I, et al. Multiplexed pancreatic genome engineering and cancer induction by transfection-based CRISPR/Cas9 delivery in mice. *Nat Commun*. (2016) 7:10770. doi: 10.1038/ncomms10770

27. Zuckermann M, Hovestadt V, Knobbe-Thomsen CB, Zapatka M, Northcott PA, Schramm K, et al. Somatic CRISPR/Cas9-mediated tumour suppressor disruption enables versatile brain tumour modelling. *Nat Commun*. (2015) 6:7391. doi: 10.1038/ncomms8391

28. Platt RJ, Chen S, Zhou Y, Yim MJ, Swiech L, Kempton HR, et al. CRISPR-Cas9 knockin mice for genome editing and cancer modeling. *Cell*. (2014) 159:440–55. doi: 10.1016/j.cell.2014.09.014

29. Rüland L, Andreatta F, Massalini S, Chuva de Sousa Lopes S, Clevers H, Hendriks D, et al. Organoid models of fibrolamellar carcinoma mutations reveal hepatocyte transdifferentiation through cooperative BAP1 and PRKAR2A loss. *Nat Commun*. (2023) 14:2377. doi: 10.1038/s41467-023-37951-6

30. Dinh TA, Jewell ML, Kanke M, Francisco A, Sritharan R, Turnham RE, et al. MicroRNA-375 suppresses the growth and invasion of fibrolamellar carcinoma. *Cell Mol Gastroenterol Hepatol*. (2019) 7:803–17. doi: 10.1016/j.jcmgh.2019.01.008

31. Dinh TA, Vitucci EC, Wauthier E, Graham RP, Pitman WA, Oikawa T, et al. Comprehensive analysis of the cancer genome atlas reveals a unique gene and non-coding RNA signature of fibrolamellar carcinoma. *(Nature) Sci Rep*. (2017) 7:44653. doi: 10.1038/srep44653

32. Dinh TA, Sritharan R, Smith FD, Francisco AB, Ma RK, Bunaciu RP, et al. Hotspots of aberrant enhancer activity in fibrolamellar carcinoma reveal candidate oncogenic pathways and therapeutic vulnerabilities. *Cell Rep*. (2020) 31:107509. doi: 10.1016/j.celrep.2020.03.073

33. Corrò C, Novellasdemunt L, Li VSW. *A brief history of organoids*. *Am J Physiol Cell Physiol*. (2020) 319:C151–c165. doi: 10.1152/ajpcell.00120.2020

34. Minuth W, Sittinger M, Kloth S. Tissue engineering: generation of differentiated artificial tissues for biomedical applications. *Cell Tissue Res*. (1998) 291:1–11. doi: 10.1007/s004410050974

35. Clevers H. Modeling development and disease with organoids. *Cell*. (2016) 165:1586–97. doi: 10.1016/j.cell.2016.05.082

36. Broutier L, Mastrogiovanni G, Verstegen MM, Francies HE, Gavarró LM, Bradshaw CR, et al. Human primary liver cancer-derived organoid cultures for disease modeling and drug screening. *Nat Med*. (2017) 23:1424–35. doi: 10.1038/nm.4438

37. Zhao Y, Li ZX, Zhu YJ, Fu J, Zhao XF, Zhang YN, et al. Single-cell transcriptome analysis uncovers intratumoral heterogeneity and underlying mechanisms for drug resistance in hepatobiliary tumor organoids. *Adv Sci (Weinh)*. (2021) 8:e2003897. doi: 10.1002/advs.202003897

38. Pamarthy S, Sabaawy HE. Patient derived organoids in prostate cancer: improving therapeutic efficacy in precision medicine. *Mol Cancer*. (2021) 20:125. doi: 10.1186/s12943-021-01426-3

39. Hu Y, Sui X, Song F, Li Y, Li K, Chen Z, et al. Lung cancer organoids analyzed on microwell arrays predict drug responses of patients within a week. *Nat Commun*. (2021) 12:2581. doi: 10.1038/s41467-021-22676-1

40. Hill SJ, Decker B, Roberts EA, Horowitz NS, Muto MG, Worley MJ Jr, et al. Prediction of DNA repair inhibitor response in short-term patient-derived ovarian cancer organoids. *Cancer Discovery*. (2018) 8:1404–21. doi: 10.1158/2159-8290.CD-18-0474

41. Sachs N, de Ligt J, Kopper O, Gogola E, Bounova G, Weeber F, et al. A living biobank of breast cancer organoids captures disease heterogeneity. *Cell*. (2018) 172:373–386.e10. doi: 10.1016/j.cell.2017.11.010

42. Narayan NJC, Requena D, Lalazar G, Ramos-Espiritu L, Ng D, Levin S, et al. Human liver organoids for disease modeling of fibrolamellar carcinoma. *Stem Cell Rep*. (2022) 17:1874–88. doi: 10.1016/j.stemcr.2022.06.003

43. Kretzschmar K. Cancer research using organoid technology. *J Mol Med (Berl)*. (2021) 99:501–15. doi: 10.1007/s00109-020-01990-z

44. Kubota H, Reid LM. Clonogenic hepatoblasts, common precursors for hepatocytic and biliary lineages, are lacking classical major histocompatibility complex class I antigen. *Proc Natl Acad Sci United States America*. (2000) 97:12132–7. doi: 10.1073/pnas.97.22.12132

45. Zhang W, Cui Y, Du Y, Yang Y, Fang T, Lu F, et al. Liver cell therapies: cellular sources and grafting strategies. *Front Med*. (2023) 17:432–57. doi: 10.1007/s11684-023-1002-1

46. Chan GKL, Maisel S, Hwang YC, Pascual BC, Wolber RRB, Vu P, et al. Oncogenic PKA signaling increases c-MYC protein expression through multiple targetable mechanisms. *Elife*. (2023) 12:e69521. doi: 10.7554/eLife.69521.sa2

47. Lalazar G, Requena D, Ramos-Espiritu L, Ng D, Bhola PD, de Jong YP, et al. Identification of novel therapeutic targets for fibrolamellar carcinoma using patient-derived xenografts and direct-from-patient screening. *Cancer Discovery*. (2021) 11:2544–63. doi: 10.1158/2159-8290.CD-20-0872

48. Tsuji W, Valentin JE, Marra KG, Donnenberg AD, Donnenberg VS, Rubin JP. An animal model of local breast cancer recurrence in the setting of autologous fat grafting for breast reconstruction. *Stem Cells Transl Med*. (2018) 7:125–34. doi: 10.1002/sctm.17-0062

49. Sugisawa N, Miyake K, Higuchi T, Oshiro H, Park JH, Kawaguchi K, et al. High incidence of lymph-node metastasis in a pancreatic-cancer patient-derived orthotopic xenograft (PDOX) NOG-mouse model. *Anticancer Res*. (2022) 42:739–43. doi: 10.21873/anticanres.15532

50. Asgharpour A, Cazanave SC, Pacana T, Seneshaw M, Vincent R, Banini BA, et al. A diet-induced animal model of non-alcoholic fatty liver disease and hepatocellular cancer. *J Hepatol*. (2016) 65:579–88. doi: 10.1016/j.jhep.2016.05.005

51. Kabeer F, Beverly LJ, Darrasse-Jèze G, Podsypanina K. Methods to study metastasis in genetically modified mice. *Cold Spring Harb Protoc*. (, 2016) 2016: pdb.top069948. doi: 10.1101/pdb.top069948

52. Fior R, Póvoa V, Mendes RV, Carvalho T, Gomes A, Figueiredo N, et al. Single-cell functional and chemosensitive profiling of combinatorial colorectal therapy in zebrafish xenografts. *Proc Natl Acad Sci United States America*. (2017) 114:E8234–43. doi: 10.1073/pnas.1618389114

53. de Oliveira S, Houseright RA, Graves AL, Golenberg N, Korte BG, Miskolci V, et al. Metformin modulates innate immune-mediated inflammation and early progression of NAFLD-associated hepatocellular carcinoma in zebrafish. *J Hepatol*. (2019) 70:710–21. doi: 10.1016/j.jhep.2018.11.034

54. Huang SJ, Cheng CL, Chen JR, Gong HY, Liu W, Wu JL. Inducible liver-specific overexpression of gankyrin in zebrafish results in spontaneous intrahepatic cholangiocarcinoma and hepatocellular carcinoma formation. *Biochem Biophys Res Commun*. (2017) 490:1052–8. doi: 10.1016/j.bbrc.2017.06.164

55. de Oliveira S, Houseright RA, Korte BG, Huttenlocher A. DnaJ-PKAc fusion induces liver inflammation in a zebrafish model of fibrolamellar carcinoma. *Dis Models Mech*. (2020) 13:dmm042564. doi: 10.1242/dmm.042564

56. Kersten K, de Visser KE, van Miltenburg MH, Jonkers J. Genetically engineered mouse models in oncology research and cancer medicine. *EMBO Mol Med*. (2017) 9:137–53. doi: 10.15252/emmm.201606857

57. Farber BA, Lalazar G, Simon EP, Hammond WJ, Requena D, Bhanot UK, et al. Non coding RNA analysis in fibrolamellar hepatocellular carcinoma. *Oncotarget*. (2018) 9:10211–27. doi: 10.18632/oncotarget.23325

58. Rangarajan A, Weinberg RA. Opinion: Comparative biology of mouse versus human cells: modelling human cancer in mice. *Nat Rev Cancer*. (2003) 3:952–9. doi: 10.1038/nrc1235

59. Santiago-Reynoso J, Zamaripa-Martínez KS, Dorantes-Loya JM, Gaytán-Fernández GJ, Apolinar-Jiménez E, Paz-Gómez F, et al. Hepatocellular carcinoma of fibrolamellar type in an adolescent: case report and literature review. *Gastrointestinal Tumors*. (2019) 6:43–50. doi: 10.1159/000499581

60. Francisco AB, Li J, Farghli AR, Kanke M, Shui B, Munn PR, et al. Chemical, molecular, and single cell analysis reveal chondroitin sulfate proteoglycan aberrancy in fibrolamellar carcinomas. *Cancer Res Commun*. (2023) 2:663–78. doi: 10.1158/2767-9764.CRC-21-0177

61. Wang Z, Arnold K, Dhurandhare VM, Xu Y, Liu J. Investigation of the biological functions of heparan sulfate using a chemoenzymatic synthetic approach. *RSC Chem Biol*. (2021) 2:702–12. doi: 10.1039/D0CB00199F

62. Nguyen TK, Raman K, Tran VM, Kuberan B. Investigating the mechanism of the assembly of FGF1-binding heparan sulfate motifs. *FEBS Lett*. (2011) 585:2698–702. doi: 10.1016/j.febslet.2011.07.024

63. Xu D, Arnold K, Liu J. Using structurally defined oligosaccharides to understand the interactions between proteins and heparan sulfate. *Curr Opin In Struct Biol*. (2018) 50:155–61. doi: 10.1016/j.sbi.2018.04.003

64. Vlodavsky I, Barash U, Nguyen HM, Yang SM, Ilan N. Biology of the heparanase-heparan sulfate axis and its role in disease pathogenesis. *Semin Thromb Hemost*. (2021) 47:240–53. doi: 10.1016/j.sbi.2018.04.003

65. Zong C, Venot A, Li X, Lu W, Xiao W, Wilkes JL, et al. Heparan sulfate microarray reveals that heparan sulfate-protein binding exhibit different ligand requirements. *J Am Chem Soc*. (2017) 139:9534–43. doi: 10.1021/jacs.7b01399

66. Zhang W, Xu Y, Wang X, Oikawa T, Su G, Wauthier E, et al. Fibrolamellar carcinomas–growth arrested by paracrine signals complexed with synthesized heparan sulfate oligosaccharides. *Matrix Biol*. (2023) 121:194–216. doi: 10.1016/j.matbio.2023.06.008

67. Zhang W, Cui Y, Lu M, Xu M, Li Y, Song H, et al. Hormonally and chemically defined expansion conditions for organoids of biliary tree Stem Cells. *Bioact Mater*. (2024) 41:672–95. doi: 10.1016/j.bioactmat.2024.08.010

68. Liu J, Linhardt RJ. Chemoenzymatic synthesis of heparan sulfate and heparin. Review. *Nat Prod Rep*. (2014) 31:1676–85. doi: 10.1039/C4NP00076E

69. Patel VN, Lombaert IM, Cowherd SN, Shworak NW, Xu Y, et al. Hs3st3-modified heparan sulfate controls KIT+ progenitor expansion by regulating 3-O-sulfotransferases. *Dev Cell*. (2014) 29:662–73. doi: 10.1016/j.devcel.2014.04.024

frontiers | Frontiers in Immunology

TYPE Review
PUBLISHED 12 December 2024
DOI 10.3389/fimmu.2024.1501659

OPEN ACCESS

EDITED BY
Yue Wang,
Second Military Medical University, China

REVIEWED BY
Huabin Ma,
First Affiliated Hospital of Fujian Medical University, China
Jingyuan Ning,
Chinese Academy of Medical Sciences and Peking Union Medical College, China

*CORRESPONDENCE
Dongxuan Li
xhyyldx@163.com
Yi Wang
cdxhyywy@163.com
Zhongyu Han
hzyczy1997@163.com

†These authors have contributed equally to this work

RECEIVED 25 September 2024
ACCEPTED 29 November 2024
PUBLISHED 12 December 2024

CITATION
Chen H, Lin Y, Chen J, Luo X, Kan Y, He Y, Zhu R, Jin J, Li D, Wang Y and Han Z (2024) Targeting caspase-8: a new strategy for combating hepatocellular carcinoma. *Front. Immunol.* 15:1501659. doi: 10.3389/fimmu.2024.1501659

Targeting caspase-8: a new strategy for combating hepatocellular carcinoma

Haoran Chen[1†], Yumeng Lin[2†], Jie Chen[1], Xuemei Luo[1], Yubo Kan[3], Yuqi He[4], Renhe Zhu[4], Jiahui Jin[5], Dongxuan Li[1*], Yi Wang[1*] and Zhongyu Han[1*]

[1]Department of General Surgery, Chengdu Xinhua Hospital Affiliated to North Sichuan Medical College, Chengdu, China, [2]Health Management Center, Nanjing Tongren Hospital, School of Medicine, Southeast University, Nanjing, China, [3]Sichuan Provincial Woman's and Children's Hospital/The Affiliated Women's and Children's Hospital of Chengdu Medical College, Chengdu, China, [4]Department of Blood Transfusion, Lu'an People's Hospital, the Affiliated Hospital of Anhui Medical University, Lu'an, China, [5]Department of gastroenterology, Baoji Central Hospital, Baoji, China

Hepatocellular carcinoma (HCC) represents the most prevalent form of primary liver cancer and has a high mortality rate. Caspase-8 plays a pivotal role in an array of cellular signaling pathways and is essential for the governance of programmed cell death mechanisms, inflammatory responses, and the dynamics of the tumor microenvironment. Dysregulation of caspase-8 is intricately linked to the complex biological underpinnings of HCC. In this manuscript, we provide a comprehensive review of the regulatory roles of caspase-8 in apoptosis, necroptosis, pyroptosis, and PANoptosis, as well as its impact on inflammatory reactions and the intricate interplay with critical immune cells within the tumor microenvironment, such as tumor-associated macrophages, T cells, natural killer cells, and dendritic cells. Furthermore, we emphasize how caspase-8 plays pivotal roles in the development, progression, and drug resistance observed in HCC, and explore the potential of targeting caspase-8 as a promising strategy for HCC treatment.

KEYWORDS

caspase-8, hepatocellular carcinoma, apoptosis, necroptosis, pyroptosis, PANoptosis, tumor microenvironment

1 Introduction

Cancer has been a grave health issue worldwide for a long time. Through remarkable advancements in medical technology, the overall survival rates for numerous cancers have significantly improved in comparison with those reported in previous decades. Nevertheless, the survival rates for certain cancers, such as liver cancer, still fall short of satisfactory levels. Liver cancer ranks among the deadliest of malignancies, with a 5-year relative survival rate of only 22% (1). Hepatocellular carcinoma (HCC), in particular, is the

foremost subtype of liver cancer, accounting for approximately 90% of all primary liver cancer cases (2). The primary risk factors contributing to HCC differ across geographical locations; however, they commonly include viral hepatitis types B and C (HBV, HCV), alcohol-related liver diseases, nonalcoholic fatty liver diseases, autoimmune hepatitis, and other related conditions (3). Regardless of the specific aetiology, ongoing damage to hepatocytes is a central factor in the development of chronic hepatitis, liver fibrosis, cirrhosis, and ultimately, the development of HCC (4). To maintain the normal functionality and homeostasis of the liver, hepatocytes require ongoing renewal and repair, and damaged hepatocytes are eliminated through programmed cell death (PCD), which helps to prevent the accumulation of potentially harmful mutations (5). However, the persistent PCD of hepatocytes results in the emission of damage-associated molecular patterns (DAMPs). These molecular signals, in turn, go on to trigger immune cell activation and inflammatory responses. This establishes a vicious inflammation-PCD cycle that exacerbates liver injury (5). Moreover, triggering PCD in tumor cells is a vital component of radiotherapy and chemotherapy for treating HCC (6). The unfavorable prognosis of HCC is closely associated with the persistent presence of cirrhosis and resistance to radiotherapy/chemotherapy. Therefore, targeting the crucial links in PCD can significantly increase the therapeutic effect on HCC, decrease the recurrence rate, and ultimately lower the mortality rate.

Caspase-8, a cysteinyl aspartate specific proteinase (caspase), plays a central role in a myriad of signaling pathways and is crucial for the regulation of PCD, immune cell homeostasis, and cytokine production (7). In HCC, dysregulation of caspase-8 expression is often observed, leading to functional imbalances within HCC cells and the tumor microenvironment (TME) (8, 9). This imbalance can have profound consequences for the progression, aggressiveness, and drug resistance of HCC (8). Consequently, a comprehensive understanding of the roles and regulatory mechanisms of caspase-8 in the context of HCC is essential for crafting impactful treatment strategies aimed at combating this cancer.

This manuscript addresses in on the latest research developments, aiming to dissect how caspase-8 orchestrates the regulation of PCD, inflammation, and the TME. Furthermore, we explore the implications of caspase-8 in the aetiology of HCC and evaluates the potential of caspase-8 as a therapeutic strategy for HCC treatment.

2 Caspase family and caspase-8

The caspase family is classified within the interleukin-1β-converting enzyme family of proteases, which are crucial components of cellular processes (10, 11). Structurally, all members of the caspase family feature an active site containing a cysteine (12). During the process of peptide bond hydrolysis, these enzymes utilize the cysteine side chain as a nucleophile, allowing them to specifically cleave the peptide bond after the specific aspartic acid residue within the target protein (13, 14). This cleavage typically results in the activation or inactivation of the substrate rather than its complete degradation (15). In cells, caspases typically exist in an inactive zymogen form known as procaspases (16). Under specific conditions, procaspases undergoes dimerization or oligomerization, leading to their activation and the formation of caspases, which perform proteolytic functions (17). The proteolytic activity of caspases is achieved through their caspase domain (16). During the activation process, the protease effector domain of pro-caspase undergoes cleavage, yielding a large subunit (approximately 20 kDa) and a small subunit (approximately 10 kDa), subsequently forming an enzymatically active complex (18). The caspase family consists of 14 members (caspase-1 to -14). On the basis of their amino acid sequence homology and functions, caspases-1 to -13 are classified into apoptosis activators, apoptosis executioners and inflammatory subfamilies (6). Caspase-14 is unrelated to apoptosis and inflammation and is instead associated with epithelial cell differentiation (19).

Caspase-8, also known as FLICE, MACH, or Mch5, belongs to the caspase family (20, 21). Inside cellular structures, the default state of caspase-8 is that of its dormant precursor, procaspase-8 (22). This includes a C-terminal domain that consists of two subunits: a larger one, p18, and a smaller one, p10 (23). P18 houses an active catalytic cysteine residue, which is crucial for its enzymatic activity, and p10 acts as a substrate-binding domain that is responsible for recognizing and binding to specific target proteins (24). Additionally, at the N-terminus, procaspase-8 possesses two death effector domains (DED1 and DED2), which are instrumental in the initial recognition of upstream signals and the subsequent activation of the zymogen (25). During the activation process, procaspase-8 is recruited by an array of upstream signals, such as the death-inducing signaling complex (DISC), leading to the formation of dimers (26, 27). These dimers then undergo two rounds of self-cleavage, culminating in the assembly of an enzymatically active tetramer consisting of two p18 and two p10 subunits, which constitute the active form of caspase-8 (24).

Caspase-8 is a multifunctional protein that is instrumental in the complex control mechanisms of PCD, inflammation, and innate immune responses. In the subsequent sections, we further explore these pivotal functions and their potential implications.

3 Caspase-8 and PCD

3.1 Caspase-8 and apoptosis

Apoptosis is a pivotal form of PCD first characterized in 1972 (28). Morphologically, apoptotic cells undergo shrinkage, display nuclear disintegration, exhibit plasma membrane blebbing, and ultimately form distinct apoptotic bodies (28–30). Apoptotic cells do not release inflammatory mediators but are quickly phagocytosed by nearby macrophages, making apoptosis a low-immunogenic form of PCD (28). Caspases are the central component of apoptosis. Apoptosis initiates upon the reception of apoptotic signals, and depending on the different sources and triggering mechanisms of these signals, apoptosis is primarily divided into extrinsic and intrinsic pathways (31, 32). The intrinsic pathway (mitochondrial pathway) is activated in response to cellular stressors or injuries such

as DNA damage and oxidative stress. Caspase-9 serves as the primary apoptosis activator in this pathway (31, 33). Conversely, the extrinsic pathway, commonly designated the death receptor (DR) pathway, is set into motion by extracellular apoptotic signals, with caspase-8 acting as the main apoptosis activator in this cascade (32). This pathway is initiated by the interaction of DRs (such as Fas and TNFR1), which are located on the cell surface, with their specific ligands (34). For example, upon binding with Fas ligand (FasL), Fas undergoes conformational alterations, facilitating the recruitment of the adaptor protein Fas-associated death domain (FADD) (35). FADD contains a DED and facilitates the assembly of procaspase-8 through the DED: DED interaction (36). As previously mentioned, procaspase-8 comprises DED1 and DED2. The interaction between FADD-DED and DED1 leads to the binding of pro-caspase-8 with FADD, culminating in the assembly of the DISC (37, 38). DED2 subsequently recruits an additional procaspase-8 and binds to its DED1, initiating dimerization and autocatalytic cleavage of procaspase-8 (39). The activated caspase-8 then cleaves multiple downstream target proteins, such as the apoptosis executioner caspases, thereby leading to activation of the extrinsic apoptosis cascade.

Moreover, caspase-8 is also instrumental in initiating the intrinsic apoptotic pathway. It achieves this by cleaving the Bcl-2 homology 3-interacting domain death agonist (BID) to generate a truncated BID (tBID), which subsequently binds to the Bcl-2-associated X protein (Bax) (40). This interaction precipitates alterations in mitochondrial membrane permeability and the release of cytochrome-c (cyt-c), culminating in the activation of caspase-9 and the induction of intrinsic apoptosis (41).

3.2 Caspase-8 and necroptosis

Necroptosis is a mixed-lineage kinase-like (MLKL)-dependent type of PCD. Once activated, MLKL enhances plasma membrane permeability, resulting in cell rupture, the liberation of intracellular contents, and the ensuing inflammatory reactions within necroptotic cells (42). Necroptosis is induced by upstream signals such as tumor necrosis factor receptor (TNFR) superfamily receptors, toll-like receptor (TLR)-3/4, and Z-DNA binding protein-1 (ZBP1) (43–46). Necroptosis is a type of caspase-8-independent PCD, yet caspase-8 plays a pivotal regulatory role in the process of necroptosis.

In the classical DR pathway, caspase-8 plays a role in inhibiting necroptosis. Using TNFR1 as an example, upon recognition of TNF-α, TNFR1 recruits receptor-interacting serine/threonine-protein kinase 1 (RIPK1) and the TNF receptor-associated death domain (TRADD) at its tail to form complex I (47, 48). In addition, proteins such as cellular inhibitor of apoptosis protein 1/2 (cIAP1/2), TNF receptor-associated factor 2/5 (TRAF2/5), transforming growth factor-β-activated kinase 1 (TAK1), and IκB kinases (IKKs) are also recruited and can regulate the activity of RIPK1 by modulating its posttranslational modifications, including deubiquitination, ubiquitination, and phosphorylation (49–52). Deubiquitination of RIPK1 promotes the dissociation of RIPK1 and TRADD from complex I and the formation of complex II (34).

Upon activation, caspase-8 initiates the assembly of the RIPK1-TRADD-FADD-caspase-8 complex (complex IIa), leading to apoptosis (53). Under conditions of high intracellular RIPK3 levels, the formation of complex IIb or IIc is dependent on the activity of caspase-8. When caspase-8 is activated, RIPK1-RIPK3-FADD-caspase-8 forms the rippoptosome (complex IIb) (54). In the rippoptosome, caspase-8 forms a heterodimer with cellular-FLICE inhibitory protein (cFLIP) to exert an inhibitory effect. cFLIP is a homologue of caspase-8 that lacks proteolytic activity (55). Owing to its low activity, the caspase-8-cFLIP heterodimer is capable of cleaving RIPK1, effectively blocking necroptosis (Figure 1) (56, 57). Additionally, this heterodimer suppresses the apoptotic-promoting function of caspase-8 while promoting cell survival (58, 59). In the absence of caspase-8, RIPK1-RIPK3-MLKL forms the necrosome (complex IIc), sequentially activating RIPK3 and MLKL, leading to the phosphorylation and oligomerization of MLKL, ultimately resulting in membrane disruption and necroptosis (60–62).

3.3 Caspase-8 and pyroptosis

Pyroptosis is a form of gasdermin (GSDM)-mediated PCD that plays a crucial role in innate immune responses and the elimination of pathogens (63, 64). The GSDM family comprises six members: GSDMA-E and PJVK. Among these, GSDMA-E feature two distinct structural domains, the N-terminal pore-forming domain (N-PFD) and the C-terminal regulatory domain (C-RD), which contribute to their unique functional roles (65, 66). The activated N-PFD mediates the formation of pores in the cell membrane, whereas the C-RD interacts with the N-PFD through a linker region to exert self-inhibition under physiological conditions (66). When the linker region is cleaved by upstream signals such as caspase and granzyme B, N-PFD is released, allowing GSDM to oligomerize at the plasma membrane and form pores, which facilitate the release of cellular contents and inflammatory mediators, ultimately triggering pyroptosis (66–68). Consequently, pyroptotic cells also display necrotic-like characteristics, including cell swelling and rupture (69).

Caspase-8 participates in the regulation of both the canonical and noncanonical pathways of pyroptosis. In the canonical pathway, an inflammasome is assembled through the interaction of pattern recognition receptors (PRRs), such as NOD-like receptor pyrin domain-containing protein 3 (NLRP3) and NLRC4, the adaptor protein ASC, and procaspase-1 (70). This complex activates caspase-1, leading to the cleavage of GSDMD and ultimately inducing pyroptosis. Furthermore, caspase-1 also mediates the cleavage of pro-IL-1β and pro-IL-18, thereby enhancing the activation and release of the inflammatory mediators interleukin-1 (IL-1β) and IL-18 (71). Caspase-8 can promote the classical pyroptosis pathway without relying on enzymatic activity. Research has shown that mutant caspase-8 ($CASP8^{C362A}$), which lacks enzymatic activity, can promote ASC activation and activate caspase-1 (7). Phylogenetic analysis revealed

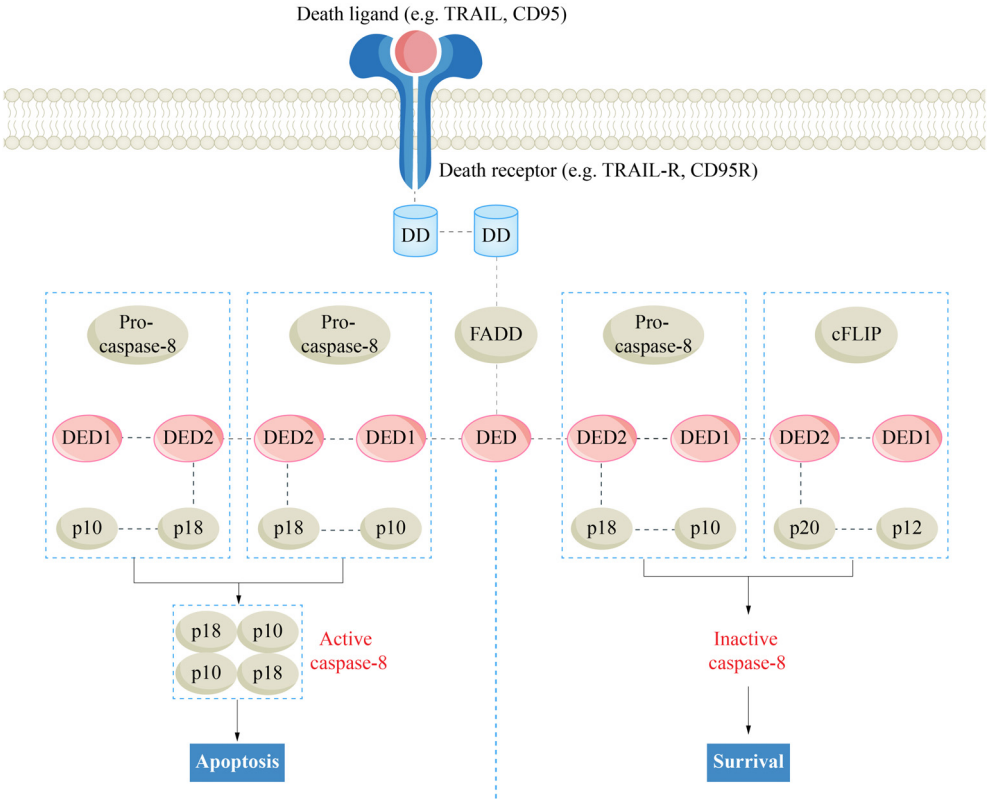

FIGURE 1
The regulatory effect of cFlip on death receptor pathway apoptosis. Caspase-8, cysteinyl aspartate specific proteinase 8; cFLIP, cellular-FLICE inhibitory protein; DD, death domain; DED, death effector domain; FADD, Fas-associated death domain.

that the DED2 domain of procaspase-8 and the pyrin domain (PYD) of ASC are located on the same branch (72). In the noncanonical pathway, caspase-8 can cleave GSDMC, GSDMD and GSDME to trigger pyroptosis. Caspase-8 can cleave GSDMD independently of caspase-1 and confer susceptibility to TNF-induced lethality (73). The metabolite α-KG elevates intracellular ROS levels, oxidizing DR6. Activated DR6 recruits caspase-8 and GSDMC, triggering the caspase-8-GSDMC pathway (74). In addition, in the presence of GSDMC and nuclear programmed cell death protein 1 (nPD-L1), TNF-α-activated caspase-8 can trigger pyroptosis through the caspase-8-GSDMC pathway (75). Furthermore, elevated TNF-α can also activate caspase-8 and caspase-3 through the DR pathway, triggering the transition from caspase-3-GSDME-mediated apoptosis to pyroptosis (76).

3.4 Caspase-8 and PANoptosis

PANoptosis is a newly discovered type of PCD that possesses the key features of pyroptosis, apoptosis, and/or necroptosis, but its mechanism cannot be solely explained by these types of PCD (77). The PANoptosome serves as the molecular platform that triggers PANoptosis, and its assembly and activation are crucial for the simultaneous involvement of pyroptosis, apoptosis, and/or necroptosis (78). A typical PANoptosome is composed of sensors (ZBP1, AIM2, RIPK1 and NLRP12), adaptors (ASC and FADD), and catalytic effectors (RIPK1, RIPK3, caspase-1 and caspase-8) (79, 80). The assembly of the PANoptosome is initiated by various factors, such as cellular stress or microbial infection. Once specific sensors are activated by these triggers, they initiate the assembly process of the PANoptosome. In this process, the interaction of conserved domains of the same or different types between proteins (such as CARD, DD, DED and PYD) provides the molecular scaffold for the assembly of the PANoptosome. The PANoptosome, once activated, initiates a cascade that activates downstream cell death effectors, culminating in a lytic form of inflammatory cell death (Figure 2) (81, 82).

Caspase-8 plays indispensable regulatory roles in PANoptosis and constitutes a fundamental part of the PANoptosome. As mentioned, caspase-8 facilitates apoptosis via the DR pathway, mitigates necroptosis by suppressing RIPK1, and further triggers pyroptosis by activating ASC and GSDMs. The dynamic activity of caspase-8 potentially shapes the plasticity of the intricate PANoptosis process. By precisely targeting the activity of caspase-8, scientists may develop innovative therapeutic approaches aimed at combating HCC.

4 Caspase-8 and inflammation

In addition to its regulatory function in PCD, caspase-8 also plays crucial roles in modulating inflammation, encompassing both anti-inflammatory and proinflammatory dual functions.

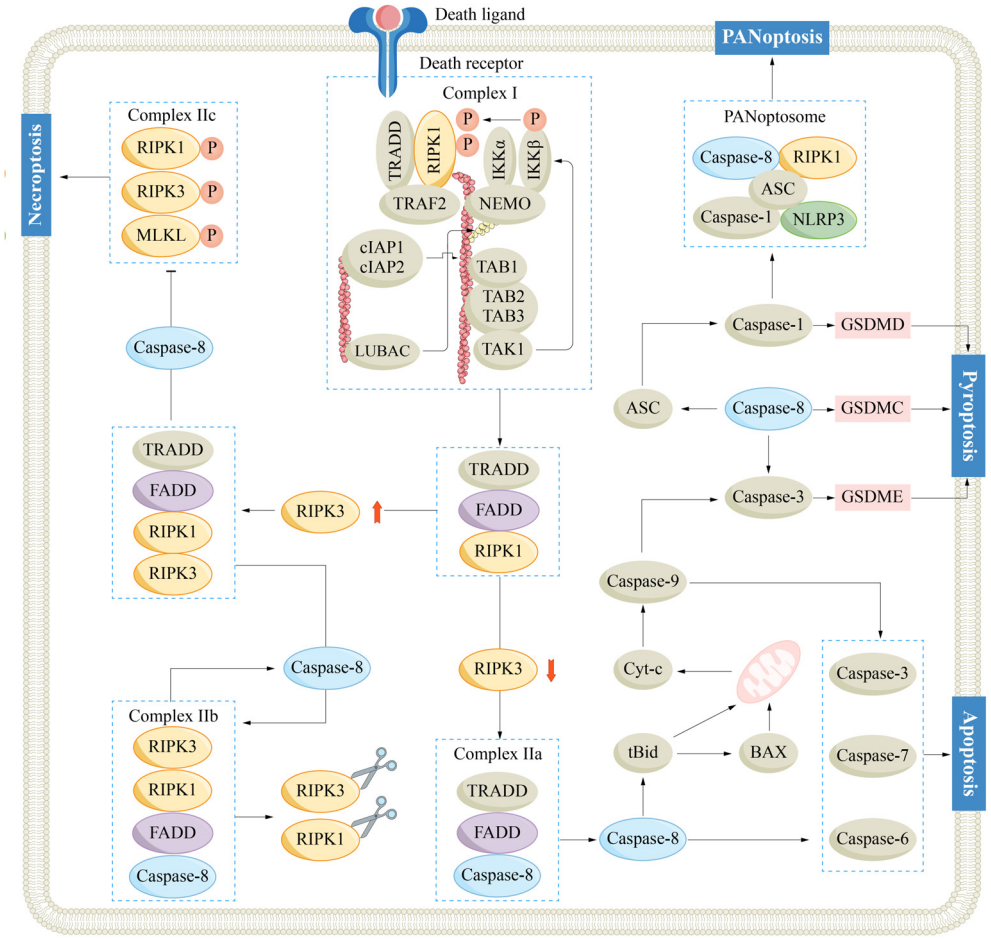

FIGURE 2
Mechanisms of caspase-8 regulated apoptosis, necroptosis, pyroptosis and PANoptosis. ASC, adaptor apoptosis-associated speck-like protein containing a CARD; BAX, Bcl-2-associated X protein; Bid, Bcl-2 homology 3 interacting domain death agonist; Caspase-1/3/6/7/8/9, cysteinyl aspartate specific proteinase 1/3/8/9; cIAP, cellular inhibitor of apoptosis protein; cyt-c, cytochrome-c; FADD, Fas-associated death domain; GSDM, gasdermin; IKK, IκB kinase; IL-1/18, interleukin-1/18; MLKL, mixed-lineage kinase-like; NEMO, nuclear factor-kappaB essential modulator; NLRP3, NOD-like receptor pyrin domain-containing protein 3; RIPK1/3, receptor-interacting serine/threonine-protein kinase 1/3; TAK, transforming growth factor-β-activated kinase 1; TNF, tumor necrosis factor receptor; TRADD, TNF receptor-associated death domain; TRAF2, TNF receptor-associated factor 2.

The anti-inflammatory role of caspase-8 is achieved primarily through promoting apoptosis, inhibiting necroptosis, and suppressing the inflammasome. Caspase-8 plays a crucial role as an important activator of apoptosis, and its activity is essential for apoptosis through the DR pathway. Apoptosis is a form of low-immunogenic PCD that eliminates damaged or infected cells, thus preventing excessive inflammation (83). Necroptosis is initiated when caspase-8 is incapacitated, leading to the activation of RIPK3 and MLKL triggered by TNFR activation. This leads to increased membrane permeability, liberating the cell contents, which triggers inflammatory responses. Caspase-8 can suppress necroptosis by cleaving RIPK1, thereby reducing inflammatory responses (84). Caspase-8 normally functions to inhibit the inflammasome. In dendritic cells (DCs), caspase-8 inhibition enhances the activation of the lipopolysaccharide-induced NLRP inflammasome and the production of IL-1β (85). This effect is related to MLKL but is distinct from the process of necroptosis. Another study revealed that the sole activation of MLKL can mediate NLRP3-dependent processes and the release of IL-1β without the involvement of GSDMD (86). In FADD$^{-/-}$RIPK3$^{-/-}$ myeloid cells, the conformation of inactive caspase-8 changes, potentially promoting the activation of caspase-1/11 and the release of IL-1β and IL-18 through autophagy and cathepsin-B pathway (87).

The proinflammatory effect of Caspase-8 is mediated through promoting pyroptosis and enhancing the maturation of IL-1β. Caspase-8 effectively promotes pyroptosis via both enzymatic and nonenzymatic pathways. Specifically, through its enzymatic activity, caspase-8 directly cleaves GSDMC, GSDMD, and GSDME. Alternatively, it may target downstream caspase-3, subsequently promoting the cleavage of GSDME, ultimately altering membrane permeability and causing the efflux of cellular contents. Furthermore, inactive caspase-8 functions as a protein scaffold, promoting the aggregation and activation of ASC and subsequently activating caspase-1 (88). Caspase-8 can activate caspase-1 via the inflammasome pathway, cleave pro-IL-1β and pro-IL-18, and release them through GSDMD-N pores (89). Caspase-8 can also

promote the maturation of IL-1β independently of caspase-1. For example, in DCs, dectin-1 recognizes fungal and mycobacterial PAMPs, resulting in the formation of the mucosa-associated lymphoid tissue lymphoma translocation protein 1 (MALT1)-caspase-8-ASC inflammasome (90). This complex can cleave pro-IL-1β, and this conversion process remains unaffected by caspase-1 inhibitors.

Caspase-8 can also regulate inflammatory responses by promoting the nuclear factor-kappa B (NF-κB) pathway. NF-κB is a highly conserved transcription factor that participates in the regulation of gene expression, cytokine production, and cell survival, among other processes (91). In normal cells, NF-κB resides in the cytoplasm in an inactive state. The inhibitor of κB (IκB) protein binds to NF-κB, masking its nuclear localization site (92). NF-κB can be activated by various upstream signals such as TNF-α. For example, when TNF-α binds to TNFR1, the IKK complex is activated through adaptor proteins such as TRAF2, mediating the phosphorylation and ubiquitination of the inhibitory protein IκBα (93, 94). This process leads to the inhibition of IκB, which in turn enables the nuclear translocation of NF-κB, subsequently leading to the transcription of downstream genes. Fianco et al. reported that caspase-8 was highly expressed in glioblastoma, which promoted the activation of NF-κB, further increasing the expression of IL-1β, IL-6, and IL-8 (24). In adipocytes, the inhibition of caspase-8 can lead to the downregulation of NF-κB signaling, subsequently causing a decrease in TNF-α levels (83). Davidovich et al. reported that the caspase-8-FADD-RIPK1 complex enhances the production of IL-6 via the NF-κB pathway (58). Caspase-8 functions as a scaffold to promote the aggregation of RIPK1 and FADD, whereas cFLIP inhibits this process owing to its lower affinity for FADD. However, Xia et al. reported that in prostate cancer, caspase-8 upregulates the NF-κB pathway to promote the upregulation of downstream IL-8. This process is independent of its proteolytic activity but requires interaction with cFLIP (95). Existing studies suggest that the assembly of caspase-8 scaffolding is an indispensable initial step for the formation of DISC and NF-κB activation. However, caspase-8's catalytic activity seems redundant for NF-κB activation and the induction of subsequent cytokines (96). How caspase-8 activates RIPK1 and phosphorylates IκBα remains to be clarified.

5 Caspase-8 and HCC

Given the intricate functions of Caspase-8, it plays a pivotal role in the pathogenesis of HCC. As previously discussed, CLDs stemming from diverse causes have been established as significant high-risk factors for HCC (3). Moreover, the chronic hepatocyte apoptosis induced by CLDs and their subsequent regenerative process serve as pivotal mechanisms underlying the pathogenesis of HCC. Caspase-8 can facilitate the timely clearance of impaired hepatocytes, thereby preserving liver health. However, an extended period of hepatocyte apoptosis can be detrimental. Boege et al. reported that caspase-8-induced hepatocyte proliferative stress is a risk factor for HCC independent of the aetiology of CLDs and that the caspase-8-dependent DNA damage response (DDR) relies on the nonapoptotic function of caspase-8 rather than its catalytic activity (8). The caspase-8-FADD-cFLIP-RIPK1 complex coordinates the regulation of cell fate, inflammasome activation, NF-κB activation, cytokine production, and other processes. Additionally, full-length caspase-8, rather than its catalytic activity, can promote the phosphorylation of H2AX (γH2AX) (8). γH2AX is a marker of DNA damage that can facilitate the initiation of DNA damage repair mechanisms (97). Therefore, caspase-8 deficiency or silencing can confer antiapoptotic ability to cells and promote the accumulation of DNA replication errors and mutations, thereby advancing the progression towards HCC.

The nonapoptotic functions of caspase-8 also play a significant role in the progression of HCC. Research has indicated that caspase-8 is overexpressed in certain malignancies, such as HCC, indicating that these tumors can resist apoptosis when caspase-8 is highly expressed (98). Consistently, cFLIP is frequently constitutively overexpressed in HCC cell lines, and its overexpression is associated with an unfavorable tumor prognosis (99). cFLIP is modulated by multiple signaling pathways such as the NF-κB pathway (100). In HCC with high expression of caspase-8, cFLIP not only blocks caspase-8-mediated apoptosis but also modulates NF-κB pathways through the caspase-8-FADD-cFLIP-RIPK1 complex, promoting the survival and drug resistance of HCC (101, 102).

Overall, caspase-8 plays a significant role in the progression of HCC, and additional research is warranted to elucidate the precise mechanisms through which caspase-8 influences HCC development.

6 Caspase-8 and the HCC TME

The TME constitutes an intricate web of diverse cellular and noncellular elements that are intertwined through sophisticated interactions (103). This intricate network profoundly influences tumor initiation, progression, invasive behavior, and resistance to therapeutic interventions. The immunosuppressive TME (ITME) is a critical component of the TME that functions to suppress immune functions. Compared with diverse cellular and acellular elements, the ITME promotes tumor growth, invasion, and metastasis through intricate interactions while simultaneously inhibiting the body's antitumor immune response (104, 105). This intricate milieu holds paramount importance in orchestrating the pathogenesis, progression, metastasis, and development of drug resistance in HCC, underscoring its pivotal role in shaping the tumor's biological behavior and therapeutic responsiveness of tumors. Caspase-8, which serves as a central hub in multiple signaling pathways, plays a pivotal role in the HCC TME, regulating HCC tumor immunity.

6.1 Caspase-8 and TAM

Tumor-associated macrophages (TAMs), which predominantly originate from circulating monocytes, are instrumental in the

progression of HCC, inflammatory response regulation, and immune suppression (106, 107). TAMs can polarize into the M1/M2 phenotype. Furthermore, owing to the plasticity and heterogeneity of macrophages, M1 and M2 TAMs can interconvert on the basis of the specific conditions within the TME (108, 109). Classically activated M1 TAMs are primarily induced by factors such as interferon gamma (IFN-γ), IL-12, and lipopolysaccharide (LPS) (110). They secrete proinflammatory cytokines, thereby stimulating immune surveillance functions. In contrast, M2 TAMs are induced by factors such as IL-4, IL-10, and TGF-β (111). M2 TAMs release inhibitory cytokines and chemokines, thereby facilitating adverse biological processes such as tumor proliferation, tumor angiogenesis, and immune evasion. In the HCC TME, the majority of cytokines tend to promote the polarization of TAMs towards the M2 phenotype, especially in advanced stages, thereby facilitating tumor progression (112). RNA-seq data revealed that HCC samples with higher levels of M2 TAMs had poorer prognoses, and several HCC prognostic markers specific to M2 TAMs were identified (113). Specifically, M2 TAMs actively promote the generation and construction of neovascular networks within tumors by secreting vascular endothelial growth factor (VEGF), providing nutritional support for HCC cell growth (114). Additionally, they release metalloproteinases (MMPs) to degrade the extracellular matrix, thereby enhancing the invasive capabilities of HCC cells (115). Moreover, M2 TAMs further consolidate the immune evasion mechanisms of HCC by suppressing the activity of antitumor immune cells such as natural killer (NK) cells and cytotoxic T lymphocytes (CTLs) and secreting inhibitory cytokines such as TGF-β and IL-10 (116). Notably, TGF-β not only participates in immune suppression but also promotes epithelial–mesenchymal transition in HCC cells. This process augments the migratory and invasive capabilities of HCC cells and may confer cancer stem cell-like properties to them (117).

Caspase-8 is instrumental in guiding macrophage differentiation. In bone marrow cell lines, caspase-8 facilitates transient activation of the NF-κB pathway through its scaffolding function, thereby promoting M0 differentiation. A deficiency in caspase-8 can block M0 differentiation (118). Cuda et al. revealed that caspase-8-mediated regulation of macrophages governs TLR activation and M1 polarization through a RIPK1-dependent mechanism. Inhibition of caspase-8 can lead to the activation of RIPK1/RIPK3, resulting in increased expression of the costimulatory factor CD86 and increased production of IL-1β upon TLR activation (119). Another study reported that CCL2 and IL-6 in the TME can promote the expression of full-length caspase-8 by inducing cFLIP but inhibit the apoptotic function of caspase-8. Subsequently, caspase-8 may function as a scaffold to promote M2 polarization, although the specific mechanism remains unclear (120). Furthermore, Caspase-8 can lead to a decrease in Kupffer cells (hepatic macrophages, KCs) after partial hepatectomy for HCC, which will facilitate tumor cell proliferation and increase the risk of HCC recurrence (121). Mechanistically, caspase-8 is activated through the TNF-α pathway, which promotes the assembly of complex IIb, thereby facilitating KC apoptosis. Additionally, it can also induce KC pyroptosis through RIPK3-dependent caspase-1 activation. Notably, this process does not involve necrosis, and there is no increase in MLKL phosphorylation. A reduction in KCs promotes the recruitment of circulating monocytes, which differentiate into Ly6C^{low} macrophages, facilitating the resolution of inflammation, suppressing T-cell activity, and promoting angiogenesis (121, 122).

6.2 Caspase-8 and T cells

T cells, which stem from lymphoid progenitor cells, undergo multiple developmental stages in the thymus, ultimately differentiating into CD4$^+$/CD8$^+$ single-positive T cells. CD8$^+$ T cells, also called cytotoxic T lymphocytes (CTLs), exhibit moderate affinity for the class I major histocompatibility complex (MHC I). Upon recognition of MHC I antigen stimulation by the T-cell receptor (TCR), CD8$^+$ T cells become activated and proliferate, killing target cells through various mechanisms (123). These include the secretion of cytokines such as IFN-γ and TNF-α, the release of perforin and granzymes, and the induction of apoptosis via Fas/FasL interactions (124, 125). In the HCC TME, CD8$^+$ cells perform immune surveillance functions, but their frequency is often lower than that in nontumorous regions. The exhaustion of CD8$^+$ T cells has been linked to a decrease in overall survival rates in patients with HCC (126–129). CD4$^+$ T cells are also called T helper (Th) cells. After recognizing MHC II antigens, naive CD4$^+$ T cells (Th0) can specialize by differentiating into various subsets of CD4$^+$ T cells. Based on their differential expression of transcription factors, CD4$^+$ T cells can be classified into various subsets (130). These diverse CD4$^+$ T-cell subsets are capable of secreting both proinflammatory and anti-inflammatory cytokines. Regulatory T cells (Tregs, CD4$^+$CD25$^+$Foxp3$^+$ T cells) are essential cells that contribute to immune suppression within the TME (131). Tregs exert immunosuppressive effects primarily through various mechanisms, including the secretion of inhibitory cytokines (such as TGF-β and IL-10) and the expression of inhibitory cell-surface molecules and competitive inhibitory cytokines (such as CTLA-4 and PD-1) (132–134). Suthen et al. reported that exhausted CD8$^+$ T cells and Treg cells are enriched in the hypoxic HCC TME, whereas active CD8$^+$ T cells are excluded (135).

Caspase-8 performs a vital function in regulating T-cell homeostasis and mediating T-cell immune responses. Salmena et al. reported that mutations in caspase-8 can lead to a decrease in the frequency of peripheral T cells, despite normal thymic cellular development (136). Furthermore, these mutations result in the absence of the ability of T cells to produce IL-2 and respond to exogenous IL-2. Similarly, in mice, the specific deletion of caspase-8 in T cells can lead to an age-dependent and fatal immune dysregulation (137). Caspase-8 also has differential effects on Tregs under diverse conditions. Under homeostatic conditions, the caspase-8-mediated DR pathway restricts the population of effector T cells (CCR7^{low}, PD-1^{high}, CTLA-4^{low}, ICOS^{high}, TIGIT^{high}). When caspase-8 expression is specifically inhibited in Treg cells, the function of Tregs remains normal, and the number of effector Tregs increases (138). During inflammation, caspase-8 promotes the survival of Tregs, whereas the inhibition of

caspase-8 leads to Treg death and excessive immune activation. Conventional T cells and Tregs exhibit different sensitivities to necroptosis (139). Compared with conventional T cells, Tregs are more sensitive to emricasan, a caspase-8/cFLIP heterodimer inhibitor, which results in high expression of RIPK3 and MLKL, thereby inducing necroptosis (138). Similarly, Carlos et al. reported that Tregs are also more sensitive to apoptosis than conventional T cells. The level of cFLIP in Tregs is significantly lower than that in control cells, and this deficiency in cFLIP markedly increases the levels of active caspase-3 and caspase-7 in Tregs, thereby increasing the rate of Treg apoptosis (140). Stimulation with TGF-β can increase the expression of cFLIP in Tregs. Caspase-8-related PCD can also regulate T-cell responses. For example, RNA-seq data analysis has revealed that the expression of the key necroptosis factors RIPK1, RIPK3, and MLKL is significantly correlated with the infiltration of HCC $CD8^+$ T cells (141). Furthermore, poly (ADP−ribose) polymerase inhibitor (PARPi) treatment can promote pyroptosis via the GSDMC−caspase-8 pathway in triple-negative breast cancer cells and mediate the infiltration of $CD8^+$ T cells in the TME (142). However, IL-18 produced by pyroptosis has also been linked to poor outcomes in HCC patients, as HCC patients with positive IL-18 receptor expression exhibit lower survival rates (143). Li et al. reported that TLR2 can inhibit caspase-8-mediated IL-18 production and increase the number of functional $CD8^+$ T cells, thereby inhibiting HCC (144). In conclusion, the complex interplay between caspase-8 and T cells needs definitive and direct evidence to elucidate the precise mechanisms by which caspase-8 regulates T cells, especially Tregs, within the HCC TME.

6.3 Caspase-8 and NK cells

NK cells are integral to the innate immune system and possess potent cytotoxic capabilities. NK cells can directly kill target cells by recognizing specific surface features of these cells without relying on antigen recognition or MHC restriction (such as tumor cells with downregulated MHC I) (145, 146). In addition, NK cells are adept at secreting a diverse array of cytokines, such as IFN-γ, GM-CSF, and the chemokines CCL4 and CCL5, which play intricate roles in coordinating immune responses, enhancing inflammatory reactions, and recruiting other immune cells (147). However, within the TME, the activity of NK cells is often severely suppressed (148). Many adverse factors within the TME, including hypoxia, adenosine, TGF-β, and prostaglandin E2, can effectively diminish the activity and function of NK cells (149). Adding to this complexity, the presence of immunosuppressive cell populations such as TAMs and Tregs further exacerbates the inhibition of NK cell immune function (150). Immunotherapy based on NK cells represents a highly promising direction in the field of HCC treatment (151, 152). Xiao et al. reported that Siglec-9 and its ligands are highly expressed on NK cells, inhibiting their antitumor immunity and correlating with poor outcomes of patients with HCC (153). They reported that the small molecule inhibitor MTX-3937, which is designed to target Siglec-9, significantly improves NK cell function and enhances HCC immune surveillance.

Caspase-8 is one of the crucial factors through which NK cells perform their cytotoxic functions. Studies have reported that NK cells can trigger apoptosis in target cells by liberating perforin and granzymes and by activating DRs such as CD95/FAS and TNF-related apoptosis-inducing ligand (TRAIL) receptors on the surface of target cells, thereby activating caspase-8-mediated apoptosis (154–156). Prager et al. reported that NK cells primarily mediate cell death through granzyme B during the first kill. In contrast, in subsequent killing processes, they shift to DR-mediated apoptosis. Prolonged cell-to-cell contact precipitates a reduction in granzyme B and perforin within NK cells, coupled with an increase in CD95L on their surface. This shift triggers a transition in the killing pathways (157). Zhao et al. reported that pyroptosis is the predominant mode of hepatocyte death in patients with HBV-related acute-to-chronic liver failure. In hepatocytes with HBV reactivation, the absence of MHC-I molecules activates cytotoxic NK cells, subsequently triggering GSDMD/caspase-8-dependent pyroptosis in hepatocytes (158). In addition, caspase-8 can modulate the immune response by curbing the overproliferation of NK cells and $CD8^+$ T cells during the expansion phase. Caspase-$8^{-/-}$RIPK$3^{-/-}$ and caspase-$8^{-/-}$RIPK$1^{-/-}$RIPK$3^{-/-}$ mice exhibit higher levels of mouse pathogen murine cytomegalovirus-specific NK cells and $CD8^+$ T cells (159).

6.4 Caspase-8 and dendritic cells

As the body's most powerful antigen-presenting cells, DCs can be classified on the basis of their origin into myeloid DCs (mDCs), plasmacytoid DCs (pDCs), or monocyte-derived DCs (MoDCs) (160, 161). DCs exhibit high levels of MHC I and MHC II, as well as the costimulatory molecules CD80 and CD86 and the adhesion molecules CD40 and CD54 on their surfaces (162, 163). This enables DCs to efficiently capture, process, and present antigens after recognizing them. In the TME, DCs recognize, process, and present tumor antigens, activating T-cell-mediated antitumor immune responses, making them one of the important targets for tumor immunotherapy (164). DC dysfunction is a pivotal contributing factor to the formation of the ITME. Galarreta et al. reported that the activation of β-catenin in HCC can elicit immune evasion and decrease the effectiveness of anti-PD-1 therapy (161). Mechanistically, the activation of b-catenin leads to a reduction in the recruitment of $CD103^+$ DCs. This decrease in DC numbers subsequently results in a decrease in HCC-specific $CD8^+$ T cells. The overexpression of the chemokine CCL5 can reverse this trend, reinstating immune surveillance. Furthermore, in the HCC TME, hypoxic conditions increase the expression of hypoxia-inducible factor-1α (HIF-1α), leading to the overexpression of CD47 and the inhibition of $CD103^+$ DC function (165). By blocking CD47, the capacity of $CD103^+$ DCs to take up tumor DNA is increased, thereby promoting the secretion of CXCL9 and IL-12, activating the cyclic GMP-AMP synthase (cGAS)-stimulator of interferon genes (STING) pathway, and facilitating the recruitment and activation of NK cells within HCC (166). Single-cell RNA sequencing has revealed that in the Scirrhous HCC (SHCC) TME, hypoxic conditions trigger the upregulation of secreted

phosphoprotein 1 (SPP1), which inhibits DC function and impedes T-cell activation through the SPP1–CD44 axis (167).

In DCs, caspase-8 can initiate the maturation of IL-1β. The administration of doxorubicin can trigger the release of IL-1β, a process intimately linked to caspase-8, which can be inhibited by caspase-8 inhibitors (168). Caspase-8-mediated maturation and release of IL-1β rely on the Toll/IL-1R domain-containing adapter-inducing IFN-γ (TRIF). TRIF is crucial in TLR4 signaling and potentially engages in the assembly of caspase-8 signaling complexes. Furthermore, in addition to antigen presentation, immature DCs also exhibit the ability to induce cell death, which is not possible for mature DCs. Vanderheyde et al. reported that MoDCs exhibit a caspase-8-dependent and FADD-independent tumor killing activity (169). This type of apoptosis does not involve the DR pathway, and blocking TNF/TNFR, CD95/CD95 ligand, or TRAIL/TRAIL receptor interactions cannot reverse this process. Conversely, overexpression of Bcl-2 increases the resistance of tumor cells. Varga et al. reported that MoDCs induce caspase-8-dependent apoptosis in Jurkat cells, and that this process can be completely blocked by caspase-8 inhibition (170).

7 Targeting caspase-8 in HCC therapy

Owing to its crucial role in PCD and tumor immunity, targeting caspase-8 presents new opportunities for treating HCC. Chemotherapy and radiotherapy precisely target HCC cells by causing DNA damage, which then initiates cell death. Apoptosis is the predominant pathway for this form of cell death. In HCC, the enzymatic activity of caspase-8 may be suppressed, which allows cancer cells to undergo apoptosis. Consequently, activating caspase-8 can induce apoptosis in these cells, thereby inhibiting the progression and metastasis of HCC. Adiponectin improves HCC partially by increasing the activity of p53 and the expression of TRAIL, and by increasing the levels of caspase-8 and caspase-3, thus promoting the apoptosis in of HCC cells (171). Che et al. reported that Cullin-associated NEDD8-dissociated 1 (CAND1) is highly expressed in HCC and can serve as an independent prognostic factor for HCC patients (172). CAND1 regulates the activity of caspase-8, and knocking down CAND1 can activate caspase-8 and amplify the apoptotic signal through the mutual activation of caspase-8-receptor interacting protein 1 (RIP1), promoting HCC apoptosis. Im et al. reported that HCC highly expresses DNA damage-induced apoptosis suppressor (DDIAS), which inhibits TRAIL-induced apoptosis by suppressing caspase-8 (173). Mechanistically, DDIAS binds to the DED of FADD, inhibiting the recruitment and oligomerization of caspase-8. Furthermore, DDIAS can promote the activation of P90 ribosomal S6 kinase 2 (RSK), leading to the phosphorylation of caspase-8 at the S227 site and promoting the ubiquitination of caspase-8. DDIAS knockdown enhances the sensitivity of HCC to the TRAIL-caspase-8 apoptosis pathway. Jin et al. reported that the long non-coding RNA (LncRNA) CASC2 promotes the expression of caspase-3/8 by acting as a sponge for miR-24 and miR-221, thereby influencing TRAIL-induced tumor cell apoptosis and drug resistance and ultimately improving TRAIL resistance in HCC (174). El-Demiry et al. reported that combined treatment with cisplatin and sunitinib significantly increased the levels of caspase-9 and caspase-8 while significantly reducing RIPK3 levels. Despite reducing necroptosis, sunitinib has been shown to intensify cisplatin-induced apoptosis and amplify oxidative stress, thereby resulting in increased cytotoxicity against HepG2 cells (175). As a key modulator of caspase-8 enzymatic activity, cFLIP is overexpressed in certain HCC patients, contributing to resistance to apoptosis. Inhibition of cFLIP is one of the proposed means to increase the responsiveness of HCC to chemotherapeutic drugs. Luan et al. reported that rocaglamide enhances the sensitivity of HepG2 cells to TRAIL by reducing the expression levels of cFLIP (176). Carlisi et al. reported that suberoylanilide hydroxamic acid (SAHA) can promote the expression of DR5 and inhibit cFLIP, facilitating the rapid activation of caspase-8 induced by TRAIL and HepG2 cell apoptosis, with no effect on primary human hepatocytes (177). Jeon et al. reported that the combined therapy utilizing maritoclax and TRAIL significantly induced apoptosis in HCC cells. Mechanistically, maritoclax enhances the susceptibility of HCC to TRAIL-mediated apoptosis through the downregulation of cFLIP by miR-708 (178). Decoy receptor 3 (DcR3) is overexpressed in various malignant tumors (179). Liang et al. reported that knocking down DcR3 can inhibit the transcription of cFLIP, promote the expression of caspase-8, and induce apoptosis in HepG2 cells (180). Furthermore, the short hairpin DcR3 can also inhibit the activation of the IKK-mediated NF-κB pathway. Overall, reactivating apoptosis in HCC cells by activating caspase-8 or inhibiting its negative regulatory factors could be an effective treatment option for HCC.

In addition to cFLIP, another key factor affecting caspase-8 targeted therapy is caspase-10. Caspase-10 also has two DED domains and is the only caspase similar to caspase-8 (181). Furthermore, caspase-10 possesses the same enzymatic active center QACQG as caspase-8 (182). These structural similarities make it challenging to target caspase-8 selectively. Z-IETD-FMK is an effective caspase-8 specific inhibitor with the sequence Z-Ile-Glu-Thr-Asp-FMK, which highly matches the substrate recognition site of caspase-8, thus allowing it to bind specifically to caspase-8 and inhibit its activity (183). Zhang et al. reported that overexpression of Z-IETD-FMK can inhibit caspase-8 and reduce apoptosis in HCC cells (184). However, there have been no reports of effective caspase-8 specific activators to date, which implies that caspase-8 activators might also inadvertently activate caspase-10. The upregulation of caspase-10 can also modulate the extrinsic apoptotic pathway. Qi et al. reported that bufalin and cinobufagin can promote apoptosis in HCC cells, and both Z-IETD-FMK and Z-AEVD-FMK (caspase-10 inhibitors) can suppress this process. This will affect the accurate assessment of the effects on caspase-8 (185). In addition, the activation of caspase-10 has a regulatory effect on the activity of caspase-8. Mohr et al. reported that 5-fluorouracil can induce caspase-8-mediated apoptosis in tumor cells (186). In this process, caspase-10 is upregulated in an ataxia telangiectasia mutated and Rad3-related kinase (ATR)-dependent manner and forms a complex known as the FADDosome with caspase-8, FADD, RIPK1, and TRAF2. This complex mediates the ubiquitination and degradation of cFLIP by TRAF2, leading to the activation of

caspase-8. Conversely, in tumor cells lacking caspase-10, TRAF2, or ATR, the mode of cell death shifts to a more effective autocrine/paracrine mode, initiated by another complex, the FLIPosome, which results in the processing of cFLIPL and the production of TNF-α, promoting p53-independent apoptosis (186). Zhang et al. reported that the POK erythroid myeloid ontogenic factor (Pokemon) is overexpressed in HCC cells (187). In HepG2 cells with silenced Pokemon, treatment with oxaliplatin can activate caspase-10 and caspase-8, promoting the release of the active fragments p18 and p10 of caspase-8. In contrast, in another study, Horn et al. reported that in HeLa cells, caspase-10 negatively regulates DISC-mediated caspase-8 activation and promotes the activation of the NF-κB pathway, converting the cell's response to CD95 into cell survival (96). Caspase-8 recruits caspase-10 through a scaffolding function, and the activation of NF-κB also depends on the scaffolding functions of both caspase-8 and caspase-10. Inhibition of caspase-10 reduces the expression of cytokines and facilitates apoptosis in tumor cells. Considering the similarities and interactions between caspase-10 and caspase-8, the development of new compounds or biomolecules that can specifically activate or inhibit caspase-8 without affecting caspase-10 may become a key direction for future research. This line of research is expected to provide a solid scientific foundation for the development of more effective treatment strategies for HCC. Furthermore, it should be noted that the absence of caspase-10 in rodents means that caution is warranted when extrapolating results related to caspase-8 from mouse studies to human contexts (188, 189).

In addition to apoptosis, the modulation of necroptosis and pyroptosis pathways by targeting caspase-8 holds immense potential as a research direction for enhancing the sensitivity of HCC cells to treatments. Xiang et al. reported that high expression of Connexin32 (Cx32) enhances the antiapoptotic capability of HCC cells, promoting the malignant progression of HCC (190). In HCC, which is characterized by high Cx32 expression, inhibiting caspase-8 to induce necroptosis represents a promising therapeutic strategy. Cx32 can bind to Src and promote Src-driven phosphorylation and inhibition of caspase-8. It can also inhibit caspase-8 activity by increasing c-FLIP expression and reducing FADD expression. The overexpression of Cx32 significantly enhances the therapeutic effect of shikonin, an activator of necroptosis (191). However, necroptosis in HCC is a double-edged sword; although necroptosis can kill HCC cells, the DAMPs and cellular debris produced by necroptosis may exacerbate the inflammatory response within the HCC TME, promoting angiogenesis and tumor metastasis (192, 193). Vucur et al. reported that the NF-κB signaling is a major cause of promoting hepatocyte necroptotic inflammation and HCC (194). In hepatocytes with naturally low expression of RIPK3 and tumors with low RIPK3 expression, when caspase-8 is underexpressed, MLKL phosphorylation is incomplete, and cells do not die immediately but instead maintain membrane leakage and inflammation for a long time, promoting the occurrence of tumors. This prolonged subnecrotic apoptosis is closely related to the simultaneous activation of NF-κB. Necroptosis without NF-κB activation does not promote the occurrence of liver cancer in mice. Therefore, targeting the reprogramming of necroptosis during caspase-8 inhibition may be a strategy for treating RIPK3-low-expressing HCC. Furthermore, determining how to specifically modulate caspase-8 inhibition and necroptosis in HCC cells to minimize the impact on normal cells is essential. Necroptosis can cause chronic inflammation in hepatocytes and contribute to liver fibrosis (195). Abnormal activation of RIPK3 due to caspase-8 deficiency can lead to midgestational death in mouse embryos, whereas caspase-8$^{-/-}$RIPK3$^{-/-}$ mice can survive but accumulate abnormal T cells (196). Targeting RNA changes that are specific to HCC may prove to be an effective approach. Visalli et al. reported a triple-miRNA signature (miR-371-5p, miR-373, and miR-543) that is overexpressed in HCC tissues and promotes the development of HCC (197). These three miRNAs can directly bind to the 3'UTR of *CASP8*, specifically inhibiting the expression of caspase-8 and promoting necroptosis in HCC cells. Targeting caspase-8-associated pyroptosis is also a potential direction for HCC treatment. Several pyroptosis-associated gene models that include *CASP8* have been established for predicting the outcome of patients with HCC (198–200). Cui et al. reported that reuterin can increase the sensitivity of HCC to sorafenib. Mechanistically, reuterin promotes pyroptosis via the cGAS–STING pathway and upregulates caspase-8. Activation of the STING pathway promotes the necroptosis and pyroptosis pathways. However, the upregulation of caspase-8 inhibits necroptosis and further promotes HCC pyroptosis through the caspase-8-GSDMD pathway (201). This interplay between necroptosis and pyroptosis, modulated by caspase-8, underscores the complexity of cellular death mechanisms in HCC and highlights the potential for novel therapeutic interventions that could selectively target these pathways.

In addition to inducing PCD, caspase-8 also regulates the TME through multiple mechanisms. DAMPs and proinflammatory cytokines released during PCD, such as necroptosis and pyroptosis can facilitate the infiltration of immune cells, potentially converting "cold" tumors into "hot" tumors and increasing the effectiveness of immunotherapy (202). However, the released DAMPs and cellular debris may trigger or exacerbate inflammatory responses within the HCC TME (193, 203). This inflammatory response may promote HCC cell proliferation, invasion, and metastasis, creating favorable conditions for HCC development and progression. Additionally, caspase-8 activates the NF-κB pathway through its scaffolding function, promoting the expression of various cytokines. Fianco et al. reported that caspase-8 activates the NF-κB pathway, promoting the expression of various cytokines, such as IL-1, IL-6, and VEGF (24). This activation fosters an inflammatory TME and neovascularization in glioblastoma, enhancing its resistance to temozolomide. In another study, Tsai et al. reported that magnolol promoted the enzymatic activity of caspase-8 and the activation of the apoptotic pathway while simultaneously inhibiting the NF-κB pathway, thus reducing the expression of VEGF and MMP-9 in HCC (204).

Furthermore, caspase-8 plays a regulatory role in the differentiation, homeostasis, and function of various immune cells. A multidimensional study revealed that high expression of caspase-8 is associated with poor outcomes in HCC patients and that patients with high caspase-8 expression have a relatively high

mutation frequency of p53. In addition, caspase-8 activity is influenced by various immune cells in the HCC TME, such as $CD4^+$ T cells, $CD8^+$ T cells, M2 macrophages, and NK cells (205). Some factors not only affect the activity of caspase-8 but also regulate immune cells. For example, the knockdown of DcR3 not only reduces the transcription of cFLIP and caspase-8 but also promotes the differentiation of Th0 cells into Th1 cells, inhibits the differentiation of Th2 and Treg cells, and enhances tumor immunity in HCC (180, 206). Nevertheless, the specific research progress on the regulation of caspase-8 by immune cells in the HCC TME is insufficient to elucidate the detailed mechanisms involved, indicating that numerous areas require further in-depth investigation (Table 1).

8 Conclusion

HCC remains as a formidable global health issue because of its elevated mortality rates and the paucity of effective therapeutic options. A thorough understanding of the complex molecular mechanisms that underpin the development of HCC is imperative for identifying innovative therapeutic avenues. Among the myriad of factors implicated in HCC pathogenesis, caspase-8 has emerged as a versatile protein with pivotal roles in modulating PCD, inflammation, and the TME.

Caspase-8 is a pivotal factor in DR pathway apoptosis, yet its dysregulation in HCC frequently culminates in chemo- and radio resistance. In addition to fostering apoptosis, caspase-8 exerts a regulatory influence on necrosis and pyroptosis, significantly contributing to the intricate PANoptosis process. In HCC, the activation of caspase-8-mediated PCD can increase the efficacy of conventional therapeutic strategies. Conversely, the emanation of DAMPs and inflammatory mediators from PCD may instigate inflammatory cascades within the TME, potentially facilitating HCC invasion and metastasis.

The TME serves as a crucial determinant of the progression and treatment response of HCC. Caspase-8 regulates the differentiation, recruitment, homeostasis, and functionality of various immune cells within the HCC TME, underscoring its potential as a therapeutic target. However, current research fails to provide a comprehensive understanding of the intricate mechanisms that drive these processes. Additional studies are imperative to shed light on the precise role that caspase-8 plays in the HCC TME.

Targeting caspase-8 in HCC therapy presents a promising yet challenging avenue. Strategies involving the reactivation of caspase-8 in apoptosis-resistant HCC cells, as well as the promotion of necroptosis and pyroptosis, are actively being explored. The development of small molecule inhibitors, antisense oligonucleotides, and other modalities aimed at modulating caspase-8 activity is a promising area of research. Additionally, the

TABLE 1 Modulators Targeting Caspase-8 in Hepatocellular Carcinoma.

Modulators	Caspase-8	HCC	Mechanisms	References
Adiponectin	Increase	Inhibit	Enhancing caspase-8 and caspase-3 levels to promote apoptosis in HCC cells.	(171)
CAND1		Inhibit	Activating caspase-8-mediated apoptosis in HCC cells.	(172)
LncRNA CASC2		Inhibit	Inhibiting miR-24 and miR-221 to promote caspase-8 and TRAIL-induced apoptosis in HCC.	(174)
Sunitinib		Inhibit	Increasing caspase-8 and caspase-9 to promote HCC apoptosis and inhibit necroptosis.	(175)
SAHA		Inhibit	Promoting DR5 and inhibiting cFLIP to enhance apoptosis in HepG2 cells	(177)
Maritoclax		Inhibit	Inhibiting cFLIP through miR-708 and promoting apoptosis.	(178)
5-fluorouracil		Inhibit	Promoting FADDosome and mediating cFLIP ubiquitination.	(185)
Reuterin		Inhibit	Up-regulating caspase-8 to inhibit necroptosis and promoting the caspase-8-GSDMD pathway to facilitate pyroptosis in HCC.	(201)
Magnolol		Inhibit	Promoting caspase-8-mediated pyroptosis and inhibiting the NF-κB pathway to reduce the expression of VEGF and MMP-9.	(203)
DDIAS	Reduce	Promote	Inhibiting caspase-8 recruitment and promoting caspase-8 ubiquitination.	(173)
Rocaglamide		Promote	Inhibiting cFLIP to promote TRAIL-induced apoptosis.	(176)
DcR3		Promote	Promoting cFLIP transcription and NF-κB pathway.	(180)
Z-IETD-FMK		Promote	Inhibiting caspase-8 expression to reduce apoptosis in HCC cells.	(184)
Cx32		Inhibit	Promoting cFLIP and reducing FADD to inhibit caspase-8.	(191)
miR-371-5p, miR-373, miR-543		Promote	Binding to the 3'UTR of *CASP8* gene to inhibit the expression of caspase-8.	(197)

CAND1, cullin-associated NEDD8-dissociated 1; Caspase-8/9, cysteinyl aspartate specific proteinase 8/9; cFLIP, cellular-FLICE inhibitory protein; Cx32, connexin32; DcR3, decoy receptor 3; DDIAS, DNA damage-induced apoptosis suppressor; DR, death receptor; FADD, Fas-associated death domain; GSDMD, gasdermin; HCC, hepatocellular carcinoma; LncRNA, long non-coding RNA; MMP-9, metalloproteinase- 9; NF-κB, nuclear factor-kappa B; SAHA, suberoylanilide hydroxamic acid; TRAIL, TNF-related apoptosis-inducing ligand; VEGF, vascular endothelial growth factor.

discovery of predictive biomarkers capable of predicting responses to caspase-8-targeted therapies could personalize treatment and improve patient outcomes. However, current research remains in its infancy. The regulatory role of caspase-8 within the complex TME of HCC is not yet fully understood, necessitating further in-depth investigation to elucidate the mechanisms by which targeting the enzymatic and scaffolding functions of caspase-8 can modulate HCC. Moreover, developing caspase-8 activators and inhibitors with high specificity and selectivity presents a significant challenge. Ensuring the effective delivery of these drugs to the tumor tissue and their ability to penetrate the richly vascularized TME of HCC is a technical hurdle that must be overcome.

In conclusion, the intricate involvement of caspase-8 in HCC pathophysiology positions it as a potential therapeutic target. Its regulatory roles in PCD, inflammation, tumor immunity, and the TME make it a compelling target for novel therapeutic strategies. Future research endeavors should focus on deciphering the exact mechanisms through which caspase-8 modulates the behavior of various immune cells within the HCC TME. It is essential to conduct clinical studies to assess the safety and efficacy of caspase-8-targeted therapies among HCC patients. With a deeper understanding of the functions and regulatory mechanisms of caspase-8, we can develop more effective treatments to improve the survival rates of HCC patients.

9 Methods

We conducted a systematic literature search using PubMed, EMBASE, Web of Science, and CENTRAL within the Cochrane Library without date or language limitations. The search terms used were "(Hepatocellular carcinoma OR HCC) AND (Caspase-8)", "(Apoptosis) AND (Caspase-8)", "(Necroptosis) AND (Caspase-8)", "(Pyroptosis) AND (Caspase-8)", "(PANoptosis) AND (Caspase-8)", "(Hepatocellular carcinoma OR HCC) AND (Apoptosis)", "(Hepatocellular carcinoma OR HCC) AND (Necroptosis)", "(Hepatocellular carcinoma OR HCC) AND (Pyroptosis)", "(Hepatocellular carcinoma OR HCC) AND (PANoptosis)", "(Hepatocellular carcinoma OR HCC) AND (Tumor microenvironment OR TME)", "(Caspase-8) AND (Tumor microenvironment OR TME)", "(Caspase-8) AND (Caspase-10)", "(Hepatocellular carcinoma OR HCC) AND (Caspase-10)".

Author contributions

HC: Writing – original draft. YL: Writing – original draft. JC: Writing – original draft. XL: Writing – original draft. YK: Writing – original draft. YH: Writing – original draft. RZ: Writing – original draft. JJ: Writing – original draft. DL: Writing – review & editing. YW: Writing – original draft. ZH: Writing – original draft, Writing – review & editing.

Funding

The author(s) declare that no financial support was received for the research, authorship, and/or publication of this article.

Conflict of interest

The authors declare that the research was conducted in the absence of any commercial or financial relationships that could be construed as a potential conflict of interest.

Publisher's note

References

1. Siegel RL, Giaquinto AN, Jemal A. Cancer statistics, 2024. *CA: Cancer J Clin.* (2024) 74:12–49. doi: 10.3322/caac.21820

2. Nagaraju GP, Dariya B, Kasa P, Peela S, El-Rayes BF. Epigenetics in hepatocellular carcinoma. *Semin Cancer Biol.* (2022) 86:622–32. doi: 10.1016/j.semcancer.2021.07.017

3. Forner A, Reig M, Bruix J. Hepatocellular carcinoma. *Lancet (London England).* (2018) 391:1301–14. doi: 10.1016/s0140-6736(18)30010-2

4. Hepatocellular carcinoma. *Nat Rev Dis Primers.* (2021) 7:7. doi: 10.1038/s41572-021-00245-6

5. Brenner C, Galluzzi L, Kepp O, Kroemer G. Decoding cell death signals in liver inflammation. *J Hepatol.* (2013) 59:583–94. doi: 10.1016/j.jhep.2013.03.033

6. Chen H, Han Z, Luo Q, Wang Y, Li Q, Zhou L, et al. Radiotherapy modulates tumor cell fate decisions: A review. *Radiat Oncol (London England).* (2022) 17:196. doi: 10.1186/s13014-022-02171-7

7. Newton K, Wickliffe KE, Maltzman A, Dugger DL, Reja R, Zhang Y, et al. Activity of caspase-8 determines plasticity between cell death pathways. *Nature.* (2019) 575:679–82. doi: 10.1038/s41586-019-1752-8

8. Boege Y, Malehmir M, Healy ME, Bettermann K, Lorentzen A, Vucur M, et al. A dual role of caspase-8 in triggering and sensing proliferation-associated DNA damage, a key determinant of liver cancer development. *Cancer Cell.* (2017) 32:342–59.e10. doi: 10.1016/j.ccell.2017.08.010

9. Soung YH, Lee JW, Kim SY, Sung YJ, Park WS, Nam SW, et al. Caspase-8 gene is frequently inactivated by the frameshift somatic mutation 1225_1226deltg in hepatocellular carcinomas. *Oncogene.* (2005) 24:141–7. doi: 10.1038/sj.onc.1208244

10. Thornberry NA, Bull HG, Calaycay JR, Chapman KT, Howard AD, Kostura MJ, et al. A novel heterodimeric cysteine protease is required for interleukin-1 beta processing in monocytes. *Nature.* (1992) 356:768–74. doi: 10.1038/356768a0

11. Cerretti DP, Kozlosky CJ, Mosley B, Nelson N, Van Ness K, Greenstreet TA, et al. Molecular cloning of the interleukin-1 beta converting enzyme. *Sci (New York NY).* (1992) 256:97–100. doi: 10.1126/science.1373520

12. Wilson KP, Black JA, Thomson JA, Kim EE, Griffith JP, Navia MA, et al. Structure and mechanism of interleukin-1 beta converting enzyme. *Nature.* (1994) 370:270–5. doi: 10.1038/370270a0

13. Sahoo G, Samal D, Khandayataray P, Murthy MK. A review on caspases: key regulators of biological activities and apoptosis. *Mol Neurobiol*. (2023) 60:5805–37. doi: 10.1007/s12035-023-03433-5

14. Lamkanfi M, Declercq W, Kalai M, Saelens X, Vandenabeele P. Alice in caspase land. A phylogenetic analysis of caspases from worm to man. *Cell Death differentiation*. (2002) 9:358–61. doi: 10.1038/sj.cdd.4400989

15. Walker NP, Talanian RV, Brady KD, Dang LC, Bump NJ, Ferenz CR, et al. Crystal structure of the cysteine protease interleukin-1 beta-converting enzyme: A (P20/P10)2 homodimer. *Cell*. (1994) 78:343–52. doi: 10.1016/0092-8674(94)90303-4

16. Chéreau D, Kodandapani L, Tomaselli KJ, Spada AP, Wu JC. Structural and functional analysis of caspase active sites. *Biochemistry*. (2003) 42:4151–60. doi: 10.1021/bi020593l

17. Keller N, Mares J, Zerbe O, Grütter MG. Structural and biochemical studies on procaspase-8: new insights on initiator caspase activation. *Structure (London England: 1993)*. (2009) 17:438–48. doi: 10.1016/j.str.2008.12.019

18. Ma C, MacKenzie SH, Clark AC. Redesigning the procaspase-8 dimer interface for improved dimerization. *Protein sci: Publ Protein Soc*. (2014) 23:442–53. doi: 10.1002/pro.2426

19. Lippens S, Kockx M, Knaapen M, Mortier L, Polakowska R, Verheyen A, et al. Epidermal differentiation does not involve the pro-apoptotic executioner caspases, but is associated with caspase-14 induction and processing. *Cell Death differentiation*. (2000) 7:1218–24. doi: 10.1038/sj.cdd.4400785

20. Boldin MP, Goncharov TM, Goltsev YV, Wallach D. Involvement of mach, a novel mort1/fadd-interacting protease, in fas/apo-1- and tnf receptor-induced cell death. *Cell*. (1996) 85:803–15. doi: 10.1016/s0092-8674(00)81265-9

21. Muzio M, Chinnaiyan AM, Kischkel FC, O'Rourke K, Shevchenko A, Ni J, et al. Flice, a novel fadd-homologous ice/ced-3-like protease, is recruited to the cd95 (Fas/apo-1) death–inducing signaling complex. *Cell*. (1996) 85:817–27. doi: 10.1016/s0092-8674(00)81266-0

22. Pop C, Fitzgerald P, Green DR, Salvesen GS. Role of proteolysis in caspase-8 activation and stabilization. *Biochemistry*. (2007) 46:4398–407. doi: 10.1021/bi602623b

23. Keller N, Grütter MG, Zerbe O. Studies of the molecular mechanism of caspase-8 activation by solution nmr. *Cell Death differentiation*. (2010) 17:710–8. doi: 10.1038/cdd.2009.155

24. Fianco G, Mongiardi MP, Levi A, De Luca T, Desideri M, Trisciuoglio D, et al. Caspase-8 contributes to angiogenesis and chemotherapy resistance in glioblastoma. *eLife*. (2017) 6:e22593. doi: 10.7554/eLife.22593

25. Henry CM, Martin SJ. Caspase-8 acts in a non-enzymatic role as a scaffold for assembly of a pro-inflammatory "Faddosome" Complex upon trail stimulation. *Mol Cell*. (2017) 65:715–29.e5. doi: 10.1016/j.molcel.2017.01.022

26. Hillert-Richter LK, Lavrik IN. Measuring composition of cd95 death-inducing signaling complex and processing of procaspase-8 in this complex. *J visualized experiments: JoVE*. (2021) 174:174. doi: 10.3791/62842

27. Schleich K, Buchbinder JH, Pietkiewicz S, Kähne T, Warnken U, Öztürk S, et al. Molecular architecture of the ded chains at the disc: regulation of procaspase-8 activation by short ded proteins C-flip and procaspase-8 prodomain. *Cell Death differentiation*. (2016) 23:681–94. doi: 10.1038/cdd.2015.137

28. Kerr JF, Wyllie AH, Currie AR. Apoptosis: A basic biological phenomenon with wide-ranging implications in tissue kinetics. *Br J Cancer*. (1972) 26:239–57. doi: 10.1038/bjc.1972.33

29. Coleman ML, Sahai EA, Yeo M, Bosch M, Dewar A, Olson MF. Membrane blebbing during apoptosis results from caspase-mediated activation of rock I. *Nat Cell Biol*. (2001) 3:339–45. doi: 10.1038/35070009

30. Chipuk JE, Kuwana T, Bouchier-Hayes L, Droin NM, Newmeyer DD, Schuler M, et al. Direct activation of bax by P53 mediates mitochondrial membrane permeabilization and apoptosis. *Sci (New York NY)*. (2004) 303:1010–4. doi: 10.1126/science.1092734

31. Marsden VS, O'Connor L, O'Reilly LA, Silke J, Metcalf D, Ekert PG, et al. Apoptosis initiated by bcl-2-regulated caspase activation independently of the cytochrome C/apaf-1/caspase-9 apoptosome. *Nature*. (2002) 419:634–7. doi: 10.1038/nature01101

32. Muzio M, Stockwell BR, Stennicke HR, Salvesen GS, Dixit VM. An induced proximity model for caspase-8 activation. *J Biol Chem*. (1998) 273:2926–30. doi: 10.1074/jbc.273.5.2926

33. Kuida K, Haydar TF, Kuan CY, Gu Y, Taya C, Karasuyama H, et al. Reduced apoptosis and cytochrome C-mediated caspase activation in mice lacking caspase 9. *Cell*. (1998) 94:325–37. doi: 10.1016/s0092-8674(00)81476-2

34. Micheau O, Tschopp J. Induction of tnf receptor I-mediated apoptosis via two sequential signaling complexes. *Cell*. (2003) 114:181–90. doi: 10.1016/s0092-8674(03)00521-x

35. Sun H, Yang Y, Gu M, Li Y, Jiao Z, Lu C, et al. The role of fas-fasl-fadd signaling pathway in arsenic-mediated neuronal apoptosis *in vivo* and *in vitro*. *Toxicol Lett*. (2022) 356:143–50. doi: 10.1016/j.toxlet.2021.11.012

36. Fu TM, Li Y, Lu A, Li Z, Vajjhala PR, Cruz AC, et al. Cryo-em structure of caspase-8 tandem ded filament reveals assembly and regulation mechanisms of the death-inducing signaling complex. *Mol Cell*. (2016) 64:236–50. doi: 10.1016/j.molcel.2016.09.009

37. Chinnaiyan AM, O'Rourke K, Tewari M, Dixit VM. Fadd, a novel death domain-containing protein, interacts with the death domain of fas and initiates apoptosis. *Cell*. (1995) 81:505–12. doi: 10.1016/0092-8674(95)90071-3

38. Kischkel FC, Lawrence DA, Chuntharapai A, Schow P, Kim KJ, Ashkenazi A. Apo2l/trail-dependent recruitment of endogenous fadd and caspase-8 to death receptors 4 and 5. *Immunity*. (2000) 12:611–20. doi: 10.1016/s1074-7613(00)80212-5

39. Kischkel FC, Hellbardt S, Behrmann I, Germer M, Pawlita M, Krammer PH, et al. Cytotoxicity-dependent apo-1 (Fas/cd95)-associated proteins form a death-inducing signaling complex (Disc) with the receptor. *EMBO J*. (1995) 14:5579–88. doi: 10.1002/j.1460-2075.1995.tb00245.x

40. Huang K, Zhang J, O'Neill KL, Gurumurthy CB, Quadros RM, Tu Y, et al. Cleavage by caspase 8 and mitochondrial membrane association activate the bh3-only protein bid during trail-induced apoptosis. *J Biol Chem*. (2016) 291:11843–51. doi: 10.1074/jbc.M115.711051

41. Chai WS, Zhu XM, Li SH, Fan JX, Chen BY. Role of bcl-2 family members in caspase-3/9-dependent apoptosis during pseudomonas aeruginosa infection in U937 cells. *Apoptosis: an Int J programmed Cell Death*. (2008) 13:833–43. doi: 10.1007/s10495-008-0197-6

42. Murphy JM, Czabotar PE, Hildebrand JM, Lucet IS, Zhang JG, Alvarez-Diaz S, et al. The pseudokinase mlkl mediates necroptosis via a molecular switch mechanism. *Immunity*. (2013) 39:443–53. doi: 10.1016/j.immuni.2013.06.018

43. Rodriguez DA, Quarato G, Liedmann S, Tummers B, Zhang T, Guy C, et al. Caspase-8 and fadd prevent spontaneous zbp1 expression and necroptosis. *Proc Natl Acad Sci United States America*. (2022) 119:e2207240119. doi: 10.1073/pnas.2207240119

44. Yang D, Liang Y, Zhao S, Ding Y, Zhuang Q, Shi Q, et al. Zbp1 mediates interferon-induced necroptosis. *Cell Mol Immunol*. (2020) 17:356–68. doi: 10.1038/s41423-019-0237-x

45. Kaiser WJ, Sridharan H, Huang C, Mandal P, Upton JW, Gough PJ, et al. Toll-like receptor 3-mediated necrosis via trif, rip3, and mlkl. *J Biol Chem*. (2013) 288:31268–79. doi: 10.1074/jbc.M113.462341

46. Lin J, Kumari S, Kim C, Van TM, Wachsmuth L, Polykratis A, et al. Ripk1 counteracts zbp1-mediated necroptosis to inhibit inflammation. *Nature*. (2016) 540:124–8. doi: 10.1038/nature20558

47. Cho YS, Challa S, Moquin D, Genga R, Ray TD, Guildford M, et al. Phosphorylation-driven assembly of the rip1-rip3 complex regulates programmed necrosis and virus-induced inflammation. *Cell*. (2009) 137:1112–23. doi: 10.1016/j.cell.2009.05.037

48. Degterev A, Hitomi J, Germscheid M, Ch'en IL, Korkina O, Teng X, et al. Identification of rip1 kinase as a specific cellular target of necrostatins. *Nat Chem Biol*. (2008) 4:313–21. doi: 10.1038/nchembio.83

49. Geng J, Ito Y, Shi L, Amin P, Chu J, Ouchida AT, et al. Regulation of ripk1 activation by tak1-mediated phosphorylation dictates apoptosis and necroptosis. *Nat Commun*. (2017) 8:359. doi: 10.1038/s41467-017-00406-w

50. Schorn F, Werthenbach JP, Hoffmann M, Daoud M, Stachelscheid J, Schiffmann LM, et al. Ciaps control ripk1 kinase activity-dependent and -independent cell death and tissue inflammation. *EMBO J*. (2023) 42:e113614. doi: 10.15252/embj.2023113614

51. Schneider AT, Gautheron J, Feoktistova M, Roderburg C, Loosen SH, Roy S, et al. Ripk1 suppresses a traf2-dependent pathway to liver cancer. *Cancer Cell*. (2017) 31:94–109. doi: 10.1016/j.ccell.2016.11.009

52. Lee CS, Hwang G, Nam YW, Hwang CH, Song J. Ikk-mediated traf6 and ripk1 interaction stifles cell death complex assembly leading to the suppression of tnf-α-induced cell death. *Cell Death differentiation*. (2023) 30:1575–84. doi: 10.1038/s41418-023-01161-w

53. Shen B, Han W, Tan X, Gu KJ, Naseem DF, Zheng G, et al. Expression of ripk1 and fadd are associated with chemosensitivity and survival in head and heck squamous cell carcinoma via tanshinone iia-mediated modulation of the ripk1-fadd-caspase 8 complex. *Mol carcinogenesis*. (2024) 63:1406–16. doi: 10.1002/mc.23734

54. Feoktistova M, Geserick P, Kellert B, Dimitrova DP, Langlais C, Hupe M, et al. Ciaps block ripoptosome formation, a rip1/caspase-8 containing intracellular cell death complex differentially regulated by cflip isoforms. *Mol Cell*. (2011) 43:449–63. doi: 10.1016/j.molcel.2011.06.011

55. Weinlich R, Oberst A, Dillon CP, Janke LJ, Milasta S, Lukens JR, et al. Protective roles for caspase-8 and cflip in adult homeostasis. *Cell Rep*. (2013) 5:340–8. doi: 10.1016/j.celrep.2013.08.045

56. Scaffidi C, Schmitz I, Krammer PH, Peter ME. The role of C-flip in modulation of cd95-induced apoptosis. *J Biol Chem*. (1999) 274:1541–8. doi: 10.1074/jbc.274.3.1541

57. Yeh WC, Itie A, Elia AJ, Ng M, Shu HB, Wakeham A, et al. Requirement for casper (C-flip) in regulation of death receptor-induced apoptosis and embryonic development. *Immunity*. (2000) 12:633–42. doi: 10.1016/s1074-7613(00)80214-9

58. Davidovich P, Higgins CA, Najda Z, Longley DB, Martin SJ. Cflip(L) acts as a suppressor of trail- and fas-initiated inflammation by inhibiting assembly of caspase-8/fadd/ripk1 nf-κb-activating complexes. *Cell Rep*. (2023) 42:113476. doi: 10.1016/j.celrep.2023.113476

59. Martinez Lagunas K, Savcigil DP, Zrilic M, Carvajal Fraile C, Craxton A, Self E, et al. Cleavage of cflip restrains cell death during viral infection and tissue injury and favors tissue repair. *Sci Adv*. (2023) 9:eadg2829. doi: 10.1126/sciadv.adg2829

60. Sun L, Wang H, Wang Z, He S, Chen S, Liao D, et al. Mixed lineage kinase domain-like protein mediates necrosis signaling downstream of rip3 kinase. *Cell*. (2012) 148:213–27. doi: 10.1016/j.cell.2011.11.031

61. Zhao J, Jitkaew S, Cai Z, Choksi S, Li Q, Luo J, et al. Mixed lineage kinase domain-like is a key receptor interacting protein 3 downstream component of tnf-induced necrosis. *Proc Natl Acad Sci United States America*. (2012) 109:5322–7. doi: 10.1073/pnas.1200012109

62. Das A, McDonald DG, Dixon-Mah YN, Jacqmin DJ, Samant VN, Vandergrift WA 3rd, et al. Rip1 and rip3 complex regulates radiation-induced programmed necrosis in glioblastoma. *Tumour biol: J Int Soc Oncodevelopmental Biol Med*. (2016) 37:7525–34. doi: 10.1007/s13277-015-4621-6

63. Brennan MA, Cookson BT. Salmonella induces macrophage death by caspase-1-dependent necrosis. *Mol Microbiol*. (2000) 38:31–40. doi: 10.1046/j.1365-2958.2000.02103.x

64. Shi J, Zhao Y, Wang K, Shi X, Wang Y, Huang H, et al. Cleavage of gsdmd by inflammatory caspases determines pyroptotic cell death. *Nature*. (2015) 526:660–5. doi: 10.1038/nature15514

65. Kayagaki N, Stowe IB, Lee BL, O'Rourke K, Anderson K, Warming S, et al. Caspase-11 cleaves gasdermin D for non-canonical inflammasome signalling. *Nature*. (2015) 526:666–71. doi: 10.1038/nature15541

66. Ding J, Wang K, Liu W, She Y, Sun Q, Shi J, et al. Pore-forming activity and structural autoinhibition of the gasdermin family. *Nature*. (2016) 535:111–6. doi: 10.1038/nature18590

67. Liu X, Zhang L, Zhu B, Liu Y, Li L, Hou J, et al. Role of gsdm family members in airway epithelial cells of lung diseases: A systematic and comprehensive transcriptomic analysis. *Cell Biol Toxicol*. (2023) 39:2743–60. doi: 10.1007/s10565-023-09799-5

68. Liu X, Zhang Z, Ruan J, Pan Y, Magupalli VG, Wu H, et al. Inflammasome-activated gasdermin D causes pyroptosis by forming membrane pores. *Nature*. (2016) 535:153–8. doi: 10.1038/nature18629

69. Mehrotra P, Maschalidi S, Boeckaerts L, Maueröder C, Tixeira R, Pinney J, et al. Oxylipins and metabolites from pyroptotic cells act as promoters of tissue repair. *Nature*. (2024) 631:207–15. doi: 10.1038/s41586-024-07585-9

70. Sun L, Ma W, Gao W, Xing Y, Chen L, Xia Z, et al. Propofol directly induces caspase-1-dependent macrophage pyroptosis through the nlrp3-asc inflammasome. *Cell Death Dis*. (2019) 10:542. doi: 10.1038/s41419-019-1761-4

71. Lalor SJ, Dungan LS, Sutton CE, Basdeo SA, Fletcher JM, Mills KH. Caspase-1-processed cytokines il-1beta and il-18 promote il-17 production by gammadelta and cd4 T cells that mediate autoimmunity. *J Immunol (Baltimore Md: 1950)*. (2011) 186:5738–48. doi: 10.4049/jimmunol.1003597

72. Vajjhala PR, Lu A, Brown DL, Pang SW, Sagulenko V, Sester DP, et al. The inflammasome adaptor asc induces procaspase-8 death effector domain filaments. *J Biol Chem*. (2015) 290:29217–30. doi: 10.1074/jbc.M115.687731

73. Demarco B, Grayczyk JP, Bjanes E, Le Roy D, Tonnus W, Assenmacher CA, et al. Caspase-8-dependent gasdermin D cleavage promotes antimicrobial defense but confers susceptibility to tnf-induced lethality. *Sci Adv*. (2020) 6:eabc3465. doi: 10.1126/sciadv.abc3465

74. Zhang JY, Zhou B, Sun RY, Ai YL, Cheng K, Li FN, et al. The metabolite α-kg induces gsdmc-dependent pyroptosis through death receptor 6-activated caspase-8. *Cell Res*. (2021) 31:980–97. doi: 10.1038/s41422-021-00506-9

75. Hou J, Zhao R, Xia W, Chang CW, You Y, Hsu JM, et al. Pd-L1-mediated gasdermin C expression switches apoptosis to pyroptosis in cancer cells and facilitates tumour necrosis. *Nat Cell Biol*. (2020) 22:1264–75. doi: 10.1038/s41556-020-0575-z

76. Wu J, Lin S, Chen W, Lian G, Wu W, Chen A, et al. Tnf-α Contributes to sarcopenia through caspase-8/caspase-3/gsdme-mediated pyroptosis. *Cell Death Discovery*. (2023) 9:76. doi: 10.1038/s41420-023-01365-6

77. Mi Y, Wei C, Sun L, Liu H, Zhang J, Luo J, et al. Melatonin inhibits ferroptosis and delays age-related cataract by regulating sirt6/P-nrf2/gpx4 and sirt6/ncoa4/fth1 pathways. *Biomed pharmacother = Biomed pharmacother*. (2023) 157:114048. doi: 10.1016/j.biopha.2022.114048

78. Christgen S, Zheng M, Kesavardhana S, Karki R, Malireddi RKS, Banoth B, et al. Identification of the panoptosome: A molecular platform triggering pyroptosis, apoptosis, and necroptosis (Panoptosis). *Front Cell infection Microbiol*. (2020) 10:237. doi: 10.3389/fcimb.2020.00237

79. Sharma BR, Karki R, Rajesh Y, Kanneganti TD. Immune regulator irf1 contributes to zbp1-, aim2-, ripk1-, and nlrp12-panoptosome activation and inflammatory cell death (Panoptosis). *J Biol Chem*. (2023) 299:105141. doi: 10.1016/j.jbc.2023.105141

80. Wang Y, Pandian N, Han JH, Sundaram B, Lee S, Karki R, et al. Single cell analysis of panoptosome cell death complexes through an expansion microscopy method. *Cell Mol Life sci: CMLS*. (2022) 79:531. doi: 10.1007/s00018-022-04564-z

81. Lee S, Karki R, Wang Y, Nguyen LN, Kalathur RC, Kanneganti TD. Aim2 forms a complex with pyrin and zbp1 to drive panoptosis and host defence. *Nature*. (2021) 597:415–9. doi: 10.1038/s41586-021-03875-8

82. Oh S, Lee J, Oh J, Yu G, Ryu H, Kim D, et al. Integrated nlrp3, aim2, nlrc4, pyrin inflammasome activation and assembly drive panoptosis. *Cell Mol Immunol*. (2023) 20:1513–26. doi: 10.1038/s41423-023-01107-9

83. Luk CT, Chan CK, Chiu F, Shi SY, Misra PS, Li YZ, et al. Dual role of caspase 8 in adipocyte apoptosis and metabolic inflammation. *Diabetes*. (2023) 72:1751–65. doi: 10.2337/db22-1033

84. Schwarzer R, Jiao H, Wachsmuth L, Tresch A, Pasparakis M. Fadd and caspase-8 regulate gut homeostasis and inflammation by controlling mlkl- and gsdmd-mediated death of intestinal epithelial cells. *Immunity*. (2020) 52:978–93.e6. doi: 10.1016/j.immuni.2020.04.002

85. Kang TB, Yang SH, Toth B, Kovalenko A, Wallach D. Caspase-8 blocks kinase ripk3-mediated activation of the nlrp3 inflammasome. *Immunity*. (2013) 38:27–40. doi: 10.1016/j.immuni.2012.09.015

86. Gutierrez KD, Davis MA, Daniels BP, Olsen TM, Ralli-Jain P, Tait SW, et al. Mlkl activation triggers nlrp3-mediated processing and release of il-1β Independently of gasdermin-D. *J Immunol (Baltimore Md: 1950)*. (2017) 198:2156–64. doi: 10.4049/jimmunol.1601757

87. Wu YH, Mo ST, Chen IT, Hsieh FY, Hsieh SL, Zhang J, et al. Caspase-8 inactivation drives autophagy-dependent inflammasome activation in myeloid cells. *Sci Adv*. (2022) 8:eabn9912. doi: 10.1126/sciadv.abn9912

88. Fritsch M, Günther SD, Schwarzer R, Albert MC, Schorn F, Werthenbach JP, et al. Caspase-8 is the molecular switch for apoptosis, necroptosis and pyroptosis. *Nature*. (2019) 575:683–7. doi: 10.1038/s41586-019-1770-6

89. Fang Y, Tian S, Pan Y, Li W, Wang Q, Tang Y, et al. Pyroptosis: A new frontier in cancer. *Biomed pharmacother = Biomed pharmacother*. (2020) 121:109595. doi: 10.1016/j.biopha.2019.109595

90. Gringhuis SI, Kaptein TM, Wevers BA, Theelen B, van der Vlist M, Boekhout T, et al. Dectin-1 is an extracellular pathogen sensor for the induction and processing of il-1β Via a noncanonical caspase-8 inflammasome. *Nat Immunol*. (2012) 13:246–54. doi: 10.1038/ni.2222

91. Napetschnig J, Wu H. Molecular basis of nf-κb signaling. *Annu Rev biophys*. (2013) 42:443–68. doi: 10.1146/annurev-biophys-083012-130338

92. Shen J, Cheng J, Zhu S, Zhao J, Ye Q, Xu Y, et al. Regulating effect of baicalin on ikk/ikb/nf-kb signaling pathway and apoptosis-related proteins in rats with ulcerative colitis. *Int Immunopharmacol*. (2019) 73:193–200. doi: 10.1016/j.intimp.2019.04.052

93. Bakshi HA, Quinn GA, Nasef MM, Mishra V, Aljabali AAA, El-Tanani M, et al. Crocin inhibits angiogenesis and metastasis in colon cancer via tnf-α/nf-kb/vegf pathways. *Cells*. (2022) 11:1502. doi: 10.3390/cells11091502

94. Zhang L, Blackwell K, Thomas GS, Sun S, Yeh WC, Habelhah H. Traf2 suppresses basal ikk activity in resting cells and tnfalpha can activate ikk in traf2 and traf5 double knockout cells. *J Mol Biol*. (2009) 389:495–510. doi: 10.1016/j.jmb.2009.04.054

95. Xia J, Zhang J, Wang L, Liu H, Wang J, Liu J, et al. Non-apoptotic function of caspase-8 confers prostate cancer enzalutamide resistance via nf-κb activation. *Cell Death Dis*. (2021) 12:833. doi: 10.1038/s41419-021-04126-4

96. Horn S, Hughes MA, Schilling R, Sticht C, Tenev T, Ploesser M, et al. Caspase-10 negatively regulates caspase-8-mediated cell death, switching the response to cd95l in favor of nf-κb activation and cell survival. *Cell Rep*. (2017) 19:785–97. doi: 10.1016/j.celrep.2017.04.010

97. Bouquet F, Muller C, Salles B. The loss of gammah2ax signal is a marker of DNA double strand breaks repair only at low levels of DNA damage. *Cell Cycle (Georgetown Tex)*. (2006) 5:1116–22. doi: 10.4161/cc.5.10.2799

98. Chen L, Park SM, Tumanov AV, Hau A, Sawada K, Feig C, et al. Cd95 promotes tumour growth. *Nature*. (2010) 465:492–6. doi: 10.1038/nature09075

99. Okano H, Shiraki K, Inoue H, Kawakita T, Yamanaka T, Deguchi M, et al. Cellular flice/caspase-8-inhibitory protein as a principal regulator of cell death and survival in human hepatocellular carcinoma. *Lab investigation; J Tech Methods Pathol*. (2003) 83:1033–43. doi: 10.1097/01.lab.0000079328.76631.28

100. Kang YC, Kim KM, Lee KS, Namkoong S, Lee SJ, Han JA, et al. Serum bioactive lysophospholipids prevent trail-induced apoptosis via pi3k/akt-dependent cflip expression and bad phosphorylation. *Cell Death differentiation*. (2004) 11:1287–98. doi: 10.1038/sj.cdd.4401489

101. Su K, Yuan Q, Hou H, Ke C, Huang C, Li S, et al. Ev-T synergizes with azd5582 to overcome trail resistance through concomitant suppression of cflip, mcl-1, and iaps in hepatocarcinoma. *J Mol Med (Berlin Germany)*. (2022) 100:629–43. doi: 10.1007/s00109-022-02180-9

102. Liu D, Fan Y, Li J, Cheng B, Lin W, Li X, et al. Inhibition of cflip overcomes acquired resistance to sorafenib via reducing er stress–Related autophagy in hepatocellular carcinoma. *Oncol Rep*. (2018) 40:2206–14. doi: 10.3892/or.2018.6606

103. Xiao Y, Yu D. Tumor microenvironment as a therapeutic target in cancer. *Pharmacol Ther*. (2021) 221:107753. doi: 10.1016/j.pharmthera.2020.107753

104. Wu T, Dai Y. Tumor microenvironment and therapeutic response. *Cancer Lett*. (2017) 387:61–8. doi: 10.1016/j.canlet.2016.01.043

105. Pitt JM, Marabelle A, Eggermont A, Soria JC, Kroemer G, Zitvogel L. Targeting the tumor microenvironment: removing obstruction to anticancer immune responses and immunotherapy. *Ann Oncol*. (2016) 27:1482–92. doi: 10.1093/annonc/mdw168

106. Ngambenjawong C, Gustafson HH, Pun SH. Progress in tumor-associated macrophage (Tam)-targeted therapeutics. *Advanced Drug delivery Rev*. (2017) 114:206–21. doi: 10.1016/j.addr.2017.04.010

107. Tang B, Zhu J, Wang Y, Chen W, Fang S, Mao W, et al. Targeted xct-mediated ferroptosis and protumoral polarization of macrophages is effective against hcc and enhances the efficacy of the anti-pd-1/L1 response. *Advanced Sci (Weinheim Baden-Wurttemberg Germany)*. (2023) 10:e2203973. doi: 10.1002/advs.202203973

108. Yu Z, Li Y, Li Y, Zhang J, Li M, Ji L, et al. Bufalin stimulates antitumor immune response by driving tumor-infiltrating macrophage toward M1 phenotype in hepatocellular carcinoma. *J immunother Cancer*. (2022) 10:e004297. doi: 10.1136/jitc-2021-004297

109. Zhang X, Lu X, Shi J, Li Y, Li Y, Tao R, et al. Bufalin suppresses hepatocellular carcinogenesis by targeting M2 macrophage-governed wnt1/β-catenin signaling. *Phytomed: Int J phytother phytopharmacol*. (2024) 126:155395. doi: 10.1016/j.phymed.2024.155395

110. Wang YN, Wang YY, Wang J, Bai WJ, Miao NJ, Wang J. Vinblastine resets tumor-associated macrophages toward M1 phenotype and promotes antitumor immune response. *J immunother Cancer*. (2023) 11:e007253. doi: 10.1136/jitc-2023-007253

111. Gunassekaran GR, Poongkavithai Vadevoo SM, Baek MC, Lee B. M1 macrophage exosomes engineered to foster M1 polarization and target the il-4 receptor inhibit tumor growth by reprogramming tumor-associated macrophages into M1-like macrophages. *Biomaterials*. (2021) 278:121137. doi: 10.1016/j.biomaterials.2021.121137

112. Han S, Bao X, Zou Y, Wang L, Li Y, Yang L, et al. D-lactate modulates M2 tumor-associated macrophages and remodels immunosuppressive tumor microenvironment for hepatocellular carcinoma. *Sci Adv*. (2023) 9:eadg2697. doi: 10.1126/sciadv.adg2697

113. Qu X, Zhao X, Lin K, Wang N, Li X, Li S, et al. M2-like tumor-associated macrophage-related biomarkers to construct a novel prognostic signature, reveal the immune landscape, and screen drugs in hepatocellular carcinoma. *Front Immunol*. (2022) 13:994019. doi: 10.3389/fimmu.2022.994019

114. Lu Y, Han G, Zhang Y, Zhang L, Li Z, Wang Q, et al. M2 macrophage-secreted exosomes promote metastasis and increase vascular permeability in hepatocellular carcinoma. *Cell communication signaling: CCS*. (2023) 21:299. doi: 10.1186/s12964-022-00872-w

115. Cui Q, Wang X, Zhang Y, Shen Y, Qian Y. Macrophage-derived mmp-9 and mmp-2 are closely related to the rupture of the fibrous capsule of hepatocellular carcinoma leading to tumor invasion. *Biol procedures Online*. (2023) 25:8. doi: 10.1186/s12575-023-00196-0

116. Xiang X, Wang J, Lu D, Xu X. Targeting tumor-associated macrophages to synergize tumor immunotherapy. *Signal transduction targeted Ther*. (2021) 6:75. doi: 10.1038/s41392-021-00484-9

117. Fan QM, Jing YY, Yu GF, Kou XR, Ye F, Gao L, et al. Tumor-associated macrophages promote cancer stem cell-like properties via transforming growth factor-beta1-induced epithelial-mesenchymal transition in hepatocellular carcinoma. *Cancer Lett*. (2014) 352:160–8. doi: 10.1016/j.canlet.2014.05.008

118. Kostova I, Mandal R, Becker S, Strebhardt K. The role of caspase-8 in the tumor microenvironment of ovarian cancer. *Cancer metastasis Rev*. (2021) 40:303–18. doi: 10.1007/s10555-020-09935-1

119. Cuda CM, Misharin AV, Khare S, Saber R, Tsai F, Archer AM, et al. Conditional deletion of caspase-8 in macrophages alters macrophage activation in a ripk-dependent manner. *Arthritis Res Ther*. (2015) 17:291. doi: 10.1186/s13075-015-0794-z

120. Roca H, Varsos ZS, Sud S, Craig MJ, Ying C, Pienta KJ. Ccl2 and interleukin-6 promote survival of human cd11b+ Peripheral blood mononuclear cells and induce M2-type macrophage polarization. *J Biol Chem*. (2009) 284:34342–54. doi: 10.1074/jbc.M109.042671

121. Hastir JF, Delbauve S, Larbanoix L, Germanova D, Goyvaerts C, Allard J, et al. Hepatocarcinoma induces a tumor necrosis factor-dependent kupffer cell death pathway that favors its proliferation upon partial hepatectomy. *Front Oncol*. (2020) 10:547013. doi: 10.3389/fonc.2020.547013

122. Nishizawa N, Ito Y, Eshima K, Ohkubo H, Kojo K, Inoue T, et al. Inhibition of microsomal prostaglandin E synthase-1 facilitates liver repair after hepatic injury in mice. *J Hepatol*. (2018) 69:110–20. doi: 10.1016/j.jhep.2018.02.009

123. Dolina JS, Van Braeckel-Budimir N, Thomas GD, Salek-Ardakani S. Cd8(+) T cell exhaustion in cancer. *Front Immunol*. (2021) 12:715234. doi: 10.3389/fimmu.2021.715234

124. Cao X, Cai SF, Fehniger TA, Song J, Collins LI, Piwnica-Worms DR, et al. Granzyme B and perforin are important for regulatory T cell-mediated suppression of tumor clearance. *Immunity*. (2007) 27:635–46. doi: 10.1016/j.immuni.2007.08.014

125. Hodge G, Barnawi J, Jurisevic C, Moffat D, Holmes M, Reynolds PN, et al. Lung cancer is associated with decreased expression of perforin, granzyme B and interferon (Ifn)-Γ by infiltrating lung tissue T cells, natural killer (Nk) T-like and nk cells. *Clin Exp Immunol*. (2014) 178:79–85. doi: 10.1111/cei.12392

126. Luo X, Zhang Z, Li S, Wang Y, Sun M, Hu D, et al. Srsf10 facilitates hcc growth and metastasis by suppressing cd8(+)T cell infiltration and targeting srsf10 enhances anti-pd-L1 therapy. *Int Immunopharmacol*. (2024) 127:111376. doi: 10.1016/j.intimp.2023.111376

127. Hofmann M, Tauber C, Hensel N, Thimme R. Cd8(+) T cell responses during hcv infection and hcc. *J Clin Med*. (2021) 10:991. doi: 10.3390/jcm10050991

128. Hu Z, Chen G, Zhao Y, Gao H, Li L, Yin Y, et al. Exosome-derived circccar1 promotes cd8 + T-cell dysfunction and anti-pd1 resistance in hepatocellular carcinoma. *Mol Cancer*. (2023) 22:55. doi: 10.1186/s12943-023-01759-1

129. Wang S, Wang R, Xu N, Wei X, Yang Y, Lian Z, et al. Sult2b1-cs-dock2 axis regulates effector T-cell exhaustion in hcc microenvironment. *Hepatol (Baltimore Md)*. (2023) 78:1064–78. doi: 10.1097/hep.0000000000000025

130. Chen H, Han Z, Fan Y, Chen L, Peng F, Cheng X, et al. Cd4+ T-cell subsets in autoimmune hepatitis: A review. *Hepatol Commun*. (2023) 7:e0269. doi: 10.1097/hc9.0000000000000269

131. Kumagai S, Koyama S, Itahashi K, Tanegashima T, Lin YT, Togashi Y, et al. Lactic acid promotes pd-1 expression in regulatory T cells in highly glycolytic tumor microenvironments. *Cancer Cell*. (2022) 40:201–18.e9. doi: 10.1016/j.ccell.2022.01.001

132. Yi C, Chen L, Lin Z, Liu L, Shao W, Zhang R, et al. Lenvatinib targets fgf receptor 4 to enhance antitumor immune response of anti-programmed cell death-1 in hcc. *Hepatol (Baltimore Md)*. (2021) 74:2544–60. doi: 10.1002/hep.31921

133. Shan F, Somasundaram A, Bruno TC, Workman CJ, Vignali DAA. Therapeutic targeting of regulatory T cells in cancer. *Trends Cancer*. (2022) 8:944–61. doi: 10.1016/j.trecan.2022.06.008

134. Marangoni F, Zhakyp A, Corsini M, Geels SN, Carrizosa E, Thelen M, et al. Expansion of tumor-associated treg cells upon disruption of a ctla-4-dependent feedback loop. *Cell*. (2021) 184:3998–4015.e19. doi: 10.1016/j.cell.2021.05.027

135. Suthen S, Lim CJ, Nguyen PHD, Dutertre CA, Lai HLH, Wasser M, et al. Hypoxia-driven immunosuppression by treg and type-2 conventional dendritic cells in hcc. *Hepatol (Baltimore Md)*. (2022) 76:1329–44. doi: 10.1002/hep.32419

136. Salmena L, Lemmers B, Hakem A, Matysiak-Zablocki E, Murakami K, Au PY, et al. Essential role for caspase 8 in T-cell homeostasis and T-cell-mediated immunity. *Genes Dev*. (2003) 17:883–95. doi: 10.1101/gad.1063703

137. Salmena L, Hakem R. Caspase-8 deficiency in T cells leads to a lethal lymphoinfiltrative immune disorder. *J Exp Med*. (2005) 202:727–32. doi: 10.1084/jem.20050683

138. Teh CE, Preston SP, Robbins AK, Stutz MD, Cooney J, Clark MP, et al. Caspase-8 has dual roles in regulatory T cell homeostasis balancing immunity to infection and collateral inflammatory damage. *Sci Immunol*. (2022) 7:eabn8041. doi: 10.1126/sciimmunol.abn8041

139. Bohgaki T, Mozo J, Salmena L, Matysiak-Zablocki E, Bohgaki M, Sanchez O, et al. Caspase-8 inactivation in T cells increases necroptosis and suppresses autoimmunity in bim-/- mice. *J Cell Biol*. (2011) 195:277–91. doi: 10.1083/jcb.201103053

140. Plaza-Sirvent C, Schuster M, Neumann Y, Heise U, Pils MC, Schulze-Osthoff K, et al. C-flip expression in foxp3-expressing cells is essential for survival of regulatory T cells and prevention of autoimmunity. *Cell Rep*. (2017) 18:12–22. doi: 10.1016/j.celrep.2016.12.022

141. Nicolè L, Sanavia T, Cappellesso R, Maffeis V, Akiba J, Kawahara A, et al. Necroptosis-driving genes ripk1, ripk3 and mlkl-P are associated with intratumoral cd3 (+) and cd8(+) T cell density and predict prognosis in hepatocellular carcinoma. *J immunother Cancer*. (2022) 10:e004031. doi: 10.1136/jitc-2021-004031

142. Wang S, Chang CW, Huang J, Zeng S, Zhang X, Hung MC, et al. Gasdermin C sensitizes tumor cells to parp inhibitor therapy in cancer models. *J Clin Invest*. (2024) 134:e166841. doi: 10.1172/jci166841

143. Gong Y, Peng Q, Gao Y, Yang J, Lu J, Zhang Y, et al. Dihydroartemisinin inhibited interleukin-18 expression by decreasing yap1 in hepatocellular carcinoma cells. *Acta histochemica*. (2023) 125:152040. doi: 10.1016/j.acthis.2023.152040

144. Li S, Sun R, Chen Y, Wei H, Tian Z. Tlr2 limits development of hepatocellular carcinoma by reducing il18-mediated immunosuppression. *Cancer Res*. (2015) 75:986–95. doi: 10.1158/0008-5472.Can-14-2371

145. He Y, Tian Z. Nk cell education via nonclassical mhc and non-mhc ligands. *Cell Mol Immunol*. (2017) 14:321–30. doi: 10.1038/cmi.2016.26

146. Liu S, Galat V, Galat Y, Lee YKA, Wainwright D, Wu J. Nk cell-based cancer immunotherapy: from basic biology to clinical development. *J Hematol Oncol*. (2021) 14:7. doi: 10.1186/s13045-020-01014-w

147. Böttcher JP, Bonavita E, Chakravarty P, Blees H, Cabeza-Cabrerizo M, Sammicheli S, et al. Nk cells stimulate recruitment of cdc1 into the tumor microenvironment promoting cancer immune control. *Cell*. (2018) 172:1022–37.e14. doi: 10.1016/j.cell.2018.01.004

148. Zheng Y, Chen Z, Han Y, Han L, Zou X, Zhou B, et al. Immune suppressive landscape in the human esophageal squamous cell carcinoma microenvironment. *Nat Commun*. (2020) 11:6268. doi: 10.1038/s41467-020-20019-0

149. Grote S, Ureña-Bailén G, Chan KC, Baden C, Mezger M, Handgretinger R, et al. *In vitro* evaluation of cd276-car nk-92 functionality, migration and invasion potential in the presence of immune inhibitory factors of the tumor microenvironment. *Cells*. (2021) 10:1020. doi: 10.3390/cells10051020

150. Parihar R, Rivas C, Huynh M, Omer B, Lapteva N, Metelitsa LS, et al. Nk cells expressing a chimeric activating receptor eliminate mdscs and rescue impaired car-T cell activity against solid tumors. *Cancer Immunol Res*. (2019) 7:363–75. doi: 10.1158/2326-6066.Cir-18-0572

151. Fisicaro P, Boni C. T and nk cell-based immunotherapy in chronic viral hepatitis and hepatocellular carcinoma. *Cells*. (2022) 11:180. doi: 10.3390/cells11020180

152. Lin X, Liu Z, Dong X, Wang K, Sun Y, Zhang H, et al. Radiotherapy enhances the anti-tumor effect of car-nk cells for hepatocellular carcinoma. *J Trans Med*. (2024) 22:929. doi: 10.1186/s12967-024-05724-4

153. Xiao R, Tian Y, Zhang J, Li N, Qi M, Liu L, et al. Increased siglec-9/siglec-9l interactions on nk cells predict poor hcc prognosis and present a targetable checkpoint for immunotherapy. *J Hepatol*. (2024) 80:792–804. doi: 10.1016/j.jhep.2024.01.028

154. Afonina IS, Cullen SP, Martin SJ. Cytotoxic and non-cytotoxic roles of the ctl/nk protease granzyme B. *Immunol Rev*. (2010) 235:105–16. doi: 10.1111/j.0105-2896.2010.00908.x

155. Screpanti V, Wallin RP, Ljunggren HG, Grandien A. A central role for death receptor-mediated apoptosis in the rejection of tumors by nk cells. *J Immunol (Baltimore Md: 1950)*. (2001) 167:2068–73. doi: 10.4049/jimmunol.167.4.2068

156. Bruning N, Bönnemann V, Watzl C. Analyzing the activity of the proteases granzyme B and caspase-8 inside living cells using fluorescence localization reporters. *Methods Cell Biol*. (2023) 178:13–24. doi: 10.1016/bs.mcb.2022.09.022

157. Prager I, Liesche C, van Ooijen H, Urlaub D, Verron Q, Sandström N, et al. Nk cells switch from granzyme B to death receptor-mediated cytotoxicity during serial killing. *J Exp Med*. (2019) 216:2113–27. doi: 10.1084/jem.20181454

158. Zhao Q, Chen DP, Chen HD, Wang YZ, Shi W, Lu YT, et al. Nk-cell-elicited gasdermin-D-dependent hepatocyte pyroptosis induces neutrophil extracellular traps that facilitate hbv-related acute-on-chronic liver failure. *Hepatol (Baltimore Md)*. (2024). doi: 10.1097/hep.0000000000000868

159. Feng Y, Daley-Bauer LP, Roback L, Potempa M, Lanier LL, Mocarski ES. Caspase-8 restricts natural killer cell accumulation during mcmv infection. *Med Microbiol Immunol*. (2019) 208:543–54. doi: 10.1007/s00430-019-00617-6

160. Palucka K, Banchereau J. Cancer immunotherapy via dendritic cells. *Nat Rev Cancer*. (2012) 12:265–77. doi: 10.1038/nrc3258

161. Prins MMC, van Roest M, Vermeulen JLM, Tjabringa GS, van de Graaf SFJ, Koelink PJ, et al. Applicability of different cell line-derived dendritic cell-like cells in autophagy research. *J Immunol Methods*. (2021) 497:113106. doi: 10.1016/j.jim.2021.113106

162. Silva Z, Ferro T, Almeida D, Soares H, Ferreira JA, Deschepper FM, et al. Mhc class I stability is modulated by cell surface sialylation in human dendritic cells. *Pharmaceutics*. (2020) 12:249. doi: 10.3390/pharmaceutics12030249

163. Han Z, Chen L, Peng H, Zheng H, Lin Y, Peng F, et al. The role of thyroid hormone in the renal immune microenvironment. *Int Immunopharmacol*. (2023) 119:110172. doi: 10.1016/j.intimp.2023.110172

164. Barry KC, Hsu J, Broz ML, Cueto FJ, Binnewies M, Combes AJ, et al. A natural killer-dendritic cell axis defines checkpoint therapy-responsive tumor microenvironments. *Nat Med*. (2018) 24:1178–91. doi: 10.1038/s41591-018-0085-8

165. Wang S, Wu Q, Chen T, Su R, Pan C, Qian J, et al. Blocking cd47 promotes antitumour immunity through cd103(+) dendritic cell-nk cell axis in murine hepatocellular carcinoma model. *J Hepatol*. (2022) 77:467–78. doi: 10.1016/j.jhep.2022.03.011

166. Ma H, Kang Z, Foo TK, Shen Z, Xia B. Disrupted brca1-palb2 interaction induces tumor immunosuppression and T-lymphocyte infiltration in hcc through cgas-sting pathway. *Hepatol (Baltimore Md)*. (2023) 77:33–47. doi: 10.1002/hep.32335

167. Chen J, Shi Z, Zhang C, Xiong K, Zhao W, Wang Y. Oroxin a alleviates early brain injury after subarachnoid hemorrhage by regulating ferroptosis and neuroinflammation. *J Neuroinflamm*. (2024) 21:116. doi: 10.1186/s12974-024-03099-3

168. Antonopoulos C, El Sanadi C, Kaiser WJ, Mocarski ES, Dubyak GR. Proapoptotic chemotherapeutic drugs induce noncanonical processing and release of il-1β Via caspase-8 in dendritic cells. *J Immunol (Baltimore Md: 1950)*. (2013) 191:4789–803. doi: 10.4049/jimmunol.1300645

169. Vanderheyde N, Aksoy E, Amraoui Z, Vandenabeele P, Goldman M, Willems F. Tumoricidal activity of monocyte-derived dendritic cells: evidence for a caspase-8-dependent, fas-associated death domain-independent mechanism. *J Immunol (Baltimore Md: 1950)*. (2001) 167:3565–9. doi: 10.4049/jimmunol.167.7.3565

170. Varga Z, Rácz E, Mázló A, Korodi M, Szabó A, Molnár T, et al. Cytotoxic activity of human dendritic cells induces ripk1-dependent cell death. *Immunobiology*. (2021) 226:152032. doi: 10.1016/j.imbio.2020.152032

171. Nazmy EA, El-Khouly OA, Zaki MMA, Elsherbiny NM, Said E, Al-Gayyar MMH, et al. Targeting P53/trail/caspase-8 signaling by adiponectin reverses thioacetamide-induced hepatocellular carcinoma in rats. *Environ Toxicol Pharmacol*. (2019) 72:103240. doi: 10.1016/j.etap.2019.103240

172. Che Z, Liu F, Zhang W, McGrath M, Hou D, Chen P, et al. Targeting cand1 promotes caspase-8/rip1-dependent apoptosis in liver cancer cells. *Am J Trans Res*. (2018) 10:1357–72.

173. Im JY, Kim BK, Lee JY, Park SH, Ban HS, Jung KE, et al. Ddias suppresses trail-mediated apoptosis by inhibiting disc formation and destabilizing caspase-8 in cancer cells. *Oncogene*. (2018) 37:1251–62. doi: 10.1038/s41388-017-0025-y

174. Jin X, Cai L, Wang C, Deng X, Yi S, Lei Z, et al. Casc2/mir-24/mir-221 modulates the trail resistance of hepatocellular carcinoma cell through caspase-8/caspase-3. *Cell Death Dis*. (2018) 9:318. doi: 10.1038/s41419-018-0350-2

175. El-Demiry SM, El-Yamany M, El-Gendy SM, Salem HA, Saber MM. Necroptosis modulation by cisplatin and sunitinib in hepatocellular carcinoma cell line. *Life Sci*. (2022) 301:120594. doi: 10.1016/j.lfs.2022.120594

176. Luan Z, He Y, He F, Chen Z. Rocaglamide overcomes tumor necrosis factor-related apoptosis-inducing ligand resistance in hepatocellular carcinoma cells by attenuating the inhibition of caspase-8 through cellular flice-like-inhibitory protein downregulation. *Mol Med Rep*. (2015) 11:203–11. doi: 10.3892/mmr.2014.2718

177. Carlisi D, Lauricella M, D'Anneo A, Emanuele S, Angileri L, Di Fazio P, et al. The histone deacetylase inhibitor suberoylanilide hydroxamic acid sensitises human hepatocellular carcinoma cells to trail-induced apoptosis by trail-disc activation. *Eur J Cancer (Oxford England: 1990)*. (2009) 45:2425–38. doi: 10.1016/j.ejca.2009.06.024

178. Jeon MY, Min KJ, Woo SM, Seo SU, Choi YH, Kim SH, et al. Maritoclax enhances trail-induced apoptosis via chop-mediated upregulation of dr5 and mir-708-mediated downregulation of cflip. *Molecules (Basel Switzerland)*. (2018) 23:3030. doi: 10.3390/molecules23113030

179. Wei Y, Chen X, Yang J, Yao J, Yin N, Zhang Z, et al. Dcr3 promotes proliferation and invasion of pancreatic cancer via a dcr3/stat1/irf1 feedback loop. *Am J Cancer Res*. (2019) 9:2618–33.

180. Liang DY, Huang W, Chang Q, Hou YQ. Shdcr3 sensitizes trail-resistant hcc cells by inducing caspase-dependent apoptosis while suppressing nf-κb dependent cflipl expression. *PloS One*. (2018) 13:e0191545. doi: 10.1371/journal.pone.0191545

181. Fan TJ, Han LH, Cong RS, Liang J. Caspase family proteases and apoptosis. *Acta Biochim Biophys Sin*. (2005) 37:719–27. doi: 10.1111/j.1745-7270.2005.00108.x

182. Fernandes-Alnemri T, Armstrong RC, Krebs J, Srinivasula SM, Wang L, Bullrich F, et al. *In vitro* activation of cpp32 and mch3 by mch4, a novel human apoptotic cysteine protease containing two fadd-like domains. *Proc Natl Acad Sci United States America*. (1996) 93:7464–9. doi: 10.1073/pnas.93.15.7464

183. Al-Rabia MW, Blaylock MG, Sexton DW, Walsh GM. Membrane receptor-mediated apoptosis and caspase activation in the differentiated eol-1 eosinophilic cell line. *J leukocyte Biol*. (2004) 75:1045–55. doi: 10.1189/jlb.0803404

184. Zhang HT, Wu J, Wen M, Su LJ, Luo H. Galangin induces apoptosis in hepatocellular carcinoma cells through the caspase 8/T-bid mitochondrial pathway. *J Asian Natural products Res*. (2012) 14:626–33. doi: 10.1080/10286020.2012.682152

185. Qi F, Inagaki Y, Gao B, Cui X, Xu H, Kokudo N, et al. Bufalin and cinobufagin induce apoptosis of human hepatocellular carcinoma cells via fas- and mitochondria-mediated pathways. *Cancer Sci*. (2011) 102:951–8. doi: 10.1111/j.1349-7006.2011.01900.x

186. Mohr A, Deedigan L, Jencz S, Mehrabadi Y, Houlden L, Albarenque SM, et al. Caspase-10: A molecular switch from cell-autonomous apoptosis to communal cell death in response to chemotherapeutic drug treatment. *Cell Death differentiation*. (2018) 25:340–52. doi: 10.1038/cdd.2017.164

187. Zhang YQ, Xiao CX, Lin BY, Shi Y, Liu YP, Liu JJ, et al. Silencing of pokemon enhances caspase-dependent apoptosis via fas- and mitochondria-mediated pathways in hepatocellular carcinoma cells. *PloS One*. (2013) 8:e68981. doi: 10.1371/journal.pone.0068981

188. Reed JC, Doctor K, Rojas A, Zapata JM, Stehlik C, Fiorentino L, et al. Comparative analysis of apoptosis and inflammation genes of mice and humans. *Genome Res*. (2003) 13:1376–88. doi: 10.1101/gr.1053803

189. Jänicke RU, Sohn D, Totzke G, Schulze-Osthoff K. Caspase-10 in mouse or not? *Sci (New York NY)*. (2006) 312:1874. doi: 10.1126/science.312.5782.1874a

190. Xiang Y, Wang Q, Guo Y, Ge H, Fu Y, Wang X, et al. Cx32 exerts anti-apoptotic and pro-tumor effects via the epidermal growth factor receptor pathway in hepatocellular carcinoma. *J Exp Clin Cancer res: CR*. (2019) 38:145. doi: 10.1186/s13046-019-1142-y

191. Xiang YK, Peng FH, Guo YQ, Ge H, Cai SY, Fan LX, et al. Connexin32 activates necroptosis through src-mediated inhibition of caspase 8 in hepatocellular carcinoma. *Cancer Sci*. (2021) 112:3507–19. doi: 10.1111/cas.14994

192. Chen J, Jin Z, Zhang S, Zhang X, Li P, Yang H, et al. Arsenic trioxide elicits prophylactic and therapeutic immune responses against solid tumors by inducing necroptosis and ferroptosis. *Cell Mol Immunol*. (2023) 20:51–64. doi: 10.1038/s41423-022-00956-0

193. Sas Z, Cendrowicz E, Weinhäuser I, Rygiel TP. Tumor microenvironment of hepatocellular carcinoma: challenges and opportunities for new treatment options. *Int J Mol Sci*. (2022) 23:3778. doi: 10.3390/ijms23073778

194. Vucur M, Ghallab A, Schneider AT, Adili A, Cheng M, Castoldi M, et al. Sublethal necroptosis signaling promotes inflammation and liver cancer. *Immunity*. (2023) 56:1578–95.e8. doi: 10.1016/j.immuni.2023.05.017

195. Mohammed S, Thadathil N, Selvarani R, Nicklas EH, Wang D, Miller BF, et al. Necroptosis contributes to chronic inflammation and fibrosis in aging liver. *Aging Cell*. (2021) 20:e13512. doi: 10.1111/acel.13512

196. Kaiser WJ, Upton JW, Long AB, Livingston-Rosanoff D, Daley-Bauer LP, Hakem R, et al. Rip3 mediates the embryonic lethality of caspase-8-deficient mice. *Nature*. (2011) 471:368–72. doi: 10.1038/nature09857

197. Visalli M, Bartolotta M, Polito F, Oteri R, Barbera A, Arrigo R, et al. Mirna expression profiling regulates necroptotic cell death in hepatocellular carcinoma. *Int J Oncol*. (2018) 53:771–80. doi: 10.3892/ijo.2018.4410

198. Shen Q, Jiang Y, Hu X, Du Z. A newly identified pyroptosis-related gene signature for predicting prognosis of patients with hepatocellular cancer. *Trans Cancer Res*. (2022) 11:3175–86. doi: 10.21037/tcr-22-366

199. Zheng S, Xie X, Guo X, Wu Y, Chen G, Chen X, et al. Identification of a pyroptosis-related gene signature for predicting overall survival and response to immunotherapy in hepatocellular carcinoma. *Front Genet*. (2021) 12:789296. doi: 10.3389/fgene.2021.789296

200. Gao X, Wang WX, Zhang XL. A novel pyroptosis risk model composed of nlrp6 effectively predicts the prognosis of hepatocellular carcinoma patients. *Cancer Med*. (2023) 12:808–23. doi: 10.1002/cam4.4898

201. Cui L, Xu X, Fan H, Wan X, Chen Q, Zhang J, et al. Reuterin promotes pyroptosis in hepatocellular cancer cells through mtdna-mediated sting activation and caspase 8 expression. *Cancer Lett*. (2024) 601:217183. doi: 10.1016/j.canlet.2024.217183

202. Dieguez HH, Romeo HE, Alaimo A, Bernal Aguirre NA, Calanni JS, Adán Aréan JS, et al. Mitochondrial quality control in non-exudative age-related macular degeneration: from molecular mechanisms to structural and functional recovery. *Free Radical Biol Med*. (2024) 219:17–30. doi: 10.1016/j.freeradbiomed.2024.03.024

203. Chen C, Wang Z, Ding Y, Qin Y. Tumor microenvironment-mediated immune evasion in hepatocellular carcinoma. *Front Immunol*. (2023) 14:1133308. doi: 10.3389/fimmu.2023.1133308

204. Tsai JJ, Chen JH, Chen CH, Chung JG, Hsu FT. Apoptosis induction and erk/nf-κb inactivation are associated with magnolol-inhibited tumor progression in hepatocellular carcinoma *in vivo*. *Environ Toxicol*. (2020) 35:167–75. doi: 10.1002/tox.22853

205. Peng F, Zhu F, Cao B, Peng L. Multidimensional analysis of panoptosis-related molecule casp8: prognostic significance, immune microenvironment effect, and therapeutic implications in hepatocellular carcinoma. *Genet Res*. (2023) 2023:2406193. doi: 10.1155/2023/2406193

206. Zhu HF, Liu YP, Liu DL, Ma YD, Hu ZY, Wang XY, et al. Role of tgfβ3-smads-sp1 axis in dcr3-mediated immune escape of hepatocellular carcinoma. *Oncogenesis*. (2019) 8:43. doi: 10.1038/s41389-019-0152-0

frontiers | Frontiers in Immunology

TYPE Original Research
PUBLISHED 20 February 2025
DOI 10.3389/fimmu.2025.1529569

OPEN ACCESS

EDITED BY
Pradeep Kumar Shukla,
University of Tennessee Health Science Center (UTHSC), United States

REVIEWED BY
Tianyi Xia,
Southeast University, China
Vibha Tripathi,
Animal and Plant Health Inspection Service (USDA), United States

*CORRESPONDENCE
Yongchao Cai
caiyongchao2007@126.com
Zhiying He
zyhe@tongji.edu.cn

RECEIVED 17 November 2024
ACCEPTED 03 February 2025
PUBLISHED 20 February 2025

CITATION
Mu X, Pan L, Wang X, Liu C, Li Y, Cai Y and He Z (2025) Development of a prognostic model for hepatocellular carcinoma based on microvascular invasion characteristic genes by spatial transcriptomics sequencing. *Front. Immunol.* 16:1529569. doi: 10.3389/fimmu.2025.1529569

Development of a prognostic model for hepatocellular carcinoma based on microvascular invasion characteristic genes by spatial transcriptomics sequencing

Xiaolan Mu[1], Lili Pan[1], Xicheng Wang[1], Changcheng Liu[1,2], Yu Li[1], Yongchao Cai[1,2]* and Zhiying He[1,2,3]*

[1]Institute for Regenerative Medicine, Medical Innovation Center and State Key Laboratory of Cardiology, Shanghai East Hospital, School of Life Sciences and Technology, Tongji University, Shanghai, China, [2]Shanghai Engineering Research Center of Stem Cells Translational Medicine, Science and Technology Commission of Shanghai Municipality, Shanghai, China, [3]Shanghai Institute of Stem Cell Research and Clinical Translation, Shanghai Municipal Education Commission, Shanghai, China

Microvascular invasion (MVI) is an independent risk factor for the recurrence and metastasis of hepatocellular carcinoma (HCC), associated with poor prognosis. Thus, MVI has significant clinical value for the treatment selection and prognosis assessment of patients with HCC. However, there is no reliable and precise method for assessing the postoperative prognosis of MVI patients. This study aimed to develop a new HCC prognosis prediction model based on MVI characteristic genes through spatial transcriptomics sequencing, distinguishing between high-risk and low-risk patients and evaluating patient prognosis. In this study, four MVI samples with different grades were selected for spatial transcriptomic sequencing to screen for MVI region-specific genes. On this basis, an HCC prognostic model was constructed using univariate Cox regression analysis, LASSO regression analysis, random survival forest, and stepwise multivariate Cox regression analysis methods. We constructed a 7-gene prognostic model based on MVI characteristic genes and demonstrated its applicability for predicting the prognosis of HCC patients in three external validation cohorts. Furthermore, our model showed superior predictive performance compared with three published HCC prediction prognostic models and could serve as an independent prognostic factor for HCC. Additionally, single nucleus RNA sequencing analysis and multiple immunofluorescence images revealed an increased proportion of macrophages in high-risk patient samples, suggesting that HCC tumor cells may promote HCC metastasis through MIF-CD74 cell interactions. To sum up, we have developed a 7-gene biomarker based on MVI that can predict the survival rate of HCC patients at different stages. This predictive model can be used to categorize into high- and low- risk groups, which is of great significance for the prognostic assessment and personalized treatment of HCC patients.

KEYWORDS

hepatocellular carcinoma, microvascular invasion, spatial transcriptome sequencing, single-nucleus RNA sequencing, prognostic model

1 Introduction

Hepatocellular carcinoma (HCC) is the primary liver cancer accounts for approximately 85 to 90% of all liver cancers (1). It has an insidious onset, and easy recurrence and metastasis. This makes HCC the sixth most common cancer and the third leading cause of cancer-related death (2). Surgical resection, liver transplantation, neoadjuvant therapy and targeted drugs are the main methods for early to intermediate stage HCC (3–5). Although these methods have improved the effectiveness of HCC treatment, over 70% of patients experience recurrence within 5 years after surgery, indicating a poor prognosis (6). Ninety percent of cases of recurrence and death are related to metastases (7). Therefore, there is an urgent need to develop new prognostic assessment methods to predict the clinical prognosis of HCC patients. Constructing prognostic models to predict survival rates and classify patients remains of great significant importance.

Tumor cells infiltrate blood vessels and form vascular cancer thrombi during the metastasis process. Microvascular invasion (MVI) refers to the presence of cancer cell nests in the lumens of blood vessels lined with endothelium under a microscope (8, 9). MVI represents an early stage of vascular infiltration and metastasis in HCC and is an independent prognostic factor for tumor recurrence and metastasis in HCC patients (10, 11). The prediction of HCC prognosis is vital for the selection of therapeutic approaches and prognostic improvement in patients with HCC. Consequently, more accurate predictive markers of MVI are needed to evaluate the risk of tumor recurrence and the prognosis of HCC patients. The tumor microenvironment (TME) plays an important role in the formation of MVI. However, conventional sequencing methods have difficulty analyzing the differential genes, microenvironmental changes and cellular heterogeneity in the MVI sites of HCC. Single-cell RNA sequencing (scRNA-seq) can reveal variations between different types and cell heterogeneity. This technology is widely used in various cancer studies, including studies of liver (12, 13), breast (14), and kidney cancer (15). Single-nucleus RNA sequencing (snRNA-seq) can also classify cells and map the cellular atlas of tissues. However, because single-cell RNA sequencing is only suitable for fresh tissue, many clinical frozen clinical samples cannot be subjected to single-cell RNA sequencing (16). Moreover, the dissociation process in single-cell RNA sequencing induces the expression of stress genes, leading to transcription biases in cells (17, 18). Furthermore, studies have shown that snRNA-seq works consistently with scRNA-seq and accurately captures the transcriptional state of cells, which has been confirmed in various tissues (16, 19, 20). Therefore, this study employs single-nucleus RNA sequencing instead of single-cell RNA sequencing. Nevertheless, single-nucleus sequencing loses spatial location information during the nucleus isolation process, making it difficult to obtain the spatial positioning of individual cells within tissues. The recent development of spatial transcriptomics (ST) has enabled the sequencing of smaller tissue samples to obtain gene expression profiles of specific locations and spatial locations of cells. Spatial transcriptomics generates complete transcriptome data from an entire tissue sample and allows the localization and differentiation of functional genes in specific tissue regions, creating spatial expression maps of cells and genes (21). This technology is now widely used in the research of various diseases, including gene expression and cell mapping during heart development (22), pancreatic cancer (23), prostate cancer (24), and skin squamous cell carcinoma (25). It is currently assumed that MVI is located mainly at the junction between the tumor and adjacent tumor. ST can obtain not only transcriptome data of the connection between the tumor and adjacent tumor but also data of the MVI region, and directly screen the characteristic genes of the MVI region. In conclusion, we combined spatial transcriptome sequencing and single-nucleus RNA sequencing techniques to obtain differentially expressed genes and determine the microenvironment composition of microvascular invasion sites. These finding are crucial for understanding the mechanism of MVI formation and finding new treatment targets.

The purpose of this study was to investigate MVI molecular markers using spatial transcriptome technology and to construct a prognostic risk assessment model for HCC patients based on MVI, with the aim of providing appropriate treatment methods for HCC patients.

2 Materials and methods

2.1 Human HCC tissues

From May 2020 to February 2021, a total of 28 early HCC tumors and adjacent normal tissues were collected from patients who underwent surgical resection at the Eastern Hepatobiliary Surgery Hospital (Shanghai, China). Each tissue sample was approximately 1 cm ×1 cm × 1 cm in size, washed in PBS, dehydrated, and quickly frozen in isopentane and liquid nitrogen. The samples were subsequently transported to the laboratory on dry ice. The tissues were embedded in optimal cutting temperature (OCT) compound (Sakura, catalog no. 4583) and stored at -80°C until use. The cryosections were then subjected to H&E staining to determine the number and distribution of MVI. The samples were sent to OE Biotech for spatial transcriptomics and single nucleus-RNA sequencing. All diagnoses were examined histologically by a specialized pathologist.

2.2 Spatial transcriptomics sequencing

This experiment utilized the 10x Genomics Visium technology platform. All reagents and consumables used in the experiment were provided by this platform. Detailed product numbers are available at www.10xgenomics.com/products/spatial-gene-expression. After fixation, H&E staining, and imaging of the sections, tissue-specific permeabilization was performed using kits provided by 10x. Library construction and sequencing were then performed using spatially barcoded mRNA-binding oligonucleotides according to standard protocols of the 10x Genomics platform.

2.3 Spatial transcriptome sequencing analysis

After the raw spatial transcriptomics data were obtained, Space Ranger was used for data quality control. The generated spot matrices were analyzed using the "Seurat7" package. Subsequently, we utilized principal component analysis (PCA) to reduce dimensions, t-distributed Stochastic Neighbor Embedding (t-SNE) to demonstrate clusters, and the mutual nearest neighbors (MNN) algorithm to eliminate batch effects. Next, genes with spatial expression patterns were identified using the FindMarkers function, followed by Gene Ontology (GO) enrichment and Kyoto Encyclopedia of Genes and Genomes (KEGG) pathway analyzes for the differentially expressed genes.

2.4 Single-nucleus RNA sequencing

The frozen liver tissue was rinsed twice with medium, and then the frozen liver tissue was minced. Then resuspend the minced liver tissue in 0.5 mL ice-cold EZ lysis buffer and homogenize on ice. The homogenized liver tissue is then successively filtered through a cell strainer. Next, centrifuge the filtered liver tissue for 5 min at 4°C and 500 g to precipitate the cell nucleus. Subsequently, resuspend the precipitated cell nucleus in 1 mL of ice-cold buffer and filter through a 20 μm cell strainer. Finally, proceed immediately to single-nucleus RNA sequencing of the obtained the cell nucleus.

2.5 Single-nucleus RNA sequencing analysis

After obtaining the raw single nucleus data, we first utilized Cell Ranger for data quality control and gene qualification. Following quantification, we filtered out low quality cells and low abundance genes. Subsequently, we applied MNN and t-SNE algorithms for dimensionality reduction and clustering. Then we annotated the cell types using the "SingleR" package and our own statistically determined specific marker genes. Finally, we selected differentially expressed genes based on the fold change and *p*-value results, and performed GO enrichment analysis and KEGG pathway enrichment analysis for these genes.

2.6 Data acquisition

A total of 424 TCGA-LIHC transcriptome sequencing datasets, 371 single nucleotide variation (SNV) datasets, and 377 clinical information datasets were downloaded from The Cancer Genome Atlas (TCGA) database (https://portal.gdc.cance.gov/). After the data were integrated, 371 primary HCC transcriptome sequencing data, 171 early Tumor Node Metastasis classification (TNM) HCC transcriptome sequencing data, and 167 early TNM HCC SNV data were obtained. In addition, 225 cases of HCC microarray data and survival information were retrieved from the GSE14520 dataset in the Gene Expression Omnibus (GEO) database (https://www.ncbi.nlm.nih.gov/geo/), including 93 cases of early-stage TNM HCC microarray data; and 115 cases of HCC microarray data and survival information were obtained from the GSE76427 dataset. From the International Cancer Genome Consortium (ICGC) LIRI-JP dataset (https://dc.icgc.org/), 240 cases of HCC transcriptomic sequencing data and survival information were collected. The TCGA dataset acted as a training set for building the predictive prognosis model, while the GSE14520, GSE76427 and LIRI-JP datasets served as validation sets for external validation of the model.

2.7 Gene set variation analysis

The HALLMARK gene sets were collected from the MSigDB database (Molecular Signature Database, http://www.gsea-msigdb.org/gsea/msigdb). Gene set variation analysis (GSVA) was employed to assess HALLMARK pathway scores in HCC patients. Pearson correlation coefficient was utilized to examine the relationships between risk scores and HALLMARK signaling pathways. A p value < 0.05 was considered statistically significant.

2.8 Evaluation and validation of the prognostic models

The "Survminer" package was used to identify the optimal risk score cutoff and calculate risk scores for HCC patients. Patients were divided into high and low risk groups according to the best cutoff value. The Kaplan-Meier survival curves show the prognosis of the high and low risk groups and the log-rank test evaluate survival differences between the two groups. The "timeROC" package was used to draw 1-year, 2-year, and 3-year Receiver Operating Characteristic (ROC) curves and calculate the Area Under the curve (AUC). The ROC and AUC curve can be used to estimate the diagnostic value of the prognostic model in predicting the prognosis of HCC patients. The survival analysis was conducted in the GSE14520 external validation cohort, and the ROC curves were plotted to verify the stability and accuracy of the prognostic model. To further assess the predictive performance of the prognostic model, we calculated the risk scores of liver cancer patients at all stages in the TCGA, GSE14520, GSE76427 and LIRI-JP cohorts and performed survival analysis for each group. The "AUCell" package was used to evaluate the expression of the prognostic model gene set in each region of the spatial transcriptome. The ssGSEA algorithm of the "GSVA" package was used to estimate the expression of the prognostic gene set in each cell type from single-nucleus transcriptome sequencing.

2.9 This model is compared with three published MVI-related models

This model was compared with three existing MVI-related models. Scores for HCC patients were calculated using scoring formulas provided in two publications, grouped by optimal cutoff values for survival analysis, and ROC curves were plotted. The

correlation between this model and the three existing MVI-related models was examined using Pearson correlation analysis, with $p < 0.05$ considered statistically significant.

2.10 Clinical characteristics of the signature

To determine the correlation between the risk score and clinical characteristics (age, gender, Grade classification, ChildPugh classification, alcohol consumption, hepatitis B), we applied the Wilcoxon test for assessment. ROC curves of the prognostic model and various clinical characteristics were plotted using the "pROC" package, and the AUC and concordance index values were compared. To determine whether the prognostic model is a prognostic factor for HCC patients, multivariate Cox regression analysis was performed on the prognostic model, age, gender, Grade classification, ChildPugh classification, alcohol consumption, Hepatitis B virus (HBV), Hepatitis C virus (HCV), alpha-fetoprotein, platelet count, prothrombin, albumin, and creatinine levels to identify prognostic factors for HCC. Nomograms for prognostic factors in HCC patients were plotted using the "rms" package, with each patient assigned points for each prognostic factor. The sum of these values resulted in a total score that was used to predict the 1-year, 3-year, and 5-year survival rates of patients with HCC. To compare the predicted survival rates with those observed and to evaluate the accuracy of the nomogram, a 5-year calibration curve was constructed.

2.11 Characteristics of different risk groups

The "DESeq2" package was used to identify genes highly expressed in the high-risk group with a fold change (FC) > 2 and an adjusted p value < 0.05. These highly expressed genes were subjected to KEGG pathway enrichment analysis, and pathways with a p value < 0.05 were considered enriched. Waterfall plots for ten most frequently mutated genes in both the high- and low-risk groups were created using the oncoplot function from the "maftools" package. The tumor mutation burden (TMB) for each patient was computed and a Pearson correlation analysis was performed between the risk score and the TMB, with a correlation coefficient and a p value < 0.05 considered statistically significant. The Tumor Immune Estimation Resource (TIMER) 2.0 database (http://timer.cistrome.org/) can assess the infiltration of six types of immune cells in TCGA, including B cells, CD4+ T cells, CD8+ T cells, neutrophils, macrophages, and dendritic cells. The Tumor Immune Dysfunction and Exclusion (TIDE) score and exclusion score are calculated via TIDE (http://tide.dfci.harvard.edu/) to predict and the immune escape ability of HCC and infer the effectiveness of immunotherapy in HCC patients.

2.12 Cell interaction analysis

Malignant cell scores in MVI samples were calculated using the ssGSEA algorithm. Malignant cells are categorized into high-score and low-score groups based on the median of these scores. The "CellChat" package was used to analyze cell the interactions between high-score and low-score malignant cells and other cell types to calculate and infer the cell interaction networks. The number of interactions, the strength of interactions, and the ability to send and receive signals are compared between high-score and low-score malignant cells.

2.13 Quantitative real-time PCR

Total RNA was isolated from liver samples using TRIzol® LS Reagent (Thermo Scientific, USA), and 250 µl of fluid was added to 750 µl TRIzol LS. Subsequently, 200 µl of chloroform was used for phase separation and 100% isopropanol and Glycogen (Beyotime, Shanghai, China) were used for RNA precipitation. Finally, the RNA was eluted in 10 µl RNase-free water after being washed twice in 75% ethanol. cDNA was synthesized by reverse transcription with a PrimeScript™ RT Master Mix (Takara, Japan). qPCR was performed using 2x SYBR Green qPCR Master Mix (bimake, USA) with ABI Prism Q7 System (Thermo Fisher Scientific, USA) in a 10 µl reaction system. Expression of different genes were normalized to GAPDH and were analyzed using the 2-ΔΔCT method. The primers used in this study are shown in Supplementary Table S1.

2.14 Gene set variation analysis

GSVA is a non-parametric and unsupervised approach for assessing the enrichment of transcriptome gene sets. It evaluates the enrichment of metabolic pathways in samples by synthesizing scores for the gene sets of interest, transforming gene-level variations into pathway-level changes to infer the biological functions of samples. In this study, we subclassify myeloid cells and use the GSVA algorithm to comprehensively score macrophages and non-macrophages within myeloid cells, thereby assessing the potential biological function changes in macrophages and non-macrophages.

2.15 Western blotting

The HCC tissues were lysed using RIPA buffer supplemented with a protease inhibitor cocktail. The protein samples were then resolved using SDS-PAGE and transferred to PVDF membranes (Millipore, no. ISEQ00010). After blocking the membranes with 5% skimmed milk (in TBST) for 1h at room temperature, they were incubated with the primary antibody overnight at 4°C. Subsequently, the membranes were incubated with the HRP-conjugated IgG at room temperature for 1h. Finally, the bands were visualized using enhanced chemiluminescence. Antibodies used are listed as follow: GAPDH (Proteintech, Cat No. 10494, 1:5000), SPLI (Abclonal, Cat No. A1897, 1:1000), GPX2(Abclonal, Cat No. A15999, 1:1000), CFL1 (Proteintech, Cat No. 10960, 1:3000), CANX (Proteintech, Cat No. 10427, 1:5000), DCN (Proteintech, Cat No. 14667, 1:2000), CARHSP1 (Proteintech, Cat No. 11672, 1:1500), PIGO (Abclonal, A18670, 1:1000).

2.16 Multiple immunofluorescence

Tissue paraffin sections were baked at 60 °C for 1 hour, and then placed in xylene I/II for 15 minutes for dewaxing. Different alcohol concentrations (95%, 80%, 70%, 50%) were used for hydration. The citrate antigen retrieval solution (PH 6.0) (MXB, China) was carried out in the microwave for 20 minutes. Endogenous peroxidase was blocked with 3% H_2O_2 at room temperature for 15 minutes in the dark. Blocking was performed with 3% BSA. The primary antibody was incubated overnight at 4°C. The next day, the primary antibody was washed off with PBST, the HRP-conjugated secondary antibody was added for 50 minutes at room temperature. A ready-to-use fluorescent dye was added and incubated for 10 minutes at room temperature (Abclonal; China). The antibody was washed, repeating the steps with 3% H_2O_2 until staining with the three primary antibodies was completed. DAPI incubation for 10 min was carried out for nuclear counterstaining, followed by slide sealing and microscopic examination. MIF (Proteintech, USA, 1:250); CD68 (CST, USA, 1:2000); CD74 (Santa Cruz; USA, 1:250).

2.17 Statistical analysis

In this study, GraphPad Prism 8.0 and R software v4.0.1 were used for the statistical analysis and plotting of the experimental data. A $p < 0.05$ was considered statistically significant.

3 Results

3.1 Identification of differentially expressed genes in MVI by spatial transcriptome analysis

To understand the causes of microvascular invasion in HCC and identify new biomarkers, we employed spatial transcriptome sequencing to discover novel targets. The workflow of this study is shown in Figure 1. We collected 25 pairs of early HCC patient tumors and adjacent normal tissues for cryo-embedding, and the MVI grade and quantity were determined by H&E staining. Complete clinical and pathological information can be found in the Supplementary Table S2. To analyze the differentially expressed genes in the MVI regions of hepatocellular carcinoma patients, we performed spatial transcriptome sequencing on 2 M0 and 2 MVI samples (P1_M0, P2_M0, P3_M1, P4_M2) (Supplementary Figure 1A). The spatial transcriptome technology in this study utilized the 10x Genomics Visium platform with spot diameters of 55 µm (containing 8-20 cells) (Figure 2A), and the 6.5 mm × 6.5 mm capture area contained 5000 spots. In this study, Space Ranger was used to assess the quality of the spatial transcriptome sequencing data, yielding a total of 13546 spots. After subsequent quality control and batch effect correction, 11620 spots remained (Supplementary Figures 1B, C). Furthermore, the data showed that the number of spots per sample was approximately 3000, with an average gene number per spot of approximately 3782 and an average Unique Molecular Identifier (UMI) number per spot of 15157 (Supplementary Table S3). Overall, UMI and gene counts were higher in tumor regions than in normal areas, which is consistent with previous studies (Supplementary Figures 1B, C).

Tissue sections were segmented by pathologists from our hospital into five different regions: tumor, normal, inflammation, MVI and fibrosis areas (Figure 2B). To verify whether the transcriptomic features matched the histological information, we compared H&E images with the corresponding spatial transcriptome data. The results confirmed that the regions defined by the expression of cell type marker genes were highly consistent with their pathological images. Specifically, ALB and CYP2E1 were highly expressed in normal areas, GPC3 and AKR1B10 were highly expressed in tumor areas, ACTA2 and COL1A1 were highly expressed in fibrostic areas, and PTPRC was highly expressed in inflammation areas (Supplementary Figure 2).

Next, we performed a differential expression analysis for the five regions using the FindAllMarkers function, with the criteria of absolute fold change (|FC|) > 1.5 and *p.adj* < 0.05. *A* total of 82 potential MVI-related genes were identified, including 49 upregulated genes and 33 downregulated genes (Figure 2C). GO enrichment analysis revealed that these genes are involved in biological processes such as the regulation of intercellular adhesion, cell growth, coagulation, and the regulation of the immune response in tumor cells (Figure 2D). These 82 differentially expressed genes were identified as MVI-related and will be used for subsequent modeling.

3.2 Construction of the HCC prognostic model on the basis MVI characteristic genes

We employed various analysis methods, including univariate Cox regression analysis, LASSO regression analysis, multivariate Cox regression analysis, CoxBoost, random survival forest, and stepwise regression analysis, to select the optimal HCC prediction model in the TCGA training cohort (Supplementary Table S4).

Univariate Cox regression analysis was conducted on the early TCGA HCC dataset to identify MVI genes associated with patient prognosis. A total of 13 MVI genes related to the prognosis of HCC patients were selected. These 13 MVI genes were then analyzed using LASSO regression, resulting in 8 genes with non-zero coefficients (Supplementary Figures 3A, B). Finally, a bidirectional stepwise multivariate Cox regression was performed for these 8 genes to obtain the best prognostic model based on the lowest AIC value.

CoxBoost was used to find the best model fit when the optimal boosting step was performed as 97 through 10-fold cross-validation, and picked out six non-zero coefficients of MVI-related genes were selected (Supplementary Figures 3C, D). Then, these 6 genes were subjected to multifactorial Cox regression analysis and bidirectional stepwise regression analysis to optimize this model, obtaining the best model based on the minimal AIC value.

Ultimately, the randomForestSRC package was utilized to perform random survival forest analysis. The error rate was lowest when the random survival forest model included 8 genes (Supplementary Figures 3E–G). These 8 genes were then subjected to multifactorial Cox regression analysis and bidirectional stepwise

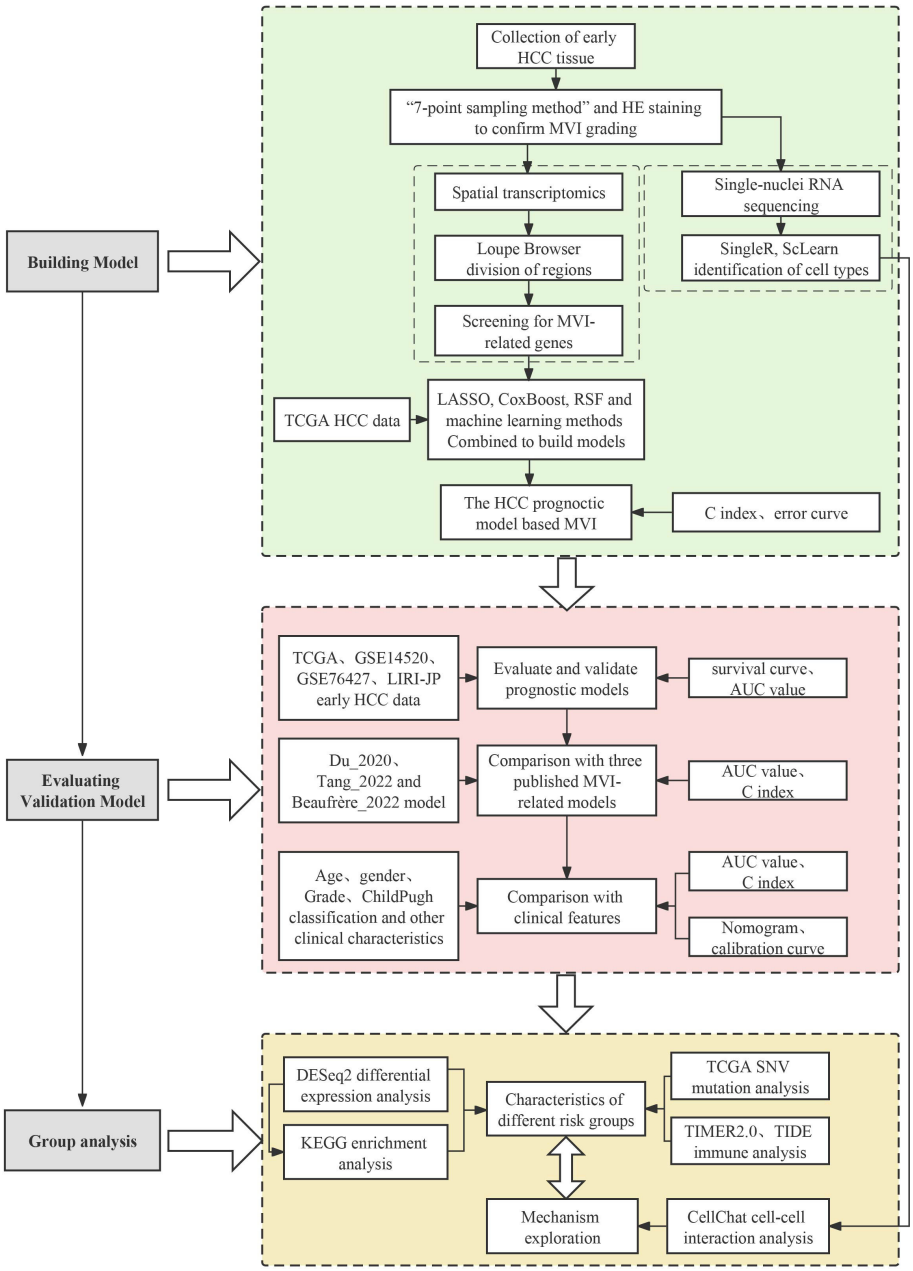

FIGURE 1
Workflow of this study.

regression analysis to optimize the model, with the best model identified based on the lowest AIC value.

The comparison revealed that the model built using a combination of random survival forest and bidirectional stepwise multifactorial Cox regression analysis achieved the highest calibration C-index (0.717107) and the lowest error rate, suggesting that the model created using the combination method has greater prognostic prediction accuracy (Figures 3A, B). We then selected 7 key MVI-related genes (GPX2, CANX, SLPI, CFL1, PIGO, CARHSP1, DCN) to construct the HCC prognostic model. The formula for the prognostic risk score was as follows: Risk Score = (0.000376 × GPX2 expression) + (0.002959 × CANX expression) + (0.000203 × SLPI expression) + (0.0045 × CFL1 expression) + (0.056461 × PIGO expression) – (0.026806 × CARHSP1 expression) – (0.0101 × DCN expression). In this model, GPX2, CANX, SLPI, CFL1, and PIGO have positive coefficients and are considered risk-related genes, whereas DCN and CARHSP1 have negative coefficients and are protective genes.

We subsequently plotted Kaplan-Meier curves based on the expression levels of the 7 MVI genes. The curves showed that high expression levels of GPX2, CANX, SLPI, CFL1 and PIGO in patients were significantly associated with lower overall survival than those in low expression groups, which correlated with worse survival rates in HCC patients. DCN expression was associated with better survival rates, whereas high expression of CARHSP1 suggested a better

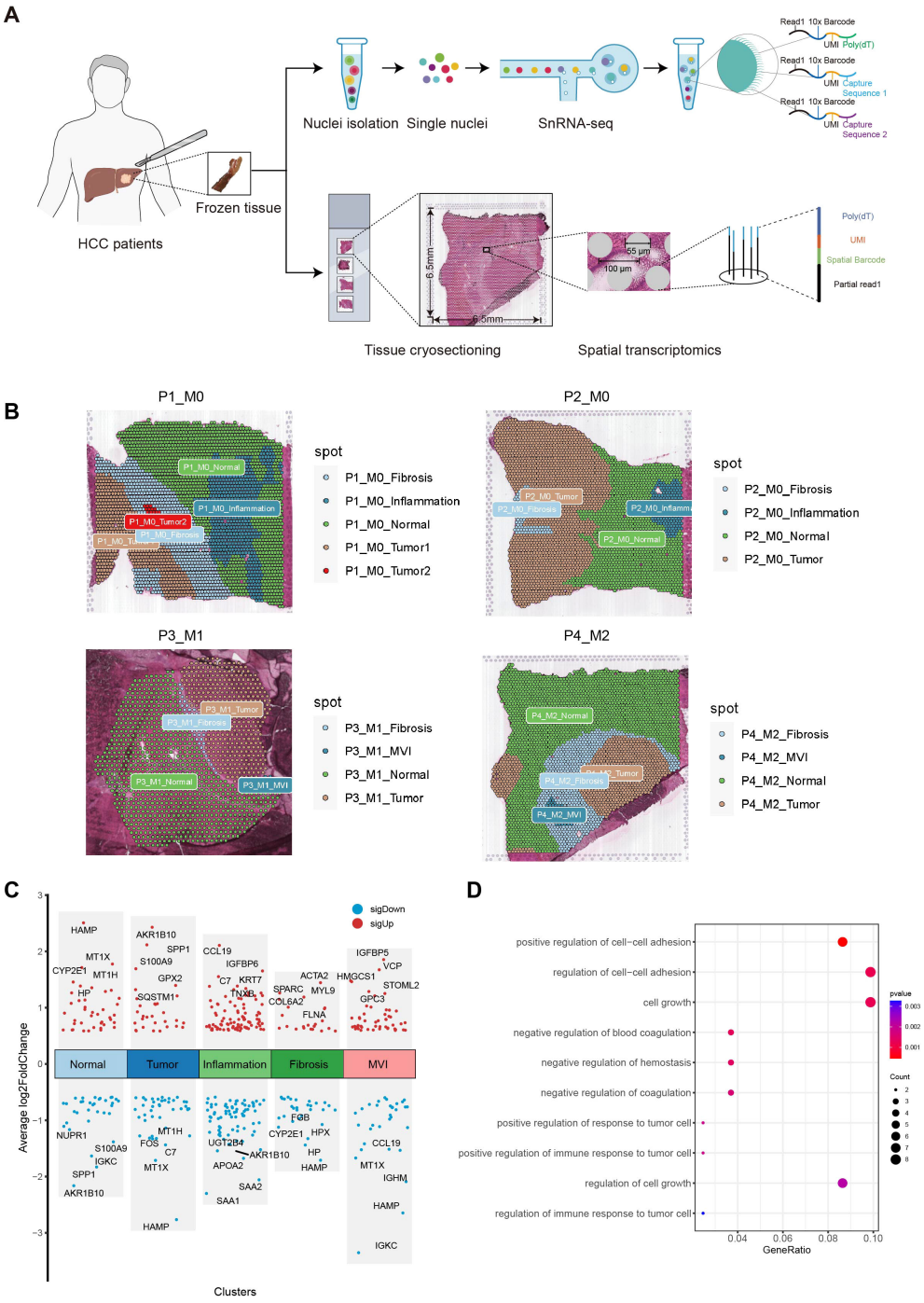

FIGURE 2
Exploration of MVI differential genes with ST. **(A)** Workflow of Hepatocellular carcinoma samples collection, processing for spatial transcriptomics sequencing, single-nuclei RNA sequencing and data analysis. **(B)** Regional division of HCC tissue sections: Tumor, Normal, MVI, Inflammation and fibrosis areas. **(C)** Plot of differential genes in five regions delineated by spatial transcriptome sequencing. Red dots indicate genes up-regulated in the five regions. Blue points indicate genes down-regulated in the five regions. **(D)** Gene Ontology enrichment analysis of MVI differential genes. MVI, Microvascular Invasion; HCC, Hepatocellular Carcinoma; GO, Gene Ontology.

prognosis for HCC patients, although the difference was not statistically significant (Figure 3C). We also found that the risk score was positively correlated with HCC-related HALLMARK signaling pathways such as mTORC1, PI3K/AKT/mTOR, and p53, suggesting that the poor prognosis of patients may be the result of a combination of multiple oncogenic pathways (Figure 3D).

3.3 The risk score based on MVI-related genes might be an independent risk factor for patients with HCC

To investigate the associations between the risk score and clinicopathological characteristics, we analyzed the correlations

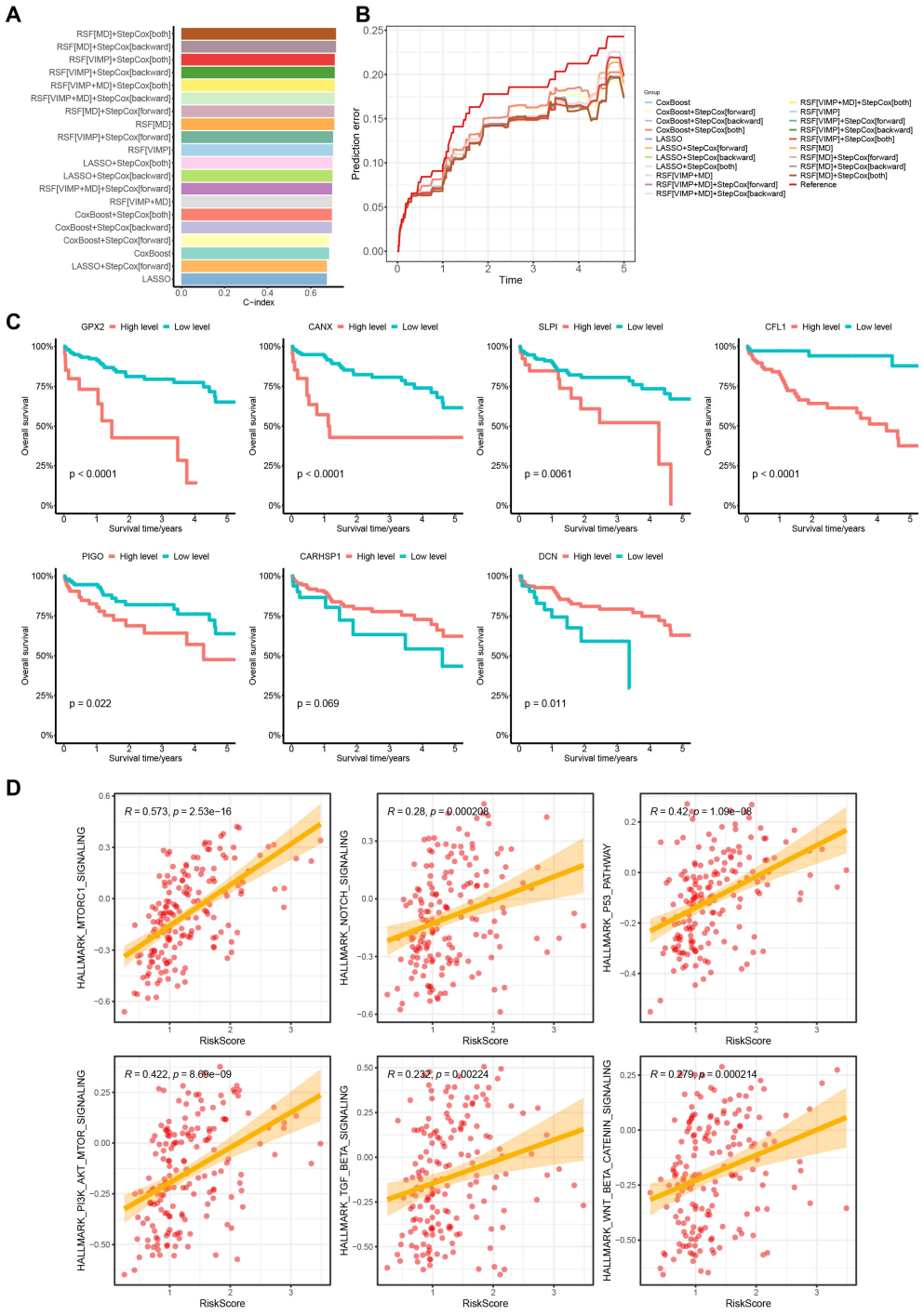

FIGURE 3
Random survival forest and bidirectional stepwise multifactorial Cox regression identification of key MVI differential genes of the model and prognostic analysis in the TCGA cohort. **(A)** C-indexes of 20 prognostic models obtained by different modeling methods. **(B)** Error curves of 20 prognostic models obtained by different modeling methods. **(C)** Survival analysis of 7 genes with the prognostic model based on the TCGA database. **(D)** Correlation analysis between early HCC patients risk scores and HALLMARK pathways. TCGA, The Cancer Genome Atlas.

between the expression of 7 MVI-related genes and clinical parameters in HCC patients (Supplementary Figure 4A). The results of the Wilcoxon test demonstrated a significant correlation between the risk score and different Grade levels. As the grade level increased, the risk score also increased. However, among other clinical characteristics, the risk score was not significant (Supplementary Figure 4B). Furthermore, we compared the AUC values and C-index of the risk score with those of various clinical characteristics. We found that the risk score had the highest AUC and C-index, indicating better predictive performance compared to individual clinical characteristics (Figures 4A, B). This suggest that the prognosis model has good predictive capability. To determine

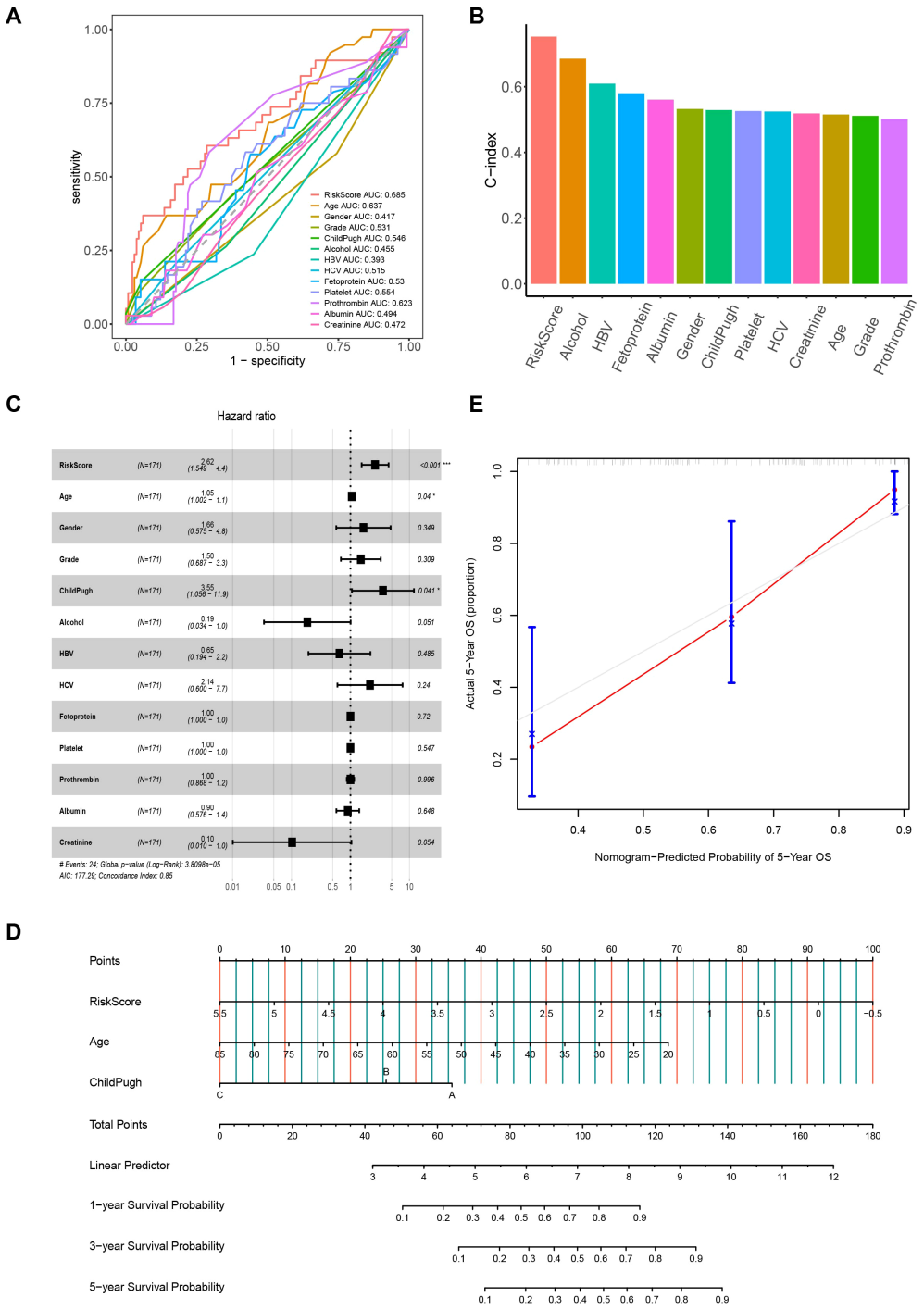

FIGURE 4
The correlation between the risk score and clinical characteristics. **(A)** ROC curves for the prognostic model and clinical characteristics. **(B)** C-index histograms for the prognostic model with different clinical characteristics. **(C)** Results of multivariate Cox regression analysis of the prognostic model and clinical characteristics. **(D)** Nomogram model created from the prognostic model, age, and Child-Pugh classification. **(E)** Five-year calibration curves. ROC, Receiver Operating Characteristic. *P< 0.05; ***P< 0.001.

whether the risk score is an independent risk factor for the prognosis of HCC patients, we also conducted a multivariate Cox regression analysis of the risk score and clinical characteristics. The results showed that the risk score, age, and Child-Pugh classification are related to the overall survival of HCC patients and can serve as independent risk factors, with the risk score being more closely associated with poor prognosis ($p < 0.001$) (Figure 4C). To make further specific predictions about individual prognosis, we integrated these independent prognostic factors to create a nomogram model. By calculating the score of each variable according to the patient's condition and summing them to get a total score. It is possible to predict the patient's 1-year, 3-year and 5-

year survival rates, allowing an intuitive assessment of the patient's prognosis and expanding its clinical applicability (Figure 4D). The calibration curve showed that the predicted 5-year survival rate was highly consistent with the actual survival rate, indicating that the nomogram is accurate and reliable (Figure 4E).

3.4 The HCC prognosis model based on MVI characteristic genes possesses good predictive value

To evaluate this prognostic model, we calculated the risk score of HCC patients in the TCGA cohort based on the prognostic model and classified the patients into low- and high-risk groups. The results indicated that the high-risk group had shorter survival times, higher mortality rates, and poorer prognosis compared to the low-risk group. The ROC curve demonstrated that the AUC values for 1-year, 2-year, and 3-year predictions were 0.81, 0.74, and 0.74, respectively, indicating that the model has good predictive ability for the prognosis of HCC patients (Figure 5A).

To further confirm the predictive value of the prognostic model in patients with HCC, we applied the same method to classify HCC patients into high- and low-risk groups in the validation cohort GSE14520. The results showed that the high-risk group in the validation cohort had shorter survival times, indicating a worse prognosis (Figure 5B), which is consistent with the above results. Moreover, the AUC values for 1-year, 2-year, and 3-year predictions in GSE14520 were 0.52, 0.59 and 0.63, respectively. These findings confirm the good predictive value of the prognostic model and its utility in assessing the survival risk of patients with HCC (Figure 5B).

In addition, we calculated the risk scores for HCC patients at all stages in the TCGA cohort and divided them into high- and low-risk groups. It turned out that the high-risk group had a worse prognosis. This was also validated in the external validation sets GSE76427 and LIRI-JP, indicating that this prognostic model can be used to predict the prognosis of HCC patients (Figure 5C). We also validated the expression of model genes using spatial transcriptomics. We found that the gene set of this prognostic model scored highest in the MVI regions of the spatial transcriptome (Figure 5D). Single-cell nuclear transcriptome UAMP plots showed the highest prognostic model gene set scores in malignant cells, validating the expression of model genes at the single-cell level (Figure 5E). Overall, this model can be used to predict the prognosis of HCC patients and has good predictive value.

Subsequently, we collected clinical tissues from HCC patients at our hospital and assessed the expression of 7 genes in 24 pairs of tumor and adjacent normal HCC tissues using qPCR. The results showed that protective genes (DCN and CARHSP1) were expressed at lower levels in tumors than in paired adjacent normal tissues (Figure 5F); risk genes (PIGO, GPX2, CFL1, SLPI, CANX) were expressed at higher levels in tumors than in paired adjacent normal tissues (Figure 5F). Moreover, we have also added qPCR and Western blot validation in samples of portal vein tumor thrombus. We examined the expression of these seven genes in seven pairs of para-tumor, tumor, and portal vein tumor thrombus (pvtt) tissues. The qPCR results indicated that the expression of protective genes (DCN and CARHSP1) gradually decreased in para-tumor, tumor, and pvtt tissues. Conversely, the expression of risk genes (PIGO, GPX2, CFL1, SLPI, CANX) gradually increased in these tissues (Figure 5G). In addition, we extracted proteins from three pairs of para-tumor, tumor, and pvtt tissues and performed western blotting (WB) experiments. The WB results showed that the expression of protective genes (DCN and CARHSP1) gradually decreased in para-tumor, tumor, and pvtt tissues. In contrast, the expression of risk-associated genes (PIGO, GPX2, CFL1, SLPI, and CANX) gradually increased in these tissues (Figure 5H). Therefore, these experiments further validated our prognostic model.

3.5 The model developed in this study outperforms other HCC models in terms of prediction performance

To further verify the prediction accuracy of our model, we compared it with three published HCC models. These models include a prognostic model of 7 MVI-related genes developed by Du et al. (26), a prognostic model of 3 MVI-related genes developed by Tang et al. (27) and a 6-gene HCC prediction model developed by Beaufrère et al. (28). We scored patients according to the scoring formulas provided in these three models and the ssGSEA algorithm, grouped them based on the optimal cutoff values, performed survival analysis, and plotted ROC curves (Figures 6A–C). We explored the correlation between our model and the three published HCC-related models using Pearson correlation analysis and considered $p < 0.05$ to indicate statistical significance. Notably, the model developed in our study showed a positive correlation with the predictive values of the models of Du and Tang et al. with consistent scoring trends (Figures 6A, B). However, it did not correlate with Beaufrère's prediction model, possibly because Beaufrère et al. developed an HCC prediction model based on data obtained using NanoString technology (Figure 6C). Finally, we compared the corrected C-index of the four models and found that the C-index of our model was greater than that of the three published HCC-related models, which clearly shows the predictive performance of our model (Figure 6D).

3.6 The high-risk group is more susceptible to genetic mutations and immune evasion

After assessing the performance of the model on various dimensions, we proceeded to evaluate the distinct characteristics of the different risk groups. Differential expression analysis was performed using the DESeq2 package for high- and low-risk groups with a threshold of FC > 2 and $p.adj < 0.05$ and identified 512 highly expressed genes in the high-risk group. KEGG pathway enrichment analysis showed that these genes were enriched in pathways related to the cell cycle, nucleocytoplasmic transport, and DNA replication

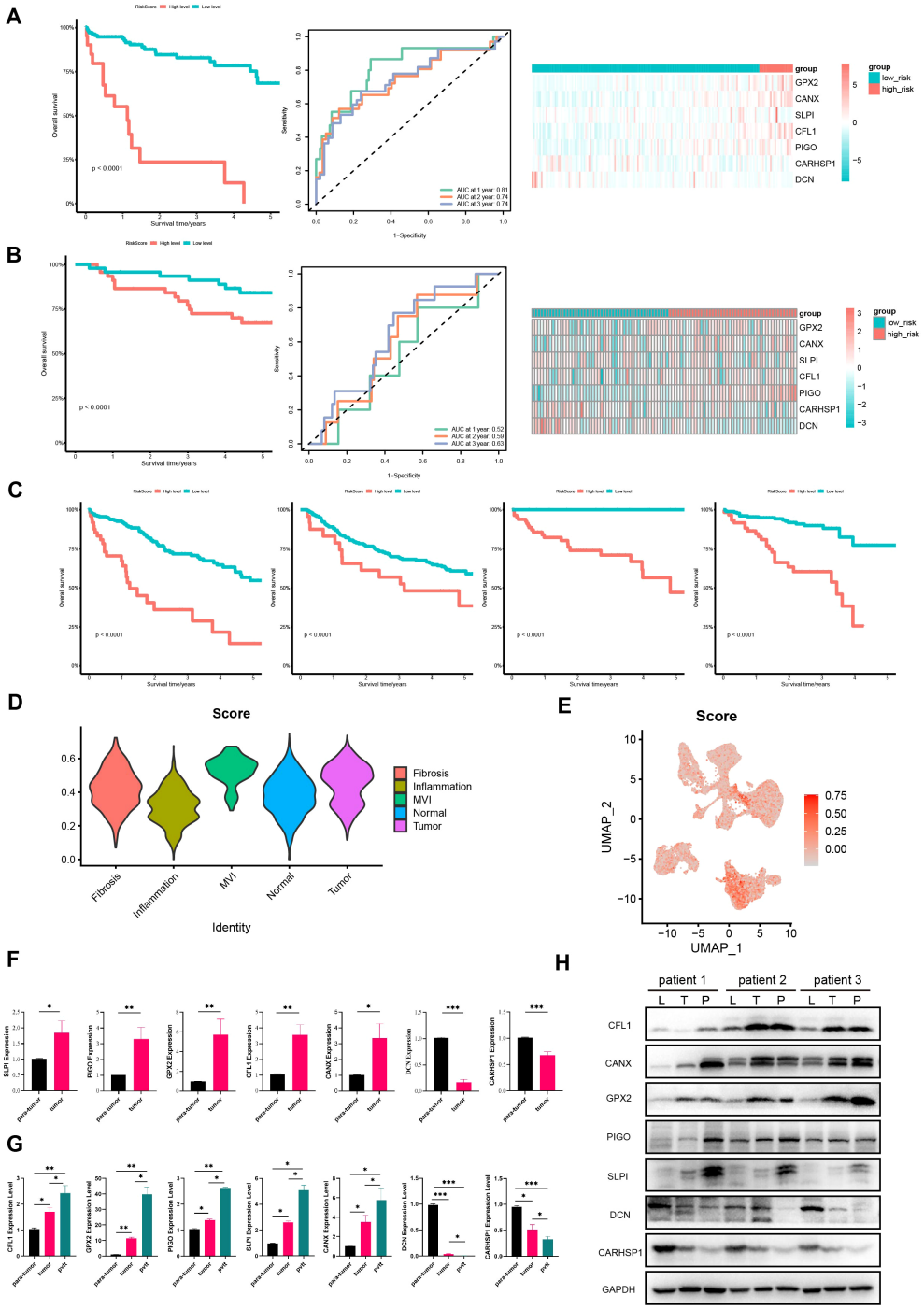

FIGURE 5
Further validation of the model in TCGA, GEO, ICGC cohorts and HCC tissues. Survival curves, ROC curves and heatmaps of model gene expression for early HCC patients from **(A)** TCGA and **(B)** GSE14520 datasets. **(C)** Survival curves for HCC patients from TCGA, GSE14520, GSE76427, and LIRI-JP databases. **(D)** Violin plots of expression of prognostic model gene set in different regions in the spatial transcriptome. **(E)** The UAMP plot of prognostic model gene set in single-nucleus transcriptomics. **(F)** The expression of protective genes and risk genes in para-tumor and tumor tissue samples. **(G)** The expression of protective genes and risk genes in para-tumor, tumor and portal vein tumor thrombus tissue samples. **(H)** Immunoblotting of proteins in the prognostic model expression (CFL1, PIGO, GPX2, SLPI, CANX, DCN, CARHSP1) in para-tumor, tumor, and portal vein tumor thrombus tissues samples. L, para-tumor; T, tumor; P, pvtt. *P* <0.05 is considered statistically significant. GEO, Gene Expression Omnibus; ICGC, International Cancer Genome Consortium. (**P* < 0.05; ***P* < 0.01; ****P* < 0.001).

(Figure 7A). Subsequently, the maftools package was used to analyze SNV data of HCC from TCGA. A waterfall chart was utilized to display information about the top 10 most frequently mutated genes in the high- and low-risk groups. Common mutation genes in the high-risk group, such as CTNNB1 (36% *vs.* 23%), TP53 (32% *vs.* 25%), TTN (27% *vs.* 20%) and MUC16 (23% *vs.* 16%), had higher mutation frequencies (Figure 7B). In addition, the TMB of early HCC patients was also calculated, which revealed a positive

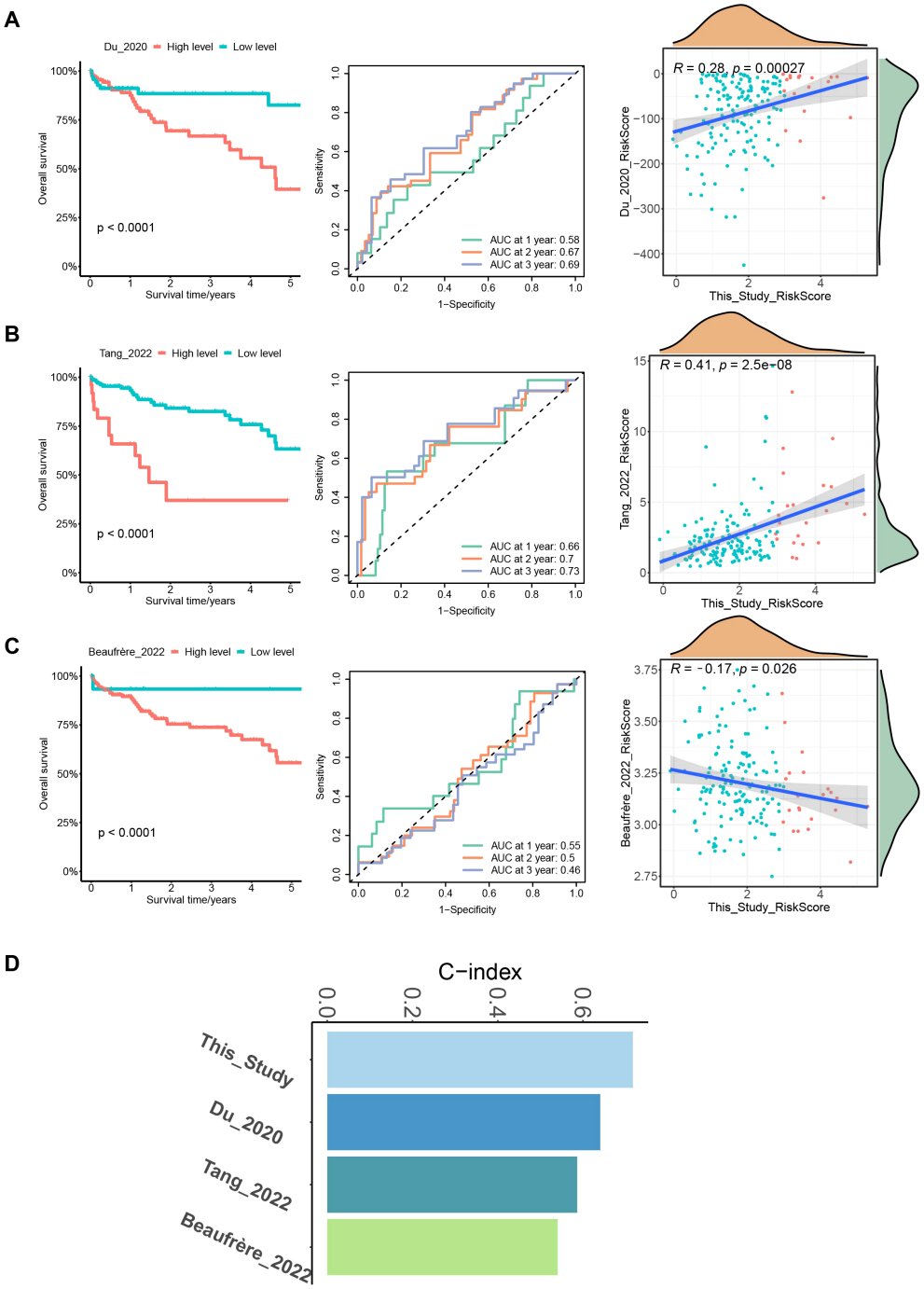

FIGURE 6
Comparison with 3 published MVI-related models. **(A)** Survival curves, ROC curves and correlation plots of risk in HCC patients predicted by the model of Du et al. compared with this model. **(B)** Survival curves, ROC curves and correlation plots of risk in HCC patients predicted by the model of Tang et al. compared with this model. **(C)** Survival curves, ROC curves and correlation plots of risk in HCC patients predicted by the model of Beaufrère et al. compared with this model. **(D)** Bar chart of C-indexes for the 4 models.

correlation between the risk score and tumor mutation burden (Figure 7C). Further investigations examined the association between the prognostic model and immune infiltration by evaluating immune cell proportions in HCC patients using TIMER 2.0. Differences in the proportions of immune cells between the high- and low-risk groups were compared. The results indicated increased proportions of macrophages, dendritic cells, and neutrophils in the high-risk group (Figure 7D). This suggests that these cells could promote early HCC metastasis, angiogenesis, and immune escape. TIDE was then used to predict the response of different risk groups to immunotherapy. The results demonstrated that the high-risk group had high TIDE scores and high exclusion scores and was susceptible to immune escape, resulting in worse immunotherapeutic effects (Figure 7E).

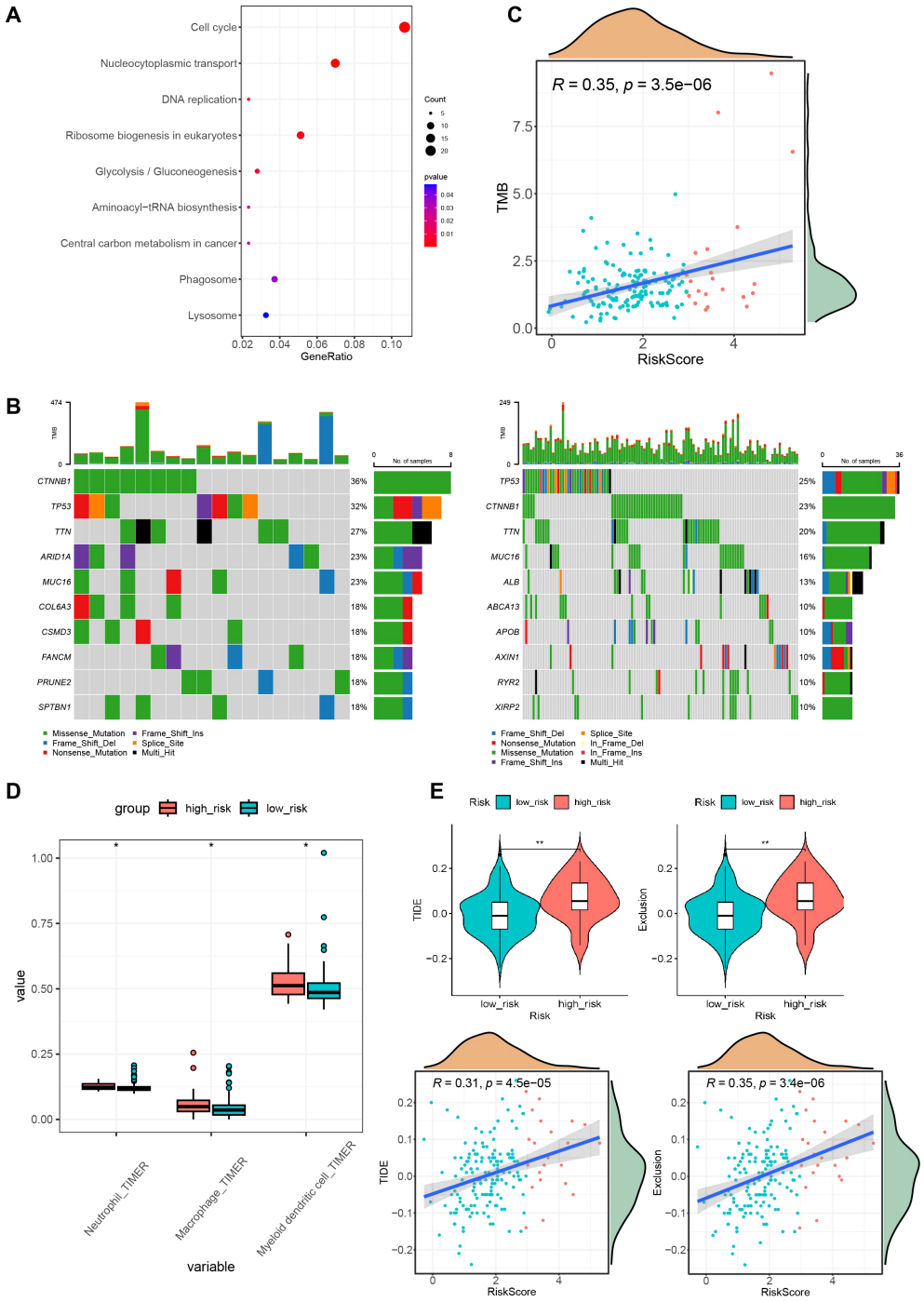

FIGURE 7
High and low-risk group mutations and immune characteristics. **(A)** KEGG enrichment results of highly expressed genes in the high-risk group. **(B)** Waterfall plots of the top 10 mutated genes in both the high- and low-risk groups. **(C)** Correlation graph between the risk score and tumor mutation burden. **(D)** Immune infiltration status in different risk groups. **(E)** TIDE scores and exclusion scores in different risk groups. KEGG, Kyoto Encyclopedia of Genes and Genomes; TIDE, Tumor Immune Dysfunction and Exclusion. *$P < 0.05$; **$P < 0.01$.

3.7 The interaction between MIF and CD74 may facilitate tumor metastasis in HCC

In the above experiments, we demonstrated that high-risk scoring patients possess a more complex immune microenvironment and are prone to immune escape. However, the mechanism of this immune evasion remains unclear. Therefore, to investigate the potential mechanisms of tumor cell immune escape and metastasis in the high-risk group, we analyzed intercellular interactions at the single-cell level. We selected 2 M0 samples and 3 MVI samples (P1_M0, P2_M0, P3_M1, P4_M2, P5_M2) for single-nucleus sequencing. The single nucleus data showed that each sample contained

approximately 10,000 nuclei, with an average of 2,324 genes per cell and an average of 4,454 UMIs per cell (Supplementary Table S5). The quality of single-nucleus transcriptome sequencing was assessed using Cell Ranger, and after quality control, doublet removal and batch effect correction, a total of 54,771 single nuclei were obtained from the 5 samples (Supplementary Figures 5A, B). Then, we used the Seurat package for dimensionality reduction and clustering obtained 25 cell clusters (Supplementary Figure 6A). Each cluster was annotated with cell types using the singleR and scLearn packages, and copy number variations in hepatic parenchymal cells were inferred using the inferCNV package to identify normal hepatocytes and malignant cells (Supplementary Figures 5C, D). We identified 8 cell types: B cells, T/NK cells, myeloid cells, fibroblasts, dendritic cells, endothelial cells, normal hepatocytes, and malignant cells (Figure 8A; Supplementary Figures 6B, C). Subsequent observation of the proportions of different cell types in

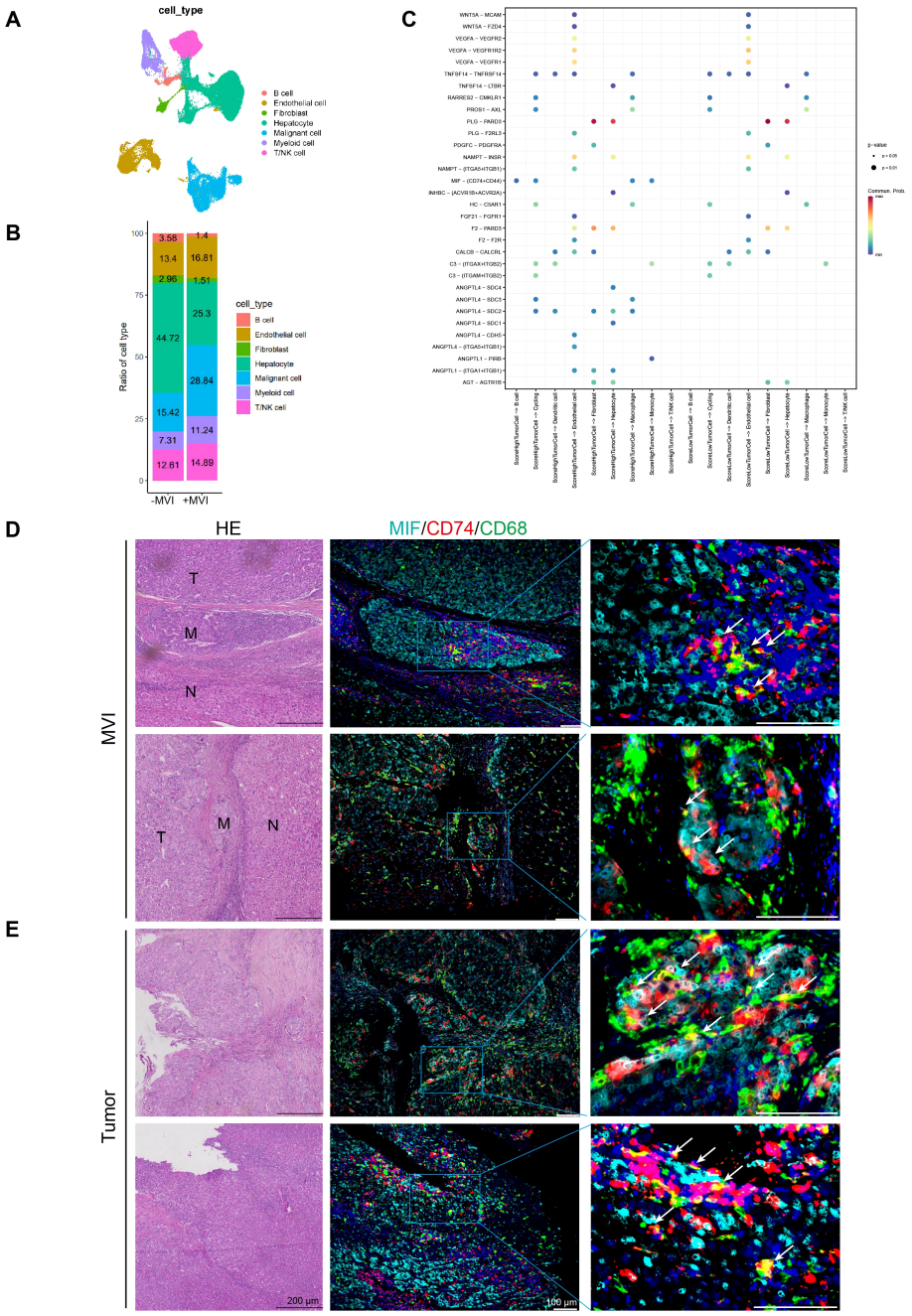

FIGURE 8
Cell interaction analysis and multiplex immunofluorescence of MVI and tumor sites. **(A)** UAMP plots of single-nuclei RNA sequencing data for various cell type markers. **(B)** Ration of cell types in MVI and no-MVI samples. **(C)** Interactions between high- and low-grade malignant cells and the receptors of other cells. **(D)** Representative HE staining and multiple immunofluorescence images of MVI sites in HCC microvascular invasion samples. **(E)** Representative HE staining and multiple immunofluorescence images of tumor sites in HCC microvascular invasion samples. UAMP, uniform manifold approximation and projection.

samples with or without MVI, it was found that the higher the degree of MVI, the higher the proportion of myeloid and T/NK cells, and that myeloid increased more (from 7.31% to 11.24%) than T/NK (from 12.61% to 14.89%) (Figure 8B). We further subclassified myeloid cells and identified five myeloid subpopulations: circulating cells, dendritic cells, plasma cell-like cells, monocytes, macrophages (Supplementary Figures 7A, B). Pathway enrichment of various myeloid subpopulations revealed that macrophages were enriched for the HIF-1 signaling pathway as well as the angiogenic pathway (Supplementary Figures 7C, D). Gene Set Variation analysis (GSVA) also revealed that macrophages were enriched for several signaling pathways associated with tumor progression, such as hypoxia, angiogenesis, and PI3K-AKT (Supplementary Figure 7E). And the Top20 gene in macrophages was associated with the prognosis of patients (Supplementary Figure 7F).

The ssGSEA algorithm was employed to compute prognostic model gene set scores in malignant cells from MVI samples. These malignant cells were then categorized into high and low score groups based on the median of these scores. The interactions of high- and low-scoring malignant cells with other cell types were examined using CellChat. Bar graphs showed that malignant cells with high scores had a higher number and stronger intensity of interactions with other cells (Supplementary Figure 8A). And heatmaps also demonstrated that high-scoring malignant cells have stronger capabilities in sending and receiving signals (Supplementary Figure 8B). Additionally, compared to low-scoring malignant cells, high-scoring malignant cells could communicate with macrophages, monocytes, and B cells through the MIF-(CD74+CD44) axis (Figure 8C). In addition intercellular interaction analysis showed that malignant cells with high and low scores had ligand-receptor interactions with macrophages but not with T/NK cells (Figure 8C). Therefore, we focused primarily on macrophages. Multiple immunofluorescence staining indicated that MIF-CD74 macrophages interact in the MVI region of MVI samples, where MIF-CD74 can promote tumor metastasis at the MVI site (Figure 8D). Furthermore, there is an interaction between MIF-CD74 macrophages in the tumor regions of the MVI samples, suggesting that their interaction may facilitate tumor progression (Figure 8E). However, there was no significant interaction between MIF-CD74 macrophages in the adjacent non-tumor tissues of the MVI samples and the tumor tissues of the non-MVI samples. (Supplementary Figures 8C, D).

The MIF-CD74 signaling pathway activates various pathways that promote cell growth and angiogenesis and inhibit the tumor suppressor protein p53 (29). Studies have shown that in kidney renal clear cell carcinoma, the strong interactions between tumor cells and tumor-associated macrophages, driven by MIF and its receptors CD74 and CD44, are critically involved in tumor progression, angiogenesis, and the mechanism of immune evasion (30). Furthermore, CD36+ cancer-associated fibroblasts (CAFs) employ MIF and CD74 to attract CD33+ myeloid-derived suppressor cells (MDSCs), creating an immunosuppressive environment that facilitates immune evasion in hepatocellular carcinoma (31). In summary, it is suggested that malignant cells in HCC could use the MIF-(CD74+CD44) interaction to promote metastasis, angiogenesis, and immune evasion.

4 Discussion

Hepatocellular carcinoma (HCC) is an extremely aggressive cancer and one of the most common causes of cancer-related death worldwide. It is characterized by its tendency to metastasize a high recurrence rate and considerable heterogeneity (32). Only 5%-10% of HCC patients are candidates for surgical treatment, with more than 70% experiencing recurrence within five years of surgery (1). Microvascular invasion (MVI) is considered a risk factor for postoperative recurrence and metastasis in HCC patients. Studies have shown that MVI is a predictive indicator of survival in HCC patients (28), therefore, the prediction of HCC prognosis is crucial for selecting treatment modalities and evaluating the prognosis of HCC patients. However, there are currently no accurate molecular markers for MVI to predict the prognosis of HCC patients. On this basis, we investigated different genes at MVI sites in HCC patients by spatial transcriptomics sequencing and constructed an HCC prognostic model.

In this study, we screened for differential genes at MVI sites by spatial transcriptomic sequencing. By comparing MVI locations with other regions, we identified 82 MVI-related genes. We then used early HCC data from TCGA as the training set to develop an HCC prediction model using various analytical approaches, including univariate Cox regression, LASSO regression, multivariate Cox regression, CoxBoost, random survival forests, and stepwise regression analysis. By comparing the C-index and error curves, we ultimately selected 7 key MVI genes (GPX2, CANX, SLPI, CFL1, PIGO, CARHSP1, DCN) to construct the HCC prognostic model. Studies have shown that the genes in the prognostic model influence metastasis and angiogenesis in HCC and other tumors. The expression of Glutathione Peroxidase 2 (GPX2) is associated with tumor metastasis of rat HCC both *in vitro* and *in vivo*. Reducing GPX2 expression in rat HCC cells leads to decreased migration; tail vein injection of cells with knocked down GPX2 results in reduced tumor formation capability and fewer lung metastases. Moreover, immunohistochemistry results of human HCC samples indicate that GPX2 is more highly expressed in tumor sites than in adjacent non-tumor tissues (33). High expression of GPX2 is associated with poor prognosis. Cox regression analysis shows that GPX2 expression is an independent prognostic factor for HCC overall survival. Cells with high GPX2 expression have stronger resistance to lenvatinib, making GPX2 a critical target for lenvatinib treatment in HCC (34). Calnexin (CANX) complexes on the cell surface can reduce the number of extracellular disulfide bonds, thereby degrading the extracellular matrix, which serves as a physical barrier to HCC growth, thereby inducing tumor growth and invasion (35). Secretory leukocyte peptidase inhibitor (SLPI) is upregulated in several cancer types and is highly expressed in liver cancer cell lines. Studies have shown that SLPI promotes metastasis (36). Cofilin 1(CFL1) is upregulated in the tumor tissues of HCC and is significantly associated with the overall survival and disease-free survival of HCC patients. Moreover, downregulation of CFL1 can inhibit the migration, invasion, and metastasis of HCC cells both *in vitro* and *in vivo* (37). CFL1 is also highly expressed in tumor tissues of HCC patients who are insensitive to sorafenib and is associated with poor prognosis. The co-delivery of siCFL1 and sorafenib via nanoparticles

could represent a new strategy for advanced HCC (38). Furthermore, CFL1 is expressed more highly in portal vein tumor thrombus (pvtt) than in HCC tumor tissues, and an increase in CFL1 expression is closely related to adverse clinical features, making it an independent risk predictor for the overall survival of HCC patients. Silencing of CFL1 can inhibit the growth viability, invasiveness, and epithelial-mesenchymal transition (EMT) of HCC cells *in vitro*, and it can also suppress the growth and lung metastasis of HCC cells in nude mice *in vivo* (39). miR-155 influences TNF-α mRNA stability by inhibiting calcium regulated heat stable protein 1 (CARHSP1), thereby modulating the inflammatory response and protecting vessels in atherosclerosis (40). Phosphatidylinositol Glycan Anchor Biosynthesis Class O (PIGO) can serve as a potential marker for the prognosis of prostate cancer (41). Decorin (DCN) is downregulated in HCC with portal vein tumor thrombus (pvtt) tissue, and low DCN expression is associated with microvascular invasion (MVI) occurrence and poor prognosis, indicating that DCN can promote vascular invasion in HCC tissues (42). Furthermore, DCN is underexpressed in tumor tissues of HCC patients, and overexpression of DCN can inhibit the proliferation of HCC cells, while knockdown of DCN can enhance HCC cell proliferation, making it a new target for HCC (43). These studies are largely consistent with the results of our prognostic genes. Thus, these seven genes are closely related to the growth and prognosis of HCC cells, which also confirms the accuracy of modeling these seven genes to some extent.

We also carried out corresponding validations for this model. First, we performed a multivariate Cox regression analysis on risk scores and clinical characteristics. The results indicated that the risk score, age, and Child-Pugh classification were associated with the overall survival of HCC patients and served as independent risk factors. And the risk score is more closely related to a worse prognosis. We also represented independent prognostic factors in a nomogram model to visually assess patient prognosis to improve its clinical applicability. Second, we calculated the risk score for each patient and divided them into high- and low-risk groups. Survival analysis revealed that the high-risk group had shorter survival times, higher mortality rates and a worse prognosis. In addition, we collected clinical samples from HCC patients at our hospital and examined the expression of 7 genes in 24 pairs of cancerous and adjacent noncancerous HCC tissues using the qPCR assay. The results showed lower expression of DCN and CARHSP1 in tumors compared to paired adjacent noncancerous tissues; PIGO, GPX2, CFL1, SLPI, and CANX were more highly expressed in tumors than in adjacent noncancerous tissues. Furthermore, we compared the model constructed in this study with three published HCC models. The results showed that the C-index of our model exceeded that of the three published HCC-related models, which demonstrated the predictive performance of our model. These results confirm that the validations conducted further clarify the reliability and predictive value of the prognostic model and support its clinical utility for personalized treatment and prognosis prediction.

In addition, we observed the relationship between the high- and low-risk groups and the immune microenvironment. The results indicated a higher proportion of macrophages, dendritic cells, and neutrophils in the high-risk group. Moreover, the high-risk group had higher immune rejection scores. These findings suggest a more complex immune microenvironment in the high-risk group, leading to increased immune evasion and worse immunotherapy outcomes. It further confirms the importance of the prognostic model in clinical decision-making regarding treatment options for patients. Subsequently, we also explored the potential mechanisms behind HCC metastasis. We found that malignant cells can interact with macrophages through the MIF-CD74 axis, thereby promoting HCC metastasis.

The advantage of this risk scoring system is that it develops an individual scoring system for patients, where those classified as high risk have an increased probability of tumor recurrence. Additionally, this risk scoring model can predict the prognosis of early HCC patients in conjunction with age and Child-Pugh classification, and can assess the possibility of postoperative recurrence. Therefore, in the era of precision medicine, this risk evaluation model not only provides a more scientific and advanced indicator for assessing tumor recurrence and prognosis risks for clinical use but also offers guidance for personalized treatment of cancer patients.

5 Conclusion

To sum up, in this study, we developed and validated a prognostic model for HCC patients based on MVI genes. This model can more accurately predict the overall survival (OS) of HCC patients at different stages. Moreover, the risk score of this model can serve as an independent prognostic factor, which is of great importance for distinguishing patient types and selecting appropriate treatment options.

Data availability statement

The data presented in the study are deposited in the Genome Sequence Archive in National Genomics Data Center, China National Center for Bioinformation/Beijing Institute of Genomics, Chinese Academy of Sciences repository, accession number BioProject ID: PRJCA035412.

Ethics statement

All human tissues used in this study were approved by the Ethics Committee of Tongji University (Shanghai, China) and Ethics Committee of Navy Medical University (Shanghai, China). Written informed consent was obtained from all patients for the use of their surgical tissue.

Author contributions

XM: Validation, Writing – original draft. LP: Writing – original draft, Formal Analysis. XW: Supervision, Writing – review &

editing. CL: Validation, Writing – review & editing. YL: Validation, Writing – original draft. YC: Conceptualization, Writing – original draft. ZH: Conceptualization, Supervision, Writing – review & editing.

Funding

The author(s) declare that financial support was received for the research, authorship, and/or publication of this article. This work was funded by the National Natural Science Foundation of China (82173019, 82203741, 82270638, 82300718), the Project of Shanghai Science and Technology Commission (22ZR1451100, 22Y11908500), Jiangxi Provincial Natural Science Foundation (20212ACB206033), Shanghai Engineering Research Center of Stem Cells Translational Medicine (20DZ2255100), and Peak Disciplines (Type IV) of Institutions of Higher Learning in Shanghai.

Acknowledgments

Thanks to all the patients who participated in this study. Thanks to the Third Affiliated Hospital of Naval Medical University (Shanghai Eastern Hepatobiliary Surgery Hospital) for providing HCC patient samples. Thanks to the OE Biotech for offering sequencing services.

Conflict of interest

The authors declare that the research was conducted in the absence of any commercial or financial relationships that could be construed as a potential conflict of interest.

Generative AI statement

The author(s) declare that no Generative AI was used in the creation of this manuscript.

Publisher's note

Supplementary material

The Supplementary Material for this article can be found online at: https://www.frontiersin.org/articles/10.3389/fimmu.2025.1529569/full#supplementary-material

References

1. Llovet JM, Kelley RK, Villanueva A, Singal AG, Pikarsky E, Roayaie S, et al. Hepatocellular carcinoma. *Nat Rev Dis Primers*. (2021) 7:6. doi: 10.1038/s41572-020-00240-3

2. Sung H, Ferlay J, Siegel RL, Laversanne M, Soerjomataram I, Jemal A, et al. Global cancer statistics 2020: GLOBOCAN estimates of incidence and mortality worldwide for 36 cancers in 185 countries. *CA Cancer J Clin*. (2021) 71:209–49. doi: 10.3322/caac.21660

3. Llovet JM, Pinyol R, Kelley RK, El-Khoueiry A, Reeves HL, Wang XW, et al. Molecular pathogenesis and systemic therapies for hepatocellular carcinoma. *Nat Cancer*. (2022) 3:386–401. doi: 10.1038/s43018-022-00357-2

4. Marrero JA, Kulik LM, Sirlin CB, Zhu AX, Finn RS, Abecassis MM, et al. Diagnosis, staging, and management of hepatocellular carcinoma: 2018 practice guidance by the american association for the study of liver diseases. *Hepatology*. (2018) 68:723–50. doi: 10.1002/hep.29913

5. European Association for the Study of the L. EASL Clinical Practice Guidelines: Management of hepatocellular carcinoma. *J Hepatol*. (2018) 69:182–236. doi: 10.1016/j.jhep.2018.03.019

6. Forner A, Reig M, Bruix J. Hepatocellular carcinoma. *Lancet*. (2018) 391:1301–14. doi: 10.1016/S0140-6736(18)30010-2

7. Shin SW, Kim TS, Ahn KS, Kim YH, Kang KJ. Effect of anatomical liver resection for hepatocellular carcinoma: a systematic review and meta-analysis. *Int J Surg*. (2023) 109:2784–93. doi: 10.1097/JS9.0000000000000503

8. Kang I, Jang M, Lee JG, Han DH, Joo DJ, Kim KS, et al. Subclassification of microscopic vascular invasion in hepatocellular carcinoma. *Ann Surg*. (2021) 274: e1170–e8. doi: 10.1097/SLA.0000000000003781

9. Hwang YJ, Bae JS, Lee Y, Hur BY, Lee DH, Kim H. Classification of microvascular invasion of hepatocellular carcinoma: correlation with prognosis and magnetic resonance imaging. *Clin Mol Hepatol*. (2023) 29:733–46. doi: 10.3350/cmh.2023.0034

10. Fares J, Fares MY, Khachfe HH, Salhab HA, Fares Y. Molecular principles of metastasis: a hallmark of cancer revisited. *Signal Transduct Target Ther*. (2020) 5:28. doi: 10.1038/s41392-020-0134-x

11. Erstad DJ, Tanabe KK. Prognostic and therapeutic implications of microvascular invasion in hepatocellular carcinoma. *Ann Surg Oncol*. (2019) 26:1474–93. doi: 10.1245/s10434-019-07227-9

12. Sun Y, Wu L, Zhong Y, Zhou K, Hou Y, Wang Z, et al. Single-cell landscape of the ecosystem in early-relapse hepatocellular carcinoma. *Cell*. (2021) 184:404–21.e16. doi: 10.1016/j.cell.2020.11.041

13. Zhang Q, He Y, Luo N, Patel SJ, Han Y, Gao R, et al. Landscape and dynamics of single immune cells in hepatocellular carcinoma. *Cell*. (2019) 179:829–45.e20. doi: 10.1016/j.cell.2019.10.003

14. Wu SZ, Al-Eryani G, Roden DL, Junankar S, Harvey K, Andersson A, et al. A single-cell and spatially resolved atlas of human breast cancers. *Nat Genet*. (2021) 53:1334–47. doi: 10.1038/s41588-021-00911-1

15. Lake BB, Menon R, Winfree S, Hu Q, Melo Ferreira R, Kalhor K, et al. An atlas of healthy and injured cell states and niches in the human kidney. *Nature*. (2023) 619:585–94. doi: 10.1038/s41586-023-05769-3

16. Slyper M, Porter CBM, Ashenberg O, Waldman J, Drokhlyansky E, Wakiro I, et al. A single-cell and single-nucleus RNA-Seq toolbox for fresh and frozen human tumors. *Nat Med*. (2020) 26:792–802. doi: 10.1038/s41591-020-0844-1

17. van den Brink SC, Sage F, Vertesy A, Spanjaard B, Peterson-Maduro J, Baron CS, et al. Single-cell sequencing reveals dissociation-induced gene expression in tissue subpopulations. *Nat Methods*. (2017) 14:935–6. doi: 10.1038/nmeth.4437

18. Adam M, Potter AS, Potter SS. Psychrophilic proteases dramatically reduce single-cell RNA-seq artifacts: a molecular atlas of kidney development. *Development*. (2017) 144:3625–32. doi: 10.1242/dev.151142

19. Lake BB, Chen S, Hoshi M, Plongthongkum N, Salamon D, Knoten A, et al. A single-nucleus RNA-sequencing pipeline to decipher the molecular anatomy and pathophysiology of human kidneys. *Nat Commun*. (2019) 10:2832. doi: 10.1038/s41467-019-10861-2

20. Alvarez M, Benhammou JN, Darci-Maher N, French SW, Han SB, Sinsheimer JS, et al. Human liver single nucleus and single cell RNA sequencing identify a hepatocellular carcinoma-associated cell-type affecting survival. *Genome Med*. (2022) 14:50. doi: 10.1186/s13073-022-01055-5

21. Saviano A, Henderson NC, Baumert TF. Single-cell genomics and spatial transcriptomics: Discovery of novel cell states and cellular interactions in liver physiology and disease biology. *J Hepatol*. (2020) 73:1219–30. doi: 10.1016/j.jhep.2020.06.004

22. Asp M, Giacomello S, Larsson L, Wu C, Furth D, Qian X, et al. A spatiotemporal organ-wide gene expression and cell atlas of the developing human heart. *Cell*. (2019) 179:1647–60e19. doi: 10.1016/j.cell.2019.11.025

23. Hwang WL, Jagadeesh KA, Guo JA, Hoffman HI, Yadollahpour P, Reeves JW, et al. Single-nucleus and spatial transcriptome profiling of pancreatic cancer identifies multicellular dynamics associated with neoadjuvant treatment. *Nat Genet*. (2022) 54:1178–91. doi: 10.1038/s41588-022-01134-8

24. Hirz T, Mei S, Sarkar H, Kfoury Y, Wu S, Verhoeven BM, et al. Dissecting the immune suppressive human prostate tumor microenvironment via integrated single-cell and spatial transcriptomic analyses. *Nat Commun*. (2023) 14:663. doi: 10.1038/s41467-023-36325-2

25. Ji AL, Rubin AJ, Thrane K, Jiang S, Reynolds DL, Meyers RM, et al. Multimodal analysis of composition and spatial architecture in human squamous cell carcinoma. *Cell*. (2020) 182:497–514.e22. 10.1016/j.cell.2020.08.043

26. Du B, Wang F, Jarad B, Wang Z, Zhang Y. A novel signature based on microvascular invasion predicts the recurrence of HCC. *J Transl Med*. (2020) 18:272. doi: 10.1186/s12967-020-02432-7

27. Tang Y, Xu L, Ren Y, Li Y, Yuan F, Cao M, et al. Identification and validation of a prognostic model based on three MVI-related genes in hepatocellular carcinoma. *Int J Biol Sci*. (2022) 18:261–75. doi: 10.7150/ijbs.66536

28. Beaufrere A, Caruso S, Calderaro J, Pote N, Bijot JC, Couchy G, et al. Gene expression signature as a surrogate marker of microvascular invasion on routine hepatocellular carcinoma biopsies. *J Hepatol*. (2022) 76:343–52. doi: 10.1016/j.jhep.2021.09.034

29. Penticuff JC, Woolbright BL, Sielecki TM, Weir SJ, Taylor JA 3rd. MIF family proteins in genitourinary cancer: tumorigenic roles and therapeutic potential. *Nat Rev Urol*. (2019) 16:318–28. doi: 10.1038/s41585-019-0171-9

30. Long Z, Sun C, Tang M, Wang Y, Ma J, Yu J, et al. Single-cell multiomics analysis reveals regulatory programs in clear cell renal cell carcinoma. *Cell Discovery*. (2022) 8:68. doi: 10.1038/s41421-022-00415-0

31. Zhu GQ, Tang Z, Huang R, Qu WF, Fang Y, Yang R, et al. CD36(+) cancer-associated fibroblasts provide immunosuppressive microenvironment for hepatocellular carcinoma via secretion of macrophage migration inhibitory factor. *Cell Discovery*. (2023) 9:25. doi: 10.1038/s41421-023-00529-z

32. Bertuccio P, Turati F, Carioli G, Rodriguez T, La Vecchia C, Malvezzi M, et al. Global trends and predictions in hepatocellular carcinoma mortality. *J Hepatol*. (2017) 67:302–9. doi: 10.1016/j.jhep.2017.03.011

33. Suzuki S, Pitchakarn P, Ogawa K, Naiki-Ito A, Chewonarin T, Punfa W, et al. Expression of glutathione peroxidase 2 is associated with not only early hepatocarcinogenesis but also late stage metastasis. *Toxicology*. (2013) 311:115–23. doi: 10.1016/j.tox.2013.07.005

34. Tan W, Zhang K, Chen X, Yang L, Zhu S, Wei Y, et al. GPX2 is a potential therapeutic target to induce cell apoptosis in lenvatinib against hepatocellular carcinoma. *J Adv Res*. (2023) 44:173–83. doi: 10.1016/j.jare.2022.03.012

35. Ros M, Nguyen AT, Chia J, Le Tran S, Le Guezennec X, McDowall R, et al. ER-resident oxidoreductases are glycosylated and trafficked to the cell surface to promote matrix degradation by tumour cells. *Nat Cell Biol*. (2020) 22:1371–81. doi: 10.1038/s41556-020-00590-w

36. Nugteren S, Samsom JN. Secretory Leukocyte Protease Inhibitor (SLPI) in mucosal tissues: Protects against inflammation, but promotes cancer. *Cytokine Growth Factor Rev*. (2021) 59:22–35. doi: 10.1016/j.cytogfr.2021.01.005

37. Zhang L, Chai Z, Kong S, Feng J, Wu M, Tan J, et al. Nujiangexanthone A inhibits hepatocellular carcinoma metastasis via down regulation of cofilin 1. *Front Cell Dev Biol*. (2021) 9:644716. doi: 10.3389/fcell.2021.644716

38. Li S, Xu L, Wu G, Huang Z, Huang L, Zhang F, et al. Remodeling serine synthesis and metabolism via nanoparticles (NPs)-mediated CFL1 silencing to enhance the sensitivity of hepatocellular carcinoma to sorafenib. *Adv Sci (Weinh)*. (2023) 10: e2207118. doi: 10.1002/advs.202207118

39. Yao B, Li Y, Chen T, Niu Y, Wang Y, Yang Y, et al. Hypoxia-induced cofilin 1 promotes hepatocellular carcinoma progression by regulating the PLD1/AKT pathway. *Clin Transl Med*. (2021) 11:e366. doi: 10.1002/ctm2.v11.3

40. Li X, Kong D, Chen H, Liu S, Hu H, Wu T, et al. miR-155 acts as an anti-inflammatory factor in atherosclerosis-associated foam cell formation by repressing calcium-regulated heat stable protein 1. *Sci Rep*. (2016) 6:21789. doi: 10.1038/srep21789

41. Mou Z, Spencer J, McGrath JS, Harries LW. Comprehensive analysis of alternative splicing across multiple transcriptomic cohorts reveals prognostic signatures in prostate cancer. *Hum Genomics*. (2023) 17:97. doi: 10.1186/s40246-023-00545-w

42. Zheng X, Wang P, Li L, Yu J, Yu C, Xu L, et al. Cancer-Associated Fibroblasts Promote Vascular Invasion of Hepatocellular Carcinoma via Downregulating Decorin-integrin beta1 Signaling. *Front Cell Dev Biol*. (2021) 9:678670. doi: 10.3389/fcell.2021.678670

43. Li Y, Gan L, Lu M, Zhang X, Tong X, Qi D, et al. HBx downregulated decorin and decorin-derived peptides inhibit the proliferation and tumorigenicity of hepatocellular carcinoma cells. *FASEB J*. (2023) 37:e22871. doi: 10.1096/fj.202200999RR

frontiers | Frontiers in Immunology

TYPE Original Research
PUBLISHED 08 April 2025
DOI 10.3389/fimmu.2025.1565486

OPEN ACCESS

EDITED BY
Zhiying He,
Tongji University, China

REVIEWED BY
Sonia Leon-Cabrera,
National Autonomous University of Mexico, Mexico
Shuman Feng,
Henan Provincial People's Hospital, China

*CORRESPONDENCE
Qiaoming Long
qmlong@suda.edu.cn

†These authors have contributed equally to this work

RECEIVED 23 January 2025
ACCEPTED 06 March 2025
PUBLISHED 08 April 2025

CITATION
Wang J, Gong P, Liu Q, Wang M, Wu D, Li M, Zheng S, Wang H and Long Q (2025) Stimulation of regulatory dendritic cells suppresses cytotoxic T cell function and alleviates DEN-induced liver injury, fibrosis and hepatocellular carcinoma.
Front. Immunol. 16:1565486.
doi: 10.3389/fimmu.2025.1565486

Stimulation of regulatory dendritic cells suppresses cytotoxic T cell function and alleviates DEN-induced liver injury, fibrosis and hepatocellular carcinoma

Junjie Wang[1†], Pixu Gong[1†], Qingqing Liu[1†], Menglei Wang[1], Dengfang Wu[1], Mengyu Li[1], Shujie Zheng[1], Han Wang[2,3] and Qiaoming Long[1*]

[1]Jiangsu Key Laboratory of Neuropsychiatric Diseases and Cam-Su Mouse Genomic Resources Center, Suzhou Medical College, Soochow University, Suzhou, Jiangsu, China, [2]Center for Circadian Clocks, Soochow University, Suzhou, Jiangsu, China, [3]School of Basic Medical Sciences, Suzhou Medical College, Soochow University, Suzhou, Jiangsu, China

Background: Dendritic cells (DCs) are versatile professional antigen-presenting cells and play an instrumental role in the generation of antigen-specific T-cell responses. Modulation of DC function holds promise as an effective strategy to improve anti-tumor immunotherapy efficacy and enhance self-antigen tolerance in autoimmune diseases.

Methods: Wild-type (WT) and TLR2 knockout (KO) mice at 2 weeks of age were injected intraperitoneally (i.p.) with a single dose of diethylnitrosamine (DEN) to induce hepatocellular carcinoma (HCC). Four weeks later, WT and KO mice were randomly divided into control and treatment groups and treated once every two days for 30 weeks with phosphate buffered saline (PBS) and a mix of 4 TLR2-activating lactic acid-producing probiotics (LAP), respectively. Mice were euthanized after 30 weeks of LAP treatment and their liver tissues were collected for gene expression, histological, flow cytometric and single-cell RNA sequencing analyses.

Results: We demonstrate here that oral administration of a mix of TLR2-activating LAP triggers a marked accumulation of regulatory DCs (rDCs) in the liver of mice. LAP-treated mice are protected from DEN-induced liver injury, fibrosis and HCC in a TLR2-dependent manner. Single-cell transcriptome profiling revealed that LAP treatment determines an immunosuppressive hepatic T-cell program that is characterized by a significantly reduced cytotoxic activity. The observed functional changes of T cells correlated well with the presence of a hepatic DC subset displaying a regulatory or tolerogenic transcriptional signature.

Conclusion: Overall, these data suggest that stimulation of regulatory dendritic cells (rDCs) in the liver by LAP suppresses cytotoxic T-cell function and alleviates DEN-induced liver damage, fibrosis and tumorigenesis.

KEYWORDS

TLR2, rDCs, T cells, hepatocellular carcinoma, lactic acid producing probiotics

1 Introduction

Hepatocellular carcinoma (HCC) is the most common primary liver malignancy. Worldwide, HCC accounts for over 800,000 deaths annually, the second leading cause of cancer-related mortality (1). HCC usually develops in the setting of chronic hepatitis and cirrhosis, conditions that are causally associated with a viral infection, alcohol consumption, endotoxin as well as metabolic dysfunction-related liver injuries (2, 3). These conditions result in hepatocyte death and compensatory hepatocyte proliferation, which, together with endoplasmic reticulum and oxidative stress, drive hepatocarcinogenesis (4–6). The global prevalence of HCC is rapidly increasing, a direct effect of the growing worldwide obesity epidemic (7). Traditional treatment options for HCC include surgical removal, local ablation, chemo- and radiotherapy (3). Therapies targeting the programmed death 1 (PD-1) and cytotoxic T lymphocyte-associated antigen 4 (CTLA-4), the immune checkpoints, have shown unprecedented rates of durable clinical responses in patients with several solid and hematological cancers (8, 9). Despite this, only a subset of HCC patients shows favorable responses to PD-1 and CTLA-4-based immunotherapies (10), underscoring the need for a deeper understanding of the cellular and molecular mechanisms underlying HCC pathogenesis, in particular the roles of hepatic immune cells.

The liver is populated by a variety of immune cells, including macrophages (Kupffer cells, KC), dendritic cells (DC), natural killer (NK) cells, neutrophils, B and T lymphocytes (11). These distinct innate and adaptive immune cells form a sophisticated immune surveillance network to protect hepatocytes against invading pathogens and from chemically or metabolically triggered hepatocellular damages (12). Growing evidence from liver disease patients and murine models indicated that dysfunction and/or dysregulation of the hepatic immune cell system plays an essential role in the pathogenesis of liver fibrosis and cirrhosis, and consequently, HCC, by producing proinflammatory cytokines such as TNFα, IL-1β and IL-6, to drive necroinflammation and hepatocyte death (4–6). From a therapeutic perspective, targeted manipulation of specific immune cells subsets, such as tumor-associated macrophages (TAMs) and neutrophils (TANs), may offer effective strategies to prevent hepatic inflammation and cell death, thus novel treatments for liver cancer (13–15).

Dendritic cells (DCs) are a diverse group of specialized immune cells developed from bone marrow hematopoietic precursors (16). DCs have been well-recognized for their ability to present various self and non-self-antigens in conjunction with major histocompatibility complex (MHC) molecules to naïve T lymphocytes to prime T cell responses (17, 18), qualifying them as essential mediators of systemic or tissue-specific adaptive immune responses. As such, there has been a persistent interest over the past few decades in developing DC-based treatment strategies for various cancer types, including HCC (18, 19), especially following the remarkable patient responses observed with novel checkpoint blockade therapies (20). It is noteworthy that aging decreases the migrating and cytokine-producing abilities of DCs, thereby negatively impacting the anti-tumor and anti-viral adaptive immune responses in elderly mice and humans (21). Of note, correcting DCs migration defect using a vaccine adjuvant reverses aging-related adaptive immune defects and improves anti-tumor immunity in aged mice (22). Thus, modulating the cross-presenting function of the DC subset represents a promising tool for improving the efficacy of next-generation cancer immunotherapies.

rDCs, are commonly found in the microenvironment of advanced solid tumors (23, 24). This discovery has fundamentally shifted the perception of DCs solely as inducers of immune reactivity. As such, DCs are now recognized to have the potential to both stimulate and inhibit immune responses (25, 26). Tumor-associated rDCs may directly or indirectly maintain antigen-specific or non-specific T cell unresponsiveness by controlling T cell polarization, myeloid-derived suppressive cell (MDSC) and regulatory T cell (Treg) differentiation and activity, consequently leading to tumor initiation and progression (23, 27). Despite these understandings, the molecular nature and function of rDCs, as well as their relationships with other myeloid and T cell subsets during HCC development, remain largely unknown thus far.

Probiotics are popular food supplements and have shown potent immunostimulatory effects in both healthy subjects (28) and gastrointestinal cancer patients (29). certain probiotic strains have also demonstrated beneficial roles of in lowering systemic inflammation and in suppressing extraintestinal tumor growth, doing so at least in part through either inhibiting T helper 17 (Th17) cell differentiation or stimulating rDC formation (30, 31). The present study aims to determine whether and how hepatic DC manipulation affects diethylnitrosamine (DEN)-induced HCC formation in mice. We show that daily oral administration of LAP, a novel mix of four live lactic acid-producing probiotics, mitigates DEN-induced liver injury, reduces hepatic fibrosis and suppresses HCC progression. The hepatoprotective effect of LAP is associated with an expanded DC population in the liver. Single-cell RNA profiling reveals that LAP treatment causes a markedly repressed cytotoxic T-cell program in the liver. Gene expression analysis indicates that the expanded hepatic DC subsets broadly display a transcriptional signature indicative of regulatory dendritic cells. Overall, our findings suggest that targeted stimulation of rDCs in the liver protects against DEN-induced tumorigenesis by attenuating T cell-mediated hepatocyte death.

2 Materials and methods

2.1 Animal experiments

In this project, C57BL/6 WT mice were purchased from Gempharmatech Co., Ltd (Nanjing, China), and TLR2 KO mice were a gift from the lab of S. Xiong (Soochow University) and bred on C57BL/6 mice.

2-week-old male mice were injected (i.p.) with a single dose of 25 mg/kg diethylnitrosamine (DEN; Sigma N0258), then fed with high-fat diet and provided with probiotics by gavage (i.g.) at 6 weeks of age, finally euthanized and harvested with tumor for analysis at 36 weeks of age. Tumor volume = length x width^2 x 1/2.

All mice were housed in a Specific Pathogen Free (SPF) facility and all animal operations were performed in accordance with the protocol approved by the Animal Ethics Committee of Soochow University.

2.2 TLR2 reporter-based probiotics screening

Lactobacillus plantarum WCFS1 (ATCC BAA-793) and Lactobacillus plantarum (BNCC 194165) were purchased from Bena culture collection (BNCC, China). Lactococcus lactis and Lactobacillus plantarum 35 were isolated from a freeze-dried probiotic powder mixture. All probiotics were grown in an MRS medium. For probiotics functional screening, HEK-Dual™ hTLR2 (NF/IL8) cells (InvivoGen) were grown in DEME High Sugar Medium containing 100 ml of DEME High Sugar Medium consisting of 10% FBS, 100 U/mL penicillin G sodium salt, 10 mg/mL streptomycin sulfate. After the cells were inoculated in 96-well plates, 10^7 CFU of PBS-resuspended bacteria were added and co-cultured for 24 h at 37°C, 5% CO_2. After 24 h, 10 μL supernatant from each well was incubated with 50 μL Quanti-Luc™ solution, and a microplate reader tested the luciferase value.

2.3 Flow cytometry

Minced liver tissues were digested by collagenase 4 for 30 min. The product was filtered through 70 μm cell sieves. Liver parenchymal cells were removed by centrifugation before erythrocytes were removed by LCK lysate. FC blocking was performed at a rate of 1 μL FC block per 1,000,000 cells. After the cells were stained by CD45, CD3, CD8, CD19, Gr-1, CD11b, CD11c, F4/80, NK1.1 Antibody and LIVE/DEAD Fixable Dead Cell Stain Kits, the cells were detected using flow cytometry.

2.4 Immunohistochemistry and multiplex immunofluorescence

Dewaxed and hydrated liver tissue sections were antigen retrieved and endogenous peroxidase activity blocked as previously described (32). The sections were then treated with primary antibodies (4°C, 16h) and secondary antibodies (RT, 2h), followed by DAB and hematoxylin staining). Images were acquired using a Nikon digital camera and analyzed by ImageJ. For the immunofluorescence assay, rehydrated liver sections were blocked in 10% goat serum for 2 hours, then incubated with primary antibodies (4°C, 16h) and Polymer-HRP secondary antibody (RT, 30min). After TSA fluorescent dye and DAPI staining, fluorescent images were acquired using a Digital Pathology Scanner (KFBIO, China).

2.5 Masson staining

Masson staining was performed according to the manufacturer's instructions (Solarbio, G1340, China). Briefly, dewaxed and rehydrated liver tissue sections were treated with a weak acid working solution for 30s. The treated sections were then incubated in Phosphomolybic Acid Solution (2min), followed by treatment with Aniline Blue Solution for 2 min. Images were acquired using a Nikon digital camera and analyzed by ImageJ.

2.6 qPCR and western blotting

Liver tissue or tumor RNA was extracted using RNAiso Plus (Takara, Japan) and reverse-transcribed using a HiScript III 1st Strand cDNA Synthesis Kit (Vazyme, China). Quantitative PCR was performed using SYBR Green (Vazyme, China) on a ViiA7 Real-Time PCR system (Applied Biosystems, USA), and β-Actin was used as an internal control. For Western blotting, liver tumor or tissue lysates were prepared as previously described (32). Lysate protein concentrations were determined by BCA assay. Twenty mg of each lysate was resolved in a 10% sodium dodecyl sulfate (SDS)-polyacrylamide gel and then transferred onto a PVDF membrane. The protein-loaded membranes were blocked in 5% milk for 2-4 hours and then incubated with primary and secondary antibodies. Immunodetection was performed using the ECL chemiluminescence kit according to the manufacturer's specifications. The following antibodies were used: β-tubulin (1:10000) (Proteintech, USA), Bcl-2 (1:1000) (Proteintech, USA), PCNA (1:5000) (Proteintech, USA), Cyclin D1 (1:5000) (Proteintech, USA), CDK4 (1:1000) (Proteintech, USA), ACSL4 (1:2000) (Proteintech, USA), GPX4 (1:1000) (Proteintech, USA), TLR4 (1:4000) (Proteintech, USA), TLR5 (1:1000) (Proteintech, USA) and P-P38 (1:1000) (Proteintech, USA), P-MLKL(1:1000) (CST, USA), MLKL(1:1000) (CST, USA), P-RIP(1:1000) (CST, USA), RIP(1:1000) (CST, USA), TLR2(1:1000) (CST, USA), P38(1:1000) (CST, USA), P-P65(1:1000) (CST, USA), P65(1:1000) (CST, USA) and Caspase3(1:1000) (CST, USA), and TLR9 (1:1000) (Abcam, USA).

2.7 Single-cell transcriptome profiling

2.7.1 Library construction and sequencing

Hepatic $CD45^+$ cells were prepared through fluorescence-activated cell sorting (FACS). A total of 10000 $CD45^+$ cells from 4 mice (2500 cells/mouse) were loaded to a 10 x GemCode Single-cell instrument to generate single-cell Gel Bead-In-Emulsions (GEMs). The GEMs were then subjected to library construction using the Chromium™ Single Cell 3'Reagent Kit (version 3.1) (10X Genomics, Pleasanton, CA) according to the manufacturer's instructions. Library construction and RNA sequencing were completed by Gene Denovo Biotechnology Co., Ltd. (Guangzhou, China) as described (33, 34).

2.7.2 Data quality control and normalization

Barcode processing, data quality control and normalization were performed using the Cell Ranger Single Cell Software v3.1 (10X Genomics, Pleasanton, CA). Briefly, raw data from the sequencer were demultiplexed into the FASTQ format with the

bcl2fastq software and then aligned in the NucleotideSequence Database https://www.ncbi.nlm.nih.gov/genbank/ using the NCBI Basic Local Alignment Search Tool (BLAST). Low-quality sequences (containing adaptor sequences, or "N" longer than 10% of the read) and low-quality cells (containing ≥ 8000 UMIs,≥ 10% mitochondrial genes, and with <500 or >4000 genes detected) were filtered out. After quality control, a dataset of 18,690 $CD45^+$ cells (8392 control and 10298 LAP) x 42145 genes was obtained for downstream analysis. The raw gene expression measurements for each cell were normalized by dividing them with the total expression followed by scale factor-multiplying (x10,000) and log-transformation.

2.7.3 Cell clustering and visualization

Data clustering was performed using the Seurat R package v4.0.4. Briefly, filtered and normalized control and LAP datasets were integrated after canonical correlation analysis-based reduction of batch effects. The integrated data were further normalized by the Z-score and then subjected to principle component analysis (PCA) to reduce dimensionality. Subsequently, the enriched PCs with low p-value genes were used in a share-nearest neighbor (SNN) graph approach to cluster cells. The FindCluster tool employing the Louvain algorithm was used to group cells into different subsets according to their expression levels. Single-cell subgroup classification results were visualized by t-distributed Stochastic Neighbor Embedding (t-SNE) using the Louge Cell Browser software. For each cell cluster, genes showing differential expression and with known functions were identified.

2.7.4 Single-cell pseudo-time analysis

Single-cell trajectory analysis was performed with the Monocle v2.10.1 package (35). Briefly, key differentially expressed genes (DEGs) related to the development and differentiation processes were identified by performing differential gene tests and subsequently used as markers to define cellular progress. Data dimension reduction was performed using DDRTress, and cells were ordered in peseudotime using the order-cells function. The trajectory was visualized in a two-dimensional tree-like structure by running the plot cell trajectory function.

2.7.5 Gene functional enrichment analysis

Differentially expressed genes (DEGs) were subjected to Gene Ontology (GO), Reactome and Gene Set Enrichment Analysis (GSEA) to identify biological functions and interacting pathways. GO and Reactome analyses were performed using the Cluster Profiler R package in RStudio (v 1.2.1335) and ClueGO plugin in Cytoscape software (v3.8.2), respectively (36). Outputs with false discovery rate (FDR)-corrected p-value <0.05 were retained. GSEA analysis was performed using GSEA v4.0.3 and thec6.all.v7.0.symbols.gmt (oncogenic signatures) and c2.cgp.v7.0.symbols.gmt (chemical and genetic perturbations) gene setlibraries as reference gene set collections (37). The statistical cutoff for this analysis wasset at $p<0.05$.

2.7.6 Identification of gene expression programs by cNMF

Gene expression programs underlying cellular activities in hepatocytes, myeloid and T cells were identified using the consensus non-negative matrix factorization (cNMF) method (https://github.com/dylkot/cNMF) (38). Briefly, normalized cell type-specific expression data from control and LAP mice were integrated and used as input to run non-negative factorization (NMF) analysis to identify clusters of highly similar clusters of components inferred as GEPs. This procedure was repeated multiple rounds for each cell type, and a consensus k-value (number of GEPs) was selected, which provided a reasonable trade-off between error and stability. Non-negative least squares (NNLS) was used to calculate the activity of NMF transcription programs in each cell based on the first 100 weighted genes of the GEP (39). Subsequently, Student's t-test or Mann-Whitney test statistical analysis was performed to compare GEP activity values between control and LAP cells and $p<0.05$ was defined as statistically different. The top 30 genes of each GEP that show significant activity difference between control and LAP cells were used in GO, KEGG and Reactome analysis to identify the biological functions associated with the GEP (36, 40). Finally, tSNE plots generated with the ggplot2 package were used to visualize the spatial distribution of the statistically different GEPs in cell subtypes.

2.8 Statistical analysis

Differences between compared groups were evaluated by performing Student's t-test or two-way repeated ANOVA using Graphpad (8.0). Data were presented as mean ± standard error, and $p<0.05$ was considered as significant.

3 Results

3.1 Dietary supplementation of LAP protected wild-type but not TLR2 knockout mice from DEN-induced liver injury, fibrosis and tumorigenesis

Probiotics are living bacteria that, when administered in adequate amounts, confer a health benefit on the host (41). The broad health benefits of probiotics and their specific effect on cancer suppression have been repeatedly demonstrated in both clinical and experimental settings (42, 43). One mechanism by which probiotics affect host physiology is the stimulation of rDC differentiation (30, 44) in a Toll-like 2 receptor (TLR2) dependent manner (45–47). To develop a probiotics-based approach to reduce hepatic inflammation and to promote liver function, we first conducted a functional screening *in vitro* using a TLR2 activity reporter to identify probiotics that specifically bind to and activate TLR2 signaling. This screening led to the identification of four TLR2-activating lactic acid-producing (LAP) probiotics (Figure 1A). To evaluate the potential effects of LAP

on hepatic function and homeostasis, we assessed whether LAP-administered mice are protected from or become more sensitive to chemically induced liver injury, fibrosis and HCC formation. For this, LAP was administered once every two days over a 30-week period into mice 4 weeks after intraperitoneal injection of diethylnitrosamine (DEN) (Figure 1B). Both control (PBS) and LAP-treated mice were placed on a high-fat diet (HFD) to accelerate tumor growth. Compared to controls, LAP-treated mice had significantly lower liver-to-body weight ratios (Figure 1C), reduced numbers and volumes of liver surface tumor (Figure 1E) and decreased serum alanine transaminase (ALT), aspartate transferase (AST) and lactate dehydrogenase (LDH) levels (Figure 1F). Histological analysis revealed that LAP mice showed markedly reduced hepatic lipid accumulation (Figures 1G, H) and fibrosis (Figures 1I, J). Notably, the observed hepatoprotective effects LAP were blunted in TLR2 KO mice (Supplementary Figures S1A–I).

Next, western blotting and quantitative RT-PCR were performed to assess the hepatic expression of critical genes functionally involved in or regulating cell death (Bcl2, Casp3, Acsl4 and Gpx4), proliferation (Pcna, Ccnd1, Cdk4, p65), inflammation (IL-1β, Il-2, Il-4, Il-6 and Tgfβ) and danger/stress signaling (Tlr2, Tlr4, Tlr5, Tlr9, Rip, Mlkl and P38). None of the listed genes was differentially expressed between the livers of control and LAP mice (Supplementary Figures S2A–H). Notably, however, immunohistochemical analysis revealed that LAP mice contained fewer Ki67$^+$ cells in their livers than control mice (Figures 1K, L). Overall, these findings indicate that mice with expanded hepatic DC subset were protected from DEN-induced liver injury, fibrosis and tumorigenesis, and this hepatoprotective effect was dependent, at least partially, on the TLR2 signaling pathway.

3.2 Dietary supplementation of LAP causes accumulation of CD11C$^+$ dendritic cells in the mouse liver

The liver is populated by a variety of immune cells, including macrophages (Kupffer cells, KC), dendritic cells (DC), natural killer (NK) cells, neutrophils, B and T lymphocytes (11). To determine whether LAP could modulate hepatic immune composition in a TLR2-dependent manner, we analyzed hepatic nonparenchymal cells (NPCs) through fluorescence-activated cell sorting (FACS) (Supplementary Figure S3). FACS analysis showed that LAP-treated and control (PBS) mice showed comparable percentages of total immune cells (Supplementary Figures S4A, G), macrophages (F4/80$^+$) (Supplementary Figures S4B, H), myeloid-derived macrophages (MDM) (F4/80$^+$/CD11b$^+$) (Supplementary Figures S4C, I), natural killer cells (NK1.1$^+$) (Supplementary Figures S4D, J), NKT (CD3$^+$NK1.1$^+$) (Supplementary Figures S4E, K) and total T cells (CD3$^+$) (Supplementary Figures S4F, L) in the liver. However, LAP-fed WT mice had a significantly higher percentage of dendritic cells (CD11c$^+$) (Figures 2A, G–J) and lower percentage of neutrophils (Gr-1$^+$CD11b$^+$) (Figure 2C) but no difference in MHCII+ dendritic cells (Figure 2B) than control mice. Notably, LAP and PBS-treated WT mice showed no difference in splenic immune composition (Supplementary Figures S6A–L), and the observed alterations in hepatic DC and neutrophils were completely blunted in TLR2 KO mice (Figures 2D–F; Supplementary Figures S5A–L). These results indicate that LAP supplementation did not alter the overall hepatic immune content and landscape of major immune cell types in the liver but selectively affected the proportion of dendritic cells and neutrophils in a TLR2-dependent manner.

3.3 LAP-treated mice harbored additional and more subtle immune compositional changes in their hepatic tumor microenvironment (TME)

To more quantitatively assess the hepatic immune composition changes induced by LAP, we isolated CD45$^+$ cells (total immune cells) from control and LAP-treated mice and performed single-cell RNA sequencing (scRNA-seq) (Figure 3A). After quality control of the raw data, a total of 18,690 cells (8392 control and 10298 LAP) were retained, and their single-cell transcriptomic data were used for further analysis. Cell clustering using integrated control and LAP cell data yielded 26 numerically distinct cell subsets (Figure 3B). Lineage-specific marker gene-based functional annotation defined these immune cell subsets into 7 functional groups: T cells, B cells, macrophages, natural killer cells, dendritic cells, granulocytes and hepatocytes, with T cells being the most dominant (62%) immune cell type in the liver (Figures 3C, D).

Cell clustering analysis was also performed using separated control and LAP cell transcriptomic data to enable a quantitative assessment of the relative abundance of each cell type between control and LAP groups. As shown in Figures 3E, F, dendritic cell abundance was increased (1.5-fold), consistent with the FACS data (Figure 2), whereas neutrophil abundance was decreased (0.64-fold) in the liver of LAP-treated mice. Notably, the abundance of two other immune cell subtypes, T and B lymphocytes, was also increased (1.27 and 1.43-fold, respectively) in LAP mice. Hence, transcriptome profiling at the single-cell resolution allowed the identification of additional and more subtle immune compositional changes in mice administered with LAP.

3.4 Hepatic T cells in LAP-treated mice exhibit increased mitochondrial oxidative phosphorylation but decreased cytotoxic activity

Because T cells were dominantly present in the TME of DEN-induced liver tumors (Figures 3C, D) and have been recognized as the significant cytotoxic immune cells (48, 49), we further analyzed the compositional and functional changes of the T cell subset resulting from LAP treatment. Cell clustering analysis using integrated control and LAP cell transcriptome data yielded 19 T cell clusters (Figure 4A), which were further defined into three functional sub-types: CD8$^+$T, CD4$^+$T and double-negative T (DNT)

10.3389/fimmu.2025.1565486

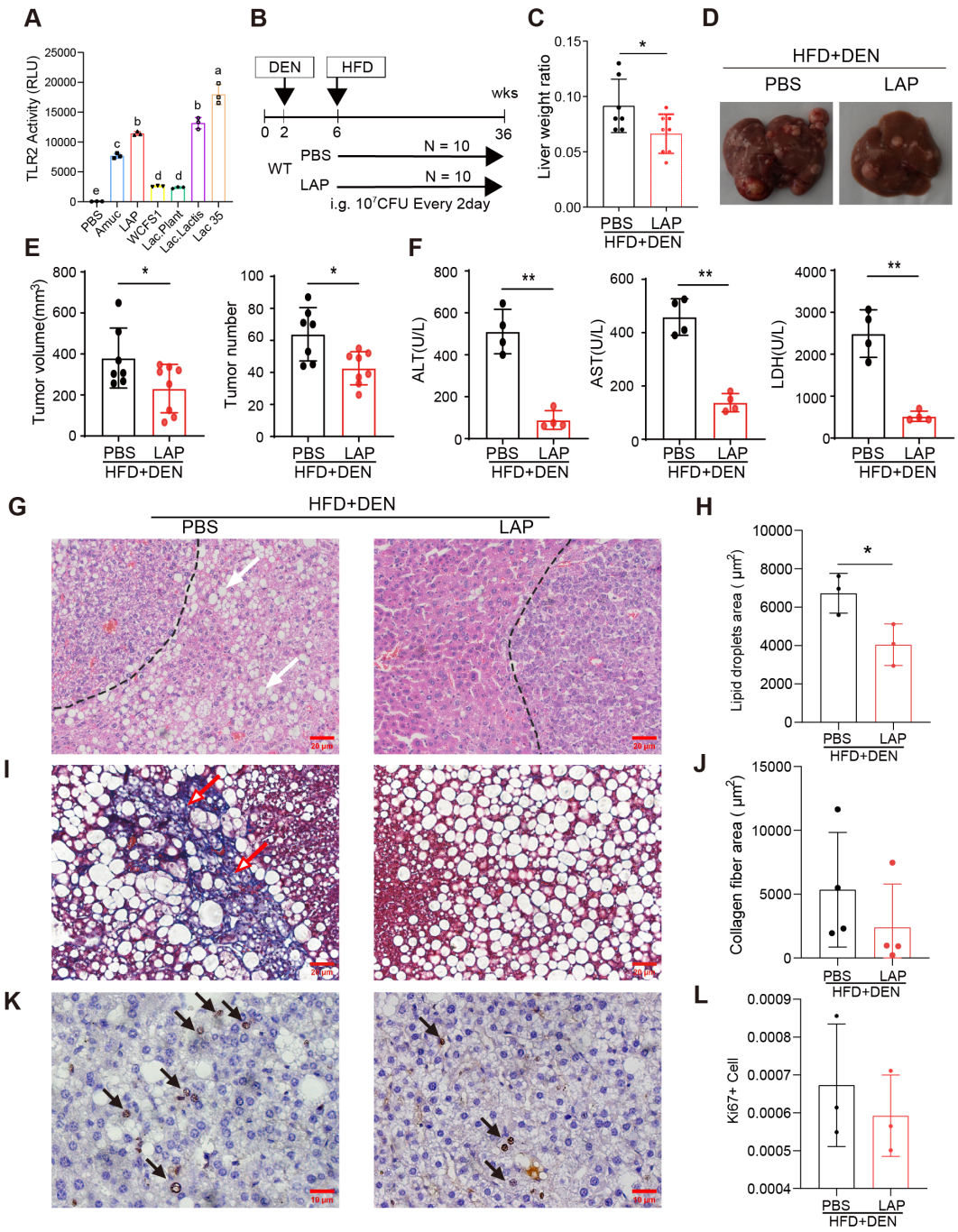

FIGURE 1
Oral administration of LAP protected mice from DEN-induced liver injury, fibrosis and HCC development. 2-week old male wild-type mice were injected (i.p.) with a single dose of DEN and kept on high fat diet for 36 weeks. Two weeks after DEN injection, mice were divided into two groups and oral garaged with PBS and LAP, respectively. At the endpoint, mouse serum samples and liver tissues were analyzed. **(A)** TLR2 luciferase reporter assay results showing increased TLR2 activity following LAP or individual probiotics treatment *in vitro*. Amuc (a recombinant *Akkermansia muciniphila* membrane protein) was used as a positive control. **(B)** Diagram of treatment timelines. **(C)** Liver-to-body weight ratios of LAP treatment vs control (PBS) groups. **(D)** Representative images of liver from negative control group and DEN-injected mice treated with and without LAP. **(E)** Quantified liver surface tumor numbers and volumes and **(F)** Serum ALT, AST and LDH levels, PBS vs LAP groups. **(G, I, K)** Representative images of H&E **(G)**, Masson's Trichrome **(I)** and immunohistochemical **(K)** staining showing decreased lipid accumulation (white arrows), fibrosis (red arrows) and Ki67+ proliferating cells (black arrow) in the liver of LAP treated mice. **(H, J, L)** Quantification of lipid droplets and collagen fiber areas in **(F, H)**, and Ki67+ cells in **(J)**, respectively. All data were presented as means ± SD, *, p<0.05; **, p<0.01.

10.3389/fimmu.2025.1565486

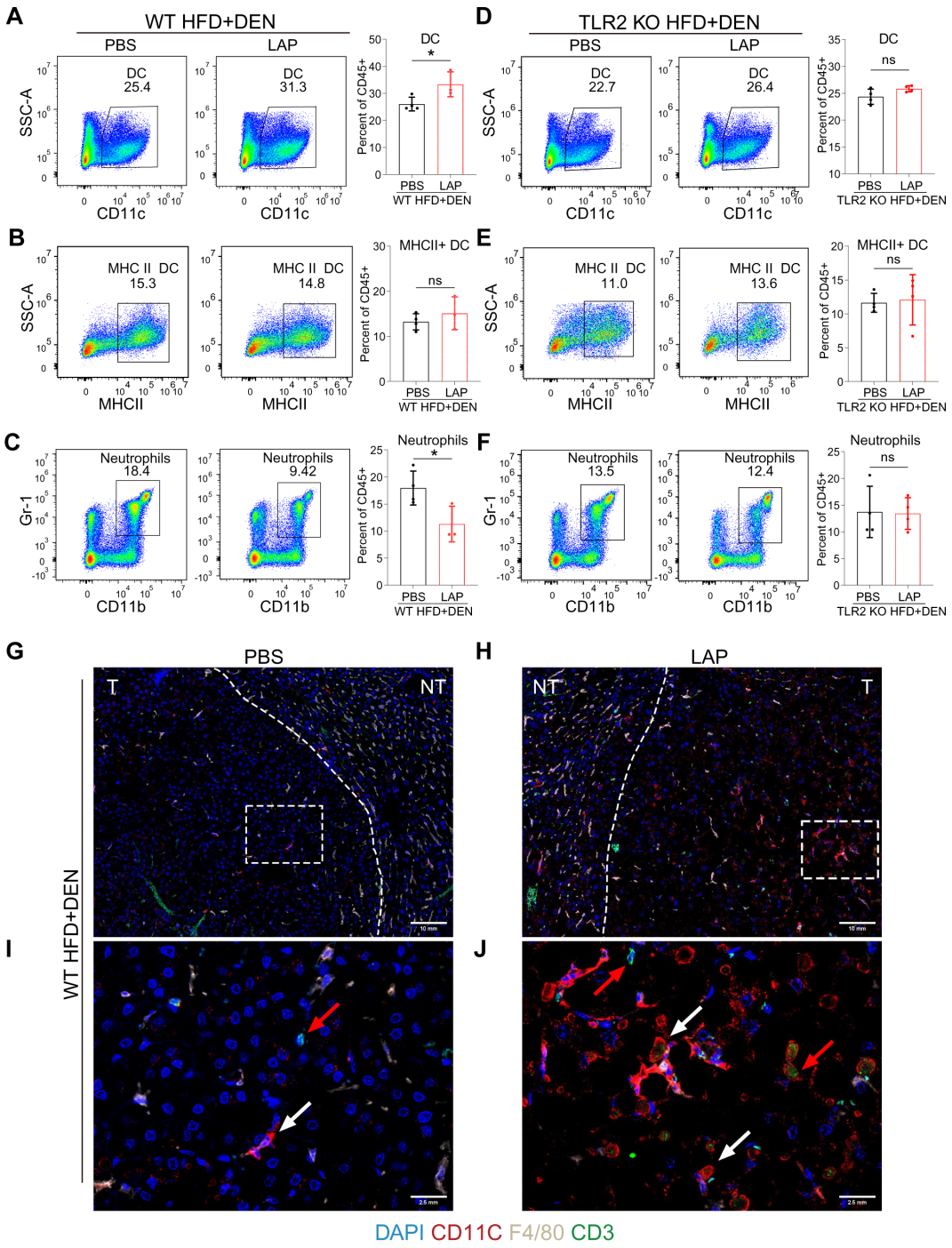

FIGURE 2
Oral LAP treatment stimulates hepatic dendritic cells in a TLR2-dependent manner. 2-week old male wild-type mice were injected (i.p.) with a single dose of DEN and kept on high fat diet for 36 weeks. Two weeks after DEN injection, mice were divided into two groups and oral garaged with PBS and LAP, respectively. At the endpoint, liver nonparenchymal cells (NPCs) were isolated and analyzed by fluorescence activated cell sorting (FACS) using immune cell type-specific antibodies. **(A–F)** FACS gating strategies and quantifications of percentages of dendritic cells **(A, D)**, MHCII dendritic cells **(B, E)**, neutrophils **(C, F)** in wild-type **(A–C)** and TLR2 knockout **(D–F)** mice treated with PBS or LAP. **(G–J)** Co-immunofluorescence staining showing increased numbers of DCs (white arrows) and T cells (red arrows) in LAP-treated liver. **(I, J)** Magnified images of the dashed squares in **(G)** and **(H)**, respectively. T and NT indicate tumor and non-tumor. All data were presented as means ± SD, *, p<0.05; **, p<0.01; ns means no significant difference.

(Figure 4E), based on marker gene expression. Cell clustering using separated control and LAP cell transcriptomic data revealed that clusters 6 and 12 (C06 and C12) were significantly diminished, whereas other T cell clusters were modestly expanded in the LAP group (Figures 4B, C). Notably, both C06 and C12 showed high expression of Pdcd1, Cd69, Ctla4, Tox, Entpd1 and Lag3, markers of exhausted T cells, as well as Ccl3 and Ccl5, genes functionally associated with effector T-cell function (50) (Figure 4F). Other

10.3389/fimmu.2025.1565486

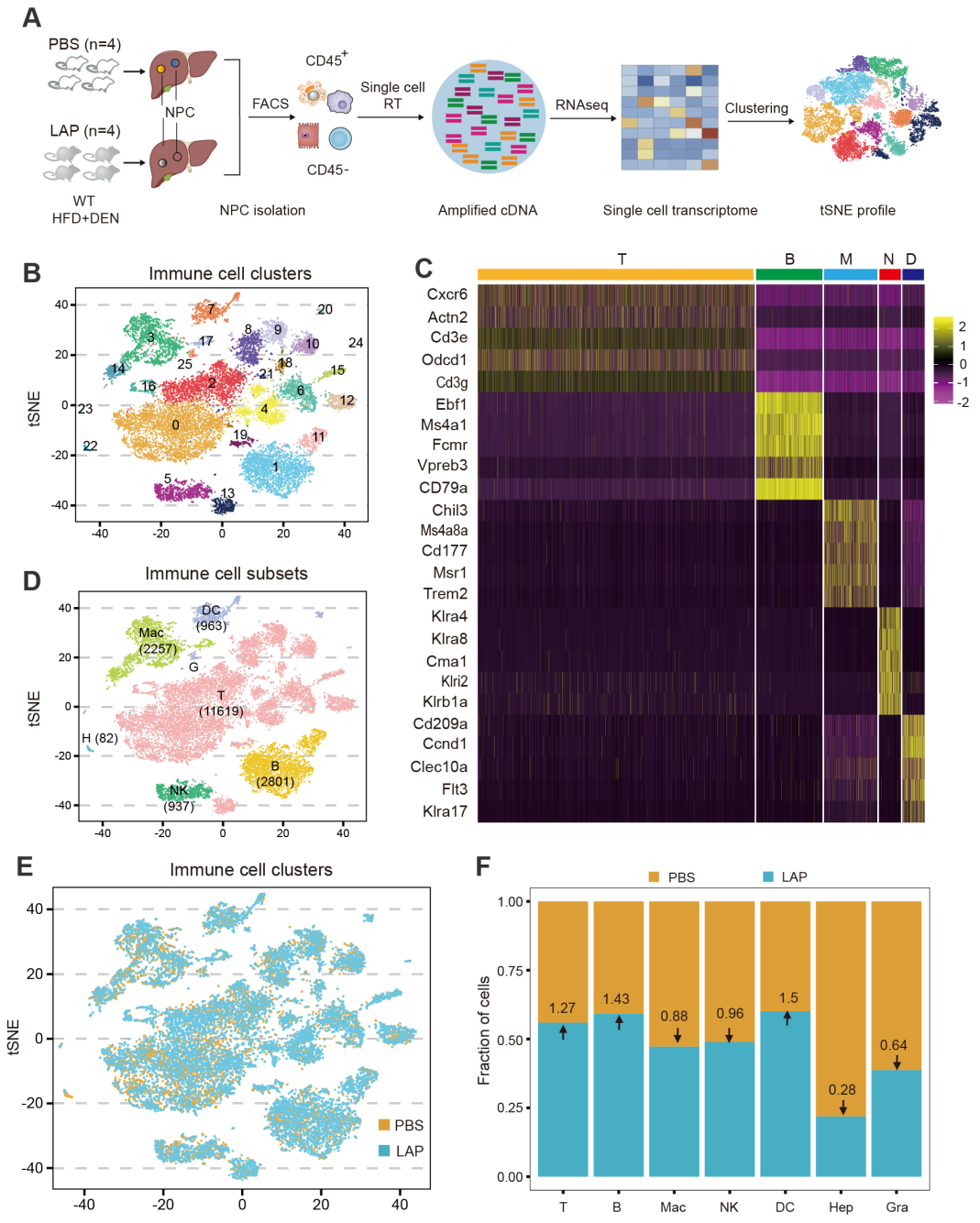

FIGURE 3
Single-cell transcriptome profiling identifies additional and more subtle LAP-induced changes in hepatic immune composition. Two-week old male wild-type mice were injected (i.p.) with a single dose of DEN and kept on high fat diet treated with PBS or LAP for 36 weeks. At the end point, liver nonparenchymal cells (NPCs) were isolated and subjected to single cell RNA sequencing. **(A)** Diagram of experimental procedures. **(B, D, E)** tSNE plots based on integrated **(B, D)** and separated **(E)** control and LAP group transcriptome data, showing hepatic immune cell clusters **(B)**, defined immune cell subsets **(D)** and differential presence of hepatic immune cell subtypes between control (PBS) vs LAP-treatment **(E)**. **(C)** The heat map shows the enhanced expression of 5 lineage marker genes in T cells, B cells, macrophages, neutrophils, and dendritic cells. **(F)** Calculated fold changes for major immune cell types and hepatocytes, control vs LAP treatment group.

clusters showed high expression of either effector or naïve T cell markers or a mixed expression of both types of markers (Figure 4F).

To understand how LAP treatment affected the functionality of T cells, consensus non-negative matrix factorization (cNMF), a novel algorithm developed to more accurately infer identity versus activity program (38), was used to establish gene expression programs (GEPs). cNMF analysis yielded 9 T cell-specific GEPs (T-GFPs) (Figure 4D). Based on functional annotation of the top 30 differentially expressed genes, these T-GFPs controlled nine distinct functional pathways: mitochondrial oxidative phosphorylation (OXPHOS) (T-GEP1), natural killer cell activation (T-GEP2), cell cycle activation (T-GEP3), antigen presentation (T-GEP4),

interferon-gamma functioning (T-GEP5), lymphoid differentiation (T-GEP6), T cell cytotoxicity (T-GEP7), ribosome assembly (T-GEP8) and co-stimulatory signaling (T-GEP9) (Figure 4D). LAP treatment, while increasing the activity of lymphocyte mitochondrial OXPHOS (T-GEP1) and co-stimulatory signaling (T-GEP9), notably decreased the activity of NK activation (T-GEP2), IFN functioning (T-GEP 5) and T cell cytotoxicity (T-GEP7). Furthermore, marker gene-based trajectory analysis for the CD8T subset and various T-cell clusters indicated that LAP feeding did not affect the differentiation of effector and exhausted T cells from naïve T progenitors (Figure 4G, Supplementary Figure S8A).

3.5 Oral supplementation of LAP induces regulatory dendritic cells in the liver

As first immune responders, myeloid cells (macrophages, dendritic cells, monocytes and granulocytes) sense infection or tissue damage and direct the recruitment, proliferation and activation of adaptive immune cells (51). Hence, we wondered whether compositional and functional alterations of the myeloid compartment caused the observed hepatic T cell activity and functional changes in LAP-treated mice. Clustering analysis showed that the hepatic myeloid compartment was composed of 16 distinct clusters, which were further defined into 3 functional groups: granulocytes, dendritic cells and macrophages, by marker gene expression analysis (Figure 5A). LAP administration increased the abundance of C01, C07, C10, C12 and C15, while decreased the abundance of C03, C05, C11 and C14 (Figures 5B, C). Notably, all clusters expanded in the LAP group were dendritic cells expressing two or more regulatory or tolerogenic dendritic cell markers (Figure 5E), such as Anxa1, C1qc, Cstb and Fth1 (52). Interestingly, these DC clusters all express TLR2 and its downstream adaptor Myd88 (Figure 5F). On the contrary, the unchanged or diminished clusters in the LAP group were either macrophages or granulocytes that expressed two or more M1-type macrophage markers (Figure 5G), such as Cd86, Il1b, Cd164, Cd74, Clqc, Ccl2 and S100a6 (53). These findings support the notion that LAP supplementation induces regulatory or tolerogenic dendritic cells in the liver.

Next, gene expression programs (GEPs) of hepatic myeloid cells were calculated and compared between the control and LAP groups. cNMF analysis produced 8 myeloid-specific GEPs (M-GEP1 to M-GEP8) (Figure 5D). These M-GEPs control eight distinct myeloid functional pathways, including inflammatory response (M-GEP1), TCR assembly (M-GEP2), complementary activation (M-GEP3), IFN signaling (M-GEP4), cell adhesion signaling ((M-GEP5), mitochondrial OXPHOS (M-GEP6), ferroptosis control (M-GEP7) and antigen presentation (M-GEP8) (Figure 5D). LAP treatment increased the activity of myeloid cell mitochondrial OXPHOS (M-GEP6) and antigen presentation (M-GEP8) while decreasing the activity of inflammatory response (M-GEP1), IFN signaling (M-GEP4), cell adhesion signaling (M-GEP5) and ferroptosis (M-GEP7) (Figure 5D). We re-examined the functions of the top 30 differentially expressed genes in M-GEP6 through Reactome pathway analysis and found that they were enriched in bioenergetic functions, such as cellular respiratory electron transport, ATP synthesis and TCA cycle (Supplementary Figures S8B, C). Collectively, these results suggest that oral administration of LAP induces regulatory or tolerogenic dendritic cells that promote an immunosuppressive tumor microenvironment in the liver.

4 Discussion

DCs are versatile antigen-presenting cells with essential roles in the initiation and regulation of "*danger*"-specific T cell responses. Thus, DCs have long been considered an attractive drug target for immune-based treatment of liver diseases (54, 55). Despite this, few clinical benefits of DC-based therapy have been demonstrated thus far, in part due to the lack of efficient DC-modulating reagents. Here, we demonstrate that LAP, a novel mix of TLR2-interacting and lactic acid-producing probiotics, are potent promoters of hepatic DCs. Mice orally administered with LAP had significantly higher numbers of DCs in the liver and were protected from diethylnitrosamine-induced liver injury, fibrosis and tumorigenesis, in a TLR2-dependent manner. Single-cell transcriptome profiling revealed that the hepatic T cells of LAP-treated mice exhibit enhanced mitochondrial oxidative phosphorylation but reduced cytotoxicity activity. LAP treatment increased mitochondrial oxidative phosphorylation and antigen presentation activities while decreasing the inflammatory response of hepatic myeloid cells. The observed LAP-responsive DCs in the liver expressed two or more regulatory or tolerogenic markers. Collectively, our data suggest that the TLR2-activating probiotics identified in the current study are potent promoters of hepatic regulatory dendritic cells and can thus be utilized to devise probiotics-based approaches for effective protection of the liver against toxin or metabolic stress-induced hepatocellular damages and tumorigenesis.

Diverse innate and adaptive immune cells, including macrophages, dendritic cells polymorphonuclear neutrophils (PMN) and lymphocytes express one family of 13 receptors, the toll-like receptors (TLRs) that recognize pathogen-associated molecular patterns (PAMPs) or endogenous danger-associated molecule patterns (DAMPs) (56). The recognition of PAMPs and/or DAMPs by different TLRs triggers distinct signaling pathways, including NF-kB, p38, JNK and ERK, causing upregulation of proinflammatory genes and immune reactions (57). Of note, one member of the TLR family, TLR2, has been shown to play a unique immune modulatory role by recognizing probiotics or other intestinal commensals to elicit immunosuppressive action (58). In line with previously reported data, we find in this study that LAP administration lowers DEN-induced liver injury in WT but not in TLR2 KO mice (Figures 1C–F; Supplementary Figures S1B–I). In addition, LAP stimulated modest upregulation of immunosuppressive cytokines IL-4 and

10.3389/fimmu.2025.1565486

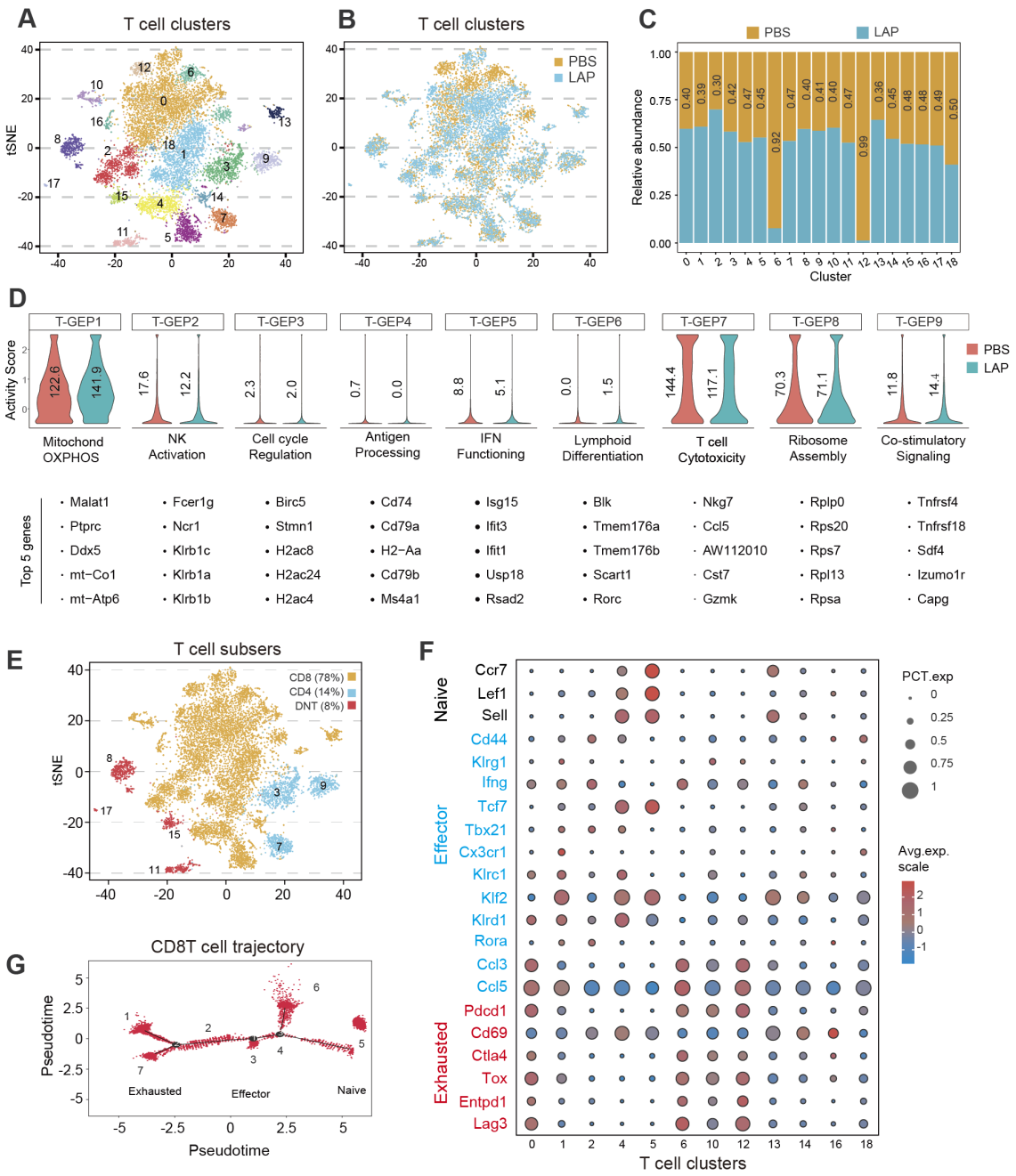

FIGURE 4
LAP treatment alters the composition and functionality of hepatic T cells. Normalized T cell-specific expression data from control and LAP mice were integrated and used as input to run non-negative factorization (NMF) analysis to identify T clusters of highly similar components inferred as T-GEPs. **(A, B, E)** tSNE plots based on integrated **(A, E)** or separated **(B)** RNAseq data showing various T cell clusters **(A)** and different functional T cell subtypes **(E)**, with differential presence of several T cell clusters between control (PBS) vs LAP treated mice **(B)**. **(C)** Bar graph showing differentially present hepatic immune cell subtypes between control (PBS) vs LAP-treatment. Horizontal numbers indicate cluster-specific cell number fold changes. **(D)** Violin plots showing altered T cell-specific gene expression programs (T-GEPs) between control and LAP mice. Vertical numbers indicate GEP activity score. Top 5 of the 100 weighted genes were listed below each GEP. **(F)** Bubble chart showing differential expression of naïve, effector and exhausted markers between the identified T cell clusters. **(G)** Marker gene-based trajectory analysis for the CD8T subset.

IL-10 in WT but not in TLR2 KO mice (Supplementary Figures S2A–D). Moreover, single cell transcriptomic profiling indicates that both TLR2 and its downstream signaling adaptor Myd88 are highly expressed in the LAP-stimulated DC clusters (Figure 5F). Together, these results suggest that one mechanism by which LAP elicits immunosuppressive effects is to bind and activate the TLR2 signaling pathway.

Dendritic cells are developmentally and functionally heterogeneous. Depending on the nature of the stimulating cues, DCs, which are commonly classified into conventional (cDC),

10.3389/fimmu.2025.1565486

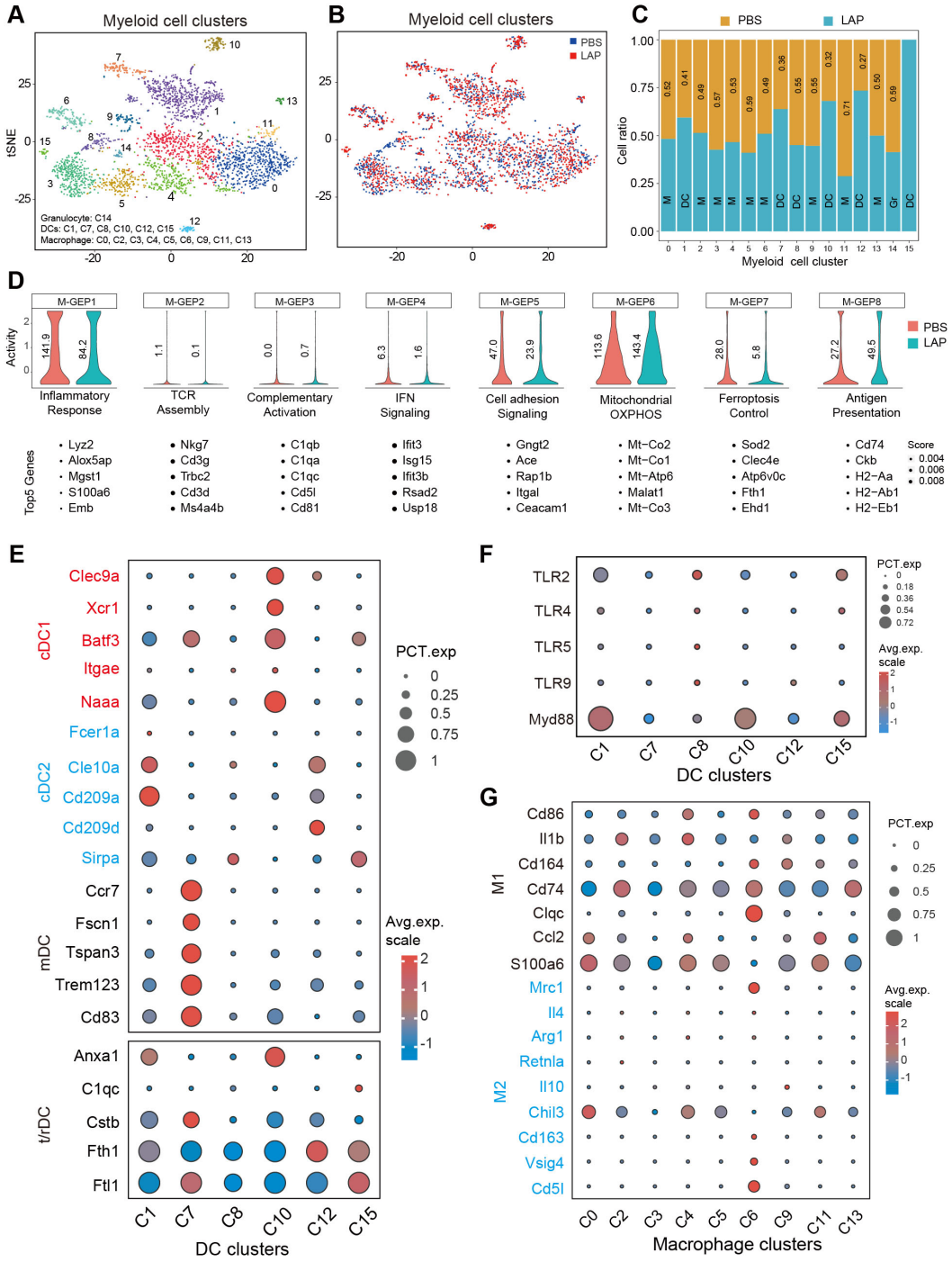

FIGURE 5
LAP treatment induces regulatory/tolerogenic dendritic cells in the liver. Normalized myeloid cell-specific expression data from control and LAP mice were integrated and used as input to run non-negative factorization (NMF) analysis to identify myeloid clusters of highly similar components inferred as M-GEPs. **(A, B)** tSNE plots of various myeloid cell clusters based on integrated **(A)** and separated **(B)** RNAseq data. **(C)** Bar graph showing differentially present hepatic immune cell subtypes between control (PBS) vs LAP-treatment. **(D)** Violin plots showing altered myeloid cell-specific gene expression programs (M-GEPs) between control and LAP mice. Vertical numbers indicate GEP activity score. Top 5 of the 100 weighted genes were listed below each GEP. **(E–G)** Bubble charts revealing differential expression of cDC1, cDC2, mDC and r/tDC, and M1 and M2-like macrophage markers **(E, G)** and TLR signaling related genes between the identified myeloid cell clusters.

plasmacytoid (pDC) and monocyte-derived (mDC), can either promote (immunogenic) or suppress (tolerogenic or regulatory) tissue inflammation (59). Through single-cell transcriptome profiling, we identified seven hepatic DC clusters. Compared to other defined myeloid cell clusters (macrophages and granulocytes), all DC clusters consistently showed high mRNA expression of Flt3 and Batf3, critical regulators of monocytes to DCs differentiation (60, 61). These findings indicate that the DC clusters observed here

were likely derived from monocytes and may function as APCs to activate $CD8^+$T cells, much as the $CD103^+$ DCs observed in other tissue microenvironments (62). It is noteworthy that oral LAP administration in mice increased the hepatic abundance of five but one DC cluster and that all expanded DCs show high mRNA expression of one or more regulatory or tolerogenic DC markers (also known as DC3) (52, 63). More importantly, gene expression program (GEP) activity analysis revealed that LAP treatment broadly decreased hepatic T cell functionality, including reduction of the inflammatory response, downregulation of IFN signaling and cytotoxicity. Based on these findings, we suggest that the LAP-responsive hepatic DCs observed in our study are regulatory or tolerogenic DCs that may directly interact with hepatic T cells to suppress immunogenicity.

Oral administration of LAP markedly diminished two hepatic T cell clusters (C06 and C12) while modestly expanded several others (Figure 4C). We wondered whether the two diminished T cell clusters are Th1, Th2 or Th17 helper cells, as these cells are proinflammatory and are readily inducible by probiotics treatment (30). Notably, both C06 and C12 are transcriptionally positive for cytotoxic T lymphocyte markers, including Cd8, Gzmk, Gzma, Gnly and Gzmb (64, 65), but negative for Il-17, a potent proinflammatory cytokine secreted by T helper 17 (Th17) T cells (66, 67). Furthermore, C06 and C12 show higher transcription of several exhausted (Pdcd1, Cd69, Ctla4, Tox, Entpd1 and Lag3) and effector (Ccl3, Ccl5 and Nkg7) T cell markers (50, 68, 69). Based on these findings, we speculate that C06 and C12 represent two immune-reactive effector $CD8^+$ T cells that are undergoing rDC-mediated T cell exhaustion. These cells are highly inflammatory but molecularly different from the IL-17-producing $CD4^+$ T helper cells, whose abundance was reportedly decreased by probiotics treatment (31). Further studies are needed to shed light on the cellular and immunological features of these cells and how they interact with antigen-presenting cells during immune coordination.

Another intriguing finding of the current study is that oral administration of LAP in mice significantly increases mitochondrial oxidative phosphorylation in both myeloid cells and T lymphocytes. This suggests that LAP supplementation may benefit innate and adaptive immune cell health by increasing mitochondrial functionality. Presently, the mechanisms underlying the LAP-mediated metabolic upregulation remain unclear. From a therapeutic or prophylactic perspective, this may be useful for improving future cancer immunotherapy. In the solid tumor microenvironment (TME), rapidly proliferating cancer cells compete, often disproportionally, with tumor-infiltrating immune cells for glucose and other nutrients (70). The decreased nutrient contents impose metabolic stress on and impair the function of immune cells, resulting in rapid tumor growth (71). Restoring nutrient supply to or reprogramming metabolic requirements of tumor infiltrating immune cells are potential strategies that can be used clinically to reverse premature immune cell exhaustion and to increase the success of immunotherapy (72, 73). In this direction, further studies are needed to test the safety and efficacy of LAP as well as other immunogenic probiotics as an immune checkpoint blockade therapy adjuvant in both preclinical models and in clinical settings. Finally, given the characterized role of LAP in stimulating regulatory DCs, we anticipate that it will have several other important clinical applications, including the prevention or treatment of autoimmune disorders (arthritis and asthma), inflammatory bowel disease and alcohol/nonalcohol-induced chronic liver diseases.

Data availability statement

The raw sequence data reported in this paper have been deposited in the Genome Sequence Archive in National Genomics Data Center, China National Center for Bioinformation / Beijing Institute of Genomics, Chinese Academy of Sciences (GSA: CRA024153) that are publicly accessible at https://ngdc.cncb.ac.cn/gsa.

Ethics statement

The animal study was approved by Animal Ethics Committee of Soochow University. The study was conducted in accordance with the local legislation and institutional requirements.

Author contributions

JW: Conceptualization, Data curation, Methodology, Visualization, Writing – original draft, Writing – review & editing. PG: Conceptualization, Data curation, Methodology, Visualization, Writing – review & editing. QLi: Conceptualization, Data curation, Methodology, Software, Visualization, Writing – review & editing. MW: Methodology, Visualization, Writing – review & editing. DW: Methodology, Visualization, Writing – review & editing. ML: Writing – original draft, Validation. SZ: Methodology, Visualization, Writing – review & editing. HW: Supervision, Writing – review & editing. QLo: Conceptualization, Funding acquisition, Project administration, Resources, Supervision, Writing – original draft, Writing – review & editing.

Funding

The author(s) declare that financial support was received for the research and/or publication of this article. This work was supported by the National Key R&D Program of China Grant 2019YFA0802400 and Natural Science Foundation of China Grant 32070762 to QLo.

Acknowledgments

We thank members of the Soochow University core facility for technical assistance; Drs. Ying Xu, Yong Zhang, Weiqi He and

Wensheng Zhang for helpful discussions and critical comments on the manuscript.

Conflict of interest

The authors declare that the research was conducted in the absence of any commercial or financial relationships that could be construed as a potential conflict of interest.

Generative AI statement

The author(s) declare that no Generative AI was used in the creation of this manuscript.

Publisher's note

Supplementary material

The Supplementary Material for this article can be found online at: https://www.frontiersin.org/articles/10.3389/fimmu.2025.1565486/full#supplementary-material

References

1. Sung H, Ferlay J, Siegel RL, Laversanne M, Soerjomataram I, Jemal A, et al. Global cancer statistics 2020: GLOBOCAN estimates of incidence and mortality worldwide for 36 cancers in 185 countries. *CA Cancer J Clin*. (2021) 71:209–49. doi: 10.3322/caac.21660

2. Sartorius K, Sartorius B, Aldous C, Govender PS, Madiba TE. Global and country underestimation of hepatocellular carcinoma (HCC) in 2012 and its implications. *Cancer Epidemiol*. (2015) 39:284–90. doi: 10.1016/j.canep.2015.04.006

3. Yang JD, Hainaut P, Gores GJ, Amadou A, Plymoth A, Roberts LR. A global view of hepatocellular carcinoma: trends, risk, prevention and management. *Nat Rev Gastroenterol Hepatol*. (2019) 16:589–604. doi: 10.1038/s41575-019-0186-y

4. Maeda S, Kamata H, Luo JL, Leffert H, Karin M. IKKbeta couples hepatocyte death to cytokine-driven compensatory proliferation that promotes chemical hepatocarcinogenesis. *Cell*. (2005) 121:977–90. doi: 10.1016/j.cell.2005.04.014

5. Nakagawa H, Umemura A, Taniguchi K, Font-Burgada J, Dhar D, Ogata H, et al. ER stress cooperates with hypernutrition to trigger TNF-dependent spontaneous HCC development. *Cancer Cell*. (2014) 26:331–43. doi: 10.1016/j.ccr.2014.07.001

6. Sakurai T, He G, Matsuzawa A, Yu GY, Maeda S, Hardiman G, et al. Hepatocyte necrosis induced by oxidative stress and IL-1 alpha release mediate carcinogen-induced compensatory proliferation and liver tumorigenesis. *Cancer Cell*. (2008) 14:156–65. doi: 10.1016/j.ccr.2008.06.016

7. Huang DQ, El-Serag HB, Loomba R. Global epidemiology of NAFLD-related HCC: trends, predictions, risk factors and prevention. *Nat Rev Gastroenterol Hepatol*. (2021) 18:223–38. doi: 10.1038/s41575-020-00381-6

8. Sharma P, Goswami S, Raychaudhuri D, Siddiqui BA, Singh P, Nagarajan A, et al. Immune checkpoint therapy-current perspectives and future directions. *Cell*. (2023) 186:1652–69. doi: 10.1016/j.cell.2023.03.006

9. Zou W, Wolchok JD, Chen L. PD-L1 (B7-H1) and PD-1 pathway blockade for cancer therapy: Mechanisms, response biomarkers, and combinations. *Sci Transl Med*. (2016) 8:328rv4. doi: 10.1126/scitranslmed.aad7118

10. Greten TF, Wang XW, Korangy F. Current concepts of immune based treatments for patients with HCC: from basic science to novel treatment approaches. *Gut*. (2015) 64:842–8. doi: 10.1136/gutjnl-2014-307990

11. Racanelli V, Rehermann B. The liver as an immunological organ. *Hepatology*. (2006) 43:S54–62. doi: 10.1002/hep.21060

12. Heymann F, Tacke F. Immunology in the liver–from homeostasis to disease. *Nat Rev Gastroenterol Hepatol*. (2016) 13:88–110. doi: 10.1038/nrgastro.2015.200

13. Geh D, Leslie J, Rumney R, Reeves HL, Bird TG, Mann DA. Neutrophils as potential therapeutic targets in hepatocellular carcinoma. *Nat Rev Gastroenterol Hepatol*. (2022) 19:257–73. doi: 10.1038/s41575-021-00568-5

14. Li X, Yao W, Yuan Y, Chen P, Li B, Li J, et al. Targeting of tumour-infiltrating macrophages via CCL2/CCR2 signalling as a therapeutic strategy against hepatocellular carcinoma. *Gut*. (2017) 66:157–67. doi: 10.1136/gutjnl-2015-310514

15. Ruf B, Heinrich B, Greten TF. Immunobiology and immunotherapy of HCC: spotlight on innate and innate-like immune cells. *Cell Mol Immunol*. (2021) 18:112–27. doi: 10.1038/s41423-020-00572-w

16. Zhou H, Wu L. The development and function of dendritic cell populations and their regulation by miRNAs. *Protein Cell*. (2017) 8:501–13. doi: 10.1007/s13238-017-0398-2

17. Banchereau J, Steinman RM. Dendritic cells and the control of immunity. *Nature*. (1998) 392:245–52. doi: 10.1038/32588

18. Wculek SK, Cueto FJ, Mujal AM, Melero I, Krummel MF, Sancho D. Dendritic cells in cancer immunology and immunotherapy. *Nat Rev Immunol*. (2020) 20:7–24. doi: 10.1038/s41577-019-0210-z

19. Hato L, Vizcay A, Eguren I, Perez-Gracia JL, Rodriguez J, Gallego-Perez-Larraya J, et al. Dendritic cells in cancer immunology and immunotherapy. *Cancers (Basel)*. (2024) 16:981. doi: 10.3390/cancers16050981

20. Audsley KM, McDonnell AM, Waithman J. Cross-presenting XCR1(+) dendritic cells as targets for cancer immunotherapy. *Cells*. (2020) 9:565. doi: 10.3390/cells9030565

21. Grolleau-Julius A, Harning EK, Abernathy LM, Yung RL. Impaired dendritic cell function in aging leads to defective antitumor immunity. *Cancer Res*. (2008) 68:6341–9. doi: 10.1158/0008-5472.CAN-07-5769

22. Zhivaki D, Kennedy SN, Park J, Boriello F, Devant P, Cao A, et al. Correction of age-associated defects in dendritic cells enables CD4(+) T cells to eradicate tumors. *Cell*. (2024) 187:3888–3903 e18. doi: 10.1016/j.cell.2024.05.026

23. Ma Y, Shurin GV, Gutkin DW, Shurin MR. Tumor associated regulatory dendritic cells. *Semin Cancer Biol*. (2012) 22:298–306. doi: 10.1016/j.semcancer.2012.02.010

24. Shurin MR, Naiditch H, Zhong H, Shurin GV. Regulatory dendritic cells: new targets for cancer immunotherapy. *Cancer Biol Ther*. (2011) 11:988–92. doi: 10.4161/cbt.11.11.15543

25. Conejo-Garcia JR, Rutkowski MR, Cubillos-Ruiz JR. State-of-the-art of regulatory dendritic cells in cancer. *Pharmacol Ther*. (2016) 164:97–104. doi: 10.1016/j.pharmthera.2016.04.003

26. Zhong H, Gutkin DW, Han B, Ma Y, Keskinov AA, Shurin MR, et al. Origin and pharmacological modulation of tumor-associated regulatory dendritic cells. *Int J Cancer*. (2014) 134:2633–45. doi: 10.1002/ijc.28590

27. Shurin GV, Ouellette CE, Shurin MR. Regulatory dendritic cells in the tumor immunoenvironment. *Cancer Immunol Immunother*. (2012) 61:223–30. doi: 10.1007/s00262-011-1138-8

28. Miller LE, Lehtoranta L, Lehtinen MJ. The Effect of Bifidobacterium animalis ssp. lactis HN019 on Cellular Immune Function in Healthy Elderly Subjects: Systematic Review and Meta-Analysis. *Nutrients*. (2017) 9:191. doi: 10.3390/nu9030191

29. Kan HX, Cao Y, Ma Y, Zhang YL, Wang J, Li J, et al. Efficacy and safety of probiotics, prebiotics, and synbiotics for the prevention of colorectal cancer and precancerous lesion in high-risk populations: A systematic review and meta-analysis of randomized controlled trials. *J Dig Dis*. (2024) 25:14–26. doi: 10.1111/1751-2980.13247

30. Kwon HK, Lee CG, So JS, Chae CS, Hwang JS, Sahoo A, et al. Generation of regulatory dendritic cells and CD4+Foxp3+ T cells by probiotics administration suppresses immune disorders. *Proc Natl Acad Sci U S A*. (2010) 107:2159–64. doi: 10.1073/pnas.0904055107

31. Li J, Sung CY, Lee N, Ni Y, Pihlajamaki J, Panagiotou G, et al. Probiotics modulated gut microbiota suppresses hepatocellular carcinoma growth in mice. *Proc Natl Acad Sci U S A*. (2016) 113:E1306–15. doi: 10.1073/pnas.1518189113

32. Hu Y, Gao Y, Zhang M, Deng KY, Singh R, Tian Q, et al. Endoplasmic reticulum-associated degradation (ERAD) has a critical role in supporting glucose-stimulated insulin secretion in pancreatic beta-cells. *Diabetes*. (2019) 68:733–46. doi: 10.2337/db18-0624

33. Wang J, Xu Y, Chen Z, Liang J, Lin Z, Liang H, et al. Liver immune profiling reveals pathogenesis and therapeutics for biliary atresia. *Cell*. (2020) 183:1867–1883 e26. doi: 10.1016/j.cell.2020.10.048

34. Wu L, Gao A, Li L, Chen J, Li J, Ye J. A single-cell transcriptome profiling of anterior kidney leukocytes from nile tilapia (Oreochromis niloticus). *Front Immunol*. (2021) 12:783196. doi: 10.3389/fimmu.2021.783196

35. Qiu X, Mao Q, Tang Y, Wang L, Chawla R, Pliner HA, et al. Reversed graph embedding resolves complex single-cell trajectories. *Nat Methods*. (2017) 14:979–82. doi: 10.1038/nmeth.4402

36. Fabregat A, Jupe S, Matthews L, Sidiropoulos K, Gillespie M, Garapati P, et al. The reactome pathway knowledgebase. *Nucleic Acids Res*. (2018) 46:D649–55. doi: 10.1093/nar/gkx1132

37. Subramanian A, Tamayo P, Mootha VK, Mukherjee S, Ebert BL, Gillette MA, et al. Gene set enrichment analysis: a knowledge-based approach for interpreting genome-wide expression profiles. *Proc Natl Acad Sci U S A*. (2005) 102:15545–50. doi: 10.1073/pnas.0506580102

38. Kotliar D, Veres A, Nagy MA, Tabrizi S, Hodis E, Melton DA, et al. Identifying gene expression programs of cell-type identity and cellular activity with single-cell RNA-Seq. *Elife*. (2019) 8:e43803. doi: 10.7554/eLife.43803

39. Pelka K, Hofree M, Chen JH, Sarkizova S, Pirl JD, Jorgji V, et al. Spatially organized multicellular immune hubs in human colorectal cancer. *Cell*. (2021) 184:4734–4752 e20. doi: 10.1016/j.cell.2021.08.003

40. Kanehisa M, Furumichi M, Tanabe M, Sato Y, Morishima K. KEGG: new perspectives on genomes, pathways, diseases and drugs. *Nucleic Acids Res*. (2017) 45: D353–61. doi: 10.1093/nar/gkw1092

41. FAO/WHO. *Health and nutritional properties of probiotics in food including powder milk with live lactic acid bacteria*. Cordoba: Prevention (2001).

42. Behnsen J, Deriu E, Sassone-Corsi M, Raffatellu M. Probiotics: properties, examples, and specific applications. *Cold Spring Harb Perspect Med*. (2013) 3: a010074. doi: 10.1101/cshperspect.a010074

43. So SS, Wan ML, El-Nezami H. Probiotics-mediated suppression of cancer. *Curr Opin Oncol*. (2017) 29:62–72. doi: 10.1097/CCO.0000000000000342

44. Rossi O, van Berkel LA, Chain F, Tanweer Khan M, Taverne N, Sokol H, et al. Faecalibacterium prausnitzii A2-165 has a high capacity to induce IL-10 in human and murine dendritic cells and modulates T cell responses. *Sci Rep*. (2016) 6:18507. doi: 10.1038/srep18507

45. Han Y, Ling Q, Wu L, Wang X, Wang Z, Chen J, et al. Akkermansia muciniphila inhibits nonalcoholic steatohepatitis by orchestrating TLR2-activated gammadeltaT17 cell and macrophage polarization. *Gut Microbes*. (2023) 15:2221485. doi: 10.1080/19490976.2023.2221485

46. Jia DJ, Wang QW, Hu YY, He JM, Ge QW, Qi YD, et al. Lactobacillus johnsonii alleviates colitis by TLR1/2-STAT3 mediated CD206(+) macrophages(IL-10) activation. *Gut Microbes*. (2022) 14:2145843. doi: 10.1080/19490976.2022.2145843

47. Lin Y, Fan L, Qi Y, Xu C, Jia D, Jiang Y, et al. Bifidobacterium adolescentis induces Decorin(+) macrophages via TLR2 to suppress colorectal carcinogenesis. *J Exp Clin Cancer Res*. (2023) 42:172. doi: 10.1186/s13046-023-02746-6

48. Chiossone L, Dumas PY, Vienne M, Vivier E. Natural killer cells and other innate lymphoid cells in cancer. *Nat Rev Immunol*. (2018) 18:671–88. doi: 10.1038/s41577-018-0061-z

49. Reina-Campos M, Scharping NE, Goldrath AW. CD8(+) T cell metabolism in infection and cancer. *Nat Rev Immunol*. (2021) 21:718–38. doi: 10.1038/s41577-021-00537-8

50. Luther SA, Cyster JG. Chemokines as regulators of T cell differentiation. *Nat Immunol*. (2001) 2:102–7. doi: 10.1038/84205

51. Bassler K, Schulte-Schrepping J, Warnat-Herresthal S, Aschenbrenner AC, Schultze JL. The myeloid cell compartment-cell by cell. *Annu Rev Immunol*. (2019) 37:269–93. doi: 10.1146/annurev-immunol-042718-041728

52. Navarro-Barriuso J, Mansilla MJ, Martinez-Caceres EM. Searching for the transcriptomic signature of immune tolerance induction-biomarkers of safety and functionality for tolerogenic dendritic cells and regulatory macrophages. *Front Immunol*. (2018) 9:2062. doi: 10.3389/fimmu.2018.02062

53. Li C, Menoret A, Farragher C, Ouyang Z, Bonin C, Holvoet P, et al. Single cell transcriptomics based-MacSpectrum reveals novel macrophage activation signatures in diseases. *JCI Insight*. (2019) 5:e126453. doi: 10.1172/jci.insight.126453

54. Henning JR, Graffeo CS, Rehman A, Fallon NC, Zambirinis CP, Ochi A, et al. Dendritic cells limit fibroinflammatory injury in nonalcoholic steatohepatitis in mice. *Hepatology*. (2013) 58:589–602. doi: 10.1002/hep.26267

55. Lurje I, Hammerich L, Tacke F. Dendritic cell and T cell crosstalk in liver fibrogenesis and hepatocarcinogenesis: implications for prevention and therapy of liver cancer. *Int J Mol Sci*. (2020) 21:7378. doi: 10.3390/ijms21197378

56. Akira S, Hemmi H. Recognition of pathogen-associated molecular patterns by TLR family. *Immunol Lett*. (2003) 85:85–95. doi: 10.1016/s0165-2478(02)00228-6

57. Takeda K, Akira S. Regulation of innate immune responses by Toll-like receptors. *Jpn J Infect Dis*. (2001) 54:209–19.

58. Zeuthen LH, Fink LN, Frokiaer H. Toll-like receptor 2 and nucleotide-binding oligomerization domain-2 play divergent roles in the recognition of gut-derived lactobacilli and bifidobacteria in dendritic cells. *Immunology*. (2008) 124:489–502. doi: 10.1111/j.1365-2567.2007.02800.x

59. Worbs T, Hammerschmidt SI, Forster R. Dendritic cell migration in health and disease. *Nat Rev Immunol*. (2017) 17:30–48. doi: 10.1038/nri.2016.116

60. Hildner K, Edelson BT, Purtha WE, Diamond M, Matsushita H, Kohyama M, et al. Batf3 deficiency reveals a critical role for CD8alpha+ dendritic cells in cytotoxic T cell immunity. *Science*. (2008) 322:1097–100. doi: 10.1126/science.1164206

61. Molina MS, Hoffman EA, Stokes J, Kummet N, Smith KA, Baker F, et al. Regulatory dendritic cells induced by bendamustine are associated with enhanced flt3 expression and alloreactive T-cell death. *Front Immunol*. (2021) 12:699128. doi: 10.3389/fimmu.2021.699128

62. Salmon H, Idoyaga J, Rahman A, Leboeuf M, Remark R, Jordan S, et al. Expansion and activation of CD103(+) dendritic cell progenitors at the tumor site enhances tumor responses to therapeutic PD-L1 and BRAF inhibition. *Immunity*. (2016) 44:924–38. doi: 10.1016/j.immuni.2016.03.012

63. Chen YP, Yin JH, Li WF, Li HJ, Chen DP, Zhang CJ, et al. Single-cell transcriptomics reveals regulators underlying immune cell diversity and immune subtypes associated with prognosis in nasopharyngeal carcinoma. *Cell Res*. (2020) 30:1024–42. doi: 10.1038/s41422-020-0374-x

64. Wu F, Fan J, He Y, Xiong A, Yu J, Li Y, et al. Single-cell profiling of tumor heterogeneity and the microenvironment in advanced non-small cell lung cancer. *Nat Commun*. (2021) 12:2540. doi: 10.1038/s41467-021-22801-0

65. Zhang Y, Song J, Zhao Z, Yang M, Chen M, Liu C, et al. Single-cell transcriptome analysis reveals tumor immune microenvironment heterogenicity and granulocytes enrichment in colorectal cancer liver metastases. *Cancer Lett*. (2020) 470:84–94. doi: 10.1016/j.canlet.2019.10.016

66. Numasaki M, Fukushi J, Ono M, Narula SK, Zavodny PJ, Kudo T, et al. Interleukin-17 promotes angiogenesis and tumor growth. *Blood*. (2003) 101:2620–7. doi: 10.1182/blood-2002-05-1461

67. Numasaki M, Watanabe M, Suzuki T, Takahashi H, Nakamura A, McAllister F, et al. IL-17 enhances the net angiogenic activity and *in vivo* growth of human non-small cell lung cancer in SCID mice through promoting CXCR-2-dependent angiogenesis. *J Immunol*. (2005) 175:6177–89. doi: 10.4049/jimmunol.175.9.6177

68. Castellino F, Huang AY, Altan-Bonnet G, Stoll S, Scheinecker C, Germain RN. Chemokines enhance immunity by guiding naive CD8+ T cells to sites of CD4+ T cell-dendritic cell interaction. *Nature*. (2006) 440:890–5. doi: 10.1038/nature04651

69. Ng SS, De Labastida Rivera F, Yan J, Corvino D, Das I, Zhang P, et al. The NK cell granule protein NKG7 regulates cytotoxic granule exocytosis and inflammation. *Nat Immunol*. (2020) 21:1205–18. doi: 10.1038/s41590-020-0758-6

70. Reinfeld BI, Madden MZ, Wolf MM, Chytil A, Bader JE, Patterson AR, et al. Cell-programmed nutrient partitioning in the tumour microenvironment. *Nature*. (2021) 593:282–8. doi: 10.1038/s41586-021-03442-1

71. Chang CH, Qiu J, O'Sullivan D, Buck MD, Noguchi T, Curtis JD, et al. Metabolic competition in the tumor microenvironment is a driver of cancer progression. *Cell*. (2015) 162:1229–41. doi: 10.1016/j.cell.2015.08.016

72. Hunt EG, Hurst KE, Riesenberg BP, Kennedy AS, Gandy EJ, Andrews AM, et al. Acetyl-CoA carboxylase obstructs CD8(+) T cell lipid utilization in the tumor microenvironment. *Cell Metab*. (2024) 36:969–983.e10. doi: 10.1016/j.cmet.2024.02.009

73. Minhas PS, Latif-Hernandez A, McReynolds MR, Durairaj AS, Wang Q, Rubin A, et al. Restoring metabolism of myeloid cells reverses cognitive decline in ageing. *Nature*. (2021) 590:122–8. doi: 10.1038/s41586-020-03160-0

frontiers | Frontiers in Immunology

TYPE Review
PUBLISHED 16 April 2025
DOI 10.3389/fimmu.2025.1569150

OPEN ACCESS

EDITED BY
Yue Wang,
Second Military Medical University, China

REVIEWED BY
Tongze Cai,
Guangxi Traditional Chinese Medical University, China
Eunjeong Kim,
Kyungpook National University Hospital, Republic of Korea

*CORRESPONDENCE
Haowen Tang
haowen_tang@163.com
Ning Zhang
ningzhang912@163.com

RECEIVED 31 January 2025
ACCEPTED 27 March 2025
PUBLISHED 16 April 2025

CITATION
Zhang T, Ren C, Yang Z, Zhang N and Tang H (2025) Exploration of the role of immune cells and cell therapy in hepatocellular carcinoma. *Front. Immunol.* 16:1569150. doi: 10.3389/fimmu.2025.1569150

Exploration of the role of immune cells and cell therapy in hepatocellular carcinoma

Tao Zhang[1], Cong Ren[2], Zhanyu Yang[1], Ning Zhang[1]* and Haowen Tang[1]*

[1]Faculty of Hepato-Pancreato-Biliary Surgery, Chinese People's Liberation Army (PLA) General Hospital, Beijing, China, [2]The Second Clinical College, Chongqing Medical University, Chongqing, China

Hepatocellular carcinoma stands as one of the foremost contributors to cancer-associated fatalities globally, and the limitations of traditional treatment methods have prompted researchers to explore new therapeutic options. Recently, cell therapy has emerged as a promising approach for HCC, showing significant potential in improving patient outcomes. This review article explores the use of cell therapy for HCC, covering different types, the mechanisms behind their effectiveness, recent advancements in clinical trials, and ongoing challenges. This article aims to provide insightful perspectives for future research and clinical applications in treating HCC by synthesizing current knowledge.

KEYWORDS

hepatocellular carcinoma, cell therapy, immune cells, immunotherapy, tumor microenvironment

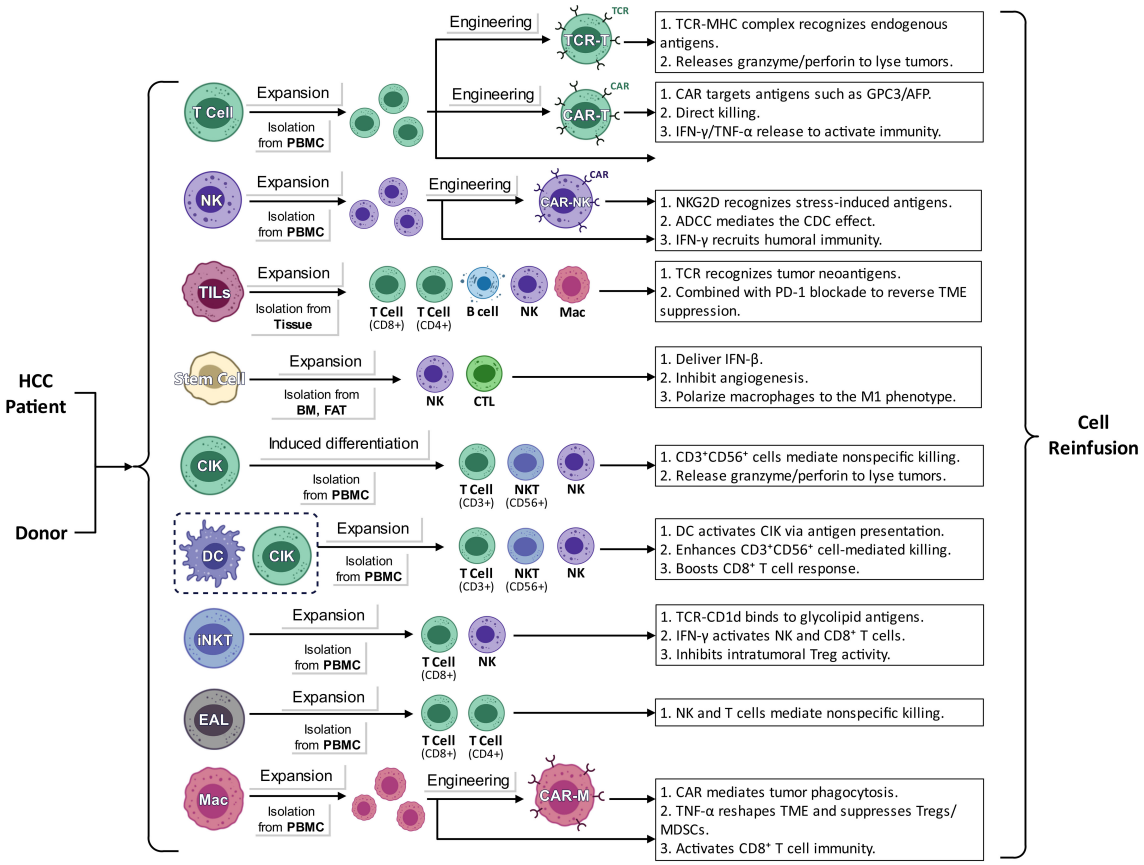

GRAPHICAL ABSTRACT

1 Introduction

Hepatocellular carcinoma (HCC) is a major global health issue, as it is the most prevalent form of primary liver cancer and a leading cause of cancer-related deaths around the world (1). The incidence of HCC varies by region, with China and East Africa reporting the highest rates, primarily due to widespread infections with hepatitis B virus (HBV) and hepatitis C virus (HCV) (2). Recently, the global burden of HCC has grown due to an increase in metabolic disorders. Among these metabolic disorders, metabolic dysfunction-associated steatotic liver disease (MASLD) is increasingly recognized as a significant risk factor for the development of HCC (3, 4). The pathogenesis of HCC is multifactorial, with chronic liver diseases, cirrhosis, and environmental factors such as aflatoxin exposure significantly contributing to its development (5–7).

Surgical approaches, including surgical resection, liver transplantation, and locoregional therapies, represent the only efficacious treatments for early-stage HCC. However, these treatments are only applicable to a small percentage of patients. For patients with advanced disease or underlying liver dysfunction, surgical options are often not viable treatment alternatives. Moreover, systemic therapies, such as chemotherapy, have primarily proven ineffective in treating HCC. HCC is characterized by its notable resistance to conventional chemotherapeutic agents (8). This underscores the urgent need for new treatment strategies to tackle the challenges of HCC. Based on in-depth research into the immune mechanisms of HCC, cell therapy has emerged as a promising alternative to treating this disease. Cell therapies use living cells to treat or prevent diseases and encompass various approaches, including stem cells, immune cells, and genetically modified cells (9).

Recent advancements in the field have highlighted the ability of specific therapies to more effectively target tumor cells and modify the tumor microenvironment, which can enhance the overall therapeutic response (10, 11). Immune cell-based therapies, particularly CAR T-cell therapy, have shown significant promise in treating hematological malignancies. They are currently being explored for their effectiveness against solid tumors, including hepatocellular carcinoma (12–19). This review aims to provide an overview of the latest insights into cellular therapies for managing HCC. By synthesizing recent findings and ongoing research efforts, we seek to clarify how cellular therapies could potentially revolutionize the treatment landscape for HCC and lead to improved patient outcomes. The following sections will examine various facets of cellular therapy,

including its mechanisms of action and clinical implications in treating HCC.

2 Types and mechanisms of cell therapy in HCC

2.1 CAR-T cell therapy

Chimeric Antigen Receptor T cell(CAR-T) therapy is designed to quickly integrate specific chimeric antigen receptors into T lymphocytes, enhancing their ability to recognize and destroy cancer cells (20, 21). A chimeric antigen receptor typically consists of two main components: an antigen-binding domain derived from a monoclonal antibody targeting tumor-associated antigens and a signaling domain that triggers T-cell activation. This structure allows CAR-T cells to identify specific antigens found on tumor cells, resulting in their swift activation and proliferation, significantly boosting their effectiveness against tumors (22–24).

The effectiveness of CAR-T cell therapy relies on accurately targeting specific proteins highly expressed on tumor surfaces. Glypican 3 (GPC3) is one such protein found at elevated levels in more than 70% of hepatocellular carcinoma (HCC) cases, while it is nearly absent in normal tissues (25, 26). This heightened expression of GPC3 is also significantly linked to poorer prognoses for patients with hepatocellular carcinoma (27, 28). Studies using animal models have confirmed the efficacy of GPC3-CAR-T cells, with initial findings indicating that these cells have promising safety profiles and effectiveness in patients with GPC3-positive relapsed or refractory conditions (29–31). To improve the ability of CAR-T cells to infiltrate tumor environments, researchers have modified GPC3-CAR-T cells to express interleukin 7 (IL-7) and chemokine CCL19, resulting in positive outcomes in experimental studies (32). Another research on Interleukin-15-armored GPC3-CAR T cells for solid tumors, including liver cancer, showed that IL15 increases the expansion, intratumoral survival, and antitumor activity of GPC3-CAR-T cells in patients (33). Several studies have indicated that GPC3-targeted CAR-T cells that overexpress GLUT1 or AGK demonstrate improved CD8 T-cell persistence *in vivo* and greater antitumor effects in HCC (34). Additionally, GPC3-specific CAR-T cells engineered with IL-21 and CXCL9, combined with PD-1 blockade, have enhanced cytotoxic capabilities against hepatocellular carcinoma (35).

A significant number of liver cancer cases show increased levels of alpha-fetoprotein (AFP) in the blood, as this protein is released into the bloodstream. Consequently, several research teams have developed TCR-T cells designed to specifically target AFP (36, 37). Furthermore, early clinical trials have indicated that CAR-T cells targeting c-Met, NKG2D, CD133, and CEA have shown encouraging antitumor effects along with a satisfactory safety profile (12, 38–44).

CAR-T cells face two main challenges as they travel to and infiltrate tumor sites. The first challenge is the lack of essential chemokine receptors on T cells, which limits their ability to interact with chemokines released by tumor cells. This deficiency makes it difficult for CAR-T cells to reach the intended tumor location (45, 46). In the case of hepatocellular carcinoma, the situation is further complicated by a dense fibrotic matrix that reduces the expression of chemokines, significantly hindering the migration and infiltration of CAR-T cells into the tumor (47). Once these cells manage to enter the tumor, they encounter additional obstacles within the harsh tumor microenvironment (TME), which is marked by low oxygen levels and a lack of nutrients (48). Moreover, the TME in HCC is filled with various immunosuppressive cell types, such as regulatory T cells, tumor-associated macrophages, and fibroblasts. These cells can weaken the effectiveness of T-cell responses by releasing immunosuppressive factors and activating immune checkpoints (49).

Nonetheless, this therapeutic approach encounters several challenges, particularly notable adverse reactions like cytokine release syndrome (CRS), off-target toxicity, and neurotoxicity. These complications necessitate careful monitoring and management of patients (50, 51). Current research efforts are aimed at improving the durability and effectiveness of CAR-T cells while also expanding the therapeutic applications of CAR technology to include solid tumors, which have demonstrated higher resistance to this treatment strategy (52–55).

2.2 NK cell therapy

In the study of hepatocellular carcinoma, natural killer (NK) cells play a crucial role in suppressing tumors by effectively identifying and targeting cancerous cells. The interactions among these cells are complex and can vary significantly. Under normal physiological conditions, NK cells are highly capable of detecting and eliminating HCC cells (56). This recognition process involves various receptors, including NKG2D, NKp30, and NKp46, which bind to specific ligands found on tumor cells, such as MICA/B and ULBP (57). However, HCC tumor cells frequently downregulate the expression of these ligands as a strategy to evade immune detection, which diminishes the ability of NK cells to recognize and attack them (58). Research has demonstrated a direct correlation between the levels of NKG2D ligands on HCC cells and the cytotoxic activity of NK cells. Importantly, activating NKG2D has been shown to enhance the cytotoxic effects of NK cells against HCC (58). Furthermore, when NK cells are activated, they boost the overall immune response to tumors by producing cytokines like interferon-γ, which further supports anti-tumor activities (59).

The tumor microenvironment associated with hepatocellular carcinoma (HCC) plays a crucial role in affecting the functionality of natural killer (NK) cells, primarily through immunosuppressive mechanisms and metabolic dysregulation (60, 61). Low oxygen levels mark this microenvironment, the presence of immunosuppressive cells like regulatory T cells and hepatic stellate cells, and the secretion of tumor-associated cytokines such as interleukin-6 (IL-6) and transforming growth factor-β (TGF-β). Together, these factors lead to a reduction in NK cell activity (62, 63). For instance, elevated levels of IL-6 have been found to hinder NK cell function, resulting in decreased cytotoxic abilities and reduced cytokine production (62). Moreover, the secretion of

soluble programmed death ligand-1 (sPD-L1) by HCC cells significantly contributes to the suppression of NK cell activity, causing NK cell exhaustion and a subsequent drop in their effectiveness (64, 65). Therefore, it is essential to either mitigate the immunosuppressive conditions within HCC or restore NK cell functionality to improve the outcomes of HCC therapies (59, 66).

Autologous natural killer cell therapy has significantly progressed in treating hepatocellular carcinoma (67). Numerous studies have shown that autologous natural killer cells can effectively recognize and eliminate tumor cells. However, the effectiveness of NK cells is often reduced in patients with HCC. Consequently, enhancing the activity of these cells has become a vital approach in HCC treatment. Recent clinical trials have demonstrated that expanding and activating autologous NK cells *in vitro*, especially when combined with cytokines like interleukin-15 (IL-15), significantly boosts their anti-tumor effectiveness (68). For instance, one study found that IL-2-activated autologous NK cells exhibited promising anti-tumor effects in a mouse model, which was also reflected in clinical responses from patients (69). Furthermore, research has highlighted a connection between NK cell functionality and the liver microenvironment, revealing that certain factors within this environment can promote NK cell growth and activation, thereby enhancing their ability to combat tumors (70).

Allogeneic natural killer cell therapy is emerging as a promising immunotherapeutic strategy, showing positive results in various clinical studies (71). Unlike autologous NK cells, which require time-consuming processes for cell expansion and activation within the patient, allogeneic NK cells can be obtained "off the shelf," allowing for a quicker start to treatment. Research has shown that allogeneic NK cells sourced from healthy donors can effectively control the progression of hepatocellular carcinoma (HCC), with clinical trials reporting fewer side effects (69). For instance, a clinical trial involving patients with advanced HCC found that combining allogeneic NK cells with other immunotherapeutic approaches improved safety and increased effectiveness, leading to significantly better survival rates for patients (72). Additionally, there is ongoing research into chimeric antigen receptor-NK (CAR-NK) cells, with early results suggesting that these cells can specifically target tumor cells and enhance the anti-tumor response, opening up new possibilities for treating HCC (17, 22, 73, 74).

The tumor microenvironment poses significant challenges for therapies that utilize natural killer cells, creating hurdles for cancer immunotherapy. This environment is often marked by high levels of inhibitory cytokines, the presence of immunosuppressive cells, and hypoxic conditions, all of which severely limit the effectiveness and lifespan of NK cells. For instance, tumor cells can release inhibitory substances such as transforming growth factor beta (TGF-β) and interleukin-10 (IL-10), which hinder the activity and proliferation of NK cells (75). Additionally, the low oxygen levels typical of the tumor microenvironment negatively impact NK cell functions, making it difficult to accurately recognize and destroy tumor cells (76). In response to these challenges, recent advancements in NK cell-based therapies have led researchers to develop various combination treatment strategies specifically for hepatocellular carcinoma (HCC). One promising approach is the combination of NK cells with immune checkpoint inhibitors (ICIs), which have shown significant effectiveness in treating HCC. These immune checkpoint inhibitors, such as anti-PD-1/PD-L1 antibodies, enhance NK cells' cytotoxic capabilities and cytokine production (76). Moreover, using these therapies together effectively counters the immune evasion strategies employed by liver cancer, promoting better tumor infiltration and activation of NK cells (59). The interaction between natural killer cells, targeted therapies, and the combination of NK cells with chemotherapy has garnered significant attention in treating hepatocellular carcinoma (HCC). Targeted therapeutic agents inhibit tumor cell growth directly and enhance anti-tumor responses by activating NK cell cytotoxicity (77). Additionally, these agents can help overcome drug resistance associated with targeted therapies (78). Chemotherapeutic drugs such as paclitaxel and cisplatin can increase the expression of ligands for NK cell-activating receptors on the surface of tumor cells. This elevation improves the ability of NK cells to recognize and eliminate tumor cells effectively (79, 80).

2.3 Tumor-infiltrating lymphocytes therapy

Tumor-infiltrating lymphocytes (TILs) are lymphocytes that infiltrate into tumor tissues, primarily T cells, B cells, natural killer cells, etc. These lymphocytes play a crucial role in immune surveillance and have anti-tumor effects within the tumor microenvironment (81, 82). They can recognize and attack cancerous cells, which has been linked to better overall survival rates (83, 84).

The process of isolating and expanding TILs is essential for their clinical application. Typically, TILs are collected from tumor tissue and then expanded *in vitro* (85). Modern techniques use specialized culture media and cytokines, particularly interleukin-2 (IL-2), to enhance TIL growth and improve functional abilities (86). Additionally, researchers are exploring more effective methods for cell separation, such as flow cytometry and magnetic bead sorting technology, to increase TIL's purity and yield (87). These advancements improve the efficiency of TIL amplification and enhance their ability to kill tumor cells, laying a strong foundation for future immunotherapy applications. In the context of hepatocellular carcinoma (HCC), the TIL subpopulations most commonly studied include Foxp3+, CD8+, and CD4+ T cells, as well as B lymphocytes, NK cells, and macrophages, all of which are associated with prognostic outcomes. These advancements improve the efficiency of TIL amplification and enhance their ability to kill tumor cells, laying a strong foundation for future immunotherapy applications. In the context of hepatocellular carcinoma (HCC), the TIL subpopulations most commonly studied include Foxp3+, CD8 +, and CD4+ T cells, as well as B lymphocytes, NK cells, and macrophages, all of which are associated with prognostic outcomes (88–91). Previous clinical trials have shown that administering TILs can significantly enhance patient survival rates after HCC hepatectomy (92, 93).

Future investigations should focus on integrating TILs with various immunotherapeutic strategies to improve treatment effectiveness. For instance, using anti-PD-1 monoclonal

antibodies together with TILs has shown promising results (94). Studies suggest that agonists targeting co-stimulatory receptors, like GITR, may enhance the functionality of TILs. When these agents are used alongside PD-1 inhibitors, they could create a synergistic effect (95). TILs can serve as a standalone treatment option and work effectively in combination with other immunotherapeutic approaches, ultimately leading to better response rates and extended survival for patients with HCC.

Applying single-cell RNA sequencing technology offers a deep insight into the complex diversity found within tumor-infiltrating lymphocytes. This understanding allows for the precise tailoring of immunotherapy, ensuring that each patient receives a treatment plan that aligns with their specific immune profile (96). Furthermore, incorporating key biomarkers, such as PD-L1 expression levels and the extent of TIL infiltration, provides a dependable way to evaluate how well patients might respond to immunotherapy. This approach has opened doors to innovative personalized treatment strategies (97). By focusing on the unique characteristics of each patient, these tailored treatment plans not only improve the effectiveness of therapies but also minimize the risk of unnecessary side effects, significantly enhancing the overall quality of life for patients (98).

2.4 Stem cell therapy

Stem cell therapy for hepatocellular carcinoma focuses on three main aspects. First, it utilizes the regenerative capabilities of stem cells to help repair liver tissue. These stem cells can transform into hepatocytes, effectively replacing damaged cells and restoring liver function. Second, the therapy takes advantage of the immunomodulatory effects of stem cells to improve the tumor microenvironment. Stem cells can release various cytokines and bioactive molecules that influence the behavior of immune cells within the tumor area, reducing the immunosuppressive conditions and enhancing the body's anti-tumor immune response. Finally, genetically modified stem cells are engineered to specifically target cancerous cells, which helps to limit tumor growth. These altered stem cells can be designed to recognize tumor cells, deliver anti-cancer agents, and induce programmed cell death in malignant cells, thereby preventing tumors' growth and spread (99–102).

Numerous investigations have explored the therapeutic potential of mesenchymal stem cells (MSCs), liver cancer stem cells (LCSCs), and induced pluripotent stem cells (iPSCs) in treating hepatocellular carcinoma. MSCs are recognized for their significant capabilities in tissue repair, and research indicates that they can enhance HCC outcomes by reducing tumor-related inflammation and promoting liver regeneration (103). For instance, in an animal study, administering MSCs derived from bone marrow led to decreased levels of pro-inflammatory cytokines, such as tumor necrosis factor-alpha (TNF-α) and interleukins (IL-2, IL-10), which markedly improved liver function in rats modeling HCC and facilitated liver regeneration (104). Furthermore, MSCs have been shown to reduce tumor-associated immunosuppression by inhibiting T cells' activation and proliferation while promoting the generation of regulatory T cells (Tregs), thereby enhancing immune tolerance and inhibiting tumor progression (103). These immunomodulatory properties of MSCs make stem cell therapy a promising strategy for HCC treatment. On the other hand, cancer stem cells (CSCs) in liver cancer possess a strong capacity for self-renewal, diverse differentiation potential, and the ability to initiate tumors. These cells play a crucial role in tumor progression, metastasis, and drug resistance, making them pivotal in the recurrence and metastasis of HCC (105). Studies have shown that a combination of 5-fluorouracil and a CD13 inhibitor can effectively suppress the proliferation of LCSCs and reduce tumor burden (106).

Induced pluripotent stem cells (iPSCs) are created by reprogramming somatic cells to express specific transcription factors, resulting in cells that can differentiate into any cell type, similar to embryonic stem cells. One of the main advantages of iPSCs is that they can be derived from various cell types, which minimizes ethical concerns. This feature allows researchers to isolate iPSCs from cells obtained from patients, paving the way for personalized treatment options. In the study of hepatocellular carcinoma (HCC), iPSCs are particularly useful as they provide models to explore the mechanisms of cancer development and to evaluate how liver cancer responds to different drugs (103). Furthermore, researchers can guide iPSCs to differentiate into hepatocyte-like cells using specific induction techniques, offering new strategies for treating HCC (107). Additionally, adipose-derived stem cells (ADSCs) hold considerable promise for HCC treatment, as they can promote liver tissue regeneration and repair by releasing various bioactive factors (103).

2.5 TCR-T cell therapy

Engineered T cell therapy, specifically T cell receptor (TCR) therapy, is an innovative approach in cellular immunotherapy designed to reprogram patients' T cells to target and destroy tumor cells. This strategy relies on the ability of TCRs to recognize tumor-specific antigens presented by major histocompatibility complex (MHC) molecules, which activate the T cell-mediated immune response against tumors. TCR-T cells can identify unique antigens found on the surfaces of tumor cells, triggering a cytotoxic response that leads to eliminating these cancerous cells. Research has shown that TCR-T cell therapy is promising in clinical applications for various solid tumors, particularly highlighting its potential effectiveness in treating resistant tumors like hepatocellular carcinoma (108, 109).

Recent advancements have been made in studying hepatitis B virus (HBV)-specific T cell receptor redirected T (HBV-TCR-T) cells, particularly in HBV-associated hepatocellular carcinoma. In a clinical trial, one participant who received HBV-TCR-T cell therapy achieved a partial remission of 27.7 months. Moreover, most patients showed a significant decrease in both HBsAg and HBV DNA levels following treatment, highlighting the targeted effectiveness of this therapeutic strategy (110). Another clinical study, identified by clinical trial number NCT05339321, demonstrated the ability of genetically modified T cells to

specifically target hepatocytes that express hepatitis B surface antigen and those involved in hepatocellular carcinoma (111). Additionally, a different clinical investigation (NCT02719782) emphasized the safety and anti-tumor efficacy of mRNA electroporated HBV-specific TCR-T cells (112). A significant challenge related to this therapeutic approach is the limited specificity that comes with T cell receptor (TCR) recognition. Most TCRs are designed to target specific antigenic epitopes, which limits their ability to recognize a broader range of targets. For example, TCRs developed to target hepatocellular carcinoma may not effectively recognize all tumor cells, especially when there are variations in the antigens present on the tumor cells.

Therapeutic strategies that combine different treatment modalities, especially those involving T-cell receptor (TCR)-engineered T cells, show significant promise in managing hepatocellular carcinoma (HCC). Integrating cytokines like interleukin-21 (IL-21) with TCR-T cell therapy can significantly enhance anti-tumor responses. IL-21 promotes the growth of TCR-T cells and supports their development into memory T cells, which boosts their effectiveness against tumors. Furthermore, IL-21 is crucial in reducing the expression of programmed cell death protein 1 (PD-1), which helps decrease cell death and strengthens the anti-tumor capabilities of TCR-T cells (113). Additionally, combining TCR-T cells with small molecule agents, such as Atovaquone, has improved treatment outcomes. Atovaquone increases the cytotoxic effects of TCR-T cells by triggering ferroptosis, which further hinders the progression of HCC (114). By enhancing the effectiveness of each therapeutic approach and reducing the chances of resistance, these combination therapy strategies pave the way for a more personalized and targeted treatment approach for HCC.

CRISPR/Cas9 technology for editing T-cell receptors (TCRs) allows for more precisely introducing these receptors into T cells. This accuracy ensures that TCRs are consistently expressed in T lymphocytes, which enhances their ability to fight tumors in living organisms (115). Simultaneously, the development of TCR-engineered T cells aimed at specific antigens, like glypican-3 (GPC3) and alpha-fetoprotein (AFP), has demonstrated promising safety and effectiveness in clinical trials (116).

2.6 CIK cell therapy

Cytokine-induced killer (CIK) cells represent an ex vivo-expanded heterogeneous immunocyte subset, mainly consisting of CD3+ and CD56+ T lymphocytes with dual T-cell and natural killer (NK)—like phenotypic characteristics (117). The expansion of CIK cells in the lab involves a specific sequence of cytokine treatments. First, interferon-γ (IFN-γ) is used to activate antigen-presenting cells. After this initial step, anti-CD3 monoclonal antibodies and interleukin-2 (IL-2) are introduced at specific times to promote the growth and development of these cells. The combined effects of these cytokines allow CIK cells to participate in adaptive and innate immune responses through two main ways of attacking. The first way involves recognizing antigens presented by major histocompatibility complex (MHC) molecules through T-cell receptors (TCRs). The second way allows CIK cells to use a receptor called NKG2D to detect stress-induced ligands like MIC-A/B and ULBP1-4, which means they can act without relying on MHC. This approach combines the activation of cytokines (IL-2 and IFN-γ) with the stimulation of anti-CD3 antibodies to create effector cells that are highly effective in killing cancer cells through perforin/granzyme pathways and producing Th1-type cytokines. As a result, CIK cells show enhanced abilities to recognize tumors compared to traditional lymphocyte therapies (118, 119).

CIK cells have become a significant focus in the field of immunotherapy for hepatocellular carcinoma. Clinical trials have highlighted the potential of CIK cells to enhance anti-tumor responses in patients with HCC. Clinical trials have highlighted the potential of CIK cells to enhance anti-tumor responses in patients with HCC. For example, a notable study involving 264 participants found that patients receiving CIK cell therapy, whether as a standalone treatment or alongside surgical procedures or transcatheter arterial chemoembolization (TACE), showed significantly improved overall survival (OS) compared to those undergoing standard therapies alone. The Kaplan-Meier analysis further revealed that patients who received both surgery and CIK therapy had better OS rates than those who only had surgery, with a statistically significant difference ($P < 0.001$). Additionally, incorporating CIK therapy into TACE regimens enhanced both OS and progression-free survival (PFS) (120). Another study demonstrated that CIK cells derived from HCC patients exhibited substantial cytotoxicity against various tumor cell lines, highlighting their effectiveness in targeting HCC cells (121). A comprehensive meta-analysis that combined results from multiple studies confirmed that CIK therapy significantly improves OS and reduces recurrence rates among HCC patients, reinforcing the therapeutic potential of CIK cells in clinical settings (122). Furthermore, the effectiveness of CIK therapy is linked to its ability to trigger a robust immune response. For instance, one study showed that CIK cells have high levels of activating receptors and low levels of immune checkpoint molecules, indicating their readiness to engage in anti-tumor activities (123).

The combination of cytokine-induced killer cell therapy with immune checkpoint inhibitors has shown promising results in treating hepatocellular carcinoma. Studies suggest that some patients who received CIK therapy before anti-PD-1 antibody treatment experienced complete responses, indicating a potential synergistic effect between these two treatment strategies (124). This synergy is thought to arise from the ability of CIK cells to enhance tumor-specific immune responses. In contrast, immune checkpoint inhibitors work to reduce the inhibitory signals that dampen T-cell activity in the tumor microenvironment. Moreover, a new strategy involves administering CIK cells with dendritic cells (DCs), leading to a DC-CIK combination therapy. This approach has been associated with increased immune activation and better anti-tumor responses in various cancers, including HCC (125, 126). In this context, DCs serve as powerful antigen-presenting cells that can further stimulate the growth and activation of CIK cells, thereby boosting their ability to effectively target and destroy HCC cells.

Novel methodologies, such as gas-permeable culture systems, have significantly enhanced the efficiency of cytokine-induced killer cell expansion while preserving their functional characteristics. A comparative analysis between traditional culture techniques and gas-permeable systems showed that CIK cells grown in these advanced systems exhibited improved proliferation rates and retained their ability to target myeloid leukemia cell lines effectively. This finding underscores these cells' potential for large-scale clinical production (127). Incorporating various cytokines and growth factors into the culture media has also been explored to enhance the functional properties of CIK cells. For instance, adding N-acetylcysteine (NAC) during the culture process has been shown to significantly increase the cytotoxicity of CIK cells against cancer cell lines by promoting their proliferation and enhancing cytokine production (128).

2.7 DC-CIK cell therapy

DC-CIK cell therapy, which combines dendritic cells (DCs) with cytokine-induced killer (CIK) cells, has emerged as a promising immunotherapeutic strategy for hepatocellular carcinoma (HCC), supported by an increasing amount of clinical evidence demonstrating its effectiveness in improving patient survival and overall quality of life. A meta-analysis involving 3,756 HCC patients revealed that adding DC-CIK therapy to standard treatment methods, such as surgical resection or locoregional therapies, significantly enhances overall survival (OS) rates compared to conventional treatment alone (129). Notably, DC-CIK therapy has been found to substantially reduce recurrence rates, especially in patients who have undergone curative procedures like hepatectomy or liver transplantation. Clinical trials have shown a 32% reduction in early postoperative recurrence (within two years) when DC-CIK therapy is used as an adjunctive treatment (130). Additionally, recent multicenter studies in Eastern China have reinforced these findings, highlighting the increased antitumor effectiveness of DC-CIK therapy when combined with multimodal approaches such as microwave ablation, chemotherapy, or transarterial chemoembolization (TACE). For instance, a phase II clinical trial indicated that the combination of DC-CIK and TACE led to a median progression-free survival (PFS) of 14.6 months, compared to 9.8 months for TACE alone (HR=0.62; P<0.01) (131). Mechanistically, DC-CIK therapy improves the presentation of tumor antigens by DCs while simultaneously activating CIK cell-mediated cytotoxicity against HCC cells that lack MHC class I, thus overcoming significant challenges associated with traditional immunotherapy methods.

The combination of dendritic cell-cytokine-induced killer (DC-CIK) cell therapy with targeted agents has shown impressive synergistic effects in treating hepatocellular carcinoma (HCC). Research indicates that immune checkpoint inhibitors, especially those targeting PD-1 like pembrolizumab, significantly boost the cytotoxic effectiveness of DC-CIK cells by blocking the PD-1/PD-L1 interaction. This blockage helps reverse T-cell exhaustion and enhances the tumor-killing activity of DC-CIK cells, which is linked to better patient survival rates (132). Moreover, immunohistochemical studies have demonstrated increased CD8+ T-cell infiltration in tumors following combination therapy, indicating a heightened immune response (129). Simultaneously using DC-CIK and targeted therapies positively impacts the tumor microenvironment (TME). Targeted therapies can modify the TME, creating a more supportive environment for immune cell infiltration and function, thereby increasing the therapeutic effects of DC-CIK cells. Evidence shows that targeted therapies significantly improve the growth and cytotoxic abilities of DC-CIK cells in patients (130). A systematic review and meta-analysis have highlighted that DC-CIK immunotherapy has considerable potential for enhancing survival and response rates in cases of solid tumors (133).

2.8 iNKT cell therapy

Natural killer T (NKT) cells represent a unique subset of T lymphocytes characterized by co-expression of T-cell receptors and natural killer cell markers (134). Although they originate from the T-cell lineage, NKT cells exhibit both morphological and functional similarities to NK cells. They play a crucial role in bridging innate and adaptive immune responses by quickly releasing cytokines, essential during the early stages of immune reactions (135).

The invariant NKT (iNKT) cell subset, a predominant subtype of NKT cells, develops from CD4+ and CD8+ double-positive thymocytes (136). These cells are notable for their invariant TCR chain, which explicitly recognizes lipid antigens presented by CD1d molecules on antigen-presenting cells (APCs) (137). Upon activation by α-galactosylceramide (α-GalCer), a synthetic glycolipid antigen loaded onto CD1d, iNKT cells exhibit dual effector functions: 1) rapid secretion of both Th1-type (e.g., IFN-γ, TNF-α) and Th2-type (e.g., IL-4, IL-13) cytokines (138); 2) direct cytotoxic activity against tumor cells via perforin/granzyme pathways (139). Furthermore, activated iNKT cells enhance antitumor immunity by facilitating interactions with NK cells and cytotoxic T lymphocytes (CTLs) through CD40L-CD40 signaling and cytokine networks, thereby strengthening immune responses across various compartments (140).

Numerous clinical investigations are currently underway to evaluate the safety and effectiveness of various treatments for hepatocellular carcinoma (HCC). One notable study is a phase I clinical trial (NCT03175679) conducted at Beijing YouAn Hospital, which enrolled ten patients diagnosed with HCC at stages B/C according to the Barcelona Clinic Liver Cancer classification. In this trial, researchers isolated autologous invariant natural killer T (iNKT) cells from the patient's peripheral blood mononuclear cells, expanded them, and pulsed them with α-GalCer before infusion. The trial results indicated that the administration of expanded iNKT cells was safe and well-tolerated, with most treatment-related adverse events classified as grade 1-2. Preliminary findings suggested that the infused iNKT cells triggered significant T-helper 1-like immune responses,

potentially contributing to antitumor activity. Additionally, assessments conducted after infusion showed increased levels of circulating iNKT cells and activated natural killer (NK) cells among the patients, indicating a likely enhancement of antitumor immune responses (141). Furthermore, a phase II randomized controlled trial explored the effects of iNKT cell infusion combined with transcatheter arterial embolization (TAE) in patients with unresectable HCC who had previously failed TACE. This combined approach significantly improved progression-free survival (PFS) compared to TAE alone, highlighting the promising role of iNKT cell therapy in managing HCC (142). These findings are further supported by additional studies that underscore the antitumor efficacy of iNKT cells across various malignancies, including gastric cancer and neuroblastoma, where iNKT cell-based therapies have shown potential in improving clinical outcomes and patient survival rates (143, 144). In conclusion, the growing body of evidence indicates that iNKT cell therapy is safe and effective. This highlights the urgent need for more extensive multicenter trials to confirm these findings across various patient demographics and cancer types.

2.9 EAL cell therapy

Expanded Activated Lymphocyte (EAL) cell therapy involves extracting and enhancing lymphocytes from a patient's own body using specialized techniques. These lymphocytes, primarily T cells and natural killer (NK) cells, are then expanded and activated in a laboratory setting before being reinfused into the patient to boost their ability to fight tumors. Both T cells and NK cells play essential roles in immune surveillance (145). Research indicates that EAL cells can recognize tumor-specific antigens and trigger tumor cell death through cytotoxic mechanisms. Additionally, they can modulate the activity of other immune cells by releasing cytokines, thereby creating a robust anti-tumor immune network (146). The proliferation of T and B lymphocytes, along with the presence of cytokines, has shown encouraging results in combating various tumors (147, 148).

One significant study highlighted a Phase I clinical trial that used autologous tumor-infiltrating lymphocytes in patients with primary hepatocellular carcinoma, providing initial evidence for the feasibility of this immunotherapeutic approach in treating this type of cancer (92). Furthermore, a multicenter, randomized, open-label pivotal Phase II study (NCT05213637) evaluated the effectiveness and safety of EAL therapy in preventing recurrence in patients with primary HCC who are at high risk for recurrence after radical resections.

2.10 CAR-macrophages cell therapy

Macrophages possess unique characteristics that make them well-suited for CAR (Chimeric Antigen Receptor) engineering. These cells are highly adaptable, allowing them to polarize into different functional states, such as M1 (pro-inflammatory) and M2 (anti-inflammatory) phenotypes. This adaptability enables macrophages to respond to the changing conditions within the tumor microenvironment effectively. As a result, CAR-engineered macrophages (CAR-Ms) can directly attack tumor cells through processes like phagocytosis, while modulating the immune response by influencing the activities of other immune cells (149, 150). CAR-M engineering equips them with remarkable antigen recognition and targeting capabilities. They are specifically designed to identify tumor-associated antigens accurately. For instance, CAR-Ms targeting Glypican-3 (GPC3) are adept at recognizing and eliminating hepatocellular carcinoma (HCC) cells due to their antigen-specific recognition domains on the cell surface (151). Beyond targeting surface antigens, CAR-Ms can also recognize additional markers, such as fibroblast activation protein (FAP), present in the tumor microenvironment. This diverse targeting ability significantly enhances the effectiveness of immune surveillance and the clearance of tumor cells (152). CAR-Ms play a crucial role in the secretion of cytokines and the modulation of the immune response. Research shows that these engineered macrophages produce a range of pro-inflammatory cytokines, such as interferon-gamma (IFN-γ), tumor necrosis factor-alpha (TNF-α), and interleukin-12 (IL-12), which are essential for generating a strong anti-tumor immune response (149, 153). Additionally, CAR-Ms enhance anti-tumor immunity by influencing the activity of other immune cells; for example, they can promote T-cell activation and proliferation through the release of cytokines, leading to a more vigorous immune response (154). Furthermore, CAR-Ms impact the immune environment within the tumor microenvironment by encouraging the polarization of M1 macrophages while suppressing M2 macrophage activity, thereby strengthening anti-tumor effects (155). This inherent ability to modify the tumor microenvironment gives CAR-Ms significant potential for cancer therapy, especially in tackling solid tumors where they can effectively address the immune suppression challenges posed by the tumor microenvironment (156).

Initial findings from clinical trials indicate promising results for using CAR macrophages in treating hepatocellular carcinoma (HCC). One study that combined GPC3-targeted CAR macrophage cells with sorafenib showed significant anti-tumor activity, particularly in smaller tumors, although the effectiveness decreased in larger tumor masses (151). Overall, this combination therapy was more advantageous for smaller tumors, yet it still demonstrated improved anti-tumor properties. Additionally, CAR macrophages targeting CD147 exhibited encouraging anti-tumor effects in laboratory studies, with early evidence hinting at their potential use in clinical applications (157). In preclinical models of HER2+ solid tumors, which generally show low responsiveness to anti-PD1 (aPD1) monotherapy, CAR macrophages with aPD1 proved exceptionally effective. This approach controls tumor growth, extends survival, and modifies the tumor microenvironment (TME). These findings suggest a synergistic relationship between CAR macrophages and T-cell checkpoint inhibitors, highlighting a potential strategy to enhance the response of tumors that usually do not respond to aPD1 therapy in patients (158).

3 Challenges and future research directions

3.1 Development of new cell therapy technologies

The utilization of CAR-T/NK/M cell therapies in treating hepatocellular carcinoma faces several challenges, particularly regarding target selection due to the tumor's heterogeneity and the immunosuppressive characteristics of the tumor microenvironment. Future efforts should focus on improving CAR construct designs, which includes identifying more specific and practical tumor-associated antigens and finding ways to mitigate the immunosuppressive effects of the tumor microenvironment. For instance, combining immune checkpoint inhibitors or other immunomodulatory agents could enhance the effectiveness of CAR-T, NK, and M cell therapies. Gene-editing technologies like CRISPR/Cas9 may be utilized to modify T, NK, and M cells, potentially increasing their ability to recognize and target specific antigens found in hepatocellular carcinoma (53, 159, 160). Several studies have attempted to engineer CAR-T, NK, and M cells targeting specific antigens in hepatocellular carcinoma, such as glypican-3 (GPC3), showing promising initial results; however, further improvements and optimizations are necessary (30, 151, 161).

Tumor-infiltrating lymphocytes hold significant potential in cancer immunotherapy, yet their application in hepatocellular carcinoma is still relatively limited. Future research should concentrate on efficiently isolating and expanding TILs from hepatocellular carcinoma tissues and optimizing TIL reinfusion protocols to enhance their therapeutic impact in managing this type of cancer (162). Studies have highlighted the considerable effectiveness of TIL therapy in treating other cancers, like melanoma, providing a helpful reference for its potential use in hepatocellular carcinoma (163).

Mesenchymal stem cells (MSCs) possess both immunomodulatory properties and the ability to regenerate tissues, making them a promising cellular source for treating hepatocellular carcinoma (164). Research has shown that MSCs can exert anti-tumor effects by regulating the tumor microenvironment and promoting apoptosis in cancerous cells. However, further studies are needed to clarify the therapeutic mechanisms through which MSCs function. Additionally, advancements in MSC-based cell therapy products, such as genetic modifications of MSCs or the incorporation of therapeutic agents, could enhance their anti-tumor effectiveness (165).

Exosomes, nanoscale vesicles secreted by cells, can transport specific proteins from their parent cells and serve as alternatives to immune cells by stimulating the production of cytotoxic T lymphocytes, thus contributing to anti-cancer responses (166, 167). More research is required to understand the mechanisms that govern exosome functionality. It is also crucial to optimize exosome preparation and modification techniques to improve their targeting abilities and therapeutic efficacy in managing hepatocellular carcinoma (168, 169). Furthermore, exosomes can be engineered to specifically target and incorporate antigen fragments associated with hepatocellular carcinoma, potentially boosting their anti-cancer properties (170).

The NIR-II laser activates nanomaterials, such as polymer nanoagonists and immunoprotease nanorestimulators, to create localized hyperthermia, reaching temperatures between 45°C and 50° C. This heat directly destroys tumor cells and initiates a process known as immunogenic cell death (ICD). As a result, damage-associated molecular patterns (DAMPs) like ATP, HMGB1, and calreticulin are released, which help mature dendritic cells (DCs) and improve antigen presentation (171). NIR-II photothermal immunotherapy presents a promising and low-toxicity strategy for cancer treatment through four main mechanisms: photothermal ablation, antigen release triggered by ICD, targeted delivery of immunomodulators using activatable nanocarriers, and the combined activation of both innate and adaptive immune responses (172).

3.2 Exploration of combination therapy strategies

The integration of cell therapy with immune checkpoint inhibitors represents a promising advancement in the treatment of hepatocellular carcinoma, particularly with the use of PD-1/PD-L1 inhibitors, which have shown significant effectiveness (173). However, there is still a pressing need to improve the response rates seen with monotherapy. By combining cell therapy with immune checkpoint inhibitors, we may achieve synergistic effects; cell therapy can activate the immune system, while immune checkpoint inhibitors can help reduce immunosuppressive mechanisms, ultimately enhancing the anti-tumor immune response (174). Currently, a clinical trial is in progress to assess the effectiveness of CAR-T cell therapy when used alongside PD-1/PD-L1 inhibitors in patients with hepatocellular carcinoma (175). Additionally, Table 1 provides a comprehensive overview of the mechanisms, benefits, limitations, and potential future directions for various cell and combination therapies.

Combining Cell Therapy with targeted therapeutics has shown promise in enhancing cancer treatment outcomes. Targeted agents like sorafenib and lenvatinib are effective in suppressing tumor cell growth and forming new blood vessels, but a major challenge is the development of drug resistance over time (176). Combining cell therapy with these targeted treatments may create a synergistic effect by utilizing different mechanisms of action, which could help reduce the chances of resistance (177). For example, studies have found that administering CAR-T cell therapy alongside sorafenib leads to better anti-tumor responses in animal models of liver cancer (178).

On the other hand, traditional treatment methods such as surgery, liver transplantation, radiotherapy, and chemotherapy remain vital in managing hepatocellular carcinoma. By integrating cell therapy with these conventional approaches, we can leverage the benefits of both to improve treatment results (179). For instance, using cell therapy as an additional treatment after surgical removal of tumors or liver transplants can help eliminate any remaining cancer cells and lower the risk of the cancer returning (180). Additionally, combining cell therapy with radiotherapy or chemotherapy may enhance the destructive effects on cancer cells while reducing the side effects commonly associated with these traditional treatments (181, 182).

TABLE 1 Presentation of the mechanisms, advantages, limitations and future development directions of different types of cell therapies and combination therapies.

Cell Therapy Type	Mechanism	Advantages	limitations	Future Research Directions
CAR-T cell therapy	Genetically engineered T cells expressing chimeric antigen receptors (CARs) to target tumor antigens.	High specificity; Potent tumor cell killing	Tumor microenvironment suppression; off-target effects; cytokine release syndrome (CRS).	Develop multi-target CAR-T cells; Combine with immune checkpoint inhibitors; Optimize persistence and activity in the TME.
NK cell therapy	NK cells recognize and kill tumor cells via innate immunity.	High safety profile; no risk of CRS; Adaptable to HCC heterogeneity.	TME suppression; limited *in vivo* expansion and persistence.	Develop CAR-NK with cytokines; Investigate the interaction between NK cells and TME.
TILs cell therapy	Tumor-infiltrating lymphocytes (TILs) are isolated, expanded ex vivo, and reinfused into patients. Naturally tumor-specific, recognize multiple tumor antigens.	Naturally tumor-specific; Recognize various tumor antigens.	Complex isolation and expansion process; TME suppression of TIL function.	Optimize isolation and expansion techniques; Combine with immune checkpoint inhibitors; Identify HCC-specific TIL targets.
Stem cell therapy	Stem cells differentiate into hepatocytes or secrete anti-inflammatory factors to repair liver damage and inhibit tumor growth.	Liver tissue repair; Immunomodulatory effects.	Potential to promote tumor growth; limited therapeutic efficacy.	Investigate stem cell roles in TME; Develop genetically engineered stem cells; Explore combination therapies.
TCR-T cell therapy	Genetically engineered T cells expressing specific T cell receptors (TCRs) to recognize tumor antigens.	Broad target range (including intracellular antigens); Adaptable to HCC heterogeneity.	Risk of autoimmune reactions; complex manufacturing process.	Develop high-efficacy, safe TCR-T cells; Combine with immune checkpoint inhibitors; Optimize target selection.
CIK cell therapy	Heterogeneous CD3+ CD56+ cells with nonspecific cytotoxicity via Fas/FasL and perforin.	Broad antitumor activity (hematologic and solid tumors); Simple preparation and high autologous safety; Mild adverse effects	High interpatient variability in efficacy; Poor *in vivo* proliferation and persistence; Lack of antigen-specific targeting.	Combine with dendritic cells (DC-CIK) to enhance antigen specificity; Engineer CIK cells to express chemokine receptors (e.g., CXCR4) for improved homing; Optimize culture conditions to enrich CD3+ CD56+ subsets.
DC-CIK cell therapy	Dendritic cells (DCs) prime T cells with tumor antigens, while CIK cells mediate MHC-unrestricted killing, synergistically enhancing antitumor immunity.	Dual-action synergy with antigen-specific responses; Applicable to advanced solid tumor; Manageable toxicity.	Complex manufacturing and high costs; Low DC antigen-loading efficiency; Inconsistent clinical outcomes.	Standardize antigen-loading techniques (mRNA electroporation); Combine with ICIs (anti-CTLA-4); Explore cryopreservation to maintain cell viability.
iNKT cell therapy	iNKT cells recognize CD1d-presented glycolipids (α-GalCer), directly killing tumors and activating NK/CD8+ T cells via IFN-γ secretion.	Allogeneic applicability (non-HLA restricted); Immune microenvironment modulation (Treg/MDSC suppression);	Low endogenous iNKT cell frequency in patients; Immature expansion protocols; CD1d expression dependency for antigen presentation.	Develop CAR-iNKT for enhanced targeting; Combine with oncolytic viruses to induce CD1d expression; Optimize ex vivo expansion (IL-7/IL-15).
EAL cell therapy	Anti-CD3 antibody-activated polyclonal T cells mediate tumor killing via perforin/FasL pathways; Enhance immunity via IFN-γ/TNF-α secretion.	Multi-target coverage reducing antigen escape; Mild self-limiting side effects	Mechanism ambiguity and lack of specificity; Efficacy dependent on patient T cell quality;	Isolate high-activity T cell subsets (e.g., CD8+ memory T cells); Combine with chemotherapy to enhance antigen release; Develop cryopreservation protocols for stable cell products.

(Continued)

TABLE 1 Continued

Cell Therapy Type	Mechanism	Advantages	limitations	Future Research Directions
CAR-M cell therapy	CAR-engineered macrophages phagocytose tumors secrete matrix metalloproteinases (MMPs) to degrade extracellular matrix; activate T cells via MHC-II antigen presentation.	Intense solid tumor infiltration; Reprogramming immunosuppressive microenvironment (M1 polarization); Low CRS risk.	Short *in vivo* persistence (days); Low gene-editing efficiency (macrophage resistance to transduction); Limited targetable surface antigens.	CAR domains fused with phagocytic signals (FcγR); Gene-edited M1 stabilization (C/EBPα overexpression)

Integrating various cell therapies showcases unique characteristics and benefits of each approach. When multiple cell therapies are combined, they can create a synergistic effect that significantly improves therapeutic outcomes (183). For example, using CAR-T cell therapy alongside cytokine-induced killer cell therapy or tumor-infiltrating lymphocyte cell therapy allows for the targeted specificity of engineered cells to work in tandem with the broad-spectrum action of natural immune cells, enhancing the management of tumor growth (184). In previous experiments, a construct known as Ad5f35-anti-GPC3-CAR, which utilized a chimeric adenoviral vector (Ad5f35), demonstrated impressive antigen-specific phagocytosis and tumor cytotoxicity (151).

3.3 Discovery and application of biomarkers

Alpha-fetoprotein (AFP) is an important biomarker used to diagnose hepatocellular carcinoma (HCC), but some patients with HCC may still test negative for AFP. This highlights the need for alternative biomarkers that provide better sensitivity and specificity. Other potential biomarkers include serum alpha-L-fucosidase (AFU), gamma-glutamyl transpeptidase isoenzyme II (γ-GT2), des-gamma-carboxy prothrombin (DCP), and Golgi protein 73 (GP73), all of which have shown promise in diagnosing and differentiating HCC (185). However, further research is needed to assess their clinical usefulness and the methods for detecting them (186). Additionally, advancements in genomics, transcriptomics, and proteomics may lead to the discovery of new biomarkers such as circulating tumor DNA (ctDNA), microRNA (miRNA), and long non-coding RNA (lncRNA) (187–189). These emerging biomarkers could provide a more accurate basis for the early diagnosis, evaluation of treatment effectiveness, and prediction of outcomes in HCC. By performing gene sequencing and analyzing biomarkers in HCC patients, researchers can gain insights into their tumors' molecular features and biological behaviors, which can help develop personalized treatment plans. For patients with specific gene mutations or abnormal biomarker levels, targeted therapies or cellular treatments may improve the effectiveness and safety of their care (190). Furthermore, these biomarkers can be used to monitor how healthy treatments are working and to assess the risk of cancer recurrence, allowing for timely adjustments to treatment strategies (191).

The absence of standardized detection methods and criteria for biomarkers presents significant challenges to the accuracy and reliability of their clinical applications (192). To ensure the precision and comparability of future test results, it is crucial to develop uniform protocols for biomarker detection and establish quality control frameworks. Furthermore, conducting multi-center, large-scale clinical studies is essential to validate these biomarkers' clinical relevance and potential applications.

4 Conclusion

Recently, cellular therapies have shown significant promise in managing hepatocellular carcinoma (HCC), leading to better outcomes for patients. This review focuses on the latest advancements in cellular therapies, such as tumor-infiltrating lymphocytes, engineered T cells, and stem cell-based strategies, all of which have yielded encouraging results in preclinical and clinical trials. The treatment landscape for HCC is complex, requiring careful consideration of various factors when incorporating cellular therapies into standard treatment plans. Despite the positive findings, several challenges remain that need further investigation. These challenges include the heterogeneity of HCC, the nature of the tumor microenvironment, and the risk of immune evasion. Moreover, a thorough assessment of the manufacturing processes for cellular products, patient selection criteria, and the long-term safety and effectiveness of these therapies is crucial. It is important to integrate diverse perspectives from various studies to develop a more nuanced understanding of the treatment landscape and avoid overestimating cellular therapies' effectiveness. Combining cellular therapies with established treatment methods, such as surgery, chemotherapy, and immunotherapy, could create synergistic effects that enhance overall treatment effectiveness. This integrative approach can potentially improve response rates in HCC patients, extend survival, and enhance quality of life. As the field progresses, promoting collaboration among researchers, clinicians, and regulatory bodies will be essential to tackle the complexities of HCC treatment and to ensure the safe and effective use of cellular therapies. In summary, cellular therapies offer promising possibilities for the future management of hepatocellular carcinoma (HCC), but ongoing research and clinical trials are essential to overcome the existing challenges. By fostering a balanced discussion around diverse research findings, we can pave the way for innovative treatment strategies to benefit patients facing this challenging cancer.

Author contributions

TZ: Writing – original draft. CR: Writing – original draft. ZY: Writing – original draft. NZ: Writing – original draft, Writing – review & editing. HT: Writing – original draft, Writing – review & editing.

Funding

The author(s) declare that no financial support was received for the research and/or publication of this article.

Acknowledgments

We thank Dr. Dai from the Department of Medicine and Therapeutics, The Chinese University of Hong Kong, Hong Kong SAR, China, for helping us prepare the figures.

Conflict of interest

The authors declare that the research was conducted in the absence of any commercial or financial relationships that could be construed as a potential conflict of interest.

Generative AI statement

The author(s) declare that no Generative AI was used in the creation of this manuscript.

Publisher's note

References

1. Bray F, Laversanne M, Sung H, Ferlay J, Siegel RL, Soerjomataram I, et al. Global cancer statistics 2022: GLOBOCAN estimates of incidence and mortality worldwide for 36 cancers in 185 countries. *CA: A Cancer J Clin*. (2024) 74:229–63.

2. Catherine DM, Damien G, Freddie B, Jacques F, Gary MC. Global burden of cancer attributable to infections in 2018: a worldwide incidence analysis. *Lancet Glob Health*. (2020) 8:e180–e90.

3. McGlynn KA, Petrick JL, El-Serag HB. Epidemiology of hepatocellular carcinoma. *Hepatology*. (2021) 73(Suppl 1):4–13.

4. Satender PS, Tushar M, Phool C. Global epidemiology of hepatocellular carcinoma. *J Clin Exp Hepatol*. (2025) 15(2):102446.

5. Cao G, Liu J, Liu M. Global, regional, and national trends in incidence and mortality of primary liver cancer and its underlying etiologies from 1990 to 2019: results from the global burden of disease study 2019. *J Epidemiol Global Health*. (2023) 13:344–60.

6. Röcken C, Carl-McGrath S. Pathology and pathogenesis of hepatocellular carcinoma. *Digestive Dis (Basel Switzerland)*. (2001) 19:269–78.

7. McGlynn K, Petrick J, El-Serag H. Epidemiology of hepatocellular carcinoma. *Hepatol (Baltimore Md)*. (2021) 73:4–13.

8. Daher S, Massarwa M, Benson A, Khoury T. Current and future treatment of hepatocellular carcinoma: an updated comprehensive review. *J Clin Trans hepatol*. (2018) 6:69–78.

9. Chancellor D, Barrett D, Nguyen-Jatkoe L, Millington S, Eckhardt F. The state of cell and gene therapy in 2023. *Mol Ther*. (2023) 31:3376–88.

10. Liu B, Zhou H, Tan L, Siu K, Guan X. Exploring treatment options in cancer: Tumor treatment strategies. *Signal transduction targeted Ther*. (2024) 9:175.

11. Xie N, Shen G, Gao W, Huang Z, Huang C, Fu L. Neoantigens: promising targets for cancer therapy. *Signal transduction targeted Ther*. (2023) 8:9.

12. Zhou Y, Wei S, Xu M, Wu X, Dou W, Li H, et al. CAR-T cell therapy for hepatocellular carcinoma: current trends and challenges. *Front Immunol*. (2024) 15:1489649.

13. Brudno J, Maus M, Hinrichs C. CAR T cells and T-cell therapies for cancer: A translational science review. *JAMA*. (2024) 332:1924–35.

14. Stewart M, Kalos M, Coutinho V, Better M, Jazayeri J, Yohrling J, et al. Accelerating the development of genetically engineered cellular therapies: a framework for extrapolating data across related products. *Cytotherapy*. (2024) 26:778–84.

15. Baker D, Arany Z, Baur J, Epstein J, June C. CAR T therapy beyond cancer: the evolution of a living drug. *Nature*. (2023) 619:707–15.

16. Kumar A, Emdad L, Das S, Fisher P. Recent advances and progress in immunotherapy of solid cancers. *Adv Cancer Res*. (2024) 164:111–90.

17. Peng L, Sferruzza G, Yang L, Zhou L, Chen S. CAR-T and CAR-NK as cellular cancer immunotherapy for solid tumors. *Cell Mol Immunol*. (2024) 21:1089–108.

18. Ismail F, Gallus M, Meuth S, Okada H, Hartung H, Melzer N. Current and future roles of chimeric antigen receptor T-cell therapy in neurology: A review. *JAMA Neurol*. (2025) 82(1):93–103.

19. Aggeletopoulou I, Kalafateli M, Triantos C. Chimeric antigen receptor T cell therapy for hepatocellular carcinoma: where do we stand? *Int J Mol Sci*. (2024) 25 (5):2631.

20. Ma S, Li X, Wang X, Cheng L, Li Z, Zhang C, et al. Current progress in CAR-T cell therapy for solid tumors. *Int J Biol Sci*. (2019) 15:2548–60.

21. Feins S, Kong W, Williams E, Milone M, Fraietta J. An introduction to chimeric antigen receptor (CAR) T-cell immunotherapy for human cancer. *Am J hematol*. (2019) 94:S3–9.

22. Yalan Z, Weilin Z, Jiangping Y, Jinrong Y, Wei W. Chimeric antigen receptor engineered natural killer cells for cancer therapy. *Exp Hematol Oncol*. (2023) 12(1):70.

23. Albert TG, Benjamine A, Charles LS. How chimeric antigen receptor design affects adoptive T cell therapy. *J Cell Physiol*. (2016) 231(12):2590–8.

24. Chabannon C, Bonini C. Structure of and signalling through chimeric antigen receptor. *The EBMT/EHA CAR-T Cell Handbook*. Cham (CH): Springer (2022) p. 3–5.

25. Jorge F, Mariana C. Glypican-3: a marker and a therapeutic target in hepatocellular carcinoma. *FEBS J*. (2013) 280(10):2471–6.

26. Arnaud C, Toshihiro S, Tetsuya N. Progress and challenges in glypican-3 targeting for hepatocellular carcinoma therapy. *Expert Opin Ther Targets*. (2024) 28 (10):895–909.

27. Jian Z, Manka Z, Huimin M, Xincheng S, Lingling H, Xiaohui Y, et al. Overexpression of glypican-3 is a predictor of poor prognosis in hepatocellular carcinoma: An updated meta-analysis. *Med (Baltimore)*. (2018) 97(24):e11130.

28. Meng G, Hailing Z, Jianming Z, Yangfang L. Glypican-3: A new target for diagnosis and treatment of hepatocellular carcinoma. *J Cancer*. (2020) 11(8):2008–21.

29. Zhao Z, Guo W, Fang S, Song S, Song J, Teng F, et al. An armored GPC3-directed CAR-T for refractory or relapsed hepatocellular carcinoma in China: A phase I trial. *J Clin Oncol*. (2021) 39:4095.

30. Shi D, Shi Y, Kaseb A, Qi X, Zhang Y, Chi J, et al. Chimeric antigen receptor-glypican-3 T-cell therapy for advanced hepatocellular carcinoma: results of phase I trials. *Clin Cancer research: an Off J Am Assoc Cancer Res*. (2020) 26:3979–89.

31. Luan S, Fang G, Zhanhui G, Lei A, Na L, Sujuan M, et al. Shed antigen-induced blocking effect on CAR-T cells targeting Glypican-3 in Hepatocellular Carcinoma. *J Immunother Cancer*. (2021) 9(4):e001875.

32. Pang N, Shi J, Qin L, Chen A, Tang Y, Yang H, et al. IL-7 and CCL19-secreting CAR-T cell therapy for tumors with positive glypican-3 or mesothelin. *J Hematol Oncol*. (2021) 14(1):118.

33. Steffin D, Ghatwai N, Montalbano A, Rathi P, Courtney A, Arnett A, et al. Interleukin-15-armored GPC3-CAR T cells for patients with solid cancers. *Nature*. (2025) 637(8047):940–6.

34. Sun R, Liu Y, Sun Y, Zhou M, Wang Y, Shi B, et al. GPC3-targeted CAR-T cells expressing GLUT1 or AGK exhibit enhanced antitumor activity against hepatocellular carcinoma. *Acta pharmacologica Sinica*. (2024) 45:1937–50.

35. Chen S, Gong F, Liu S, Xie Y, Ye X, Lin X, et al. IL-21- and CXCL9-engineered GPC3-specific CAR-T cells combined with PD-1 blockade enhance cytotoxic activities against hepatocellular carcinoma. *Clin Exp Med*. (2024) 24:204.

36. Liu H, Xu Y, Xiang J, Long L, Green S, Yang Z, et al. Targeting alpha-fetoprotein (AFP)-MHC complex with CAR T-cell therapy for liver cancer. *Clin Cancer research: an Off J Am Assoc Cancer Res*. (2017) 23:478–88.

37. Wang Y, Zhao Y, Li M, Hou H, Jian Z, Li W, et al. Conversion of primary liver cancer after targeted therapy for liver cancer combined with AFP-targeted CAR T-cell therapy: a case report. *Front Immunol*. (2023) 14:1180001.

38. Huang X, Guo J, Li T, Jia L, Tang X, Zhu J, et al. c-Met-targeted chimeric antigen receptor T cells inhibit hepatocellular carcinoma cells in *vitro and in vivo*. *J Biomed Res*. (2021) 36:10–21.

39. Sun B, Yang D, Dai H, Liu X, Jia R, Cui X, et al. Eradication of hepatocellular carcinoma by NKG2D-based CAR-T cells. *Cancer Immunol Res*. (2019) 7:1813–23.

40. Jiang W, Li T, Guo J, Wang J, Jia L, Shi X, et al. Bispecific c-met/PD-L1 CAR-T cells have enhanced therapeutic effects on hepatocellular carcinoma. *Front Oncol*. (2021) 11:546586.

41. Tao K, He M, Tao F, Xu G, Ye M, Zheng Y, et al. Development of NKG2D-based chimeric antigen receptor-T cells for gastric cancer treatment. *Cancer chemotherapy Pharmacol*. (2018) 82:815–27.

42. Hu Q, Hu X, Zhang L, Zhao Y, Li L. Targeting Hedgehog signalling in CD133-positive hepatocellular carcinoma: improving Lenvatinib therapeutic efficiency. *Med Oncol (Northwood London England)*. (2021) 38:41.

43. Yang C, You J, Pan Q, Tang Y, Cai L, Huang Y, et al. Targeted delivery of a PD-1-blocking scFv by CD133-specific CAR-T cells using nonviral Sleeping Beauty transposition shows enhanced antitumour efficacy for advanced hepatocellular carcinoma. *BMC Med*. (2023) 21:327.

44. Katz S, Hardaway J, Prince E, Guha P, Cunetta M, Moody A, et al. HITM-SIR: phase Ib trial of intraarterial chimeric antigen receptor T-cell therapy and selective internal radiation therapy for CEA liver metastases. *Cancer Gene Ther*. (2020) 27:341–55.

45. Xu N, Palmer D, Robeson A, Shou P, Bommiasamy H, Laurie S, et al. STING agonist promotes CAR T cell trafficking and persistence in breast cancer. *J Exp Med*. (2020) 27(5):341–55.

46. Spranger S, Dai D, Horton B, Gajewski T. Tumor-residing batf3 dendritic cells are required for effector T cell trafficking and adoptive T cell therapy. *Cancer Cell*. (2017) 31:711–23.e4.

47. Caruana I, Savoldo B, Hoyos V, Weber G, Liu H, Kim E, et al. Heparanase promotes tumor infiltration and antitumor activity of CAR-redirected T lymphocytes. *Nat Med*. (2015) 21:524–9.

48. Liu L, Zhang R, Deng J, Dai X, Zhu X, Fu Q, et al. Construction of TME and Identification of crosstalk between Malignant cells and macrophages by SPP1 in hepatocellular carcinoma. *Cancer immunol immunother: CII*. (2022) 71:121–36.

49. Chen C, Wang Z, Ding Y, Qin Y. Tumor microenvironment-mediated immune evasion in hepatocellular carcinoma. *Front Immunol*. (2023) 14:1133308.

50. Guzman G, Reed M, Bielamowicz K, Koss B, Rodriguez A. CAR-T therapies in solid tumors: opportunities and challenges. *Curr Oncol Rep*. (2023) 25:479–89.

51. Cappell K, Kochenderfer J. Long-term outcomes following CAR T cell therapy: what we know so far. *Nat Rev Clin Oncol*. (2023) 20:359–71.

52. Ghorai S, Pearson A. Current strategies to improve chimeric antigen receptor T (CAR-T) cell persistence. *Cureus*. (2024) 16:e65291.

53. Dimitri A, Herbst F, Fraietta J. Engineering the next-generation of CAR T-cells with CRISPR-Cas9 gene editing. *Mol cancer*. (2022) 21:78.

54. Sterner R, Sakemura R, Cox M, Yang N, Khadka R, Forsman C, et al. GM-CSF inhibition reduces cytokine release syndrome and neuroinflammation but enhances CAR-T cell function in xenografts. *Blood*. (2019) 133:697–709.

55. Sun M, Xu P, Wang E, Zhou M, Xu T, Wang J, et al. Novel two-chain structure utilizing KIRS2/DAP12 domain improves the safety and efficacy of CAR-T cells in adults with r/r B-ALL. *Mol Ther oncolytics*. (2021) 23:96–106.

56. Juengpanich S, Shi L, Iranmanesh Y, Chen J, Cheng Z, Khoo A, et al. The role of natural killer cells in hepatocellular carcinoma development and treatment: A narrative review. *Trans Oncol*. (2019) 12:1092–107.

57. Hassouna M, Radwan E, Abdelsameea E, Estaphan S, Abd Elrhman H, Abdel-Samiee M, et al. The putative role of natural killer cells in patients with hepatitis C virus-related hepatocellular carcinoma. *Asian Pacific J Cancer prevention: APJCP*. (2021) 22:2559–67.

58. Mantovani S, Varchetta S, Mele D, Donadon M, Torzilli G, Soldani C, et al. An anti-MICA/B antibody and IL-15 rescue altered NKG2D-dependent NK cell responses in hepatocellular carcinoma. *Cancers*. (2021) 22(8):2559–67.

59. Wang X, Yang T, Shi X. NK cell-based immunotherapy in hepatocellular carcinoma: An attractive therapeutic option for the next decade. *Cell signalling*. (2024) 124:111405.

60. Lu C, Rong D, Zhang B, Zheng W, Wang X, Chen Z, et al. Current perspectives on the immunosuppressive tumor microenvironment in hepatocellular carcinoma: challenges and opportunities. *Mol cancer*. (2019) 18:130.

61. Mantovani S, Oliviero B, Varchetta S, Mele D, Mondelli M. Natural killer cell responses in hepatocellular carcinoma: implications for novel immunotherapeutic approaches. *Cancers*. (2019) 18(1):130.

62. Lee H, Kang H, Cho H. Role of interleukin(IL)-6 in NK activity to hypoxic-induced highly invasive hepatocellular carcinoma(HCC) cells. *J Microbiol Biotechnol*. (2023) 33:864–74.

63. Su X, Yin H, Bai M, Liu J, Liu R, Zeng H, et al. A novel trxR1 inhibitor regulates NK and CD8+ T cell infiltration and cytotoxicity, enhancing the efficacy of anti-PD-1 immunotherapy against hepatocarcinoma. *J Immunol (Baltimore Md: 1950)*. (2023) 210:681–95.

64. Shi X, Chen W, Yin Y, Cao H, Wang X, Jiang W, et al. RAC1 NK cell-based immunotherapy in hepatocellular carcinoma via STAT3-NKG2D axis. *Cancer letters*. (2024) 592:216909.

65. Yang Y, Chen D, Zhao B, Ren L, Huang R, Feng B, et al. The predictive value of PD-L1 expression in patients with advanced hepatocellular carcinoma treated with PD-1/PD-L1 inhibitors: A systematic review and meta-analysis. *Cancer Med*. (2023) 12:9282–92.

66. Nguyen T, Chen P, Pham J, Kaur K, Raman S, Jewett A, et al. Current and future states of natural killer cell-based immunotherapy in hepatocellular carcinoma. *Crit Rev Immunol*. (2024) 44:71–85.

67. Park H, Kim G, Kim N, Ha S, Yim H. Efficacy and safety of natural killer cell therapy in patients with solid tumors: a systematic review and meta-analysis. *Front Immunol*. (2024) 15:1454427.

68. Lizana-Vasquez G, Torres-Lugo M, Dixon R, Powderly J, Warin R. The application of autologous cancer immunotherapies in the age of memory-NK cells. *Front Immunol*. (2023) 14:1167666.

69. Pan S, Wang F, Jiang J, Lin Z, Chen Z, Cao T, et al. Chimeric antigen receptor-natural killer cells: A new breakthrough in the treatment of solid tumours. *Clin Oncol (Royal Coll Radiologists (Great Britain))*. (2023) 35:153–62.

70. Hu X, Shui Y, Shimizu S, Sakamoto S, Kasahara M, Okada S, et al. Targeted immune cell therapy for hepatocellular carcinoma using expanded liver mononuclear cell-derived natural killer cells. *Neoplasia (New York NY)*. (2024) 58:101061.

71. Berrien-Elliott M, Jacobs M, Fehniger T. Allogeneic natural killer cell therapy. *Blood*. (2023) 141:856–68.

72. Rimassa L, Finn R, Sangro B. Combination immunotherapy for hepatocellular carcinoma. *J hepatol*. (2023) 79:506–15.

73. Dagher O, Posey A. Forks in the road for CAR T and CAR NK cell cancer therapies. *Nat Immunol*. (2023) 24:1994–2007.

74. Pan K, Farrukh H, Chittepu V, Xu H, Pan C, Zhu Z. CAR race to cancer immunotherapy: from CAR T, CAR NK to CAR macrophage therapy. *J Exp Clin Cancer research: CR*. (2022) 41:119.

75. Wenhua Q, Peng D, Hui C, Jianmin Z. Advances in induced pluripotent stem cell-derived natural killer cell therapy. *Cells*. (2022) 41(1):119.

76. Nicholas L-R, Nina MH, Rebecca MD. Structural basis for the activity and specificity of the immune checkpoint inhibitor lirilumab. *Sci Rep*. (2024) 13(23):1976.

77. Jia Y, Aydin E, Alessandro S, Kejia C, Zhuoli Z. Combination of NK-based immunotherapy and sorafenib against hepatocellular carcinoma. *Am J Cancer Res*. (2024) 14(1):742.

78. Ashok Kumar J, Sungjun K, Hyun Jin K, Kyobum K. Biomaterial-mediated exogenous facile coating of natural killer cells for enhancing anticancer efficacy toward hepatocellular carcinoma. *Bioconjug Chem*. (2021) 11(2):337–49.

79. Shuojiong P, Tianyu L, Yizheng T, Huaping X. Selenium-containing nanoparticles synergistically enhance Pemetrexed&NK cell-based chemoimmunotherapy. *Biomaterials*. (2023) 34(10):1789–801.

80. Woo Kyun B, Byung Chan L, Hyeon-Jong K, Je-Jung L, Ik-Joo C, Sung Bum C, et al. A phase I study of locoregional high-dose autologous natural killer cell therapy with hepatic arterial infusion chemotherapy in patients with locally advanced hepatocellular carcinoma. *Front Immunol*. (2022) 13.

81. Fridman W, Pagès F, Sautès-Fridman C, Galon J. The immune contexture in human tumours: impact on clinical outcome. *Nat Rev Cancer*. (2012) 12:298–306.

82. Reardon S. First cell therapy for solid tumours heads to the clinic: what it means for cancer treatment. *Nature*. (2024).

83. Brummel K, Eerkens AL, de Bruyn M, Nijman HW. Tumour-infiltrating lymphocytes: from prognosis to treatment selection. *Br J Cancer*. (2022) 128:451–8.

84. Liu T, Tan J, Wu M, Fan W, Wei J, Zhu B, et al. High-affinity neoantigens correlate with better prognosis and trigger potent antihepatocellular carcinoma (HCC) activity by activating CD39CD8 T cells. *Gut*. (2021) 70:1965–77.

85. Sarnaik A, Hwu P, Mulé J, Pilon-Thomas S. Tumor-infiltrating lymphocytes: A new hope. *Cancer Cell*. (2024) 42:1315–8.

86. Shen H, Sun T, Hoang H, Burchfield J, Hamilton G, Mittendorf E, et al. Enhancing cancer immunotherapy through nanotechnology-mediated tumor infiltration and activation of immune cells. *Semin Immunol*. (2017) 34:114–22.

87. Wang Z, Ahmed S, Labib M, Wang H, Hu X, Wei J, et al. Efficient recovery of potent tumour-infiltrating lymphocytes through quantitative immunomagnetic cell sorting. *Nat Biomed engineering*. (2022) 6:108–17.

88. Hiraoka N. Tumor-infiltrating lymphocytes and hepatocellular carcinoma: molecular biology. *Int J Clin Oncol*. (2010) 15:544–51.

89. Fu J, Zhang Z, Zhou L, Qi Z, Xing S, Lv J, et al. Impairment of CD4+ cytotoxic T cells predicts poor survival and high recurrence rates in patients with hepatocellular carcinoma. *Hepatol (Baltimore Md)*. (2013) 58:139–49.

90. Shi J, Gao Q, Wang Z, Zhou J, Wang X, Min Z, et al. Margin-infiltrating CD20 (+) B cells display an atypical memory phenotype and correlate with favorable prognosis in hepatocellular carcinoma. *Clin Cancer research: an Off J Am Assoc Cancer Res*. (2013) 19:5994–6005.

91. Zhu L, Zhou J, Liu Y, Pan W. Prognostic significance of natural killer cell infiltration in hepatocellular carcinoma. *Chin J Cancer*. (2009) 28:1198–202.

92. Jiang S, Tang Y, Zhang Y, Weng D, Zhou Z, Pan K, et al. A phase I clinical trial utilizing autologous tumor-infiltrating lymphocytes in patients with primary hepatocellular carcinoma. *Oncotarget*. (2015) 6:41339–49.

93. Takayama T, Sekine T, Makuuchi M, Yamasaki S, Kosuge T, Yamamoto J, et al. Adoptive immunotherapy to lower postsurgical recurrence rates of hepatocellular carcinoma: a randomised trial. *Lancet (London England)*. (2000) 356:802–7.

94. Peña-Asensio J, Calvo H, Torralba M, Miquel J, Sanz-de-Villalobos E, Larrubia J. Anti-PD-1/PD-L1 based combination immunotherapy to boost antigen-specific CD8 T cell response in hepatocellular carcinoma. *Cancers*. (2000) 356(9232):802–7.

95. van Beek A, Zhou G, Doukas M, Boor P, Noordam L, Mancham S, et al. GITR ligation enhances functionality of tumor-infiltrating T cells in hepatocellular carcinoma. *Int J cancer*. (2019) 145:1111–24.

96. Li Y, Huang H, Wang Q, Zheng X, Zhou Y, Kong X, et al. Identification of prognostic risk model based on plasma cell markers in hepatocellular carcinoma through single-cell sequencing analysis. *Front Genet*. (2024) 15:1363197.

97. Nie H, He T, Wang L, Zhang L. Expression and prognostic value of tumor-infiltrating lymphocytes and PD-L1 in hepatocellular carcinoma. *OncoTargets Ther*. (2021) 14:1377–85.

98. Wang X, Yuan Z, Li Z, He X, Zhang Y, Wang X, et al. Key oncogenic signaling pathways affecting tumor-infiltrating lymphocytes infiltration in hepatocellular carcinoma: basic principles and recent advances. *Front Immunol*. (2024) 15:1354313.

99. Zhou G, Wilson G, George J, Qiao L. Targeting cancer stem cells as a therapeutic approach in liver cancer. *Curr Gene Ther*. (2015) 15:161–70.

100. Lee H, Hong I. Targeting liver cancer stem cells: an alternative therapeutic approach for liver cancer. *Cancers*. (2015) 15(2):161–70.

101. Liu Y, Yeh C, Lin K. Cancer stem cell functions in hepatocellular carcinoma and comprehensive therapeutic strategies. *Cells*. (2020) 12(10):2746.

102. Zhang N, Bai S, Zhang F, Shi M, Wang L, Wang L, et al. Molecular markers and mechanisms for stemness maintenance of liver cancer stem cells: a review. *Chin J Biotechnol*. (2021) 37:2719–36.

103. Abdellateif M, Zekri A. Stem cell therapy for hepatocellular carcinoma and end-stage liver disease. *J Egyptian Natl Cancer Institute*. (2023) 35:35.

104. Mansour W, Kamel M, Elzayat E, Atta S, Kamel M, Mahmood D, et al. Therapeutic role of bone marrow-derived mesenchymal stem cells in controlling prognosis of hepatocellular carcinoma in a murine model. *Exp Clin transplantation: Off J Middle East Soc Organ Transplantation*. (2022) 20:62–8.

105. Lee T, Guan X, Ma S. Cancer stem cells in hepatocellular carcinoma - from origin to clinical implications. *Nat Rev Gastroenterol hepatol*. (2022) 19:26–44.

106. Li M, Mu X, Song J, Zhai P, Cheng Y, Le Y, et al. PAF enhances cancer stem cell properties via β-catenin signaling in hepatocellular carcinoma. *Cell Cycle (Georgetown Tex)*. (2021) 20:1010–20.

107. Elkhenany H, Shekshek A, Abdel-Daim M, El-Badri N. Stem cell therapy for hepatocellular carcinoma: future perspectives. *Adv Exp Med Biol*. (2020) 1237:97–119.

108. Hussein M, Li Q, Mao R, Peng Y, He Y. TCR T cells overexpressing c-Jun have better functionality with improved tumor infiltration and persistence in hepatocellular carcinoma. *Front Immunol*. (2023) 14:1114770.

109. Wu D, Li Y. Application of adoptive cell therapy in hepatocellular carcinoma. *Immunology*. (2023) 170:453–69.

110. Meng F, Zhao J, Tan A, Hu W, Wang S, Jin J, et al. Immunotherapy of HBV-related advanced hepatocellular carcinoma with short-term HBV-specific TCR expressed T cells: results of dose escalation, phase I trial. *Hepatol Int*. (2021) 15:1402–12.

111. Wan X, Wisskirchen K, Jin T, Yang L, Wang X, Wu X, et al. Genetically-modified, redirected T cells target hepatitis B surface antigen-positive hepatocytes and hepatocellular carcinoma lesions in a clinical setting. *Clin Mol hepatol*. (2024) 30:735–55.

112. Yang F, Zheng X, Koh S, Lu J, Cheng J, Li P, et al. Messenger RNA electroporated hepatitis B virus (HBV) antigen-specific T cell receptor (TCR) redirected T cell therapy is well-tolerated in patients with recurrent HBV-related hepatocellular carcinoma post-liver transplantation: results from a phase I trial. *Hepatol Int*. (2023) 17:850–9.

113. Zhu W, Zhang Z, Chen J, Chen X, Huang L, Zhang X, et al. A novel engineered IL-21 receptor arms T-cell receptor-engineered T cells (TCR-T cells) against hepatocellular carcinoma. *Signal transduction targeted Ther*. (2024) 9:101.

114. Chen A, Yu Z, Ma N, Lu X, Zhang Y, Xu W, et al. Atovaquone enhances antitumor efficacy of TCR-T therapy by augmentation of ROS-induced ferroptosis in hepatocellular carcinoma. *Cancer immunol immunother: CII*. (2024) 73:49.

115. Müller T, Jarosch S, Hammel M, Leube J, Grassmann S, Bernard B, et al. Targeted T cell receptor gene editing provides predictable T cell product function for immunotherapy. *Cell Rep Med*. (2021) 2:100374.

116. Vercher E, Covo-Vergara Á, Conde E, Hernández-Rueda M, Elizalde E, Mancheño U, et al. Human T cells engineered with an HLA-A2-restricted murine T-cell receptor targeting Glypican 3 effectively control human hepatocellular carcinoma in mice. *Hepatol (Baltimore Md)*. (2024).

117. Schmidt-Wolf I, Lefterova P, Mehta B, Fernandez L, Huhn D, Blume K, et al. Phenotypic characterization and identification of effector cells involved in tumor cell recognition of cytokine-induced killer cells. *Exp hematol*. (1993) 21:1673–9.

118. Guo Y, Han W. Cytokine-induced killer (CIK) cells: from basic research to clinical translation. *Chin J cancer*. (2015) 34:99–107.

119. Zhang Q, Liu X, Zhang T, Zhang X, Zhao L, Long F, et al. The dual-functional capability of cytokine-induced killer cells and application in tumor immunology. *Hum Immunol*. (2015) 76:385–91.

120. Jia C, Chen Y, Cai X, Li Y, Zheng X, Yao Z, et al. Efficacy of cytokine-induced killer cell-based immunotherapy for hepatocellular carcinoma. *Am J Cancer Res*. (2019) 9:1254–65.

121. Yang C, Huang C, Hu C, Fang J, Chen T, Lin Y, et al. Immunophenotype and antitumor activity of cytokine-induced killer cells from patients with hepatocellular carcinoma. *PloS One*. (2023) 18:e0280023.

122. Wang J, Feng L, Zhang L. Combining cellular immunotherapy was an optional choice for unresectable advanced HCC: A systematic review and meta-analysis. *Clinics Res Hepatol gastroenterol*. (2021) 45:101440.

123. Wu X, Sharma A, Oldenburg J, Weiher H, Essler M, Skowasch D, et al. NKG2D engagement alone is sufficient to activate cytokine-induced killer cells while 2B4 only provides limited coactivation. *Front Immunol*. (2021) 12:731767.

124. Wu T, Zhang L, Zeng Z, Yan T, Cheng J, Miao X, et al. Complete response to PD-1 inhibitor in primary hepatocellular carcinoma patients post-progression on bi-specific antibody conjugated CIK cell treatment: A report of two cases. *OncoTargets Ther*. (2021) 14:5447–53.

125. Zhang X, Yang J, Zhang G, Song L, Su Y, Shi Y, et al. 5 years of clinical DC-CIK/NK cells immunotherapy for acute myeloid leukemia - a summary. *Immunotherapy*. (2020) 12:63–74.

126. Lee Y, Luo S, Lee C, Tang C, Shen C, Cheng W, et al. Optimizing tumor-associated antigen-stimulated autologous dendritic cell and cytokine-induced killer cell coculture to enhance cytotoxicity for cancer immunotherapy in manufacturing. *BMC Immunol*. (2023) 24:14.

127. Tawinwung S, Tudsamran S, Thaiwong R, Asawapanumas T, Wudhikarn K, Chanswangphuwana C, et al. Improving cytokine-induced killer cell expansion using a gas-permeable culture method for clinical-scale production. *Asian Pacific J Allergy Immunol*. (2023).

128. Ek-Eudomsuk P, Chalermrujinanant C, Soontrapa K. N-acetylcysteine potentiates the tumor cytotoxicity of cytokine-induced killer cells. *Asian Pacific J Allergy Immunol*. (2022).

129. Cao J, Kong F, Liu X, Wang X. Immunotherapy with dendritic cells and cytokine-induced killer cells for hepatocellular carcinoma: A meta-analysis. *World J gastroenterol*. (2019) 25:3649–63.

130. Yue S, Xiaoping M, Xueting L, Zhicun Y, Hongjuan W. Research progress and clinical prospect of immunocytotherapy for the treatment of hepatocellular carcinoma. *Int Immunopharmacol*. (2019) 25(27):3649–3663.

131. Luo W, Xin L, Xue-Juan D, Xiao-Ling Y, Jing Z, Zhi-Gang C, et al. Dendritic cell-cytokine killer combined with microwave ablation reduced recurrence for hepatocellular carcinoma compared to ablation alone. *Technol Health Care*. (2020) 82(0):106351.

132. Wan Z, Zhenghui S, Jianpeng X, Xinhui L, Yue L, Zike Y, et al. Blocking the PD-1/PD-L1 axis in dendritic cell-stimulated Cytokine-Induced Killer Cells with pembrolizumab enhances their therapeutic effects against hepatocellular carcinoma. *J Cancer*. (2024) 32(3):1819–34.

133. Jiang W, Wang Z, Luo Q, Dai Z, Zhu J, Tao X, et al. Combined immunotherapy with dendritic cells and cytokine-induced killer cells for solid tumors: a systematic review and meta-analysis of randomized controlled trials. *J Trans Med*. (2024) 22:1122.

134. Bendelac A, Savage P, Teyton L. The biology of NKT cells. *Annu Rev Immunol*. (2007) 25:297–336.

135. Godfrey D, Kronenberg M. Going both ways: immune regulation via CD1d-dependent NKT cells. *J Clin Invest*. (2004) 114:1379–88.

136. Gapin L. Development of invariant natural killer T cells. *Curr Opin Immunol*. (2016) 39:68–74.

137. Brigl M, Brenner M. CD1: antigen presentation and T cell function. *Annu Rev Immunol*. (2004) 22:817–90.

138. Borowski C, Bendelac A. Signaling for NKT cell development: the SAP-FynT connection. *J Exp Med*. (2005) 201:833–6.

139. Wei B, Wingender G, Fujiwara D, Chen D, McPherson M, Brewer S, et al. Commensal microbiota and CD8+ T cells shape the formation of invariant NKT cells. *J Immunol (Baltimore Md: 1950)*. (2010) 184:1218–26.

140. Fujii S, Shimizu K, Okamoto Y, Kunii N, Nakayama T, Motohashi S, et al. NKT cells as an ideal anti-tumor immunotherapeutic. *Front Immunol*. (2013) 4:409.

141. Yao G, Jia G, Xuli B, Fang X, Yanpin M, Bingqin T, et al. Adoptive transfer of autologous invariant natural killer T cells as immunotherapy for advanced hepatocellular carcinoma: A phase I clinical trial. *Oncologist*. (2013) 4:409.

142. Jia G, Xuli B, Fuquan L, Jiang G, Yifan W, Fang X, et al. Efficacy of invariant natural killer T cell infusion plus transarterial embolization vs transarterial embolization alone for hepatocellular carcinoma patients: A phase 2 randomized clinical trial. *J Hepatocell Carcinoma*. (2021) 26(11):e1919–30.

143. Dezhao L, Mei L, Jinhuan W, Jia G, Ningzhi X, Jun L. SOX chemotherapy with anti-PD-1 and iNKT cell immunotherapies for stage IV gastric adenocarcinoma with liver metastases: A case report. *Front Immunol*. (2022) 13.

144. Kevin OM, Spyridon AK, Michael DH, Hamid B. Enhancing neuroblastoma immunotherapies by engaging iNKT and NK cells. *Front Immunol*. (2020) 11.

145. Oscar Fabian G-A, Christoph H, Bence K. Lymphocyte expansion in bioreactors: upgrading adoptive cell therapy. *J Biol Eng*. (2020) 11:873.

146. Le-Ping Z, Ai-Dong L, Jun W, Yue-Ping J, Ying-Xi Z, Yong-Hua Z, et al. Expanded activated autologous lymphocyte infusions improve outcomes of low- and intermediate-risk childhood acute myeloid leukemia with low level of minimal residual disease. *Cancer Lett*. (2021) 15(1):13.

147. Subramani B, Pullai C, Krishnan K, Sugadan S, Deng X, Hiroshi T, et al. Efficacy of *ex vivo* activated and expanded natural killer cells and T lymphocytes for colorectal cancer patients. *Biomed Rep*. (2014) 2:505–8.

148. Zhang G, Li F, Sun S, Hu Y, Wang G, Wang Y, et al. Adoptive immunotherapy for small cell lung cancer by expanded activated autologous lymphocytes: a retrospective clinical analysis. *Asian Pacific J Cancer prevention: APJCP*. (2015) 16:1487–94.

149. Christopher S, Saar G, Michael K. Engineered CAR-macrophages as adoptive immunotherapies for solid tumors. *Front Immunol*. (2021) 12.

150. Jialin L, Yuqing M, Qiuxin L, Yihuan X, Yiquan X, Sheng X. CAR Macrophages: a promising novel immunotherapy for solid tumors and beyond. *biomark Res*. (2015) 6 (38):41339–49.

151. Guan L, Wu S, Zhu Q, He X, Li X, Song G, et al. GPC3-targeted CAR-M cells exhibit potent antitumor activity against hepatocellular carcinoma. *Biochem biophysics Rep*. (2024) 39:101741.

152. Mao Y, Yao C, Zhang S, Zeng Q, Wang J, Sheng C, et al. Targeting fibroblast activation protein with chimeric antigen receptor macrophages. *Biochem Pharmacol*. (2024) 230:116604.

153. Abdin S, Paasch D, Lachmann N. CAR macrophages on a fast track to solid tumor therapy. *Nat Immunol*. (2024) 25:11–2.

154. Shi Y, Li X, Dong Y, Yuan H, Wang Y, Yang R. Exploring the potential of CAR-macrophage therapy. *Life Sci*. (2025) 361:123300.

155. Lei A, Yu H, Lu S, Lu H, Ding X, Tan T, et al. A second-generation M1-polarized CAR macrophage with antitumor efficacy. *Nat Immunol*. (2024) 25:102–16.

156. Klichinsky M, Ruella M, Shestova O, Lu X, Best A, Zeeman M, et al. Human chimeric antigen receptor macrophages for cancer immunotherapy. *Nat Biotechnol*. (2020) 38:947–53.

157. Chupradit K, Muneekaew S, Wattanapanitch M. Engineered CD147-CAR macrophages for enhanced phagocytosis of cancers. *Cancer immunol immunother: CII*. (2024) 73:170.

158. Pierini S, Gabbasov R, Oliveira-Nunes M, Qureshi R, Worth A, Huang S, et al. Chimeric antigen receptor macrophages (CAR-M) sensitize HER2+ solid tumors to PD1 blockade in pre-clinical models. *Nat Commun*. (2025) 16:706.

159. Stefanoudakis D, Kathuria-Prakash N, Sun A, Abel M, Drolen C, Ashbaugh C, et al. The potential revolution of cancer treatment with CRISPR technology. *Cancers*. (2024) 73(9):170.

160. Zhang X, Cheng C, Sun W, Wang H. Engineering T cells using CRISPR/cas9 for cancer therapy. *Methods Mol Biol (Clifton NJ)*. (2020) 2115:419–33.

161. Zheng X, Liu X, Lei Y, Wang G, Liu M. Glypican-3: A novel and promising target for the treatment of hepatocellular carcinoma. *Front Oncol*. (2022) 12:824208.

162. Kobayashi T, Kumagai S, Doi R, Afonina E, Koyama S, Nishikawa H. Isolation of tumor-infiltrating lymphocytes from preserved human tumor tissue specimens for downstream characterization. *STAR Protoc*. (2022) 3:101557.

163. Tas L, Jedema I, Haanen J. Novel strategies to improve efficacy of treatment with tumor-infiltrating lymphocytes (TILs) for patients with solid cancers. *Curr Opin Oncol*. (2023) 35:107–13.

164. Pittenger M, Discher D, Péault B, Phinney D, Hare J, Caplan A. Mesenchymal stem cell perspective: cell biology to clinical progress. *NPJ Regenerative Med*. (2019) 4:22.

165. Hassanzadeh A, Shamlou S, Yousefi N, Nikoo M, Verdi J. Genetically-modified stem cell in regenerative medicine and cancer therapy; A new era. *Curr Gene Ther*. (2022) 22:23–39.

166. Théry C, Zitvogel L, Amigorena S. Exosomes: composition, biogenesis and function. *Nat Rev Immunol*. (2002) 2:569–79.

167. Cao Y, Xu P, Shen Y, Wu W, Chen M, Wang F, et al. Exosomes and cancer immunotherapy: A review of recent cancer research. *Front Oncol*. (2022) 12:1118101.

168. Ge Y, Jiang L, Dong Q, Xu Y, Yam JWP, Zhong X. Exosome-mediated crosstalk in the tumor immune microenvironment: critical drivers of hepatocellular carcinoma progression. *J Clin Trans Hepatol*. (2024) 000:000–.

169. Chen W, Mao Y, Liu C, Wu H, Chen S. Exosome in hepatocellular carcinoma: an update. *J Cancer*. (2021) 12:2526–36.

170. GuoYun W, GaiXiang L, MeiJing Z, HuiLai M. Significance of exosomes in hepatocellular carcinoma. *Front Oncol*. (2022) 12.

171. Xu M, Zhang C, He S, Xu C, Wei X, Pu K. Activatable immunoprotease nanorestimulator for second near-infrared photothermal immunotherapy of cancer. *ACS nano*. (2023) 17:8183–94.

172. Jiang Y, Huang J, Xu C, Pu K. Activatable polymer nanoagonist for second near-infrared photothermal immunotherapy of cancer. *Nat Commun*. (2021) 12:742.

173. El-Khoueiry A, Sangro B, Yau T, Crocenzi T, Kudo M, Hsu C, et al. Nivolumab in patients with advanced hepatocellular carcinoma (CheckMate 040): an open-label, non-comparative, phase 1/2 dose escalation and expansion trial. *Lancet (London England)*. (2017) 389:2492–502.

174. Wardell C, Boardman D, Levings M. Harnessing the biology of regulatory T cells to treat disease. *Nat Rev Drug discov*. (2024) 24:93–111.

175. Yi M, Zheng X, Niu M, Zhu S, Ge H, Wu K. Combination strategies with PD-1/PD-L1 blockade: current advances and future directions. *Mol cancer*. (2022) 21:28.

176. Shi T, Iwama H, Fujita K, Kobara H, Nishiyama N, Fujihara S, et al. Evaluating the effect of lenvatinib on sorafenib-resistant hepatocellular carcinoma cells. *Int J Mol Sci*. (2017) 389(10088):2492–502.

177. Liu Z, Liu J, Staiculescu D, Chen J. Combination of molecularly targeted therapies and immune checkpoint inhibitors in the new era of unresectable hepatocellular carcinoma treatment. *Ther Adv Med Oncol*. (2021) 13:17588359211018026.

178. Wu X, Luo H, Shi B, Di S, Sun R, Su J, et al. Combined antitumor effects of sorafenib and GPC3-CAR T cells in mouse models of hepatocellular carcinoma. *Mol therapy: J Am Soc Gene Ther*. (2019) 27:1483–94.

179. Butterfield L, Najjar Y. Immunotherapy combination approaches: mechanisms, biomarkers and clinical observations. *Nat Rev Immunol*. (2024) 24:399–416.

180. Gu Y, Xu S, Wang Z, Yang J, Zheng S, Wei Q, et al. When immunotherapy meets liver transplantation for hepatocellular carcinoma: A bumpy but promising road. *Chin J Cancer Res = Chung-kuo yen cheng yen chiu*. (2023) 35:92–107.

181. Tojjari A, Yu J, Saeed A. Immunotherapy and radiation therapy combinatorial approaches in hepatocellular carcinoma. *Cancers*. (2019) 27(8):1483–94.

182. Wang A, Ong X, D'Souza C, Neeson P, Zhu J. Combining chemotherapy with CAR-T cell therapy in treating solid tumors. *Front Immunol*. (2023) 14:1140541.

183. Goswami S, Pauken K, Wang L, Sharma P. Next-generation combination approaches for immune checkpoint therapy. *Nat Immunol*. (2024) 25:2186–99.

184. Albarrán V, San Román M, Pozas J, Chamorro J, Rosero D, Guerrero P, et al. Adoptive T cell therapy for solid tumors: current landscape and future challenges. *Front Immunol*. (2024) 15:1352805.

185. Junna Z, Gongde C, Jinying X, Xiu Z. Serum AFU, 5'-NT and AFP as biomarkers for primary hepatocellular carcinoma diagnosis. *Open Med (Warsaw Poland)*. (2017) 12:354–8.

186. Wang T, Zhang K. New blood biomarkers for the diagnosis of AFP-negative hepatocellular carcinoma. *Front Oncol*. (2020) 10:1316.

187. Attia A, Rezaee-Zavareh M, Hwang S, Kim N, Adetyan H, Yalda T, et al. Novel biomarkers for early detection of hepatocellular carcinoma. *Diagnostics (Basel Switzerland)*. (2024) 15:1352805.

188. Fares S, Wehrle C, Hong H, Sun K, Jiao C, Zhang M, et al. Emerging and clinically accepted biomarkers for hepatocellular carcinoma. *Cancers*. (2017) 12:354–8.

189. Solhi R, Pourhamzeh M, Zarrabi A, Hassan M, Mirzaei H, Vosough M. Novel biomarkers for monitoring and management of hepatocellular carcinoma. *Cancer Cell Int*. (2024) 24:428.

190. Yu L, Xu F, Gao L. Predict new therapeutic drugs for hepatocellular carcinoma based on gene mutation and expression. *Front bioengineer Biotechnol*. (2020) 8:8.

191. Zheng Z, Guan R, Zou Y, Jian Z, Lin Y, Guo R, et al. Nomogram based on inflammatory biomarkers to predict the recurrence of hepatocellular carcinoma-A multicentre experience. *J Inflammation Res*. (2022) 15:5089–102.

192. Pepe M, Li C, Feng Z. Improving the quality of biomarker discovery research: the right samples and enough of them. *Cancer epidemiol Biomarkers prevention: Publ Am Assoc Cancer Research cosponsored by Am Soc Prev Oncol*. (2015) 24:944–50.

frontiers | Frontiers in Immunology

TYPE Methods
PUBLISHED 10 December 2025
DOI 10.3389/fimmu.2025.1609732

OPEN ACCESS

EDITED BY
Yan-Ru Lou,
Shanghai Jiao Tong University, China

REVIEWED BY
Martin R. Goodier,
MRC Unit The Gambia at London School of Hygiene and Tropical Medicine UK, Gambia
Achille Anselmo,
San Raffaele Scientific Institute, Italy

*CORRESPONDENCE
Alberta Gerarda Antonia Paul
apaul@cytekbio.com
Yacine Kharraz
ykharraz@cytekbio.com

RECEIVED 10 April 2025
REVISED 31 October 2025
ACCEPTED 10 November 2025
PUBLISHED 10 December 2025

CITATION
Paul AGA, Reichel KHH, Garcia-Vallejo JJ, Heij LR, Jaimes MC and Kharraz Y (2025) A 41-marker 37-color full spectrum flow cytometry panel for the deep immunophenotyping of human peripheral and liver natural killer cells.
Front. Immunol. 16:1609732.
doi: 10.3389/fimmu.2025.1609732

A 41-marker 37-color full spectrum flow cytometry panel for the deep immunophenotyping of human peripheral and liver natural killer cells

Alberta Gerarda Antonia Paul[1]*, Konrad H. H. Reichel[2,3], Juan J. Garcia-Vallejo[2], Lara R. Heij[3,4,5], Maria C. Jaimes[1] and Yacine Kharraz[1]*

[1]Scientific Commercialization Team (SCT), Cytek Biosciences Inc, Fremont, CA, United States, [2]Department of Molecular Cell Biology and Immunology (MCBI), Amsterdam Infection and Immunity and Cancer Center Amsterdam, Amsterdam University Medical Centers, Free University of Amsterdam, Amsterdam, Netherlands, [3]Department of General, Visceral and Transplant Surgery, University Hospital Essen, Essen, Germany, [4]Department of Pathology, University Hospital Rotterdam, Rotterdam, Netherlands, [5]Institute of Pathology, University Hospital Essen, Essen, Germany

Natural killer cells (NK cells) are granular lymphocytes with cytotoxic activity that have a role in both innate and adaptive immune responses. NK cells consist of a diverse array of phenotypes with specific functions imposed by the microenvironment. Liver NK cells are an abundant lymphocyte population playing a key role in tuning immune responses under physiological and pathological conditions. For example, NK cell functional and phenotypic changes occur during liver cancer progression and correlate with disease prognosis. As liver cancer has the second-highest mortality rate among solid cancers, it is important to define the composition and the dynamics of the liver and peripheral NK cell compartment both in health and disease state. In-depth analysis of the phenotypes and functional status of NK cells and their frequencies will expand our knowledge on their role in maintaining immune tolerance, disease progression, and aid the development of novel treatments. We present here a 41-marker 37-color spectral flow cytometry panel for the in-depth phenotyping of human peripheral and liver NK cells. This paper describes the first spectral flow cytometry panel with 35 markers potentially co-expressed on one cell type (NK cells) including the panel design process, sample preparation, staining protocol, quality control metrics, acquisition protocol and workflows to analyze NK cells in the periphery and liver. NK cell subsets and phenotypes were distinguished by including markers of differentiation, maturation, tissue residency, migratory potential, functional status, key transcription factors, and immune checkpoint molecules. Liver-type ILC1s (Lt-ILC1s) could be identified by inclusion of additional markers and modification of published gating strategies. Furthermore, we describe the dynamics of peripheral and liver NK cells. Finally, we show the validity of markers included to indicate NK cell dysfunction in

samples of patients with Hepatocellular Carcinoma (HCC). This high parameter high resolution panel provides a key tool for in-depth delineation of distinct NK cell subsets in the periphery and in liver, in health and disease state. It allows for the robust identification of NK cells subsets with low frequencies and can effectively be used for samples with limited cell numbers.

KEYWORDS

Aurora, high dimensional, flow cytometry, spectral, human NK cell, PBMCs, liver, cancer

1 Introduction

In-depth NK cell phenotyping is crucial to identify NK subsets and phenotypes that exert positive or detrimental effector functions under different pathological conditions. Furthermore, NK cell phenotyping would benefit the development of NK-targeting therapies and chimeric antigen receptor (CAR-NK) cell-based therapies that have become a major focus of the pharmaceutical industry and academic research (1, 2). Peripheral NK cells are classically divided into three main subsets based upon the relative expression of CD56 and CD16, namely $CD56^{bright}CD16^{-}$ (early NK cells), $CD56^{dim}CD16^{+}$ (mature NK cells) and $CD56^{-}CD16^{+}$ (terminal NK cells). Early NK cells are limited in cytotoxic function, produce proinflammatory cytokines, and express different cytokines, chemokine, adhesion and NK cell receptors than mature NK cells (3–6). Mature NK cells have high cytolytic capacity, produce proinflammatory cytokines, and mediate antibody-dependent cytotoxicity (ADCC) (3–7). Terminal NK cells proliferate less than mature NK cells, have limited cytokine responsiveness and accumulate with age and during chronic viral infections (8–10). Besides the classical NK cell subsets defined by CD16 and CD56 expression levels, other functional states have been identified with distinct expression of inhibitory (CD159a, CD159c, CD85j, KIRs), activating (CD337), chemokine (CD183, CX3CR1) and cytokine receptors (CD195), adhesion molecules (CD49e) and proteins that indicate differentiation (CD57, CD161) by using a variety of technologies (7, 11–17). Recently, a new NK cell classification was proposed dividing NK cells into 6 major subsets resembling subsets of mature (NK1A-C), early-stage $CD56^{dim}$ (NKint), early (NK2) and adaptive $CD159c^{+}$ (NK3) NK cells respectively (16). However, liver NK cells have not yet been investigated and classified with the same level of detail.

The liver receives 80% of its blood supply from the portal vein that drains the gastrointestinal tract. Consequently, it is constantly exposed to foreign antigens. Therefore, the liver immune compartment must maintain a status of local homeostasis and prevent activation and inflammation while in parallel it must aid the efficient clearance of pathogens. NK cells are an abundant population of the liver immune compartment as compared to the periphery (they represent almost 50% of liver lymphocytes) and play a key role in maintaining immune homeostasis in health and disease state (18–22). Liver NK cells are generally divided into two main phenotypes: $CD56^{dim}CD16^{bright}$ and $CD56^{bright}CD16^{-}$ that are present in relatively equal proportions. This is in contrast to the periphery where most NK cells are $CD56^{dim}CD16^{bright}$ (18). Based upon the site of residency and origin, three types of hepatic NK cells can be further distinguished: long-lived liver tissue resident NK cells (tr-NK) that are $CD56^{bright}CD16^{-}$ $CD69^{+}CD186^{+}CD195^{+/-}CD183^{+/-}$ $CD49a^{+/-}Eomes^{Hi}Tbet^{low}$, short-lived circulating conventional NK cells (cNK; $CD56^{dim}CD16^{bright}$), and adaptive/memory-like NK cells (ml-NK; $CD56^{bright}CD16^{-}$). Tr-NK cells are believed to have a key function in controlling viral infections, local tolerance and tissue homeostasis due to their expression of molecules that enforce their unique location close to liver sinusoidal endothelial cells (LSECs) lining the hepatic sinusoids that receive blood from the portal vein (23–26). Ml-NK cells are prone to respond upon re-exposure to viral antigens and include a population of $CD159c^{+}$ NK cells that expand upon human cytomegalovirus infection (HCMV) (18, 26). The prevalence of chronic liver diseases (CLD) and liver cancer is increasing with Hepatocellular Carcinoma (HCC) being the most frequent liver tumor type (27, 28). Besides HCC, liver metastasis are also common in colorectal cancer (CRC) and a major cause of death. As a crucial role has been attributed to NK cells in disease progression and survival rates, both in HCC and CRC liver metastasis (20, 22, 29, 30), a clear understanding of the dynamics of peripheral and liver NK cell subsets, phenotypes and functional status is key for the development and monitoring of NK-based therapies. This reported diversity of NK cells also suggests that discrete subpopulations and/or distinct molecules need to be targeted and can vary per individual, disease state, and tissue type. Thus, it emphasizes the need for in-depth immunophenotyping of NK cells in the periphery and in tissues.

We report here on the development of a comprehensive 41-marker 37-color spectral flow cytometry panel that allows the identification of distinct NK cell subsets and phenotypes in the periphery and in the liver. This panel was based on two high dimensional NK panels previously described for conventional flow cytometry platforms (11, 31). Taking advantage of the resolution and multiplexing capacity of spectral cytometry, we expanded the published panels to include 35 markers potentially expressed on NK cells. Additionally, we established for each marker the sensitivity to enzyme digestion that was needed to isolate cells from liver tissues.

We included CD94, CD49a, CD161, CD158b, CD158a-h, Eomes, Tbet and CD127 to distinguish NK cells from ILCs (32). Markers of tissue homing/residency and co-stimulation (CX3CR1, CD49e, CD69, CD186, CD49a, CD103, CD183, CD195, CD2, PLZF) were incorporated to identify tr-NK cells subsets/phenotypes (23, 31–37). Furthermore, the panel includes HLA-DR, CD38, Ki-67, Granzyme B and Perforin to evaluate functional responses to inflammation, activation and cytotoxic potential. By incorporating CD27, CD11b, CD159a, CD159c and CD57, it also allows detailed characterization of NK cell maturation and memory status (9, 38–42). Finally, antibodies directed to the immune checkpoint molecules TIGIT and CD226 (DNAM-1), inhibitory receptors CD85j and CD161, and activating receptor CD314 were added as they modulate NK cell functionality and are potential targets of cancer immunotherapies (43–49). As such, we present a panel that can serve as a key tool for NK cell functional studies in health and disease. In this method paper, we describe the process of sample preparation, panel design, panel optimization, panel verification, and provide a detailed description of the staining protocol and methods for data quality control. Additionally, we provide a workflow for sample analysis and NK cell subset/phenotype annotation.

2 Materials

2.1 Biological samples

Human PBMC were isolated from buffy coats (Sanquin Blood Bank, Amsterdam, The Netherlands) by means of density centrifugation with Lymphoprep (Axis-Shield, Oslo, Norway). Cells were resuspended to 10-20x10^6/ml in 20% DMSO in Fetal Bovine Serum (FBS) and 1ml aliquots were stored at -80 °C for future use. Liver biopsies from healthy livers were obtained from liver transplant donors, and liver biopsies from patients with HCC were sampled from the tumor site. Liver cell suspensions were generated from liver biopsies as described in (50). Briefly, biopsies were mechanically disrupted into small pieces using a scalpel. The resulting pieces were transferred into a 15 mL conical tube, with 9 mL of complete RPMI (10% FBS, 1% Pen/Strep and 1 mM Glutamine) and 1 mL of 10× hyaluronidase/collagenase solution (StemCell, 07912, Vancouver, BC, Canada). The first round of tissue dissociation by enzymatic digestion was done at 37 °C for 30 min in a pre-warmed shaker. The supernatant was collected without disrupting the tissue and a fresh digestion media was added (10 ml complete RPMI containing 128 U/ml of collagenase IV (Lorne Laboratories, LS004194, Danhill, Berkshire, UK), 40 U/ml of DNaseI (Sigma, DN25, Gillingham, Dorset, UK) and 25 U/ml of universal nuclease (Pierce, 88702, Waltham, MA, USA) for an additional 30 min of digestion. The supernatant was combined with the one from the first digestion step and the remaining liver pieces were squeezed through a 70 µm tissue strainer and rinsed with 10 mL of complete RPMI. The supernatants from all digestion steps were combined and centrifuged for 10 min at 300 g. Red blood cells (RBCs) were removed with ACK lysing buffer (Gibco™, A10492-01, Paisley, UK). Isolated cells were resuspended in 20% DMSO in FBS and aliquots (2.2-5.6x10^6 cells/vial) were stored at -80 °C for future use. As the high parameter flow cytometry panel was designed to determine NK cell phenotypes both in the periphery and in liver cell suspensions, obtained after digesting liver biopsies, it was key to verify that the expression of the chosen markers was not affected by the enzyme digestion method used. To determine which markers were affected, freshly isolated PBMC were treated with the same protocol as used for obtaining liver cell suspensions, frozen and stored at -80 °C until use.

2.2 Ancillaries and reagents for flow cytometric staining

Falcon® FACS tubes 12x75 mm, 5 ml (Corning, catalogue #352063) or equivalent.
10, 200 and 1000 µl pipet tips (ThermoFisher Scientific, catalogue #9400310, 94300220, 9401030) or equivalent.
10, 20, 200 and 1000 µl pipettors (ThermoFisher Scientific, catalogue #4642030, 4642050, 4642080, 4642090) or equivalent.
1.5 ml eppendorf tube (ThermoFisher Scientific, catalogue #3451PK) or equivalent.
RPMI 1640 (Sigma-Aldrich®, catalogue # R8758).
FBS (Corning GmbH, catalogue #35-079-CV).
PBS (Gibco™, catalogue #20012-027).
BD Horizon™ Brilliant Stain Buffer Plus (BD Biosciences, catalogue #566385).
True-Stain Monocyte Blocker™ (BioLegend, catalogue #426101).
UltraComp eBeads™ Compensation Beads (ThermoFisher Scientific, catalogue #01-2222-41).
eBioscience™ Foxp3/Transcription Factor Staining Buffer Set (ThermoFisher Scientific, catalogue #00-5523-00).
4% Paraformaldehyde (Santa Cruz Biotechnology, catalogue# 30525-89-4) or equivalent.
Thawing medium (RPMI 1640 supplemented with 10% FBS).
Staining and washing buffer (PBS with 0.05% Bovine Serum Albumin).
Vendor and catalogue numbers of antibody reagents used in the panel are listed in Supplementary Table 1.

2.3 Equipment

This panel was developed for a Cytek® Aurora (Cytek Biosciences Inc., Fremont, California) equipped with 5 lasers (355, 405, 488, 561, 640 nm) and 64 detectors. The complete configuration with laser power, number of detectors per laser module, center wavelength, bandwidth of the filters, is detailed in (51, 52).

3 Methods

A summary of the major steps in the panel verification process that are addressed in this chapter is depicted in Figure 1.

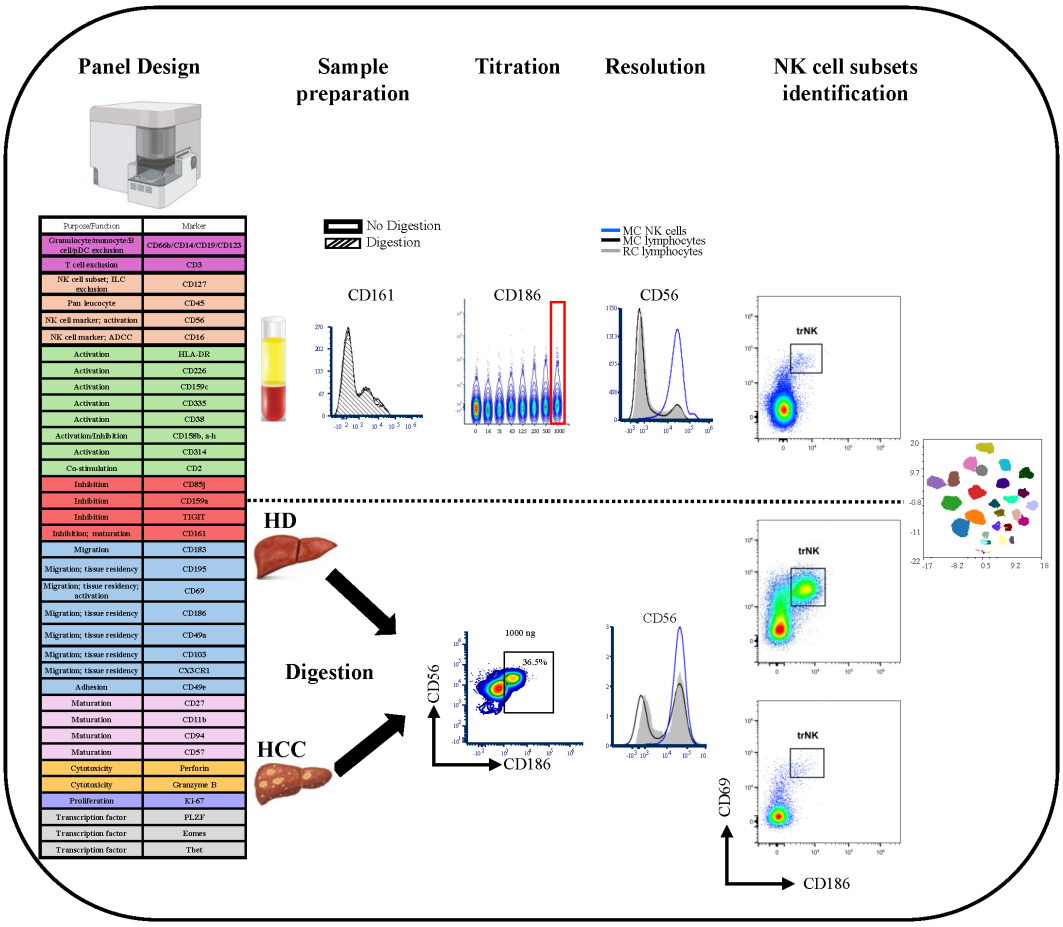

FIGURE 1
Summary of the major steps in the panel development and verification process. The major steps in panel development were as follows: First a panel design was generated using estabilshed metrics. Secondly preservation of the staining patterns/percentages of all markers was confirmed after sample preparation (digestion). Further optimization involved titration of all reagents, confirming preservation of resolution in the MC sample and establishing gating strategies for PBMCs and liver samples. Finally, manual gating and multidimensional analysis was performed for NK cell subset identification.

3.1 Clone selection and panel design

The panel design (markers, clones, and fluorochromes) was based on two high dimensional panels for NK cells that were developed for conventional flow cytometry platforms (11, 31). We expanded those panels to accommodate additional markers while preserving the overall resolution. We followed the rules for panel redesign as described in (51, 52). First, we classified markers that were added as primary, secondary, and tertiary (53). Secondly, we assessed the level of co-expression on peripheral and liver NK cells based upon the literature. Thirdly, we used the Cytek® Cloud to select unique fluorochrome spectra to accommodate all the markers of the panel thereby avoiding fluorochromes with a high cosine similarity index and avoiding a high condition number as described in (51, 52). Finally, we limited the use of custom reagents. Based on the criteria stated above (51) we selected 37 fluorochromes (Supplementary Figures 1A, C). Of the 37 fluorochromes selected, and as depicted in Supplementary Figure 1B, the pairs with the highest Similarity™ indices were Vio® Bright B515 and Vio® Bright FITC (0.93), BV421 and Super Bright™ 436 (0.96) and PE and cFluor® YG584 (0.91). However, the condition number of the panel was low (16.82; Supplementary Figure 1B; black arrow) and hence this metric gave us confidence that this fluorochrome combination was appropriate. We next generated the Spillover Spread Matrix (SSM; Supplementary Figure 2C) from PBMCs stained with anti-CD4 antibodies available for the selected fluorochromes, except for RealBlue™744 (RB744) and RealBlue™780 (RB780) which were CD3 and CD2 conjugates respectively. The SSM was used to predict areas of spread and to guide further marker-fluorochrome assignment when needed.

Despite the high Similarity™ indices between the combinations of fluorochromes stated above, these fluorochromes pairs could still be sufficiently discriminated from each other both in PBMCs (Supplementary Figure 2A) and in the liver (Supplementary Figure 2B) when stained with the final panel. Markers that were added to this panel as compared to (11, 31) were the exclusion markers CD123 (for pDCs) and CD66b (for granulocytes). Although this panel was run on frozen/thawed samples, the addition of CD66b allows to exclude granulocytes in case fresh samples are analyzed. Additionally, we added CD226, CD183 and CD94 as they indicate the functional status and/or distinguish

specific NK cell phenotypes and can be used in the gating strategy to exclude ILCs ($CD94^-$). Some markers needed to be reassigned to different fluorochromes and/or clones due to performance issues after initial testing. For example, CD161 was first assigned to BV605 and clone DX12 was chosen. As the ability of this reagent to discriminate $CD161^+$ from $CD161^-$ was suboptimal, we switched to clone HP-3G10 conjugated to cFluor® R720. Another example was CD195, originally assigned to BUV395, that was reassigned to the brighter fluorochrome BUV661 because of the dim expression of CD195 on NK cells. Final markers, clones and fluorochromes that were used in this panel are listed in Table 1.

3.2 Antibody titrations

All selected reagents were titrated using frozen PBMC from healthy donors (HD). An average of 1.10^6 cells were used per test and subjected to fixation/permeabilization method as described in

TABLE 1 Markers included in the panel design (in alpha numeric order) and their specifics.

Specificity	Alternative name	Fluorochrome	Clone	Purpose/function
CD103	Integrin alpha E	BUV805	Ber-ACT8	Migration, tissue residency
CD11b	Integrin alpha M, ITGB2 subunit A	BV570	ICRF44	Maturation, NK cell subsets
CD123	IL-3 receptor alpha, IL-3RA	cFluor V450	6H6	Exclusion plasmacytoid dendritic cells
CD127	IL-7Ra	BV421	A019D5	Exclusion ILC, NK cell subsets
CD14	N.A.	cFluor V450	M5E2	Exclusion monocytes
CD158a-h	KIR2DL1, KIR2DS1	PE-Cy5.5	EB6 (11PB6)	Activating/inhibitory receptor
CD158b	KIR2DL2, KIR2DL3, KIR2DS2	PE-Cy5.5	GL183	Activating/inhibitory receptor
CD159a	NKG2A	PE-Vio 615	REA110	Inhibitory receptor
CD159c	NKG2C	BV480	134591	Activating receptor, NK subsets
CD16	FcgRIII	BUV496	3G8	NK subsets, Antibody Dependent Cellular Cytotoxicity (ADCC)
CD161	NKR-P1	cFluor R720	HP-3G10	Inhibitory receptor, maturation marker; NK cell subsets
CD183	CXCR3	PE-Cy5	1C6/ CXCR3	Migration
CD186	CXCR6	BV711	13B1E5	Migration, tissue residency
CD19	N.A.	cFluor V450	HIB19	Exclusion B cells
CD195	CCR5	BUV661	2D7/CCR5	Migration, tissue residency
CD2	Cluster of differentiation 2	Super Bright 436	RPA-2.10	Co-stimulatory receptor
CD226	DNAM-1, DNAX accessory molecule	BUV615	DX11	Activating receptor
CD27	Tumor necrosis factor receptor superfamily 7	cFluor YG584	O323	Maturation, NK cell subsets
CD3	N.A.	RB744	UCHT1	Exclusion T cells
CD314	NKG2D, KLRK1	cFluor BYG750	1D11	Activating receptor
CD335	NKp46, NCR1	Vio Bright B515	REA808	Activating receptor
CD38	Cyclic ADP ribose hydrolase	APC-Fire 810	HIT2	Activation marker
CD45	Protein tyrosine phosphatase receptor C	PerCP	HI30	Pan leucocyte marker
CD49a	Integrin alpha 1, VLA-1, ITGA1, ITA1	BV750	SR84	Migration, tissue residency
CD49e	integrin α5	Vio Bright FITC	REA686	Cell adhesion
CD56	Neural cell adhesion molecule (NCAM)	BUV563	NCAM16.2	NK subsets, activation
CD57	HNK-2, Leu-7	APC-Vio 770	REA769	Maturation marker
CD66b	CEACAM8, CGM6, NCA-95	Pacific Blue	G10F5	Exclusion granulocytes

(Continued)

TABLE 1 Continued

Specificity	Alternative name	Fluorochrome	Clone	Purpose/function
CD69	Cluster of differentiation 69	BUV737	FN50	Migration, tissue residency, activation
CD85j	ILT2, LIR-1	RB780	GHI/75	Inhibitory receptor
CD94	killer cell lectin-like receptor subfamily D member 1, KP43	PE-Cy7	DX22	Exclusion ILC, NK subsets
CX3CR1	Fractalkine receptor	BV650	2A9-1	Migration, tissue residency
Eomes	Eomesodermin, T-box brain protein 2 (Tbr2)	eFluor 660	WD1928	Transcription factor
Granzyme B	N.A.	BV510	GB11	Cytotoxic potential
HLA-DR	MHC Class II	BUV395	G46-6 (L243)	NK cell activation marker
Ki-67	N.A.	BV605	B56	Proliferation marker
Perforin	N.A.	PerCP-eFluor 710	dG9	Cytotoxic potential
PLZF	Zinc finger and BTB domain Domain containing 16	PE	R17-809	Transcription factor
Tbet	T-box transcription factor, Tbx21	BV785	4B10	Transcription factor
TIGIT	T-cell immunoreceptor with Ig and ITIM domains, WUCAM, VSTM3	APC	MBSA43	Checkpoint inhibitor molecule
Viability	N.A.	Live Dead UV Blue	NA	Viability

Antigens included in the panel annotated according to the CD classification (where applicable) with their alternative name, assigned fluorochrome, clone and the purpose/function in the panel.

the staining protocol. 5 µl of True-Stain Monocyte Blocker was added before adding dilutions of antibodies. Antibodies, whether bottled at µg/test or ul/test, were tested starting at two-fold the manufacturer recommended titer, followed by seven serial dilutions (except PLZF; 6 serial dilutions). All titrations were done in a total volume of 250 µl for 25 minutes at RT. Optimal titers were selected based on highest staining index, saturation of percentage positives and signal intensities (Median Fluorescence Intensity, MFI) as described (54). Files were unmixed with autofluorescence (AF) extraction and concatenated for analysis using FCS Express™ version 7. Concatenated plots of titration results as well as the stain indices and the frequencies of the positive populations are depicted in Supplementary Figures 3A, B respectively. The selected titers for all reagents are listed in Supplementary Table 1. Two markers that were detected at very low frequency in PBMCs (CD49a and CD186) were additionally titrated on liver samples from a HD, confirming that the selected titer for PBMCs also applied to liver samples (data not shown). In addition, we carefully evaluated non-specific binding in parallel to the selection of the optimal titers based upon the criteria mentioned above. As expected, the use of True-Stain Monocyte Blocker™ significantly eliminated non-specific staining on monocytes for cyanine-based fluorochromes. Therefore, all titrations and multicolor staining were done with the inclusion of True-Stain Monocyte Blocker™. Of note, the inclusion of Fc-block had no effect on monocytes background staining and did not improve further the effect of adding True-Stain Monocyte Blocker™ (data not shown).

3.3 Effect of the digestion protocol on reagent performance

As liver samples preparation required digestion steps, it was important to verify that the expression of the markers in the panel was not affected by this treatment. We therefore assessed the impact of the dissociation protocol on the antigen integrity on PBMCs by comparing the percentage of positive populations and staining intensities to untreated PBMCs of the same donor after staining with the optimal titers. Although liver samples might be less sensitive to the digestion procedure, either because some cell epitopes can be hidden due to the association of cells to the extracellular matrix or because of the presence of tissue polyphenols that can partially inhibit digestive enzymes, PBMCs that undergo enzymatic digestion does provide important information on whether the antigens detected in the panel contain a peptide substrate for the digestion enzymes used in the protocol. Supplementary Figure 4A shows markers that were not affected by enzyme treatment. Pseudocolor plots were used for CD159c, CD69 and CD49a, as the frequency of these populations was low in the tested samples. CD159c showed no changes in MFI and frequency after digestion. On the other hand, CD69 and CD49a showed an increase in percentage positive events but similar staining intensities after digestion (Supplementary Figure 4B). We observed a decrease in the MFI of CD56 after digestion, as previously described (11). However, the percentage of $CD56^+$ events remained the same (Supplementary Figure 4C) which confirmed that this marker can be used with

confidence for NK cell phenotyping in digested tissues. Supplementary Figures 4D, E illustrate the loss of signal of NKp80 and CD337 (NKp30) after the digestion protocol, regardless of the antibody clone used to stain the cells. While we originally intended to target these antigens in our panel, we decided to exclude them based on these findings. Of note, loss of NKp80 and CD337 staining upon treatment of PBMCs with different commercially available digestion kits has been documented by the manufacturer (Miltenyi Biotech; https://static.miltenyibiotec.com/asset/150655405641/document_a8tksr6uf95id9ohsujoh08q0o?content-disposition=inline,https://static.miltenyibiotec.com/asset/150655405641/document_p5pedude156p1dta8vo2aelc7s?content-disposition=inline).

3.4 Sequential staining

Sequential staining has been shown to be beneficial when working with high dimensional flow cytometry panels either due to effects of different staining volumes or steric hindrance of antibody-fluorochrome conjugates combinations (51, 52). Optimization of the staining protocol was therefore performed, and we concluded that the staining for CD161 and CD314 needed to be done as a first staining step (cocktail A). Similarly, addition of NK cell receptors antibodies in a separate staining step (cocktail B) improved the resolution for CD159a, CD335 and CD85j when compared with the staining including those antibodies in the master mix (cocktail C) (Supplementary Figure 5A). MFI and frequencies of positive populations are provided in Supplementary Figure 5B. Although NKG2c was not evaluated the decision was made to add this antibody at the same step as other NK cell receptors (cocktail B). Based on previous reports that the resolution of the chemokine receptors CD195, CX3CR1 and CD183 is negatively impacted when stained alongside other antigens (51, 52, 55), we decided to also add these antibodies sequentially. In order to respect the order of addition of these antibodies as described, CD183 was added to cocktail A while CX3CR1 and CD195 were added sequentially after cocktail B. As sequential staining leads to longer incubation times than the 25 min set for titrations, we also decided to rerun antibody titrations with incubation times matching those of the multicolor tube staining: 35 min for CD195, 45 min for CX3CR1, 55 min for antibodies of cocktail B and 65 min for antibodies of cocktail A. Although the stain indices were overall improved with longer times of incubation, no difference was observed in positive population frequencies or optimal titers (data not shown). The final order of addition is presented in the protocol and outlined in Supplementary Figure 6E and Supplementary Table 1.

3.5 Thawing PBMCs and liver samples

After thawing, cell recovery and viability must be assessed to ensure no artifacts are introduced in the data. The cell recoveries and viability of the samples used in this study, and the final number of NK cells acquired is provided in Supplementary Table 2.

Note: Handling of human biological components should be done in accordance with regional and institutional biosafety policies and/or requirements.

1. Pre-warm thawing medium at 37 °C for at least 30 minutes.
2. Thaw cells as quickly as possible.
3. Thaw cryo-vial in a 37 °C water bath, until only a small piece of ice remains.
4. Transfer the contents of cryo-vial to 50 ml conical tube.
5. Add 1 ml of warm thawing medium to the empty cryo-vial. Leave aside until step 8.
6. Drop-by-drop add 5 ml of thawing medium to the cells in the 50 ml tube. While adding, gently mix the 50 ml tube (with a pipette in one hand and in the other the 50 ml tube, add the thawing medium while you gently swirl the tube).
7. After the first 5 ml of thawing medium has been added, add the next 5 ml a little bit faster (a few drops at a time).
8. After 10 ml have been added, pour the 1 ml content of the cryo-vial into the 50 ml tube.
9. Add an additional volume of thawing medium to bring the total volume to 20 ml.
10. Spin at 400 g for 5 minutes.
11. Decant supernatant carefully without disturbing the pellet.
12. Gently resuspend the pellet in 2 ml of thawing medium. Take 5 µl for counting.
13. Complete to 20 ml.
14. Repeat steps 10 and 11.
15. Resuspend in staining buffer supplemented with 5 µl of True-Stain Monocyte Blocker/100µl of cell suspension to reach an approximate concentration of $10x10^6$/ml for PBMCs. Liver samples ($0.4\text{-}1.5x10^6$ cells) were resuspended in 500 µl staining buffer supplemented with 5 µl True-Stain Monocyte Blocker™/100 µl cell suspension and filtered through a 70 µm tissue strainer before staining.
16. Once the staining has begun, samples need to be processed without delay.

3.6 Viability dye, antibody dilutions and multicolor (MC) antibody cocktails preparation

1. Thaw an aliquot of Live/Dead Fixable Blue viability dye (aliquoted according to manufacturer recommendations).
2. Prepare a 1:40 dilution in PBS by adding 5 µl of the viability dye to 195 µl PBS.
3. Keep in the dark until usage.
4. Prepare antibody dilutions as needed in staining buffer.
5. Prepare MC antibody cocktails A, B and C (surface) and D (intracellular) according to Supplementary Table 1 by adding 10 µl Brilliant Stain Buffer Plus into an Eppendorf tube and adding each antibody at the determined titer. Mix gently after adding each antibody.

6. Add 10 µl of prediluted viability dye to the pellet, vortex gently and incubate for 15 minutes in the dark at RT.

3.7 Staining protocol for MC samples and reference controls

A summary of the staining protocol is depicted in Supplementary Figure 6.

Samples were aliquoted over the different tubes before staining. For MC tubes 300 µl PBMCs (± $3x10^6$ PBMCs) and 400 µl liver cells (± 0.32 – 1.36 $x10^6$ liver cells) were aliquoted and 100 ul for each RC (± $1x10^6$ cells PBMC). Additionally, 100 ul of each sample was aliquoted to be used as a sample specific unstained. For the RC on beads, the manufacturer recommended volume of beads was aliquoted per tube (1 drop per tube after vigorous vortexing of the stock vial) and washed once in staining buffer before addition of antibodies. Both the MC tubes and RC for viability staining should be washed with 3 ml PBS to remove any protein before viability staining.

1. Add 3 ml PBS and centrifuge at 400 g for 5 minutes at RT.
2. Decant supernatant and vortex gently.
3. Repeat step 1 and 2
4. Add 10 µl of prediluted viability dye to the pellet, vortex gently and incubate for 15 minutes in the dark at RT.
5. Wash the MC tubes and all the RC with 3 ml staining buffer
6. Centrifuge at 400 g for 5 minutes at RT
7. Decant supernatant and vortex gently.
8. In the meantime, stain the RC (cells or beads) for surface markers with the appropriate titers of antibodies: for the RC on cells, add 5 µl of True-Stain Monocyte Blocker to all RC tubes before adding the antibodies.
9. Add 300 µl of staining buffer to the viability RC and store in the dark.
10. Add 10 µl of Brilliant Stain Buffer Plus and 5 µl of True-Stain Monocyte Blocker™ to all the MC tubes and vortex gently.
11. Add MC antibody cocktail A and incubate for 10 minutes in the dark at RT; vortex gently.
12. Add the MC antibody cocktail B (see Supplementary Table 1, calculate how much volume is needed per sample based on the volumes of each of the individual antibodies), vortex gently and incubate for 10 minutes in the dark at RT.
13. Add anti-CX3CR1 BV650 and incubate for 10 minutes in the dark at RT; vortex gently.
14. Add anti-CD195 BUV661 and incubate for 5 minutes in the dark at RT; vortex gently.
15. Add the MC antibody cocktail C (see Supplementary Table 1, calculate how much volume is needed per sample based on the volumes of each of the antibodies) and incubate for 25 minutes in the dark; vortex gently.
16. Add 3 ml staining buffer.
17. Centrifuge at 400 g for 5 minutes at RT
18. Decant supernatant and vortex gently
19. Repeat steps 16, 17 and 18.
20. Add 250 µl of 4x prediluted fixative solution (eBioscience™ Foxp3/Transcription Factor Staining Buffer Set), prewarmed to RT, to all the MC tubes and RC and vortex gently. Incubate for 40 minutes at RT; repeat vortexing after 20 min. NOTE: if beads are used for intracellular markers, they should not be treated with fixative but only stained after washing with permeabilization buffer to ensure that the intracellular antibody reagent is exposed to the same condition/buffers as in the MC sample.
21. Add 2 ml of 10x prediluted permeabilization buffer (eBioscience™ Foxp3/Transcription Factor Staining Buffer Set), prewarmed to RT, to the MC tubes and all the RC.
22. Centrifuge at 800 g for 5 minutes (it is important to increase the centrifugation speed at this step and thereafter as cellular weight decreases after fixation and particularly permeabilization).
23. Decant supernatant and vortex gently.
24. Repeat step 21 and leave the tubes in the dark at RT for 5–10 minutes before proceeding with step 25 (waiting before centrifugation ensures that cells are permeabilized before adding the antibodies for intracellular staining). The RC on beads can be washed once.
25. Repeat step 22–23.
26. Add the MC antibody cocktail D (see Supplementary Table 1, calculate how much volume is needed per sample based on the volumes of each of the intracellular antibodies), vortex gently, and incubate for 30 minutes in the dark at RT. At the same time add the intracellular antibodies to the RC on cells or beads at the indicated titers.
27. Add 2 ml of 10x prediluted permeabilization buffer and leave the tubes in the dark at RT for 5-10 minutes before proceeding with step 28 (waiting before centrifugation helps reduce unspecific staining).
28. Centrifuge at 800 g for 5 minutes.
29. Decant supernatant and vortex gently.
30. steps 27, 28 and 29.

If samples are immediately acquired, follow the steps below:

31. Wash with 2 ml of staining buffer.
32. Centrifuge at 800 g for 5 minutes.
33. Decant supernatant and vortex gently.
34. Add 150 µl of staining buffer and acquire using CytekAssaySetting (CAS) at medium flowrate.

If samples are acquired after 4 h follow the steps below:

35. Add 200 µl of 1% paraformaldehyde (4% diluted to 1% with PBS) and incubate for 15 minutes in the dark at RT; vortex gently.
36. Wash with 2 ml of staining buffer.
37. Centrifuge at 800 g for 5 minutes.
38. Decant supernatant and vortex gently
39. Add 150 µl of staining buffer and acquire or store at 4 degrees in the dark until analysis within 24h (longer times until acquisition were not tested).

3.8 Instrument set-up and QC

Daily Instrument Quality Control (Daily QC) was run before each new experiment acquisition using SpectroFlo® QC beads, lot 2005. Settings provided by the manufacturer (referred to as CytekAssaySetting in SpectroFlo® software) were used as a starting point for instrument setup with adjustments in FSC-A and SSC-A gains and FSC threshold settings for optimal visualization of lymphocytes vs. monocyte populations and reducing the collection of debris.

3.9 Determination of optimal controls for unmixing

Optimal single stained controls (named Reference Controls in SpectroFlo software, RC) are essential to ensure accurate unmixing. As a first step of RC optimization, determining if beads lead to accurate unmixing is essential. Indeed, the spectrum of antibody-conjugated fluorochromes can differ when binding to cells or beads. As these emission spectrum mismatches can lead to unmixing errors in an assay specific manner, the use of beads must be assessed empirically (51). To do so, we stained both beads and cells in parallel, applying the same protocol, reagents and titers as for the MC sample. Optimal RC were selected by the method described in (51). Description of optimal RC (cells or beads) and cell numbers to be acquired to ensure collection of enough positive events are listed in Supplementary Table 3. This panel also includes a combination of two markers in PE-Cy5.5, namely CD158b and CD158a-h. As PE-Cy5.5 is a tandem-dye, its spectrum can vary from lot to lot due to differences in energy transfer between donor and acceptor molecules. We therefore assessed whether the two spectra were different. We observed a perfect overlap between both signatures (data not shown) showing that both markers in PE-Cy5.5 have identical spectra and can therefore be used as RC indifferently.

3.10 Autofluorescence extraction and exclusion of RBCs

Cellular suspensions from digested solid tissues can be highly and heterogeneously autofluorescent. Several publications reported that including multiple autofluorescence (AF) spectra as reference controls to perform the unmixing might be indispensable to ensure that data is exempt of any artifact and leads to correct result interpretation (56–60). The liver being a highly AF tissue, we then wondered whether our samples needed the application of such approach. In the case of this study, although liver samples displayed a high and heterogenous AF (Supplementary Figure 7A), we found that applying multiple AF extraction was not required for accurate unmixing and resolution of the NK markers as lymphoid cells showed homogenous AF as opposed to cell types such as myeloid or mesenchymal cells. Despite a great variability in the morphology of the cells extracted from the liver, lymphocytes were easily identified by SSC and FSC. We found that gating tightly on the corresponding population was enough to clean up most of the irrelevant AF spectral signatures and obtain a well-defined AF spectrum (Supplementary Figure 7B). We therefore applied a default unmixing with AF extraction with the gate set on the lymphocytes. However, despite the successful cleaning of irrelevant AF using the SSC and FSC parameters, one a small population still appeared to be unproperly unmixed (red arrows in top and middle lanes, Supplementary Figure 7C) (61). This was evidenced by its super negative median fluorescence intensities (MFI) in several fluorescence parameters, suggesting that a specific cell lineage lying in the lymphocyte gate had a different AF. Because of their small FSC-SSC overlapping partially with lymphocytes, we hypothesized these could be RBCs. One of the advantages of the Aurora spectral analyzer used in this study is the possibility to measure light scattering using both the violet and the blue laser simultaneously. Because RBCs lack a nucleus, their absorbance of the light at these wavelengths is different from nucleated cells allowing for their easy discrimination as already reported in a previous publication (61). After further investigation, this population was identified as RBCs based on their scattering of the blue and violet laser light. We could therefore easily eliminate them with an appropriate gating strategy (Supplementary Figure 7C bottom lane). Once an accurate gating strategy was applied to the data, we found that a default AF extraction is highly beneficial, especially for those fluorochromes emitting in high AF area (Supplementary Figure 7D).

3.11 Evaluation of the unmixing accuracy of MC samples

MC samples were unmixed with the SpectroFlo® software V3.2.1. To check the unmixing accuracy of the MC tube steps were followed as in (51). Briefly, the data were cleaned up (cleaning gates included time, singlets, live, and aggregate exclusion when needed), and NxN permutations were displayed. The multicolor samples were screened for unmixing errors by visually inspecting the NxN plots of one fluorochrome versus all the other fluorochromes in the panel. Spillover corrections were only applied when the observed unmixing errors were between fluorochromes with known spillover and were guided based on well-characterized and described staining patterns. Unmixing accuracy was very high with 3–16 corrections below 5% in the 1722 combinations (including the AF parameter) except for BUV661 into BV605 for which corrections between 3.2 and 7.2 % were needed. The relatively high correction for BUV661 into BV605 was confirmed by Fluorescence Minus One controls (data not shown).

3.12 Panel resolution assessment

To ensure that the theoretical panel design resulted in limited areas of spread and, if spread occurred, this was in regions in which markers are not coexpressed or at dim levels, we first assessed spread by calculating the SSM of PBMC stained with the final panel reagents at established titers. Of the 1,369 possible combinations of

fluorochromes, only 17 marker fluorochrome combinations had a spillover and spread value (SSV) above 6 (Supplementary Figure 8A). The limited number of combinations exhibiting relatively high spread confirmed the robustness of the fluorochrome selection and panel design. Supplementary Figure 8B, C show a few marker combinations with SSV above 6 for PBMCs **(B)** and liver from a HD **(C)**. The highest SSV was for the Granzyme BV510 and CD16 BUV496 combination, but its impact on data resolution was negligible.

Resolution loss can also occur because of interactions between reagents, such as steric hindrance. We therefore systematically compared the resolution of each marker in the MC tube with its corresponding RC, both on PBMCs and on liver. For the resolution comparison we overlayed the histograms of gated singlets/lymphocytes or singlets/monocytes (when applicable) of single stained samples (grey filled) with the MC sample (bold black line). Additionally, we overlayed the gated total NK cells (bold blue line; defined by sequentially gating on $CD45^+CD3^-$Lin- and subsequently gating out ILC's ($CD94^-CD127^+$), $CD56^-$HLA-DR^+ and $CD56^-CD16^-$ events) for NK cell markers. Note that the single stained sample and the MC sample were obtained from the same donor and stained with the exact same protocol (incubation time, volume, fixation and permeabilization methods) in order to make an accurate comparison. Supplementary Figures 9A, B show a perfect match for all markers both in PBMCs and HCC liver. Importantly, the NK cell gated population demonstrated excellent resolution of all NK cell markers, therefore confirming appropriate panel design.

3.13 Multidimensional analysis

After gating on lymphocytes using FSC-A/SSC-A, excluding the doublets by gating on FSC-A/FSC-H, excluding the RBCs by gating on SSC-A/SSC-B-A, gating on viable leukocytes ($CD45^+$ Live $Dead\ Blue^-$), getting rid of B-cells/monocytes/pDC/granulocytes (Lin^-) and T-cells ($CD3^-$), gated $CD94^{+/-}CD127^{+/-}$ events were exported (from SpectroFlo®; see gating strategy Figures 2A, B) into the OMIQ platform (https://www.omiq.ai/). Files were further analyzed using an OMIQ pipeline according to (52) with adjustments of using FlowCut (62) and Phenograph (63). After scaling optimization (Arcsinh), the FlowCut algorithm was applied to remove outlier events due to abnormal flow behaviors. All files were then further manually gated to exclude $CD127^+CD94^-$ and HLA-DR^+CD56^- events (as in Figures 2A, B) and finally gated on total NK cells ($CD56^{+/-}CD16^+$ encompassing early, mature and terminal NK cells). Files were then concatenated before running the Phenograph clustering algorithm, Unified Manifold Approximation and Projection (UMAP) algorithm and heatmap generation. Clustering analysis of total NK cells with the PhenoGraph algorithm, included all markers (except Live Dead Blue, CD45, Lin, and CD3) with using 40 K Nearest Neighbors and Euclidean distance metrics. After PhenoGraph analysis, dimensionality was reduced by means of UMAP with the following parameters and settings: all markers as parameters (except Live Dead Blue, CD45, Lin and CD3) and including the PhenoGraph parameter, Neighbors 80, Minimum Distance 0.7, components 2, Euclidean metric, Learning rate 1, Epochs 250, Random Seed 5320 and spectral embedding initialization. PhenoGraph clusters were overlayed on the UMAP for visualization of the distribution of the clusters between sample types and individual samples. Following the UMAP analysis, a heatmap was generated by combining all files and hierarchically ordering the PhenoGraph clusters.

4 Results

4.1 Manual gating strategy to identify major NK cells subsets in the periphery and liver

The manual gating strategies used to define NK cells in PBMCs and liver samples are illustrated in Figures 2A, B. First several cleaning gates were applied: gating on lymphocytes using FSC-A/SSC-A, exclusion of doublets by gating on FSC-A/FSC-H, followed by RBC exclusion gate using the SSC-A and SSC-B-A parameters, gating on viable leucocytes and finally, exclusion of B cells/monocytes/pDCs/ granulocytes and T cells. Further gating was performed by gating on **1)** $CD94^{+/-}CD127^{dim/-}$ as described in (64, 65) and subsequently **2)** by including only $CD56^{+/-}$HLA-DR^{dim} events and **3)** gating total NK cells based on $CD56^{+/-}CD16^+$ events.

4.2 Subsets and phenotypes of peripheral NK cells

The gated total NK cells in PBMCs were classified into 3 subsets by means of CD56 and CD16 expression levels. Using this gating strategy, we clearly identified the three classical subsets described in PBMCs, namely early, mature, and terminal NK cells as illustrated in Figure 2A. Further details of the expression profiles of NK cell markers in the three main subsets are also shown in Figure 2A in which the antigens are classified according to the functional properties of the markers. Early NK cells were enriched for expression of the inhibitory receptor CD159a, expressed high levels of the activating receptor CD335 and low levels of granzyme B and were negative for perforin. Expression of CD158b, a-h, as well as CD57 was absent or too low to be resolved, indicating the absence of clonal expansion and maturation respectively. The pattern of CD11b and CD27 expression showed enrichment of the $CD11b^+CD27^+$ population, a population described to be the most efficient in secreting cytokines in early NK cells (39). Furthermore, early NK cells were enriched for CD161 expression when compared to the other NK cell subsets, the engagement of which inhibits cytotoxicity and triggers IFN-ɣ production (66, 67). Adding another nuance to the definition of the functional properties of early NK cells was the detection of a subset expressing high levels of CD183. Interestingly, this phenotype has been described as producing higher levels of IFN-γ and having higher degranulation capacity (68).

In accordance with previous publications, mature NK cells expressed CD57 and CD158b, a_h, indicating maturation and clonal expansion, and higher levels of CX3CR1 as compared to

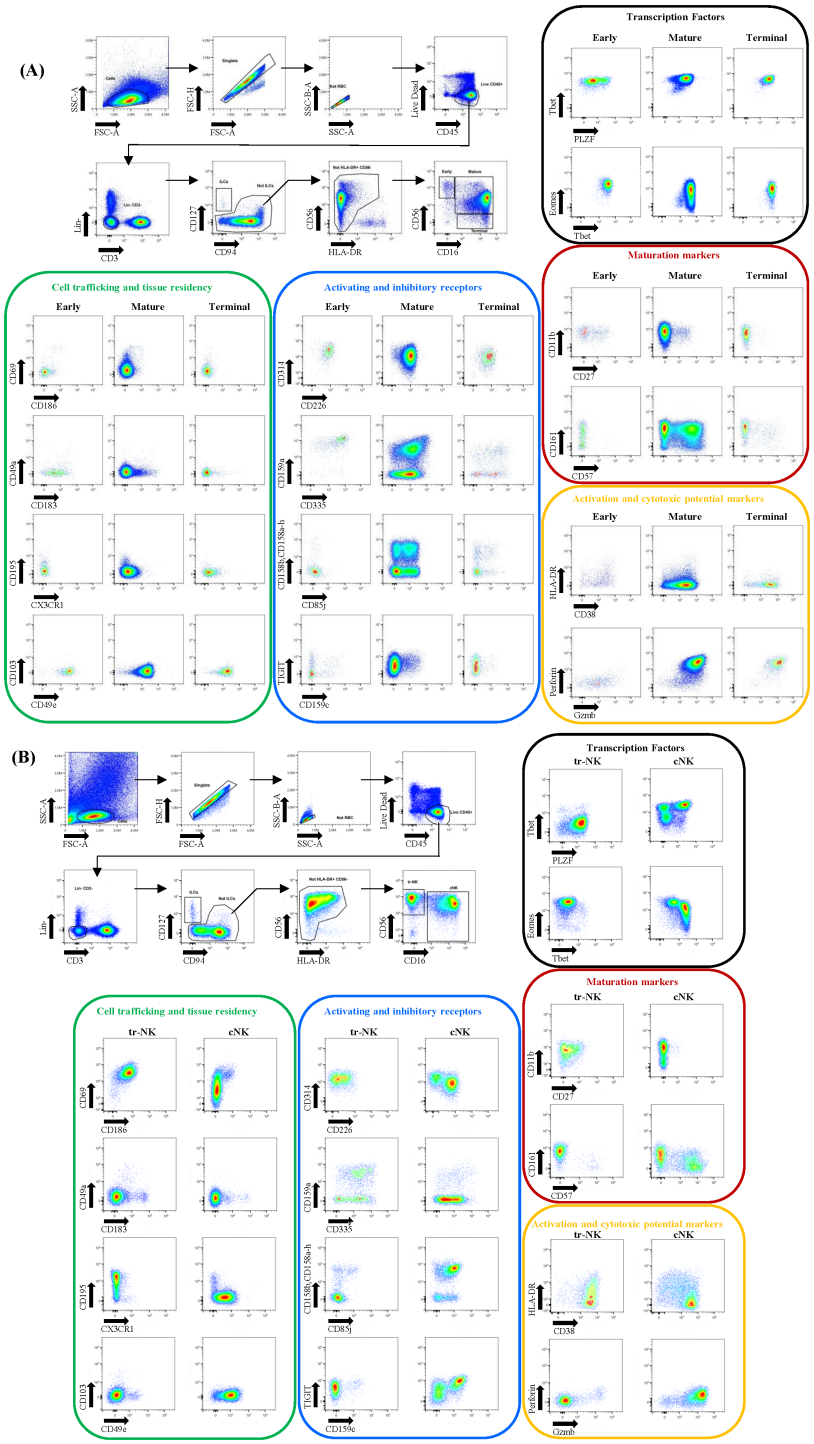

FIGURE 2
Gating strategy for NK cell identification in PBMCs and liver samples. **(A)** Gating strategy for NK cell identification in PBMCs. Three major NK cell subsets were gated: Early, Mature and Terminal NK cells. **(B)** Gating strategy for NK cell identification in HD liver. Two major NK cell subsets were gated: tr-NK and cNK cells. The expression levels of markers indicating cell trafficking/tissue residency, activation and inhibitory receptors, maturation, transcription factors and activation and cytotoxic potential are shown for each gated major subset.

early NK cells (5, 16, 40, 69). The cytotoxic molecules Granzyme B and Perforin were highly expressed as compared to early NK cells as described before (3, 5, 69). However, expression patterns of CD57/CD161, CD159a/CD335, TIGIT/CD158b, a_h/CD85j, CD11b/CD27, and TIGIT/CD159c could indicate the presence of different phenotypes within mature NK cells (Figure 2A). Additionally, some mature NK cells coexpressed CD186 and CD69 and were found in all 5 donors and were also observed in early NK cells. These $CD69^{+}CD186^{+}$ NK cells, detected in both the periphery and the liver, might represent a rare subset of NK cells with liver/tissue homing

capacity (37, 70). The panel also captured a mature NK cell subset with enhanced effector responses and clonal expansion: the so-called adaptive NK cells that are $CD56^{dim}CD16^{+}CD159c^{+}CD159a^{-}CD57^{+}CD161^{+}PLZF^{low}CD85j^{+}CD158b$, a_h^{+}, a phenotype enforced by HCMV exposure and detected at higher frequencies in HCMV-positive individuals (16, 41, 42, 71–74). The sample used as an example of the panel performance in Figure 2A shows the expression of CD159c in mature NK cells that, with the markers present in the panel, could potentially be further defined in terms of the expression of markers associated with adaptive NK cells. Terminal $CD56^{-}CD16^{-}$ NK cells are believed to be derived from mature NK cells with interchangeable phenotypes reflected by modulation of CD159a and KIRs expression (9). Those cells express higher levels of KIRs, CD57, CD85j, TIGIT, lower levels of the activating receptors CD314 and CD335 and expand with age and under chronic infection or lymphopenic conditions like hematopoietic stem cell transplantation (HSCT (75–78). Terminal NK cells, although dysfunctional in terms of expressing lower levels of cytotoxic molecules and presenting a lower responsiveness to cytokines, can still exert cytotoxicity through other mechanisms like ADCC or death-receptor mediated cytotoxicity. As expected, we detected terminal NK cells at low frequencies in the PBMC of all donors with variable expression patterns of CD159a, KIRs, CD57, CD314, CD335 as well as TIGIT and CD85j. In terms of transcription factors (TF), the expression of Eomes was higher in early NK cells as compared to mature and terminal NK cells related to the different roles these TFs have in the process of NK cell maturation (79).

4.3 Subsets and phenotypes of liver NK cells

Liver NK cells are divided into two main subsets based upon CD56 and CD16 expression, namely the $CD56^{bright}CD16^{-}$ and $CD56^{dim}CD16^{+}$ subset. In the healthy liver, the two subsets are present at equal frequencies in contrast to the distribution seen in PBMCs (18, 34). The $CD56^{bright}CD16^{-}$ subset has been further defined as $CD56^{bright}CD16^{-}CD69^{+}CD186^{+}Eomes^{Hi}Tbet^{low}PLZF^{Hi}TIGIT^{+}CD49e^{-}CX3CR1^{-}$ (23, 31, 33–37, 80, 81) and are called tr-NK cells. Tr-NK cells possibly originate from peripheral $CD56^{dim}CD16^{+}CD69^{+}CD186^{+}Eomes^{low}Tbet^{hi}PLZF^{hi}$ NK cells (35, 37). The $CD56^{dim}CD16^{+}$ subset represents phenotypes very similar to peripheral mature NK cells as they are mainly NK cells recirculating from the periphery and annotated as transient conventional NK cells (cNK). The cNK subsets express CD49e high levels of T bet and low levels of Eomes in contrast to tr-NK cells (18, 31, 33). Within the tr-NK and cNK subsets, additional populations are distinguished based upon CD159c expression with $CD159c^{+}$ NK cells representing adaptive NK cells prone to respond upon viral rechallenge (18, 26, 36). Given this information, we based the manual gating strategy upon expression levels of CD56 and CD16, after gating on $CD94^{+/-}CD127^{+/-}CD56^{+/-}$HLA-$DR^{dim/-}$ events. Figure 2B shows that liver NK cells can be clearly divided into the two described main populations of tr-NK and cNK with a near equal distribution in terms of frequencies. Most $CD69^{+}CD186^{+}$ liver NK cells are found in the $CD56^{bright}CD16^{-}$ subset, the latter also being predominantly $Eomes^{hi}Tbet^{low}CD49e^{-}CX3CR1^{-}$. In 2 out of 3 HD livers, we observed adaptive NK cells in both the $CD56^{bright}CD16^{-}$ and $CD56^{dim}CD16$ subsets of which one example is shown in Figure 2B. In this example, the adaptive NK cells expressed high levels of the inhibitory receptor CD85j and checkpoint inhibitor TIGIT, as also observed in adaptive NK cells present in PBMCs (Figure 2A). Additional markers showed even more granularity within the three populations of tr-NK, cNK and liver adaptive NK cells. For example, CD49a and CD103 were detected at higher frequencies in the gated tr-NK subset which both are markers of tissue residency. Furthermore, $CD11b^{+}CD27^{+}$ NK cells were enriched in the tr-NK subset and displayed a dominant expression of the inhibitory receptors CD159a, CD161 and low to no expression of CD57 and CD158b, a_h as compared to cNK cells. As described previously (31, 36), liver NK cells (tr-NK, cNK and adaptive NK cells) expressed low levels of perforin as compared to peripheral NK cells and most tr-NK cells did not express granzyme B. Additionally, we confirmed the dominance of Eomes over Tbet expression and strong PLZF expression in tr-NK cells as compared to cNK (Figure 2B), reflecting the role of Eomes and PLFZ in enforcing a tissue-resident phenotype (35, 37).

4.4 Additional phenotype information derived from multidimensional analysis

While manual gating is commonly used to demonstrate the ability to resolve populations of interest, it is generally not practical, time consuming, and can lead to a biassed and incomplete phenotyping of the samples when working with 37 parameters. Therefore, we proceeded with multidimensional analysis of total NK cells (early, mature and terminal) as outlined in Figures 2A, B, by applying the Phenograph clustering algorithm followed by the UMAP reduction algorithm. For the multidimensional analysis, we included two additional HCC liver samples. Including HCC liver samples allowed us to verify the use of the panel not only in health but also in disease state, in particular liver cancer. The gating strategy applied to define total NK cells from liver samples with HCC is the same as shown in Figure 2B. Applying the clustering algorithm to 5 PBMC donors, 3 HD liver and 2 HCC liver identified a total of 29 clusters. Before proceeding further with the analysis of cluster identity and dynamics, the significance of each cluster was verified by setting the following requirements: each cluster needed to consist of at least 100 events and/or be present in at least 3 samples, either in PBMC or liver. All clusters fulfilled these requirements (depicted in Supplementary Table 4), and we therefore proceeded with the assignment of clusters to phenotypes and/or known populations. The 29 identified clusters are illustrated in Figure 3A overlayed on the concatenated UMAP of all 10 samples.

4.5 Cluster tissue-prevalence

One of the purposes of the panel design was to be able to distinguish peripheral and tissue (liver) specific NK cells. We therefore first determined the prevalence of clusters in each

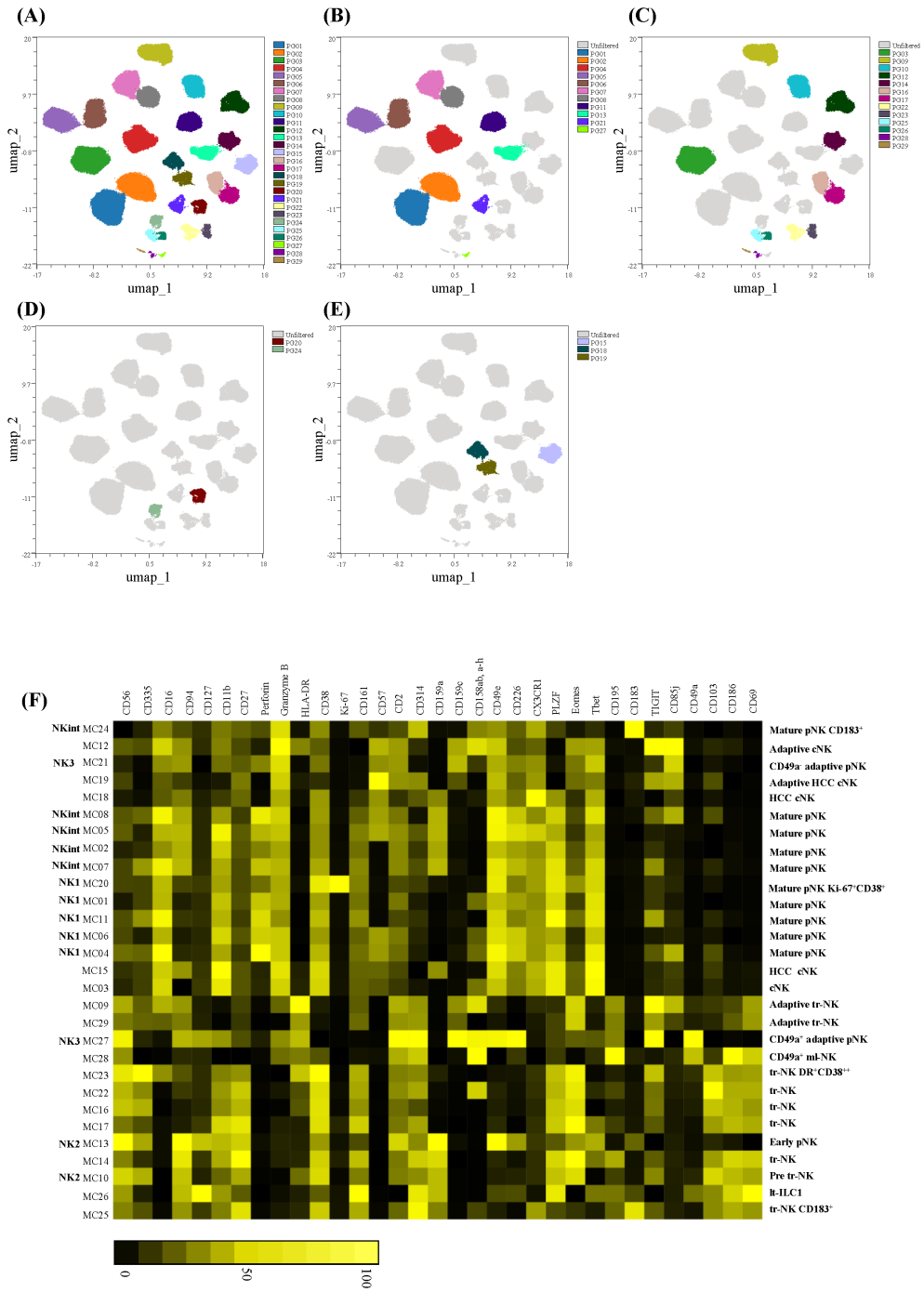

FIGURE 3
Multidimensional analysis of NK cells. Data were analyzed using the OMIQ platform with the analysis pipeline as described in the methods section. Phenograph clusters are overlayed on the concatenated UMAP of all samples for ease of visualization as in **(A)** all clusters identified, **(B)** clusters enriched in PBMCs, **(C)** clusters enriched in HD Liver, **(D)** clusters shared between PBMC and HD Liver and **(E)** clusters enriched in HCC Liver samples. **(F)** Heat-map generated of the different clusters and ordered hierarchically. The annotation of each metacluster (MC) is shown on the left with the annotation of NK1, NK2, NK3 and NKint. Annotation according to early, mature, adaptive peripheral (pNK; CD49a$^-$ or CD49a$^+$), pre tr-NK, tr-NK, CD49a$^+$ ml-NK, adaptive cNK, cNK, and lt-ILC is indicated on the right with indication of a distinct feature of the cluster when applicable. Marker intensity is depicted from black (negative) to yellow (positive) on a scale from zero to 100 percentile based on intensity per column.

sample type, as percentages of total NK cells. Our data indicated that certain clusters were either more prevalent in PBMCs as compared to HD liver (clusters 1, 2, 4-8, 11, 13, 21 and 27; Figure 3B) or in HD liver as compared to PBMCs (clusters 3, 9-10, 12, 14, 16-17, 22-23, 25-26, and 28-29; Figure 3C). Other clusters were shared between PBMCs and liver samples (clusters 20 and 24; Figure 3D), at equal percentages of total NK cells. Three clusters were prevalent in HCC liver (clusters 15, 18 and 19; Figure 3E) and

a detailed analysis of the biological significance of these clusters is provided in section 4.6.

Given the reported dynamic phenotype of NK cells based upon environmental cues (vaccination/infection history, tissue health status) and genetics (12, 82–86) we determined donor-dependent prevalence of each cluster. The percentages of each cluster of total NK cells, per individual PBMC or liver donor is displayed in Supplementary Figure 10 and events assigned to each cluster in Supplementary Table 4. This analysis shows the dominance of certain clusters in the periphery versus liver but also donor-dependent differences. For example, in the case of clusters 4 and 8 that are more prevalent in PBMCs, cluster 4 was nearly absent in PBMCs of donor 3 (1.3 %) and cluster 8 was detected at low percentages in PBMCs of donors 1, 2 and 3 (respectively 2.4%, 2.5%, and 1.4%). Clusters 9 and 10, two out of 13 clusters that were more prevalent in HD liver, represented more than 15% of total NK cells in donors 1 and 3 but were hardly detectable (<1%) in donor 2. Clusters that were prevalent in the HCC liver represented 46.5% of total NK cells for cluster 15 in HCC donor 1 (1.3% in HCC donor 2) and 44.6% for cluster 18 (1.2% in HCC donor 1) and 37.6% for cluster 19 in HCC donor 2 (0% in HCC donor 1). These three clusters were present at a low percentage in both HD liver and PBMC. Testing of the HCC liver samples was performed as proof of concept of the utility of this panel although we acknowledge the limitations of sample size.

4.6 Cluster assignment and verification

Next, we proceeded with displaying the identified clusters hierarchically by means of a heatmap for the purpose of cluster assignment and verification (Figure 3F). To facilitate further data exploration, UMAP color-continuous scatterplots of each NK cell marker in the panel are presented in Supplementary Figure 11A. The extended phenotype of each cluster is shown in Supplementary Figure 11B as overlayed scatter plots displaying the expression of each marker defining the metaclusters (left) and the position of the cluster on the UMAP (right). The final assignment of different NK cell clusters, elaborated in detail in the section below, is indicated on the left of the heatmap in Figure 3F and are annotated as peripheral early NK cells (early pNK), peripheral mature NK cells (mature pNK), peripheral adaptive NK cells (adaptive pNK either $CD49a^+$ or $CD49a^-$), liver tr-NK, adaptive/memory liver resident NK cells (ml-NK), liver circulating NK (cNK), liver circulating adaptive NK (adaptive cNK), tr-NK precursor (pre tr-NK), liver circulating NK cells or adaptive cNK prevalent in HCC (HCC cNK, adaptive HCC cNK) and Lt-ILC1s. A summary of peripheral and HD liver NK cell subsets described in the literature is given in Supplementary Table 5 that lists core markers identifying the subsets, markers enriched or expressed on additional subsets/phenotypes, their reported frequencies and specific function/properties. The information listed was used as a guide for the final Phenograph cluster assignments which is also indicated in Supplementary Table 5.

From the heatmap it could be deduced that the three main NK cell subsets in the periphery were represented in cluster 13 for early NK cells ($CD56^{bright}CD16^-CD69^+CD186^+CD335^{bright}CD127^+CD11b^+CD27^+CD183^+CD159a^+CD159c^-CD161^{low}CD57^-CD158b$, $a\_h^-CD49e^+CX3CR1^-Eomes^{low}Tbet^{low}$) and in clusters 1-2, 4-8, 11, 20 and 24 for mature non-adaptive NK cells ($CD56^{dim}CD16^-CD69^-CD186^-Eomes^{Int}Tbet^+PLZF^+CD127^-CD11b^+CD27^{dim}CD49e^+CX3CR1^+CD226^+$). Mature NK cell clusters had variable expression levels of CD335, CD94, CD161, CD57, CD158b, a_h. Some non-adaptive mature NK cells were distinctive in expressing high levels of CD183 (cluster 24) or high levels of Ki-67 and CD38 (cluster 20). No specific cluster(s) could be assigned to terminal NK cells in agreement with their described highly variable phenotype (9). NK cells that corresponded to the described peripheral "classical" adaptive NK cells ($CD49a^-CD127^-$ $CD56^{dim}CD16^+CD159c^+CD159a^-CD57^+CD2^+CD161^-CD49e^+CX3CR1^+CD69^-CD186^-Eomes^+Tbet^+PLZF^{low}$ CD158b, $a\_h^+Perforin^+GranzymeB^+CD85j^+$) resided in cluster 21 and were detected in the PBMCs of donor 3 (24.8%) and donor 5 (2%).

Tr-NK cells, defined as $CD56^+CD16^-CD57^-CD69^+CD186^+Eomes^{hi}Tbet^{low}PLZF^{bright}CD2^+CD49e^-CX3CR1^-CD226^-$, were clearly distinguished from the rest of the clusters in the heatmap and resided in clusters 10, 14, 16-17, 22-23, 25. These clusters could be distinguished by different expression levels of CD94, absence or presence of CD159a, and differences in expression levels of CD335, CD195, HLA-DR. All tr-NK cells were enriched for TIGIT and CD103 expression as described previously (31, 35, 81). Additionally, all tr-NK clusters were $CD11b^+CD27^+CD161^{bright}CD38^{bright}Perforin^-GranzymeB^-$ indicating that tr-NK cells have less cytotoxic capacity but might have enhanced pro-inflammatory potential as described for peripheral $CD11b^+CD27^+$NK cells (39). The absence of CD49e, CX3CR1 and increased CD195 expression indicated tissue residency, as described for tr-NK cells (23, 31, 33). Overall, the cluster designations of tr-NK cells were in accordance with their previously described phenotype.

As CD49a has been described to identify a liver-specific NK cells subset (36) and because the frequency of intrahepatic $CD49a^+$ NK cells has been shown to be associated with tumor progression and clinical outcome in HCC (87) we analyzed the $CD49a^+$ clusters in further detail. Two clusters expressed high levels of CD49a, namely clusters 27 and 28, one being more prevalent in PBMCs (cluster 27) and the other one in HD liver (cluster 28). We then proceeded with a detailed cluster verification of cluster 27 and 28 in several manners. First, we visualized the prevalence of the clusters per sample type by superimposing the location of the 2 clusters on concatenated UMAPs for PBMC (Figure 4A) and HD liver samples (Figure 4B). Additionally, the expression of all NK markers in each cluster is illustrated as color-coded clusters superimposed on total NK cells (unfiltered) of all concatenated files in PBMCs (Figure 4C) and HD liver (Figure 4D). Furthermore, we generated bi-exponential plots of selected markers defining the clusters, either on total NK cells (unfiltered; grey) of concatenated PBMC (Figure 4E) or concatenated HD liver samples (Figure 4F) with the color-coded clusters superimposed. UMAPs of each PBMC donor (Figure 4G) or HD liver donor (Figure 4H) visualize the presence of the clusters per individual sample and donor-dependent variety. The phenotype of cluster 28 was confirmed as being $CD56^{bright}CD16^-CD69^+CD186^+$

10.3389/fimmu.2025.1609732

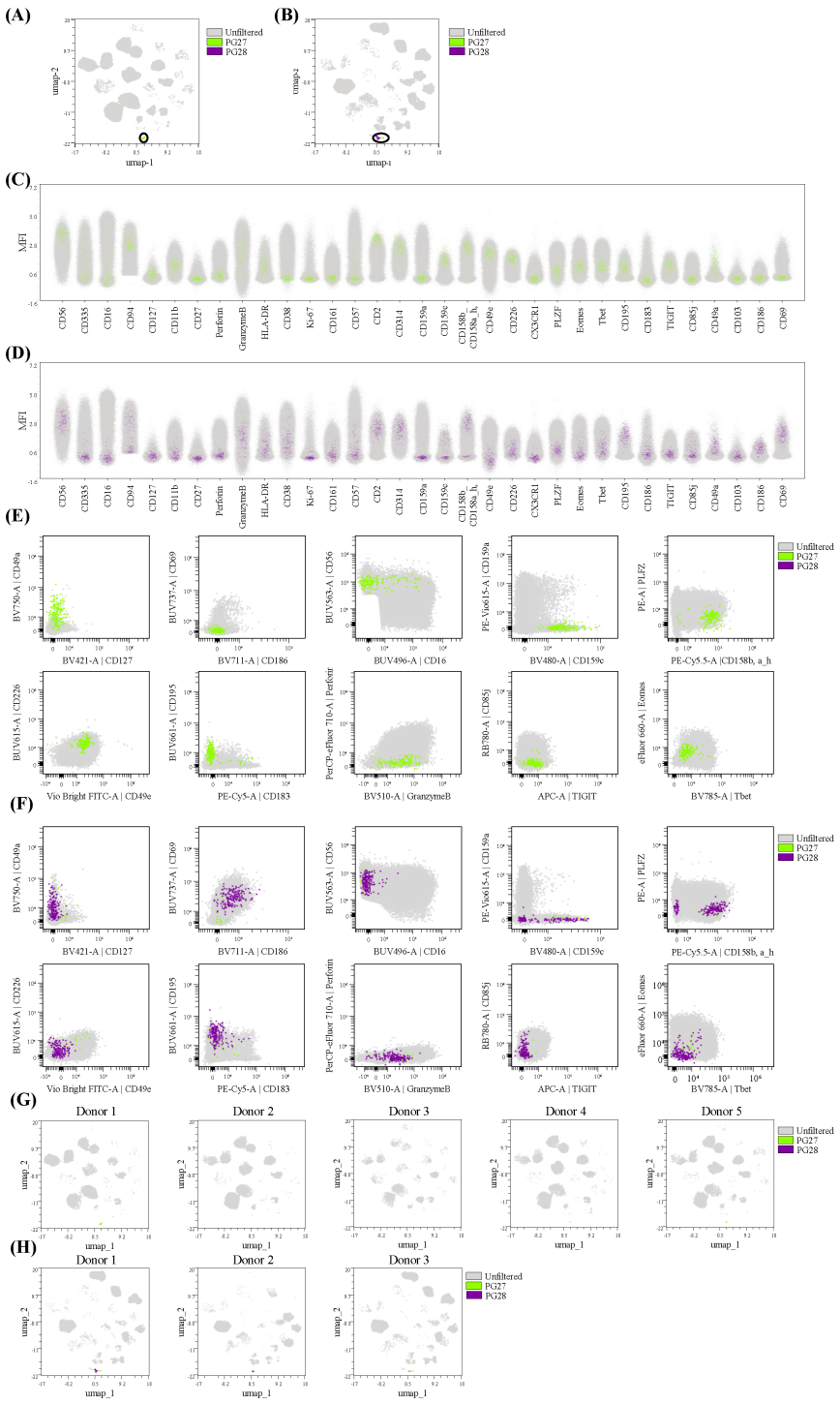

FIGURE 4
Detailed cluster verification. Verification of clusters 27 and 28 was performed by **(A)** superimposing the color-coded clusters (green; cluster 27, purple: cluster 28) on the concatenated UMAPs (grey; unfiltered) of PBMCs and **(B)** HD liver samples. Displaying the expression levels of all NK cell markers in **(C)** cluster 27 and **(D)** cluster 28 by superimposing the color-coded clusters on all concatenated files (grey; unfiltered). Generating biexponential plots of the color-coded clusters with markers unique and/or differentially expressed between the two clusters as indicated in the heatmap and superimposed on **(E)** concatenated PBMCs and **(F)** concatenated HD liver samples. Superimposing the color-coded clusters on the UMAP per individual donor in **(G)** PBMC and **(H)** HD liver samples to confirm tissue-specificity and donor-dependency of each cluster.

Eomes^{low}Tbet^{low}PLZF^{low}CD159c^{+}CD158b, a_h^{+}CD49e^{-}CX3CR1^{-}CD226^{-}CD195^{+}CD183^{-}TIGIT^{-}CD85j^{dim} (Figures 4C–F) and represents the described CD49a^{+} liver specific ml-NK subset (36). The UMAPs in Figures 4G, H confirmed that cluster 28 is only present in HD liver. Cluster 27 resembled peripheral early NK cells being CD56^{bright}CD16$^{-/low}$CD127^{low}CD69^{-}CD186^{-}Eomes^{int}Tbet^{int}PLZF^{low}CD158b, a_h^{+}CD49e^{+}CX3CR1^{-}CD226^{+}CD195^{+}CD183^{-}TIGIT^{+}CD85j^{-} (Figures 4C–F) but additionally expressed CD159c. As such, this cluster corresponded to the described CD56^{bright}CD16^{-} adaptive NK cells, detectable in blood and tissues, with features of tissue-residency (88). Accordingly, cluster 27 was detected at low frequencies in both PBMC (3 out of 5 donors) and in HD livers (2 out of 3 donors) (Figures 4C, D). We confirmed the presence of cluster 27 in three independent experiments in the PBMC of donor 1 (data not shown) for additional validation.

Additional verification of two clusters (clusters 9 and 10) with a similar phenotype as tr-NK cells is presented in Supplementary Figure 12. Both clusters were CD49a^{-} and CD69^{+}CD186^{+} Eomes^{hi}Tbet$^{low/+}$CD49e^{-}CX3CR1^{-}CD226^{-}, with cluster 9 being CD159c^{+} and cluster 10 being CD159c^{-}. Supplementary Figures 12C-F confirmed the differential expression of CD159c between the two clusters and high expression of CD158b, a_h, TIGIT, CD85j and HLA-DR and low expression of PLZF in cluster 9. Although the phenotype of cluster 9 was similar to the described peripheral CD56^{dim}CD16^{+} adaptive NK cells this cluster displayed an expression profile reminiscent of tissue residency (CD69^{+} CD186^{+}Eomes^{hi}Tbet^{low}CD49e^{-}CX3CR1^{-}CD226^{-}), expressed Granzyme B but not perforin, was negative for CD57, and was HLA-DR^{hi} thereby indicating activation. Cluster 9 was detected in all HD liver donors, but only at low percentage in 2 out 5 PBMCs (Supplementary Figures 12G, H). Given the expression of markers of tissue residency and despite the expression of CD16, we designated this cluster, as well as cluster 29, as adaptive tr-NK cells. Cluster 10 was further defined as CD56^{+}CD16^{-}CD57^{-}CD69^{+} CD186^{+}Eomes^{hi}Tbet^{low}PLZF^{bright}CD49e^{-}CX3CR1^{-}CD226 (Supplementary Figure 12D-F). Cluster 10 was also detected at low percentages in the PBMCs of all 5 donors (Supplementary Figure 12G-H) and resembles the described peripheral precursors of tr-NK cells (pre tr-NK) (35, 37, 70). We identified cluster 10 in PBMCs of three independent acquisitions in donor 3 (data not shown) which reinforced the validity of this cluster. Notably, cluster 9 and other liver adaptive NK cells (clusters 12 and 29) all expressed higher levels of TIGIT as well as lower levels of CD226 than CD49a^{-} adaptive NK present in PBMCs (cluster 21). The pattern of TIGIT and CD226 expression might contribute to a unique role of liver adaptive NK cells in maintaining immune homeostasis as previously suggested (81). Additionally, different expression levels of CD158b, a_h were observed among liver adaptive NK cells which might be due to differences in clonal expansion related to HCMV exposure (26).

An important adjustment to our panel design and gating strategy was to include CD127 and CD94. This adjustment was made to distinguish between NK cells (CD127$^{+/-}$CD94^{+}) and ILCs (CD127^{+}CD94^{-}). However, CD49a^{+} lt-ILC1 were recently described, with a phenotype similar to tr-NK cells, including CD94 expression (32). Lt-ILCs could be further identified by expression levels of NKp80 (negative on lt-ILC1s) and Eomes (negative to low on Lt-ILC1s) and being CD200R1^{+}CD127^{low}CD161^{Bright}. Despite the absence of NKp80 in our panel, we were able to identify lt-ILCs in cluster 26. In line with the description of lt-ILC1s, cluster 26 was enriched for CD49a expression and was CD127$^{+/dim}$CD56^{bright}CD16^{-} CD94^{+}CD57^{-}CD69^{+}CD186^{+}CD94^{+}CD161^{bright}CD158b, a_h^{-} Eomes^{low}Tbet^{+}PLZF^{bright}CD2^{-}CD49e^{low}CX3CR1^{-}CD226^{low} (Figure 3F). Additionally, cells in cluster 26 were CD183^{+} and contained heterogenous expression of CD103^{+} cells as in (32) and expressed CD195, two markers of tissue residency. As CD183 plays a role in tissue homing of NK cells under homeostatic conditions and aids in recruiting NK cells to diverse tumor and inflammatory environments (89), this observation suggests that CD183 might also aid the localization of lt-ILCs in combination with other tissue-homing receptors.

In HCC liver samples, derived from the tumor site, we found three clusters to be highly prevalent (clusters 15, 18, 19; Figure 3E) as compared to HD liver and PBMCs. These clusters were CD56^{dim}CD16^{+}CD69^{-}CD186^{-}CD49e^{+}CX3CR1^{+}, and did not express markers of tissue residency, which indicated that these three clusters were cNKs. The HCC liver prevalent clusters represented respectively adaptive NK cells in cluster 19 (37.6% of total NK cells in HCC liver donor 2; CD56^{dim}CD16^{+}CD314^{+} CD159a^{-}CD159c^{+}CD158b, a_h^{-} CD161^{-}CD159a^{-}CD57^{Hi}GranzymeB^{+}Perforin^{-}TIGIT^{+}CD85j^{+}), and mature NK cells in both cluster 18 (44.6% of total NK cells in HCC liver donor 2; CD56^{dim}CD16^{+}CD159c^{-}CD158b, a_h^{-}CD161^{+} CD314^{+}CD159a^{+}CD159c^{-}CD57^{+}GranzymeB^{+}Perforin^{-}TIGIT^{-} CD85j$^{-/low}$) and cluster 15 (46.5% of total NK cells in HCC liver donor 1; CD56^{dim}CD16^{+}CD159c^{-}CD158b, a_h^{-}CD161^{+}CD314^{-}CD159a^{+} CD159c^{-}CD57^{+}GranzymeB^{+}Perforin^{-}TIGIT^{-}CD85j^{-}). Notably, cluster 15 was distinct from the clusters representing peripheral mature NK by their low expression of the NK cell activating receptors CD314 and CD226 and their high levels of the inhibitory receptor CD159a. This combination of NK cell receptors suggests that NK cells belonging to cluster 15 have impaired functionality, as already described in HCC (30, 48, 90). Cluster 19 was CD159c^{+} and distinct from adaptive NK cells prevalent in the periphery (cluster 21) or HD liver (cluster 12) as they expressed high levels of CD57 and CD314 and higher levels of the checkpoint inhibitory molecule TIGIT and the inhibitory receptor CD85j as compared to cluster 21. Cluster 18 was similar to the mature NK cells prevalent in PBMCs (cluster 8), with the distinction that cluster 18 was negative for perforin, TIGIT and CD85j, and express lower levels of CD226, CD335, and CD2 and higher levels of CD314. As such, cluster 15 and 18 expressed a mixture of molecules involved in either NK cell activation or dysfunction. We did not detect CD49a^{+} NK cells in the two HCC liver donors analyzed, in contrast to their reported increased frequency in HCC patients with poor prognosis (87, 91). This might be due to the limited number of samples included in the analysis.

Interestingly, NK cells were recently reclassified by means of scRNAseq and CITE-seq into 6 subsets, namely NK1A-C, NKint, NK2, and NK3 (16). These subsets represent mature NK cells with different metabolic activity (NK1A-C), early NK cells (NK2), adaptive NK cells (NK3) and a NKint subset that is transitional between NK2 and NK1C. These subsets were detected in different

tissues and tumor samples, including HCC, although NK cells in healthy liver samples were not analyzed and markers ascribed to tr-NK cells were not included. With our panel, we were able to identify subpopulations resembling NK1, NK2, NK3, and NKint subsets in PBMCs based on expression levels of CD56, CD16, CD159C, CD159a, CD335, CD314, CD158b, a_h, CD183, PLZF and TIGIT. NKint were described as expressing lower levels of CD335, CD56, CD158_ah, intermediate levels of CD159a, TIGIT and high levels of CD183. Therefore, we annotated clusters 2, 5, 7–8 and 24 as NKint using a combination of these markers. NK2 were defined as being $CD56^{bright}CD16^{-}CD127^{+}CD159a^{+}CD159c^{-}CD183^{dim}$ and were assigned to clusters 10 and 13. NK1 were assigned to clusters 1, 4, 6, 11 and 20 based on the described absence of CD159a and CD159c as well as variable expression of CD158b, a_h and TIGIT. Finally, clusters 21 and 27 matched the phenotype of NK3, as they were $CD159c^{+}CD159a^{-}TIGIT^{+}PLZF^{-}$ as described (16). Designation of clusters according to this newly proposed classification in PBMCs is indicated on the right of the heatmap in Figure 3F and in Supplementary Table 5.

5 Discussion

We present in this method paper the development of a high dimensional full spectral flow cytometric human NK cell panel that can **1)** identify all the NK cell subsets that have been described as present in the periphery and liver; **2)** identify nuances in the different NK cell subsets described as present in the periphery and liver obtained from healthy donors; **3)** distinguish NK cells from ILCs and lt-ILCs; **4)** be used for samples with limited cell numbers and NK cell frequencies; **5)** identify NK cell phenotypes prevalent in health and disease and; **6)** resolve each marker optimally in this high dimensional application focused on one leucocyte lineage. As such, this panel is a valuable tool for NK cell phenotyping in the liver and in the periphery under different pathological conditions. It is likely that this panel can also be used for phenotyping of NK in other sample (tissue) types if the same digestion protocol is applied.

We based the design of this panel on two published panels designed for conventional platforms with key improvements to the gating strategy and panel design. Well established metrics for panel design were used, namely Similarity Index (51), SSM (92), and antigen classification (53). All reagents used in the panel were titrated to ensure optimal target identification and tested for digestion sensitivity. Additionally, we verified the final panel performance by confirming optimal resolution of each marker on both PBMC and liver samples using previously published strategies (51, 52). Despite the limited number of PBMCs and liver samples tested, we confirmed that our panel was able to identify described peripheral and liver (tr-NK and c-NK) NK cells, lt-ILC1s and clusters prevalent in the liver of HCC donors A key improvement that was made in this panel is the inclusion of CD94, HLA-DR and CD127. All NK cells are $CD94^{+}$ which can distinguish them from peripheral $CD94^{-}$ ILCs and can additionally define functional NK cell subsets (93). More importantly, CD127 combined with expression levels of CD94, Eomes and CD49a, allowed us to distinguish tr-NK cells from the recently described $CD94^{+}$ lt-ILC1s (32). Although NKp80 has been designated as a key marker to distinguish NK cells from ILCs and lt-ILC1s (32, 94), we showed that NKp80 is sensitive to our enzyme digestion protocol and noted that this limitation has also been described for commercially available enzyme cocktails. Despite this shortcoming, our panel design provides an alternative gating strategy allowing the distinction between NK cells, ILCs and lt-ILC1s in case enzymatic digestion of samples is needed. Additionally, the inclusion of CD94, instead of using CD127 as unique exclusion marker for classical ILC subsets (11, 64, 65, 95, 96), allowed us to better define the phenotype of early NK cells as being $CD56^{bright}CD16^{-}CD127^{+}CD94^{bright}CD183^{+}$, as described by a variety of technologies (65, 69, 97), and distinguishing them from the rare $CD127^{-}$ peripheral precursors of tr-NKs (35, 37, 70). By using CD127 in combination with CD49a we also identified the $CD49a^{+}$ adaptive NK cell subset present a low frequency in both liver and PBMCs. HLA-DR is often used as an exclusion marker when analyzing NK cells (11, 98, 99). However, it has now been clearly documented that HLA-DR^{+} NK cells represent NK cells with enhanced effector function (100, 101). By including the $CD94^{+}CD56^{+}$HLA-DR^{dim} population in our gating strategy, we confirmed that HLA-DR expression is confined to specific clusters, namely clusters representing adaptive cNK, adaptive tr-NK, $CD49a^{+}$ adaptive pNK, $CD49a^{+}$ ml-NK, pre-tr-NK and $CD49a^{-}$ tr-NK cells. Possibly, these HLA-DR^{+} clusters exert enhanced effector functions like increased production of proinflammatory cytokines or other granzymes and/or enhanced antigen presentation (100).

Although we acknowledge that the number of HCC liver (n=2) and HD liver (n=3) samples used in this study is limited, it was important to confirm that the panel performed optimally on these sample types, as well as to validate the performance of markers associated with NK cell dysfunction. The fact that for HCC liver the cluster distribution was very different between the two donors is not surprising due to the diverse etiology of the disease. Additionally, cancer stage, specific tumor location sampled, treatment strategy, viral infection history, age, gender and other factors could influence the NK cell clusters found in each donor and would need expansion to a larger cohort with clear patient/sample stratification in order to correlate NK cell clusters with patient/sample specific features. However, the results of our study constitute proof of concept of the usefulness of all the markers included in our panel in the context of liver cancer. We incorporated several markers with clinical relevance that affect NK cell functional status including two immune checkpoint molecules, TIGIT and CD226. TIGIT is an inhibitory receptor that decreases NK cell cytotoxic capacity and is upregulated on liver tr-NK. CD226 is an activating receptor mediating anti-tumor responses through recognition of its ligands that are upregulated in tumor cells. Both TIGIT and CD226 share the same ligands, with TIGIT having a higher binding affinity. As such, the balance of TIGIT and CD226 expression levels can

influence the function of NK cells. For example, dysfunctional NK cells that express TIGIT in combination with lower levels of CD226 have been observed in liver cancer, correlate with disease prognosis and are increased in the periphery of hepatitis B-related HCC patients (21, 43, 44, 81, 102–105). In addition, other molecules that have been linked to decreased NK cell function like CD85j, CD161, CD159a and CD314 were also included. CD85j is an inhibitory NK cell receptor of which one of the ligands is a viral ligand encoded by HCMV (106). CD85j identifies dysfunctional NK cells in chronic HBV and HCMV infection (72, 73, 107, 108), conditions often associated with the development of liver cancer. We detected CD85j on liver-specific adaptive NK cells, peripheral adaptive NK cells and subsets of peripheral mature NK cells, allowing to further define distinct functional subsets. CD161 is known to inhibit NK cytolytic function and is a potential target for immunotherapy of HCC (109, 110). CD314 is an activating NK cell receptor triggering NK cell cytotoxicity which downregulation has been correlated with a diminished anti-tumor response (48, 111–113). CD159a is an inhibitory NK cell receptor correlated with poor prognosis in liver cancer (21, 90). Notably, we found three NK cell clusters to be more prevalent in HCC liver samples with specific combinations and expression levels of markers associated with NK cell functionality. The clinical relevance of several markers included in this panel is further emphasized by a recent study in which the presence of NK cells with a specific expression profile (expressing higher levels of CD57, NKG2c, CD314 and CD335 and lower levels of TIGIT and NKG2a) could predict HCC recurrence risk and was related to the specific tumor location sampled (114).

Recently, subsets of NK cells were reclassified as NK1A-C, NK2, NK3 and NKint representing mature, early, adaptive and an intermediate stage between NK2 and NK1 cells (16). We started developing this panel before the publication of this NK cell reclassification and for this reason markers that could further distinguish between the different NK1 subsets (chemotaxis receptors; CXCR4, S1PR1, and SP1PR4) were not included in our panel. However, we were able to define NK1, NK2, NK3, NKint subsets based on the combination of expression levels of CD56, CD16, CD159c, CD159a, CD335, CD314, CD158b, a_h, CD183, PLZF and TIGIT. In summary, with this optimized panel we were able to accurately identify NK cell subsets previously defined in the literature in PBMCs of HDs and liver biopsies, as summarized in Supplementary Table 5. In the near future, it would be interesting to incorporate additional and newly described markers into this panel for a deeper characterization of newly defined subsets.

In conclusion, this is the first high dimensional spectral flow cytometric panel designed for in-depth characterization of NK cells, including 35 markers that can all potentially be coexpressed. We present data supporting the robustness and utility of this panel by providing data supporting the optimal performance of the panel and by showing the effective identification of human NK cell subsets/phenotypes previously described to be present in the circulation and in the liver. We believe that this panel could be a useful tool in studies aimed at understanding the dynamics of NK cells in health and disease states as well as at the development of NK cell-targeted immunotherapies.

Data availability statement

The original contributions presented in the study are included in the article/Supplementary Material. Further inquiries can be directed to the corresponding authors.

Ethics statement

The studies involving humans were approved by Ethics Advisory Council of Sanquin Blood Supply Foundation. The studies were conducted in accordance with the local legislation and institutional requirements. The participants provided their written informed consent to participate in this study.

Author contributions

AP: Conceptualization, Data curation, Formal analysis, Investigation, Methodology, Project administration, Resources, Software, Supervision, Validation, Visualization, Writing – original draft, Writing – review & editing. KR: Resources, Writing – review & editing. JG-V: Conceptualization, Methodology, Writing – review & editing. LH: Conceptualization, Methodology, Writing – review & editing. MJ: Methodology, Supervision, Writing – review & editing. YK: Conceptualization, Data curation, Formal analysis, Methodology, Supervision, Validation, Visualization, Writing – original draft, Writing – review & editing.

Funding

The author(s) declared that financial support was not received for this work and/or its publication.

Acknowledgments

The authors would like to thank Sebastian Lunemann for technical input with the panel design.

Conflict of interest

Authors AP, YK, and MJ are employees of the company Cytek Biosciences Fremont, California, USA.

The remaining authors declare that the research was conducted in the absence of any commercial or financial relationships that could be construed as a potential conflict of interest.

Generative AI statement

The author(s) declare that no Generative AI was used in the creation of this manuscript.

Any alternative text (alt text) provided alongside figures in this article has been generated by Frontiers with the support of artificial intelligence and reasonable efforts have been made to ensure accuracy, including review by the authors wherever possible. If you identify any issues, please contact us.

Publisher's note

All claims expressed in this article are solely those of the authors and do not necessarily represent those of their affiliated organizations, or those of the publisher, the editors and the reviewers. Any product that may be evaluated in this article, or claim that may be made by its manufacturer, is not guaranteed or endorsed by the publisher.

Supplementary material

The Supplementary Material for this article can be found online at: https://www.frontiersin.org/articles/10.3389/fimmu.2025.1609732/full#supplementary-material

References

1. Maskalenko NA, Zhigarev D, Campbell KS. Harnessing natural killer cells for cancer immunotherapy: dispatching the first responders. *Nat Rev Drug Discov*. (2022) 21:559–77. doi: 10.1038/s41573-022-00413-7

2. Zhang B, Yang M, Zhang W, Liu N, Wang D, Jing L, et al. Chimeric antigen receptor-based natural killer cell immunotherapy in cancer: from bench to bedside. *Cell Death Dis*. (2024) 15:50. doi: 10.1038/s41419-024-06438-7

3. Schwane V, Huynh-Tran VH, Vollmers S, Yakup VM, Sauter J, Schmidt AH, et al. Distinct signatures in the receptor repertoire discriminate CD56bright and CD56dim natural killer cells. *Front Immunol*. (2020) 11:568927. doi: 10.3389/fimmu.2020.568927

4. Cooper MA, Fehniger TA, Caligiuri MA. The biology of human natural killer-cell subsets. *Trends Immunol*. (2001) 22:633–40. doi: 10.1016/S1471-4906(01)02060-9

5. Jacobs R, Hintzen G, Kemper A, Beul K, Kempf S, Behrens G, et al. CD56bright cells differ in their KIR repertoire and cytotoxic features from CD56dim NK cells. *Eur J Immunol*. (2001) 31:3121–6. doi: 10.1002/1521-4141(2001010)31:10<3121::AID-IMMU3121>3.0.CO;2-4

6. Nagler A, Lanier LL, Cwirla S, Phillips JH. Comparative studies of human FcRIII-positive and negative natural killer cells. *J Immunol*. (1989) 143:3183–91. doi: 10.4049/jimmunol.143.10.3183

7. Dogra P, Rancan C, Ma W, Toth M, Senda T, Carpenter DJ, et al. Tissue determinants of human NK cell development, function, and residence. *Cell*. (2020) 180:749–763.e13. doi: 10.1016/j.cell.2020.01.022

8. Björkström NK, Ljunggren H-G, Sandberg JK. CD56 negative NK cells: origin, function, and role in chronic viral disease. *Trends Immunol*. (2010) 31:401–6. doi: 10.1016/j.it.2010.08.003

9. Béziat V, Descours B, Parizot C, Debré P, Vieillard V. NK cell terminal differentiation: correlated stepwise decrease of NKG2A and acquisition of KIRs. *PloS One*. (2010) 5:e11966. doi: 10.1371/journal.pone.0011966

10. Cocker ATH, Liu F, Djaoud Z, Guethlein LA, Parham P. CD56-negative NK cells: Frequency in peripheral blood, expansion during HIV-1 infection, functional capacity, and KIR expression. *Front Immunol*. (2022) 13:992723. doi: 10.3389/fimmu.2022.992723

11. Frutoso M, Mair F, Prlic M. OMIP-070: NKp46 -based 27-color phenotyping to define natural killer cells isolated from human tumor tissues. *Cytometry Part A*. (2020) 97:1052–6. doi: 10.1002/cyto.a.24230

12. Horowitz A, Strauss-Albee DM, Leipold M, Kubo J, Nemat-Gorgani N, Dogan OC, et al. Genetic and environmental determinants of human NK cell diversity revealed by mass cytometry. *Sci Transl Med*. (2013) 5:208ra145. doi: 10.1126/scitranslmed.3006702

13. Seo S, Mace EM. Diversity of human NK cell developmental pathways defined by single-cell analyses. *Curr Opin Immunol*. (2022) 74:106–11. doi: 10.1016/j.coi.2021.11.001

14. Yang C, Siebert JR, Burns R, Gerbec ZJ, Bonacci B, Rymaszewski A, et al. Heterogeneity of human bone marrow and blood natural killer cells defined by single-cell transcriptome. *Nat Commun*. (2019) 10:3931. doi: 10.1038/s41467-019-11947-7

15. Ben Amara A, Rouviere M-S, Fattori S, Wlosik J, Gregori E, Boucherit N, et al. High-throughput mass cytometry staining for deep phenotyping of human natural killer cells. *STAR Protoc*. (2022) 3:101768. doi: 10.1016/j.xpro.2022.101768

16. Rebuffet L, Melsen JE, Escalière B, Basurto-Lozada D, Bhandoola A, Björkström NK, et al. High-dimensional single-cell analysis of human natural killer cell heterogeneity. *Nat Immunol*. (2024) 25:1474–88. doi: 10.1038/s41590-024-01883-0

17. Vendrame E, McKechnie JL, Ranganath T, Zhao NQ, Rustagi A, Vergara R, et al. Profiling of the human natural killer cell receptor-ligand repertoire. *J Visualized Experiments*. (2020) 165. doi: 10.3791/61912

18. Mikulak J, Bruni E, Oriolo F, Di Vito C, Mavilio D. Hepatic natural killer cells: organ-specific sentinels of liver immune homeostasis and physiopathology. *Front Immunol*. (2019) 10:946. doi: 10.3389/fimmu.2019.00946

19. Yang M, Vanderwert E, Kimchi ET, Staveley-O'Carroll KF, Li G. The important roles of natural killer cells in liver fibrosis. *Biomedicines*. (2023) 11:1391. doi: 10.3390/biomedicines11051391

20. Fionda C, Scarno G, Stabile H, Molfetta R, Di Censo C, Gismondi A, et al. NK cells and other cytotoxic innate lymphocytes in colorectal cancer progression and metastasis. *Int J Mol Sci*. (2022) 23:7859. doi: 10.3390/ijms23147859

21. Wang J, Cao Y, Tian Y, Dai C, Jin T, Xu F. A novel prognostic nomogram based on TIGIT and NKG2A can predict relapse-free survival of hepatocellular carcinoma after hepatectomy. *Cancer Med*. (2024) 13:e70419. doi: 10.1002/cam4.70419

22. Xue J-S, Ding Z-N, Meng G-X, Yan L-J, Liu H, Li H-C, et al. The prognostic value of natural killer cells and their receptors/ligands in hepatocellular carcinoma: A systematic review and meta-analysis. *Front Immunol*. (2022) 13:872353. doi: 10.3389/fimmu.2022.872353

23. Hudspeth K, Donadon M, Cimino M, Pontarini E, Tentorio P, Preti M, et al. Human liver-resident CD56bright/CD16neg NK cells are retained within hepatic sinusoids via the engagement of CCR5 and CXCR6 pathways. *J Autoimmun*. (2016) 66:40–50. doi: 10.1016/j.jaut.2015.08.011

24. Jameson G, Harmon C, Santiago RM, Houlihan DD, Gallagher TK, Lynch L, et al. Human hepatic CD56bright NK cells display a tissue-resident transcriptional profile and enhanced ability to kill allogenic CD8+ T cells. *Front Immunol*. (2022) 13:921212. doi: 10.3389/fimmu.2022.921212

25. Doyle EH, Aloman C, El-Shamy A, Eng F, Rahman A, Klepper AL, et al. A subset of liver resident natural killer cells is expanded in hepatitis C-infected patients with better liver function. *Sci Rep*. (2021) 11:1551. doi: 10.1038/s41598-020-80819-8

26. Forrest C, Chase TJG, Cuff AO, Maroulis D, Motallebzadeh R, Gander A, et al. Control of human cytomegalovirus replication by liver resident natural killer cells. *Nat Commun*. (2023) 14:1409. doi: 10.1038/s41467-023-37181-w

27. Singh SP, Madke T, Chand P. Global epidemiology of hepatocellular carcinoma. *J Clin Exp Hepatol*. (2025) 15:102446. doi: 10.1016/j.jceh.2024.102446

28. Llovet JM, Kelley RK, Villanueva A, Singal AG, Pikarsky E, Roayaie S, et al. Hepatocellular carcinoma. *Nat Rev Dis Primers*. (2021) 7:6. doi: 10.1038/s41572-020-00240-3

29. Sajid M, Liu L, Sun C. The dynamic role of NK cells in liver cancers: role in HCC and HBV associated HCC and its therapeutic implications. *Front Immunol*. (2022) 13:887186. doi: 10.3389/fimmu.2022.887186

30. Shin SK, Oh S, Chun S, Ahn M, Lee S, Kim K, et al. Immune signature and therapeutic approach of natural killer cell in chronic liver disease and hepatocellular carcinoma. *J Gastroenterol Hepatol*. (2024). 9:1717–1727. doi: 10.1111/jgh.16584

31. Filipovic I, Sönnerborg I, Strunz B, Friberg D, Cornillet M, Hertwig L, et al. 29-color flow cytometry: unraveling human liver NK cell repertoire diversity. *Front Immunol*. (2019) 10:2692. doi: 10.3389/fimmu.2019.02692

32. Krämer B, Nalin AP, Ma F, Eickhoff S, Lutz P, Leonardelli S, et al. Single-cell RNA sequencing identifies a population of human liver-type ILC1s. *Cell Rep*. (2023) 42:111937. doi: 10.1016/j.celrep.2022.111937

33. Aw Yeang HX, Piersma SJ, Lin Y, Yang L, Malkova ON, Miner C, et al. Cutting edge: human CD49e– NK cells are tissue resident in the liver. *J Immunol*. (2017) 198:1417–22. doi: 10.4049/jimmunol.1601818

34. Harmon C, Robinson MW, Fahey R, Whelan S, Houlihan DD, Geoghegan J, et al. Tissue-resident Eomes hi T-bet lo CD56 bright NK cells with reduced proinflammatory potential are enriched in the adult human liver. *Eur J Immunol*. (2016) 46:2111–20. doi: 10.1002/eji.201646559

35. Cuff AO, Robertson FP, Stegmann KA, Pallett LJ, Maini MK, Davidson BR, et al. Eomeshi NK cells in human liver are long-lived and do not recirculate but can be replenished from the circulation. *J Immunol*. (2016) 197:4283–91. doi: 10.4049/jimmunol.1601424

36. Marquardt N, Béziat V, Nyström S, Hengst J, Ivarsson MA, Kekäläinen E, et al. Cutting edge: identification and characterization of human intrahepatic CD49a+ NK cells. *J Immunol*. (2015) 194:2467–71. doi: 10.4049/jimmunol.1402756

37. Hess LU, Martrus G, Ziegler AE, Langeneckert AE, Salzberger W, Goebels H, et al. The transcription factor promyelocytic leukemia zinc finger protein is associated with expression of liver-homing receptors on human blood CD56bright natural killer cells. *Hepatol Commun*. (2020) 4:409–24. doi: 10.1002/hep4.1463

38. Vossen MTM, Matmati M, Hertoghs KML, Baars PA, Gent M-R, Leclercq G, et al. CD27 defines phenotypically and functionally different human NK cell subsets. *J Immunol*. (2008) 180:3739–45. doi: 10.4049/jimmunol.180.6.3739

39. Fu B, Wang F, Sun R, Ling B, Tian Z, Wei H. CD11b and CD27 reflect distinct population and functional specialization in human natural killer cells. *Immunology*. (2011) 133:350–9. doi: 10.1111/j.1365-2567.2011.03446.x

40. Björkström NK, Riese P, Heuts F, Andersson S, Fauriat C, Ivarsson MA, et al. Expression patterns of NKG2A, KIR, and CD57 define a process of CD56dim NK-cell differentiation uncoupled from NK-cell education. *Blood*. (2010) 116:3853–64. doi: 10.1182/blood-2010-04-281675

41. Hendricks DW, Balfour HH, Dunmire SK, Schmeling DO, Hogquist KA, Lanier LL. Cutting edge: NKG2ChiCD57+ NK cells respond specifically to acute infection with cytomegalovirus and not epstein–barr virus. *J Immunol*. (2014) 192:4492–6. doi: 10.4049/jimmunol.1303211

42. Lopez-Vergès S, Milush JM, Schwartz BS, Pando MJ, Jarjoura J, York VA, et al. Expansion of a unique CD57 + NKG2C hi natural killer cell subset during acute human cytomegalovirus infection. *Proc Natl Acad Sci*. (2011) 108:14725–32. doi: 10.1073/pnas.1110900108

43. Zheng Q, Xu J, Gu X, Wu F, Deng J, Cai X, et al. Immune checkpoint targeting TIGIT in hepatocellular carcinoma. *Am J Transl Res*. (2020) 12:3212–24.

44. Chiang EY, Mellman I. TIGIT-CD226-PVR axis: advancing immune checkpoint blockade for cancer immunotherapy. *J Immunother Cancer*. (2022) 10:e004711. doi: 10.1136/jitc-2022-004711

45. Du X, De Almeida P, Manieri N, De Almeida Nagata D, Wu TD, Harden Bowles K, et al. CD226 regulates natural killer cell antitumor responses via phosphorylation-mediated inactivation of transcription factor FOXO1. *Proc Natl Acad Sci*. (2018) 115:E11731-E11740. doi: 10.1073/pnas.1814052115

46. Conner M, Hance KW, Yadavilli S, Smothers J, Waight JD. Emergence of the CD226 axis in cancer immunotherapy. *Front Immunol*. (2022) 13:914406. doi: 10.3389/fimmu.2022.914406

47. Hu Z, Zhang Q, He Z, Jia X, Zhang W, Cao X. MHC1/LILRB1 axis as an innate immune checkpoint for cancer therapy. *Front Immunol*. (2024) 15:1421092. doi: 10.3389/fimmu.2024.1421092

48. Wang J, Li C-D, Sun L. Recent advances in molecular mechanisms of the NKG2D pathway in hepatocellular carcinoma. *Biomolecules*. (2020) 10: 301. doi: 10.3390/biom10020301

49. Childs A, Aidoo-Micah G, Maini MK, Meyer T. Immunotherapy for hepatocellular carcinoma. *JHEP Rep*. (2024) 6:101130. doi: 10.1016/j.jhepr.2024.101130

50. Sivakumar S, Abu-Shah E, Ahern DJ, Arbe-Barnes EH, Jainarayanan AK, Mangal N, et al. Activated regulatory T-cells, dysfunctional and senescent T-cells hinder the immunity in pancreatic cancer. *Cancers (Basel)*. (2021) 13:1776. doi: 10.3390/cancers13081776

51. Park LM, Lannigan J, Jaimes MC. OMIP-069: forty-color full spectrum flow cytometry panel for deep immunophenotyping of major cell subsets in human peripheral blood. *Cytometry Part A*. (2020) 97:1044–51. doi: 10.1002/cyto.a.24213

52. Park LM, Lannigan J, Low Q, Jaimes MC, Bonilla DL. OMIP-109: 45-color full spectrum flow cytometry panel for deep immunophenotyping of the major lineages present in human peripheral blood mononuclear cells with emphasis on the T cell memory compartment. *Cytometry Part A*. (2024) 105:807–15. doi: 10.1002/cyto.a.24900

53. Mahnke YD, Roederer M. Optimizing a multicolor immunophenotyping assay. *Clin Lab Med*. (2007) 27:469–85. doi: 10.1016/j.cll.2007.05.002

54. Bonilla DL, Paul A, Gil-Pulido J, Park LM, Jaimes MC. The power of reagent titration in flow cytometry. *Cells*. (2024) 13:1677. doi: 10.3390/cells13201677

55. Jalbert E, Shikuma CM, Ndhlovu LC, Barbour JD. Sequential staining improves detection of CCR2 and CX3CR1 on monocytes when simultaneously evaluating CCR5 by multicolor flow cytometry. *Cytometry Part A*. (2013) 83:280–6. doi: 10.1002/cyto.a.22257

56. Ferrer-Font L, Small SJ, Lewer B, Pilkington KR, Johnston LK, Park LM, et al. Panel optimization for high-dimensional immunophenotyping assays using full-spectrum flow cytometry. *Curr Protoc*. (2021) 1:e222. doi: 10.1002/cpz1.222

57. Kharraz Y, Lukesova V, Serrano AL, Davison A, Muñoz-Cánoves P. Full spectrum cytometry improves the resolution of highly autofluorescent biological samples: Identification of myeloid cells in regenerating skeletal muscles. *Cytometry Part A*. (2022) 101:862–76. doi: 10.1002/cyto.a.24568

58. Chang MY, Brune JE, Black M, Altemeier WA, Frevert CW. Multicompartmental analysis of the murine pulmonary immune response by spectral flow cytometry. *Am J Physiology-Lung Cell Mol Physiol*. (2023) 325:L518–35. doi: 10.1152/ajplung.00317.2022

59. Baumann Z, Wiethe C, Vecchi CM, RiChina V, Lopes T, Bentires-Alj M. Optimized full-spectrum flow cytometry panel for deep immunophenotyping of murine lungs. *Cell Rep Methods*. (2024) 4:100885. doi: 10.1016/j.crmeth.2024.100885

60. Lambooij JM, Tak T, Zaldumbide A, Guigas B. OMIP-104: A 30-color spectral flow cytometry panel for comprehensive analysis of immune cell composition and macrophage subsets in mouse metabolic organs. *Cytometry Part A*. (2024) 105:493–500. doi: 10.1002/cyto.a.24845

61. Rico LG, Salvia R, Ward MD, Bradford JA, Petriz J. Flow-cytometry-based protocols for human blood/marrow immunophenotyping with minimal sample perturbation. *STAR Protoc*. (2021) 2:100883. doi: 10.1016/j.xpro.2021.100883

62. Meskas J, Yokosawa D, Wang S, Segat GC, Brinkman RR. flowCut: An R package for automated removal of outlier events and flagging of files based on time versus fluorescence analysis. *Cytometry A*. (2023) 103:71–81. doi: 10.1002/cyto.a.24670

63. Levine JH, Simonds EF, Bendall SC, Davis KL, Amir ED, Tadmor MD, et al. Data-driven phenotypic dissection of AML reveals progenitor-like cells that correlate with prognosis. *Cell*. (2015) 162:184–97. doi: 10.1016/j.cell.2015.05.047

64. Bianca Bennstein S, Riccarda Manser A, Weinhold S, Scherenschlich N, Uhrberg M. OMIP-055: characterization of human innate lymphoid cells from neonatal and peripheral blood. *Cytometry Part A*. (2019) 95:427–30. doi: 10.1002/cyto.a.23741

65. Ohne Y. OMIP-066: identification of novel subpopulations of human group 2 innate lymphoid cells in peripheral blood. *Cytometry Part A*. (2020) 97:1028–31. doi: 10.1002/cyto.a.24046

66. Mathew SO, Chaudhary P, Powers SB, Vishwanatha JK, Mathew PA. Overexpression of LLT1 (OCIL, CLEC2D) on prostate cancer cells inhibits NK cell-mediated killing through LLT1-NKRP1A (CD161) interaction. *Oncotarget*. (2016) 7:68650–61. doi: 10.18632/oncotarget.11896

67. Mathew P. The LLT1 receptor induces IFN-γ production by human natural killer cells. *Mol Immunol*. (2004) 40:1157–63. doi: 10.1016/j.molimm.2003.11.024

68. Eisenhardt M, Glässner A, Krämer B, Körner C, Sibbing B, Kokordelis P, et al. The CXCR3(+)CD56Bright phenotype characterizes a distinct NK cell subset with anti-fibrotic potential that shows dys-regulated activity in hepatitis C. *PloS One*. (2012) 7:e38846. doi: 10.1371/journal.pone.0038846

69. Wendt K, Wilk E, Buyny S, Buer J, Schmidt RE, Jacobs R. Gene and protein characteristics reflect functional diversity of CD56dim and CD56bright NK cells. *J Leukoc Biol*. (2006) 80:1529–41. doi: 10.1189/jlb.0306191

70. Angelo LS, Hogg GD, Abeynaike S, Bimler L, Vargas-Hernandez A, Paust S. Phenotypic and functional plasticity of CXCR6+ Peripheral blood NK cells. *Front Immunol*. (2021) 12:810080. doi: 10.3389/fimmu.2021.810080

71. López-Botet M, De Maria A, Muntasell A, Della Chiesa M, Vilches C. Adaptive NK cell response to human cytomegalovirus: Facts and open issues. *Semin Immunol*. (2023) 65:101706. doi: 10.1016/j.smim.2022.101706

72. Béziat V, Dalgard O, Asselah T, Halfon P, Bedossa P, Boudifa A, et al. CMV drives clonal expansion of NKG2C + NK cells expressing self-specific KIRs in chronic hepatitis patients. *Eur J Immunol*. (2012) 42:447–57. doi: 10.1002/eji.201141826

73. Schlums H, Cichocki F, Tesi B, Theorell J, Beziat V, Holmes TD, et al. Cytomegalovirus infection drives adaptive epigenetic diversification of NK cells with altered signaling and effector function. *Immunity*. (2015) 42:443–56. doi: 10.1016/j.immuni.2015.02.008

74. Hammer Q, Romagnani C. OMIP-039: Detection and analysis of human adaptive NKG2C + natural killer cells. *Cytometry Part A*. (2017) 91:997–1000. doi: 10.1002/cyto.a.23168

75. Forconi CS, Oduor CI, Oluoch PO, Ong'echa JM, Münz C, Bailey JA. Moormann AM. A new hope for CD56negCD16pos NK cells as unconventional cytotoxic mediators: an adaptation to chronic diseases. *Front Cell Infect Microbiol*. (2020) 10:162. doi: 10.3389/fcimb.2020.00162

76. Gonzalez VD, Falconer K, Michaëlsson J, Moll M, Reichard O, Alaeus A, et al. Expansion of CD56– NK cells in chronic HCV/HIV-1 co-infection: Reversion by antiviral treatment with pegylated IFNα and ribavirin. *Clin Immunol*. (2008) 128:46–56. doi: 10.1016/j.clim.2008.03.521

77. Gonzalez VD, Falconer K, Bjorkstrom NK, Blom KG, Weiland O, Ljunggren H-G, et al. Expansion of functionally skewed CD56-negative NK cells in chronic hepatitis C virus infection: correlation with outcome of pegylated IFN-α and ribavirin treatment. *J Immunol*. (2009) 183:6612–8. doi: 10.4049/jimmunol.0901437

78. Hu PF, Hultin LE, Hultin P, Hausner MA, Hirji K, Jewett A, et al. Natural killer cell immunodeficiency in HIV disease is manifest by profoundly decreased numbers of CD16+CD56+ cells and expansion of a population of CD16dimCD56- cells with low lytic activity. *J Acquir Immune Defic Syndr Hum Retrovirol*. (1995) 10:331–40. doi: 10.1097/00042560-199511000-00005

79. Wong P, Foltz JA, Chang L, Neal CC, Yao T, Cubitt CC, et al. T-BET and EOMES sustain mature human NK cell identity and antitumor function. *J Clin Invest*. (2023) 133:e162530. doi: 10.1172/JCI162530

80. Stegmann KA, Robertson F, Hansi N, Gill U, Pallant C, Christophides T, et al. CXCR6 marks a novel subset of T-betloEomeshi natural killer cells residing in human liver. *Sci Rep*. (2016) 6:26157. doi: 10.1038/srep26157

81. Ziegler AE, Fittje P, Müller LM, Ahrenstorf AE, Hagemann K, Hagen SH, et al. The co-inhibitory receptor TIGIT regulates NK cell function and is upregulated in human intrahepatic CD56bright NK cells. *Front Immunol*. (2023) 14:1117320. doi: 10.3389/fimmu.2023.1117320

82. Polidoro MA, Mikulak J, Cazzetta V, Lleo A, Mavilio D, Torzilli G, et al. Tumor microenvironment in primary liver tumors: A challenging role of natural killer cells. *World J Gastroenterol*. (2020) 26:4900–18. doi: 10.3748/wjg.v26.i33.4900

83. Shi F-D, Ljunggren H-G, La Cava A, Van Kaer L. Organ-specific features of natural killer cells. *Nat Rev Immunol*. (2011) 11:658–71. doi: 10.1038/nri3065

84. Rückert T, Lareau CA, Mashreghi M-F, Ludwig LS, Romagnani C. Clonal expansion and epigenetic inheritance of long-lasting NK cell memory. *Nat Immunol*. (2022) 23:1551–63. doi: 10.1038/s41590-022-01327-7

85. Ferron E, David G, Willem C, Legrand N, Salameh P, Anquetil L, et al. Multifactorial determinants of NK cell repertoire organization: insights into age, sex, KIR genotype, HLA typing, and CMV influence. *Front Immunol*. (2024) 15:1389358. doi: 10.3389/fimmu.2024.1389358

86. Gibert-Ramos A, Sanfeliu-Redondo D, Aristu-Zabalza P, Martínez-Alcocer A, Gracia-Sancho J, Guixé-Muntet S, et al. The hepatic sinusoid in chronic liver disease: the optimal milieu for cancer. *Cancers (Basel)*. (2021) 13:5719. doi: 10.3390/cancers13225719

87. Sun H, Liu L, Huang Q, Liu H, Huang M, Wang J, et al. Accumulation of tumor-infiltrating CD49a+ NK cells correlates with poor prognosis for human hepatocellular carcinoma. *Cancer Immunol Res*. (2019) 7:1535–46. doi: 10.1158/2326-6066.CIR-18-0757

88. Brownlie D, Scharenberg M, Mold JE, Hård J, Kekäläinen E, Buggert M, et al. Expansions of adaptive-like NK cells with a tissue-resident phenotype in human lung and blood. *Proc Natl Acad Sci*. (2021) 118:e2016580118. doi: 10.1073/pnas.2016580118

89. Ran G, Lin YQ, Tian L, Zhang T, Yan DM, Yu JH, et al. Natural killer cell homing and trafficking in tissues and tumors: from biology to application. *Signal Transduct Target Ther*. (2022) 7:205. doi: 10.1038/s41392-022-01058-z

90. Sun C, Xu J, Huang Q, Huang M, Wen H, Zhang C, et al. High NKG2A expression contributes to NK cell exhaustion and predicts a poor prognosis of patients with liver cancer. *Oncoimmunology*. (2017) 6:e1264562. doi: 10.1080/2162402X.2016.1264562

91. Zecca A, Barili V, Boni C, Fisicaro P, Vecchi A, Rossi M, et al. High CD49a+ NK cell infiltrate is associated with poor clinical outcomes in Hepatocellular Carcinoma. *Heliyon*. (2023) 9:e22680. doi: 10.1016/j.heliyon.2023.e22680

92. Nguyen R, Perfetto S, Mahnke YD, Chattopadhyay P, Roederer M. Quantifying spillover spreading for comparing instrument performance and aiding in multicolor panel design. *Cytometry Part A*. (2013) 83:306–15. doi: 10.1002/cyto.a.22251

93. Yu J, Mao HC, Wei M, Hughes T, Zhang J, Park I, et al. CD94 surface density identifies a functional intermediary between the CD56bright and CD56dim human NK-cell subsets. *Blood*. (2010) 115:274–81. doi: 10.1182/blood-2009-04-215491

94. Freud AG, Keller KA, Scoville SD, Mundy-Bosse BL, Cheng S, Youssef Y, et al. NKp80 defines a critical step during human natural killer cell development. *Cell Rep*. (2016) 16:379–91. doi: 10.1016/j.celrep.2016.05.095

95. Doyle CM, Fewings NL, Ctercteko G, Byrne SN, Harman AN, Bertram KM. OMIP 082: A 25-color phenotyping to define human innate lymphoid cells, natural killer cells, mucosal-associated invariant T cells, and γδ T cells from freshly isolated human intestinal tissue. *Cytometry Part A*. (2022) 101:196–202. doi: 10.1002/cyto.a.24529

96. Calvi M, Di Vito C, Frigo A, Trabanelli S, Jandus C, Mavilio D. Development of human ILCs and impact of unconventional cytotoxic subsets in the pathophysiology of inflammatory diseases and cancer. *Front Immunol*. (2022) 13:914266. doi: 10.3389/fimmu.2022.914266

97. Hertoghs N, Schwedhelm KV, Stuart KD, McElrath MJ, De Rosa SC. OMIP-064: A 27-color flow cytometry panel to detect and characterize human NK cells and other innate lymphoid cell subsets, MAIT cells, and γδ T cells. *Cytometry Part A*. (2020) 97:1019–23. doi: 10.1002/cyto.a.24031

98. Dintwe O, Rohith S, Schwedhelm KV, McElrath MJ, Andersen-Nissen E, De Rosa SC. OMIP-056: evaluation of human conventional T cells, donor-unrestricted T cells, and NK cells including memory phenotype by intracellular cytokine staining. *Cytometry Part A*. (2019) 95:722–5. doi: 10.1002/cyto.a.23753

99. Liechti T, Roederer M. OMIP-058: 30-parameter flow cytometry panel to characterize iNKT, NK, unconventional and conventional T cells. *Cytometry Part A*. (2019) 95:946–51. doi: 10.1002/cyto.a.23850

100. Erokhina SA, Streltsova MA, Kanevskiy LM, Grechikhina MV, Sapozhnikov AM, Kovalenko EI. HLA-DR-expressing NK cells: Effective killers suspected for antigen presentation. *J Leukoc Biol*. (2021) 109:327–37. doi: 10.1002/JLB.3RU0420-668RR

101. Evans JH, Horowitz A, Mehrabi M, Wise EL, Pease JE, Riley EM, et al. A distinct subset of human NK cells expressing HLA-DR expand in response to IL-2 and can aid immune responses to BCG. *Eur J Immunol*. (2011) 41:1924–33. doi: 10.1002/eji.201041180

102. Yu L, Liu X, Wang X, Yan F, Wang P, Jiang Y, et al. TIGIT + TIM-3 + NK cells are correlated with NK cell exhaustion and disease progression in patients with hepatitis B virus-related hepatocellular carcinoma. *Oncoimmunology*. (2021) 10:e1942673. doi: 10.1080/2162402X.2021.1942673

103. Ge Z, Peppelenbosch MP, Sprengers D, Kwekkeboom J. TIGIT, the next step towards successful combination immune checkpoint therapy in cancer. *Front Immunol*. (2021) 12:699895. doi: 10.3389/fimmu.2021.699895

104. Sanchez-Correa B, Valhondo I, Hassouneh F, Lopez-Sejas N, Pera A, Bergua JM, et al. DNAM-1 and the TIGIT/PVRIG/TACTILE axis: novel immune checkpoints for natural killer cell-based cancer immunotherapy. *Cancers (Basel)*. (2019) 11:877. doi: 10.3390/cancers11060877

105. Stanietsky N, Simic H, Arapovic J, Toporik A, Levy O, Novik A, et al. The interaction of TIGIT with PVR and PVRL2 inhibits human NK cell cytotoxicity. *Proc Natl Acad Sci*. (2009) 106:17858–63. doi: 10.1073/pnas.0903474106

106. Valeís-Goímez M, Shiroishi M, Maenaka K, Reyburn HT. Genetic variability of the major histocompatibility complex class I homologue encoded by human cytomegalovirus leads to differential binding to the inhibitory receptor ILT2. *J Virol*. (2005) 79:2251–60. doi: 10.1128/JVI.79.4.2251-2260.2005

107. Zhang Y, Tong S, Li S, Wang X, Ren H, Yin W. Increased ILT2 expression contributes to dysfunction of CD56dimCD16+NK cells in chronic hepatitis B virus infection. *Antiviral Res*. (2022) 205:105385. doi: 10.1016/j.antiviral.2022.105385

108. Gumaí M, Angulo A, Vilches C, Goímez-Lozano N, Malats N, Loípez-Botet M. Imprint of human cytomegalovirus infection on the NK cell receptor repertoire. *Blood*. (2004) 104:3664–71. doi: 10.1182/blood-2004-05-2058

109. Kurioka A, Cosgrove C, Simoni Y, Van Wilgenburg B, Geremia A, Björkander S, et al. CD161 defines a functionally distinct subset of pro-inflammatory natural killer cells. *Front Immunol*. (2018) 9:486. doi: 10.3389/fimmu.2018.00486

110. Mathew P. The LLT1 receptor induces IFN-γ production by human natural killer cells. *Mol Immunol*. (2004) 40:1157–63. doi: 10.1016/j.molimm.2003.11.024

111. Cosman D, Müllberg J, Sutherland CL, Chin W, Armitage R, Fanslow W, et al. ULBPs, novel MHC class I–related molecules, bind to CMV glycoprotein UL16 and stimulate NK cytotoxicity through the NKG2D receptor. *Immunity*. (2001) 14:123–33. doi: 10.1016/S1074-7613(01)00095-4

112. Sutherland CL, Chalupny NJ, Schooley K, VandenBos T, Kubin M, Cosman D. UL16-binding proteins, novel MHC class I-related proteins, bind to NKG2D and activate multiple signaling pathways in primary NK cells. *J Immunol*. (2002) 168:671–9. doi: 10.4049/jimmunol.168.2.671

113. Bauer S, Groh V, Wu J, Steinle A, Phillips JH, Lanier LL, et al. Activation of NK cells and T cells by NKG2D, a receptor for stress-inducible MICA. *Science*. (1999) 285:727–9. doi: 10.1126/science.285.5428.727

114. Jia G, He P, Dai T, Goh D, Wang J, Sun M, et al. Spatial immune scoring system predicts hepatocellular carcinoma recurrence. *Nature*. (2025). 8060:1031–1041. doi: 10.1038/s41586-025-08668-x

Frontiers in Immunology

Explores novel approaches and diagnoses to treat immune disorders.

The official journal of the International Union of Immunological Societies (IUIS) and the most cited in its field, leading the way for research across basic, translational and clinical immunology.

Discover the latest Research Topics

See more →

Frontiers

Avenue du Tribunal-Fédéral 34
1005 Lausanne, Switzerland
frontiersin.org

Contact us

+41 (0)21 510 17 00
frontiersin.org/about/contact